Technical Report Documentation Page

1. Report No. FHWA/TX-07/0-4650-1	2. Government Accession No.	3. Recipient's Catalog No.	
4. Title and Subtitle A Probabilistic Analysis of the Frequency of Bridge Collapses due to Vessel Impact		5. Report Date November 2006	
		6. Performing Organization Code	
7. Author(s) Lance Manuel, Loukas F. Kallivokas, Eric B. Williamson, Michael Bomba, Kenneth B. Berlin, Adam Cryer, Wyatt R. Henderson		8. Performing Organization Report No. 0-4650-1	
9. Performing Organization Name and Address Center for Transportation Research The University of Texas at Austin 3208 Red River, Suite 200 Austin, TX 78705-2650		10. Work Unit No. (TRAIS)	
		11. Contract or Grant No. 0-4650	
12. Sponsoring Agency Name and Address Texas Department of Transportation Research and Technology Implementation Office P.O. Box 5080 Austin, TX 78763-5080		13. Type of Report and Period Covered Technical Report September 1, 2003–August 31, 2005	
		14. Sponsoring Agency Code	
15. Supplementary Notes Project performed in cooperation with the Texas Department of Transportation and the Federal Highway Administration.			
16. Abstract The collapse of the Queen Isabella Causeway in 2001, caused by a vessel collision, sent an alarming message to the state of Texas that vessel impact on bridges is a serious issue and that the possibility of such accidents needs to be considered in the design and evaluation of any bridge spanning a waterway. The Texas Department of Transportation (TxDOT) funded this research project at The University of Texas at Austin seeking to re-evaluate the current vessel collision calculations (both on the load and resistance side), create a database of vessel traffic in the state of Texas, and design a stand-alone computer program to perform the vessel collision risk calculations. Currently the 2004 American Association of State Highway and Transportation Officials (AASHTO) Load and Resistance Factor Design (LRFD) design code regulates vessel collision analysis. Bridges are designed to meet a specified annual frequency of collapse based on a probabilistic model. While the basis for the computation of the probability of aberrancy and geometric probability are well justified, little research has been performed on barge to pier collisions to support the AASHTO LRFD method for probability of collapse. Using two models, one that determines the force imparted on a bridge pier by a vessel and another that determines what the ultimate lateral strength of a pier is, an enhanced method for determining probability of collapse was developed.			
17. Key Words Vessel impact, bridge, barge, pier, vessel collision analysis, probability of collapse, modeling		18. Distribution Statement No restrictions. This document is available to the public through the National Technical Information Service, Springfield, Virginia 22161; www.ntis.gov.	
19. Security Classif. (of report) Unclassified	20. Security Classif. (of this page) Unclassified	21. No. of pages 454	22. Price

Form DOT F 1700.7 (8-72) Reproduction of completed page authorized

A Probabilistic Analysis of the Frequency of Bridge Collapses due to Vessel Impact

Lance Manuel
Loukas F. Kallivokas
Eric B. Williamson
Michael Bomba
Kenneth B. Berlin
Adam Cryer
Wyatt R. Henderson

Disclaimers

Author's Disclaimer: The contents of this report reflect the views of the authors, who are responsible for the facts and the accuracy of the data presented herein. The contents do not necessarily reflect the official view or policies of the Federal Highway Administration or the Texas Department of Transportation (TxDOT). This report does not constitute a standard, specification, or regulation.

Patent Disclaimer: There was no invention or discovery conceived or first actually reduced to practice in the course of or under this contract, including any art, method, process, machine manufacture, design or composition of matter, or any new useful improvement thereof, or any variety of plant, which is or may be patentable under the patent laws of the United States of America or any foreign country.

Notice: The United States Government and the State of Texas do not endorse products or manufacturers. If trade or manufacturers' names appear herein, it is solely because they are considered essential to the object of this report.

Engineering Disclaimer

NOT INTENDED FOR CONSTRUCTION, BIDDING, OR PERMIT PURPOSES.

Project Engineer: Lance Manuel, Ph.D., P.E.
Professional Engineer License State and Number: Texas No. 95990
P. E. Designation: Research Supervisior

v

Acknowledgments

Table of Contents

Introduction

Introduction

The collapse of the Queen Isabella Causeway in 2001, caused by a vessel collision, sent an alarming message to the state of Texas that vessel impact on bridges is a serious issue and that the possibility of such accidents needs to be considered in the design and evaluation of any bridge spanning a waterway. The Texas Department of Transportation (TxDOT) funded this research project at The University of Texas at Austin seeking to re-evaluate the current vessel collision calculations (both on the load and resistance side), create a database of vessel traffic in the state of Texas, and design a stand-alone computer program to perform the vessel collision risk calculations.

Currently the 2004 American Association of State Highway and Transportation Officials (AASHTO) Load and Resistance Factor Design (LRFD) design code regulates vessel collision analysis. Bridges are designed to meet a specified annual frequency of collapse based on a probabilistic model. While the basis for the computation of the probability of aberrancy and geometric probability are well justified, little research has been performed on barge to pier collisions to support the AASHTO LRFD method for probability of collapse. Using two models, one that determines the force imparted on a bridge pier by a vessel and another that determines what the ultimate lateral strength of a pier is, an enhanced method for determining probability of collapse is developed.

Volume I   Development of a Software Program for Vessel Impact Risk Calculations

Because of the extensive calculations that need to be carried out to determine the return period for just one bridge, a user-friendly stand-alone computer program, named VIOB (Vessel Impact On Bridges), is created. Using a comprehensive vessel traffic database created for this research project, VIOB performs an entire bridge analysis efficiently. Like most analysis programs, VIOB consists of three parts: a pre-processing component, a solver component, and a post-processing component. A database assembled for these analyses is integrated with the software and is extensively used in the preprocessing phase. The solver component is where the various calculations leading up to the estimation of probability of bridge collapse are carried out. In the post-processing component, results can be viewed and extensive reports can be printed and studied.

In order to carry out all the calculations involved in estimating the probability of bridge collapse due to vessel impact, the software program developed here builds upon vessel impact force analysis, bridge ultimate strength analysis, and the development of a database on waterways, vessels, traffic, and bridges.

A comprehensive study entitled, "Structural Reliability Analysis for Vessel Impact on Bridges," by Kenneth B. Berlin and Lance Manuel, summarizes all of the work carried

out that relates to the structural reliability analysis and the development of the computer program, VIOB, for vessel impact on bridges. This study makes up <u>Volume I</u> of this report.

Volume II   Vessel Impact Forces

The 2001 Interim AASHTO LRFD Bridge Design Specifications contain design provisions that account for waterway vessel collisions on bridge piers and that were adapted from the 1991 AASHTO Guide Specifications and Commentary for Vessel Collision Design of Highway Bridges. Recent vessel collisions with bridge piers, however, have brought renewed attention to the code specifications, especially in light of the fact that the 1991 AASHTO Specifications draw heavily from two sets of physical experiments conducted 2 to 4 decades ago, which may not be representative of actual field conditions and may lead to either conservative or inadequate designs.

Among the various aspects of the design specifications, the way in which one estimates the impact force that the bridge piers will experience during a collision is clearly of significance in the overall design process. In the current specifications, the imparted force is computed through simplified kinetic energy arguments that require a priori knowledge or an estimate of the vessel bow deformation. The estimated energy is then transformed to an equivalent static force that is used for design. Such a process, though designer-friendly due to its simplicity, overlooks, among other issues, the dynamic behavior inherent in an impact problem.

It is therefore the purpose of this research to provide the framework for obtaining rational estimates of the impact forces a pier may experience during a collision with a waterway vessel. In the absence of a (costly) large-scale experimental program that will allow a field-based comparison of the design provisions, the only path to such estimates is through computational simulations. To this end, this study reports on the finite-element-based modeling of collision events and provides, for a representative field scenario, a comparison between the AASHTO code provisions and the computational results.

A comprehensive study entitled, "Modeling of Waterway Vessel Impact on Bridge Piers," by Adam J. Cryer and Loukas F. Kallivokas, summarizes all of the work carried out that related to vessel impact forces. This study makes up <u>Volume II</u> of this report.

Volume III Ultimate Strength of Bridges Subjected to Vessel Impact

The AASHTO-recommended design procedure for vessel collision is a probability-based calculation that returns an annual frequency of collapse for a given bridge. One of the important calculations in estimating the annual frequency of collapse is the ultimate lateral strength of a bridge element, which AASHTO defines as that of a bridge pier or bridge span. The current AASHTO Design Specifications provide little guidance in the calculation of this value. An objective of one part of this study is to provide engineers with the necessary tools to calculate the ultimate lateral strength of bridge elements. This study outlines procedures for modeling and analyzing bridge piers and bridge systems

subject to vessel impact loads using a typical structural analysis software package. The methods presented focus on modeling reinforced concrete bridge piers, both with and without shear walls. In addition, the effect of considering system-wide response on the ultimate lateral strength of a bridge is investigated by including the bridge superstructure and adjacent bridge piers in the models.

A comprehensive study entitled, "Modeling and Analysis of Bridges Subjected to Vessel Impact," by Wyatt R. Henderson and Eric B. Williamson, summarizes all of the work carried out that related to ultimate strength of bridges subjected to vessel impact. This study makes up Volume III of this report.

Volume IV Development of a Database to Support Calculations on Vessel Impact Risks

As part of this research study, a significant effort is undertaken to collect the data required by the research engineers so that they can estimate the probability and the effect of vessel collisions on bridges along the Gulf Intracoastal Waterway and Texas' inland waterways using the most realistic dataset that could be produced. The data assembled for this study include information on vessel types (barges, towboats, barge groups, and ships), waterways (including the GIWW, the Houston Ship Channel, the Neches River and the Victoria Barge Canal), a selected number of bridges and vessel traffic density in two directions there, digital aerial photographs for geometric information on waterway transitions at the bridges, and current velocity data. Actual data is supplemented with simulated information based on realistic assumptions when necessary.

A comprehensive study entitled, "Data Collection for the Model for Vessel Impact on Bridges," by Michael Bomba, summarizes all of the work carried out that development of the database to support vessel impact risk calculations. This study makes up Volume IV of this report.

Structural Reliability Analysis for Vessel Impact on Bridges

Kenneth B. Berlin
Lance Manuel

Executive Summary

The collapse of the Queen Isabella Causeway in 2001 due to a vessel collision was an alarming message to the state of Texas that vessel impact on bridges is a serious issue and may need to be considered for all bridges that span waterways. The Texas Department of Transportation funded this research project that was aimed at examining in detail the AASHTO LRFD code provisions for vessel impact on bridges. The goals of the present study are to develop a stand-alone computer program that utilizes information on waterways, vessels, traffic, and bridges in a probabilistic analysis that estimates the annual frequency of collapse.

According to today's code provisions for vessel impact on bridges, a bridge is required to have a specific minimum return period associated with collapse depending on its importance classification. A user-friendly stand-alone computer program, VIOB (Vessel Impact on Bridges), is developed to make it possible to carry out the required calculations that lead to estimates of the return period.

Given information related to the bridge and pier geometry, the waterway, and the vessel traffic at a given mile marker of a waterway where the bridge is located, VIOB produces an in-depth report detailing all the calculations. This report provides information on the analysis performed and also includes summaries that allow the user to determine sources of vulnerability for the bridge. Such information is useful in improving a bridge design when, for example, code specifications are not met. VIOB integrates databases with analysis capabilities and makes it possible to carry out calculations related to an important problem – the safety of bridges against vessel impact.

Table of Contents

List of Figures

List of Tables

Chapter 1. Introduction

1.1 Background

The Queen Isabella Causeway allows vehicles to drive from Port Isabella, Texas along Park Road 100 over the Gulf Intracoastal Waterway to South Padre Island. On September 15, 2001 a four-barge tow collided with the Queen Isabella Causeway triggering a collapse of Bent 32. The collapse can be seen in Figure 1.1. The catastrophe left a gaping 160-foot fissure in the bridge and caused the deaths of eight people as their cars plunged 87 feet into the water below (Schwartz, 2001; Texas Civil Engineer, 2004).
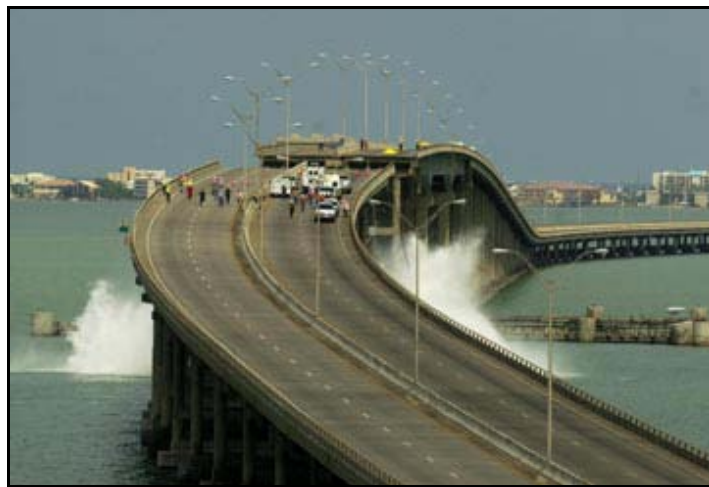
*Figure 1.1: The Queen Isabella Causeway Collapses in September 2001
(Source: http://pages.sbcglobal.net/calzada/newsqueen1.html).*

At the time of the accident, the Queen Isabella Causeway was the only means of transportation for visitors to and from South Padre Island. The destruction of this bridge, shown in Figure 1.2, effectively stranded thousands of people on the island until ferries could be brought in to transport them to the mainland. Given the importance of this bridge to the surrounding communities, the tragedy due to the loss of life was exacerbated by the economic crippling of an entire region.

Figure 1.2: The Collapsed Portion of the Queen Isabella Causeway
(Source: South Texas Business Directory).

When the captain and crew of the barge tow were questioned about the incident, it was determined that neither drugs nor alcohol were involved in the accident; however, the barge tow was several hundred feet off course when it slammed into the Queen Isabella Causeway. One possible explanation that has been suggested is that there might have been some particularly high currents in the curved channel leading up to the bridge at the time of the accident that the captain of the barge tow was unaware of (Schwartz, 2001).

Vessel collisions are not unique to Texas. Months after the Queen Isabella Causeway disaster, Oklahoma experienced a similar bridge collapse. On May 27, 2002 a barge captain blacked out as his barge tow was approaching Interstate 40 where it crosses over the Arkansas River in Webbers Falls, Oklahoma. The collision caused 600 feet of the bridge to collapse (See Figure 1.3), killing fourteen people when their vehicles drove off the collapsed bridge (National Transportation Safety Board, 2004).

*Figure 1.3: Bridge in Webbers Falls Oklahoma Collapses Due to Vessel Collision
(Source: The Anniston Star).*

While the Webbers Falls and Queen Isabella Causeway vessel collisions were fairly recent, the history of vessel collisions with bridges in the United States is quite extensive. Possibly the largest bridge collapse due to vessel impact in the U.S. occurred in 1980 in Tampa Bay where a 1400-foot span of the Sunshine Skyway Bridge was destroyed when a ship collided into one of the main piers killing thirty-five people. In 1993, a barge tow collided with the Judge William Seeber Bridge in New Orleans killing three people.

Vessel collisions with bridge piers have occurred in the past and they will likely continue to occur in the future. According to Frandsen (1983), the annual rate of catastrophic collisions during the period 1960-1970 was 0.5 bridges per year. However, that number tripled to 1.5 bridges per year during the period 1971-1982. This increased number of bridge failures over time resulted due to an increase in the number of bridges over navigable waterways as well as an increased volume of vessels using those waterways (AASHTO, 1991).

The recent Queen Isabella Causeway bridge collapse and other vessel collisions on bridges motivated the present research study, supported by the Texas Department of Transportation (TxDOT), which aims to evaluate bridges spanning waterways in Texas for safety against vessel collisions.

Having experienced the horrific disaster resulting from the Queen Isabella Causeway collapse, TxDOT decided to analyze each of the state's bridges that span waterways to determine if rehabilitation might be needed to prevent a similar accident. Using available software that can assess the likelihood of a bridge collapse due to vessel collisions, TxDOT performed the appropriate AASHTO calculations which also helped identify bridges that require attention. A shortcoming of the analyses that were carried out was that the data, especially on vessel traffic and waterways, were not generally available.

This report is part of a research study that is comprised of three separate tasks: structural reliability analysis, bridge ultimate strength models, and finite element modeling to assess impact forces. In addition, a comprehensive database development effort is an integral part of this research project. The parts of the project are combined together in one report to help identify Texas bridges that might be at risk of failure due to vessel collision.

1.1.1 Bridge ultimate strength models

In order to accurately assess the vulnerability of a bridge against vessel impacts, it is necessary to determine the strength of exposed bridge piers. By taking into account such factors as the superstructure stiffness, soil stiffness, vessel force, and pier geometry, models have been developed (Henderson, 2005) to determine the ultimate lateral strength of a bridge pier. Additionally, different structural analysis computer programs such as ANSYS and SAP2000 have been used to perform nonlinear static pushover analyses to determine the ultimate strength of a pier.

1.1.2 Finite element modeling to assess impact forces

Using LS-DYNA, a finite element analysis program, models have been developed (Cryer, 2005) to determine the characteristics of the force transferred from a vessel to a pier during a collision. Important variables include the vessel speed, current velocity, pier stiffness, vessel hull stiffness, and angle of impact. Taking into consideration these variables, a model has been developed to provide descriptions of the impact force for the reliability study.

1.1.3 Data Collection

Because data on waterway characteristics and vessel traffic on Texas waterways are not easily available, a database has been developed as part of this research study. Using information from sources such as the Army Corps of Engineers and commercial towing companies, vessel traffic and channel data have been assembled at various mile markers on Texas waterways. The data include information regarding channel profile, channel currents, vessel traffic, and vessel geometry. These data are essential in assessing the return period for bridge collapse due to vessel impact.

1.1.4 Structural Reliability Analysis

Using models developed for vessel impact forces and for ultimate strength of piers along with data on vessel traffic and on the channels, a probabilistic framework is developed to estimate the return period associated with bridge collapse due to vessel impacts. Calculations also involve the use of databases developed along with formulations for estimating the probability of aberrant vessels, consideration of the channel geometry, and the vessel traffic. Estimates of the return period help transportation agencies identify bridges that might be vulnerable to collisions and are useful in prioritizing resources for retrofitting of at-risk bridges that span waterways.

1.2 Scope of Report

There are many different factors that influence vessel impact analysis for bridges including the bridge geometry and structural properties, channel characteristics, and vessel traffic data. This report focuses on the structural reliability analysis calculations which are integrated into a stand-alone analysis program that makes use of databases and models to evaluate bridge against vessel

impact. The entire numerical framework for estimating return periods for bridge collapse due to vessel impact involving various models as well as Texas-specific databases has been conveniently incorporated in a user-friendly software program, VIOB (Vessel Impact on Bridges), which is developed as part of this study. This software program allows the user to complete detailed calculations of the type needed when following the AASHTO LRFD specifications (AASHTO, 2004). The ease of use of this software is a major improvement over existing computational tools for such analyses.

1.3 Organization of Report

This volume of the report is organized in the same way that the research itself progressed. First, a literature review describing past research efforts is presented in Chapter 2. This is followed in Chapter 3 by a detailed description of the AASHTO LRFD methodology currently in use when evaluating bridges for vessel impact loads. Next, some changes to the AASHTO methods that we propose for the reliability analysis based on our understanding of vessel impact forces and bridge pier ultimate strength models are described in Chapter 4. A set of example calculations is included in Chapter 5. Building on the example calculations, Chapter 6 compares results for different bridges. A presentation of VIOB, the computer software developed for this research is outlined in Chapter 7. Finally, some general conclusions arising from this research are included in Chapter 8.

Chapter 2. Literature Review

2.1 Previous Vessel Impact Studies

Consideration for the design of bridges against vessel impact is important in many countries around the world. Land-locked countries must be concerned with vessel traffic in rivers, channels and lakes, while countries by the ocean must account for vessel traffic entering and leaving its ports. Vessels have been known to collide with other vessels, with bridge piers, and with other obstacles. Countries like the United States, Japan, and Germany have, over the years, carried out numerous research studies dealing with vessel impact on bridges and other obstacles.

In Japan, Fuji and Shiobara (1978) reported on tests representing ship-to-ship collisions to determine the annual economic losses occurring in Tokyo Bay. Their studies related the probability of collision between two vessels at sea and the associated rate of damage caused. Due to a lack of vessel-to-pier collision data at the time of the writing of the 1991 AASHTO Guide Specification (AASHTO, 1991), studies of ship-ship collisions including the one by Fuji and Shiobara (1978) were modified to apply to vessel-pier collisions.

The commentary in both the AASHTO LRFD Specifications (AASHTO, 2004) and the earlier 1991 Guide Specification (AASHTO, 1991) refers to two sets of experiments conducted in Europe that were used as a basis for establishing critical relationships provided in the Specifications for computing vessel damage and impact forces. For ships, these experiments were largely based on the work of Woisin, conducted in Germany in the late 1960s to the mid 1970s (Woisin, 1970, 1971, 1976). Similarly, for barges, the expressions in the two AASHTO documents provided for vessel damage and collision force were based on the experimental work of Meir-Dornberg, published in German in 1983 (Meir-Dornberg, 1983).

Inland waterways in Germany have bridges that are very old and were not originally designed for vessel impact. A recent study (Proske et al., 2003) discusses an approach for strengthening of such old bridges. Probabilistic analysis techniques are used to correlate bridge damage to the number of ship impacts for different bridge structures.

As far as experience with vessel impact studies in the United States is concerned, all states have bridges crossing waterways and hence, vessel collision is a problem in every state, not simply coastal states. While national codes have been established to design against vessel collisions, research has been mostly performed in states that are at greatest risk. Florida and Louisiana have led vessel collision research efforts in the U.S., but other states such as New Jersey and Kentucky have also influenced code development. Texas, too, has undertaken its own research into vessel collision design.

The state of Louisiana and the Federal Highway Administration introduced one of the first comprehensive code criteria for vessel impact (Modjeski and Masters Consulting Engineers, 1984). These criteria describe in detail how to perform a vessel collision probabilistic analysis based on bridge, vessel, and channel data. The model uses a dynamic analysis to determine

vessel forces and also provides a simplified approach for design. This model was one of the primary sources that led to the development of the 1991 AASHTO Guide Specifications (AASHTO, 1991).

In the state of Florida, a significant amount of research has been done on the topic of vessel impact on bridges. The University of Florida and the Florida Department of Transportation have recently performed extensive tests relating to vessel impact on bridges (Consolazio et al., 2005). In the area of probabilistic analysis for the return period of bridge collapse due to vessel impact, a Mathcad spreadsheet that could be linked to a vessel traffic database was developed to enable estimation of the annual frequency of collapse of susceptible bridges in the state of Florida (Florida Department of Transportation, 2000).

The state of New Jersey has also dealt with vessel collision situations in practice. For example, when Parsons Brinckerhoff was involved in the design of the Ocean City – Longport Bridge in the state, vessel collision forces controlled the design of several piers. It was found to be most economical to use longer spans in the center portion of the bridge and the use of a fender system had a significant reduction in the annual frequency of collapse of the bridge (Rue et al., 2002).

In the state of Kentucky, the use of various types of data with Method II as given in the AASHTO Guide Specification is demonstrated by Whitney et al. (1996) for a cable-stayed bridge in the state.

2.2 Changes in the Design Code

While research into vessel impact design had been performed for many years around the world, vessel impact design did not seriously begin in the United States until 1980 when the Sunshine Skyway Bridge, in Tampa Bay, Florida, collapsed due to a ship collision (see Figure 2.1). This catastrophic event forced researchers and officials to take a closer look at the frequency of vessel collisions and methods to prevent further accidents from occurring.

Figure 2.1: 1980 Sunshine Skyway Bridge Collapse (Source: Time Magazine).

2.2.1 The 1991 AASHTO Guide Specification and Commentary for Vessel Collision Design of Highway Bridges

The first attempts by AASHTO to formally address the design of bridges for vessel collision forces were made in 1991. Following the Sunshine Skyway Bridge disaster, research into vessel collision was thought to be necessary. AASHTO examined the results from several research projects in other countries (see, for example, Fuji and Shiobara, 1978; Woisin, 1970, 1971, 1976; and Meir-Dornberg, 1983) and in the United States (e.g., by Modjeski and Masters, 1984) and developed their first guide specifications (AASHTO, 1991). These specifications, while not required for bridge design, include a large commentary component and propose guidelines for determining vessel impact loads and a procedure for designing a protective bridge barrier. The guide specifications also attempt to create a preliminary vessel database that encompasses the most common types of vessels in use on waterways in the U.S.

2.2.2 The 2004 AASHTO LRFD Bridge Design Specifications

Starting in 2004, vessel collision was formally incorporated into the primary AASHTO LRFD design code for bridges (AASHTO, 2004). The guidelines here were adapted from the 1991 AASHTO Guide Specification with minor modifications made to streamline the design process and keep it consistent with the rest of the LRFD code. Also, only Method II from the 1991 Guide Specification was retained in the 2004 AASHTO LRFD code. This method is the optimal method of vessel collision design in terms of complexity and is similar in principle with the overall LRFD probabilistic design philosophy. These AASHTO 2004 LRFD guidelines for vessel collision are discussed in further detail in Chapter 3.

Chapter 3. The AASHTO Specifications for Vessel Impact on Bridges

3.1 Implementation of AASHTO Guide Specification

Developed from the *AASHTO Guide Specifications and Commentary for Vessel Collision Design of Highway Bridges* (AASHTO, 1991), the AASHTO LRFD code Section 3.14 outlines a procedure for estimating a bridge's likelihood of collapse, given that a vessel collides with it.

The vessel collision requirements are aimed at preventing a vessel from impacting a bridge over a navigable waterway and causing excessive damage. A probabilistic model, based on a worst-case-scenario, where a fully loaded fast-moving vessel collides with a pier, while moving unimpeded, is used to determine whether a bridge is adequately designed. In determining the feasibility of a given bridge, it is necessary to consider the waterway geometry, the types of vessels using the waterway, the speed and load state of the waterway vessels, and the response of the structure in the event of a vessel collision. If a structure is unable to resist the vessel collision forces, it needs to be protected by a fender system.

The acceptable probability for any given bridge depends on the importance that the bridge serves to the community. Bridges may be categorized as either "critical" or "regular" according to AASHTO LRFD code Section 3.14.3. If a bridge is classified as critical, it must remain operational after a vessel collision. Once a bridge's classification has been established, it is determined to have met the criteria according to its completed annual frequency of collapse.

3.1.1 Annual Frequency of Collapse

The AAHSTO LRFD code uses annual frequency of collapse to determine whether a bridge design is satisfactory. An alternative way of representing a bridge's vulnerability is with the inverse of annual frequency of collapse, or return period. A bridge's return period is the number of years on average that a bridge may be expected to stand before a vessel collides with it and causes it to collapse. The annual frequency of collapse resulting from collision of a single pier by a vessel is calculated as follows:

$$AF_{ij} = (N_i)(PA_{ij})(PG_{ij})(PC_{ij}) \qquad\qquad (3.1)$$

where:

AF_{ij} = Annual frequency of collapse of pier *j* caused by vessel type *i*,
N_i = Annual number of vessel type *i* (a vessel must pass all piers),
PA_{ij} = Probability of aberrancy of vessel type *i* with respect to pier *j*,
PG_{ij} = Geometric probability associated with vessel type *i* and pier *j*,
PC_{ij} = Probability of collapse of pier *j* due to vessel type *i*.

Equation 3.1 suggests that the annual frequency of collapse is based on a number of different probabilities. In sequence, we need to know the probability that a vessel becomes aberrant; then, the probability that a vessel will strike the bridge given that it becomes aberrant; and finally the probability that the bridge will collapse given that a vessel is aberrant *and* strikes the bridge.

The overall annual frequency of collapse of a bridge, AF_{Total}, is the sum of the annual frequencies that result from collisions of the various vessel types with the various bridge piers that one deems vulnerable due to their location relative to the channel. Thus, we have:

$$AF_{Total} = \sum_{i=1}^{NV} \sum_{j=1}^{NP} AF_{ij} \qquad (3.2)$$

where:

AF_{Total} = Annual frequency of collapse of the bridge,
NV = Number of vessel types (i.e., including the same loading condition, size, etc.) that pass the bridge,
NP = Number of bridge piers within three times the overall length (LOA) of the vessel from the navigable channel centerline.

The sequence of computations is such that the annual frequency of collapse is determined for each pier, and the sum of these frequencies for all piers provides the overall annual frequency of collapse of the bridge. For a bridge classified as "critical," the annual frequency of collapse must be not greater than 0.0001, or its return period must be not shorter than 10,000 years. The required annual frequency of collapse for a bridge designated as "regular" must be no larger than 0.001 corresponding to a return period of 1,000 years. In terms of these acceptable levels, we have:

$$AF_{Total} < AF_{Acp} \qquad (3.3)$$

where:

AF_{Total} = Annual frequency of collapse of the bridge,
AF_{Acp} = Acceptable annual frequency of collapse of the bridge.

3.1.2 Probability of Aberrancy (*PA*)

The probability of aberrancy is the likelihood that a vessel deviates off course due to pilot error, poor weather conditions, or mechanical failure. One of the three main components to determining the annual frequency of bridge collapse, the probability of aberrancy can be calculated by two different methods. The first method involves performing a statistical analysis of historical data from a given channel. While this method is the most accurate, it can be time-consuming and difficult. The simplified approach detailed in AASHTO LRFD 3.14.5.2.3 is an approximate method and can be written as follows:

$$PA = (BR)(R_B)(R_C)(R_{XC})(R_D) \qquad (3.4)$$

where:

PA = Probability of aberrancy,
BR = Aberrancy base rate,
R_B = Correction factor for bridge location,

R_C = Correction factor for current acting parallel to vessel transit path,
R_{XC} = Correction factor for cross-current acting perpendicular to vessel transit path,
R_D = Correction factor for vessel traffic density.

Aberrancy Base Rate

From Equation 3.4, it can be seen that probability of aberrancy is calculated by starting with a base rate and then modifying it by four different factors. The four correction factors adjust for bridge location, parallel current, perpendicular current, and traffic density. Each of the five variables that influence probability of aberrancy is based on historical data for the waterway.

The aberrancy base rate is the fraction of vessels that become aberrant. Ships are less likely to become aberrant than barges; therefore, the base rate as given by the AASHTO LRFD code for a ship is 0.00006, as opposed to 0.00012 for barges.

Correction for Bridge Location

A correction factor for bridge location is necessary to adjust for the different types of channel geometry in the vicinity of the bridge. Different turn regions exist in any channel and the sharper the turn angle the more difficult it becomes for the vessel operator to keep the vessel on course. The AASHTO LRFD code distinguishes channel regions into three types: straight, transition, and turn/bend.
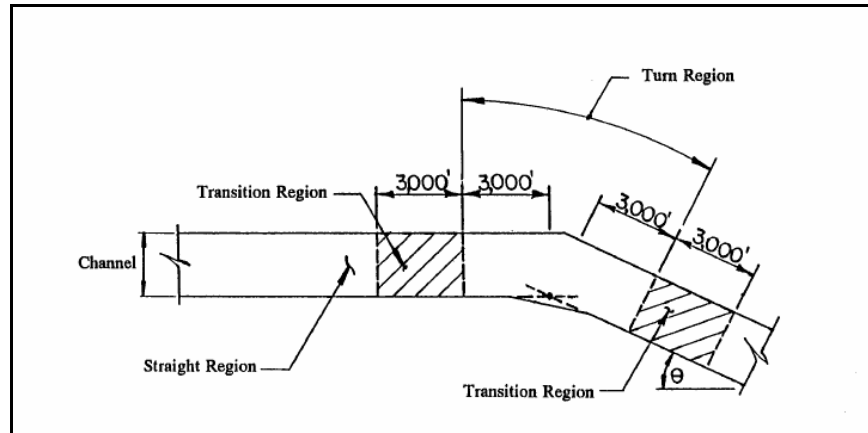
Figure 3.1: Channel turn region (from AASHTO LRFD Figure 3.14.5.2.3-1a)
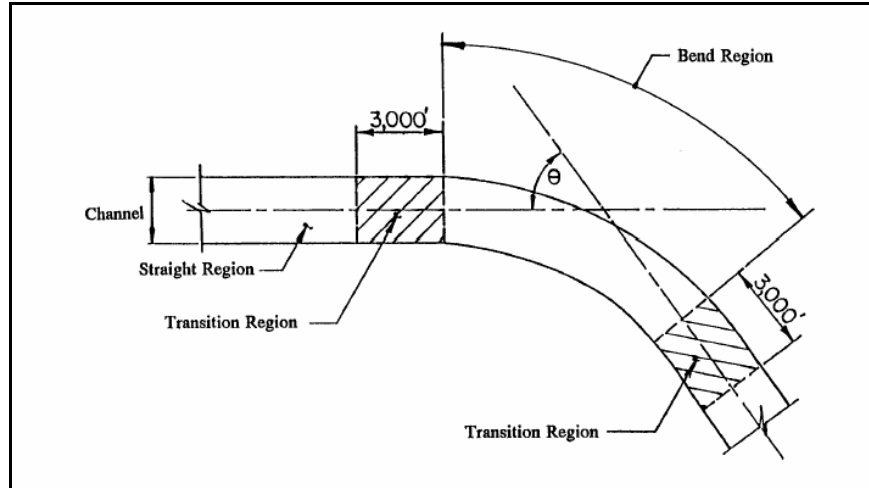
Figure 3.2: Channel bend region (from AASHTO LRFD Figure 3.14.5.2.3-1b)

A straight region is the simplest; here, a vessel has a clear straight path underneath the bridge. A turn or bend region, shown in Figure 3.2, would be a place where the bridge crosses the channel, while the channel is changing directions (See Figure 3.1 for an illustration of a turn region and Figure 3.2 for a channel bend region.). The transition region is a 3,000-foot long region before and after the turn or bend region. If a bridge is located in a transition region, it is more difficult for a vessel to navigate the channel than with a straight channel, but not quite as challenging as it would be in a turn or bend region. The difference between a turn region and a bend region is only that a turn region has a sharp-angled change in channel geometry, while a bend region has a smoother, curved-angle change. However, both turn and bend regions are handled the same way in the AASHTO LRFD code.

For straight regions:
$$R_B = 1.0 \tag{3.5}$$

For transition regions:
$$R_B = \left(1 + \frac{\theta}{90°}\right) \tag{3.6}$$

For turn/bend regions:
$$R_B = \left(1 + \frac{\theta}{45°}\right) \tag{3.7}$$

where:

R_B = Correction factor for bridge location,
θ = Angle of turn or bend (°) as shown in Figure 3.1 and Figure 3.2.

Correction for Current

In the computation of the probability of aberrancy, these are the next two corrections that account for the velocity of the water current. It is necessary to correct for both the current flow parallel to the vessel traffic and the current flow perpendicular to the vessel traffic. As the

current velocity increases, it becomes more difficult to maintain the vessel's heading. Currents in the two directions do not have an equal effect on vessel aberrancy. The correction factor for the cross current has ten times the influence of that for parallel currents.

$$R_C = \left(1 + \frac{V_C}{10}\right)$$

(3.8)

where:

R_C =   Correction factor for current parallel to the direction of vessel traffic,
V_C =   Velocity of current parallel to the direction of vessel traffic (knots).

$$R_{XC} = \left(1 + V_{XC}\right)$$

(3.9)

where:

R_{XC} =   Correction factor for current perpendicular to the direction vessel traffic,
V_{XC} =   Velocity of current perpendicular to the direction of vessel traffic (knots).

Correction Factor for Vessel Traffic Density

The final correction factor in the computation of probability of aberrancy is due to vessel traffic density in the waterway. Higher traffic density equates to an increased probability that a vessel will become aberrant. The AASHTO LRFD code categorizes traffic density very broadly into low, medium, and high levels.

Low traffic density:

$$R_D = 1.0$$

(3.10)

Average traffic density:

$$R_D = 1.3$$

(3.11)

High traffic density:

$$R_D = 1.6$$

(3.12)

where:

R_D =   Correction factor for traffic density.

The combination of the aberrancy base rate and the four correction factors described above yields an estimate for the probability of aberrancy. In general, a higher probability of aberrancy can directly lead to a higher annual frequency of collapse or a lower return period.

Limitations

The equations for probability of aberrancy in the AASHTO LRFD code were developed in the AASHTO Guide Specifications (AASHTO, 1991). Data from bridges around the world were collected and led to estimated base rates of aberrancy for ships and barges. The base rate for barges was found to be two to three times higher than that for ships. The limitations associated

with probability of aberrancy stem mostly from the quality and quantity of available data and the lack of ability to make appropriate site-specific modifications. The four correction factors used in the AASHTO LRFD code are just a few of the many different variables that determine whether a vessel becomes aberrant. Other variables such as wind, visibility conditions, navigation aids, and human error can have a strong influence on the probability of aberrancy but they were not directly included in the AASHTO LRFD code as they were considered too difficult to quantify. Such factors were indirectly accounted for in the base rate; however, if any one of these is particularly significant at a given waterway and bridge location, its influence on the results would not be indicated. Human error which accounts for 60 to 85 percent of all aberrant vessels is the most difficult variable to quantify.

It is expected that advances in technology such as computer-guided vessels and warning technologies would be able to vastly improve the base rate for vessels. Technological improvements should also decrease the influence of the four correction factors that were accounted for.

3.1.3 Geometric Probability (*PG*)

Once a vessel has become aberrant, it is then necessary to estimate the probability that the vessel will strike the bridge. To do this, geometric considerations are necessary. The geometric probability is based on a number of parameters including the geometry of the waterway, water depth, location of bridge piers, span clearance, sailing path of vessel, maneuvering characteristics of the vessel, location, heading and velocity of vessel, rudder angle at time of failure, environmental conditions, width, length, and shape of vessel, and vessel draft.

The AASHTO LRFD code uses a normal distribution to account for geometric probability. The standard deviation is taken as the overall length of the vessel (LOA). The probability density function for a normally distributed random variable is expressed as follows:

$$f(x) = \frac{1}{\sigma\sqrt{2\pi}}e^{-\frac{1}{2}\left(\frac{x-\mu}{\sigma}\right)^2} \qquad (3.13)$$

where:

σ =   Standard deviation (For *PG*, σ = LOA),

μ =   Mean (For *PG*, μ = 0).

To determine the geometric probability, two points are plotted on the *x*-axis. The variable *x* refers to the possible location of the center of a vessel relative to the centerline of a channel. This can be viewed in Figure 3.3.
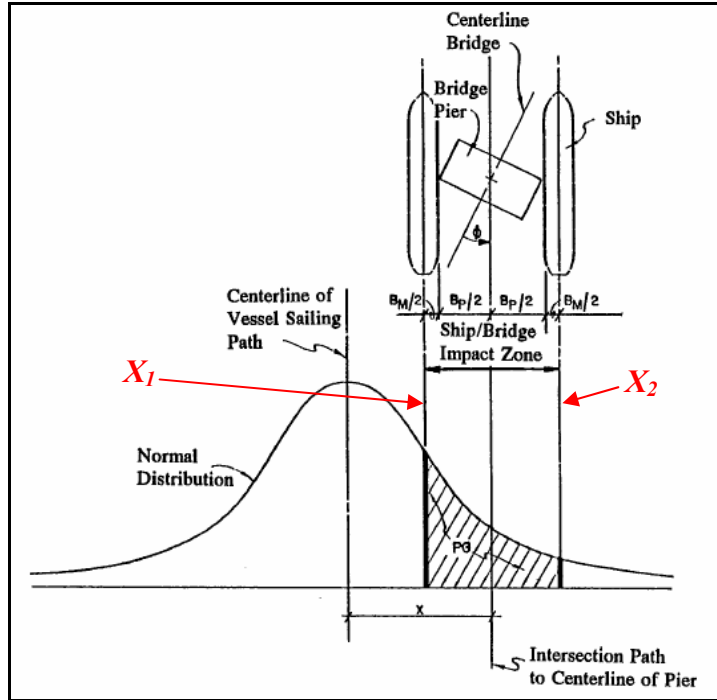
Figure 3.3: Normal distribution curve for geometric probability.
(*AASHTO LRFD code Figure 3.14.5.3-1*)

The geometric probability represents the probability that the vessel lies between X_1 and X_2 (See Figure 3.3).

$$X_1 = \frac{x - \dfrac{B_P + B_M}{2}}{LOA} \qquad (3.14)$$

$$X_2 = \frac{x + \dfrac{B_P + B_M}{2}}{LOA} \qquad (3.15)$$

where:

X_1	=	Lower bound for location of vessel that can collide with the pier,
X_2	=	Upper bound for location of vessel that can collide with the pier,
x	=	Distance from centerline of navigable channel to centerline of pier,
B_P	=	Width of pier,
B_M	=	Width of vessel,
LOA	=	Length overall of vessel.

The geometric probability, *PG*, is the area under the normal distribution curve between X_1 and X_2:

$$PG = \Phi(X_2) - \Phi(X_1) \qquad (3.16)$$

where:

PG = Geometric Probability,

$\Phi(X_i)$ = Standard normal cumulative distribution function evaluated at X_i.

It has been shown in various studies, most notably in the development of the AASHTO Guide specification (AASHTO, 1991), that piers outside of 3LOA from the navigable channel centerline are unlikely to be struck by a vessel. Therefore, any piers more than 3LOA away from the centerline of the navigable channel are not considered in the computation of *PG*.

Limitations

The limitations of estimating the geometric probability of geometry are due to lack of data on barge collisions. In developing a model for estimating geometric probability, a wide variety of ship data was available, however very few data referring to barge collisions exist. The AASHTO LRFD code recommends that the same standard deviation of LOA be used for barge groups, even though there is no statistical evidence to support that value.

3.1.4 Probability of Collapse (*PC*)

Given that a vessel has gone aberrant and has struck a pier, it is then necessary to estimate the probability that the bridge will collapse. Several variables including vessel size, type, configuration, speed, direction of impact, and mass influence the probability of collapse. The stiffness of the bridge pier and the nature of bridge superstructure also influence the probability of bridge collapse.

The AASHTO LRFD code Section 3.14.5.4 which addresses probability of collapse was developed by Cowiconsult (1987) based of studies performed by Fujii and Shiobara (1978) using Japanese historical damage data on vessels colliding at sea (AASHTO LRFD C3.14.5.4). The ratio of ultimate lateral resistance to the vessel impact force is computed in order to estimate the probability of collapse. The LRFD equations governing probability of collapse are as follows:

If $0.0 \leq H/P < 0.1$:

$$PC = 0.1 + 9\left(0.1 - \frac{H}{P}\right) \qquad (3.17)$$

If $0.1 \leq H/P < 1.0$:

$$PC = \frac{1}{9}\left(1 - \frac{H}{P}\right) \qquad (3.18)$$

If $H/P \geq 1.0$:

$$PC = 0.0 \qquad (3.19)$$

where:

PC = Probability of collapse,
H = Ultimate lateral resistance of pier (kips),
P = Vessel impact force (kips).

The ultimate strength of a single pier is typically conservatively assumed to be the ultimate strength of the entire bridge. A plot of Equations 3.17 to 3.19 provides a better picture of how the probability of collapse is computed. As seen in Figure 3.4, working from right to left, if the bridge element strength, H, is greater than the vessel impact force, P, there is a zero probability that the bridge will collapse. As the H/P ratio increases, the probability of collapse remains low until the vessel impact force becomes greater than one-tenth the ultimate lateral pier strength. From then on, small reductions in the H/P ratio cause the probability of collapse to increase quite sharply. Eventually, the probability of collapse reaches 1.0 where the vessel impact force exceeds the ultimate lateral pier strength.
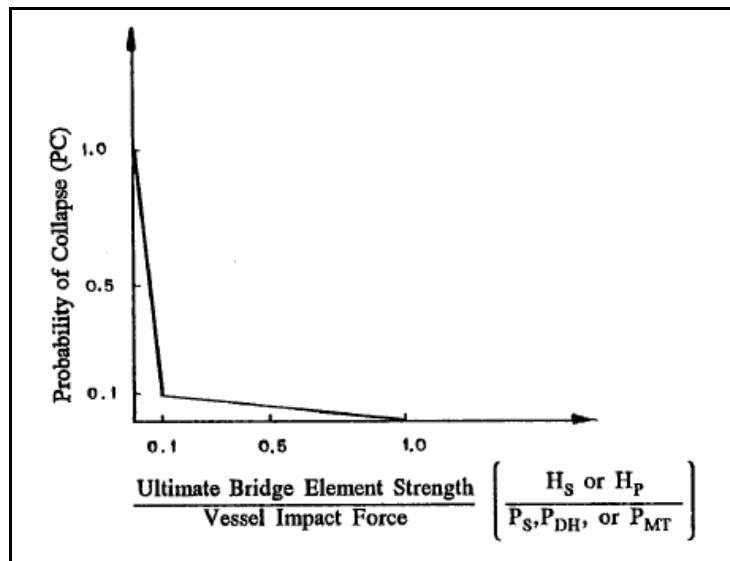
Figure 3.4: Probability of collapse distribution.
(*from AASHTO LRFD code Figure C3.14.5.4-1*)

Ultimate Lateral Pier Strength

In order to determine the ultimate lateral strength of each pier, a separate analysis must be done outside of the AASHTO LRFD code calculation for annual frequency of collapse due to vessel impact. Either a nonlinear static pushover analysis or a nonlinear dynamic analysis may be employed for this purpose.

Vessel Impact Force

The impact force of a vessel on a pier is based on a number of different variables including vessel type, vessel impact velocity, strength and stiffness of the pier, and the angle of collision. The kinetic energy of the moving vessel must be computed to determine how much force is

transferred from the vessel to the pier. In order to calculate kinetic energy, the impact velocity of the vessel must be estimated.

Vessel velocity is difficult to establish because the velocity of the vessel must be combined with the velocity of the current. In any given waterway, the water speed is not constant at all locations across the channel. In addition, it is necessary that the velocity of the vessel be considered when it has become aberrant. Often a vessel that has strayed considerably off course will no longer maintain its original speed but will rather be moving with the channel current velocity.

Based on various studies performed in the past, the AASHTO LRFD code Section 3.14.6 proposes a means for determination of the vessel velocity. A linear interpolation is used to represent the variation in velocity from the centerline of the waterway to the edges of the channel. Figure 3.5 shows the velocity distribution used in the code.
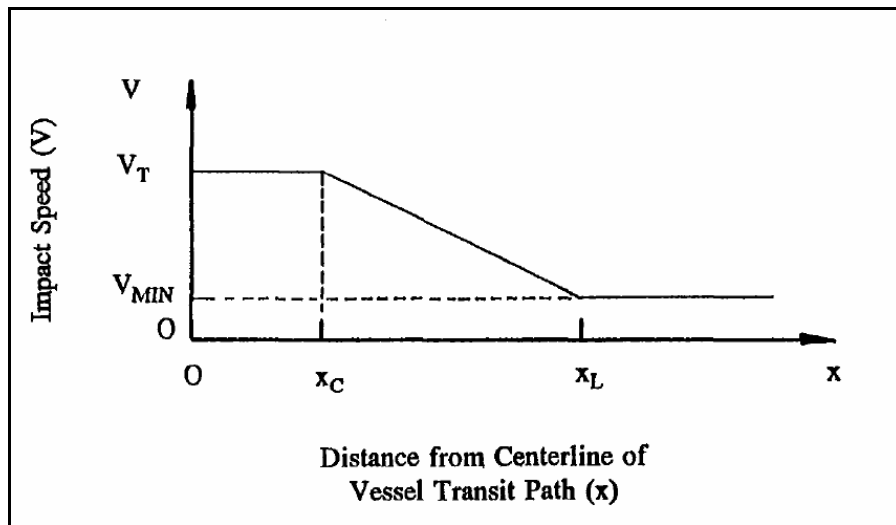
Figure 3.5: Variation of design collision velocity with distance from navigable channel centerline.
(*from AASHTO LRFD code Figure 3.14.6-1*)

where:

V = Design impact velocity,
V_T = Typical vessel transit velocity (under normal environmental conditions),
V_{MIN} = Minimum design impact velocity (not less than the yearly mean current velocity),
x = Distance to face of pier from centerline of channel,
x_C = Distance to edge of channel,
x_L = Distance equal to three times the overall length of the vessel.

Vessel velocity should be determined using typical current velocities and taking into account wind and other external forces. The velocity of a vessel may be different for upbound and downbound vessels. This velocity can be accounted for by running two separate calculations, one for each direction. It would seem logical to add the velocities of the vessel and channel current velocity for downbound and subtract them for upbound vessels; however this is not done. No distinction is made regarding vessel motion direction in the AASHTO LRFD code. This is because a minimum velocity, V_{MIN}, is required, as seen in Figure 3.5, and it must be greater than the yearly mean current velocity. In other words, a negative velocity that might result from a large current opposite to the vessel traffic direction is not permitted in the AASHTO LRFD code.

Once the velocity of the vessel in known, the kinetic energy of the vessel can be determined. Kinetic energy is based on a number of parameters including vessel displacement tonnage, impact velocity, and a hydrodynamic mass coefficient that accounts for the influence of the surrounding water upon the moving vessel. This is detailed in AASHTO LRFD code Section 3.14.7. The kinetic energy of a moving vessel is computed as follows:

$$KE = \frac{C_H W V^2}{29.2} \tag{3.20}$$

where:

KE = Vessel collision energy (kip-ft.),
W = Vessel displacement tonnage (tonnes),
C_H = Hydrodynamic mass coefficient,
V = Design impact velocity (ft./sec.).

Equation 3.20 is based on the standard $\frac{1}{2}mV^2$ formula for kinetic energy along with consideration of the hydrodynamic mass coefficient and necessary unit conversion factors. A separate calculation is required for the vessel in loaded and unloaded condition. Vessel displacement tonnage will usually differ based on the loading state of the vessel.

Using the kinetic energy of the vessel, the impact force transferred from the vessel to the pier can be calculated. A different set of equations is used to determine the impact force from ships and barge groups as the geometry and other properties of these vessels are significantly different.

Vessel Impact Force for Ships

The impact force of a ship colliding with a pier is based on the ship impact velocity and the deadweight tonnage of the ship. According to the AASHTO LRFD code Section 3.14.8 the force is computed as follows:

$$P_S = 8.15V \sqrt{DWT} \qquad (3.21)$$

where:

P_S =   Equivalent static vessel impact force (kips),
DWT =   Deadweight tonnage of vessel (tonnes),
V =   Design impact velocity (ft./sec.).

While it is not required for the LRFD calculations for annual frequency of bridge collapse, the ship bow damage length can be calculated as well. The bow damage depth is the horizontal length of the ship's bow that is crushed by the impact with the pier. It is computed based on impact force averaged against the work path. The AASHTO LRFD code Section 3.14.9 quantifies ship bow damage depth as follows:

$$a_S = 1.54 \left(\frac{KE}{P_S} \right) \qquad (3.22)$$

where:

a_S =   Bow damage length of the ship (ft.),
KE =   Vessel collision energy (kip-ft.),
P_S =   Ship impact force (kips) as determined from Equation 3.21.

The multiplier 1.54 in Equation 3.22 results from the product of three other coefficients: a factor of 1.25 accounts for the increase in average impact force over time; a factor of 1.11 accounts for the increase in average impact force to the 70 percent design fractile; and another factor of 1.11 provides an increase in the damage length to provide a similar level of design safety as that used to compute the ship collision force.

Vessel Impact Force for Barges

While the bow damage depth is not required for calculating impact forces of ships, for a barge it is a key component of the calculation. Barge impact force is directly obtained from the barge bow damage depth. The AASHTO LRFD code Section 3.14.12 expresses barge bow damage depth as follows:

$$a_B = 10.2 \left(\sqrt{1 + \frac{KE}{5,672}} - 1 \right) \qquad (3.23)$$

where:

a_B =   Barge bow damage length (ft.),

KE　　=　　Vessel collision energy (kip-ft.).

Based on the barge bow damage length, the force imparted by the barge group on a pier can be calculated. The expressions for barge collision force on a pier are outlined in the AASHTO LRFD code Section 3.14.11 and are as follows:

If $a_B < 0.34$:

$$P_B = 4,112a_B \qquad\qquad (3.24)$$

If $a_B \geq 0.34$:

$$P_B = 1,349 + 110a_B \qquad\qquad (3.25)$$

where:

P_B　　=　　Equivalent static barge impact force (kips),
a_B　　=　　Barge bow damage length (ft.).

Limitations

As with geometric probability, the probability of collapse methodology outlined above was based on data acquired from ship-to-ship collisions. Fujii and Shiobara (1978) reported on ship-to-ship collisions and Cowiconsult (1987) adapted their results to allow the estimation of the probability of collapse caused by any vessel including barge groups for which no data were used in the code development. The AASHTO LRFD code acknowledges in the commentary that the procedure is proposed only due to a lack of data available on vessel collision with bridges.

In addition to the lack of data on barge collisions, the AASHTO LRFD method for calculating probability of collapse does not take into consideration the effects of progressive collapse nor the importance of a specific pier in the overall bridge collapse. The AASHTO LRFD code implies that if one pier is considered failed, then the entire bridge has failed. This is a very conservative approach. It is likely that, in some situations, a pier may be completely removed and the bridge could still remain operational and could be repaired before a collapse occurred. Also, losing one pier could cause a progressive collapse mechanism. Redundancy is not accounted for in the code calculations. Consideration for the conditional probability of bridge collapse given that a single pie has failed or is removed would add accuracy to the calculation of the annual frequency of collapse.

3.2 AASHTO LRFD Code Limitations

While the AASHTO LRFD code guidelines provide a comprehensive analysis approach to determining a return period for bridge collapse due to vessel impact, there are several limitations in the code. The AASHTO LRFD code attempts to simplify the modeling considerably based on past vessel impact studies. In most cases, the simplification allows the engineer to perform easier calculations. However, in several areas, the code simplification leads to an overly conservative approach. Some sections of the AASHTO LRFD code are based on sparse data and limited studies – e.g. computing the probability of bridge collapse due to impact from barge groups is based on data on ship-to-ship collision studies.

3.2.1 Data Limitations

One of the most significant weaknesses of the AASHTO LRFD code guidelines for vessel collision is the heavy reliance on actual data. While the AASHTO LRFD code equations can sometimes offer a reasonable estimate, the ability to obtain an estimate of the annual frequency of bridge collapse due to vessel impact relies on the availability of a plethora of actual data about the bridge, the channel, and the vessel traffic. It can be either very difficult to accumulate the necessary data and some data will change frequently. For instance, the depth of the water in a channel constantly changes as the channel fills with deposits and is dredged on a regular basis. It is difficult to know what the depth of the channel is at any give time. Other factors likely to change include vessel traffic, types of vessels, and channel currents.

3.3 Conclusion

The AASHTO LRFD design code attempts to provide a framework for the probability-based analysis of vessel impact on bridges. This framework is employed in example studies that follow and in the development of a standalone analysis program that will be discussed.

Chapter 4. Modifications to the AASHTO LRFD Approach

4.1 Areas of Modification

While the AASHTO LRFD method for the design of bridges for vessel collision can often provide reasonable answers, some of its limitations can be addressed. One such area relates to improving the calculation of probability of collapse. Very little research has been performed in the past on barge-to-pier collisions; therefore, the code bases calculations for probability of collapse entirely on ship-to-ship collision studies. To address this limitation, some preliminary work based on analysis (not testing) is proposed in order to yield different probability of collapse curves that might be of interest especially for barge impact on bridges.

4.2 Modification Procedure

To develop a probability of collapse curve to be used as an alternative to Figure 3.4, it is necessary to carry out a series of analyses that will assess the likelihood that the bridge will collapse under different barge collision scenarios. The test runs are selected based upon a random sampling of important input variables for the analyses, which yield impact forces and ultimate bridge strengths.

4.2.1 Test Variables

The input variables that will be modified include material properties, angle of impact, height or elevation of impact, and vessel loading. Separate analyses that yield vessel impact forces and ultimate strength for each sampled set of impact variables need to be carried out.

Variability of Material Properties

The material properties of the concrete and the steel reinforcement used in most bridge piers can vary considerably. In order to account for this, a normal distribution for concrete compressive strength is used. According to ACI (ACI, 2002) Table 5.3.2.2, the mean concrete compressive strength must exceed the specified concrete strength by 1,200 psi. Therefore, the mean for 4,000 psi concrete would be 5,200 psi. The coefficient of variation for concrete compressive strength is taken as 10%. Thus, we have:

$$\sigma = 0.1\mu \qquad\qquad (4.1)$$

where σ and μ are the standard deviation and the mean, respectively, of concrete compressive strength.

To insure that a range of concrete compressive strengths are sampled, random numbers are generated from ten bins evenly distributed based on the cumulative distribution function of a normal random variable. Compressive strength values are thus obtained randomly in this statistical stratified sampling procedure. The modulus of elasticity can be determined based on a function relationship with the compressive strength of the concrete. Table 4.1 presents the set of concrete compressive strength and modulus of elasticity values obtained for the test analyses.

Table 4.1: Sampled Material Properties for Concrete.

Step	f'c	E
	(ksi)	(ksi)
1	4.19	3689.6
2	4.65	3888.5
3	4.79	3943.8
4	4.94	4005.5
5	5.08	4063.0
6	5.28	4140.1
7	5.35	4167.6
8	5.59	4263.5
9	5.76	4324.4
10	5.91	4381.9

Variability of the Angle of Impact

As a given barge group approaches a bridge and becomes aberrant, the angle at which it strikes a given bent or pier can vary. While it is possible to strike the bent at any angle between zero and 90 degrees, realistic angles of impact are likely to be far more limited. In order to have a manageable number of analyses to perform, the angle of impact for this study is limited to a maximum of 15 degrees in each direction from a head-on collision. A zero degree angle is considered a head-on collision and the range of impact angles is 30 degrees split into five steps of 7.5 degrees each. Since in most situations, positive and negative angles will yield the same results, only three values, 15, 7.5 and 0 degrees are needed here. See Table 4.2.

Table 4.2: Angles of Impact Considered in the Analyses.

Step	Angle
	(deg)
1	15.0
2	7.5
3	0.0
4	-7.5
5	-15.0

Variability of Height/ Elevation of Impact

Because the water level in the channel changes at all times, the height or elevation along a pile where a barge group or vessel may strike is variable. The probability of collapse is expected to vary depending on the height of impact as the ultimate strength of the pier is different, depending on the location where the load is applied. The load will be applied at two different locations, the normal water line and the high water line (See Table 4.3). In many cases, these two locations will be fairly close and, hence, additional impact locations are not considered.

Table 4.3: Impact Heights used in the Analyses.

Step	Location
1	HWL
2	NWL

Variability of Vessel Loading

At the time of the impact, a vessel may be fully loaded, completely unloaded, or at any loading condition in between. Analyses will be carried out only for the two extreme cases – loaded fully and unloaded (See Table 4.4).

Table 4.4: Vessel Loadings used in the Analyses.

Step	Loading
1	Loaded
2	Unloaded

Variable Limitations

While material properties, angle of impact, impact height, and vessel loading are being varied in the analyses, these are not the only variables that could be changed. Superstructure stiffness, boundary conditions, vessel velocity, vessel type, pier geometry, and degradation of materials properties could also have been modified. However, a limit on the number of variables is considered in order to have a manageable number of analyses to perform. While some variables (such as superstructure stiffness, boundary conditions, degradation of material properties) are easier to change and reflect modeling uncertainty, consideration for other variables such as vessel type, speed, and pier geometry would require an extremely large number of analyses. Again, in the interest of having a manageable number of analyses to perform that focus on some of the key sources of variability, only the previously described analysis sets are proposed.

4.2.2 A Proposal for Improved Probability of Collapse Calculations

Considering all combinations of input parameters that are variable (Table 4.1 to Table 4.4), a total of 200 different analyses need to be performed. In each analysis, the ultimate lateral strength (H) of a pier and the impact force (P) transmitted by the vessel (barge) to the pier are determined. If P is found to be greater than H, a failure is deemed to have occurred. The fraction of analyses out of the 200 proposed that lead to failure is an alternative estimate to the probability of collapse value suggested by the AASHTO LRFD code.

Such estimates for the probability of bridge collapse due to vessel impact clearly have limitations in that they are model-based and not data-based. Moreover, numerous analyses are necessary for a single scenario in order to estimate the probability of collapse. Nevertheless, in this study, a software program for estimation of the annual frequency of bridge collapse due to vessel impact is developed to offer the user the option of alternative probability of collapse (PC) estimates, which can be obtained using the method outlined in this chapter.

Chapter 5. Example Calculations

5.1 Calculation Method

As shown in Equation 3.2, the total annual frequency of bridge collapse due to vessel impacts is equal to the sum of the annual frequencies of collapse for each vessel-pier combination. A detailed example calculation is presented in this chapter. The calculations are performed using the program VIOB that was developed and discussed in Chapter 7. To facilitate the understanding of all the calculations, the data for each vessel-pier combination are first presented. Bridge and traffic data are *simulated* here in order to illustrate the 2004 AASHTO LRFD method. All of the equations used for these calculations and some background for their development can be found in Chapter 3.

5.2 The Colorado River - FM 521 Bridge

5.2.1 Description of Data

Bridge and Channel Diagrams

Figure 5.1 shows a stick drawing of the Colorado River – FM 521 Bridge located in Matagorda County. The navigable waterway boundary and centerline are shown as are the high water line and the normal water line. Figure 5.2 shows a satellite image of the bridge and the surrounding region of interest.

Figure 5.1: Colorado River – FM 521 Bridge Geometry

*Figure 5.2: Satellite Image of the Colorado River – FM 521 Bridge
and the Surrounding Region of Interest.*

Bridge Data

The first step in performing the vessel collision analysis is to determine basic bridge properties and the importance classification of the bridge. Table 5.1 lists the name of the bridge, the TxDOT structure ID for the bridge, the waterway the bridge crosses, the mile marker on the waterway that the bridge is situated at, the roadway over the bridge, and the importance classification. Of all of these fields, only the importance classification will be needed later. The importance classification is determined in accordance with AASHTO LRFD code Section 3.14.3.

Table 5.1: Bridge Information

Bridge Name:	Colorado River - FM 521
TxDOT Structure ID:	131580084603009
Waterway:	Colorado River
Mile Marker:	100
Roadway:	FM 521
Importance Classification:	Regular

Once the basic information on the bridge is defined, additional information about the piers is collected. Each pier is first labeled for reference. In this case the bridge has four piers labeled from left to right (See Figure 5.1). For each pier, its distance from the navigable waterway centerline, the depth of the channel at the high water line (HWL) at that pier, the radius of the

pier at where the high water line crosses, and the ultimate lateral strength (*H*) are recorded. All of this information is summarized in Table 5.2.

Table 5.2: Pier Data

Pier	Distance from CL	HWL Channel Depth	Diameter at HWL	H
	(ft)	(ft)	(ft)	(kips)
1	62.5	22.7	4	450
2	62.5	24.7	4	330
3	152.5	18.7	4	200
4	192.5	13.7	2	200

Channel Data

To perform the analysis, it is necessary to record the channel data. The parallel current velocity, perpendicular current velocity, minimum impact speed, navigable channel width, channel region type, channel turn angle, and the traffic density need to be defined. It is important to be careful with units as the AASHTO LRFD code equations contain empirical parameters that are often unit-specific. The channel data are summarized in Table 5.3.

Table 5.3: Channel Data

Parallel Current Velocity:	2 ft/s
Perpendicular Current Velocity:	1 ft/s
Minimum Impact Speed:	1.689 ft/s
Navigable Channel Width:	100 ft
Channel Region Type:	Transition
Channel Turn Angle:	34 deg
Traffic Density:	Low

Vessel Traffic Data

In addition to bridge, pier, and channel data, traffic data must also be collected. Table 5.4 is a list of all of the vessels that will pass under the bridge. The class of vessel, the size of the vessel, and the specific type of vessel are all recorded. For more details on vessel class, size, and type see Chapter 7. It is also important to note how many times each vessel passes under the bridge, whether the vessel is loaded or unloaded, and the velocity of the vessel.

Table 5.4: Vessel Fleet Description[*]

Vessel Name	Vessel Class	Vessel Size	Vessel Type	# Trips	Loaded of Unloaded	Velocity
				(Trips/Yr)		(knots)
V1	Barge Group	TXDOT BG 1	N/A	101	Loaded	6
V2	Barge Group	TXDOT BG 2	N/A	29	Loaded	6
V3	Barge Group	TXDOT BG 3	N/A	15	Loaded	6

[*] The Vessel Size labels such as "TXDOT BG 1" are only to be understood as designators used in this example. These designators do not refer to any specific TxDOT barges or ferries and they can be changed by the user of the program.

The specific geometry related to each vessel that passes under the bridge is detailed in Table 5.5, Table 5.6, and Table 5.7. The specific configuration of each of the barge groups is displayed in Figure 5.3, Figure 5.4, and Figure 5.5.

Table 5.5: Barge Group Description

Name	Barge Group Type	LOA	Width	Draft	Displacement
		(ft)	(ft)	(ft)	(tonne)
V1	TXDOT BG 1	452.0	35.0	9.0	3628.1
V2	TXDOT BG 2	655.0	35.0	9.0	5442.2
V3	TXDOT BG 3	850.0	35.0	9.0	7165.5
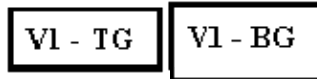
Figure 5.3: Vessel 1 – TXDOT BG 1 – Formation
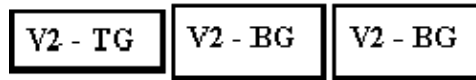
Figure 5.4: Vessel 2 – TXDOT BG 2 – Formation
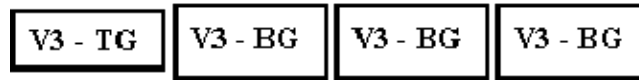
Figure 5.5: Vessel 3 – TXDOT BG 3 – Formation

Table 5.6: Tug Information

Name	Type	Horsepower	Length	Width	Draft	Displacement
			(ft)	(ft)	(ft)	(ton)
V1 - TG	TXDOT Tug	1	62.0	20.0	9.0	181.4
V2 - TG	TXDOT Tug	2	70.0	27.0	9.0	272.1
V3 - TG	TXDOT Tug	2	70.0	27.0	9.0	272.1

Table 5.7: Barge Information

Name	Type	Size	Length	Width	Draft	Displacement
			(ft)	(ft)	(ft)	(tonne)
V1 - BG	Covered Hopper	Jumbo	195.0	35.0	8.7	1723.4
V2 - BG	Covered Hopper	Jumbo	195.0	35.0	8.7	1723.4
V3 - BG	Covered Hopper	Jumbo	195.0	35.0	8.7	1723.4

5.2.2 Calculations

Using the data assembled in Section 5.2.1, computations leading to estimates of the annual frequency of collapse can now be carried out. The formulations for all the required calculations are detailed in Chapter 3.

Probability of Aberrancy (PA)

The expression for calculating probability of aberrancy is given in Equation 3.4. Each of the components that are involved in computing the probability of aberrancy is shown in Table 5.8. Probability of aberrancy is calculated for every vessel-pier combination.

Table 5.8: Probability of Aberrancy Calculations

Vessel	Pier	BR	R_B	R_C	R_{XC}	R_D	PA
							(1/Yrs)
1	1	0.00012	1.378	1.118	1.592	1.0	**0.000294**
1	2	0.00012	1.378	1.118	1.592	1.0	**0.000294**
1	3	0.00012	1.378	1.118	1.592	1.0	**0.000294**
1	4	0.00012	1.378	1.118	1.592	1.0	**0.000294**
2	1	0.00012	1.378	1.118	1.592	1.0	**0.000294**
2	2	0.00012	1.378	1.118	1.592	1.0	**0.000294**
2	3	0.00012	1.378	1.118	1.592	1.0	**0.000294**
2	4	0.00012	1.378	1.118	1.592	1.0	**0.000294**
3	1	0.00012	1.378	1.118	1.592	1.0	**0.000294**
3	2	0.00012	1.378	1.118	1.592	1.0	**0.000294**
3	3	0.00012	1.378	1.118	1.592	1.0	**0.000294**
3	4	0.00012	1.378	1.118	1.592	1.0	**0.000294**

The base rate is assigned depending on the type of vessel that is passing the pier. If the vessel is a ship or tug, the base rate is equal to .00006, for a barge or barge group the base rate is .00012. Table 5.9 shows the base rate for each vessel pier combination.

Table 5.9: Base Rate (*BR*) Selection

Vessel	Pier	Vessel	BR
1	1	Barge	**0.00012**
1	2	Barge	**0.00012**
1	3	Barge	**0.00012**
1	4	Barge	**0.00012**
2	1	Barge	**0.00012**
2	2	Barge	**0.00012**
2	3	Barge	**0.00012**
2	4	Barge	**0.00012**
3	1	Barge	**0.00012**
3	2	Barge	**0.00012**
3	3	Barge	**0.00012**
3	4	Barge	**0.00012**

The correction factor for bridge location uses Equations 3.5, 3.6, and 3.7 depending on the region type. Chapter 3 also explains how one can determine what region type the bridge is located in.

Table 5.10 displays the correction factor for bridge location for each of the vessel-pier combinations. The angle θ in Table 5.10 is computed for the study region using the satellite image in Figure 5.2.

Table 5.10: Correction Factor for Bridge Location (R_B) Calculations

Vessel	Pier	Region	θ	R_B
			(deg)	
1	1	Transition	34	**1.378**
1	2	Transition	34	**1.378**
1	3	Transition	34	**1.378**
1	4	Transition	34	**1.378**
2	1	Transition	34	**1.378**
2	2	Transition	34	**1.378**
2	3	Transition	34	**1.378**
2	4	Transition	34	**1.378**
3	1	Transition	34	**1.378**
3	2	Transition	34	**1.378**
3	3	Transition	34	**1.378**
3	4	Transition	34	**1.378**

The correction factors for parallel current and perpendicular current are given in Equations 3.8 and 3.9, respectively. It is important to note that these formulas involve unit-dependent empirical constants. The current velocity values and resulting correction factors used to determine probability of aberrancy are summarized in Table 5.11 and Table 5.12 for each vessel-pier combination.

Table 5.11: Correction Factor for Parallel Current (R_C) Calculations

Vessel	Pier	V_C	V_C	R_C
		(ft/sec)	(knots)	
1	1	2.0	1.185	**1.118**
1	2	2.0	1.185	**1.118**
1	3	2.0	1.185	**1.118**
1	4	2.0	1.185	**1.118**
2	1	2.0	1.185	**1.118**
2	2	2.0	1.185	**1.118**
2	3	2.0	1.185	**1.118**
2	4	2.0	1.185	**1.118**
3	1	2.0	1.185	**1.118**
3	2	2.0	1.185	**1.118**
3	3	2.0	1.185	**1.118**
3	4	2.0	1.185	**1.118**

Table 5.12: Correction Factor for Perpendicular Current (R_{XC}) Calculations

Vessel	Pier	V_{XC} (ft/sec)	V_{XC} (knots)	R_{XC}
1	1	1.0	0.592	**1.592**
1	2	1.0	0.592	**1.592**
1	3	1.0	0.592	**1.592**
1	4	1.0	0.592	**1.592**
2	1	1.0	0.592	**1.592**
2	2	1.0	0.592	**1.592**
2	3	1.0	0.592	**1.592**
2	4	1.0	0.592	**1.592**
3	1	1.0	0.592	**1.592**
3	2	1.0	0.592	**1.592**
3	3	1.0	0.592	**1.592**
3	4	1.0	0.592	**1.592**

The final correction factor for determining the probability of aberrancy is due to vessel traffic density. Chapter 3 explains how traffic density is represented and the resulting correction factors due to vessel traffic density are summarized in Table 5.13.

Table 5.13: Correction Factor for Traffic Density (R_D) Calculations

Vessel	Pier	Traffic Density	R_D
1	1	Low	**1.0**
1	2	Low	**1.0**
1	3	Low	**1.0**
1	4	Low	**1.0**
2	1	Low	**1.0**
2	2	Low	**1.0**
2	3	Low	**1.0**
2	4	Low	**1.0**
3	1	Low	**1.0**
3	2	Low	**1.0**
3	3	Low	**1.0**
3	4	Low	**1.0**

Geometric Probability (PG)

To determine the geometric probability, *PG*, the approach presented in Chapter 3 Section 3.1.3 is employed. The various parameters involved in the geometric probability calculations for each vessel-pier combination are summarized in Table 5.14.

Table 5.14: Geometric Probability (*PG*) Calculations

Vessel	Pier	X_P	B_P	B_V	LOA	X_1	X_2	PG
		(ft)	(ft)	(ft)	(ft)			(1/Yrs)
1	1	62.5	4.0	35.0	452.0	0.095	0.181	0.034084
1	2	62.5	4.0	35.0	452.0	0.095	0.181	0.034084
1	3	152.5	4.0	35.0	452.0	0.294	0.381	0.032509
1	4	192.5	2.0	35.0	452.0	0.385	0.467	0.029819
2	1	62.5	4.0	35.0	655.0	0.066	0.125	0.023642
2	2	62.5	4.0	35.0	655.0	0.066	0.125	0.023642
2	3	152.5	4.0	35.0	655.0	0.203	0.263	0.023115
2	4	192.5	2.0	35.0	655.0	0.266	0.322	0.021581
3	1	62.5	4.0	35.0	850.0	0.051	0.096	0.018253
3	2	62.5	4.0	35.0	850.0	0.051	0.096	0.018253
3	3	152.5	4.0	35.0	850.0	0.156	0.202	0.018011
3	4	192.5	2.0	35.0	850.0	0.205	0.248	0.016925

Probability of Collapse (PC)

Probability of collapse is determined by the method described in Section 3.1.4. While the ultimate lateral strength (*H*) is determined outside of the AASHTO LRFD calculations, the load due to the vessel impact may be estimated using the AASHTO LRFD code procedure. Table 5.15 shows the values of *H* and *P* used to estimate the probability of collapse for each of the vessel-pier combinations.

Table 5.15: Probability of Collapse (*PC*) Calculations

Vessel	Pier	H	P	H/P	PC
		(kip)	(kip)		(1/Yrs)
1	1	450	2274.7	0.198	0.089041
1	2	330	2274.7	0.145	0.094896
1	3	200	2192.6	0.091	0.179043
1	4	200	2155.7	0.093	0.165002
2	1	450	2610.0	0.172	0.091862
2	2	330	2610.0	0.126	0.096966
2	3	200	2537.4	0.079	0.290605
2	4	200	2504.5	0.080	0.281296
3	1	450	2889.9	0.156	0.093716
3	2	330	2889.9	0.114	0.098325
3	3	200	2824.1	0.071	0.362635
3	4	200	2794.3	0.072	0.355830

To determine the force, *P*, Equation 3.25 is used. The kinetic energy, *KE*, and barge bow damage length, a_B, needed to compute *P* for each vessel-pier calculation are given in Table 5.16. In this example, all of the vessels in this calculation are barge groups; hence, the same procedure

for computing *P* is used for all vessel-pier combinations. Chapter 3 describes how the calculation would differ if ships were involved.

Table 5.16: Vessel Impact Force Calculations

Vessel	Pier	KE	a_B	P
		(kip ft)	(ft)	(kip)
1	1	13219.4	8.415	**2274.7**
1	2	13219.4	8.415	**2274.7**
1	3	11735.0	7.669	**2192.6**
1	4	11088.1	7.334	**2155.7**
2	1	19914.2	11.464	**2610.0**
2	2	19914.2	11.464	**2610.0**
2	3	18378.0	10.803	**2537.4**
2	4	17698.6	10.505	**2504.5**
3	1	26276.7	14.008	**2889.9**
3	2	26276.7	14.008	**2889.9**
3	3	24718.4	13.410	**2824.1**
3	4	24024.3	13.139	**2794.3**

Table 5.17 shows how the kinetic energy (*KE*) is computed for each vessel-pier combination based on Equation 3.20. The hydrodynamic mass coefficient is determined using the method described in the AASHTO LRFD code Section 3.14.7.

Table 5.17: Kinetic Energy (*KE*) Calculations

Vessel	Pier	HWL Depth	Draft	Underkeel Clearance	CH	W	V	KE
		(ft)	(ft)	(ft)		(tonne)	(ft/s)	(kip ft)
1	1	22.7	9.0	13.7	1.05	3628.1	10.066	**13219.4**
1	2	24.7	9.0	15.7	1.05	3628.1	10.066	**13219.4**
1	3	18.7	9.0	9.7	1.05	3628.1	9.484	**11735.0**
1	4	13.7	9.0	4.7	1.05	3628.1	9.219	**11088.1**
2	1	22.7	9.0	13.7	1.05	5442.2	10.088	**19914.2**
2	2	24.7	9.0	15.7	1.05	5442.2	10.088	**19914.2**
2	3	18.7	9.0	9.7	1.05	5442.2	9.691	**18378.0**
2	4	13.7	9.0	4.7	1.05	5442.2	9.510	**17698.6**
3	1	22.7	9.0	13.7	1.05	7165.5	10.099	**26276.7**
3	2	24.7	9.0	15.7	1.05	7165.5	10.099	**26276.7**
3	3	18.7	9.0	9.7	1.05	7165.5	9.795	**24718.4**
3	4	13.7	9.0	4.7	1.05	7165.5	9.656	**24024.3**

The method for determining vessel velocity (*V*) needed in computing kinetic energy is described in Section 3.1.4.2. The various parameters needed for the calculations are summarized in Table 5.18.

Table 5.18: Velocity (*V*) Calculations

Vessel	Pier	VT	V_{Min}	XC	LOA	XL	CLX	Pier Width	FaceX	V
		(ft/s)	(ft/s)	(ft)	(ft)	(ft)	(ft)	(ft)	(ft)	(ft/s)
1	1	10.134	1.689	50.0	452.0	1356.0	62.5	4.0	60.5	**10.066**
1	2	10.134	1.689	50.0	452.0	1356.0	62.5	4.0	60.5	**10.066**
1	3	10.134	1.689	50.0	452.0	1356.0	152.5	4.0	150.5	**9.484**
1	4	10.134	1.689	50.0	452.0	1356.0	192.5	2.0	191.5	**9.219**
2	1	10.134	1.689	50.0	655.0	1965.0	62.5	4.0	60.5	**10.088**
2	2	10.134	1.689	50.0	655.0	1965.0	62.5	4.0	60.5	**10.088**
2	3	10.134	1.689	50.0	655.0	1965.0	152.5	4.0	150.5	**9.691**
2	4	10.134	1.689	50.0	655.0	1965.0	192.5	2.0	191.5	**9.510**
3	1	10.134	1.689	50.0	850.0	2550.0	62.5	4.0	60.5	**10.099**
3	2	10.134	1.689	50.0	850.0	2550.0	62.5	4.0	60.5	**10.099**
3	3	10.134	1.689	50.0	850.0	2550.0	152.5	4.0	150.5	**9.795**
3	4	10.134	1.689	50.0	850.0	2550.0	192.5	2.0	191.5	**9.656**

Vessel Frequency (N)

For each vessel-pier combination, the number of trips per year by each vessel is multiplied by a growth factor to account for increased future vessel traffic. This calculation is summarized in Table 5.19.

Table 5.19: Projected Vessel Frequency (*N*) Calculations

Vessel	Pier	Growth Factor	# Trips	N
			(Trips/Yr)	(Trips/Yr)
1	1	1.2	101	**121.2**
1	2	1.2	101	**121.2**
1	3	1.2	101	**121.2**
1	4	1.2	101	**121.2**
2	1	1.2	29	**34.8**
2	2	1.2	29	**34.8**
2	3	1.2	29	**34.8**
2	4	1.2	29	**34.8**
3	1	1.2	15	**18.0**
3	2	1.2	15	**18.0**
3	3	1.2	15	**18.0**
3	4	1.2	15	**18.0**

Return Period

Finally, using Equation 3.1, the annual frequency of bridge collapse is computed for each vessel-pier combination. Then, all of these annual frequencies of collapse are summed, and the reciprocal of this frequency yields the return period associated with bridge collapse due to vessel impact. This calculation is summarized in Table 5.20.

Table 5.20: Return Period Calculations

Vessel	Pier	N	PA	PG	PC	AFC
		(Trips/Yr)	(1/Yrs)	(1/Yrs)	(1/Yrs)	(1/Yrs)
1	1	121.2	0.000294	0.034084	0.089041	0.000108
1	2	121.2	0.000294	0.034084	0.094896	0.000115
1	3	121.2	0.000294	0.032509	0.179043	0.000208
1	4	121.2	0.000294	0.029819	0.165002	0.000176
2	1	34.8	0.000294	0.023642	0.091862	0.000022
2	2	34.8	0.000294	0.023642	0.096966	0.000023
2	3	34.8	0.000294	0.023115	0.290605	0.000069
2	4	34.8	0.000294	0.021581	0.281296	0.000062
3	1	18.0	0.000294	0.018253	0.093716	0.000009
3	2	18.0	0.000294	0.018253	0.098325	0.000010
3	3	18.0	0.000294	0.018011	0.362635	0.000035
3	4	18.0	0.000294	0.016925	0.355830	0.000032

| | | | | **Sum AFC:** | **0.000869** | **1 /Yrs** |
| | | | | **Return Period:** | **1150.7** | **Years** |

$$1150.7 > 1000 \qquad\qquad (5.1)$$

This bridge passes the AASHTO LRFD specifications.

Since this bridge is classified as "Regular" in terms of importance, its return period must be larger than 1000 years. Since this bridge has a return period of 1150.7 years, it passes the AASHTO LRFD requirements.

5.3 San Jacinto River – Eastbound IH-10 Bridge

This second example using the Eastbound IH-10 Bridge located in Harris County is provided to reiterate the methods used in Section 5.2. Only the tables and figures are provided as the equations and methods are identical to those used in the previous example.

5.3.1 Description of Data

The bridge and channel diagrams are summarized in Figure 5.6 and Figure 5.7.
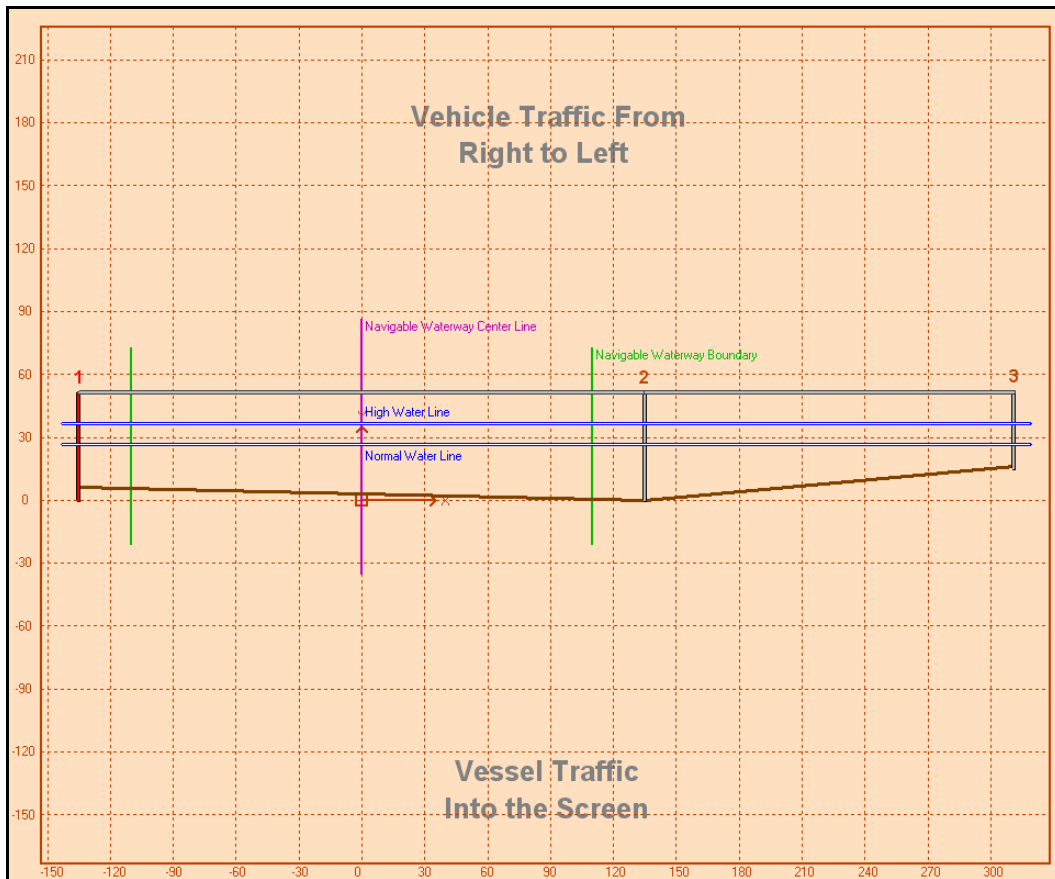
Figure 5.6: San Jacinto River – IH 10 Bridge Geometry

Figure 5.7: Satellite View of the San Jacinto River – IH 10 Bridge

Bridge Data

Table 5.21: Bridge Information

Bridge Name:	San Jacinto River - Eastbound IH-10
TxDOT Structure ID:	121020050801317
Waterway:	San Jacinto River
Mile Marker:	1
Roadway:	Eastbound IH-10
Importance Classification:	Regular

Table 5.22: Pier Data

Pier	Distance from CL	HWL Channel Depth	Diameter at HWL	H
	(ft)	(ft)	(ft)	(kips)
1	135.0	30.7	4.75	997
2	135.0	36.7	4.75	997
3	311.0	20.7	3.75	815

Channel Data

Table 5.23: Channel Data

Parallel Current Velocity:	2.0 ft/s
Perpendicular Current Velocity:	1.0 ft/s
Minimum Impact Speed:	1.689 ft/s
Navigable Channel Width:	220 ft
Channel Region Type:	Bend
Channel Turn Angle:	15 deg
Traffic Density:	Low

Vessel Traffic Data

Table 5.24: Vessel Fleet Description

Vessel Name	Vessel Class	Vessel Size	Vessel Type	# Trips	Loaded of Unloaded	Velocity
				(Trips/Yr)		(knots)
V1	Barge Group	TXDOT BG 4	N/A	677	Loaded	6
V2	Barge Group	TXDOT BG 4	N/A	677	Unloaded	6

Table 5.25: Barge Group Description

Name	Barge Group Type	LOA	Width	Draft	Displacement
		(ft)	(ft)	(ft)	(tonne)
V1	TXDOT BG 4	257.0	35.0	9.0	1542.0
V2	TXDOT BG 4	257.0	35.0	9.0	568.0

V1 - TG   V1 - BG
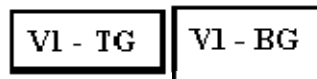
Figure 5.8: Vessel 1 – TXDOT BG 4 (V1 Loaded) – Formation

V2 -TG   V2 -BG

Figure 5.9: Vessel 1 – TXDOT BG 4 (V2 Empty) – Formation

Table 5.26: Tug Information

Name	Type	Horsepower	Length	Width	Draft	Displacement
			(ft)	(ft)	(ft)	(ton)
V1 - TG	TXDOT Tug	1	62.0	20.0	9.0	200.0
V2 - TG	TXDOT Tug	1	62.0	20.0	9.0	200.0

Table 5.27: Barge Information

Name	Type	Size	Length	Width	Draft	Displacement
			(ft)	(ft)	(ft)	(ton)
V1 - BG	Covered Hopper	Jumbo	195.0	35.0	7.0	1500.0
V2 - BG	Covered Hopper	Jumbo	195.0	35.0	2.0	425.8

5.3.2 Calculations

Probability of Aberrancy (PA)

Table 5.28: Table Probability of Aberrancy Calculations

Vessel	Pier	BR	R_B	R_C	R_{XC}	R_D	PA
							(1/Yrs)
1	1	0.00012	1.333	1.118	1.592	1.0	**0.000285**
1	2	0.00012	1.333	1.118	1.592	1.0	**0.000285**
1	3	0.00012	1.333	1.118	1.592	1.0	**0.000285**
2	1	0.00012	1.333	1.118	1.592	1.0	**0.000285**
2	2	0.00012	1.333	1.118	1.592	1.0	**0.000285**
2	3	0.00012	1.333	1.118	1.592	1.0	**0.000285**

Table 5.29: Base Rate (*BR*) Selection

Vessel	Pier	Vessel	BR
1	1	Barge	**0.00012**
1	2	Barge	**0.00012**
1	3	Barge	**0.00012**
2	1	Barge	**0.00012**
2	2	Barge	**0.00012**
2	3	Barge	**0.00012**

Table 5.30: Correction Factor for Bridge Location (R_B) Calculations

Vessel	Pier	Region	θ	R_B
			(deg)	
1	1	Bend	15	**1.333**
1	2	Bend	15	**1.333**
1	3	Bend	15	**1.333**
2	1	Bend	15	**1.333**
2	2	Bend	15	**1.333**
2	3	Bend	15	**1.333**

Table 5.31: Correction Factor for Parallel Current (R_C) Calculations

Vessel	Pier	V_C	V_C	R_C
		(ft/sec)	(knots)	
1	1	2.0	1.185	**1.118**
1	2	2.0	1.185	**1.118**
1	3	2.0	1.185	**1.118**
2	1	2.0	1.185	**1.118**
2	2	2.0	1.185	**1.118**
2	3	2.0	1.185	**1.118**

Table 5.32: Correction Factor for Perpendicular Current (R_{XC}) Calculations

Vessel	Pier	V_{XC}	V_{XC}	R_{XC}
		(ft/sec)	(knots)	
1	1	1.0	0.592	**1.592**
1	2	1.0	0.592	**1.592**
1	3	1.0	0.592	**1.592**
2	1	1.0	0.592	**1.592**
2	2	1.0	0.592	**1.592**
2	3	1.0	0.592	**1.592**

Table 5.33: Correction Factor for Traffic Density (R_D) Calculations

Vessel	Pier	Traffic Density	R_D
1	1	Low	**1.0**
1	2	Low	**1.0**
1	3	Low	**1.0**
2	1	Low	**1.0**
2	2	Low	**1.0**
2	3	Low	**1.0**

Geometric Probability (PG)

Table 5.34: Geometric Probability (*PG*) Calculations

Vessel	Pier	X_P	B_P	B_V	LOA	X_1	X_2	PG
		(ft)	(ft)	(ft)	(ft)			(1/Yrs)
1	1	135	4.75	35.0	257.0	0.448	0.603	**0.053713**
1	2	135	4.75	35.0	257.0	0.448	0.603	**0.053713**
1	3	311	3.75	35.0	257.0	1.135	1.286	**0.028937**
2	1	135	4.75	35.0	257.0	0.448	0.603	**0.053713**
2	2	135	4.75	35.0	257.0	0.448	0.603	**0.053713**
2	3	311	3.75	35.0	257.0	1.135	1.286	**0.028937**

Probability of Collapse (PC)

Table 5.35: Probability of Collapse (*PC*) Calculations

Vessel	Pier	H	P	H/P	PC
		(kip)	(kip)		(1/Yrs)
1	1	997	1792.8	0.556	**0.049271**
1	2	997	1792.8	0.556	**0.049271**
1	3	815	1629.8	0.500	**0.055493**
2	1	997	1530.2	0.652	**0.038677**
2	2	997	1530.2	0.652	**0.038677**
2	3	815	1459.9	0.558	**0.049033**

Table 5.36: Vessel Impact Force (*P*) Calculations

Vessel	Pier	KE	a_B	P
		(kip ft)	(ft)	(kip)
1	1	5374.2	4.034	**1792.8**
1	2	5374.2	4.034	**1792.8**
1	3	3194.3	2.553	**1629.8**
2	1	1979.6	1.647	**1530.2**
2	2	1979.6	1.647	**1530.2**
2	3	1176.6	1.008	**1459.9**

Table 5.37: Kinetic Energy (*KE*) Calculations

Vessel	Pier	HWL Depth	Draft	Underkeel Clearance	CH	W	V	KE
		(ft)	(ft)	(ft)		(tonne)	(ft/s)	(kip ft)
1	1	30.7	9.0	21.7	1.05	1542.0	9.845	**5374.2**
1	2	36.7	9.0	27.7	1.05	1542.0	9.845	**5374.2**
1	3	20.7	9.0	11.7	1.05	1542.0	7.590	**3194.3**
2	1	30.7	9.0	21.7	1.05	568.0	9.845	**1979.6**
2	2	36.7	9.0	27.7	1.05	568.0	9.845	**1979.6**
2	3	20.7	9.0	11.7	1.05	568.0	7.590	**1176.6**

Table 5.38: Velocity (*V*) Calculations

Vessel	Pier	VT	V_{Min}	XC	LOA	XL	CLX	Pier Width	FaceX	V
		(ft/s)	(ft/s)	(ft)	(ft)	(ft)	(ft)	(ft)	(ft)	(ft/s)
1	1	10.134	1.689	110.0	257.0	771.0	135.0	4.75	132.625	**9.845**
1	2	10.134	1.689	110.0	257.0	771.0	135.0	4.75	132.625	**9.845**
1	3	10.134	1.689	110.0	257.0	771.0	311.0	3.75	309.125	**7.590**
2	1	10.134	1.689	110.0	257.0	771.0	135.0	4.75	132.625	**9.845**
2	2	10.134	1.689	110.0	257.0	771.0	135.0	4.75	132.625	**9.845**
2	3	10.134	1.689	110.0	257.0	771.0	311.0	3.75	309.125	**7.590**

Vessel Frequency (N)

Table 5.39: Projected Vessel Frequency (*N*) Calculations

Vessel	Pier	Growth Factor	# Trips	N
			(Trips/Yr)	(Trips/Yr)
1	1	1.2	677	**812.4**
1	2	1.2	677	**812.4**
1	3	1.2	677	**812.4**
2	1	1.2	677	**812.4**
2	2	1.2	677	**812.4**
2	3	1.2	677	**812.4**

Return Period

Table 5.40: Return Period Calculations

Vessel	Pier	N	PA	PG	PC	AFC
		(Trips/Yr)	(1/Yrs)	(1/Yrs)	(1/Yrs)	(1/Yrs)
1	1	812.4	0.000285	0.053713	0.049271	0.000613
1	2	812.4	0.000285	0.053713	0.049271	0.000613
1	3	812.4	0.000285	0.028937	0.055493	0.000372
2	1	812.4	0.000285	0.053713	0.038677	0.000481
2	2	812.4	0.000285	0.053713	0.038677	0.000481
2	3	812.4	0.000285	0.028937	0.049033	0.000329
				Sum AFC:	0.002888	1 /Yrs
				Return Period:	346.3	Years

$$346.3 < 1000 \qquad\qquad (5.2)$$

This bridge does not pass the AASHTO LRFD specifications.

This bridge has a return period for collapse due to vessel impact that is shorter than 1,000 years and, hence, fails to meet the AASHTO LRFD specification for a "regular" bridge.

5.4 Conclusions

The preceding examples illustrate the procedure involved in Method II of the AASHTO LRFD code specifications. This method aims to provide estimates of the annual frequency of collapse of a bridge due to vessel impact. The computations such as those summarized are included in a computer analysis program that was developed for this study and is discussed in Chapter 7.

Chapter 6. Discussion of Results

6.1 Bridge Performance and Recommendations

This chapter will focus on the results of a complete analysis of three distinct bridges. For each bridge, the return period is provided and a discussion detailing important parameters influencing the bridge vulnerability is included. Figure 6.1 lists the bridges that will be discussed in this chapter along with the results from the analysis using the AASHTO LRFD approach.

Throughout this chapter, various screenshots from the VIOB program are presented for the three bridges studied. All of these screenshots will be referred to as figures even when they might appear to be better classified as tables; this is done mainly to emphasize that they were obtained directly from images or output from VIOB.

Bridge Name	Return Period (years)	Pass/Fail
Colorado River - FM 521	1152	Pass
San Jacinto River - EB IH 10	346	Fail
GIWW - PR 22	12019	Pass

Figure 6.1: Summary of Bridges Analyzed

6.1.2 Colorado River – FM 521

The Colorado River – FM 521 Bridge has a return period of 1152 year which passes the AASHTO LRFD requirements of a 1000-year return period for a bridge with an importance classification of "Regular." While this bridge has a return period which is acceptable, it is still useful to examine which piers and vessels most influence the annual frequency of bridge collapse. Figure 6.2 shows the bridge geometry and Figure 6.3 shows a satellite image of the bridge and the surrounding region of interest.
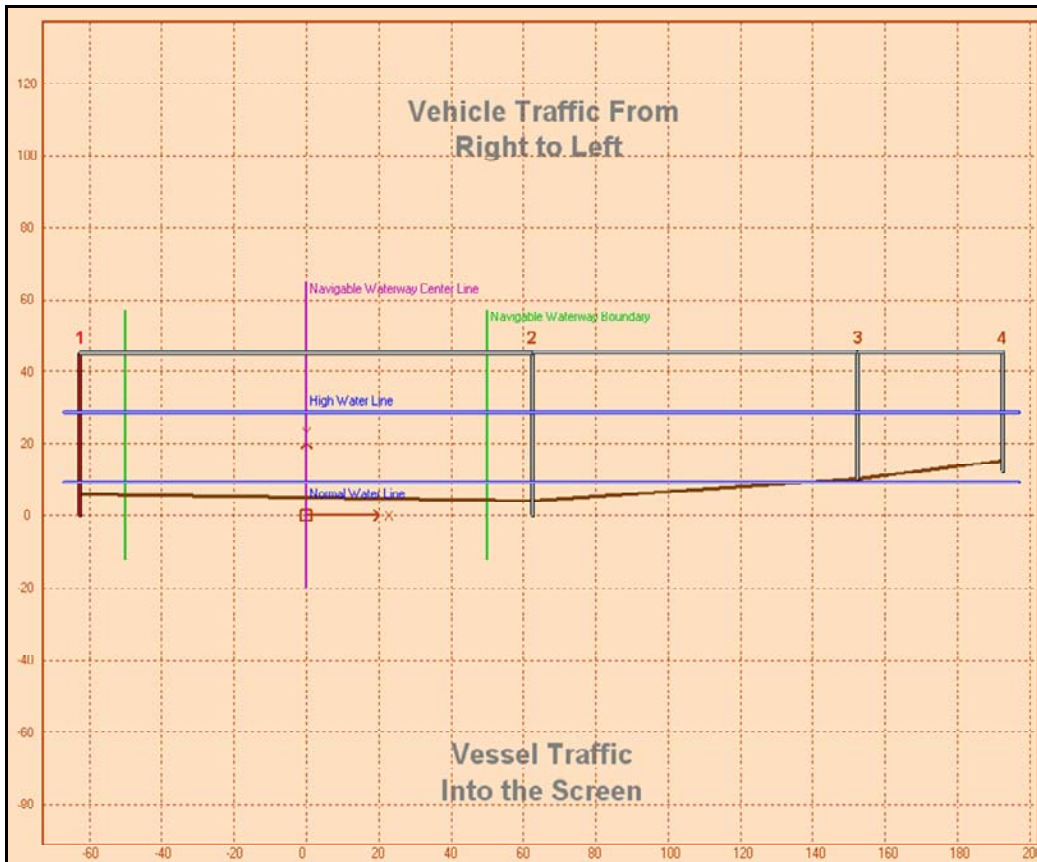
Figure 6.2: Colorado River – FM 521 Bridge Geometry.

Figure 6.3: Satellite Image of the Colorado River – FM 521 Bridge and the Surrounding Region of Interest.
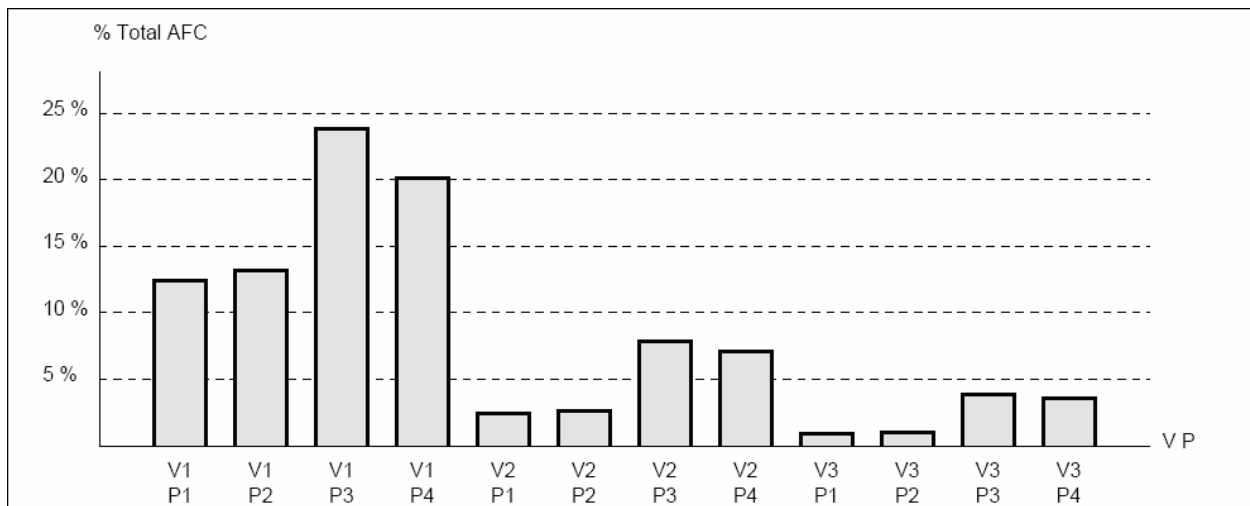
Figure 6.4: Contribution towards the annual frequencies of collapse of a particular vessel passing a particular pier of the Colorado River – FM 521 Bridge (from the VIOB Report).
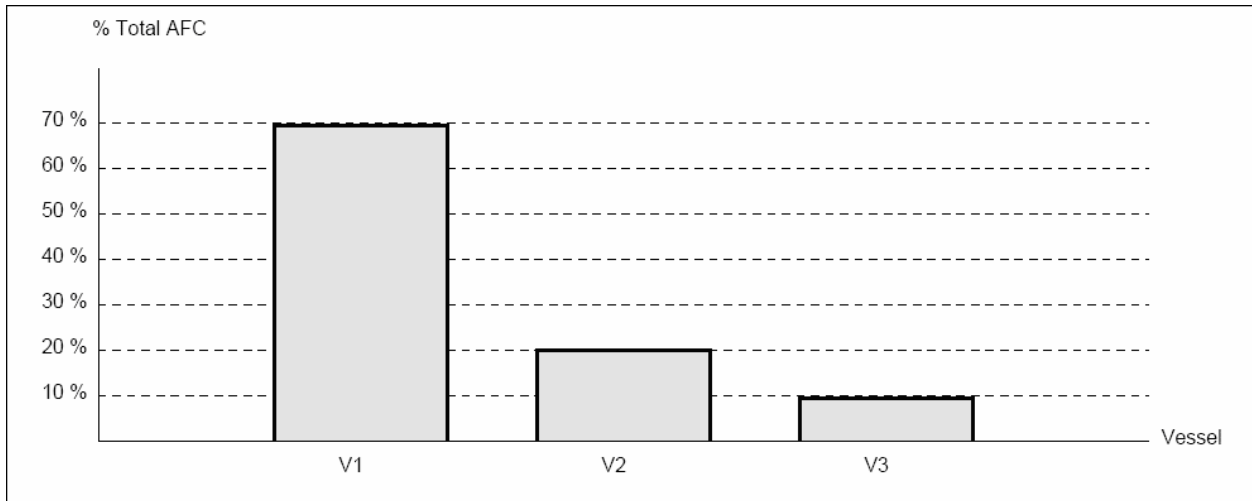
Figure 6.5: Contribution towards the annual frequencies of collapse of each vessel passing all piers of the Colorado River – FM 521 Bridge (from the VIOB Report).

Figure 6.6: Contribution towards the annual frequencies of collapse of all vessels passing a particular pier of the Colorado River – FM 521 Bridge (from the VIOB Report).

Vessel Name	Vessel Class	Vessel Type	Vessel Size	Vessel Frequency	Loaded or Unloaded	Vessel Velocity
				(Trips/Year)		(knots)
V1	Barge Group	TXDOT BG 1	N/A	101	Loaded	6
V2	Barge Group	TXDOT BG 2	N/A	29	Loaded	6
V3	Barge Group	TXDOT BG 3	N/A	15	Loaded	6

Figure 6.7: Vessel fleet components for the Colorado River – FM 521 Bridge (from the VIOB Report).

Pier Number:		Pier 1	Pier 2	Pier 3	Pier 4
Pier Height:	ft	45	45	35	33
Pier Bottom Elevation:	ft	0	0.16	10.16	12.16
Channel Elevation:	ft	6.16	4.16	10.16	15.16
User X Location:	ft	-62.5	62.5	152.5	192.5
Ultimate Transverse Pier Strength:	kips	450	330	200	200
Pier X-Section Shape:		Circle	Circle	Circle	Circle
Pier X-Section Depth:	ft	4	4	4	2
Pier X-Section Width:	ft	4	4	4	2
Pier X-Section Angle:	deg	0	0	0	0

Figure 6.8: Pier Information for the Colorado River – FM 521 Bridge
(from the VIOB Report).

From the results comparison section of the VIOB Report (discussed further in Chapter 7) for the Colorado River – FM 521 Bridge, several trends may be noted. First, by studying Figure 6.4 and 6.5, it can be seen that Vessel 1 has a much greater influence on the return period than does Vessels 2 and 3. However, Vessel 3 has a much larger displacement than Vessel 1 and both vessels move at the same velocity (See Chapter 5). It can be concluded that the dominant variable in the calculations is vessel trip frequency. Figure 6.7 lists the trip frequency of each type of vessel that passes this bridge. Each year, Vessel 1 travels past the bridge 101 times while Vessel 3 travels past it only 15 times. Vessel 2 travels past the bridge 29 times per year. There is almost a direct relationship between the vessel frequency and the percentage contribution to the total annual frequency of collapse of the bridge.

Upon studying Figure 6.6, it can be seen that Piers 3 and 4 have a far greater influence on the return period than Piers 1 and 2. At first, this seems unexpected because Piers 1 and 2 are closer to the centerline of the navigable channel than Piers 3 and 4. Piers closer to the centerline generally have a higher geometric probability. However, upon further inspection, it is clear that the controlling factor in this calculation is the probability of collapse, and as seen in Figure 6.8, Piers 3 and 4 both have considerably lower ultimate lateral strengths (*H*) than do Piers 1 and 2. A low *H* value leads to a high probability of collapse and hence, Piers 3 and 4 have a strong influence on the final return period associated with collapse of the Colorado River – FM 521 Bridge. By studying Figure 6.4, both factors identified, namely the vulnerability of Piers 3 and 4 and the importance of Vessel 1, are seen to dominate the risk to this bridge.

6.1.3 San Jacinto River – IH 10

The San Jacinto River – IH10 Bridge (eastbound) is not as straightforward as the Colorado River – FM 521 Bridge. The return period for this bridge is only 346 years, considerably lower than the AASHTO LRFD required 1,000 years for a "regular" bridge. By interpreting the results, a feasible solution for increasing the return period may be determined. Figure 6.9 shows the bridge geometry and Figure 6.10 shows a satellite image of the bridge and the surrounding region of interest.
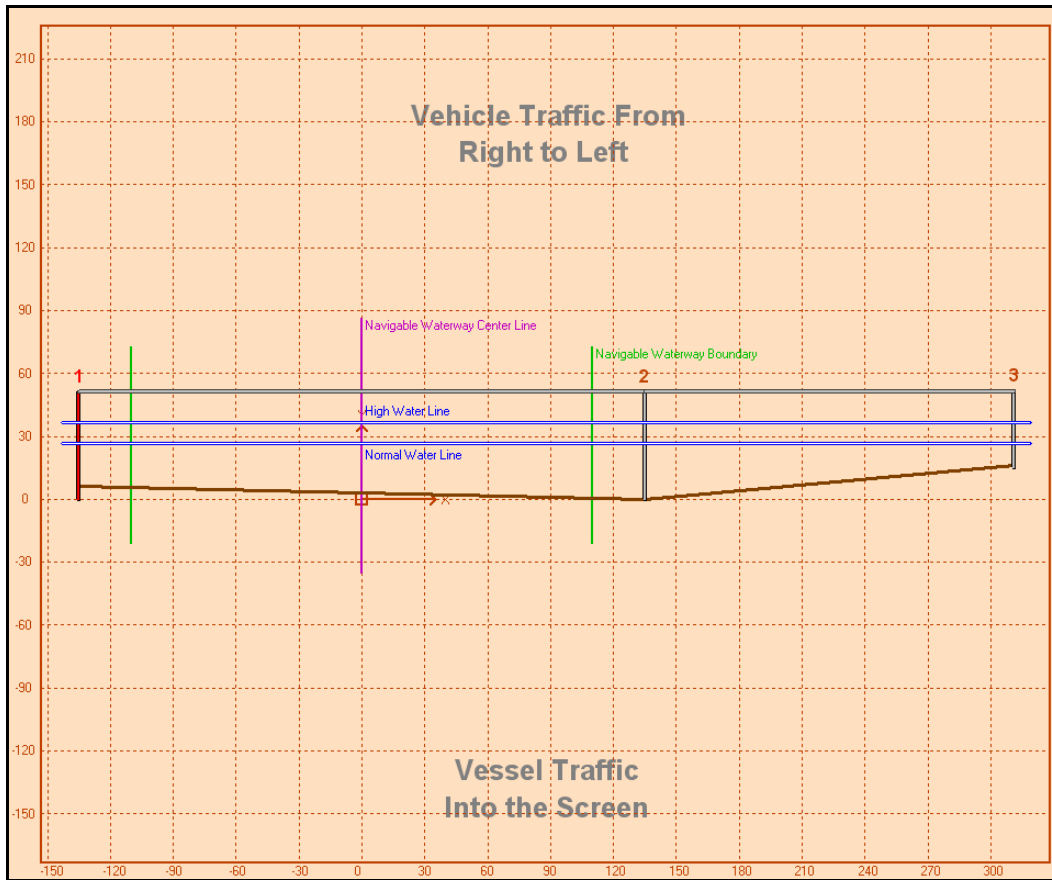
Figure 6.9: San Jacinto River – IH 10 Bridge Geometry.

Figure 6.10: Satellite Image of the San Jacinto River – IH 10 Bridge and the Surrounding Region of Interest.

Figure 6.11: Contribution towards the annual frequencies of collapse of a particular vessel passing a particular pier of the San Jacinto River – IH 10 Bridge (from the VIOB Report).
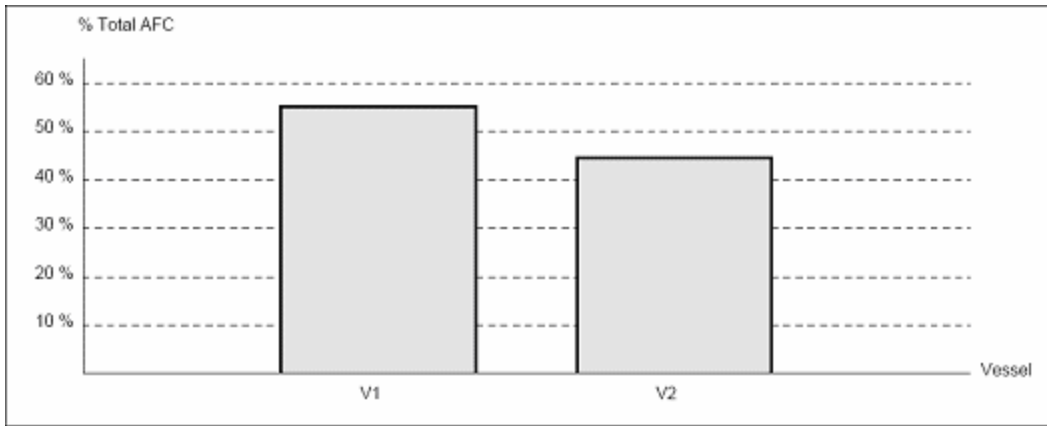
Figure 6.12: Contribution towards the annual frequencies of collapse of each vessel passing all piers of the San Jacinto River – IH 10 Bridge (from the VIOB Report).
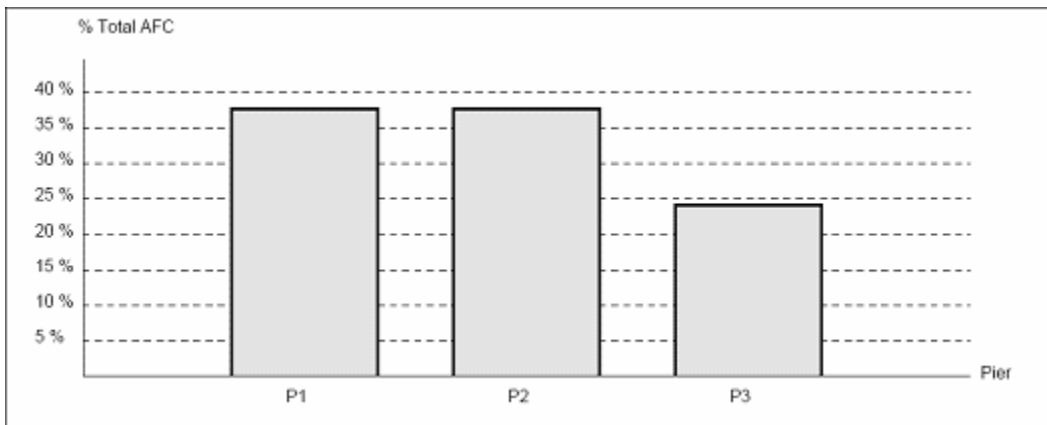
Figure 6.13: Contribution towards the annual frequencies of collapse of all vessels passing a particular pier of the San Jacinto River – IH 10 Bridge (from the VIOB Report).

Vessel i - Pier j	N	PA	PG	PC	AFC
Vessel 1 - Pier 1	812.4	0.000285	0.053714	0.049254	0.000613
Vessel 1 - Pier 2	812.4	0.000285	0.053714	0.049254	0.000613
Vessel 1 - Pier 3	812.4	0.000285	0.028937	0.055482	0.000372
Vessel 2 - Pier 1	812.4	0.000285	0.053714	0.038662	0.000481
Vessel 2 - Pier 2	812.4	0.000285	0.053714	0.038662	0.000481
Vessel 2 - Pier 3	812.4	0.000285	0.028937	0.049025	0.000329
				Total AFC:	**0.002889**

Figure 6.14: Annual frequency of collapse values for each vessel-pier combination for the San Jacinto River – IH 10 Bridge (from the VIOB Report).

56

Upon studying Figure 6.11, Figure 6.12, and Figure 6.13, no obvious trends can be seen. Figure 6.11 shows that there is a fairly equal contribution towards the bridge's risk from each of the vessel-pier combinations. However, it is necessary to increase the return period associated with collapse of this bridge since it is considerably lower than the acceptable value of 1,000 years. The most obvious way to improve an existing bridge is to place a dolphin in front of the piers to mitigate vessel collision effects significantly. Placing a dolphin in front of a pier effectively changes that pier's probability of collapse to almost zero and therefore makes its annual frequency of collapse also zero. Installation of a dolphin is very expensive though and, therefore, minimizing the number of piers that need to be protected can save a considerable amount of money. Figure 6.13 and Figure 6.14 clearly indicate that Piers 1 and 2 are of greater risk than Pier 3. Therefore, placing dolphins in front of those two piers could solve the problem of the low return period. In this case, the new return period increases to 1,426 years and therefore makes this bridge acceptable under the 2004 AASHTO LRFD standards. The completion of this analysis suggests that a dolphin is not needed to protect Pier 3.

6.1.4 GIWW – PR 22 (Nueces County)

The GIWW – PR 22 Bridge in Nueces County illustrates a few different issues that are not a concern for the first two bridges discussed. With a return period of 12,019 years, the GIWW – PR 22 Bridge clearly passes the AASHTO LRFD requirement of 1000 years for a "regular" bridge. A detailed study of how this bridge achieves such a high return period is still useful. Figure 6.15 shows the bridge geometry and Figure 6.16 shows a satellite image of the bridge and the surrounding region of interest.
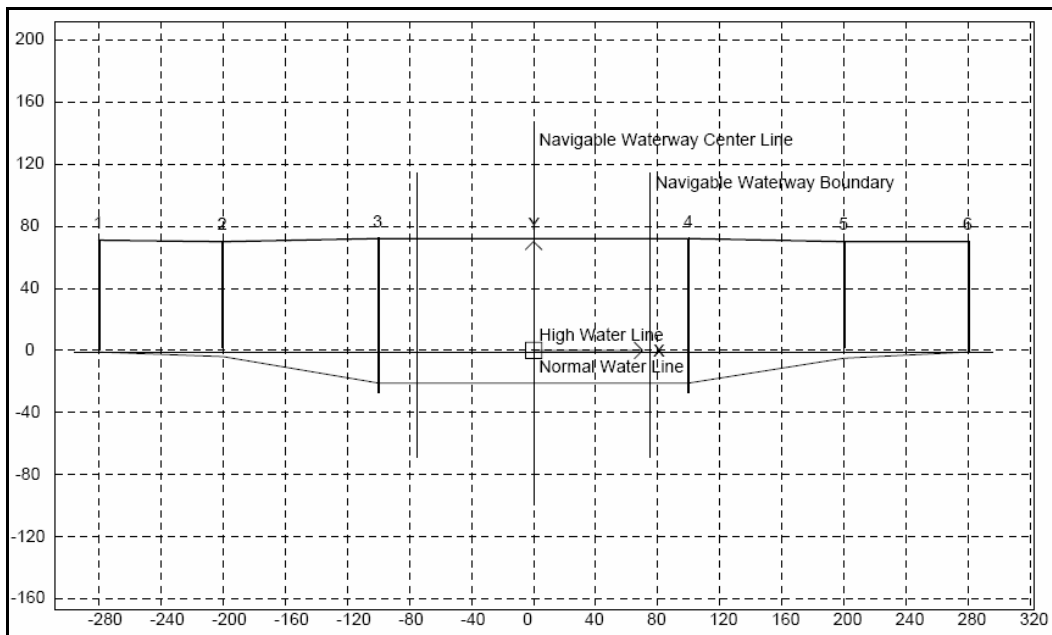
Figure 6.15: GIWW – PR 22 Bridge Geometry.
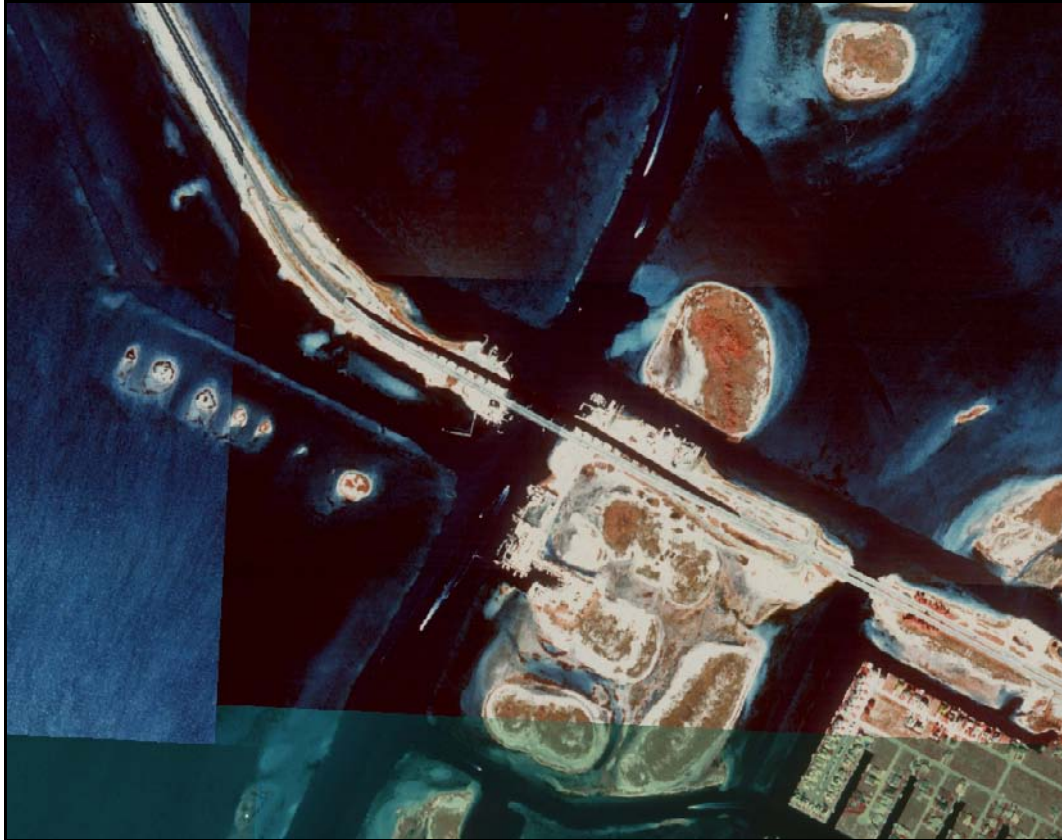
*Figure 6.16: Satellite Image of the GIWW – PR 22 Bridge and
the Surrounding Region of Interest.*
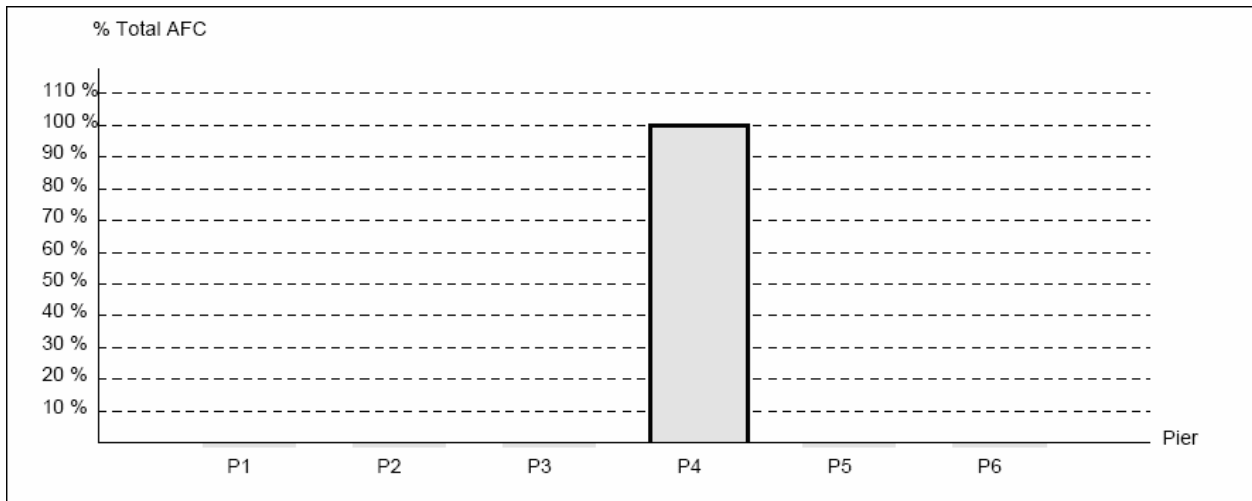
*Figure 6.17: Contribution towards the annual frequencies of collapse of all vessels
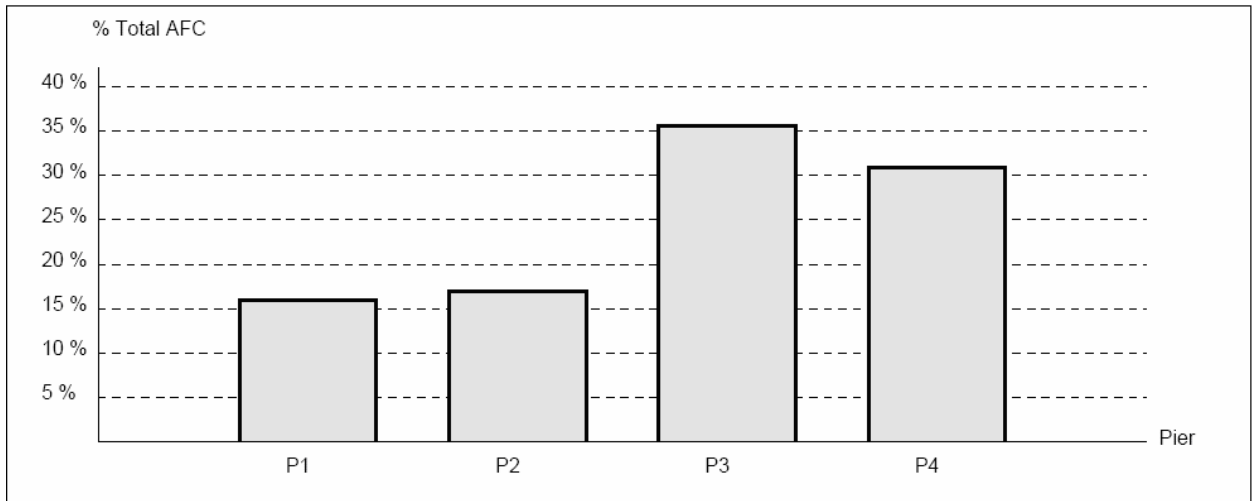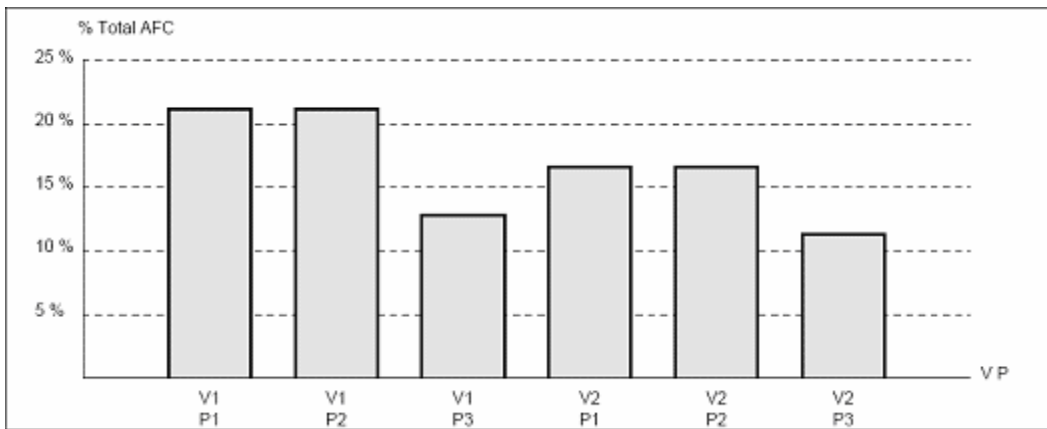passing a particular pier of the GIWW – PR 22 Bridge (from the VIOB Report).*

Vessel i - Pier j	N	PA	PG	PC	AFC
Vessel 1 - Pier 1	1008	0.000251	0.028043	0	0
Vessel 1 - Pier 2	1008	0.000251	0.031204	0	0
Vessel 1 - Pier 3	1008	0.000251	0.041323	0	0
Vessel 1 - Pier 4	1008	0.000251	0.041323	0.002633	0.000028
Vessel 1 - Pier 5	1008	0.000251	0.031204	0	0
Vessel 1 - Pier 6	1008	0.000251	0.028043	0	0
Vessel 2 - Pier 1	288	0.000251	0.021399	0	0
Vessel 2 - Pier 2	288	0.000251	0.022669	0	0
Vessel 2 - Pier 3	288	0.000251	0.02889	0	0
Vessel 2 - Pier 4	288	0.000251	0.02889	0.016654	0.000035
Vessel 2 - Pier 5	288	0.000251	0.022669	0	0
Vessel 2 - Pier 6	288	0.000251	0.021399	0	0
Vessel 3 - Pier 1	144	0.000251	0.017114	0	0
Vessel 3 - Pier 2	144	0.000251	0.017803	0	0
Vessel 3 - Pier 3	144	0.000251	0.02237	0	0
Vessel 3 - Pier 4	144	0.000251	0.02237	0.025842	0.000021
Vessel 3 - Pier 5	144	0.000251	0.017803	0	0
Vessel 3 - Pier 6	144	0.000251	0.017114	0	0
				Total AFC:	0.000084

Figure 6.18: Annual frequency of collapse values for each vessel-pier combination for the GIWW – PR 22 Bridge (from the VIOB Report).

It can be seen from Figure 6.17 that only Pier 4 contributes to the annual frequency of collapse of the bridge. Also, it can be seen in Figure 6.18 that the reason for this is that the probability of collapse is zero for all of the other piers. The reason the probability of collapse is zero though is not the same for all piers. Pier 3 is at the same distance from the centerline of the navigable channel line as Pier 4, but it has a probability of collapse of zero while Pier 4 has a non-zero probability of collapse because the ultimate lateral strength of Pier 4 is 2,210 kips and that of Pier 3 is 3,900 kips. Figure 6.19 shows the effect that the high pier strength of Pier 3 has on its probability of collapse, causing it to go to zero. The slightly lower pier strength of Pier 4, shown in Figure 6.20, causes the probability of collapse to have a non-zero (albeit small) value.
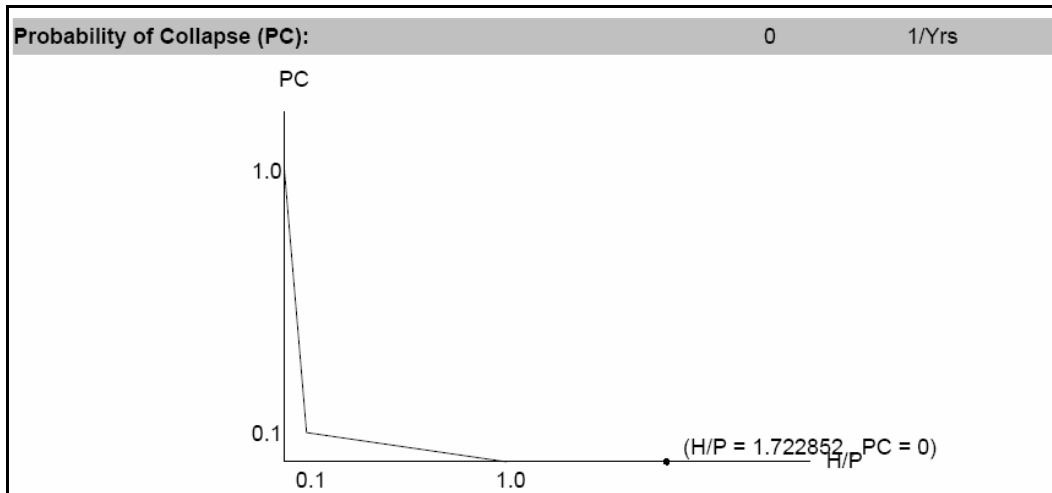
Figure 6.19: Probability of collapse for Vessel 1 Pier 3 for the GIWW – PR 22 Bridge (from the VIOB Report).
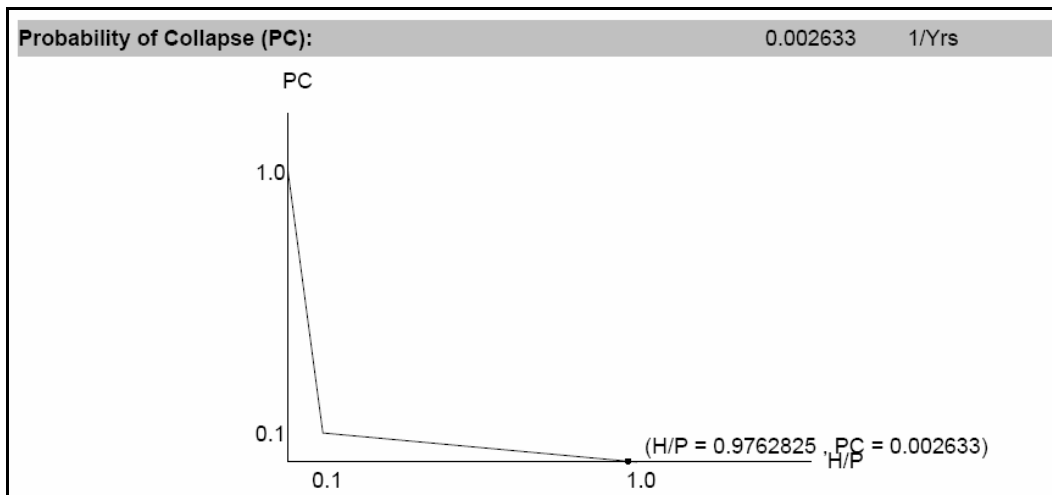
Figure 6.20: Probability of collapse for Vessel 1 Pier 4 for the GIWW – PR 22 Bridge (from the VIOB Report).

While Pier 3's negligible influence on the bridge risk can be explained by its high ultimate lateral pier strength, Piers 1, 2, 5, and 6 cannot be explained similarly. These outer piers all have an ultimate lateral pier strength of 1,000 kips, not nearly high enough to drive the probability of collapse to zero. Rather, outer piers have a zero probability of collapse because they are all situated in the very low water depths of the channel. None of the vessels passing this bridge has an underkeel clearance that would allow them to strike any of the four outer piers.

It should also be noted that even though the return period is very high, the probability of collapse of this bridge is still not insignificant. If this bridge were still in the design stage, it might be beneficial to increase the ultimate lateral strength of Pier 4 so that it too has a negligible probability of collapse. If this were done, the bridge would effectively have an almost infinite

return period. Often, an infinite return period is optimal when future vessel traffic is difficult to predict or when trends suggest rapid growth in traffic.

Chapter 7. VIOB (Vessel Impact on Bridges)

7.1 Introduction to the Software Program, VIOB

If one considers computational effort involved in just one annual frequency of collapse calculation, for just one type of vessel passing one pier of one bridge, there can be upwards of 100 calculations depending on the type of vessel. If one then assumes a modest number of different vessels, say five, and an average number of bridge piers, say four, then over 2,000 calculations would be required for each bridge to determine the total annual frequency of collapse. Due to the large number of calculations needed to determine the return period of a bridge, it is necessary to create an automated solution to the problem.

7.1.1 Past Vessel Impact Tools

The Florida Department of Transportation (FDOT) has made available a Mathcad spreadsheet which can be used to determine the annual frequency of collapse of a bridge on a Florida waterway using the AASHTO LRFD specifications. While FDOT's spreadsheet can help to perform the desired vessel collision analysis, the program has some limitations in terms of general applicability. Most importantly, it is not a standalone program, the data are Florida-specific, the program is difficult to change, it allows only one type of analysis, it does not provide a comprehensive output, and it does not allow the user to create reports summarizing salient details of the analysis.

7.1.2 The Program VIOB and its Features

VIOB is a completely standalone program that reads data from a standard Microsoft Access database and carries out all of the analysis required to evaluate bridges against vessel impact according to the AASHTO LRFD code. It was developed as part of this TxDOT-funded research study.

The straightforward approach of VIOB and its conveniently designed user interface allow the user to easily insert necessary data and perform calculations using the data. Modifying the database is simple as the vessel libraries provide quick viewing and retrieval of data. Most importantly, the enhanced graphical capabilities of VIOB make trouble-shooting complicated geometric problems a routine task. Finally, comprehensive reports can be produced and the output allows clear understanding and insights into the results as was seen in Chapter 6.

7.2 User Flow Chart

Figure 7.1 shows a flow chart of the steps that a user would take to analyze a bridge in VIOB. This rest of this chapter provides a detailed explanation of each of the features of VIOB. For a step-by-step example see Appendix B.
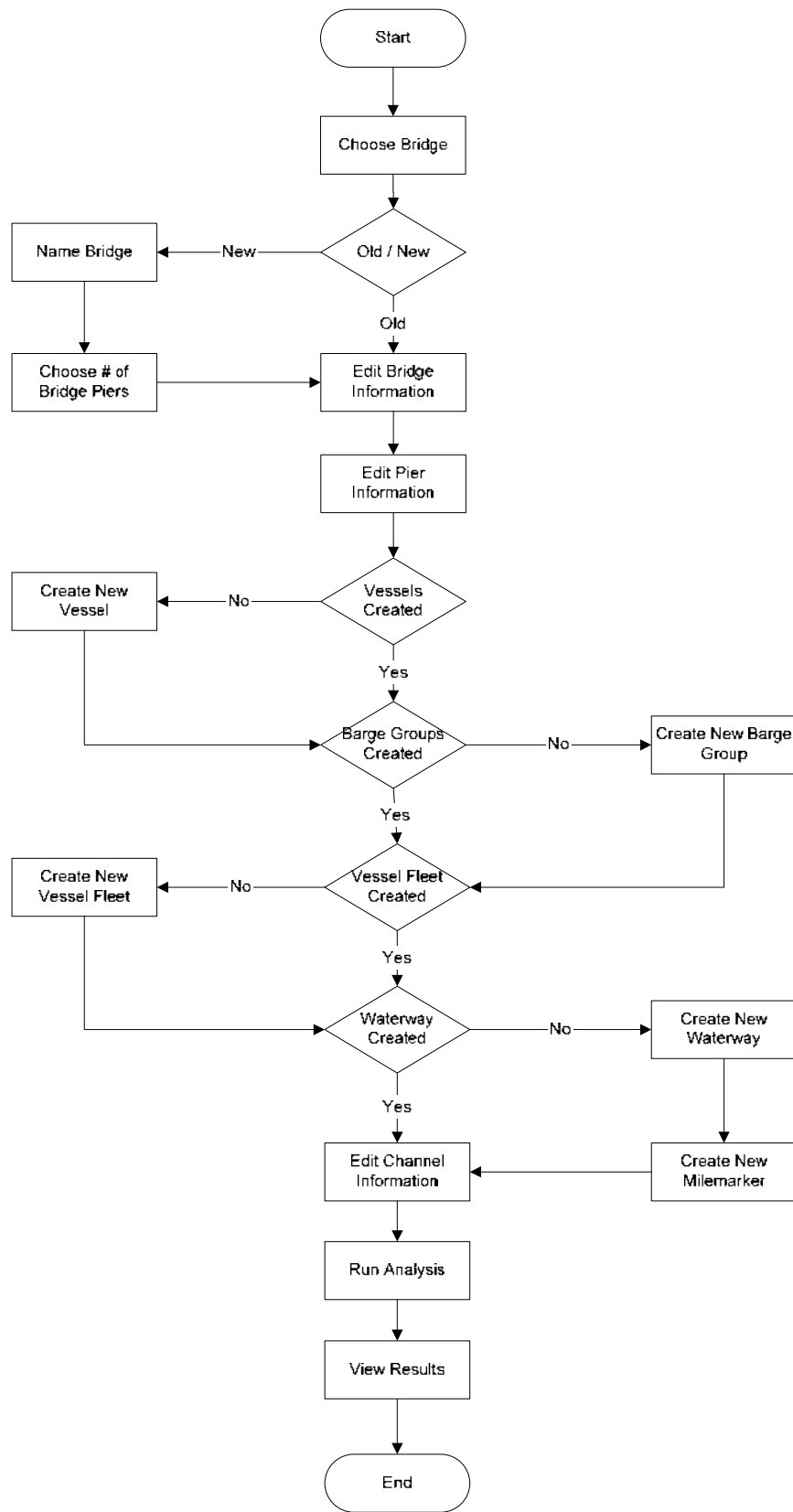
Figure 7.1: User Flow Chart for Analysis of a Single Bridge in VIOB

7.3 Description of Program

Like most analysis programs, VIOB consists of three parts: a preprocessing component, a solver component, and a postprocessing component. Each stage of the program performs different functions and involves different relative amounts of user work and computer work.

7.3.1 Preprocessor

The preprocessor stage of VIOB is where most of the user input occurs. The user inputs all of the data that will be used for the calculations and VIOB takes all of the information that the user enters and stores it in a database until the calculations are run.

Start Menu

On first opening the program, the user is greeted by the start menu page, shown in Figure 7.2. On this start menu page, the user has the option to analyze an existing bridge, create a new bridge, or delete an existing bridge.
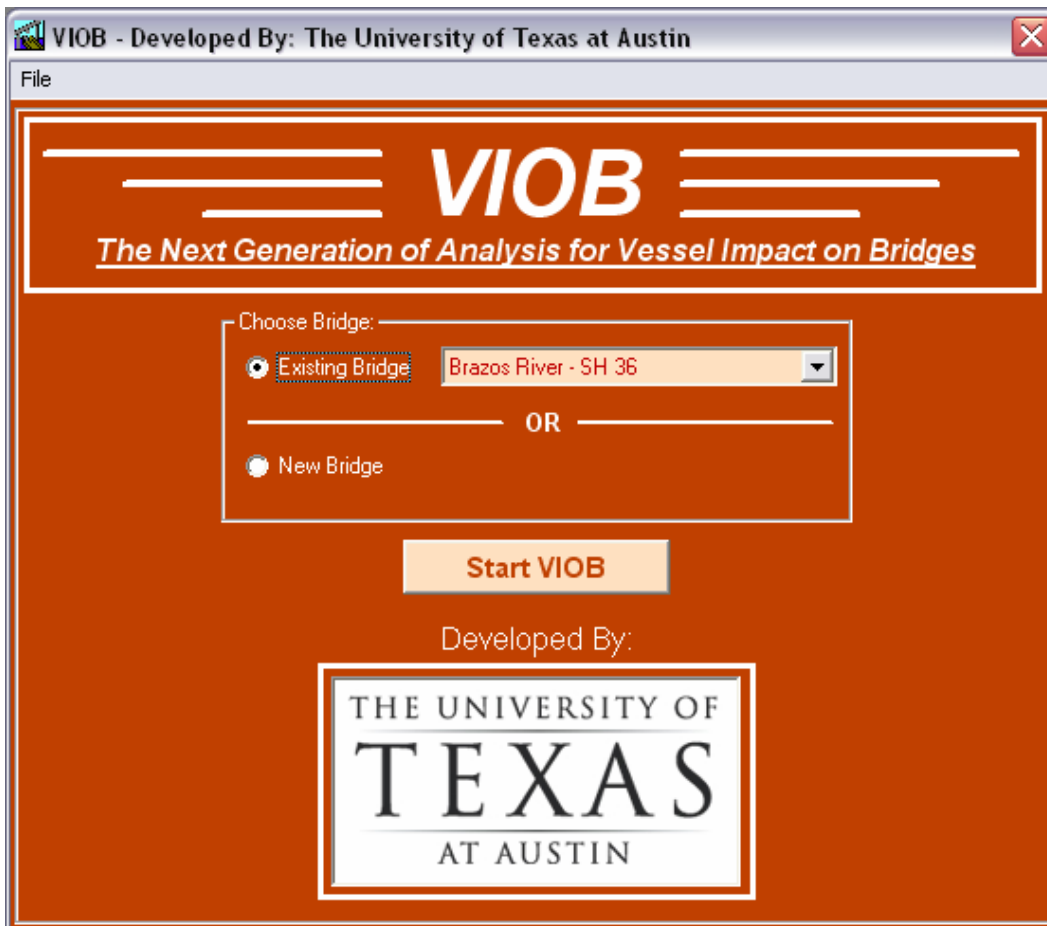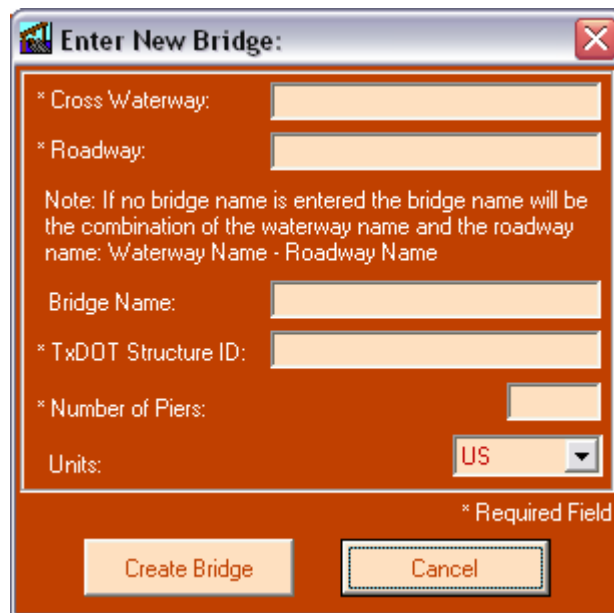
Figure 7.2: Start Menu screen shot

Work With Existing Bridge

If the objective is to work with an existing bridge, the user must simply select the "Existing Bridge" option button and then select the bridge that he/she wishes wish to use from the pull-down menu. In order to begin working with the bridge, the user then clicks the "Start VIOB" button.

Create New Bridge

If the user wants to create a new bridge, he/she selects the "New Bridge" option and the clicks the "Start VIOB" button to enter information about the new bridge. The new bridge form, shown in Figure 7.3, will pop up and the user is asked to enter information about the bridge he/she wishes to create. The user must enter the waterway which the bridge crosses, the roadway that the bridge is part of, the TxDOT Structure ID of the bridge, the number of piers that the bridge has, and the unit system with which the user wishes to work.

Figure 7.3: New Bridge Screen Shot

If the user does not enter a bridge name, a name will be created from the Cross Waterway and the Roadway in the form: Waterway Name – Roadway Name. In some cases such as with the Queen Isabella Causeway Bridge, an actual name for the bridge exists so the user has the option to enter that. The TxDOT Structure ID is a unique number given to the bridge by TxDOT and can be entered at this time. It is not necessary to provide a number that is a given length or even a real number, but something must be entered into the field for the user to be allowed to continue.

The most important number entered at this point in the program is the number of piers that the bridge has. The program will allow the user to enter any number between 1 and 50. However, it is important to realize that for each of these piers, some additional information will need to be

entered subsequently. It is not recommended to include piers that are not in the waterway or are extremely far from the centerline of the channel as they will be unnecessary for the calculations and will be mostly wasted effort. Adding extra piers will not make a significant difference in the computation time as the program executes a single analysis nearly instantaneously. It is not possible to change the number of piers in the bridge at a later stage; therefore, the user should make sure to enter this number correctly.

The final information added on the New Bridge form is a selection of the unit system that will be used in the computations. There are seven physical quantities for which units are needed; the user can select either the SI or US system of units. The different unit schemes are listed in Table 7.1. As with the number of piers, the selected unit system may not be changed at a later stage.

Table 7.1: Different unit schemes

Category	US	SI
Length	ft	mm
Mass 1	ton	Mg
Mass 2	tonne	Mg
Velocity 1	knots	km / hr
Velocity 2	ft / s	m / s
Force	kips	N
Energy	kip - ft	J

Delete an Existing Bridge

To delete an existing bridge the user first goes to the pull-down menu and selects the desired bridge. Next the user goes to the **File > Delete Bridge...** A message box, shown in Figure 7.4, asking the user, "Are you sure you want to delete the bridge: Example Bridge?" pops up on the screen. If the user clicks "Yes" then the bridge is deleted and the user is returned to the Start Menu page. If the user clicks "No" the bridge is not deleted and the user is returned to the Start Menu page.
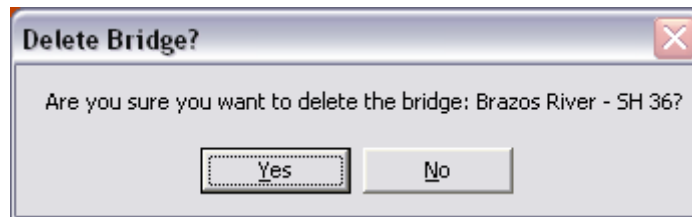
Figure 7.4: Delete Bridge pop up screen shot

Main Page

Once the user has either selected to use an existing bridge, or created a new bridge, the start page closes and the main page, shown in Figure 7.5, is presented. The main page has many different features on it including: data display, bridge selection, edit features, plot display, run

calculations, and database manipulation. A stick plot based on user input geometry shows the bridge. In this plot, vessel traffic moves into or out of the page and vehicle traffic moves from left to right or vice versa.
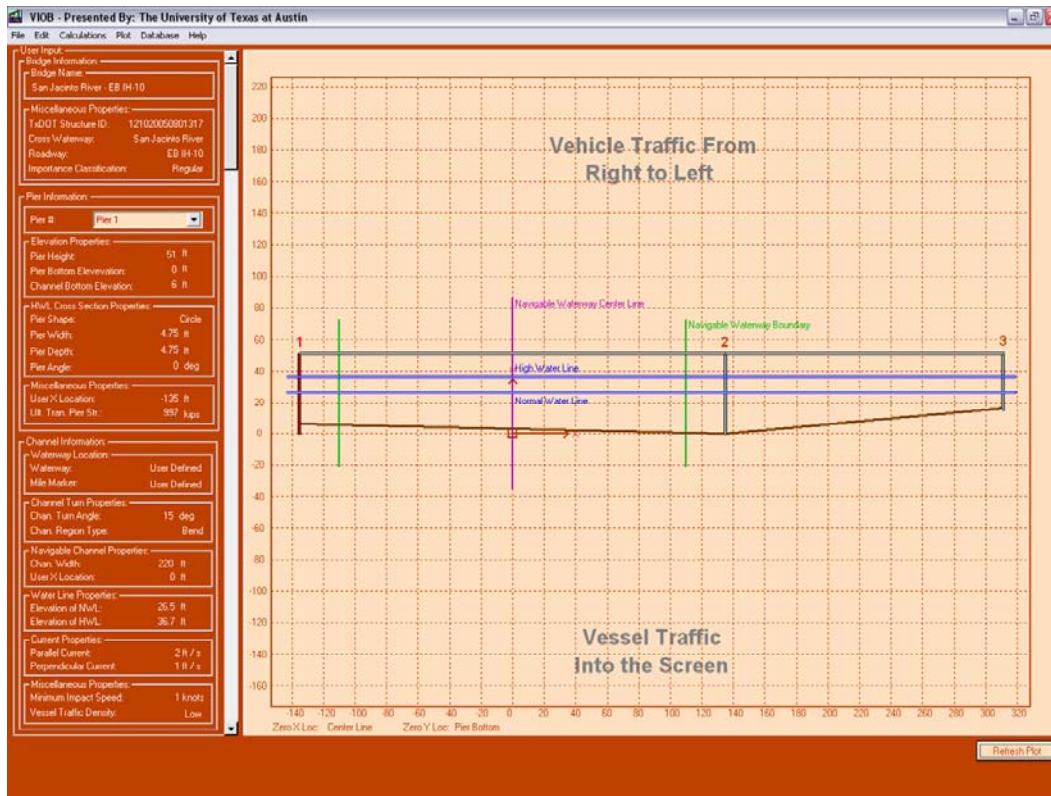
Figure 7.5: Main Page Screen Shot

Data Display

On the left hand side of the screen, all of the data about the bridge and the channel are displayed so that the user can quickly see this information. By selecting the pier pull-down menu, the user can scroll through the various piers. When a pier is selected, the plotted pier on the right corresponding to the selected pier will be highlighted in red. Numbers appearing above the plotted piers indicate the index number of the pier and this number will also turn red when that pier is selected by the user.

On the lower left hand corner of the plot, the origin *x* and origin *y* locations are noted. The location of the origin is also indicated by the origin icon. The location of any point on the plot can be determined quickly by moving the mouse over a point. The coordinates of the point over which the mouse is located will be displayed in the lower right hand corner of the plot display.

Changing the Origin

The user can change the origin location by clicking on **Plot > Origin Location…** from the Main Page. The user has the ability to change both the X origin location and Y origin location independently (See Figure 7.6). The X origin location can be selected to be at any of the piers or at the centerline of the navigable channel. The Y origin can be selected as the pier bottom, pier top, channel bottom, normal water line or high water line. All of the Y origin locations are associated with Pier 1. So, if "Pier Top" is selected, the Y origin will be the top of Pier 1 even if the X origin is located at the centerline of the navigable channel or at a different pier.
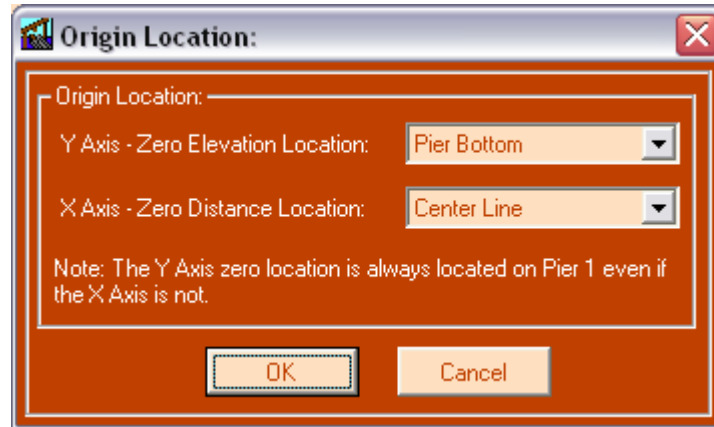
Figure 7.6: Origin Location Screen Shot

The user selects the desired origin from the pull-down menu. Once the user selects a new origin, all of the geometry data are automatically updated with reference to the new origin location.

Plot Display

On the plot itself, several features are displayed and can be turned on or off. Displayed features include: channel bottom, navigable channel boundaries, navigable channel centerline, piers, bridge deck, traffic direction labels, normal water line, and high water line. All of these features and their labels can be toggled on or off by going to **Plot > Display Options…** That will bring up a Display Options window, shown in Figure 7.7, which allows the user to check which features and labels they would like displayed. The origin and axes can also be toggled on and off in this window.

The user has the ability to change the spacing of the grid lines from the Display Options menu. VIOB offers an Auto Spacing option for both the X and Y grids. If the Auto Spacing feature is turned on, VIOB will automatically space the grid lines in an optimal manner.
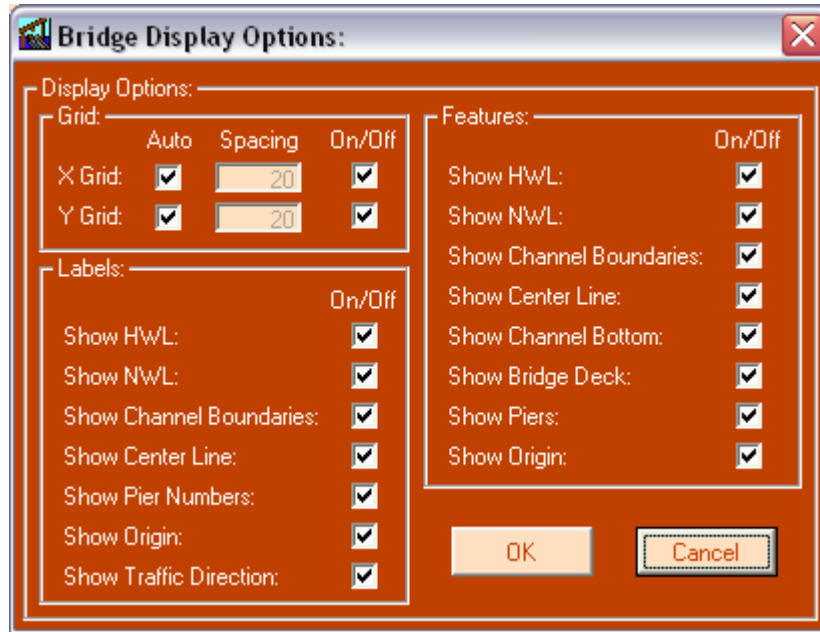
Figure 7.7: Display Options Screen Shot

Refreshing the Plot

It is possible that the bridge plot will sometimes become "smudged" by other programs or windows that are moved over the bridge plot. In some cases, the plot may even disappear completely. If plot smudging occurs, the user can refresh the plot in two ways. The user can click **Plot > Refresh Plot**, or he/she can click the Refresh Plot button in the lower right hand corner of the Main Page window. Both of these actions will restore the plot of the bridge in the Main Page window.

Switching to a Different Bridge

While the main page currently shows the bridge that was selected on the Start Page, the user may want to switch bridges or start working on a new bridge. The user has bridge-switching capabilities under the **File** menu. In order to start a new bridge, the user goes to **File > New Bridge…** from the Main Page. Choosing the "New Bridge" option will close the Main Page window and reopen the start page window. The "Create New Bridge" option button will already be selected for the user. If the user wants to close the current bridge, he/she clicks on **File > Close Bridge…** If the user chooses the "Close Bridge" option, the Main Page is closed and the Start Page is opened again with the "Select Existing Bridge" option selected. If the user wants to open a different bridge, he/she goes to **File > Open Bridge…** Selecting the "Open Bridge" option has the same effect as selecting the "Close Bridge" option. The Main Page is closed and the Start Page is opened with the "Select Existing Bridge" option pre-selected. Finally, the user can exit VIOB by clicking **File > Exit**.

Edit Features

Input data is divided into three categories: bridge information, pier information, and channel information. The user can access all three of these features under the **Edit** tab. Further information on these features is provided later.

Run Calculations

To run calculations the user clicks on **Calculations > Run…** Further information on this feature is provided in Section 7.3.2

Database Manipulation

All the vessel information is stored in a database and that information is accessed under the **Database** tab. Under the Database tab, the user can edit the Vessel Library, Barge Group Library, Vessel Fleet Library, and the Waterway Library. Further information about each of these databases is provided later.

Edit Bridge Information

To edit bridge information, the user goes to **Edit > Bridge Data…** from the Main Page. This will bring up the "Edit Bridge" window, shown in Figure 7.8, and the user can change several bridge-related variables. The Bridge Name, TxDOT Structure ID, Cross Waterway, Roadway, and Importance Classification are all input in the Edit Bridge window.

Bridge name, cross waterway, and roadway should all have been entered earlier when the user first created the bridge. These values will automatically be displayed when the user opens the Edit Bridge window. As stated earlier, the TxDOT Structure ID is a unique identification number that each structure is given by the Texas Department of Transportation. This number may be in any format the user chooses. If the user does not know the true TxDOT Structure ID, this number a dummy number may be entered instead. The TxDOT Structure ID is not used for any calculations or as a reference in any other part of the program.
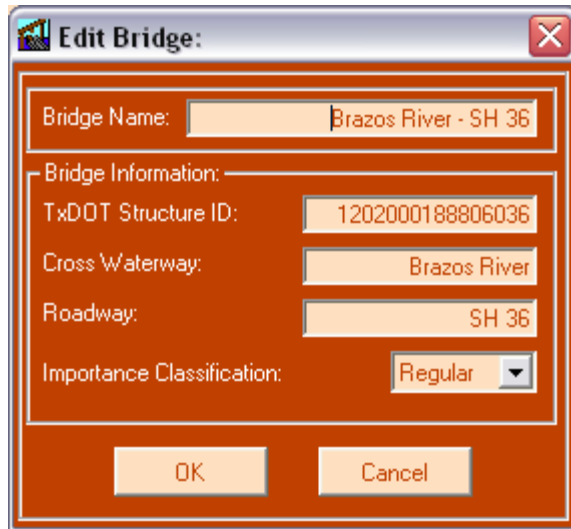
Figure 7.8: Edit Bridge Screen Shot

Importance classification is defined in the AASHTO LRFD code Section 3.14.3. The user may enter this value as either "Critical" or "Regular," where the default value is "Regular." The program will later use this importance factor to determine whether the bridge passes the AASHTO LRFD code specifications. Pressing the "OK" button will close the window and save any changes the user made. If the user presses the "Cancel" button, data changes made will not have been saved.

Edit Pier Information

To edit individual pier data, the user must click on the **Edit > Pier Data…** tab on the Main Page which will open the "Edit Pier" window, shown in Figure 7.9. The "Edit Pier" window allows the user to edit pier height, pier bottom elevation, channel bottom elevation, cross-sectional properties, x-location, and ultimate transverse pier strength.
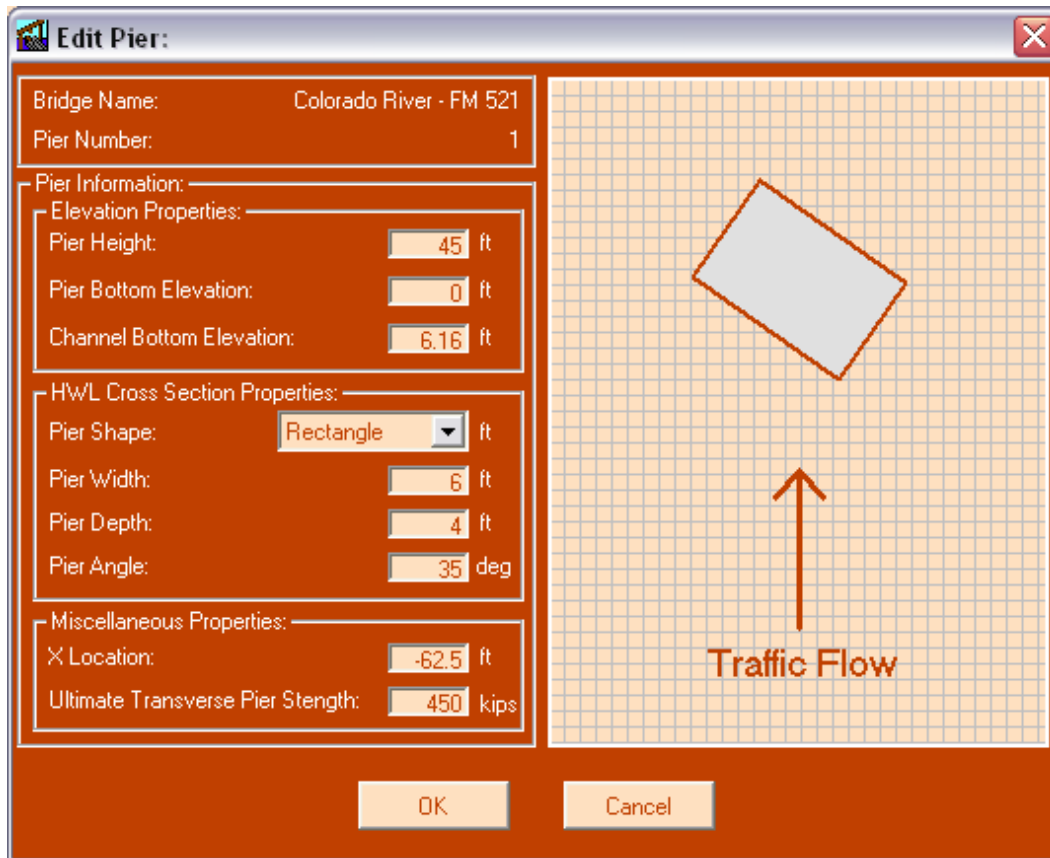
Figure 7.9: Pier Info Screen Shot

The pier height is the distance from the top of the foundation to the bridge deck. This value is not used for the calculations but is used to accurately draw the bridge on the screen. Pier bottom elevation is the location of the top of the pier foundation.. Similar to pier height, this value is not used in any calculations. It is only needed so that a relative top of the bridge can be determined for plotting purposes.

Channel bottom elevation is the location of the channel bottom at the same *x*-location as the pier. It is necessary to know this value in determining the depth of water at the pier. The user can enter channel bottom elevation and water levels and the program will automatically determine what the channel depth is.

The cross-sectional properties of the pier are entered into the program in the "Edit Pier" window. The cross-sectional properties are used to determine B_P, the effective width of the pier if the pier is turned at an angle. This effective width, B_P, is defined in the AASHTO LRFD code section 3.14.5.3 and is indicated in Figure 7.10. To aid the user in entering cross-section properties, the "Edit Pier" form will draw a scaled version of the pier cross-section.

73
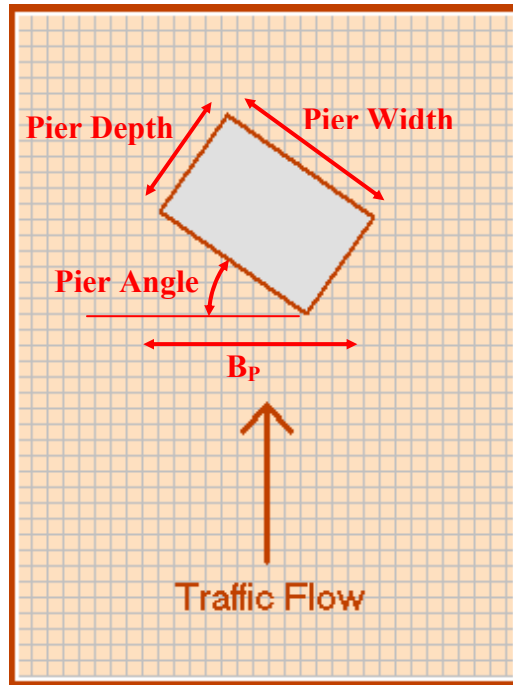
Figure 7.10: Definition of Pier Cross-Sectional Properties

There are four cross-sectional properties necessary for determining B_P. These include the pier shape, width, depth, and angle. Since it is possible that the pier's cross-sectional dimensions can change along its height, the AASHTO LRFD code recommends using the cross-section at the high water line level to represent the worst-case scenario. If the user wants to use a different location, that is possible through data manipulation within VIOB. The program will perform the calculations by using the values entered as high water line values. If the user puts in cross-sectional values at the normal water line and enters the normal water line elevation as the high water line elevation, the program would perform the calculations for these normal water line cross-sectional values.

The user has the ability to enter either a circular or rectangular cross-section into VIOB. For a circular cross-section, the width and depth are equal, and VIOB will automatically make the two values the same. It is also not necessary to enter a pier angle for a circular cross-section. For a rectangular cross-section, the pier width, pier depth, and pier angle are defined as shown in Figure 7.10.

In the event that the user wants to enter a cross-section that is neither a circle nor a rectangle, he/she could independently determine the effective width of the pier and enter it as a circular pier with a diameter equal to the effective width of the actual polygonal cross-section.

The *x*-location of the pier is the distance in the *x* direction that the pier is from the origin. The origin is defined by the user on the Main Page, and the user needs to make sure that the *x*-location entered is appropriate. The program will not permit the user to enter an *x*-location that would place the piers at a location that is inconsistent in any manner.

Finally, the Ultimate Transverse Pier Strength is entered in the "Edit Pier" window. Defined in AASHTO LRFD code Section 3.14.5.4, the ultimate lateral pier strength is determined by the user outside of VIOB, and then entered into the program at this time.

Edit Channel Information

To edit channel information the user clicks on **Edit > Channel Data…** from the Main Page. The "Edit Channel" page, shown in Figure 7.11, allows the user to edit all information related to the channel such as width, turn angle, region type, navigable channel properties, high water line, normal water line, current velocities, minimum impact speed, and vessel traffic density.
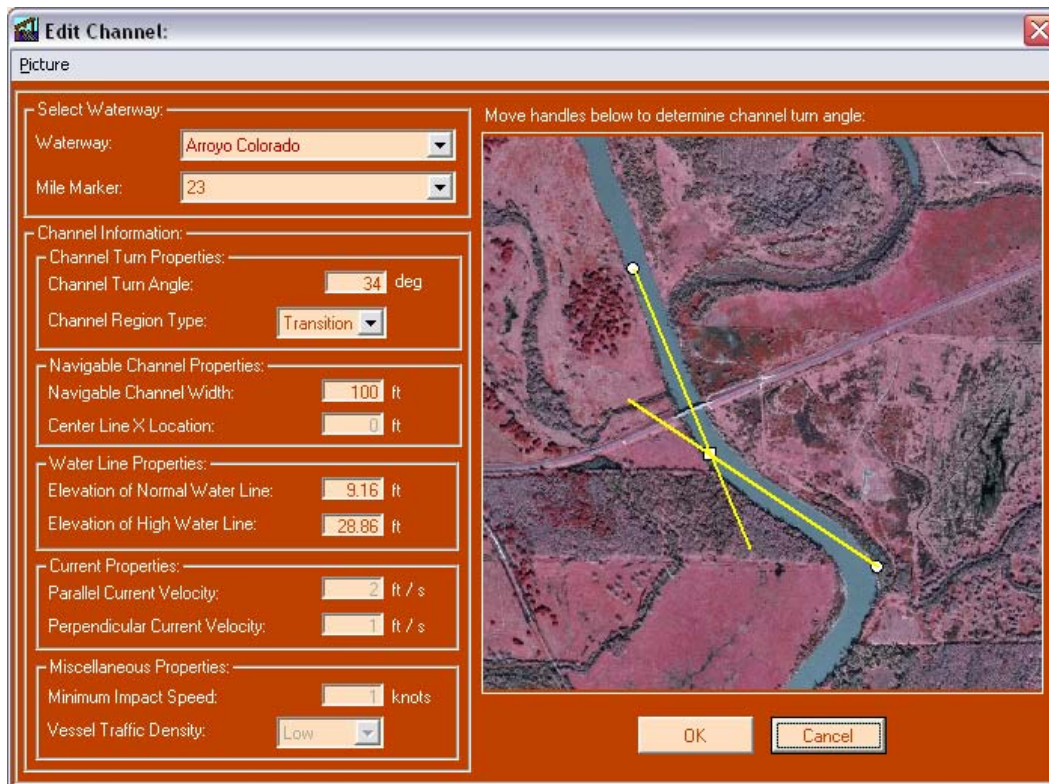
Figure 7.11: Edit Channel Screen Shot

When a bridge is first created, its cross waterway is selected. However, the user will need to select the waterway in the "Edit Channel" window to link the waterway to any given vessel traffic. In the Waterway pull-down menu will be a list of all waterways that are stored in the database. If the waterway does not exist, the user has the option of choosing a "User Defined" waterway, in which case information normally stored in the waterway database and automatically entered for the user is manually entered instead.

Once the user chooses a waterway, the Mile Marker pull-down menu will automatically load with all the mile markers that are stored in the database for the given waterway. Choosing a mile marker automatically fills in parallel current velocity, perpendicular current velocity, minimum impact speed, and vessel traffic density.

The user can determine the channel turn angle in two ways. The first is to measure the channel turn angle by hand, independent of the program, and enter the value into the turn angle box. The second way is for the user to load a picture of the channel into VIOB and use the built-in protractor to determine the turn angle. To load a picture into the VIOB "Edit Channel" window, the user goes to **Picture > Load Picture…** which will bring up a prompt. The user then selects the picture and it will appear beneath a protractor. The user can then move the square handle to adjust the origin of the cross hairs and move the circular handles to rotate the two protractor arms. The turn angle will always indicate the smaller angle between the cross hairs. The turn angle is defined in AASHTO LRFD Section 3.14.5.2.3-1. The turn region, also defined in AASHTO LRFD code Section 3.14.5.2.3-1, can be selected as either straight, transition, turn, or bend.

The navigable waterway is defined as the dredged part of the channel where a given vessel can safely pass under the bridge. The navigable channel width and navigable channel centerline need to be entered by the user.

The high water line and normal water line are both entered by the user and required by VIOB; however, only the high water line is used. The user can enter a dummy number in the normal water line box as that number is not used by the program for any calculations. Entering the correct normal water line can be useful visually as both waterlines are plotted on the Main Page.

The parallel current velocity is the velocity of the current parallel to the vessel traffic, and the perpendicular current velocity is the velocity of the current perpendicular to vessel traffic. If the user chooses a waterway, both current velocities will be automatically entered from the waterway database. Minimum impact speed, also stored in the waterway database, is defined in the AASHTO LRFD code Section 3.14.6 and must not be less than the yearly mean current velocity for the bridge location.

Vessel traffic density is the density level of vessels in the waterway in the immediate vicinity of the bridge. If vessels *rarely* meet or pass each other, the density is considered low. The density is considered average if vessels *occasionally* meet or pass each other. A bridge where vessels *routinely* meet or pass each other would have a density classified as high. VIOB will automatically determine the vessel density correction factor based on AASHTO LRFD code Section 3.14.5.2.3-7, 3-8, and 3-9.

Understanding the Vessel Database

Figure 7.12 shows the hierarchy of the VIOB database. It is important to understand this hierarchy when working with the VIOB database. The most basic items are vessels. A vessel can be a ship, a tug, or a barge. Each vessel has properties such as length, width and draft. A barge group is a combination of a tug and a series of barges. A barge group can be considered a fourth type of vessel. A vessel fleet is a combination of all vessels that pass under a given bridge. Hence, a vessel fleet is described in terms of a series of vessels that comprise it and the frequency and loading of those vessels as they pass the bridge.

Database Flow Chart
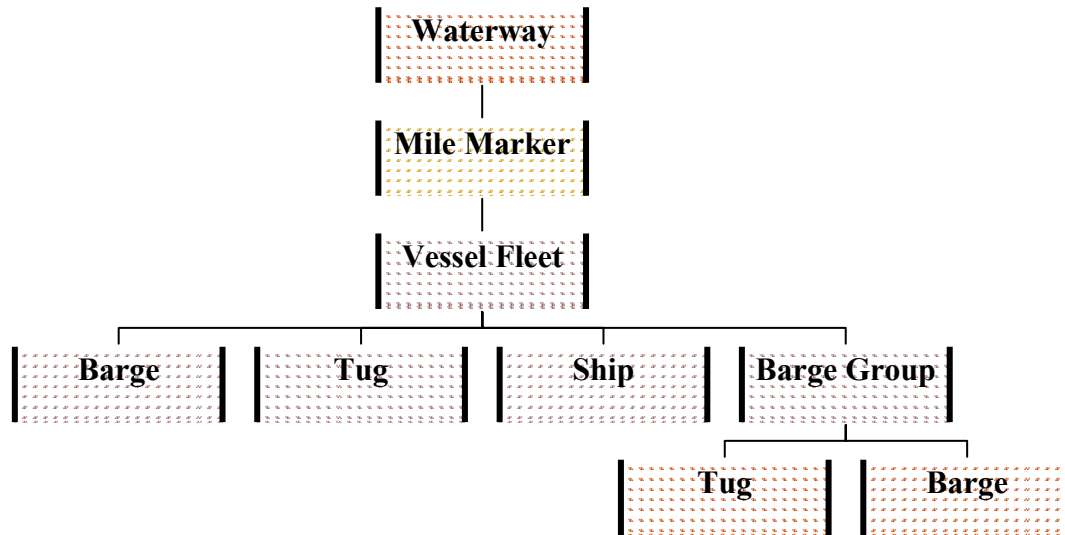
Figure 7.12: Hierarchy of VIOB Database

At any given channel location or mile marker, a certain traffic pattern occurs. That traffic pattern is defined by the vessel fleet; hence, each mile marker has a specific vessel fleet that passes it. A waterway is described by a list of all mile markers on its channel. Understanding the terminology that is associated with each type of vessel and vessel group is critical to the user creating and editing the database.

Vessel Library

The "Vessel Library" is where all of the different barges, tugs, and ships are stored. The user can access the "Vessel Library" by going to **Database > Vessel Library…** from the "Main Page." Once the "Vessel Library" window, shown in Figure 7.13, has been opened, the user has the option to add, edit, or delete barges, tugs, or ships. Data can be entered into the vessel library in either US or SI units; however, all units are stored in the database in US units. An alternative method for populating the database is presented in Appendix A.
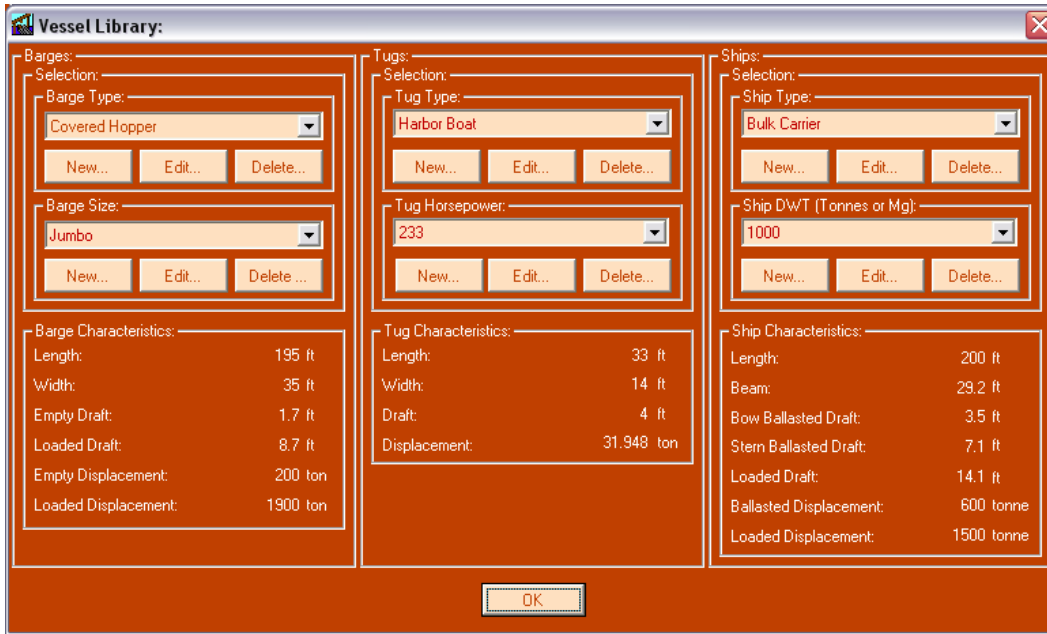
Figure 7.13: Vessel Library Screen Shot

If the user has a bridge opened for which information is specified in SI units and he/she then enters a new vessel, the input will be assumed to be in SI units as well. Although VIOB converts all numbers entered by the user for vessels to US units and stores them in this manner in the database, the numbers will still be displayed to the user in SI units. This is only the case for vessel data; all bridge and channel data are stored in the units in which they are entered.

It is necessary to store vessel data in this manner since the data must be available for all bridges. The user may have opened a bridge and selected US or SI units, and the vessel data should be presented accordingly. Storing the data in two separate databases is another option but it is inconvenient for a user trying to recreate the database outside of VIOB. It is not necessary to perform the same operations for bridge and channel data because they are unique to a bridge. Once a bridge is created, its units cannot be changed; therefore, the data can be stored in any units that it was entered in and it will never have to be converted.

Create or Edit Barge

Barges are sorted by Barge Type with a subset for Barge Size. The user has the ability to create a new barge type, edit the barge type or delete the barge type. If the user clicks on the "New…" button in the barge type section, a window, shown in Figure 7.14, will pop up asking the user what the name of the new barge type is.
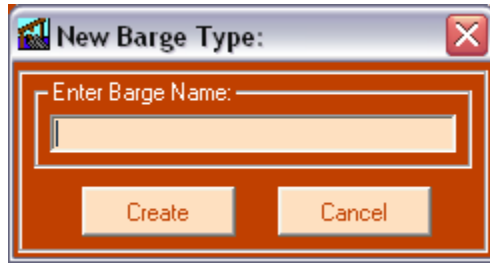
Figure 7.14: New Barge Screen Shot

The user enters the name of the barge type, and the "Barge Dimensions" window, Figure 7.15, will pop up. All barge types must have at least one barge size; therefore, since a new barge type has been created, the user must input the first new barge size. On the "Barge Dimensions" window, the user enters the barge size, length, width, empty draft, loaded draft, empty displacement, and loaded displacement.
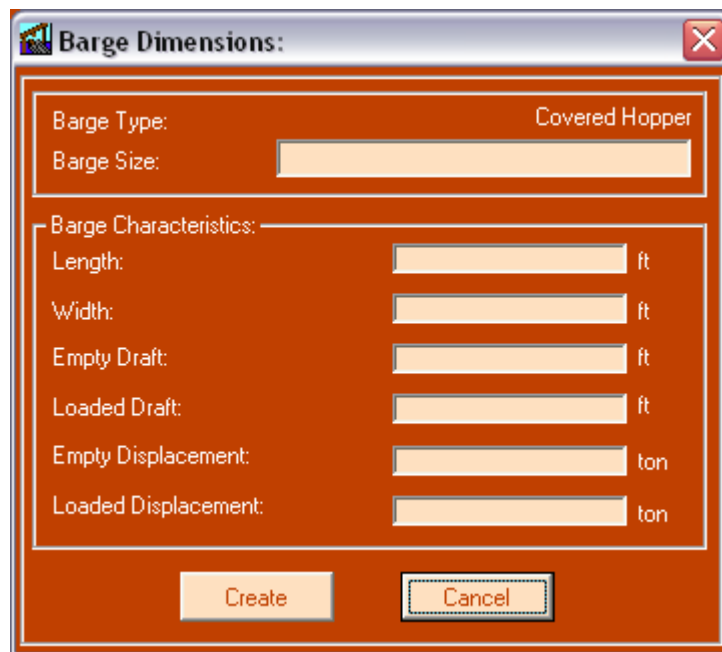
Figure 7.15: New Barge Size Screen Shot

Once the user presses the "Create" button, the new barge type and barge size are added to the vessel library. The user can then add any other barge sizes that are associated with the new barge type by clicking the "New…" button in the barge size box on the "Vessel Library" window. If the user wants to change a barge size there is an option to edit the data. If the user chooses to delete a barge type, all the associated barge sizes will be deleted as well.

Create or Edit a Tug

Creating a tug works in the same way as for a barge as the user has all of the same options with a tug that exist for barges. Tugs are uniquely identified by a type and a horsepower. The

horsepower that is entered for the tug is only a label, and the actual value does not matter at all. If the user wants to assign the horsepower as 1 or 9000, it will only serve as a way of distinguishing between different horsepowers for the same type of tugs. When the user clicks on the Tug Type pull-down menu and selects a type of tug, e.g. "Line Haul," the horsepower pull-down menu is automatically filled with all horsepower tugs that exist for the tug type "Line Haul." The user can create new tug types, edit tug types, and delete tug types. The user can create, edit, and delete tug horsepowers as well. Figure 7.16 shows the window used to enter a new tug name.

Figure 7.16: New Tug Type Screen Shot

Tug dimensions that need to be entered are length, width, draft, and displacement. Since a tug is never loaded, there is no distinction between loaded and empty draft or loaded and empty displacement. Figure 7.17 shows the window used to enter a new tug horsepower.
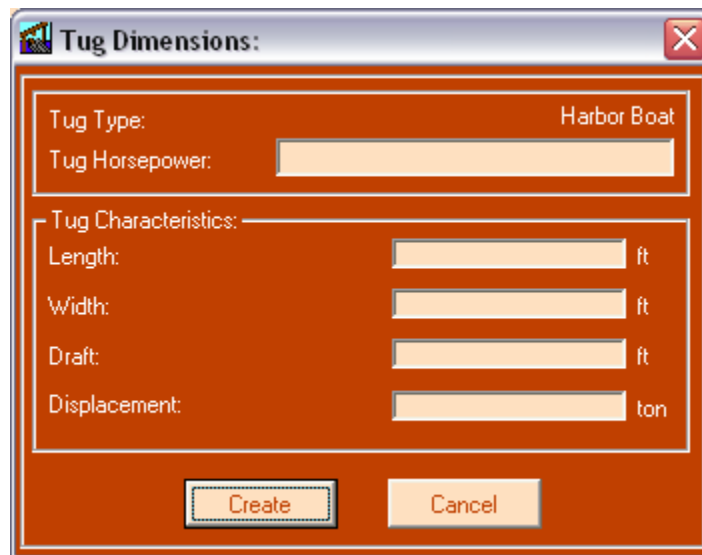
Figure 7.17: New Tug Horsepower Screen Shot

Create or Edit a Ship

As with barges and tugs, the user has the ability to create new ships for the vessel library. Ships are sorted by a two-level system: Type and Dead Weight Tonnage (DWT). Each ship type is

comprised of a set of ship DWTs. The user can create, edit, and delete both ship types and ship DWTs. Figure 7.18 shows the window used to edit a ship name.
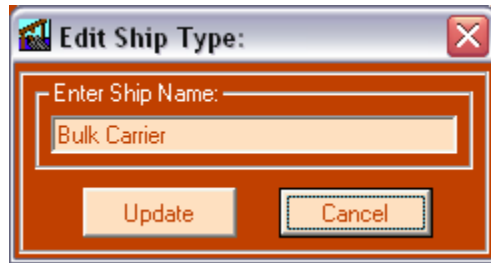
Figure 7.18: Edit Ship Type Screen Shot

For a ship, the user must enter the length, beam, ballasted draft and displacement, and loaded draft and displacement. For the ballasted draft, the user must enter the draft at both the bow and the stern of the ship. The program uses the stern draft as it is larger. The number the user enters for the bow ballasted draft is never used by VIOB. The dead weight tonnage should also be entered accurately as it is used by VIOB in the calculations; DWT is not simply a label as horsepower is for a tug. Figure 7.19 shows the window for entering a new ship DWT.

Figure 7.19: New Ship DWT Screen Shot

Assemble Barge Group

Once the user is satisfied with the vessels in the "Vessel Library," he/she can create barge groups. To work with the "Barge Group Library," the user clicks on **Database > Barge Group Library…** from the "Main Page." This will bring up the "Barge Group Library" window, shown in Figure 7.20. In this window, the user can scroll through different barge groups that have been previously assembled and see what their dimensions are. The user can also create new barge groups or delete existing barge groups.
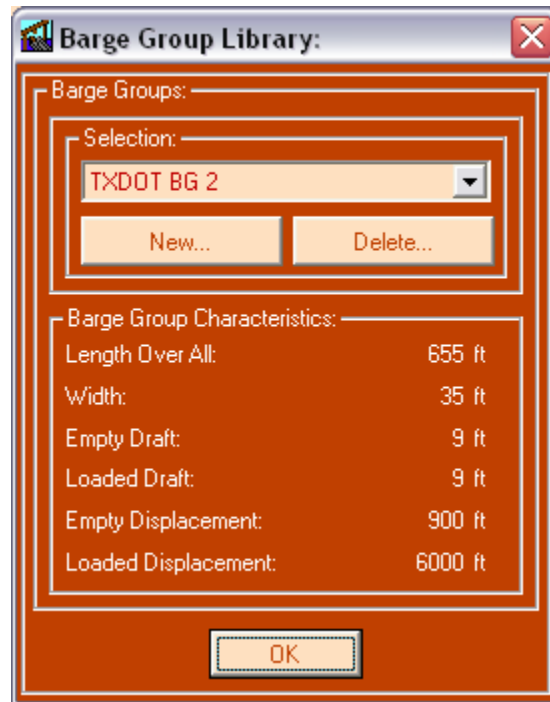
Figure 7.20: Barge Group Library Screen Shot

To create a new barge group, the user clicks on the "New…" button on the "Barge Group Library" window which will open the "Create Barge Group" window. A barge group is an assembly of a set of barges pulled or pushed by a tug. The user can name the barge group as he/she pleases, but it must be a unique name as no two barge groups can have identical names. It is necessary for the user to specify how many barges long and wide the barge group is. For both the number of barges long and the number wide, the user may enter a number between 1 and 10 as long as the total number of barges is less than 24. As the user enters the configuration of barges, VIOB automatically draws a layout of the barge group in the "Create Barge Group" window, shown in Figure 7.21. Seeing a layout of the barge group can help the user ensure that the information entered is appropriate.
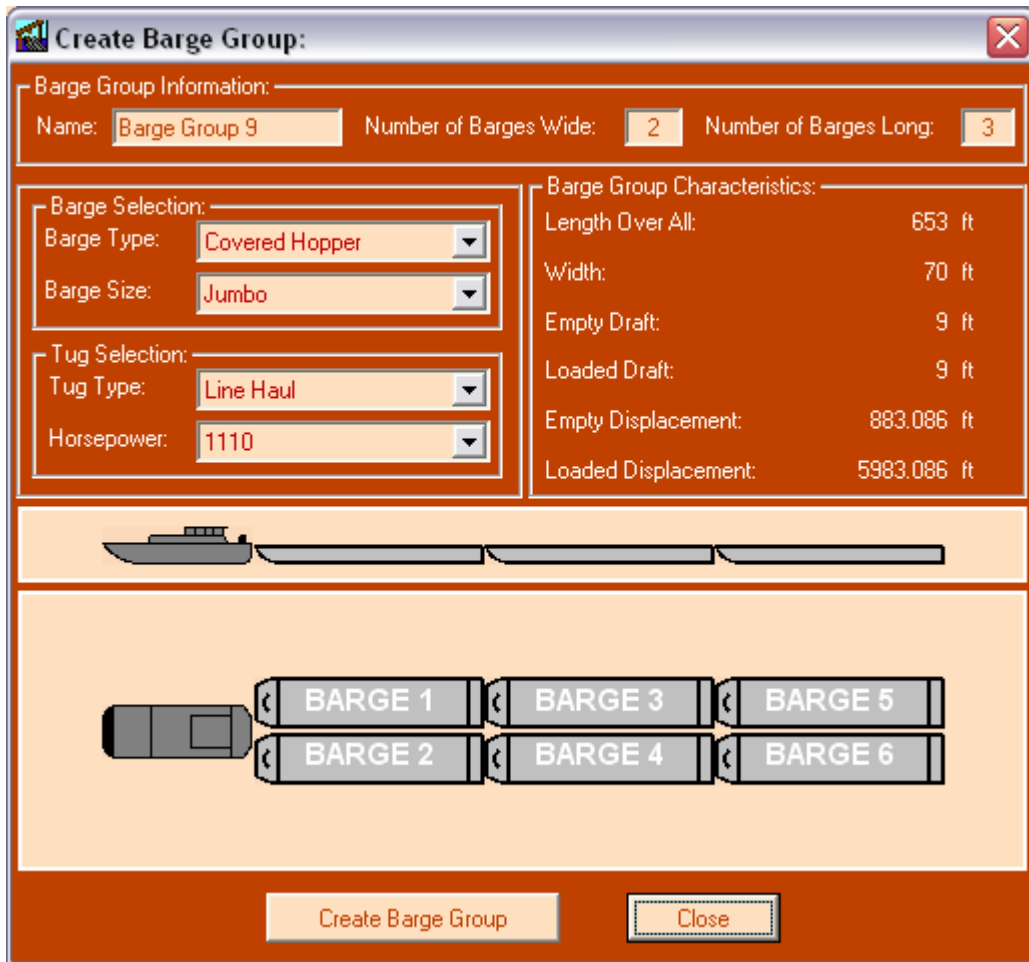
Figure 7.21: Create Barge Group Screen Shot

The user must specify the type and size of barges that are used in the barge group as well as the tug type and tug horsepower that are being used in the barge group. The barge group will have only one type of barge. Only one barge type is allowed because in practice most barge groups are configured that way and the data input is greatly simplified. As the user picks which tug and barge type will be used, the "Create Barge Group" window will update the statistics for the barge group on the screen. Again, seeing real-time statistics of the barge group characteristics can assure the user that the barge group is assembled as desired.

Once the user has the appropriate information entered into the "Create Barge Group" window, pressing the "Create Barge Group" button will save the barge group to the database. The "Create Barge Group" window will reset itself upon clicking the "Create Barge Group" button, and the user can enter other barge groups. Once the user has created all of the desired barge groups, pressing the "Close" button will close the "Create Barge Group" window and the user will be brought back to the "Barge Group Library."

Create Vessel Fleet

With the vessels and barge groups stored in the libraries, the user can now create the vessel fleet. To create a vessel fleet, the user clicks on **Database > Vessel Fleet Library…** from the "Main Page." This will open the "Vessel Fleet Library" window, shown in Figure 7.22. The "Vessel Fleet Library" window has a pull-down menu with all the vessel fleets that are stored in the database. If the user selects one of these vessel fleets, all of the vessels which make up the vessel fleet will be displayed on the "Vessel Fleet Library" window. The window also shows the vessel's frequency, loading, and velocity. For the first time, the user is introduced to the term "vessel class," which simply refers to the kind of vessel that is being displayed: barge, tug, ship, or barge group. A barge group does not have a vessel size; so, if it is displayed, its vessel size will be "N/A."
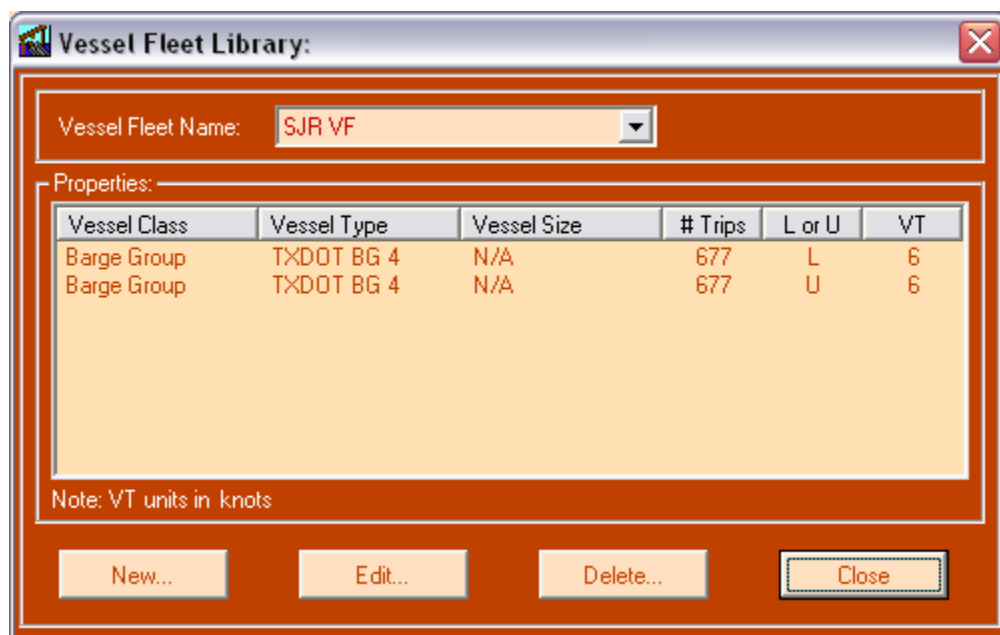
Figure 7.22: Vessel Fleet Library Screen Shot

As with all of the other libraries, the user has the ability to work with the "Vessel Fleet Library." The user can create a new vessel fleet, edit an existing vessel fleet, or delete a vessel fleet. When finished with the "Vessel Fleet Library," clicking the "Close" button returns the user to the "Main Page."

If the user clicks on the "New…" button, the "Create Vessel Fleet" window, shown in Figure 7.23, will appear. The user must name the new vessel fleet with a unique name because no two vessel fleets can have the same name. Also to be entered in the "Create New Vessel Fleet" window are the vessels (that will be part of the vessel fleet) and information about each vessel. For each vessel, the user must specify its class, type, size, frequency, loading configuration, and velocity.

Figure 7.23: Create New Vessel Fleet Form

When the user selects the vessel class from the vessel class pull-down menu, the type and size pull-down menus will automatically reload. If "barge" is selected, the user can select a barge type and barge size; if "tug" is selected, the user can select tug type and tug horsepower; and if "ship" is selected, the user can choose a ship type and ship DWT. The user can also select "barge group" from the vessel class pull-down menu; in this case, the user only needs to select the barge group type.

Once the user has selected the vessel he/she wants to add to the vessel fleet, information about that vessel's traffic pattern needs to be input. The user must specify the number of trips per year that the vessel makes past a given location, whether the vessel is loaded or unloaded during those trips, and what velocity the vessel has during each passage. If a vessel is sometimes loaded and sometimes unloaded, the user should add the vessel to the vessel fleet twice, once with "loaded" selected and once with "unloaded" selected. Each time the vessel is added, the number of trips for each loading and speed configuration is added with it.

To add the vessel to the vessel fleet, the "Add Vessel to Fleet" button is clicked. The vessel information entered by the user will be transferred to the viewing window and the input boxes will be reset. The user can remove a vessel from the fleet by clicking the "Remove Vessel from Fleet" button. When all of the vessels the user wants in the vessel fleet have been added, the user clicks the "Create Vessel Fleet" button to create the vessel fleet.

Create Waterway

Now that the user has created a vessel fleet, it is necessary to place that vessel fleet at a given mile marker on a waterway. At various mile markers of a waterway, there are specific channel characteristics and traffic patterns. The user has already created the traffic patterns; now it is necessary to assign them to the mile marker. To do this, the user clicks on **Database > Waterway Library…** from the "Main Page." The "Waterway Library" window, shown in Figure 7.24, will pop up. The user has the ability to create a waterway and any mile markers that are a part of that waterway. For any waterway and mile marker that is selected, information about that location is displayed in the window.

Figure 7.24: Waterway Library Screen Shot

To add a new waterway, the user clicks the "New…" button under the waterway category on the "Waterway Library" window. Once the user creates the waterway he/she will have the opportunity to add mile markers to it.

Create Mile Marker

If the user clicks the new mile marker button on the "Waterway Library" window, a window allowing the user to input information about that waterway will pop up, as seen Figure 7.25. The same window (only with data in it) will pop up if the user clicks the Edit Mile Marker button. When the "Edit Mile Marker" window opens, the user must enter several key statistics about the mile marker.
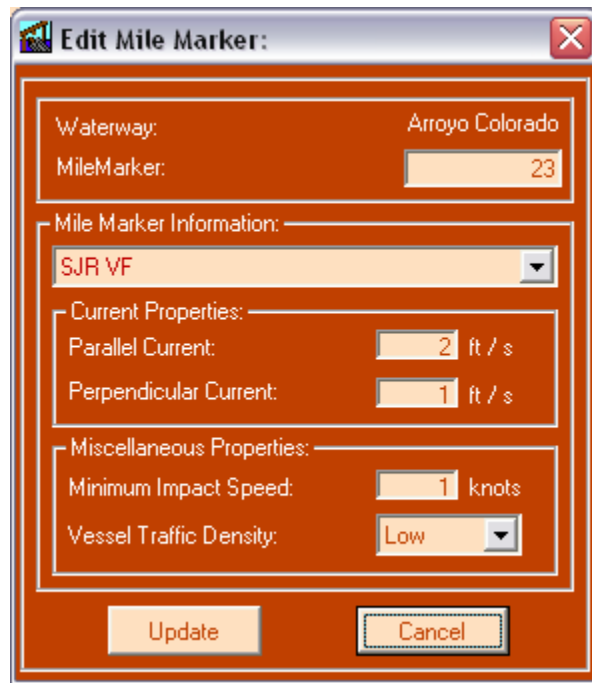
Figure 7.25: Edit Mile Marker Screen Shot

The user must link a vessel fleet to the mile marker and enter the parallel and perpendicular currents, the traffic density, and the minimum impact speed. When the user edits channel data at a later time and links the channel to a specific waterway and mile marker, all of the data entered for the mile marker is automatically entered into the "Edit Channel" window.

7.3.2 Solver

The solver part of VIOB is where all of the calculations are performed. In the code, all of the calculation procedures are located in the "RunAnlaysisCalcs" module. If at any time modifications are made to the AASHTO LRFD code or a new calculation is formulated, adjustments to the VIOB solver would be made in this module. Each separate calculation is performed as its own function; so functions can be easily swapped in and out to reflect updates to the AASTHO LRFD specifications.

Run Analysis

With all of the data entered into VIOB, the user can now begin the calculations. To run the analyses, the user clicks on **Calculations > Run…** from the "Main page." This will bring up the "Analysis Wizard" window where the user can enter a few key pieces of information and determine if the bridge is acceptable based on its return period associated with collapse due to vessel impact.

In the "Analysis Wizard" window, shown in Figure 7.26, the only piece of information the user must enter is his/her name. All the other pieces of information will be selected automatically. However, the user can change some of the selections that VIOB has pre-selected. The growth

factor that the program uses for vessel frequency is input here; the default value is 1.2. The growth factor accounts for possible increases in vessel traffic in future years. Using a value of 1.2 for the growth factor is conservative, but it is important to use a growth factor as vessel traffic is always changing. If the user wants to use a less conservative value, they can change that value at this point.
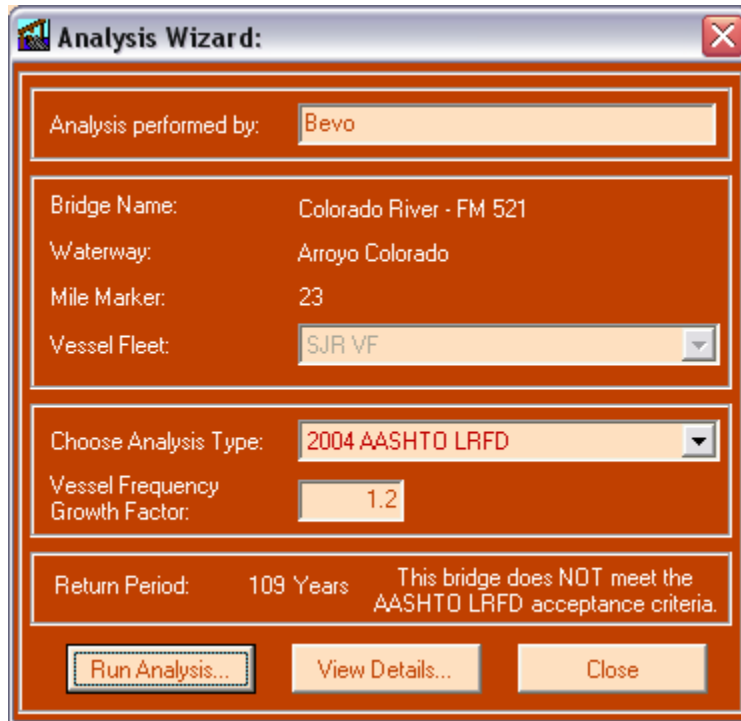
Figure 7.26: Analysis Wizard Screen Shot

If the user selected a user-defined waterway in the "Edit Channel" window, then the vessel fleet that passes the bridge of choice will not be known. If that is the case, then the vessel fleet pull-down menu will not be disabled and the user will pick the appropriate vessel fleet. If the user had already selected the waterway and mile marker, VIOB automatically chooses the correct vessel fleet.

Analysis Type only offers two options, "2004 AASHTO LRFD" and "2005 University of Texas," each with its own assumptions. The "2004 AASHTO LRFD" analysis is exactly the analysis in the 2004 AASHTO LRFD code, and it will yield the same results as the Guide Specifications. The 2005 University of Texas method is based on an alternative approach for computing the probability of collapse as outlined in Chapter 4.

Once the user has selected all of the options that are desired for the calculation, the final step is to click the "Run Analysis…" button on the "Analysis Wizard" page. This will run the VIOB analysis and yield a result almost instantaneously. The return period and Pass/Fail message will be displayed on the "Analysis Wizard" window. Once the analysis has been run, the "View Details" button will be enabled and the user will have the option to look at details in the VIOB calculations.

7.3.3 Postprocessor

The post-processing section of VIOB allows the user to study the results graphically and manipulate it in different ways for interpretation. Having advanced post-processing features makes the results easier to review than is possible with only numerical summaries. Indeed, the various output formats provide useful insights into factors that influence the frequency of bridge collapses. VIOB has numerous advanced post-processing features that help the user make an educated data-supported decision about the best way to increase the return period associated with bridge collapses.

View Detailed Results

When the user clicks the "View Details…" button from the "Analysis Wizard" window the "Results Viewer" window, shown in Figure 7.27, appears. Results are split up into several categories and the user can review them in several different ways. In the upper left hand corner of the "Results Viewer" window is basic information including the bridge name, vessel fleet, waterway, mile marker, analysis type, and waterway. To the right of the basic information is a box that includes summary results such as the annual frequency of collapse, return period, importance classification, and whether or not the bridge passes the AASHTO LRFD code specifications.
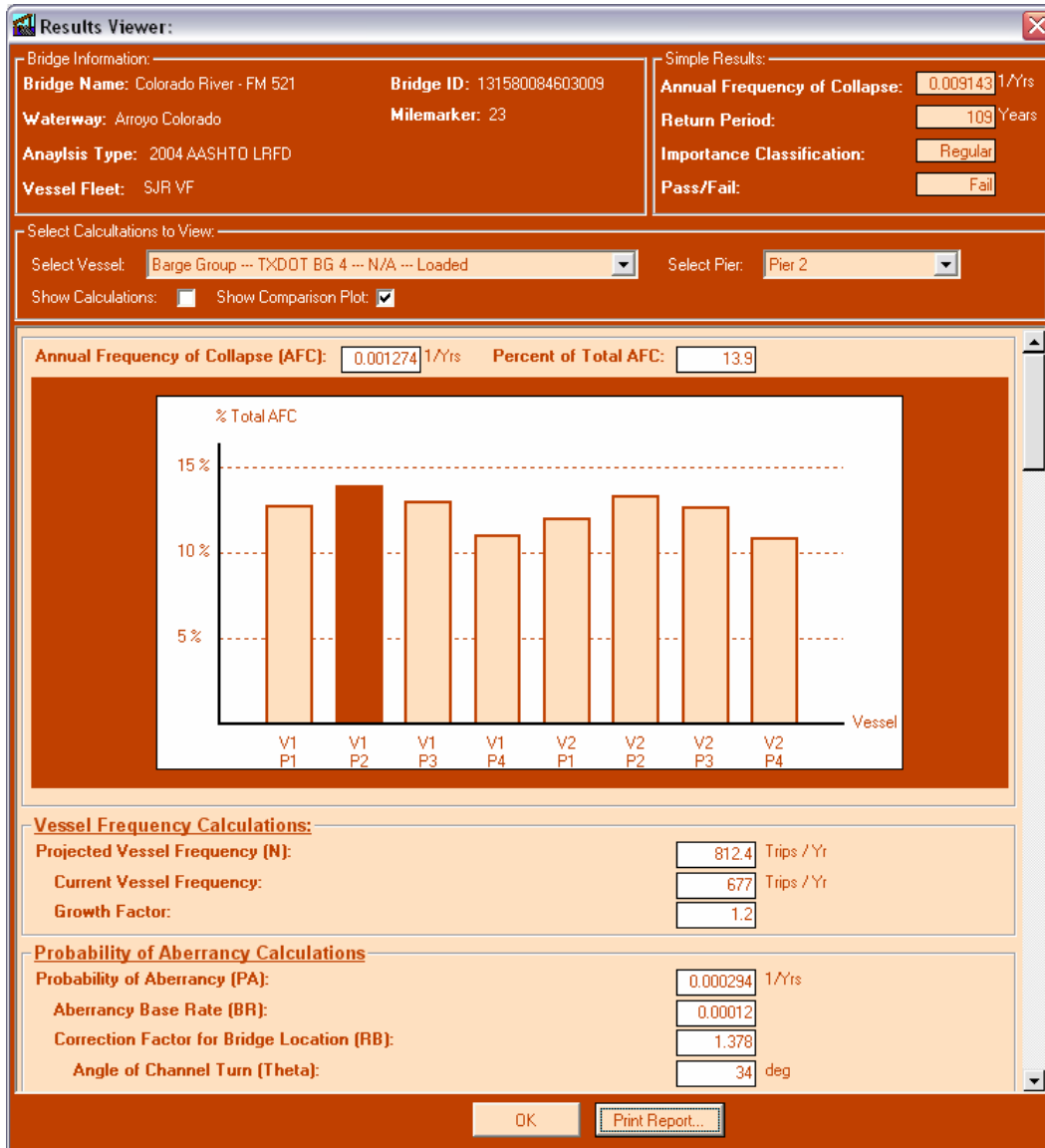
Figure 7.27: Results Viewer Screen Shot

The user may want to see more detailed information about how each calculation is performed. For any vessel impact analysis, a separate calculation is performed for every vessel-pier combination. Therefore, if there are four piers and three vessels, twelve separate calculations of annual frequency of collapse are performed, and the results are then summed to get the total annual frequency of collapse. The user can select any vessel-pier combination on the "Results Viewer" window, and details about that calculation will appear. The user can also select all piers with a given vessel, or all vessels with a given pier, and see how much one specific pier or one specific vessel influences the overall frequency of bridge collapse.

Beneath the box where the user selects the vessel and pier that he/she wants to review, are the actual values used by VIOB. It is important that VIOB display these numbers so that the user can ensure that the numbers were entered properly and that they seem reasonable. Every single

number used in all of the calculations can be reviewed if necessary. The results are split into categories of vessel frequency, probability of aberrancy, geometric probability, and probability of collapse.

If the user clicks on a specific pier and a specific vessel, all of the numbers used for that specific calculation are displayed. However, if the user selects all vessels for a specific pier or all piers for a specific vessel, some of the variables will be displayed as dashes. This is because in the group modes, only variables that are common to all runs for that group can be shown. For instance, pier height will be shown if all vessels for Pier 2 are requested. The height of Pier 2 does not change for any of the calculations in that group. On the other hand, if the same group is requested, vessel length will not be shown, because each of the vessels potentially has a different length; therefore, VIOB displays that variable as "-."

The variables are all grouped together by indents. So variables indented under another variable are used for computation of that variable. In this way, the user can tell which variables are used to get any specific results. This is also helpful when reviewing the calculations/results.

View Calculations

One unique feature of VIOB is that it will display every calculation that was made in equation form. This is a useful way to check the results numerically and to read them in a standard way as opposed to from an excessively long table. To view the calculations, the user clicks the check box "Show Calculations" on the "Results Viewer" window. This will cause the window to reassemble itself and all of the calculations and plots used to determine the annual frequency of collapse will be displayed. Each calculation shows the equation that was used and beneath that, the equation with actual numbers substituted for the different variables involved.

Three plots are also visible when the calculations are shown: the first shows the normal distribution curve used for calculating geometric probability; the second shows the method for determining velocity; and the third shows the formulation of the probability of collapse computation. Each of these plots shows the points relevant to their use that correspond to the actual analysis completed.

Compare Results

Finally, the user can compare different vessel-pier combinations with each other to see which ones have an influence on the total annual frequency of collapse. To review this analysis, the user clicks on the check box labeled "Show Comparison Plot." This allows the user to review the results and determine how to improve the return period of the bridge when necessary. The plot shows each vessel-pier combination and the percentage contribution to the total annual frequency of collapse that resulted from that vessel-pier combination. The user can also separate the calculations so as to compare each pier and each vessel.

Print Report

VIOB provides the user with the ability to print a report detailing the results. To print a report, the user clicks the "Print Report…" button on the "Results Viewer" window. There are six

different sections that VIOB prints out as part of the report. When the Print Report window, shown in Figure 7.28, first appears, the checkboxes for all six sections are checked but the user has the ability to remove any section from the report. The six report sections include the cover page, summary page, pier and channel information, vessel fleet description, results comparison, and detailed calculations. A sample report from a VIOB analysis is included in APPENDIX C of this report. The objective of the VIOB report is to produce a comprehensive outline of the analysis that can serve as both an informative report and a hard copy of all data used in the analysis. The computer-generated VIOB report is designed to be easy to read while, at the same time, not sacrificing the details of a handwritten report.
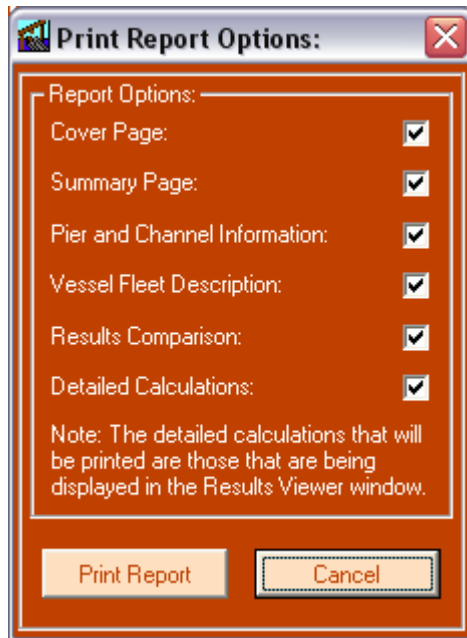
Figure 7.28: Print Report Screen Shot

The cover page is simply a front page to the report which details the name of the bridge, the TxDOT Structure ID, the waterway, the roadway, the engineer involved, and the date the report was created.

The summary page is a quick overview or abstract of what the geometry of the bridge looks like, some very basic data about the channel and the vessel fleet, and the basic results of the analysis.

All data about each pier are displayed in tabular format; similarly, all data about the channel are also displayed.

A set of tables with all of the vessel information is presented in the vessel fleet description section of the VIOB Report. A table with all of the vessel fleet components is always included in the report. Separate tables for barge groups, ships, tugs, and barges are presented. If a specific class of vessel is not in the vessel fleet, a table is not included in the report for that vessel class. The tug and barge tables list all tugs and barges that are in the vessel fleet as well as all tugs and barges that are part of any barge groups that are in the vessel fleet.

The results comparison section of the VIOB Report includes a set of three figures. The first figure shows a comparison of every vessel-pier combination and how much it influences the overall results. The second figure is a comparison of the contribution to bridge collapse due to each of the vessels. A comparison of all of the piers is shown in the third figure in the results comparison section.

The final section of the VIOB Report includes the detailed calculations. For every vessel-pier combination, VIOB produces a detailed listing of all of the calculations and expressions used to get each result. The report looks similar to the "Results Viewer" display. All of the plots that are produced for the results viewer also appear in the detailed calculation section. The first page of the detailed calculation section is a summary of all of the annual frequency of collapse estimates for every set of vessel-pier combinations.

The user should be cautious when printing reports as the print volume can get very large if there are many vessels and piers. The detailed calculation section prints six pages for every unique vessel-pier combination. Therefore, the size of this report can grow rapidly. If the user selects a specific vessel and pier before clicking the "Print Report" button on the "Results Viewer" window, only that detailed calculation will be printed. This can often be a better approach to studying the results, especially in preliminary understanding for a single bridge.

7.4 VIOB Conclusion

Performing a vessel impact analysis on a bridge can be time-consuming and tedious; it also requires a large amount of data and inputs of different types. VIOB turns this difficult problem into a manageable one. It is a useful software program for performing vessel impact analysis that offers a convenient graphical user interface, an integrated database, and convenient analysis and postprocessing features.

Chapter 8. Conclusions

8.1 Summary of Research

The collapse of the Queen Isabella Causeway in 2001 due to a vessel collision sent an alarming message to the state of Texas that vessel impact on bridges is a serious issue and may need to be a consideration for all bridges spanning waterways. The failure of the Queen Isabella Causeway resulted in the stranding of thousands of people on South Padre Island, economic losses, and most disturbingly, several fatalities. The Texas Department of Transportation funded a research project at The University of Texas that was aimed at evaluating the AASHTO LRFD code specifications for vessel impact on bridges.

The goals of the present study were to help develop a database on bridges, waterways, and vessel traffic for Texas, and to make use of this database in computations of the annual frequency of bridge collapses due to vessel impact. A standalone computer program, VIOB, was developed to meet the objectives of this research. The program incorporates a database and performs analysis using Method II of the AASHTO LRFD code Specifications.

Past research related to vessel impact on bridges is sparse. Such research did not begin in the United States until the Sunshine Skyway Bridge in Tampa Bay, Florida collapsed in 1980 when a ship collided with one of the bridge's main piers. Today, numerous states such as Florida, Louisiana, and Texas to name a few are actively involved in efforts for safety of bridges against vessel impacts.

Currently the 2004 AASHTO LRFD design code is used to evaluate bridges against vessel impact. Bridges are required to meet a specified maximum allowable annual frequency of collapse which is computed using a probabilistic analysis. A "regular" bridge must have a return period associated with collapse due to impact of at least 1,000 years. The total annual frequency of collapse of a bridge is the sum of the annual frequencies of collapse considering each pier in the bridge and each vessel passing it.

The annual frequency of collapse is evaluated as the product of the number of vessels passing a bridge per year, the probability of aberrancy, the geometric probability, and the probability of collapse. Probability of aberrancy is the probability that a vessel will stray off its intended course. If a vessel becomes aberrant, the probability that it will strike the bridge is defined as the geometric probability. The probability of collapse is defined as the probability that the bridge will collapse given that it is struck by an aberrant vessel. An assumption is usually made that the collapse of the pier in question leads to bridge collapse.

While the underlying basis for probability of aberrancy and geometric probability calculations is well justified, little research has been performed on barge-to-pier collisions to support the AASHTO LRFD code method for evaluating probability of collapse. The code has, due to lack of data on barge-pier collisions, relied on older ship-ship collision studies, for example. In the

present study, an alternative approach based on modeling is discussed for assessing the probability of collapse.

The alternative approach that can be implemented into the software program requires finite element studies to obtain vessel impact forces and nonlinear static pushover analysis to obtain pier ultimate strengths. Consideration for the variability in material properties, vessel loading condition, angle of impact, and height of impact is included in the procedure.

A user-friendly standalone computer program, named VIOB, has been developed. Using a comprehensive database that includes information on waterways, vessels, and traffic, VIOB can perform an entire bridge analysis for vessel impacts.

Given information related to the bridge and pier geometry, the waterway, and the vessel traffic at a given mile marker of a waterway, VIOB is able to produce an in-depth report detailing the calculations performed. The VIOB report not only provides information about the analysis performed, but also arranges the data so that the user can determine which vessels and piers most influence the vulnerability of the bridge. This allows the user to make educated decisions about ways to improve bridges that might not meet the AASHTO LRFD acceptance criteria.

8.2 Recommendations for Future Research

There are many areas where further research can be carried out to attempt to improve the AASHTO LRFD vessel collision design procedure. The approach for calculating probability of collapse is an extremely difficult one to support because very few actual tests have been performed involving barge-to-pier collisions. While the computer models generated in this overall research study can simulate barge-to-pier collisions, it is impossible to know if the results are accurate without a real test to use as a reference. Validation using field tests (though very expensive) are needed for realistic vessel velocities and bridge impact scenarios. Further development of analytical models to determine vessel impact loads and ultimate strength of bridges that can be validated with such full-scale test results is also necessary.

VIOB is a very robust program but there are still many improvements that can be made to it. Future versions of VIOB could include a more detailed library, enhanced features, and a better user interface. New features could include 3D plotting of the bridge, built-in structural analysis capabilities, and a library with real-time updating especially on traffic trends.

References

1. AASHTO, "Guide Specification and Commentary for Vessel Collision Design of Highway Bridges, Volume 1: Final Report," Washington D.C., 1991.
2. AASHTO, "LRFD Bridge Design Specifications – Customary US. Units," Third Edition, 2004.
3. Bell, D., "A blinding squall, then death," *St. Petersburg Times,* 1999. <http://www2.sptimes.com/weather/SW.2.html>
4. Bellamy, C., "Bridge collapses: Rescuers pull vehicles from river." The Anniston Star, 27 May 2002. <http://www.annistonstar.com/news/2002/as-nation-0527-0-2e27d0011.htm>
5. Calzada, A. W., "Queen Isabella Causeway Collapse," 2001. <http://pages.sbcglobal.net/calzada/newsqueen1.html>.
6. Consolazio, G. R. et al., "Full-Scale Experimental Measurement of Barge Impact Loads on Bridge Piers," 2005 Transportation Research Board Meeting, Washington, DC.
7. Cowiconsult. 1987. "General Principles for Risk Evaluation of Ship Collisions, Strandings, and Contact Incidents." Technical note, January 1987.
8. Cryer, A., "Brdlskajdlksajdlkas," M.S. Thesis, The University of Texas at Austin, May 2005.
9. Florida Department of Transportation, "Vessel Impact Analysis, V 3.05," 2000. < http://www.dot.state.fl.us/structures/proglib.htm>
10. Frandsen, A.G., "Accidents Involving Bridges," IABSE Colloquium, Copenhagen, Denmark, Vol. 1, 1983.
11. Fuji, Y. and Shiobara, R. (1978). "The Estimation of Losses Resulting from Marine Accidents," Journal of Navigation, Vol. 31, No. 1.
12. Henderson, W.R., "Modeling and Analysis of Bridges subjected to Vessel Impact Design," M.S. Thesis, The University of Texas at Austin, May 2005.
13. IABSE Colloquium, "Ship Collision with Bridges and Offshore Structures," 3 volumes, Copenhagen, Denmark, 1983.
14. Meir-Dornberg, K.E., "Ship Collisions, Safety Zones, and Loading Assumptions for Structures on Inland Waterways," VDI-Berichte, 496, 1-9, 1983.
15. Modjeski and Masters, Consulting Engineers. 1984. "Criteria for the Design of Bridge Piers with Respect to Vessel Collision in Louisiana Waterways." Prepared for the Louisiana Department of Transportation and Development and the Federal Highway Administration, Harrisburg, PA, November 1984.
16. National Transportation Safety Board, "U.S. Towboat *Robert Y. Love* Allision With Interstate 40 Highway Bridge Near Webbers Falls, Oklahoma May 26, 2002," NTSB/HAR-04/05, August, 2004.
17. Proske, D., S. Weiland, and M. Curbach. "Risk to old bridges due to ship impact on German Island waterways." *Applications of Statistics and Probability in Civil Engineering* (2003): 1695-1701.
18. Rue, D. L., J. Mumber, and A. J. Foden. "Vessel Impact Design for the new Ocean City-Longport Bridge." *Sixth International Conference on Short & Medium Span Bridges, Vancouver, Canada,* 2002.
19. Schwartz, J. "Expert Witness Says Bridge Collapse Due to Lack of Awareness." *Corpus Christi Caller-Times,* 12 Oct 2001.

<http://www.caller2.com/2001/october/12/today/localnew/14358.html>
20. South Texas Business Directory, "South Padre Island is Open and Ready for Visitors."
    STEXASBIZ.com. *South Texas Business Online,* 2001.
    <http://www.stexasbiz.com/TXBIZ/COLLAPSE/collapse.html>.
21. Texas Civil Engineer, "Reconstructing the Past: The Queen Isabella Causeway," Vol. 74, No.
    2, Spring 2004.
22. Whitney, M.W., I.E. Harik, J.J. Griffin, and D.L. Allen. "Barge Collision Design of Highway
    Bridges." *Journal of Bridge Engineering* May 1996: 47-58.
23. Woisin, G., Gerlach, W. (1970). "On the Estimation of Forces Developed in Collisions
    Between Ships and Offshore Lighthouses," IALA Conference, Stockholm.
24. Woisin, G., (1971). "Ship-Structural Investigation for the Safety of Nuclear Powered Trading
    Vessels," Jahrbuch der Schiffbautechnishen Gesellshaft, Volume 65, 225-263, Berlin.
25. Woisin, G., (1976). "The Collision Tests of the GKSS," Jahrbuch der Schiffbautechnishen
    Gesellshaft, Volume 70, 465-487, Berlin.

Appendix A
Description of VIOB Database Tables

Alternative Method for Assembling Database

For most data being input into the program, it is easy to use the VIOB database libraries to enter the data and then choose which vessels are to be used. However, if one is entering a large amount of data, it can sometimes be easier to create the database in Microsoft Access outside of VIOB, and simply have VIOB read in the database. This appendix describes how each of the vessel-related tables needs to be created in the VIOB database.

For each of the tables below, the names used must be entered exactly as shown. If the tables and table headers are not properly formatted and named, VIOB will not be able to understand them. For each table, a description of the table, the database table name, the index for the table, and a list of the column headers is given.

To study some examples of how the tables should look, one can open the existing VIOB database in Microsoft Access and review the format in which the tables are assembled. Besides the seven tables listed below, there will be others in the VIOB database. Those tables are used for various parts of the program; the user should be very cautious about modifying those tables. If the tables are incorrectly changed, VIOB will no longer understand them and will not function properly.

Waterways

Description

This table is a list of waterway names, the mile markers associated with each waterway, and the channel information associated with those mile markers.

Database Table Name

The database table name is "WaterwayInfo"

Index

The "WaterwayInfo" table should be indexed by "Name" and then "Milemarker"

Column Headers

Table A-1: Column headers for "WaterwayInfo" database table

Column Header	Units	Data Type	Description
Name	-	text	The name of the waterway. i.e. Gulf Intercoastals Waterway (GIWW)
Milemarker	-	number	A given mile marker on a waterway
VesselFleet	-	text	The name of the vessel fleet that passes that mile marker
ParCurrent	knots	number	The current velocity parallel to the direction of vessel traffic
PerpCurrent	knots	number	The current velocity perpendicular to the direction of vessel traffic
TrafficDensity	-	text	The traffic density at any given mile marker. Entered as High, Average, or Low. See AAHSHTO G.S. 4.8.3.2
MinimumImpactSpeed	ft / s	number	See AASHTO LRFD 3.14.6

Vessel Fleets

Description

This table contains a list of all vessel fleets, the vessels associated with each vessel fleet, and the properties associated with each vessel as they relate to the vessel fleet.

Database Table Name

The database table name is "VesselFleets"

Index

The "VesselFleet" table should be indexed by "Name" then "VesselClass" then "VesselType" then "VesselSize" and then "LoadorUnload"

Column Headers

Table A-2: Column headers for "VesselFleet" database table

Column Header	Units	Data Type	Description
Name	-	text	The name of the vessel fleet
VesselClass	-	text	The Class of vessel. Four options: Barge, Tug, Ship, Barge Group
VesselType	-	text	The Type of vessel If VesselClass = Barge Group, use BargeGroupName for VesselType
VesselSize	-	text	The Size of vessel If VesselClass = Ship, VesselSize = DWT If VesselClass = Tug, VesselSize = Horsepower If VesselClass = Barge, VesselSize = Barge Size If VesselClass = Barge Group, VesselSize = N/A
NumTrips	Trips/Yr	number	The numer of trips a given vessel makes per year past the bridge
LoadorUnload	-	True/False	Whether the vessel is loaded or unloaded. True if Loaded, False if Unloaded
VesselSpeed	knots	number	The velocity of the vessel

Barge Group Description

Description

This table describes the tug type and size and the number of barges in the barge group.

Database Table Name

The database table name is "BargeGroupDescrip"

Index

The "BargeGroupDescrip" table should be indexed by "Name"

Column Headers

Table A-3: Column headers for "BargeGroupDescrip" database table

Column Header	Units	Data Type	Description
Name	-	text	The name of the barge group
TugType	-	text	The type of tug in the barge group
TugSize	-	text	The horsepower of tug in the barge group
Width	barges	number	The number of barges wide the barge group is. In the y or j direction
Length	barges	number	The number of barges long the barge group is. In the x or i direction

Barge Group Arrangement

Description

This table describes the type and size of each barge and where it is located spatially in the barge group.
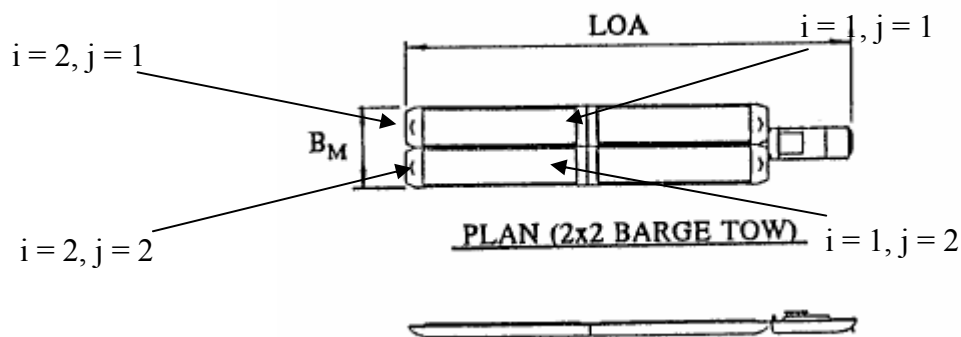
Figure A-1: Designation of i and j in a barge group

Database Table Name

The database table name is "BargeGroupArrange"

Index

The "BargeGroupArrange" table should be indexed by "Name" then by "i" and then by "j"

Column Headers

Table A-4: Column headers for "BargeGroupArrange" database table

Column Header	Units	Data Type	Description
Name	-	text	The name of the barge group
BargeType	-	text	The type of barge that is in this i,j position
BargeSize	-	text	The size of barge that is in this i,j position
i	-	number	The x position of a barge in a barge group
j	-	number	The y position of a barge in a barge group

Barges

Description

This table consists of all of the different types of barges that are in any waterway and the dimensions of those barges.

Database Table Name

The database table name is "Barges"

Index

The "Barges" table should be indexed by "Type" and then by "Size"

Column Headers

Table A-5: Column headers for "Barges" database table

Column Header	Units	Data Type	Description
Type	-	text	The type of barge. e.g. "Covered Hopper"
Size	-	text	The size of the barge. e.g. "Jumbo"
Length	ft	number	See AASHTO G.S. Figure 3.5.1-1
Width	ft	number	See AASHTO G.S. Figure 3.5.1-1
EmptyDraft	ft	number	See AASHTO G.S. Figure 3.5.1-1
LoadedDraft	ft	number	See AASHTO G.S. Figure 3.5.1-1
EmptyDisplacement	ton	number	See AASHTO G.S. Figure 3.5.1-1
LoadedDisplacement	ton	number	See AASHTO G.S. Figure 3.5.1-1

Tugs

Description

This table consists of all of the different types of tugs that are in any waterway and the dimensions of those tugs.

Database Table Name

The database table name is "TugBoats"

Index

The "TugBoats" table should be indexed by "Type" and then by "Horsepower"

Column Headers

Table A-6: Column headers for "TugBoats" database table

Column Header	Units	Data Type	Description
Type	-	text	The type of tug. e.g. "Line Haul"
Horsepower	-	number	The horsepower of the tug. e.g. "2000"
Length	ft	number	See AASHTO G.S. 3.5 Table 3.5.1-2
Width	ft	number	See AASHTO G.S. 3.5 Table 3.5.1-2
Draft	ft	number	See AASHTO G.S. 3.5 Table 3.5.1-2
Displacement	ton	number	See AASHTO G.S. 3.5 Table 3.5.1-2

Ships

Description

This table consists of all of the different types of ships that are in any waterway and the dimensions of those ships.

Database Table Name

The database table name is "Ships"

Index

The "Ships" table should be indexed by "Type" and then by "DWT"

Column Headers

Table A-7: Column headers for "Ships" database table

Column Header	Units	Data Type	Description
Type	-	text	The type of ship. e.g. "Bulk Carrier"
DWT	tonne	number	The DWT of the ship e.g. "1000"
Length	ft	number	See AASHTO G.S. Figure 3.5.2-4
Beam	ft	number	See AASHTO G.S. Figure 3.5.2-4
BallDraftB	ft	number	See AASHTO G.S. Figure 3.5.2-4
BallDraftS	ft	number	See AASHTO G.S. Figure 3.5.2-4
LoadedDraft	ft	number	See AASHTO G.S. Figure 3.5.2-4
BallDisplacement	tonne	number	See AASHTO G.S. Figure 3.5.2-4
LoadedDisplacement	tonne	number	See AASHTO G.S. Figure 3.5.2-4

Appendix B
VIOB Example

Description of VIOB Example

A step-by-step example is presented to give the user some instructions for entering a new bridge, assigning bridge properties to the new bridge, and performing an analysis on the newly entered bridge. This example will not show how to use all of the features of VIOB or how to enter information into the vessel library. For an extensive look at all of the features of VIOB, refer to Chapter 7.

Example Bridge Description

In order to determine the return period for a bridge collapse due to vessel impact using VIOB, some basic information must be known by the user. The bridge data, pier geometry, and channel data must be known. For this example, the information has been summarized in Table B-1, Table B-2, and Table B-3.

Table B-1: Bridge Data

Bridge Name:	Colorado River - FM 521
TxDOT Structure ID:	131580084603009
Waterway:	Colorado River
Mile Marker:	100
Roadway:	FM 521
Importance Classification:	Regular

Table B-2: Pier Geometry

Pier	x Distance [1]	Pier Height	Pier Bottom Elevation [2]	Channel Bottom Elevation [2]	Diameter at HWL	H
	(ft)	(ft)	(ft)	(ft)	(ft)	(kips)
1	0	45	0	6.16	4	450
2	125	45	0.16	4.16	4	330
3	215	35	10.16	10.16	4	200
4	255	33	12.16	15.16	2	200

[1] Measured from Pier 1
[2] Measured from Bottom of Pier 1

Table B-3: Channel Data

Parallel Current Velocity:	1.185 knots
Perpendicular Current Velocity:	0.592 knots
Minimum Impact Speed:	1.689 ft/s
HWL Elevation [2] **:**	28.86 ft
NWL Elevation [2] **:**	9.16 ft
Navigable Channel Width:	100 ft
Navigable Channel CL [1] **:**	62.5 ft
Channel Region Type:	Transition
Channel Turn Angle:	34 deg
Traffic Density:	Low

[1] Measured from Pier 1

[2] Measured from Bottom of Pier 1

Create New Bridge

The first step in creating a new bridge is to select the "New Bridge" option from the "Start Menu." Once the "New Bridge" option is selected, the user should click the "Start VIOB" button to bring up the "New Bridge" window. See Figure B-1.
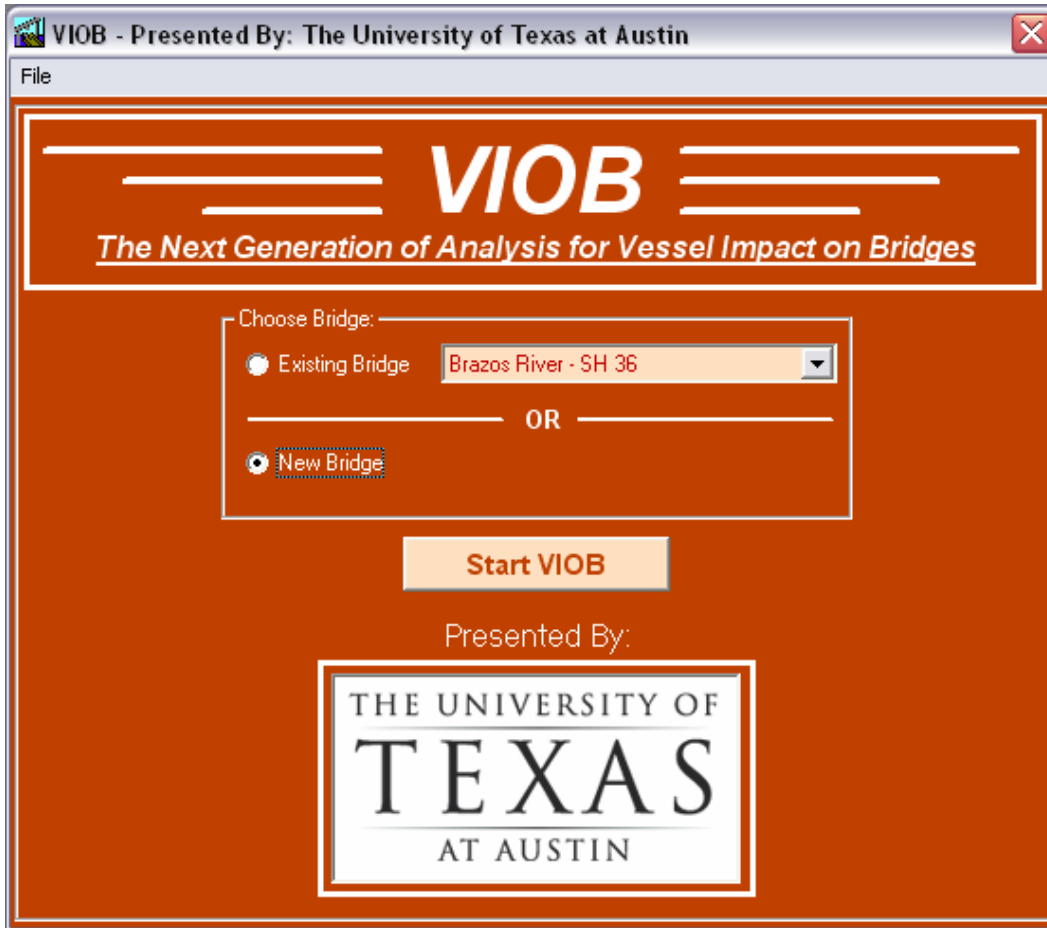
Figure B-1: "New Bridge" option selected from the "Start Menu"

When the "New Bridge" window pops up, the user should then enter the bridge information. The user must enter the cross waterway, the roadway, the TxDOT Structure ID, the number of piers, and the unit system that the user intends to use. See Figure B-2.

Figure B-2: Bridge information entered into the "New Bridge" window

Once the user has entered all of the information into the "New Bridge" window, the "Create Bridge" button is pressed. The "New Bridge" window will then be out of view and the user will be taken to the "Main Page." The initial display is a standardized bridge showing the number of piers that the user entered. In this case four piers each with a default height of 50 feet and spaced 100 feet from each other will be shown. The default centerline of the navigable channel is the midpoint of the center span of the bridge. See Figure B-3.
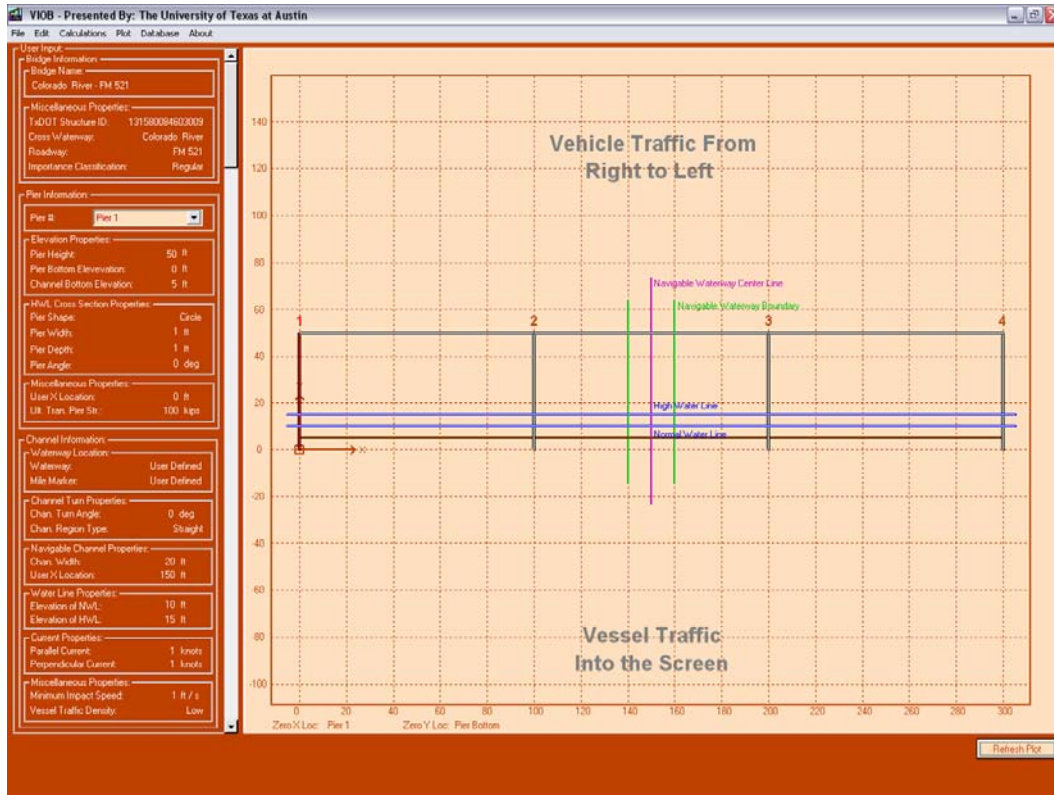
Figure B-3: The "Main Page" showing the newly created bridge

Edit Bridge Information

With the new bridge created, one can now edit the bridge information. To do this, the user clicks on **Edit > Bridge Data…** to open the "Edit Bridge" window. In the "Edit Bridge" window, the user needs to select the bridge's importance classification. The default value is "Regular." Once the importance classification is selected, the user clicks the "OK" button to return to the "Main Page." See Figure B-4and Figure B-5.
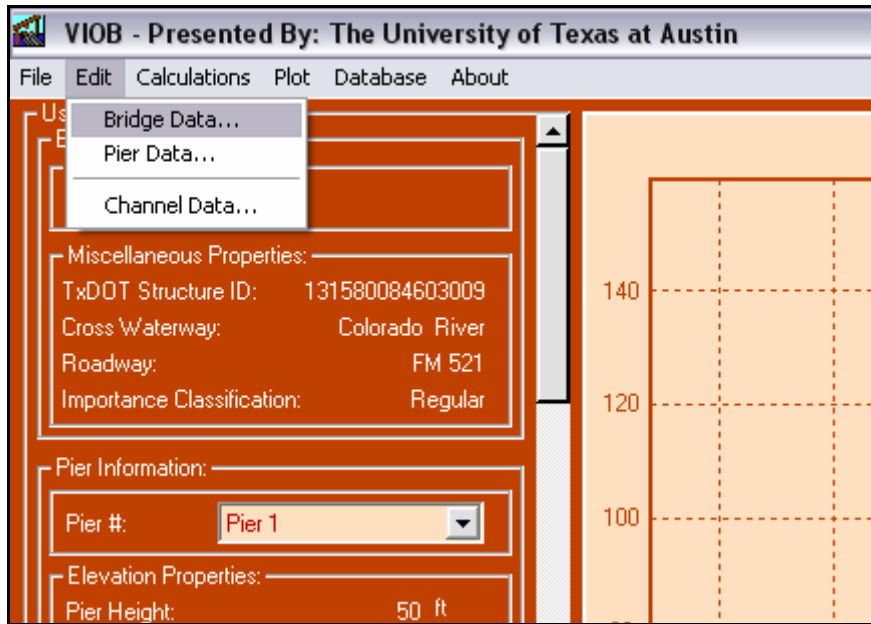
Figure B-4: Selecting Bridge Data… from the "Edit" menu
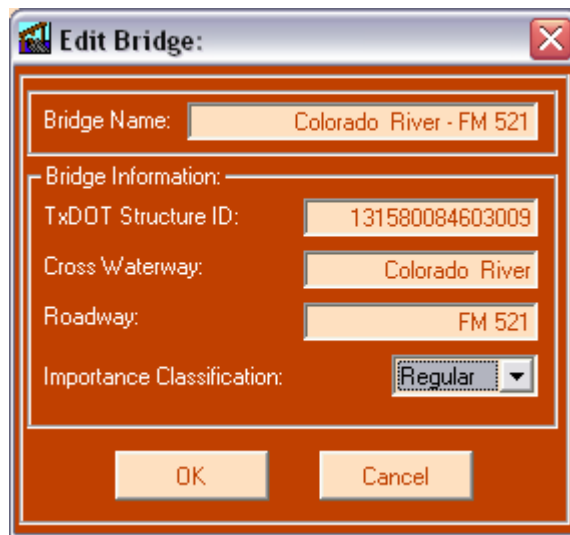
Figure B-5: "Edit Bridge" window with importance classification entered

Edit Pier Geometry

With the bridge data entered properly, the user can now edit the pier geometry. To edit the pier geometry, the user first selects the pier that he/she wants to edit in the pier pull-down menu on the "Main Page" and then clicks on **Edit > Pier Data…** which will bring up the "Edit Pier" window. The user must do this for each of the four piers. See Figure B-6 to Figure B-10. After

the information for each pier is entered, the user clicks the "OK" button to return to the "Main Page."
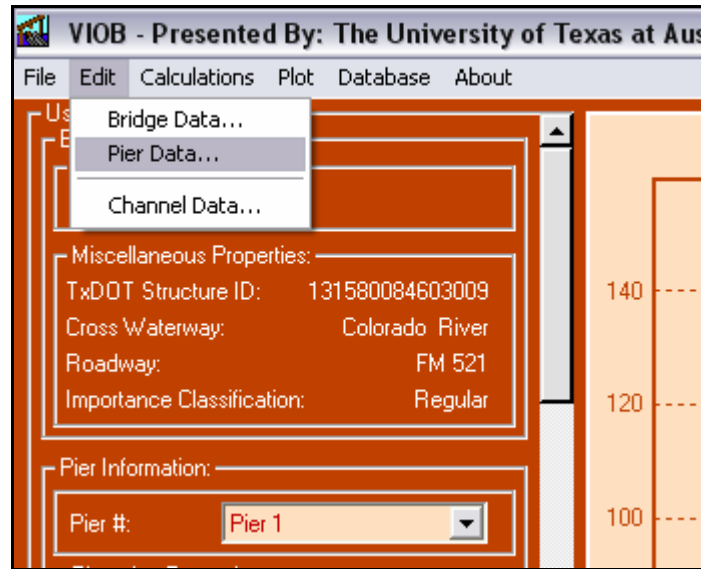
Figure B-6: Selecting Pier Data… from the "Edit" menu
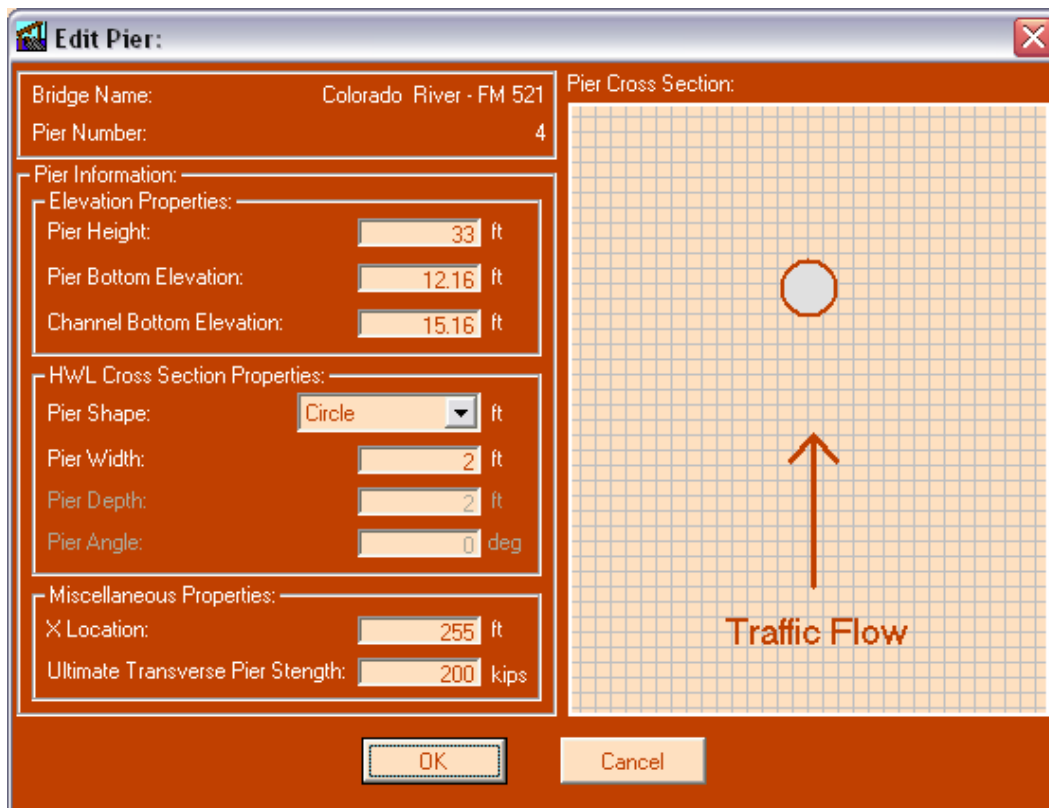
Figure B-7: Pier 4 being edited in the "Edit Pier" window
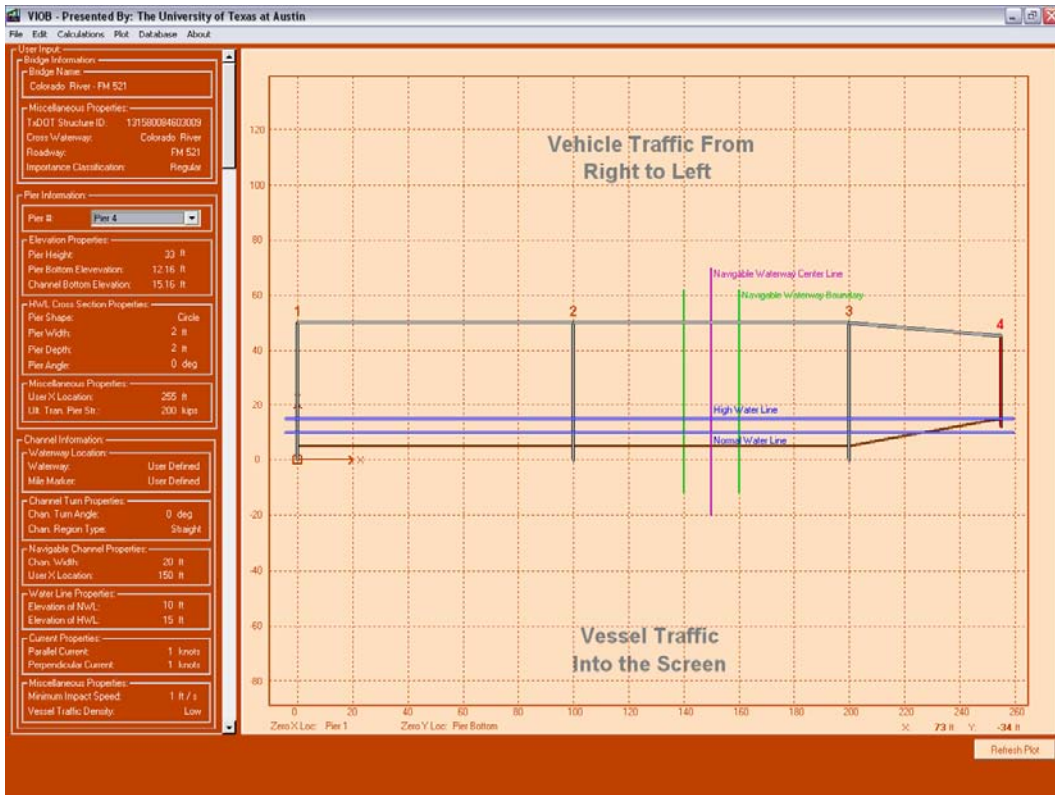
Figure B-8: "Main Page" after Pier 4 has been edited
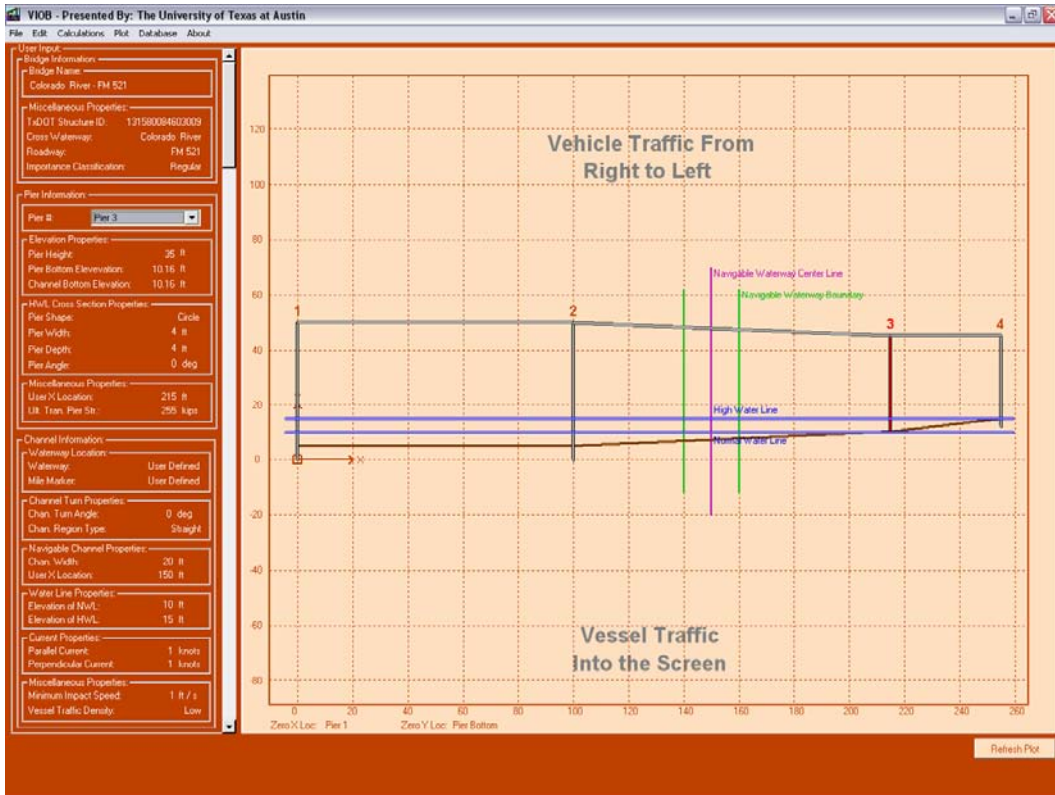
Figure B-9: "Main Page" after Pier 3 has been edited
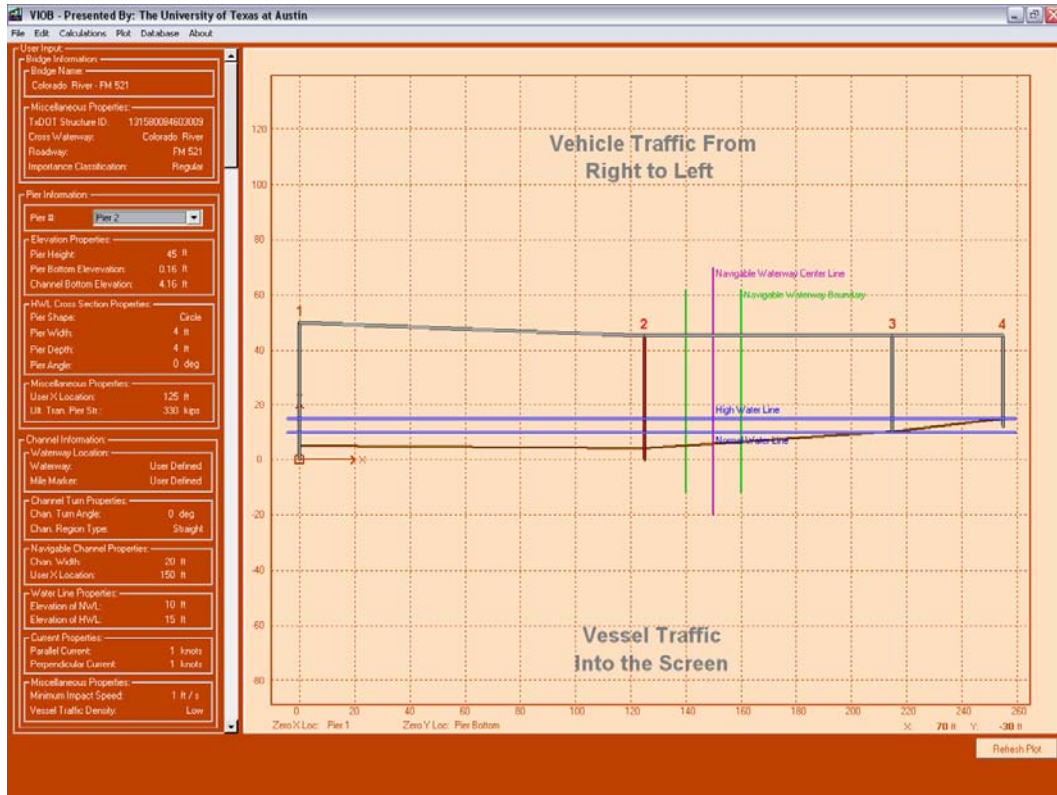
Figure B-10: "Main Page" after Pier 2 has been edited

114
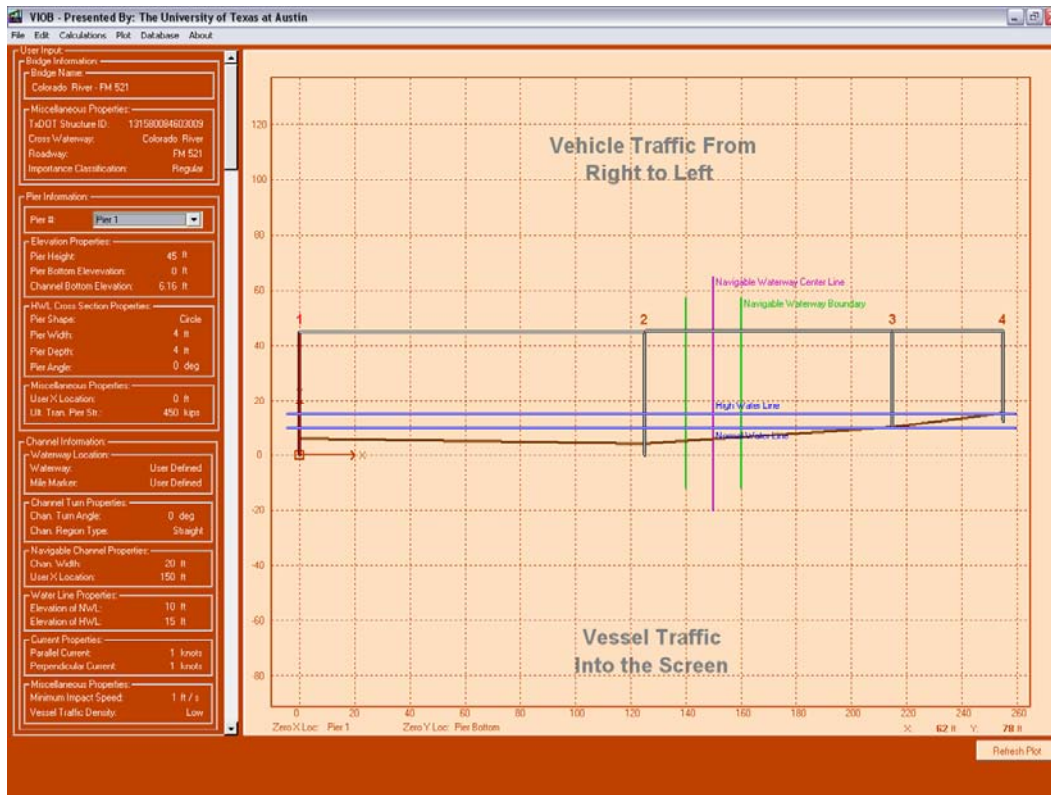
Figure B-11: "Main Page" after Pier 1 has been edited

Edit Channel Data

After the pier geometry has been entered, the next step is to edit the channel data. To do this, the user clicks on **Edit > Channel Data…** to open the "Edit Channel" window. See Figure B-12 and Figure B-13.
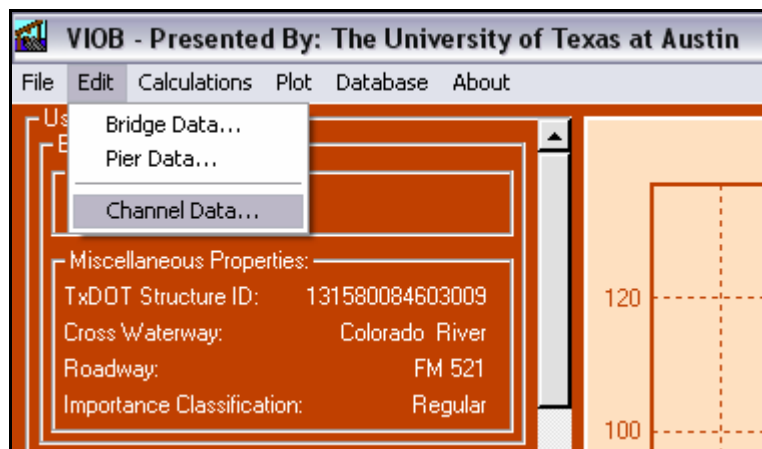
Figure B-12: Selecting channel data from the "Edit" menu
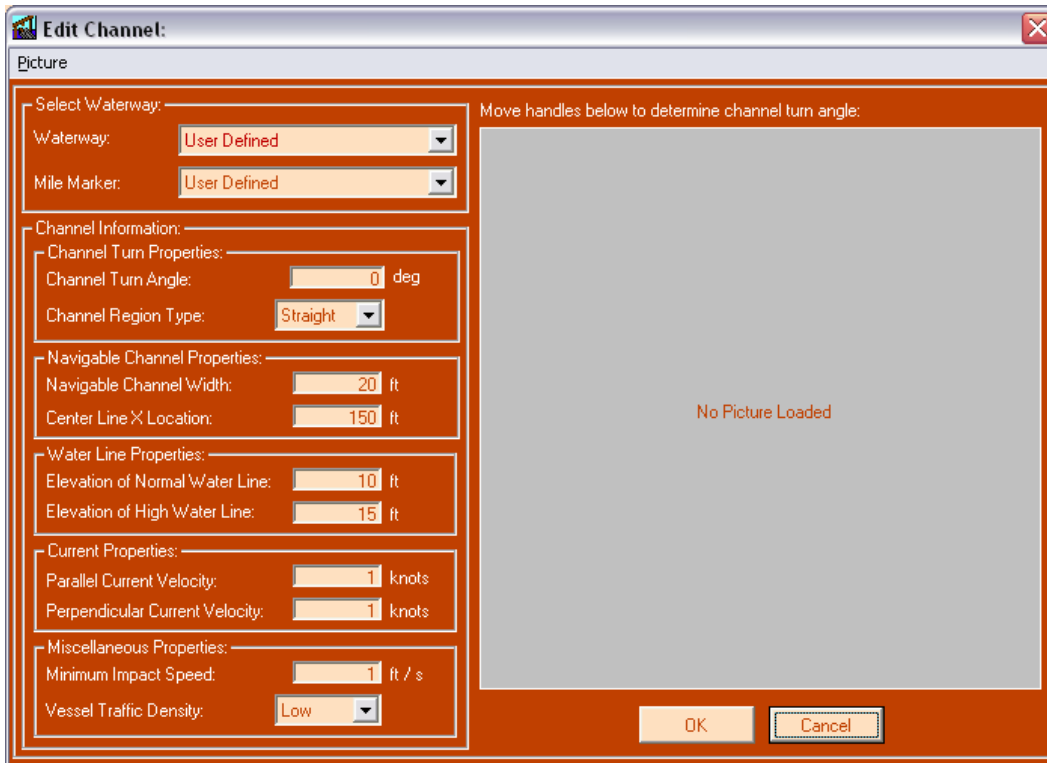
Figure B-13: Default "Edit Channel" window

When the user opens the "Edit Channel" window for the first time on a bridge, the aerial photo of that bridge will not be loaded. To do this, the user can click **Picture > Load…** which will bring up the file browse window to allow the user to select any available bitmap image of the aerial photo for this bridge. See Figure B-14. Once the aerial photo of the bridge has been loaded, the channel window will include the built-in protractor for determining the channel angle. The user can now enter all of the channel information. See Figure B-15.
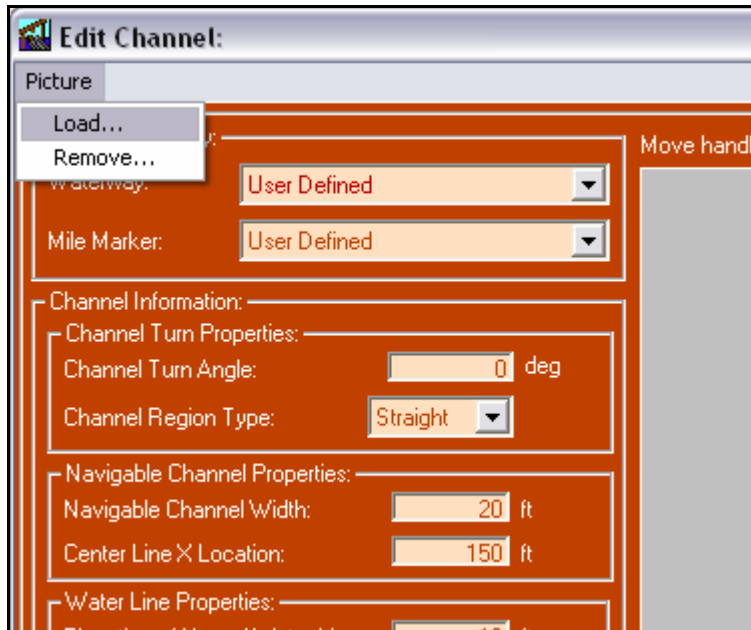
Figure B-14: Selecting the load option from the "Picture" menu

In this example, the waterway and mile marker already exist in the VIOB library; therefore, the user can select the waterway and mile marker from the pull-down menu in the "Edit Channel" window. Selecting the waterway and the mile marker will automatically fill in the current velocities, minimum impact speed, and traffic density. To edit the channel turn angle, the user moves the square handle to adjust the protractor's origin and then moves the circular handles to determine the angle of the channel. If no aerial photo exists, the user can enter the angle manually instead. Once all of the channel data is entered, the user clicks the "OK" button to return to the "Main Page."
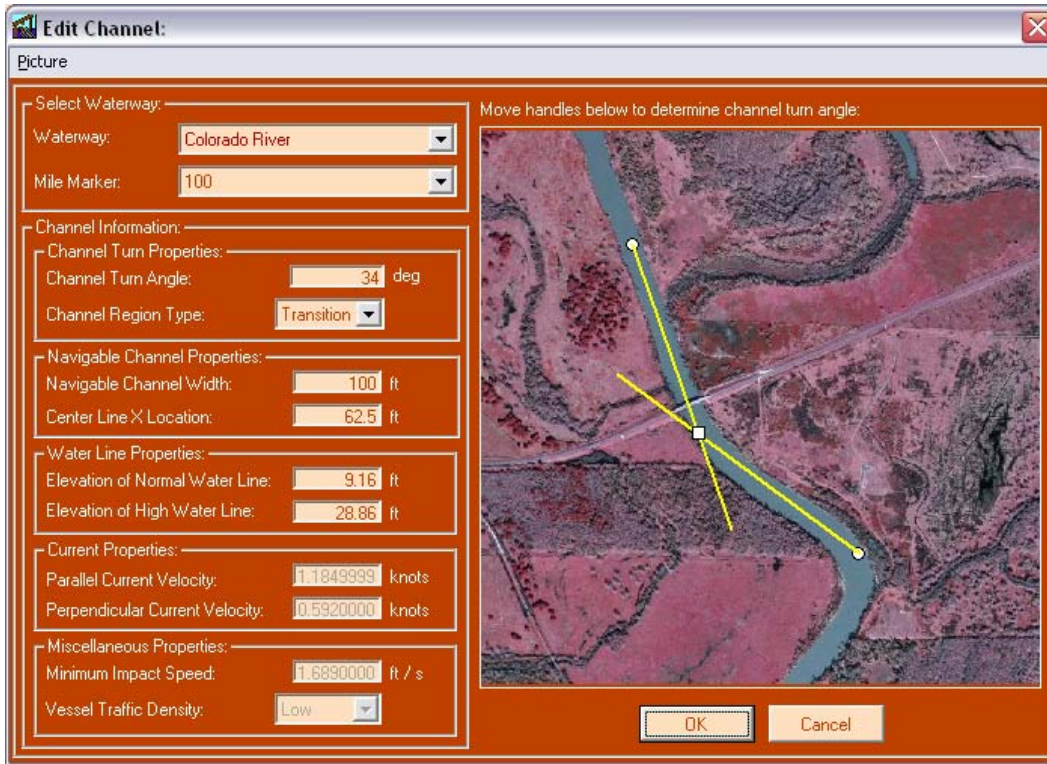
Figure B-15: "Edit Channel" window with information entered and aerial picture loaded

At this point, all of the necessary information is available and the "Main Page" is displayed. See Figure B-16.
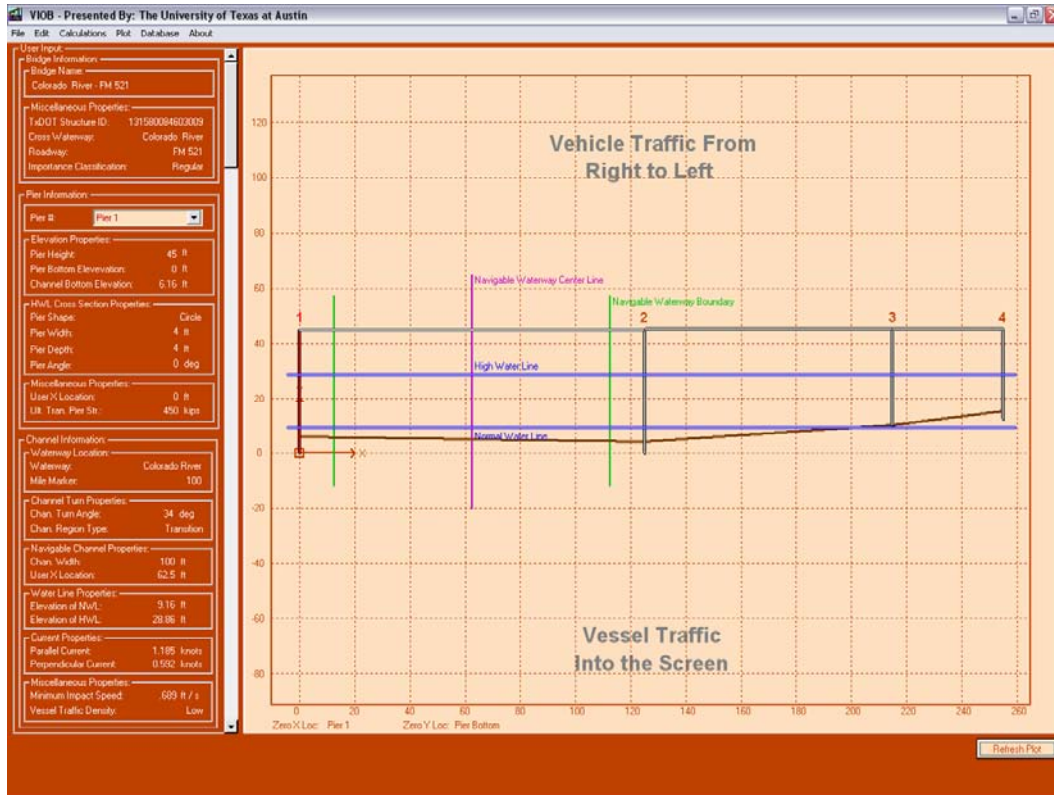
Figure B-16: The "Main Page" after the channel data has been edited

Run Analysis

With all of the information about the bridge entered into VIOB, the analysis can now be run. To run an analysis, the user clicks on **Calculations > Run…** on the "Main Page" which will open the "Analysis Wizard." See Figure B-17 and Figure B-18. In the "Analysis Wizard" the user must enter his/her name only as all of the other information will have been automatically filled out for the user. VIOB knows the vessel fleet because the vessel fleet is assigned to the waterway and mile marker assigned to the bridge previously.
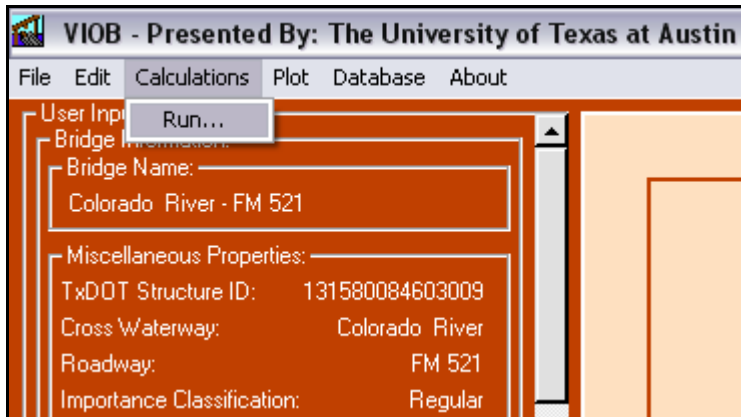
Figure B-17: Selecting the run option from the "Calculations" menu
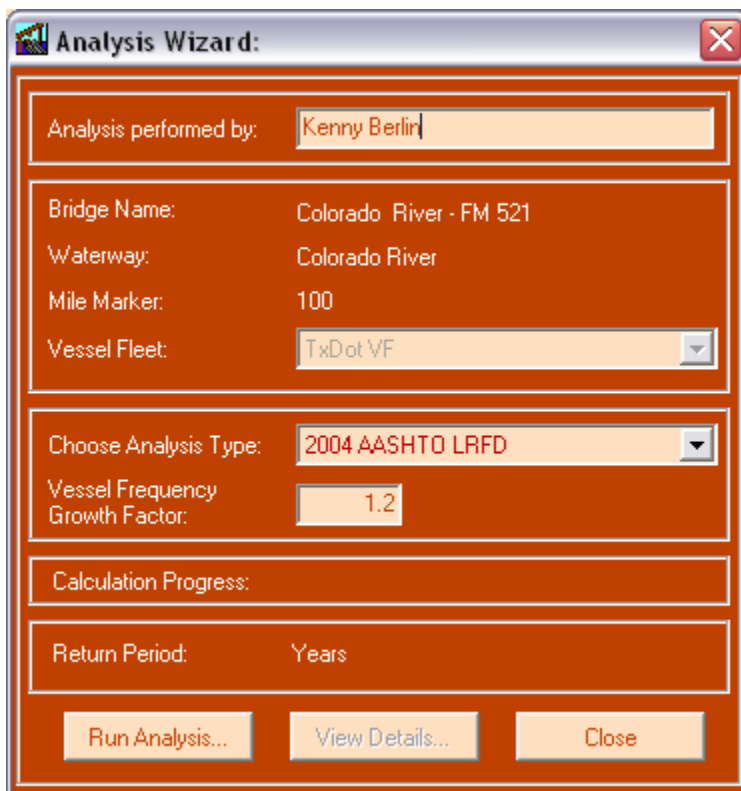
Figure B-18: "Analysis Wizard" before the analysis is run

The user must next click the "Run Analysis…" button on the "Analysis Wizard" window. VIOB will then determine the return period of the bridge and summarize the results on the same window. The user can track the progress of the calculations by looking at the calculation progress bar.
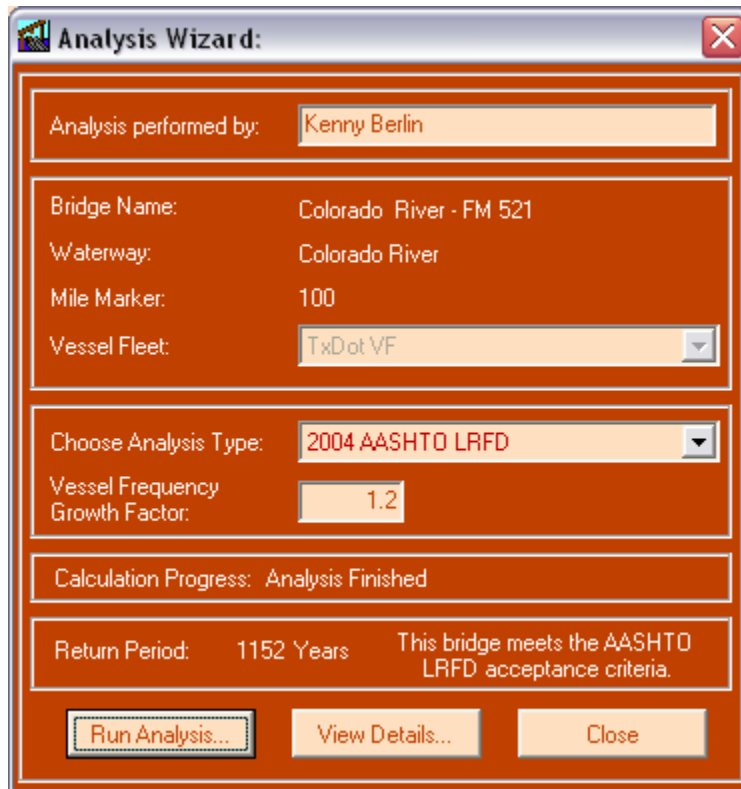
Figure B-19: "Analysis Wizard" window after "Run Analysis…" has been clicked

Once the analysis has been run, the user can view a detailed set of results by clicking on the "View Details" button. For more information about detailed results, refer to Chapter 7.

Appendix C
Sample VIOB Report

Description of Appendix

This appendix contains a sample VIOB Report for a single bridge analysis. For this example, all six sections of the report were printed. To limit the number of pages here, the VIOB report has been reproduced to show two report pages on every one page that follows.

VIOB Presented By: The University of Texas at Austin
The Next Generation of Analysis for Vessel Impact on Bridges

Results Summary:

Bridge Name:	San Jacinto River - EB IH-10	**TxDOT Structure ID:**	12102005080l317
Waterway:	User Defined	**Vessel Fleet:**	SJR VF
Roadway:	EB IH-10	**Milemarker:**	User Defined
Analysis Performed By:	Kenny Berlin	**Analysis Date:**	5/3/2005
Analysis Type:	2004 AASHTO LRFD	**Analysis Time:**	11:03:50 AM
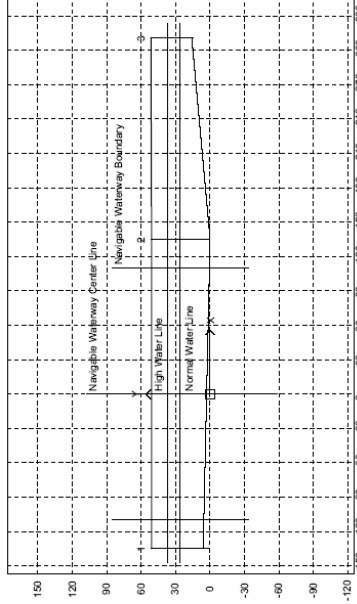
Annual Frequency of Collapse:	2.887757E-03	1/Yr
Return Period:	346	Years
Importance Classification:	Regular	
Pass/Fail:	Fail	

This bridge does NOT meet the AASHTO LRFD acceptance criteria.

Page 1

VIOB REPORT

Bridge Name:	San Jacinto River - EB IH-10
TxDOT Structure ID:	12102005080l317
Waterway:	User Defined
Roadway:	EB IH-10
Report Created By:	Kenny Berlin

May 3, 2005

VIOB Presented By: The University of Texas at Austin
The Next Generation of Analysis for Vessel Impact on Bridges

VIOB Presented By: The University of Texas at Austin
The Next Generation of Analysis for Vessel Impact on Bridges

Vessel Fleet Description:

Table 2: Vessel Fleet Components

Vessel Name	Vessel Class	Vessel Type	Vessel Size	Vessel Frequency (Trips/Year)	Loaded or Unloaded	Vessel Velocity (knots)
V1	Barge Group	TXDOT BG 4	N/A	677	Loaded	6
V2	Barge Group	TXDOT BG 4	N/A	677	Unloaded	6

Table 3: Barge Group Information

Vessel Name	Barge Group Type	Barge Group Size	Length (ft)	Width (ft)	Displacement (tonne)	Draft (ft)
V1	TXDOT BG 4	N/A	257	35	1542.214	9
			V1-TG V1-BG			
V2	TXDOT BG 4	N/A	257	35	567.7162	9
			V2-TG V2-BG			

Table 4: Tug Information

Vessel Name	Tug Type	Tug Horsepower	Length (ft)	Width (ft)	Displacement (tonne)	Draft (ft)
V1-TG	TXDOT Tug	1	62	20	181.4369	9
V2-TG	TXDOT Tug	1	62	20	181.4369	9

Table 5: Barge Information

Vessel Name	Barge Type	Barge Size	Length (ft)	Width (ft)	Displacement (tonne)	Draft (ft)
V1-BG	Covered Hopper	TXDOT Jumbo	195	35	1360.777	7
V2-BG	Covered Hopper	TXDOT Jumbo	195	35	386.2792	2

VIOB Presented By: The University of Texas at Austin
The Next Generation of Analysis for Vessel Impact on Bridges

Pier and Channel Information:

Channel Information:

Waterway Name:	User Defined				
Mile Marker:	User Defined				
Normal Water Line:	26.5	ft	Channel Width:	220	ft
High Water Line:	36.7	ft	Channel Region Type:	Bend	
Parallel Current:	1.185	knots	Channel Turn Angle:	15	deg
Perpendicular Current:	0.593	knots	Traffic Density:	Low	
Minimum Impact Speed:	1.688	ft / s			

Table 1: Pier Information

Pier Number:		Pier 1	Pier 2	Pier 3
Pier Height:	ft	51	51	36.5
Pier Bottom Elevation:	ft	0	0	15
Channel Elevation:	ft	6	0	16
User X Location:	ft	-135	135	311
Ultimate Transverse Pier Strength:	kips	997	997	815
Pier X-Section Shape:		Circle	Circle	Circle
Pier X-Section Depth:	ft	4.75	4.75	3.75
Pier X-Section Width:	ft	4.75	4.75	3.75
Pier X-Section Angle:	deg	0	0	0

VIOB Presented By: The University of Texas at Austin
The Next Generation of Analysis for Vessel Impact on Bridges

Detailed Calculations:

Table 6: AFC Summary

(AASHTO LRFD 3.14.5-1)

$$AFC = (N)(PA)(PG)(PC)$$

Vessel i - Pier j	N	PA	PG	PC	AFC
Vessel 1 - Pier 1	812.4	0.000285	0.053714	0.049254	0.000613
Vessel 1 - Pier 2	812.4	0.000285	0.053714	0.049254	0.000613
Vessel 1 - Pier 3	812.4	0.000285	0.028937	0.055482	0.000372
Vessel 2 - Pier 1	812.4	0.000285	0.053714	0.038662	0.000481
Vessel 2 - Pier 2	812.4	0.000285	0.053714	0.038662	0.000481
Vessel 2 - Pier 3	812.4	0.000285	0.028937	0.049025	0.000329
				Total AFC:	0.002889

Page 5

VIOB Presented By: The University of Texas at Austin
The Next Generation of Analysis for Vessel Impact on Bridges

Results Comparison:

Figure 1: Comparison of Particular Vessel Passing a Particular Pier

Figure 2: Comparison of Particular Vessel Passing All Piers

Figure 3: Comparison of All Vessels Passing a Particular Pier

Page 4

VIOB Presented By: The University of Texas at Austin
The Next Generation of Analysis for Vessel Impact on Bridges

Detailed Calculations (Continued):

Geometric Probability Calculations (V1-P1):

Geometric Probability (PG):	0.053714	1/Yrs

(AASHTO LRFD 3.14.5.3-1)

Centerline of Pier
X1 X2
Centerline of Vessel Sailing Path   x = 135

$$PG = NSD(Z2) - NSD(Z1)$$

Normal Standard Distribution at Z1 (NSD(Z1)):	0.673	
Z1:	0.448	
Normal Standard Distribution at Z2 (NSD(Z2)):	0.727	
Z2:	0.603	

$$X_1 = x - \left(\frac{B_P}{2} + \frac{B_M}{2} \right)$$

$$Z_1 = \frac{X_1}{LOA}$$

$$X_2 = x + \left(\frac{B_P}{2} + \frac{B_M}{2} \right)$$

$$Z_2 = \frac{X_2}{LOA}$$

Impact Pier Width (BP):	4.75	ft

$$B_P = PierWidth \times cos(\phi) + PierDepth \times sin(\phi)$$

Pier Width:	4.75	ft
Pier Depth:	4.75	ft
Pier Angle (φ):	0	deg
Vessel Width (BM):	35	ft
Vessel Length Over All (LOA):	257	ft
Distance From Pier CL to Bridge CL (x):	135	ft
User Pier x Distance:	-135	ft
User Center Line x Distance:	0	ft

$$x = |UserPier - UserCL|$$

VIOB Presented By: The University of Texas at Austin
The Next Generation of Analysis for Vessel Impact on Bridges

Detailed Calculations (Continued):

Vessel 1 - Pier 1

Vessel Frequency Calculations (V1-P1):

Projected Vessel Frequency (N):	812.4	Trips/Yr
Current Vessel Frequency:	677	Trips/Yr
Growth Factor:	1.2	

Probability of Aberrancy Calculations (V1-P1):

Probability of Aberrancy (PA):	0.000285	1/Yrs

(AASHTO LRFD 3.14.5.2.3-1)

$$PA = (BR)(R_B)(R_C)(R_{XC})(R_D)$$

Aberrancy Base Rate (BR):	0.00012
Correction Factor for Bridge Location (RB):	1.333

(AASHTO LRFD 3.14.5.2.3-4)

$$R_B = \left(1 + \frac{\theta}{45°} \right)$$

Angle of Channel Turn (θ):	15	deg
Region Type:	Bend	
Correction Factor for Parallel Current (RC):	1.118	

(AASHTO LRFD 3.14.5.2.3-5)

$$R_C = \left(1 + \frac{V_C}{10} \right)$$

Velocity of Parallel Current (VC):	1.185	knots
Correction Factor for Perpendicular Current (RXC):	1.593	

(AASHTO LRFD 3.14.5.2.3-6)

$$R_{XC} = (1 + V_{XC})$$

Velocity of Perpendicuar Current (VXC):	0.593	knots
Correction Factor for Traffic Density (RD):	1	
Traffic Density:	Low	

The Next Generation of Analysis for Vessel Impact on Bridges

Detailed Calculations (Continued):

Probability of Collapse Calculations (V1-P1) (Continued):

| Vessel Impact Speed (V): | 9.838 | ft / s |

Typical Vessel Transit Speed in the Channel (VT):	10.127	ft / s
Minimum Design Impact Speed (VMin):	1.688	ft / s
Distance from Chan. Edge to Vessel Path (XC):	110	ft
Channel Width:	220	ft
3 LOA (XL):	771	ft
Distance From Pier Face to Bridge CL (x):	132.625	ft

The Next Generation of Analysis for Vessel Impact on Bridges

Detailed Calculations (Continued):

Probability of Collapse Calculations (V1-P1):

| Probability of Collapse (PC): | 0.049254 | 1/Yrs |

$$PC = 0.1 + 9\left(0.1 - \frac{H}{P}\right)$$

(AASHTO LRFD 3.14.5.4-1)

Ultimate Bridge Element Strength (H):	997	kips
Vessel Impact Force (P):	1792.301	kips
Kinetic Energy (KE):	5367.421	kip - ft

$$KE = \frac{C_H W V^2}{29.2}$$

(AASHTO LRFD 3.14.7-1)

Vessel Displacement Tonnage (W):	1542.214	tonne
Hydrodynamic Mass Coefficient (CH):	1.05	
Draft:	9	ft
Underkeel Clearence:	21.7	ft
Draft:	9	ft
Channel Depth:	30.7	ft
User Channel Elevation:	6	ft
User High Water Line:	36.7	ft

VIOB Presented By: The University of Texas at Austin
The Next Generation of Analysis for Vessel Impact on Bridges

Detailed Calculations (Continued):

Vessel 1 - Pier 2

Vessel Frequency Calculations (V1-P2):

Projected Vessel Frequency (N):	812.4	Trips/Yr
Current Vessel Frequency:	677	Trips/Yr
Growth Factor:	1.2	

Probability of Aberrancy Calculations (V1-P2):

$$PA = (BR)(R_B)(R_C)(R_{XC})(R_D)$$

Probability of Aberrancy (PA):	0.000285	1/Yrs

(AASHTO LRFD 3.14.5.2-1)

Aberrancy Base Rate (BR):	0.00012	
Correction Factor for Bridge Location (RB):	1.333	

(AASHTO LRFD 3.14.5.2-3-4)

$$R_B = \left(1 + \frac{\theta}{45°}\right)$$

Angle of Channel Turn (θ):	15	deg
Region Type:	Bend	
Correction Factor for Parallel Current (RC):	1.118	

(AASHTO LRFD 3.14.5.2-3-5)

$$R_C = \left(1 + \frac{V_C}{10}\right)$$

Velocity of Parallel Current (VC):	1.185	knots
Correction Factor for Perpendicular Current (RXC):	1.593	

(AASHTO LRFD 3.14.5.2-3-6)

$$R_{XC} = (1 + V_{XC})$$

Velocity of Perpendicular Current (VXC):	0.593	knots
Correction Factor for Traffic Density (RD):	1	
Traffic Density:	Low	

VIOB Presented By: The University of Texas at Austin
The Next Generation of Analysis for Vessel Impact on Bridges

Detailed Calculations (Continued):

Probability of Collapse Calculations (V1-P1) (Continued):

Ship Collision Force on Pier (PS):	NA	kips

(AASHTO LRFD 3.14.8-1)

$$P_S = 8.15 V \sqrt{DWT}$$

Deadweight Tonnage of Ship (DWT):	NA	tonne
Vessel Impact Speed (V):	9.838	ft / s
Ship Damage Depth (AS):	NA	ft

(AASHTO LRFD 3.14.9-1)

$$a_S = 1.54 \left(\frac{KE}{P_S}\right)$$

Kinetic Energy (KE):	5367.421	kip - ft
Ship Collision Force on Pier (PS):	NA	kips
Barge Collision Force on Pier (PB):	1792.301	kips

(AASHTO LRFD 3.14.11-2)

$$P_B = 1349 + 110 a_B$$

Barge Damage Depth (AB):	4.03	ft

(AASHTO LRFD 3.14.12-1)

$$a_B = 10.2 \left(\sqrt{1 + \frac{KE}{5672}} - 1\right)$$

Kinetic Energy (KE):	5367.421	kip - ft

VIOB — Presented By: The University of Texas at Austin
The Next Generation of Analysis for Vessel Impact on Bridges

Detailed Calculations (Continued):

Geometric Probability Calculations (V1-P2):

Geometric Probability (PG):	0.053714	1/Yrs

(AASHTO LRFD 3.14.5.3-1)

Centerline of Pier — Centerline of Vessel Sailing Path — x = 135 — X1 — X2

$$PG = NSD(Z2) - NSD(Z1)$$

Normal Standard Distribution at Z1 (NSD(Z1)):	0.673
Z1:	0.448
Normal Standard Distribution at Z2 (NSD(Z2)):	0.727
Z2:	0.603

$$X_1 = x - \left(\frac{B_P}{2} + \frac{B_M}{2}\right) \qquad X_2 = x + \left(\frac{B_P}{2} + \frac{B_M}{2}\right)$$

$$Z_1 = \frac{X_1}{LOA} \qquad Z_2 = \frac{X_2}{LOA}$$

Impact Pier Width (BP):	4.75	ft

$$B_P = PierWidth \times \cos(\phi) + PierDepth \times \sin(\phi)$$

Pier Width:	4.75	ft
Pier Depth:	4.75	ft
Pier Angle (φ):	0	deg
Vessel Width (BM):	35	ft
Vessel Length Over All (LOA):	257	ft
Distance From Pier CL to Bridge CL (x):	135	ft
User Pier x Distance:	135	ft
User Center Line x Distance:	0	ft

$$x = |UserPier - UserCL|$$

VIOB — Presented By: The University of Texas at Austin
The Next Generation of Analysis for Vessel Impact on Bridges

Detailed Calculations (Continued):

Probability of Collapse Calculations (V1-P2):

Probability of Collapse (PC):	0.049254	1/Yrs

(H/P = 0.5562682, PC = 0.049254)

$$PC = 0.1 + 9\left(0.1 - \frac{H}{P}\right)$$

(AASHTO LRFD 3.14.5.4-1)

Ultimate Bridge Element Strength (H):	997	kips
Vessel Impact Force (P):	1792.301	kips
Kinetic Energy (KE):	5367.421	kip - ft

(AASHTO LRFD 3.14.7-1)

$$KE = \frac{C_H W V^2}{29.2}$$

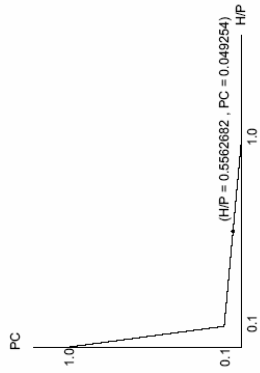|		
Vessel Displacement Tonnage (W):	1542.214	tonne
Hydrodynamic Mass Coefficient (CH):	1.05	
Draft:	9	ft
Underkeel Clearance:	27.7	ft
Draft:	9	ft
Channel Depth:	36.7	ft
User Channel Elevation:	0	ft
User High Water Line:	36.7	ft

VIOB Presented By: The University of Texas at Austin
The Next Generation of Analysis for Vessel Impact on Bridges

Detailed Calculations (Continued):

Probability of Collapse Calculations (V1-P2) (Continued):

Ship Collision Force on Pier (PS):	NA	kips

(AASHTO LRFD 3.14.8-1)

$$P_S = 8.15V\sqrt{DWT}$$

Deadweight Tonnage of Ship (DWT):	NA	tonne
Vessel Impact Speed (V):	9.838	ft / s
Ship Damage Depth (AS):	NA	ft

(AASHTO LRFD 3.14.9-1)

$$a_S = 1.54\left(\frac{KE}{P_S}\right)$$

Kinetic Energy (KE):	5367.421	kip - ft
Ship Collision Force on Pier (PS):	NA	kips
Barge Collision Force on Pier (PB):	1792.301	kips

(AASHTO LRFD 3.14.11-2)

$$P_B = 1349 + 110a_B$$

Barge Damage Depth (AB):	4.03	ft

(AASHTO LRFD 3.14.12-1)

$$a_B = 10.2\left(\sqrt{1+\frac{KE}{5672}} - 1\right)$$

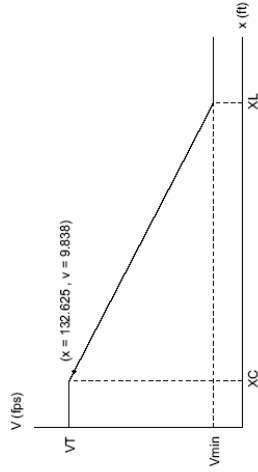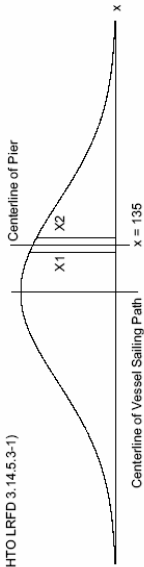| Kinetic Energy (KE):	5367.421	kip - ft

---

VIOB Presented By: The University of Texas at Austin
The Next Generation of Analysis for Vessel Impact on Bridges

Detailed Calculations (Continued):

Probability of Collapse Calculations (V1-P2) (Continued):

Vessel Impact Speed (V):	9.838	ft / s

Typical Vessel Transit Speed in the Channel (VT):	10.127	ft / s
Minimum Design Impact Speed (VMin):	1.668	ft / s
Distance from Chan. Edge to Vessel Path (XC):	110	ft
Channel Width:	220	ft
3 LOA (XL):	771	ft
Distance From Pier Face to Bridge CL (x):	132.625	ft

131

VIOB Presented By: The University of Texas at Austin
The Next Generation of Analysis for Vessel Impact on Bridges

Detailed Calculations (Continued):

Geometric Probability Calculations (V1-P3):

Geometric Probability (PG):	0.028937	1/Yrs

(AASHTO LRFD 3.14.5.3-1)

Centerline of Pier

X_1 X_2

Centerline of Vessel Sailing Path

$x = 311$

$$PG = NSD(Z2) - NSD(Z1)$$

Normal Standard Distribution at Z1 (NSD(Z1)):	0.872
Z1:	1.135
Normal Standard Distribution at Z2 (NSD(Z2)):	0.901
Z2:	1.286

$$X_1 = x - \left(\frac{B_P}{2} + \frac{B_M}{2}\right) \qquad X_2 = x + \left(\frac{B_P}{2} + \frac{B_M}{2}\right)$$

$$Z_1 = \frac{X_1}{LOA} \qquad Z_2 = \frac{X_2}{LOA}$$

Impact Pier Width (BP):	3.75	ft

$$B_P = PierWidth \times cos(\phi) + PierDepth \times sin(\phi)$$

Pier Width:	3.75	ft
Pier Depth:	3.75	ft
Pier Angle (φ):	0	deg
Vessel Width (BM):	35	ft
Vessel Length Over All (LOA):	257	ft
Distance From Pier CL to Bridge CL (x):	311	ft
User Pier x Distance:	311	ft
User Center Line x Distance:	0	ft

$$x = |UserPier - UserCL|$$

VIOB Presented By: The University of Texas at Austin
The Next Generation of Analysis for Vessel Impact on Bridges

Vessel 1 - Pier 3

Detailed Calculations (Continued):

Vessel Frequency Calculations (V1-P3):

Projected Vessel Frequency (N):	812.4	Trips/Yr
Current Vessel Frequency:	677	Trips/Yr
Growth Factor:	1.2	

Probability of Aberrancy Calculations (V1-P3):

Probability of Aberrancy (PA):	0.000285	1/Yrs

(AASHTO LRFD 3.14.5.2.3-1)

$$PA = (BR)(R_B)(R_C)(R_{XC})(R_D)$$

Aberrancy Base Rate (BR):	0.00012
Correction Factor for Bridge Location (RB):	1.333

(AASHTO LRFD 3.14.5.2.3-4)

$$R_B = \left(1 + \frac{\theta}{45°}\right)$$

Angle of Channel Turn (θ):	15	deg
Region Type:	Bend	
Correction Factor for Parallel Current (RC):	1.118	

(AASHTO LRFD 3.14.5.2.3-5)

$$R_C = \left(1 + \frac{V_C}{10}\right)$$

Velocity of Parallel Current (VC):	1.185	knots
Correction Factor for Perpendicular Current (RXC):	1.593	

(AASHTO LRFD 3.14.5.2.3-6)

$$R_{XC} = (1 + V_{XC})$$

Velocity of Perpendicuar Current (VXC):	0.593	knots
Correction Factor for Traffic Density (RD):	1	
Traffic Density:	Low	

132

VIOB Presented By: The University of Texas at Austin
The Next Generation of Analysis for Vessel Impact on Bridges

Detailed Calculations (Continued):
Probability of Collapse Calculations (V1-P3) (Continued):

Vessel Impact Speed (V):	7.585	ft / s

Graph: V (fps) vs x (ft); VT, Vmin, XC, XL, $(x = 309.125, v = 7.585)$

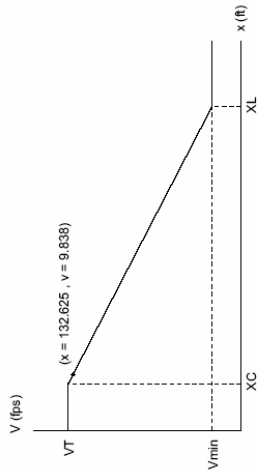| Typical Vessel Transit Speed in the Channel (VT):	10.127	ft / s
Minimum Design Impact Speed (VMin):	1.688	ft / s
Distance from Chan. Edge to Vessel Path (XC):	110	ft
Channel Width:	220	ft
3 LOA (XL):	771	ft
Distance From Pier Face to Bridge CL (x):	309.125	ft

VIOB Presented By: The University of Texas at Austin
The Next Generation of Analysis for Vessel Impact on Bridges

Detailed Calculations (Continued):
Probability of Collapse Calculations (V1-P3):

Probability of Collapse (PC):	0.055482	1/Yrs

Graph: PC vs H/P; $(H/P = 0.5001596, PC = 0.055482)$

$$PC = 0.1 + 9\left(0.1 - \frac{H}{P}\right)$$

(AASHTO LRFD 3.14.5.4-1)

Ultimate Bridge Element Strength (H):	815	kips
Vessel Impact Force (P):	1629.48	kips
Kinetic Energy (KE):	3190.247	kip-ft

(AASHTO LRFD 3.14.7-1)

$$KE = \frac{C_H W V^2}{29.2}$$

Vessel Displacement Tonnage (W):	1542.214	tonne
Hydrodynamic Mass Coefficient (CH):	1.05	
Draft:	9	ft
Underkeel Clearance:	11.7	ft
Draft:	9	ft
Channel Depth:	20.7	ft
User Channel Elevation:	16	ft
User High Water Line:	36.7	ft

VIOB Presented By: The University of Texas at Austin
The Next Generation of Analysis for Vessel Impact on Bridges

Detailed Calculations (Continued):

Vessel 2 - Pier 1

Vessel Frequency Calculations (V2-P1):

Projected Vessel Frequency (N):	812.4	Trips/Yr
Current Vessel Frequency:	677	Trips/Yr
Growth Factor:	1.2	

Probability of Aberrancy Calculations (V2-P1):

Probability of Aberrancy (PA):	0.000285	1/Yrs

(AASHTO LRFD 3.14.5.2.3-1)

$$PA = (BR)(R_B)(R_C)(R_{XC})(R_D)$$

Aberrancy Base Rate (BR):	0.00012
Correction Factor for Bridge Location (RB):	1.333

(AASHTO LRFD 3.14.5.2.3-4)

$$R_B = \left(1 + \frac{\theta}{45°}\right)$$

Angle of Channel Turn (θ):	15 deg
Region Type:	Bend
Correction Factor for Parallel Current (RC):	1.118

(AASHTO LRFD 3.14.5.2.3-5)

$$R_C = \left(1 + \frac{V_C}{10}\right)$$
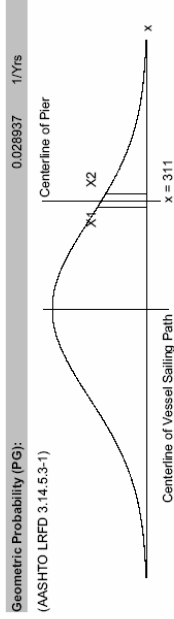
Velocity of Parallel Current (VC):	1.185 knots
Correction Factor for Perpendicular Current (RXC):	1.593

(AASHTO LRFD 3.14.5.2.3-6)

$$R_{XC} = (1 + V_{XC})$$

Velocity of Perpendicular Current (VXC):	0.593 knots
Correction Factor for Traffic Density (RD):	1
Traffic Density:	Low

VIOB Presented By: The University of Texas at Austin
The Next Generation of Analysis for Vessel Impact on Bridges

Detailed Calculations (Continued):

Probability of Collapse Calculations (V1-P3) (Continued):

Ship Collision Force on Pier (PS):	NA	kips

(AASHTO LRFD 3.14.8-1)

$$P_S = 8.15\,V\sqrt{DWT}$$

Deadweight Tonnage of Ship (DWT):	NA	tonne
Vessel Impact Speed (V):	7.585	ft / s
Ship Damage Depth (AS):	NA	ft

(AASHTO LRFD 3.14.9-1)

$$a_S = 1.54\left(\frac{KE}{P_S}\right)$$

Kinetic Energy (KE):	3190.247	kip - ft
Ship Collision Force on Pier (PS):	NA	kips
Barge Collision Force on Pier (PB):	1629.48	kips

(AASHTO LRFD 3.14.11-2)

$$P_B = 1349 + 110\,a_B$$

Barge Damage Depth (AB):	2.55	ft

(AASHTO LRFD 3.14.12-1)

$$a_B = 10.2\left(\sqrt{1 + \frac{KE}{5672}} - 1\right)$$

Kinetic Energy (KE):	3190.247	kip - ft

The Next Generation of Analysis for Vessel Impact on Bridges

Detailed Calculations (Continued):

Probability of Collapse Calculations (V2-P1):

Probability of Collapse (PC):	0.038662	1/Yrs

(H/P = 0.6516982 ; PC = 0.038662)

(AASHTO LRFD 3.14.5.4-1)

$$PC = 0.1 + 9\left(0.1 - \frac{H}{P}\right)$$

Ultimate Bridge Element Strength (H):	997	kips
Vessel Impact Force (P):	1529.849	kips
Kinetic Energy (KE):	1975.842	kip - ft

(AASHTO LRFD 3.14.7-1)

$$KE = \frac{C_H W V^2}{29.2}$$

Vessel Displacement Tonnage (W):	567.716	tonne
Hydrodynamic Mass Coefficient (CH):	1.05	
Draft:	9	ft
Underkeel Clearance:	21.7	ft
Draft:	9	ft
Channel Depth:	30.7	ft
User Channel Elevation:	6	ft
User High Water Line:	36.7	ft

The Next Generation of Analysis for Vessel Impact on Bridges

Detailed Calculations (Continued):

Geometric Probability Calculations (V2-P1):

Geometric Probability (PG):	0.053714	1/Yrs

(AASHTO LRFD 3.14.5.3-1)

Centerline of Pier

Centerline of Vessel Sailing Path   x = 135

$$PG = NSD(Z2) - NSD(Z1)$$

Normal Standard Distribution at Z1 (NSD(Z1)):	0.673
Z1:	0.448
Normal Standard Distribution at Z2 (NSD(Z2)):	0.727
Z2:	0.603

$$X_1 = x - \left(\frac{B_P}{2} + \frac{B_M}{2}\right) \qquad X_2 = x + \left(\frac{B_P}{2} + \frac{B_M}{2}\right)$$

$$Z_1 = \frac{X_1}{LOA} \qquad Z_2 = \frac{X_2}{LOA}$$

Impact Pier Width (BP):	4.75	ft

$$B_P = PierWidth \times cos(\phi) + PierDepth \times sin(\phi)$$

Pier Width:	4.75	ft
Pier Depth:	4.75	ft
Pier Angle (φ):	0	deg
Vessel Width (BM):	35	ft
Vessel Length Over All (LOA):	257	ft
Distance From Pier CL to Bridge CL (x):	135	ft
User Pier x Distance:	-135	ft
User Center Line x Distance:	0	ft

$$x = |UserPier - UserCL|$$

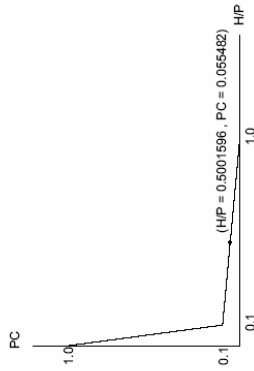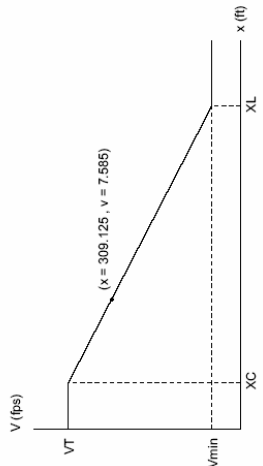**VIOB** Presented By: The University of Texas at Austin
The Next Generation of Analysis for Vessel Impact on Bridges

Detailed Calculations (Continued):

Probability of Collapse Calculations (V2-P1) (Continued):

Ship Collision Force on Pier (PS):	NA	kips

(AASHTO LRFD 3.14.8-1)

$$P_S = 8.15 V \sqrt{DWT}$$

Deadweight Tonnage of Ship (DWT):	NA	tonne
Vessel Impact Speed (V):	9.838	ft / s
Ship Damage Depth (AS):	NA	ft

(AASHTO LRFD 3.14.9-1)

$$a_S = 1.54\left(\frac{KE}{P_S}\right)$$

Kinetic Energy (KE):	1975.842	kip - ft
Ship Collision Force on Pier (PS):	NA	kips
Barge Collision Force on Pier (PB):	1529.849	kips

(AASHTO LRFD 3.14.11-2)

$$P_B = 1349 + 110 a_B$$

Barge Damage Depth (AB):	1.644	ft

(AASHTO LRFD 3.14.12-1)

$$a_B = 10.2\left(\sqrt{1 + \frac{KE}{5672}} - 1\right)$$

Kinetic Energy (KE):	1975.842	kip - ft

VIOB Presented By: The University of Texas at Austin
The Next Generation of Analysis for Vessel Impact on Bridges

Detailed Calculations (Continued):

Probability of Collapse Calculations (V2-P1) (Continued):

Vessel Impact Speed (V):	9.838	ft / s

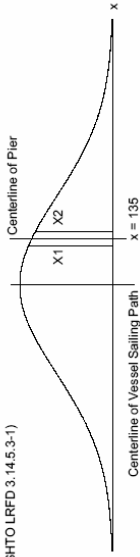|		
Typical Vessel Transit Speed in the Channel (VT):	10.127	ft / s
Minimum Design Impact Speed (VMin):	1.688	ft / s
Distance from Chan. Edge to Vessel Path (XC):	110	ft
Channel Width:	220	ft
3 LOA (XL):	771	ft
Distance From Pier Face to Bridge CL (x):	132.625	ft

VIOB — Presented By: The University of Texas at Austin
The Next Generation of Analysis for Vessel Impact on Bridges

Detailed Calculations (Continued):

Vessel 2 - Pier 2

Vessel Frequency Calculations (V2-P2):

Projected Vessel Frequency (N):	812.4	Trips/Yr
Current Vessel Frequency:	677	Trips/Yr
Growth Factor:	1.2	

Probability of Aberrancy Calculations (V2-P2):

Probability of Aberrancy (PA):	0.000285	1/Yrs

(AASHTO LRFD 3.14.5.2.3-1)

$$PA = (BR)(R_B)(R_C)(R_{XC})(R_D)$$

Aberrancy Base Rate (BR):	0.00012	
Correction Factor for Bridge Location (RB):	1.333	

(AASHTO LRFD 3.14.5.2.3-4)

$$R_B = \left(1 + \frac{\theta}{45°}\right)$$

Angle of Channel Turn (θ):	15	deg
Region Type:	Bend	
Correction Factor for Parallel Current (RC):	1.118	

(AASHTO LRFD 3.14.5.2.3-5)

$$R_C = \left(1 + \frac{V_C}{10}\right)$$

Velocity of Parallel Current (VC):	1.185	knots
Correction Factor for Perpendicular Current (RXC):	1.593	

(AASHTO LRFD 3.14.5.2.3-6)

$$R_{XC} = (1 + V_{XC})$$

Velocity of Perpendicuar Current (VXC):	0.593	knots
Correction Factor for Traffic Density (RD):	1	
Traffic Density:	Low	

VIOB — Presented By: By: The University of Texas at Austin
The Next Generation of Analysis for Vessel Impact on Bridges

Detailed Calculations (Continued):

Geometric Probability Calculations (V2-P2):

Geometric Probability (PG):	0.053714	1/Yrs

(AASHTO LRFD 3.14.5.3-1)

$$PG = NSD(Z2) - NSD(Z1)$$

Normal Standard Distribution at Z1 (NSD(Z1)):	0.673	
Z1:	0.448	
Normal Standard Distribution at Z2 (NSD(Z2)):	0.727	
Z2:	0.603	

$$X_1 = x - \left(\frac{B_P}{2} + \frac{B_M}{2}\right) \qquad X_2 = x + \left(\frac{B_P}{2} + \frac{B_M}{2}\right)$$

$$Z_1 = \frac{X_1}{LOA} \qquad Z_2 = \frac{X_2}{LOA}$$

Impact Pier Width (BP):	4.75	ft

$$B_P = PierWidth \times \cos(\phi) + PierDepth \times \sin(\phi)$$

Pier Width:	4.75	ft
Pier Depth:	4.75	ft
Pier Angle (φ):	0	deg
Vessel Width (BM):	35	ft
Vessel Length Over All (LOA):	257	ft
Distance From Pier CL to Bridge CL (x):	135	ft
User Pier x Distance:	135	ft
User Center Line x Distance:	0	ft

$$x = |UserPier - UserCL|$$

Detailed Calculations (Continued):

Probability of Collapse Calculations (V2-P2) (Continued):

Vessel Impact Speed (V):	9.838	ft / s

Graph axes: V (fps), V_T, (x = 132.625, v = 9.838), V_{min}, XC, XL, x (ft)

Typical Vessel Transit Speed in the Channel (VT):	10.127	ft / s
Minimum Design Impact Speed (VMin):	1.688	ft / s
Distance from Chan. Edge to Vessel Path (XC):	110	ft
Channel Width:	220	ft
3 LOA (XL):	771	ft
Distance From Pier Face to Bridge CL (x):	132.625	ft

VIOB Presented By: The University of Texas at Austin

The Next Generation of Analysis for Vessel Impact on Bridges

Detailed Calculations (Continued):

Probability of Collapse Calculations (V2-P2):

Probability of Collapse (PC):	0.038662	1/Yrs

Graph: PC vs H/P, (H/P = 0.6516982 , PC = 0.038662)

$$PC = 0.1 + 9\left(0.1 - \frac{H}{P}\right)$$

(AASHTO LRFD 3.14.5.4-1)

Ultimate Bridge Element Strength (H):	997	kips
Vessel Impact Force (P):	1529.849	kips
Kinetic Energy (KE):	1975.842	kip - ft

$$KE = \frac{C_H W V^2}{29.2}$$

(AASHTO LRFD 3.14.7-1)

Vessel Displacement Tonnage (W):	567.716	tonne
Hydrodynamic Mass Coefficient (CH):	1.05	
Draft:	9	ft
Underkeel Clearence:	27.7	ft
Draft:	9	ft
Channel Depth:	36.7	ft
User Channel Elevation:	0	ft
User High Water Line:	36.7	ft

Detailed Calculations (Continued):

Vessel 2 - Pier 3

Vessel Frequency Calculations (V2-P3):

Projected Vessel Frequency (N):	812.4	Trips/Yr
Current Vessel Frequency:	677	Trips/Yr
Growth Factor:	1.2	

Probability of Aberrancy Calculations (V2-P3):

Probability of Aberrancy (PA):	0.000285	1/Yrs

(AASHTO LRFD 3.14.5.2.3-1)

$$PA = (BR)(R_B)(R_C)(R_{XC})(R_D)$$

Aberrancy Base Rate (BR):	0.00012	
Correction Factor for Bridge Location (RB):	1.333	

(AASHTO LRFD 3.14.5.2.3-4)

$$R_B = \left(1 + \frac{\theta}{45°}\right)$$

Angle of Channel Turn (θ):	15	deg
Region Type:	Bend	
Correction Factor for Parallel Current (RC):	1.118	

(AASHTO LRFD 3.14.5.2.3-5)

$$R_C = \left(1 + \frac{V_C}{10}\right)$$

Velocity of Parallel Current (VC):	1.185	knots
Correction Factor for Perpendicular Current (RXC):	1.593	

(AASHTO LRFD 3.14.5.2.3-6)

$$R_{XC} = (1 + V_{XC})$$

Velocity of Perpendicular Current (VXC):	0.593	knots
Correction Factor for Traffic Density (RD):	1	
Traffic Density:	Low	

Detailed Calculations (Continued):

Probability of Collapse Calculations (V2-P2) (Continued):

Ship Collision Force on Pier (PS):	NA	kips

(AASHTO LRFD 3.14.8-1)

$$P_S = 8.15 V \sqrt{DWT}$$

Deadweight Tonnage of Ship (DWT):	NA	tonne
Vessel Impact Speed (V):	9.838	ft / s
Ship Damage Depth (AS):	NA	ft

(AASHTO LRFD 3.14.9-1)

$$a_S = 1.54 \left(\frac{KE}{P_S}\right)$$

Kinetic Energy (KE):	1975.842	kip - ft
Ship Collision Force on Pier (PS):	NA	kips
Barge Collision Force on Pier (PB):	1529.849	kips

(AASHTO LRFD 3.14.11-2)

$$P_B = 1349 + 110 a_B$$

Barge Damage Depth (AB):	1.644	ft

(AASHTO LRFD 3.14.12-1)

$$a_B = 10.2 \left(\sqrt{1 + \frac{KE}{5672}} - 1\right)$$

Kinetic Energy (KE):	1975.842	kip - ft

139

The Next Generation of Analysis for Vessel Impact on Bridges

Detailed Calculations (Continued):

Probability of Collapse Calculations (V2-P3):

Probability of Collapse (PC):   0.049025   1/Yrs

(AASHTO LRFD 3.14.5.4-1)

$$PC = 0.1 + 9\left(0.1 - \frac{H}{P}\right)$$

Ultimate Bridge Element Strength (H):	815	kips
Vessel Impact Force (P):	1459.694	kips
Kinetic Energy (KE):	1174.386	kip - ft

(AASHTO LRFD 3.14.7-1)

$$KE = \frac{C_H W V^2}{29.2}$$

Vessel Displacement Tonnage (W):	567.716	tonne
Hydrodynamic Mass Coefficient (CH):	1.05	
Draft:	9	ft
Underkeel Clearance:	11.7	ft
Draft:	9	ft
Channel Depth:	20.7	ft
User Channel Elevation:	16	ft
User High Water Line:	36.7	ft

The Next Generation of Analysis for Vessel Impact on Bridges

Detailed Calculations (Continued):

Geometric Probability Calculations (V2-P3):

Geometric Probability (PG):   0.028937   1/Yrs

(AASHTO LRFD 3.14.5.3-1)

$$PG = NSD(Z2) - NSD(Z1)$$

Normal Standard Distribution at Z1 (NSD(Z1)):	0.872
Z1:	1.135
Normal Standard Distribution at Z2 (NSD(Z2)):	0.901
Z2:	1.286

$$X_1 = x - \left(\frac{B_P}{2} + \frac{B_M}{2}\right) \qquad X_2 = x + \left(\frac{B_P}{2} + \frac{B_M}{2}\right)$$

$$Z_1 = \frac{X_1}{LOA} \qquad Z_2 = \frac{X_2}{LOA}$$

Impact Pier Width (BP):	3.75	ft

$$B_P = PierWidth \times cos(\phi) + PierDepth \times sin(\phi)$$

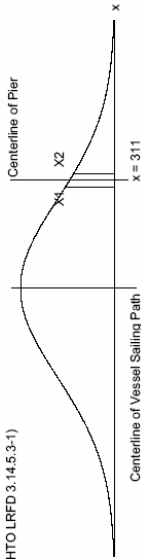|		
Pier Width:	3.75	ft
Pier Depth:	3.75	ft
Pier Angle (φ):	0	deg
Vessel Width (BM):	35	
Vessel Length Over All (LOA):	257	ft
Distance From Pier CL to Bridge CL (x):	311	ft
User Pier x Distance:	311	ft
User Center Line x Distance:	0	ft

$$x = \left|UserPier - UserCL\right|$$

140

VIOB — Presented By: The University of Texas at Austin
The Next Generation of Analysis for Vessel Impact on Bridges

Detailed Calculations (Continued):

Probability of Collapse Calculations (V2-P3) (Continued):

Ship Collision Force on Pier (PS):	NA	kips

(AASHTO LRFD 3.14.8-1)

$$P_S = 8.15\, V \sqrt{DWT}$$

Deadweight Tonnage of Ship (DWT):	NA	tonne
Vessel Impact Speed (V):	7.585	ft / s
Ship Damage Depth (AS):	NA	ft

(AASHTO LRFD 3.14.9-1)

$$a_S = 1.54\left(\frac{KE}{P_S}\right)$$

Kinetic Energy (KE):	1174.386	kip - ft
Ship Collision Force on Pier (PS):	NA	kips
Barge Collision Force on Pier (PB):	1459.695	kips

(AASHTO LRFD 3.14.11-2)

$$P_B = 1349 + 110\, a_B$$

Barge Damage Depth (AB):	1.006	ft

(AASHTO LRFD 3.14.12-1)

$$a_B = 10.2\left(\sqrt{1 + \frac{KE}{5672}} - 1\right)$$
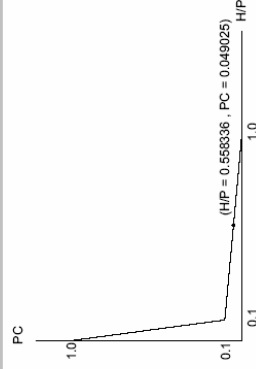
Kinetic Energy (KE):	1174.386	kip - ft

VIOB — Presented By: The University of Texas at Austin
The Next Generation of Analysis for Vessel Impact on Bridges

Detailed Calculations (Continued):

Probability of Collapse Calculations (V2-P3) (Continued):

Vessel Impact Speed (V):	7.585	ft / s

Typical Vessel Transit Speed in the Channel (VT):	10.127	ft / s
Minimum Design Impact Speed (VMin):	1.688	ft / s
Distance from Chan. Edge to Vessel Path (XC):	110	ft
Channel Width:	220	ft
3 LOA (XL):	771	ft
Distance From Pier Face to Bridge CL (x):	309.125	ft

Modeling of Waterway Vessel Impact on Bridge Piers

Adam Cryer
Loukas F. Kallivokas

Executive Summary

The *2001 Interim AASHTO LRFD Bridge Design Specifications* contain design provisions accounting for waterway vessel collisions on bridge piers, as those were adapted from the *1991 AASHTO Guide Specifications and Commentary for Vessel Collision Design of Highway Bridges*. Recent vessel collisions with bridge piers, however, have brought renewed attention to the code specifications, especially in light of the fact that the 1991 AASHTO Specifications draw heavily from two sets of physical experiments conducted two to four decades ago that may not be representative of actual field conditions and may lead to either conservative or inadequate designs.

Among the various aspects of the design specifications, the way by which one estimates the impact force the bridge piers will experience during a collision is clearly of significance to the overall design process. In the current specifications the imparted force is computed through simplified kinetic energy arguments that require a-priori knowledge or an estimate of the vessel bow deformation.

The estimated energy is then transformed to an equivalent static force that is used for design. Such a process, though designer-friendly due to its simplicity, overlooks, amongst other issues, the dynamic behavior inherent in an impact problem.

It is therefore the purpose of this research to provide the framework for obtaining rational estimates of the impact forces a pier may experience during a collision with a waterway vessel. In the absence of a (costly) large-scale experimental program that will allow a field-based comparison of the design provisions, the only path to such estimates is through computational simulations. To this end, this document reports on the finite-element-based modeling of collision events and provides, for a representative field scenario, a comparison between the AASHTO code provisions and the computational results.

Table of Contents

List of Figures

List of Tables

CHAPTER 1

Introduction

1.1 MOTIVATION

Worldwide the number of catastrophic bridge failures due to aberrant vessel impact, though still small, appears to be growing steadily over the last few decades (AASHTO, 1991). In the United States the number of inland vessels traversing the nation's navigable waterways has consistently risen as a result of population growth and the associated commercial activities. It appears that this increased density and frequency of travel has resulted in the observed rise in the number of accidental vessel collisions with highway bridges. Naturally, such accidents are undesirable; from an engineering perspective, the interest is in reducing their impact on a bridge's service life through sound design guidelines.

The current code specifications, intended to prevent catastrophic failure of a bridge or bridge component during a collision event, are based on the 2001 *Interim AASHTO LRFD Bridge Design Specifications* (henceforth referred to as 2001 AASHTO Specifications). As described therein, key provisions pertaining to the calculation of the impact forces during a collision, which are central to the design process, are based on two- to four-decade old physical experiments. The purpose of this work is to provide the framework for studying the impact process computationally, in an attempt to critique and quantify the adequacy of the design specifications.

1.2   VESSEL IMPACT ON BRIDGE PIERS

1.2.1   Background

Over the last few decades several waterway vessel to bridge pier collisions have been reported worldwide. Of these, a few cases really stand out, primarily due to the catastrophic nature of the events. For example, the Sunshine Skyway Bridge case: the bridge, in Florida's Tampa Bay, connects the cities of St. Petersburg and Bradenton. On May 9, 1980, an empty freighter, the *Summit Venture*, collided with the main pier on the southbound side of the span approximately 800 feet off of the center of the channel it was traversing (Fig. 1.1). The impact then triggered the collapse of over 1200 feet of the superstructure, resulting in 35 fatalities. The ship was attempting to pass beneath the bridge in inclement weather when it struck the pier well off of its course. Following the catastrophic collapse, the State of Florida's Department of Transportation (FDOT) funded research over the last ten years, to thoroughly evaluate the design and analysis of bridges that are susceptible to vessel impact.   The Florida DOT's efforts have arguably been the catalyst for further research across the country, including our own investigations.

Figure 1.1 Aftermath of the 1980 Sunshine Skyway Collapse

Three years after the Florida incident, a colloquium was held in Copenhagen, Denmark, by the International Association of Bridge and Structural Engineers (IABSE) to assess the growing problem of vessel-to-bridge collisions. Data submitted by Frandsen (1983) during the colloquium revealed that the number of catastrophic collisions per year worldwide had increased from 0.5 collisions per year in the 1960s to 1.5 per year in the period from 1971-1982. As predicted by many, this rising trend would continue in the following years.

More recently, the Queen Isabella Causeway Bridge, which connects South Padre Island (located in Southern Texas) to the state mainland, suffered massive collapse due to vessel impact (Fig. 1.2, Calzada 2001). A barge tow that had veered from its course impacted one of the piers of the 2.5 mile long bridge in the early morning of September 15, 2001. The 8 people that perished in this tragedy were unaware that anything was out of the ordinary before they drove off into the missing gap of the superstructure, plummeting to the channel below.

The IH-10 Bridge crossing the San Jacinto River shares many similar characteristics with the Queen Isabella Causeway Bridge. The Causeway Bridge's multi-level column supports, separated by lateral beams, reflect similar geometry to the selected IH-10 test bent (Fig. 3.8). This is a popular design among Texas bridges and is one of the primary reasons that the San Jacinto Bridge was chosen for our investigations.
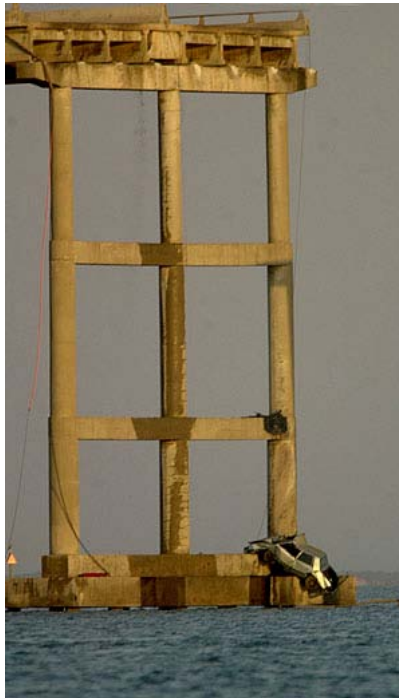
Figure 1.2 Missing section of Queen Isabella Causeway Bridge Superstructure

1.2.2 Design considerations

The current design requirements for vessel collision on bridge components are outlined in Section 3.14 of the 2001 AASHTO Specifications; the specifications therein have been adapted from the *AASHTO Guide Specification and Commentary for Vessel Collision Design of Highway Bridges*, of 1991 (henceforth referred to as 1991 AASHTO Specifications). Whereas the 1991 AASHTO Specifications provided three candidate methods (I, II and III) for designing against potential vessel impact on bridges, only Method II survived in the 2001 AASHTO Specifications. Method II relies heavily on probabilistic analysis for assessing the probability of impact and provides simple expressions for the various parameters of interest to the designer. With respect to the impact forces bridge components will experience, the 2001 AASHTO Specifications

4

provide, for design purposes, relations for two broad categories of vessels, namely, for ships and barges.

The commentary in both the 2001 AASHTO Specifications and the earlier 1991 AASHTO Specifications refers to two sets of experiments conducted in Europe that were used as the basis for establishing the critical relationships that are provided in the 2001 AASHTO Specifications for computing the bow damage length and the impact force on a bridge pier. For ships, the experiments are largely based on the experimental work of Woisin, conducted in Germany in the late 1960s to the mid 1970s (Woisin 1971). It is noteworthy that the focus of Woisin's experiments was not on ship-to-pier collisions, but rather on ship-to-ship collisions; his experiments, at scales 1:12 and 1:7.5, focused on ship-bow-to-ship-hull collisions. Similarly, for barges, the expressions provided for the bow damage length and the collision force are based on the experimental work of Meir-Dornberg, published in German in 1983 (Meir-Dornberg), and later also adopted by IABSE (1983). The Meir-Dornberg experiments were conducted at scales 1:4.5 (dynamic) and 1:6 (static), using a pendulum hammer on barge models. None of the reported experiments included true-scale models.

Thus, in summary, the critical relations entering the guidelines are based on experimental work on scale models conducted twenty to forty years ago that entertained collisions that may not be realistically extrapolated to ship-to-pier or barge-to-pier collisions. It is further noteworthy that, contrary to the now common knowledge of the presence of significant differences between dynamic versus static loading effects, even at the low vessel speeds of interest to the proposed study, the commentary of the 1991 AASHTO Specifications reports that the Meir-Dornberg experiments found no appreciable difference between dynamic and static loading. Thus, in the 2001 AASHTO Specifications, the dynamic effect of an impulse-type force, such as the one exerted on a bridge pier during a collision,

which can effectively double the imparted force's amplitude, is not taken into account. Furthermore, important parameters that may significantly alter the end effect of the collision are similarly not taken into account: for example, whereas in the 1991 AASHTO Specifications, the effect of the impact angle was, to an extent, taken into account (it had a reducing effect on the imparted kinetic energy), it is not accounted for in the 2001 AASHTO Specifications. And though by neglecting the impact angle, from a kinetic energy point of view the 2001 AASHTO Specifications are conservative, they, at the same time, neglect the effect an eccentric to the centerline of the pier force will have on both the pier and the superstructure, even if its amplitude is reduced due to the oblique incidence of the barge to the pier.

The dynamics of a ship-to-pier or barge-to-pier collision are considerably complex: during impact, part of the kinetic energy is imparted on the pier and part of it is consumed into plastic deformation of the barge- or ship-bow. The primary assumption in the 2001 AASHTO Specifications is that the amount of kinetic energy imparted on the pier is equal to the total kinetic energy reduced by the amount consumed in the bow deformation. However, the bow deformation has been calculated based on experiments (e.g. for barges) that used rigid contact surfaces (hammer), which do not account for the complexity of the actual phenomenon (deformable contact surface), thus effectively leading to larger part of the kinetic energy imparted on the pier and, in turn, larger impact forces. There is no consideration in the experiments (and therefore in the 2001 AASHTO Specifications) for local crushing or local pier deformation, or for the energy consumed in the supports of the pier (soil-structure interaction), etc, that effectively will reduce the amount of bow damage and the resulting impact force. The net effect of these omissions is likely a conservative design of the pier due to larger than actual impact forces. Furthermore, during impact (assuming that the

6

vessel is moving with the same velocity even after the initial contact), the vessel will strike the pier multiple times: in a few seconds or fractions of a second, the vessel will strike, bounce off somewhat while still in contact, strike again (smaller energy and smaller force amplitude), bounce off again, and so on and so forth, thus giving rise to a decaying amplitude cyclic loading of the pier. Consideration of these dynamics is absent from the 2001 AASHTO Specifications.

In summary, the limitations of the 2001 AASHTO Specifications we have identified, which may result to either an over- or an under-estimation of the impact forces, emanate from the reliance of the 2001 AASHTO Specifications on scale-model experimental results conducted two to four decades ago that may serve as initial approximations, but nevertheless fail to take into account all the complexities of the impact problem. In the absence of a comprehensive experimental program (the one exception is the on-going experimental program of the Florida DOT), the only remaining avenue for realistic estimation of the pier impact forces is a computational approach. Such an approach allows for the parametric consideration of all parameters of importance to the determination of the pier impact forces (flexible-to-flexible contact, time-dependent behavior, inelastic bow deformation, effect of the pier foundation, effect of the surrounding water, impact angle, vessel velocity and real geometry, etc). This work is based on such an approach without, however, taking into account all possible parameter combinations. This study is meant to provide a preliminary estimate of the impact forces for a prototype bridge in order to allow for the ready comparison with the forces provided in the 2001 AASHTO Specifications.

1.2.3 The Florida DOT experiments

Finite-element-based modeling was selected as the primary tool for the analysis in this project because of the method's flexibility and ability to provide

reasonable approximations to physical problems. As with any approach, the reliability of the model had to be calibrated against known results to ensure sufficient fidelity. The recent studies by the University of Florida (UFL) were available for such a comparison. UFL's work included both full-scale physical tests and numerical computations of vessel-to-pier impact (Consolazio 2005).

Until recently, very few full-scale tests had been conducted to examine the impact loads that a bridge element experiences during a collision event. Even the data that were available dealt primarily with ship collisions and rarely focused on barge impact, which is of primary interest here. However, in March and April of 2004, the first known impact tests using a full-scale barge against a bridge pier were carried out for the State of Florida.

The St. George Island Causeway Bridge, located in northwestern Florida, was recently replaced with a newly constructed bridge, which opened in February 2004. This new construction created a unique opportunity to use two of the piers on the existing substructure of the bridge for full-scale impact tests. Both piers were outfitted with impact load cells and high-speed data acquisition systems to properly measure the dynamic nature of the loads that they were to be subjected to. Tests were performed both with and without the superstructure mounted atop the piers to examine the damping/stiffening effects that the overhead spans typically provide.

Figure 1.3 Florida DOT's impact test on Causeway pier to be demolished

Tugboats were utilized to give the barge an initial velocity and simultaneously guide it into direct impact with the bent, as shown in Figure 1.3. Care was taken to ensure that the tugs were no longer imparting any force to the vessel at the time of impact. This monitoring was essential to prevent any external forces, aside from that of the surrounding water, from being included in the data recordings. The tests were carried out at a variety of speeds, although velocities above 4 knots were generally avoided to prevent extensive damage to the barge and to the load cell equipment. This limitation was included to expedite the subsequent repair of the barge after testing so that it could be returned to a usable condition. In addition, portions of the removed superstructure deck were placed on the barge for a subset of the tests to simulate partially-loaded scenarios (Consolazio 2005).

In order to predict the magnitude of forces that the Causeway-experiment piers would experience, and hopefully prevent excess barge damage, the University of Florida created a finite element model simulating the full-scale tests before the testing actually occurred (Consolazio 2002). These finite element

simulations were similar in nature to the simulations that are reported herein, so much was gained by comparing and contrasting data from the two projects. Our research was aimed at defining a more generalized procedure for bridge analysis, as opposed to the modeling of one particular system. In seeking more breadth than depth for the procedure, some of the computationally expensive details that the UFL model focused on are not included in our parametric studies. Chapter 4 includes a discussion and comparison between our results and those obtained by the UFL model.

1.2.4   Present scope – Modeling elections

The primary focus of this work is the estimation of the impact forces on a prototype bridge pier using computational simulations. The goal is to be able to compare for a prototype scenario (vessel type, vessel velocity, angle of attack, specific pier geometry, etc.) the impact force computed using the 2001 AASHTO Specifications against the one predicted computationally.

To this end, we chose the jumbo hopper barge as the prototype vessel, since it is the most frequently employed type of inland cargo vessel across the country. It is generally used to haul cargo in a modular fashion and requires the assistance of standard tug boats for its maneuvering since it has no power of its own.

We chose the eastbound section of the Interstate-10 Bridge at the San Jacinto River in Houston, Texas as the prototype bridge since its primary characteristics are commonly encountered among Texas bridges: its bents are anchored below the water surface and have two tiers of columns separated by a beam at mid-height, as well as a top beam supporting the superstructure. The base of the bents consists of a pier cap poured atop a number of pre-cast concrete

piles, as shown in Figure 1.4 (the drawing was taken from a copy of the original set of plans for the bridge).
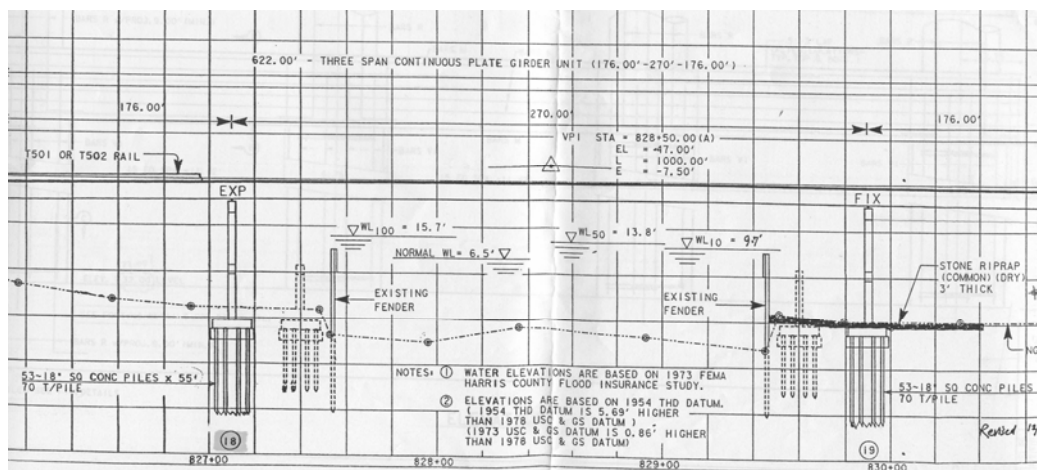
Figure 1.4 IH-10 San Jacinto Bridge schematic profile

The typical water height, as well as several high-water elevations corresponding to different return periods, is also included on the bridge profile. The water elevations result in impact locations along the span of the first column on the top tier of the bent.

To conduct the numerical simulations, we chose ANSYS, a general-purpose commercial finite element software package. ANSYS is seamlessly integrated with LS-DYNA, the most-widely used software for impact analysis, originally developed at the Lawrence Livermore National Laboratory; LS-DYNA provided the main computational engine of our simulations.

1.3   REPORT ORGANIZATION

Chapter 2 discusses the 2001 AASHTO Specifications currently being used for the majority of bridge designs in the United States. This review includes

a look at the theoretical foundation for the methodology used in the Specifications, as well as a breakdown of the Method II criteria for determining annual frequency of collapse. Chapter 3 reviews all considerations taken into account for the finite element modeling process. Contact component geometries, mesh and material properties, initial conditions, and boundary conditions are described, amongst other key items. The chapter also pinpoints the most important parameters for modeling vessel-to-pier impact phenomena and the respective values that we assumed for our trial computations. Chapter 4 presents the results of our modeling efforts and illustrates the effect of the key parameters on the response of the pier to vessel impact. Convergence of tests, equivalent static load calculation procedures, and information concerning calibration of our model against previous models are also presented. We also include animations and stress contours of the impact process to allow a quick visual assessment of the collision event. Chapter 5 provides a summary of our findings and discusses recommendations for further research.

CHAPTER 2

Review of Current Design Specifications

2.1 INTRODUCTION

Current code provisions aim at the estimation of the risk of catastrophic bridge collapse by requiring that designers consider the impact forces resulting from vessel collisions. Accordingly, "failure" of a bridge is defined as the loss of use resulting from a vessel collision, which may occur well before collapse. The calculation of the probability that a bridge will fail requires the consideration of many variables. Currently, the probability is calculated by taking into account the probability of failure of individual bridge components under impact loading. To calculate the individual probabilities, the force generated by a typical vessel colliding with a particular member of the bridge system must be calculated. In the 2001 AASHTO Specifications, the calculations are based on energy conservation principles, which in turn are based on expressions derived from scale-model experiments performed two to four decades ago. Below, we review these experiments and discuss the associated code provisions.

2.2 WOISIN EXPERIMENTS

In the late 1960s and early 1970s, scale-model vessel collision tests were carried out in Hamburg, (West) Germany by Woisin (1971). These investigations assisted in the development of measures to protect the reactors contained within nuclear submarines from ship-to-ship collisions. There were 12 ship models built at scales of 1:12 and 1:7.5. Each model consisted of two components, a ship bow model and a ship side hull model, as shown in Figure 2.1 (1991 AASHTO Specifications).

13
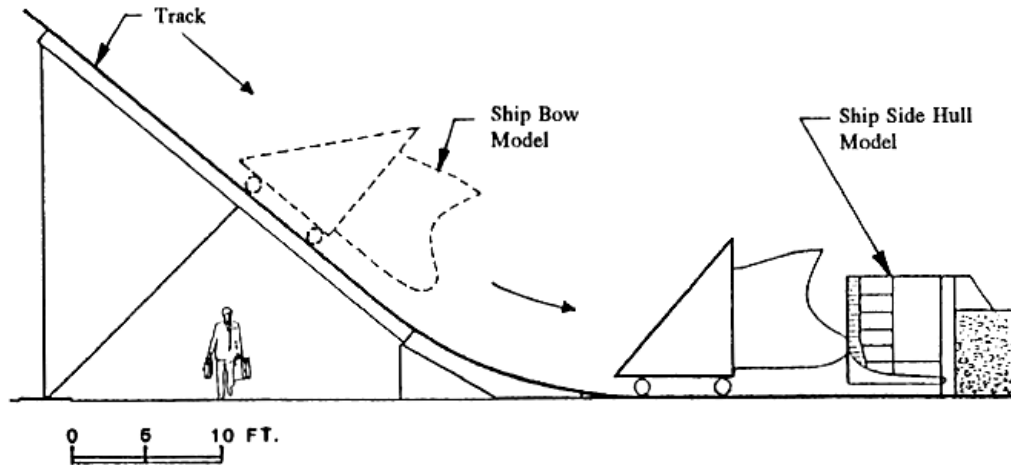
Figure 2.1 Woisin's ship model collision setup

In total, 24 collision tests were performed and collision force data were collected to produce force histories for each test. Unfortunately, issues with the electronic measuring equipment and vibrations during the test prevented accurate depictions of the force time-histories. However, Woisin was able to compute the impact force *P(a)* in an average sense by dividing the kinetic energy that was dissipated during the collision by the bow damage depth *a*, measured at the conclusion of each test. He then developed the following relationship between the mean impact force over time, *P(t)*, and the mean impact force over damage depth, *P(a)*:

$$P(t) = 1.25 \times P(a) \tag{2.1}$$

Woisin observed a ±50% scatter in the data when compared to Equation 2.1; he then evaluated the key factors that he subjectively determined were

14

influencing the magnitude of the mean impact force.   In descending order of importance, they were: ship size dead weight tonnes (DWT), ship type, bow characteristics, ballast water, and impact speed.   The scatter that these main variables produced was approximated as a triangular probability density distribution by Woisin, shown in Figure 2.2 (1991 AASHTO Specifications).
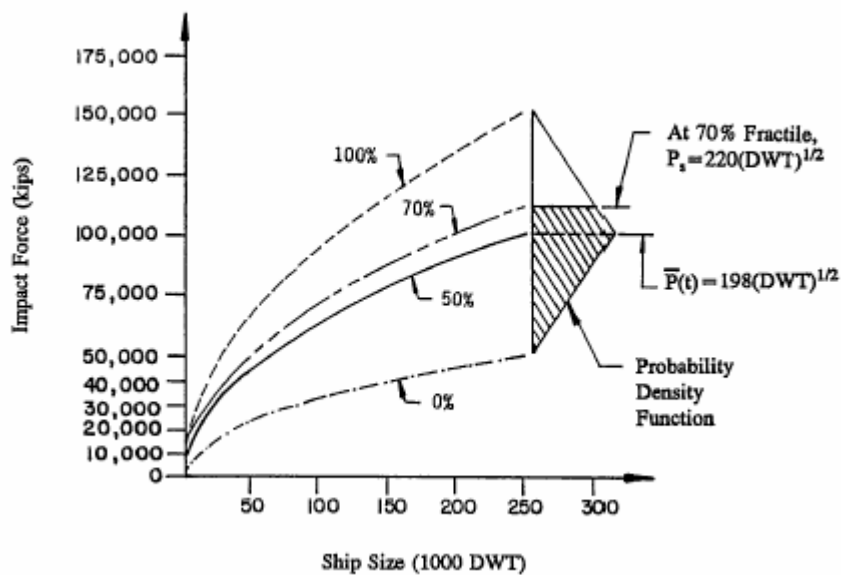
Figure 2.2 Probability density function of impact force (Woisin experiments)

Notice that the 0% and 100% fractile lines represent the upper and lower bounds of the ±50% estimated scatter about the mean impact force. From the data, Woisin developed an expression for the mean ship impact force over the duration of the collision (Equation 2.2).

$$P(t) = 198(DWT)^{\frac{1}{2}} \pm 50\% \quad \text{(kips)} \qquad (2.2)$$

It should be noted that Equation 2.2 was developed for bulk carriers, over 40,000 DWT, colliding with a rigid body at approximately 16 knots. This was originally the result of work done by Saul and Svensson (1980). Reviewers of the Woisin results, during the development of the AASHTO *Guide Specification and Commentary for Vessel Collision Design of Highway Bridges* in 1991, made a few adjustments to this basic equation. First, the reaction force *P(t)* was effectively reduced for collisions at impact speeds less than 16 knots, using the reduction factor *V*/27, where *V* denotes the vessel's velocity. The restrictions proposed earlier by Woisin with respect to vessel size and type and to the minimum impact speed of 8 knots, were eliminated. However, AASHTO warns that Equation 2.2 will be less accurate for circumstances that vary greatly from Woisin's test parameters, e.g., forces will be underestimated for impact at very low speeds. Moreover, to avoid the complications of using an envelope associated with the density function, a single equation was developed using the 70% fractile (as shown in Equation 2.3). This procedure results in an 11% increase over the mean impact force found from Woisin's observed data scatter (V, below, is expressed in feet per second (AASHTO, 1991)).

$$P(t) = 220(DWT)^{\frac{1}{2}}\left(\frac{V}{27}\right) \qquad \text{(kips)} \qquad\qquad (2.3)$$

The code allows the use of Equation 2.3 for all design calculations but cautions on its accuracy. As the design conditions vary from Woisin's testing conditions (speed, DWT, etc.), the results too will vary. The code suggests extrapolation be used in evaluating impact forces using Equation 2.3 and that further research is required to create a more accurate and appropriate expression.

16

It is interesting to note that Equation 2.3 is based on ship capacity rather than the actual load the ship is carrying. Thus, it does not account for a worst-case scenario (maximum kinetic energy). In fact, Woisin noticed that when a ballasted ship, of the same geometry and volume, was used in place of a loaded ship, the reduced mass did not result in a reduction of the impact forces. He deduced that when a ship is ballasted the water that has filled the bow tanks provides an increased stiffness to the hull and prevents energy loss associated with bow deformation. The result is a trade-off between ballast and load that renders the ship's cargo loading essentially irrelevant (AASHTO, 1991).

The use of Equation 2.3 implies that a weighted average impact force is being used to determine design impact forces. For some this might cause concern as the actual (dynamic) impact force is larger than the estimate provided by Equation 2.3. This 70% fractile force takes into account the high end of the scatter while avoiding being overly conservative. Nevertheless, the force is applied as an equivalent static load.

2.3 MEIR-DORNBERG EXPERIMENTS

At the time that the 1991 AASHTO Specifications were written, it was decided that the studies conducted by Meir-Dornberg (1983) in (West) Germany during 1983 provided a good foundation on which to base the code provisions. The original experiments were carried out to find out what happens when barges collide with bridge substructures.

Accordingly, three scale-models of barge bottoms were created. The models were built based on the characteristics of a standard European barge and were subsequently subjected to the impact of a pendulum hammer. Two expressions, dependent on the length of damage to the bow, were then derived from the physical tests.

17

For $a_B < 0.34$, $P_B = 4,112\,a_B$ (2.4)

For $a_B \geq 0.34$, $P_B = 1,349 + 110a_B$ (2.5)

where,

a_B = barge bow damage length, inches

P_B = equivalent static barge impact force, kips

A factor of $R_B = B_B/35$ (where B_B represents the beam of a European barge) was later added to the original equations to account for the difference between the European and jumbo barge beams. This factor effectively assumes a linear relationship between the barge width and the magnitude of the impact force. However, the 2001 AASHTO Specifications do not include this additional factor, citing the minimal difference between the European and standard hopper barge bow dimensions.

The barge bow damage length parameter a_B implicated in Equations 2.4 and 2.5 was calculated/estimated based on energy conservation arguments. Specifically, Equation 2.6 below estimates the deformation length using a transformation of the kinetic energy to deformation energy of the vessel bow.

$$a_B = 10.2\left[\left(1 + \frac{KE}{5672}\right)^{1/2} - 1\right] \qquad \text{(ft)} \qquad (2.6)$$

where,

$$KE = \frac{C_H m(V)^2}{2} = \frac{1}{2}C_H\frac{2.205(W)}{32.2}V^2 = \frac{C_H W V^2}{29.2} \qquad (2.7)$$

m = mass of vessel, kip-sec^2/ft

g = acceleration of gravity, ft/sec^2

W = vessel displacement tonnage, tonne

V = vessel impact speed, ft/sec

C_H = hydrodynamic mass coefficient, dimensionless

KE = kinetic energy, kip-ft

Equation 2.7 is the basic equation for the calculation of the kinetic energy, modified by the hydrodynamic mass coefficient (see below for a discussion). It should be noted that W represents the actual loading of the vessel at the time of impact. The 1991 AASHTO Specifications assume that the crush depth (deformation energy) is directly related to the pre-impact kinetic energy of the vessel. The size of the bow deformation is then directly correlated to the force required to create it. Figure 2.3, from the University of Florida research (Consolazio 2005), illustrates the relationship between bow crush depth and resultant impact force (per AASHTO, 1991). As it can be seen, at 4 inches of crush depth, buckling of internal bow trusses near the contact zone has occurred and the bow's stiffness reduces significantly.
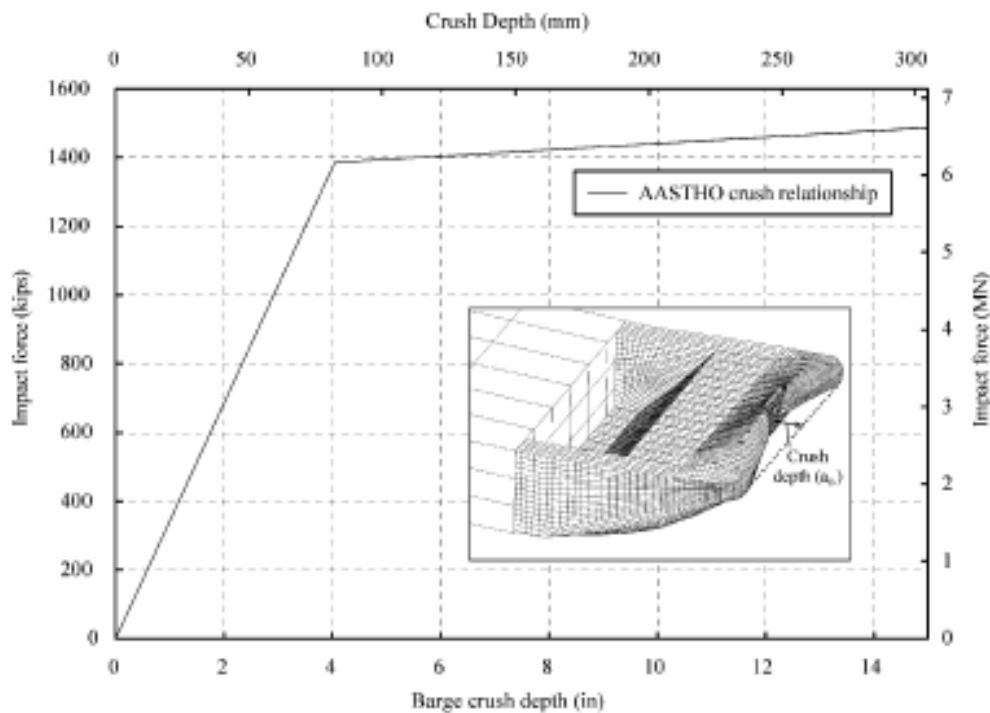
Figure 2.3 AASHTO Relationship for impact force versus bow crush depth

The C_H term appearing in Equation 2.7 accounts for the effect of the surrounding water on the collision forces (AASHTO, 1991). Specifically: when a solid body moves through a fluid, it displaces the fluid that lies in its path. To conserve mass, fluid is constantly filling the void the moving body leaves behind. The moving mass of water has its own inertia which is transferred to the rear of the body upon an abrupt change in its velocity. The result of this effect is an amplification of the impact force in the direction of motion. The 2001 AASHTO Specifications recommend that forces be multiplied by a factor C_H that lies somewhere within the range of 1.05 to 1.25, as determined by Saul and Svensson (1980). Higher values represent a large amount of water being displaced relative to the overall size of the vessel. For design purposes, the code assigns this factor

by considering the distance from the bottom of the vessel (underkeel) to the bottom of the channel through which the vessel is traveling. The 2001 AASHTO Specifications recommend a value of 1.05 for vessels with large underkeel clearances ($\geq 0.5 \times$ draft). The 'draft' value is equal to the depth of the loaded vessel in the water. A value of 1.25 is given for vessels with small underkeel clearances ($\leq 0.2 \times$ draft). Values falling between the two extremes are calculated through interpolation.

2.4 AASHTO GUIDE SPECIFICATION – METHOD II

Current code provisions require the selection of a "design vessel" for analysis of a bridge's impact resistance. This procedure, as well as many of the other provisions found in the code, was introduced in the report by Modjeski and Masters in 1984 concerning vessel impact in Louisiana waterways (Modjeski 1984). The 1991 AASHTO Specifications provide three methods (Methods I, II, and III) for designing a bridge while taking into account potential vessel impact. Methods I and III involved a semi-deterministic procedure, and a cost-effectiveness analysis procedure, respectively. Method II was the more thorough, probability-based analysis procedure for selecting a design vessel. The latter was the only method to survive and be offered in the 2001 AASHTO Specifications.

2.4.1 Acceptance criteria

The 2001 AASHTO Specifications require that the designer group bridges into one of two available Importance Categories. Bridges that must continue to serve some function after a collision are classified as *critical*. All other bridges are designated as *regular*. Accordingly, bridges are then assigned an allowable probability of collapse. The acceptable risk for *critical* bridges is equal to or less than 0.01 in 100 years, or an annual frequency of 1 in 10,000. For *regular* bridges, the rate is 0.1 in 100 years, or an annual frequency of 1 in 1,000. These

21

probabilities represent the chance that the bridge will fail as a whole. As a result, the acceptable annual frequency should be distributed throughout the elements of the bridge that are susceptible to impact. This only includes the elements that lie within a distance equal to 3 times the overall length of the barge tow (LOA) outside of the transit path centerlines, as prescribed by the 2001 AASHTO Specifications.

2.4.2 Annual frequency of collapse

The probability that any bridge element will fail in a given year is given by Equation 2.8.

$$AF = (N)(PA)(PG)(PC) \tag{2.8}$$

where,

AF = annual frequency of bridge element collapse due to vessel collision

N = annual number of vessels classified by type, size, and loading which can strike the bridge element

PA = probability of vessel aberrancy

PG = geometric probability of a collision between an aberrant vessel and a bridge pier or span

PC = probability of bridge collapse due to a collision with an aberrant vessel

2.4.2.1 Vessel frequency distribution, N

For each bridge site, a distribution of the frequency with which each vessel traverses the waterway is required. This parameter N must be determined for each bridge element by type of vessel, its size, the typical water depth at that bridge element, whether the vessel is loaded or ballasted, and in some cases the

direction of travel. The water depth used for design is measured up to the annual mean high water level, as a minimum. Future changes in the vessel frequency should be taken into account for the estimated bridge service life.

2.4.2.2   *Probability of aberrancy, PA*

In determining the likelihood that a vessel will be involved in a collision with a pier, one must first decide what the chance is that the vessel will depart from its intended path of travel.   The likelihood that it will wander, or become aberrant, is found by examining recorded data along the waterway in question. Typically, whenever accidents occur in water they are recorded by the NTSB (National Transportation Safety Board), the corresponding waterway authority, or some other agency. But, often times the recorded data, if they exist at all, may be inaccurate.

To provide an alternative means for calculating the probability of aberrancy, the 2001 AASHTO Specifications allow this probability to be approximated using Equation 2.9 below.

$$PA = BR(R_B)(R_C)(R_{XC})(R_D) \qquad\qquad (2.9)$$

where,

PA = probability of aberrancy

BR = aberrancy base rate

R_B = correction factor for bridge location

R_C = correction factor for current acting parallel to vessel transit path

R_{XC} = correction factor for crosscurrents acting perpendicular to vessel transit path

R_D = correction factor for vessel traffic density

Base rate, BR

This is a statistical value determined from historical data of the typical rate of aberrancy on a number of U.S. waterways. The rate is set at 0.6×10^{-4} events/year for ships and 1.2×10^{-4} events/year for barges. This number is then modified by the factors discussed below to yield the final aberrancy rate specific to a given waterway at a specific location.

Bridge location

Often times the location of a bridge within a waterway can be an influential factor in whether an accident is likely to occur. Geometric characteristics, such as a turn or bend in the channel, will make maneuvering through the bridge piers much more difficult. As barge tows grow in size they become more difficult to steer. In addition, channel currents only compound the problem and tend to force tows on a tangent from their regular transit path.

The 2001 AASHTO Specifications provide modification factors, depending on the severity of the turn or bend, which range between 1.0 and 2.0. A factor of 1.0 represents any straight portion of the waterway. The closer a bridge is located to a turn and the greater the angle of the turn is, the greater the location factor is.

Current effects

At locations where currents are strong the reaction time an operator has to prevent a collision is considerably diminished. This difficulty is accounted for in the 2001 AASHTO Specifications through two independent factors. First, the current is resolved into two components, namely, one acting parallel to and one perpendicular to the direction of vessel travel.

The correction factor for parallel currents, R_C, is computed using Equation 2.10. By examining the equation we can see that a current of 10 knots effectively doubles the probability of aberrancy for the vessel. For comparison, the typical travel speed for the vessel in our research was 5.83 knots. Using the 2001 AASHTO Specifications this results in an R_C factor of 1.583.

The correction factor for currents perpendicular to the direction of vessel travel, R_{XC}, is computed using Equation 2.11. Clearly, the correction factor R_{XC} is greater than R_C for the same current velocity. The difference between the influence the two factors have on the probability of aberrancy can be easily understood when one considers the difficulty of maneuvering a vessel that is being pushed by a strong current in a direction perpendicular to its direction of travel.

$$R_C = \left[1 + \frac{V_C}{10} \right] \qquad (2.10)$$

$$R_{XC} = \left(1 + V_{XC} \right) \qquad (2.11)$$

where,

V_C = current component parallel to vessel path, knots

V_{XC} = current component perpendicular to vessel path, knots

Vessel density

This factor is a little more subjective than the others in that it requires the engineer to categorize vessel traffic. The goal is to determine how much clutter of vessels there is in the immediate vicinity of the bridge on a daily basis. Consideration is given to how often vessels meet, pass, and overtake each other

near the bridge. The bridge is then categorized as either low density ($R_D = 1.0$), average density ($R_D = 1.3$), or high density ($R_D = 1.6$) and the appropriate factor is then included.

2.4.2.3   *Geometric probability, PG*

Once a vessel has become aberrant, the likelihood that it will come into contact with a bridge element must be determined. This would be virtually impossible to do on a case-by-case basis, and thus the 2001 AASHTO Specifications suggest a distribution based on historical data from across the U.S. This conditional probability was most accurately represented by a normal distribution. The 2001 AASHTO Specifications assume the standard deviation σ of the distribution to be equal to LOA (the overall length of the ship or barge tow). The mean of the distribution μ is correlated with the centerline of the vessel travel path. The corresponding geometric probability is then represented as the area under the normal distribution from the centerline of the pier to a distance, perpendicular to the travel path, equal to half of the pier width plus the vessel beam. Figure 2.4 (AASHTO, 1991) gives a graphical representation of this calculation for clarification.
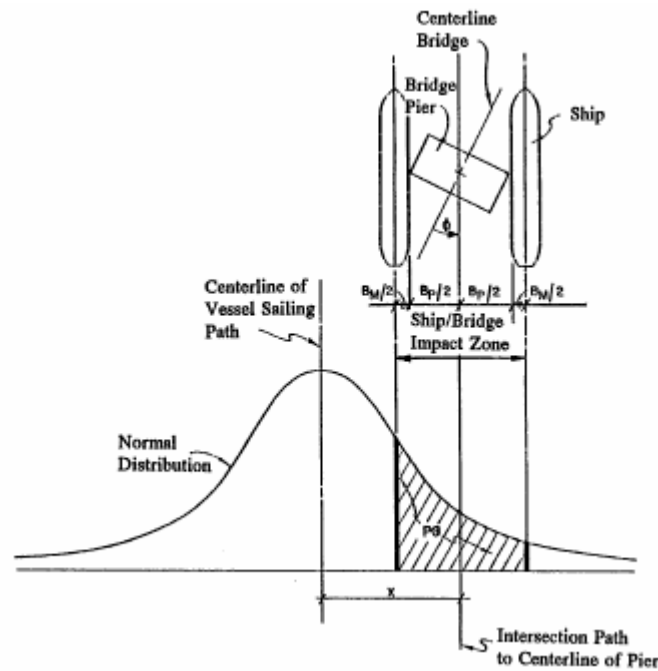
Figure 2.4 Schematic of geometric probability tabulation

2.4.2.4 Probability of collapse, PC

Once it has been determined that a collision is imminent, i.e. the vessel is aberrant and will impact the structure, the question remains whether catastrophic failure will be the final result. In most cases, the collision only results in minimal damages to the barge and/or bridge structure. So the probability that a collapse will indeed occur is calculated from either Equation 2.12, 2.13 or 2.14.

$$\text{for } 0.0 \le H/P < 0.1, \quad PC = 0.1 + 9\left[0.1 - \frac{H}{P}\right] \tag{2.12}$$

$$\text{for } 0.1 \le H/P < 1.0, \quad PC = \frac{1}{9}\left[1 - \frac{H}{P}\right] \tag{2.13}$$

27

for $H/P>1.0$ $\qquad$ $PC=0$ $\qquad$ (2.14)

where,

PC = probability of collapse

H = ultimate bridge element strength, kips

P = vessel impact force imparted to bridge element, kips

This bilinear relationship (Fig. 2.5) was the product of Woisin's ship-to-ship collision experiments, described in Section 2.2. The value H represents the resistance that a bridge element can develop before reaching failure. However, the way in which this number is calculated is not prescribed by the 2001 AASHTO Specifications. So the method for choosing this single parameter is left in the hands of the designer. Since this value has significant impact on the probability of collapse calculation, an objective approach is needed to determine the ultimate bridge element strengths.
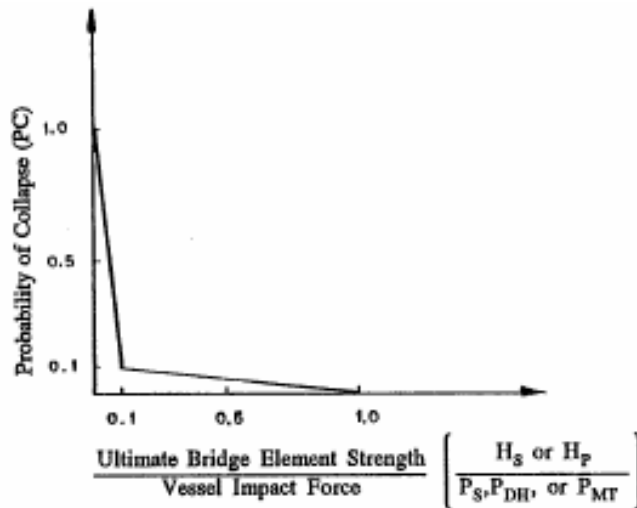
Figure 4.8.3.4-1. Probability of Collapse Distribution.

Figure 2.5 AASHTO graphic for probability of collapse determination

One of the primary goals of this study was to replace this overly simplistic curve with criteria that are more accurate for each particular bridge system being investigated. In our studies, the lateral resistance of the pier is determined by considering multiple parameters that directly factor into its strength and stiffness properties. By using data for the particular waterway and performing numerical simulations to include multiple parameter values, the true likelihood of element failure is better captured.

CHAPTER 3

Modeling Considerations

3.1 INTRODUCTION

A primary goal of this study is the calculation of the force imparted on a bridge pier during a collision, in an attempt to compare computational results with the current code provisions, which were primarily based on physical experiments. Prior to comparing our results with the estimates of the code provisions, we also attempted to calibrate/validate our models with the published data/modeling recently completed at the University of Florida (UFL) (Consolazio 2005). We chose to model the impact using finite elements. The complexity associated with the task is considerable: there is contact between two deformable surfaces, the problem is time-dependent and three-dimensional, the material behavior is non-linear, there is uncertainty or variability associated with the boundary conditions, there are hydrodynamic and soil-structure interaction effects to be accounted for, etc. To keep the modeling within the preliminary nature of this study's scope, a number of simplified assumptions were made. These modeling considerations are discussed in the sections that follow.

For all the simulations reported herein we used the commercial finite element package ANSYS. To allow for parametric studies, we opted to bypass the graphical user interface of ANSYS and instead used the ANSYS command structure to create parametric input files that could be repeatedly executed. These files are provided in Appendix C. The actual elements and solution engine for the simulations were provided by LS-DYNA. In fact, ANSYS provides a wrap

around LS-DYNA, long-dominant in crash-type simulations, that we exploited to parameterize the modeling.

3.2   Vessel Modeling

3.2.1   General assumptions

A standard jumbo hopper barge was chosen as the typical vessel for our simulations because it is the most frequently used barge type for inland waterway transportation of goods. This type of vessel is used both in single and in multiple barge tow configurations and is usually propelled with the assistance of a tug boat. Typically, during a collision event, barge tows break apart. Therefore, for our purposes, the model was setup assuming impact from one barge driven by one tug boat. Moreover, since modeling the tug boat would have added unnecessary complexity without appreciable difference in the results, it was eliminated from the modeling. However, the mass contributed by the tug boat was represented via an increase in the mass of the barge (Section 3.6.5 discusses how the tug boat mass and the cargo mass were included in the model). Due to the preliminary nature of this study we chose to neglect gravity and buoyancy effects.

3.2.2   Geometry

The overall dimensions and capacity of the jumbo hopper barge were taken directly from the 2001 AASHTO Specifications (Fig. 3.1).

PLAN

ELEVATION

			Jumbo Hopper	Oversize Tank	Special Deck
L_B	=	length (feet)	195	290	250
B_M	=	width (feet)	35	53	72
D_V	=	depth of vessel (feet)	12	12	17
D_E	=	empty [light] draft (feet)	1.7	1.7	2.5
D_L	=	loaded draft (feet)	8.7	8.7	12.5
D_B	=	depth of bow (feet)	13	13	18
R_L	=	bow rake length	20	25	30
H_L	=	head log height (feet)	2-3	2-3	3-5
C_C	=	cargo capacity (tons)	1700	3700	5000
W_E	=	empth displacement (tons)	200	600	1300
W_L	=	loaded displacement (tons)	1900	4300	6300

Figure 3.1 Typical jumbo hopper barge geometry

The finer geometric features of the barge were simplified. For example, the oblique angles at the ends of the barge were straightened to lessen the meshing demands. The plates forming the exterior of the vessel were all modeled with a realistic 3/8" thickness. This thickness was used to accurately depict the plate properties at the bow. The 3/8" value was used all around the vessel, for simplicity, and to avoid stress discontinuities at the transition zones between different sections of the vessel. The top and bottom of the bow, as well as the headlog, were all modeled using 3/8" thick shell. The internal trusses that serve to stiffen the bow were modeled using thin steel plates (an approximation to the actual geometry (Fig 3.2)). The plate stiffeners were modeled at a spacing of 2'-6" on-center (somewhat larger than the actual truss spacing which is 2'-2" on-

33

center). We used the thickness of the plate stiffeners as a parameter to properly calibrate the overall stiffness of the bow through comparisons with the UFL computational and physical models.
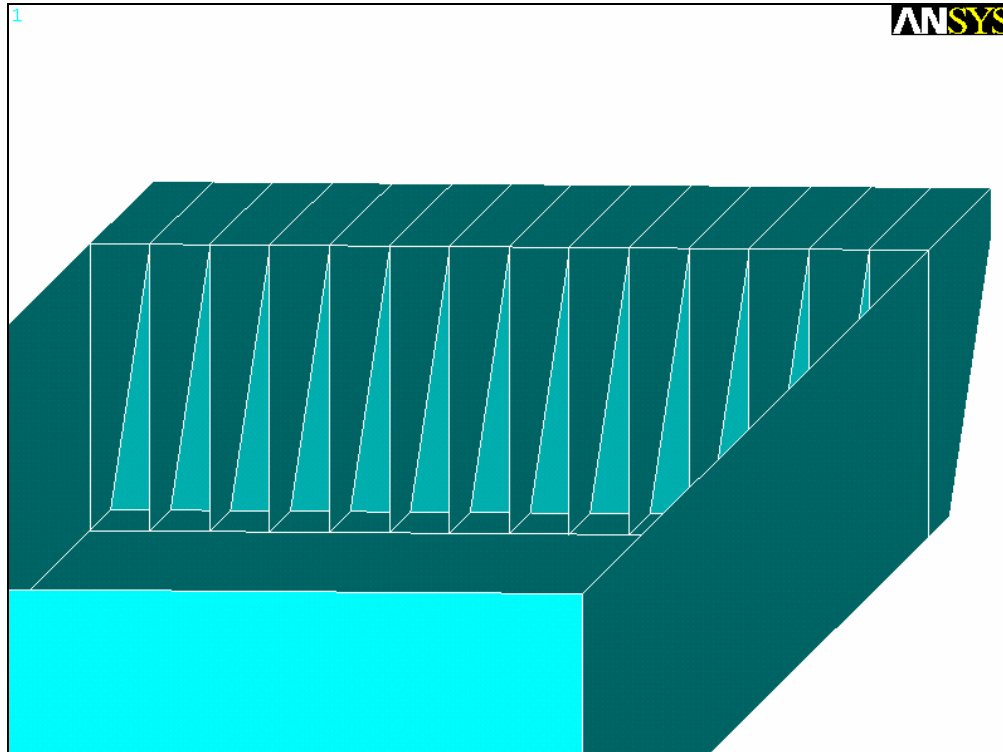
Figure 3.2 Jumbo hopper barge plate bow stiffeners

3.2.3   Meshing

Unstructured meshes were used for the discretization of the solid model. We used both 3D solid elements (SOLID164), and 2D shell elements (SHELL163).   Both element types are linear (trilinear hexahedron, bilinear quadrilateral, linear tetrahedron, and linear triangles).   Wherever possible, hexahedra/quadrilateral elements were preferred over tetrahedral/triangular

elements. At the expected contact regions we refined using an adaptive approach that allowed for a smooth transition to a coarser mesh away from the impact zone (Fig. 3.3, 3.4). Care was taken to satisfy all ANSYS internal shape quality criteria.
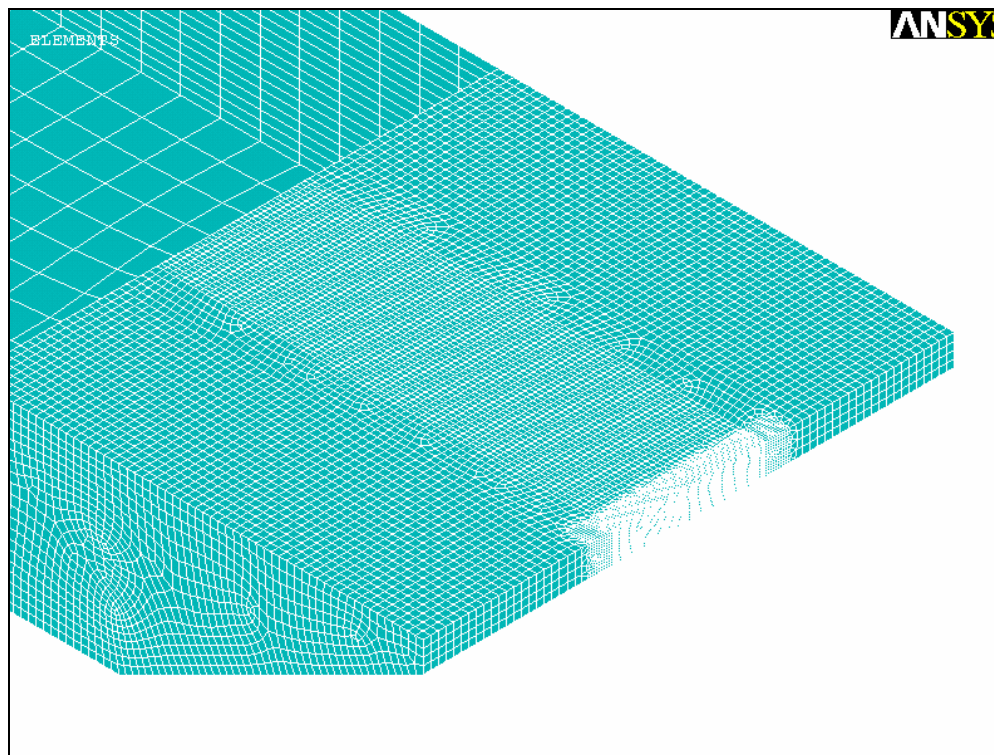
Figure 3.3 Jumbo hopper barge bow mesh
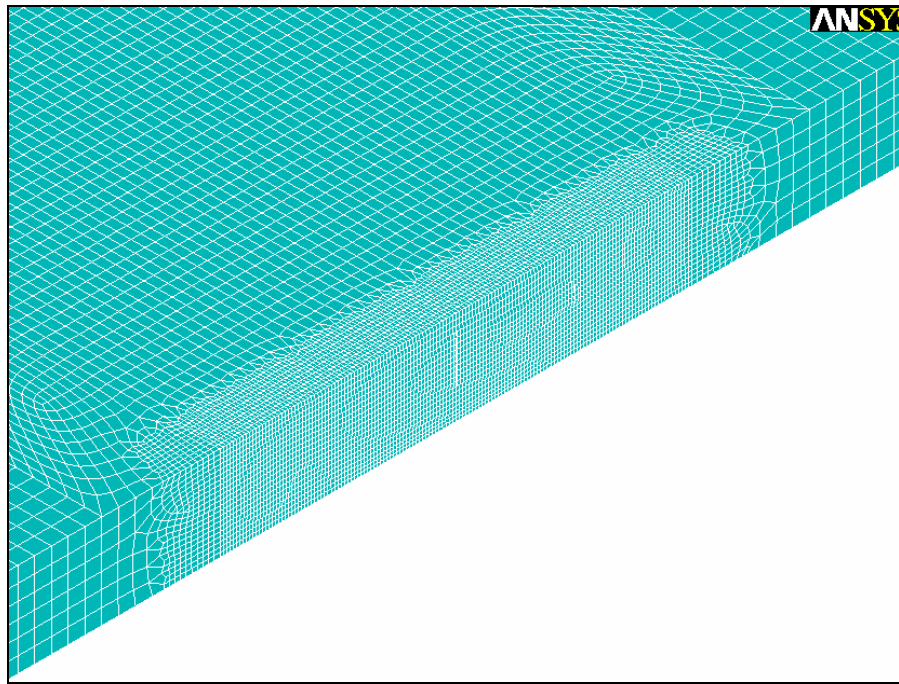
Figure 3.4 Jumbo hopper barge mesh at headlog
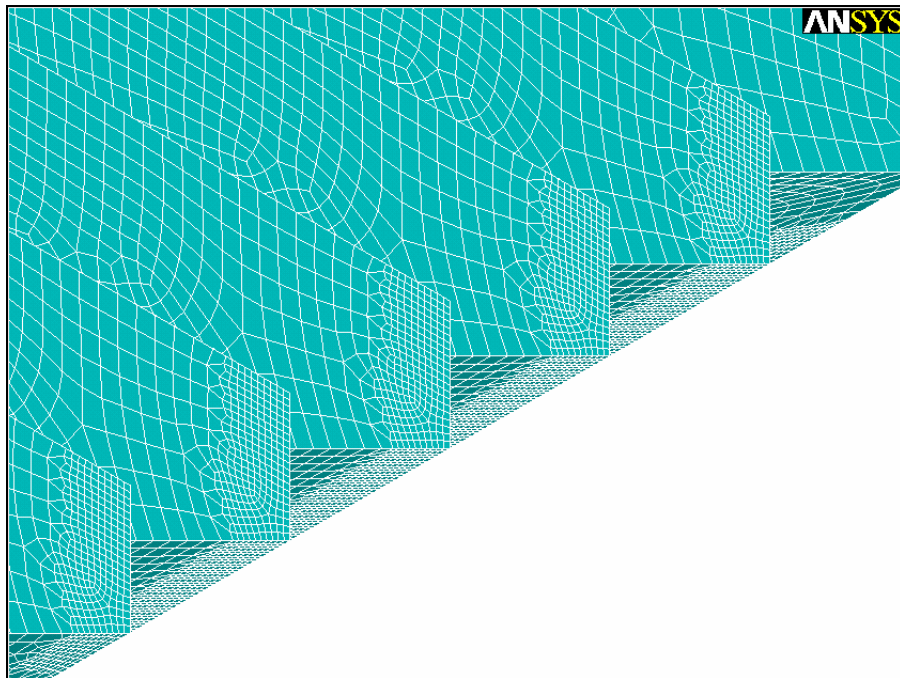
Figure 3.5 Jumbo hopper barge mesh - stiffeners at headlog

3.2.4 Material properties

To determine the geometry and material properties of the jumbo hopper barge, a standard hopper barge fabricator in the United States was contacted: upon consultation with the fabricator, we chose A36 steel as the material model for modeling the entire barge (Basci 2005). Although different material grades may have been introduced in recent years, the majority of jumbo hopper barges in operation are relatively old and were built while A36 steel was the dominant material used for vessel construction. Several material models were examined for replication of the A36 steel properties, including models with linear elastic and bilinear kinematic hardening behavior. However, the final model chosen was a piecewise linear plasticity model with strain hardening effects. This model allowed for the most accurate depiction of material behavior, which was desirable since the material properties had a significant impact on the results. To allow for calibration/validation of our results with the UFL model we chose the same (true) stress/strain curve (Consolazio 2002) as the UFL study (Fig. 3.6).

The piecewise linear plasticity model required input of discrete stress and strain values; ANSYS interpolates (linearly) between the entered data points to retrieve values along the curve. In addition, ANSYS requires the data be input as effective plastic strain ε_P versus total true stress σ_T. To calculate the effective plastic strain ε_P, the elastic true strain must be subtracted from the true strain (Equation 3.1), where $\sigma_T^{(1)}$ refers to the true stress at the elastic limit.

$$\varepsilon_P = \varepsilon_T - \frac{\sigma_T^{(1)}}{E} \qquad \text{(in/in)} \tag{3.1}$$

The material model input details can be seen in the input files of Appendix C.
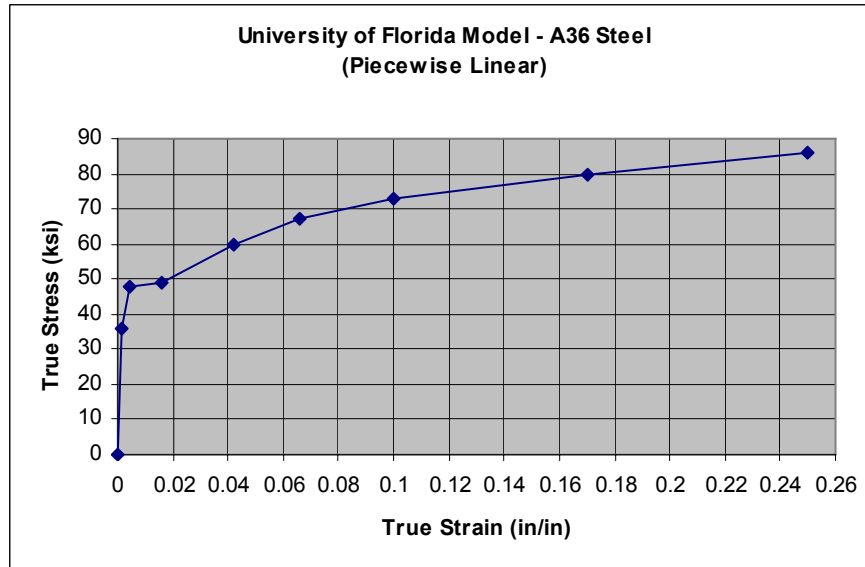
Figure 3.6 A36 steel material curve used for barge model

Loading rate effects were ignored for the explicit dynamic modeling. Typically the velocity of an aberrant vessel is relatively small compared to its cruising speed in an open channel. Because the accidents most often occur in river bends and during inclement weather conditions, vessel velocities have already been significantly reduced. Thus the rate at which deformation of the material occurs is not large enough to warrant the addition of loading rate effects to the material model and, as a consequence, the strain rate parameters were left as null.

We used a constant value for the mass density of the A36 steel ($\rho = 490$ lb/ft^3). To account for cargo loaded barges, point masses were added to the model. The procedure used to include the masses and determine each of their values is discussed in Section 4.5.

3.2.5 Initial conditions

The initial conditions for the entire model consist of an initial velocity imparted to the vessel. For certain waterways, velocities are often recorded for vessels passing a specific location. Whenever the data are available, all of the velocities for a particular type of vessel can be averaged to produce a mean velocity for that vessel type. This mean value is then used to determine a typical impact force associated with that vessel type (per the 2001 AASHTO Specification). The probability that that vessel type will produce bridge element failure can then be tabulated based on the mean velocity. Section 3.6.4 discusses how this velocity is determined, according to the 2001 AASHTO Specifications, and how it is used to calculate the design vessel velocity for each bridge element.

3.3 PIER MODELING

Piers from two bridges were selected for modeling. First we considered the St. George Island Causeway Bridge, Apalachicola, Florida, to allow for direct comparison/calibration with the published data from the UFL studies. The San Jacinto Bridge, Baytown, Texas, was chosen as a prototype case for comparing the computational results against the code provisions.

3.3.1 General assumptions

The geometry of the piers, both for the San Jacinto Bridge, and the St. George Island Bridge, were modeled as accurately as possible. Dimensions were taken directly from the bridge drawings. We assumed the piers to be in their virgin state, that is, deterioration effects such as corrosion, scouring, concrete aging, etc., were not considered in these analyses.

3.3.2 Geometry

3.3.2.1 St. George Island Causeway Bridge

      The St. George Island Causeway Bridge includes two main piers that support the deck which spans the Intracoastal Waterway (ICWW). Of these two piers, the bent on the south side of the channel was used in the UFL studies. It consists of two main columns, a beam supporting the deck above, a massive 4-foot thick shear wall spanning the columns, and a 5-foot deep pile cap, as shown in Figure 3.7. All member dimensions were taken from the UFL report, which included the original drawings.
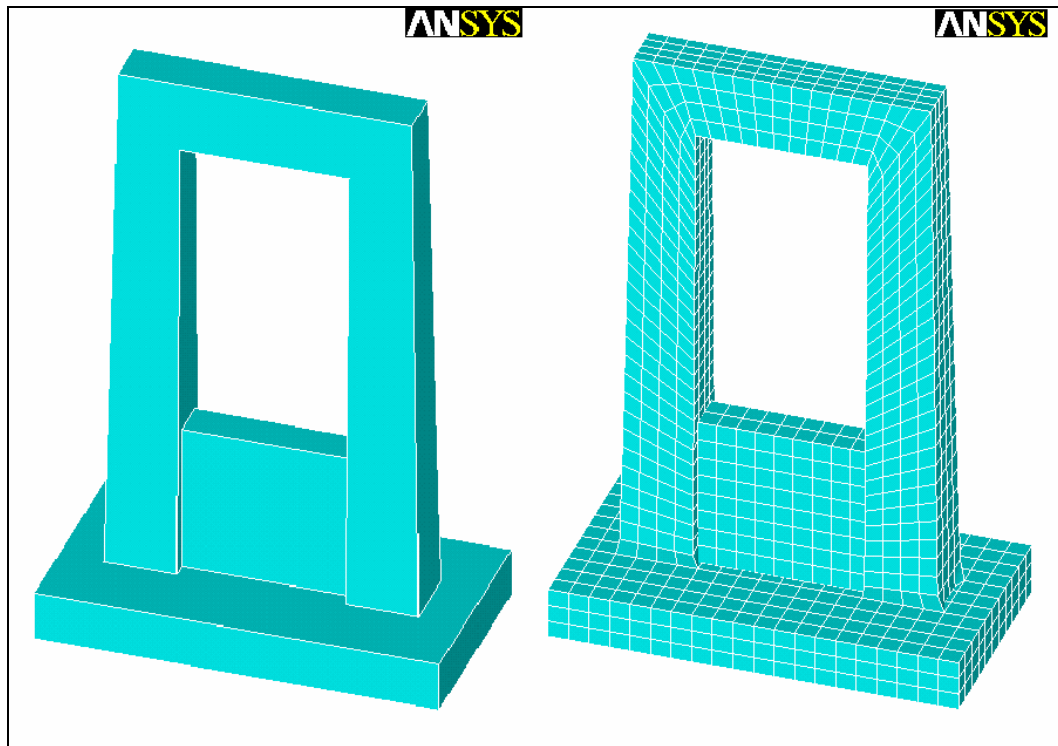
Figure 3.7 St. George Island Causeway Pier Geometry & Preliminary Mesh

3.3.2.2 IH-10 Eastbound Bridge at the San Jacinto River

The San Jacinto Bridge Bent 18 has geometry typical of Texas bridges. The bent comprises two tiers of columns, a top beam, a mid beam, a pier cap, and concrete piles. The bent member dimensions were taken directly from the details supplied in the original drawings (Fig. 3.9). The pier cap measures 18'-0"x67'-6"x4'-0" and is centered in both directions under the remainder of the bent. The columns on the bottom row are 6'-6" square and those on the top row are 4'-6" in diameter. The top beam measures 4'-9" in width by 7'-0" in depth, while the mid beam measures 7'-0" in width by 4'-0" in depth.
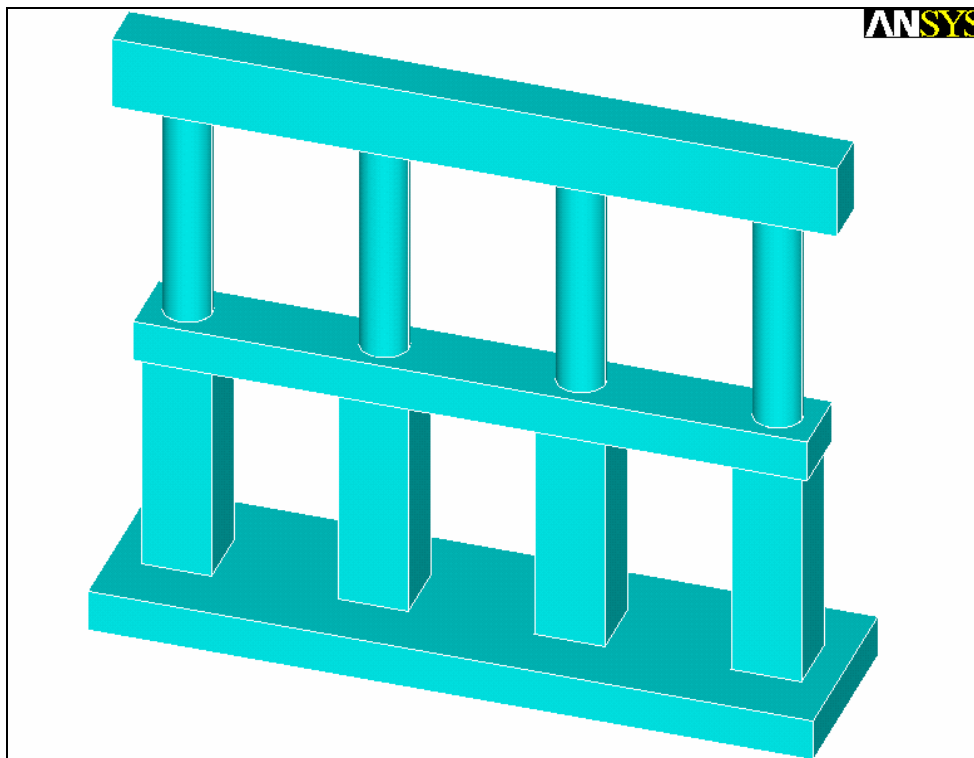
Figure 3.8 Geometry of IH10 at San Jacinto River Bent 18

Concrete cover dimensions and rebar spacing information were not included in the geometry, but rather in the material properties (Sec. 3.3.4). The concrete piles that provide the foundation for the bent were not modeled directly, since information regarding the soil was not available (see Section 3.3.5 for the boundary conditions).
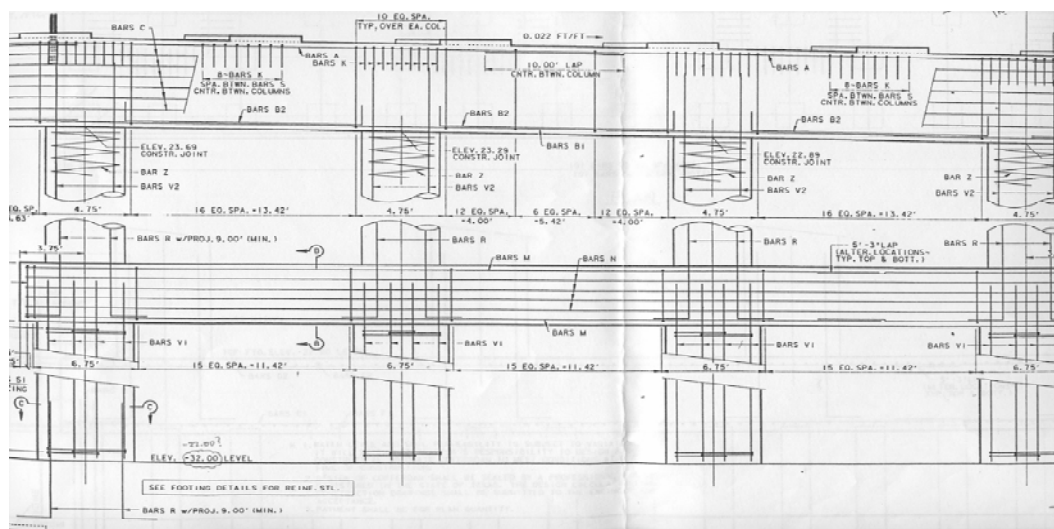
Figure 3.9 Sample of Bent 18 Schematic Drawings

All members were assumed to be monolithically constructed. Although in some cases this may not be the case, the assumption should be conservative, since a stiffer, monolithic structure will generally result in higher reaction forces.
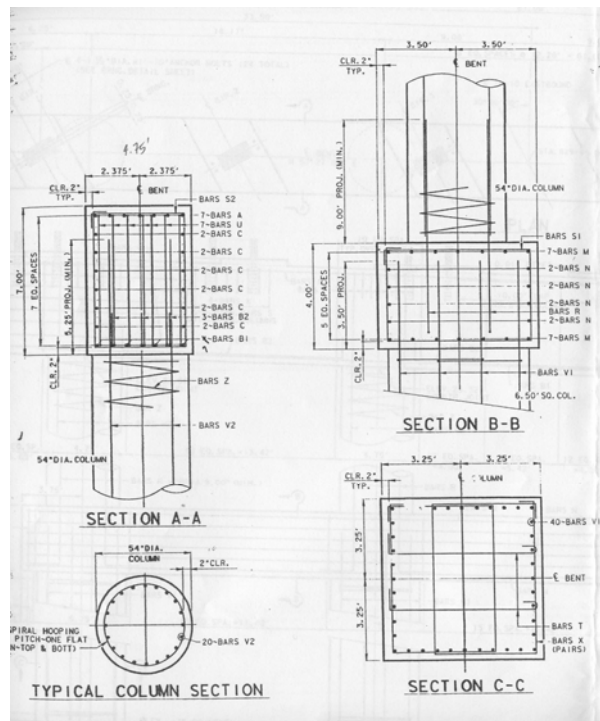
Figure 3.10 Cross-sections of Bent 18 Members

The "Typical Column Section" detail was taken through the upper tier of columns, while the "Section C-C" detail was taken through the lower tier of columns. Sections A-A and B-B are cut through the top and mid-height beams, respectively.

3.3.3 Meshing

Piers were modeled using eight-node hexahedra elements (SOLID164). All of the piers were modeled as monolithic, cast-in-place, reinforced concrete structures. This approximation may not represent the actual case for all piers, since often times joints are required for ease of construction. However, since we had no specific information regarding the joints, we felt that it was a reasonable assumption to model the piers as monolithic structures

The pier mesh was refined at the neighborhood of contact for all simulations. The level of refinement was determined, as with the vessel meshing, by reducing the size of the elements until convergence was achieved. Representative meshes of the two piers are shown in Figures 3.7 and 3.11, respectively.
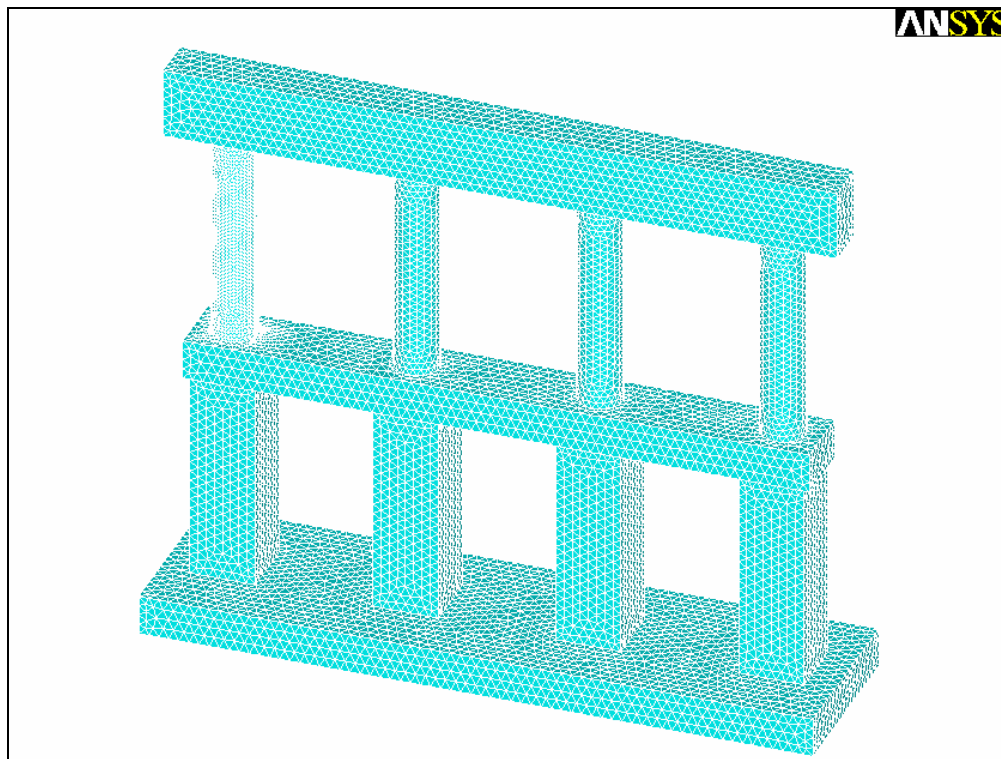
Figure 3.11 IH-10 San Jacinto Bent 18 Mesh

3.3.4   Material properties

ANSYS offers a reinforced concrete element, labeled SOLID65, which accurately models the independent steel and concrete material properties as well as the physical layout of the bars within a reinforced concrete cross-section.

44

However, this element is not part of the LS-DYNA element library. Thus, a true reinforced concrete material model was not an option for our explicit dynamic analysis (LS-DYNA). Instead, we chose SOLID164 and used smeared/equivalent properties by assuming material homogeneity across the entire cross-section. This approach had been used previously with acceptable results and simplified the input/output data for the bridge pier.

To this end, we used a concrete section analysis program (RESPONSE) to perform the material homogenization. The first step in using this tool is to input the individual properties for all of the materials to be used in the section. The cross-sectional properties of the element as well as the geometry of the reinforcing bars are then input. The layout of the bars within the section, including cover dimensions, are then included in the analysis. RESPONSE calculates the flexural properties of the section and outputs moment capacities for the proportional limit of the section as well as for the ultimate bending moment. Both a yield stress and an ultimate stress could then be back-calculated for a section with the same moment capacities and overall dimensions but consisting of homogeneous material.

For our modeling, this procedure was carried out for both the top beam and the mid beam, as well as for the upper columns and lower columns (Fig. 3.10). Thus a total of four equivalent property sets were generated and integrated into the model.

Unlike previous studies on vessel impact which employed simple linear elastic material properties for concrete, we utilized a multi-linear inelastic material model. Initially, a tri-linear curve (engineering stress versus engineering strain) was used to approximate the non-linear stress-strain relationship of the concrete, which included an ACI designated ultimate strain of 0.003. For ANSYS input purposes, the material model engineering stress-strain curve had to be

45

converted to a true stress versus effective plastic strain curve (Table 3-1) using the following expressions.

$$\sigma_T = \sigma_E (1 + \varepsilon_E) \qquad \text{(ksi)} \tag{3.2}$$

$$\varepsilon_T = \ln(1 + \varepsilon_E) \qquad \text{(in/in)} \tag{3.3}$$

The resulting tri-linear material model values are shown in Table 3-1 and the engineering stress-strain relationship used for concrete is plotted in Figure 3.12.

Table 3-1 Concrete material model data conversion

Engineering Values		True Values		
ε_E	σ_E	ε_T	σ_T	ε_P
0	0	0	0	0
0.001	2.5	0.0010	2.503	0.0003
0.002	3.0	0.0020	3.006	0.0012
0.003	2.5	0.0030	2.508	0.0023
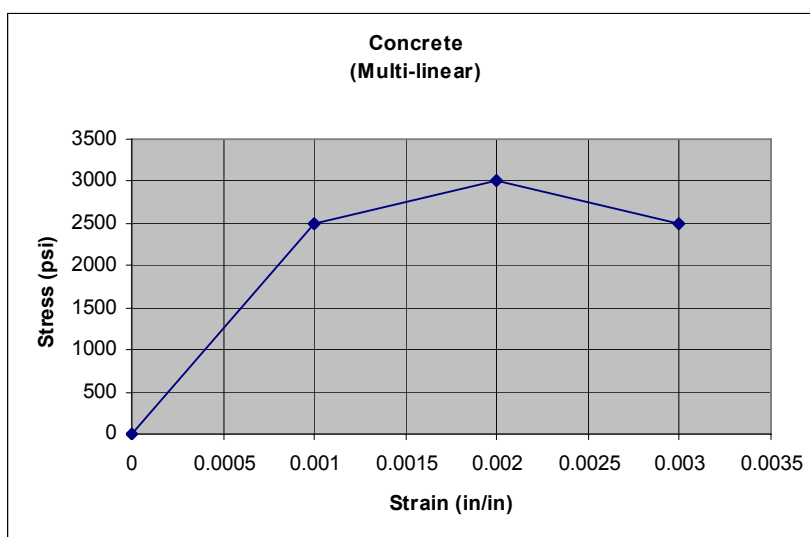
Figure 3.12 Concrete material curve used for pier material model

46

3.3.5 Boundary conditions

Two sets of boundary conditions were tested for both bridge pier models. First, the base of the pier (the bottom of the pile cap) and the top of the pier were fixed, forcing zero displacements and rotations in all three directions. In the second case, the base of the pier was fixed while the top of the pier remained free to displace and rotate in all directions. The true behavior is, of course, more complex than the simplicity of our boundary conditions betrays: for example, the superstructure provides some resistance that could be modeled using elastic linear/nonlinear springs at the top of the pier. Again, due to the preliminary nature of this study, we opted for a free condition at the pier top for all of our final simulations of this work.

To simulate the soil surrounding the pier's anchorage, COMBI165 elements were initially used to provide vertical and horizontal support at the pier foundation level. These discrete linear, elastic spring elements are an over-simplification of the actual soil-structure interaction conditions; however, no approximation of the inelastic properties of the soil was possible due to the unavailability of soil data at the bridge location. The springs were thus subsequently removed from the model (in certain cases soil-structure interaction effects can be significant and should not be, in general, neglected).

3.4 THE UFL MODEL

The barge model used in our research was developed with two goals in mind. First, the stiffnesses and reaction forces were to be matched as closely as possible to the UFL's numerical tests for calibration purposes. Our goal was to simplify the modeling process without substantial loss to the modeling of the physical processes in order to limit the computational cost. The latter is key to future parametric studies.

The UFL barge model accounted for both gravity and buoyancy effects. Discrete translational springs were included to simulate the buoyancy effects of the surrounding water. They were initially positioned such that once gravitational forces were applied the vessel would come to rest in vertical alignment with the specified contact point on the pier face. Although this is a desirable representation of the physical situation, we found that the effect of these forces on (the horizontal component of) the impact force was negligible.

In (Consolazio 2002) it was also mentioned that the additional stiffness provided by certain construction techniques used in assembling the barge should be included in the model. Plates typically overlap each other and are welded together to form the plates of the barge. This procedure is quicker and less expensive than the non-overlapping technique, since fillet welds are less labor intensive than full-penetration butt welds. The additional stiffness associated with the overlapping plates and the welds was included in the UFL model. However, we chose to simply use a constant cross-section so that shell elements could be used to form the entire section.

The loading conditions for the barge were accounted for in the UFL simulations by varying the density of the hexahedra elements that simulated the payload for the barge. To reduce the number of elements, these elements were replaced in our model with a limited number of nodal mass elements positioned at the corners of the cargo bay. Additionally, the masses were placed at mid-height to represent an average location of a typical cargo mass distribution.

The UFL model's heavily refined mesh along the internal bow truss members provided an adequate description of buckling phenomena that could occur on the backside of the headlog. In our model, as mentioned in Section 3.2.2, thin plates were added to replace the trusses and reduce the size of the model. The length and thickness of the plates were calibrated to match the initial

48

stiffness of the trusses prior to impact as well as the loss in stiffness after buckling had occurred.

3.5   ANSYS CONSIDERATIONS

3.5.1   Duration of analysis/time step

In trial simulations we found that the duration of the impact is approximately 1.5 seconds.   Thus the termination times for our numerical experiments were usually set close to 2 seconds.

The use of an explicit solver requires that the time step be small.   This requirement helps to avoid computational stability difficulties associated with large deformations over short periods of time.

To calculate the size of the minimum time step for a specific model, ANSYS LS-DYNA uses Equation 3.4 which is based on the Courant-Friedrichs-Levy criterion.   In physical terms, the value Δt represents the time required for a wave to propagate through an element of length l.

$$\Delta t = 0.9 \frac{l}{c} \tag{3.4}$$

where (e.g. for shell elements),

$$c = \sqrt{\frac{E}{\rho(1-\nu^2)}}$$

$$l = \frac{A}{\max(l_1, l_2, l_3, l_4)}$$

l_i = the length of side i of a typical element

A = area of shell element

E = Young's modulus

ρ = material unit density

ν = Poisson's ratio

The wave propagation velocity, c, is based solely on the element material properties. The element geometry is represented through the variable l. This parameter converts 2D and 3D elements into theoretical elements of finite length l. This process is necessary to simplify calculations for the numerical solver. The factor of 0.9 is included to decrease the time step size for purposes of computational stability.

Stability issues were encountered early in the modeling process at the contact region between the vessel and the pier. Large deformations in the impact zone produced element distortions that resulted in shape errors. These difficulties were remedied by reducing the mesh size at the contact region and thereby effectively reducing the time step size as well. The explicit solution requires that the step size be below the threshold described by Equation 3.5.

$$\Delta t \leq \Delta t^{crit} = \frac{2}{\omega_{max}}$$
(3.5)

where,

ω_{max} = largest natural circular frequency

3.5.2 Substeps

The post-processor requires that a certain number of solutions be read in to create an accurate depiction of the analysis over a certain time interval. Explicit dynamic analyses require very small time step increments and thus a very large

50

number of solutions. The EDRST command was issued to set the number of selected substeps to be written to the .RST result file. The result file is utilized by the POST1 post-processor to create animations, etc. The EDHTIME command was issued to set the number of results that were written to the .HIS history file. The history file is typically used by the POST26 post-processor to depict load histories over time, etc. Most of the results presented herein were extracted from the time-history postprocessor. The number of output steps written to both the result file and the output file was set at 50. This number was sufficient to capture all relevant characteristics of the impact event over the duration of the simulation.

3.5.3   Contact definition

One of the benefits of using LS-DYNA is the flexibility allowed in modeling contact between individual entities. The explicit dynamic analysis allows definition of contact surfaces which can consist of any of the eight element types found in the LS-DYNA element library. For a typical finite element analysis, actual "contact" elements must be defined. Large deformations often associated with an explicit dynamic analysis are also accommodated.

3.5.4   Contact algorithm

For any explicit dynamic analysis involving contact between two boundaries, an algorithm must be specified to describe how the interaction between the two entities will be characterized. The contact algorithm chosen for these simulations was Automatic Surface-to-Surface (ASTS) Contact. As one of the most common algorithms in use, it was chosen because it allowed both surfaces to be relatively large in area. The "automatic" portion of this operation alludes to the fact that it automatically orients shell elements such that the "contact" side of the element properly faces the side encountering impact. Flexible-to-flexible contact was required, as both component bodies were

deformable in nature. Frictional effects were ignored throughout the analysis since the spotlighted value was a force normal to the plane of contact. The more computationally efficient asymmetric contact was permitted since the barge consisted entirely of contact elements and the bridge pier entirely of target elements. Additionally, the barge mesh near the contact zone was more heavily refined than that of the pier and thus supported the choice of the asymmetric procedure.

3.5.5 Component generation

Component models were created for both the vessel and the bridge element and consisted of all the nodes generated from meshing the solid model entities. The bridge pier component also incorporated the elastic supports. ANSYS requires that one entity be designated as the "contact" surface and the other, the "target" surface. The difference being that contact elements cannot penetrate the target surface, whereas the target elements may penetrate the contact surface. Together they are referred to as the "contact pair" and are associated with one another via a real constant set. The birth time for contact definitions was set to zero and the death time was set well beyond the analysis' termination time.

Creating components is useful beyond just the need for definition of contact. ANSYS LS-DYNA also uses component information to write requested output data to the results and time-history files. The POST26 post-processor can then display desired data for any component in graphical format. In our case, two components were required to complete the analysis but only one was needed for analysis of the results. For analyzing the contact forces between the two entities, only the results for one component are necessary since the force magnitudes should be the same for both and will only differ in sign.

3.5.6 Contact forces

In determining the contact forces developed during an impact event, ANSYS LS-DYNA develops a stiffness relationship between the contact components. This relationship is idealized as an elastic spring with a stiffness k, called the contact stiffness, and a deflection δ, called the penetration. The contact stiffness of an individual entity is determined from either Equation 3.6 or 3.7.

$$k = \frac{f_p A^2 K}{V} \quad \text{for segments on solid elements} \tag{3.6}$$

$$k = \frac{f_p A K}{D_M} \quad \text{for segments on shell elements} \tag{3.7}$$

where,

f_p = penalty factor (0.1 by default)

A = face area of contact segment

K = bulk modulus of contacted element

D_M = minimum diagonal

V = volume of contact segment

The contact stiffness is multiplied by the amount of penetration to produce the resultant contact force. Ideally, there would be no penetration between surfaces, however this implies that $k = \infty$ which results in numerical instabilities. Instead, the contact stiffness is effectively adjusted by changing the value of the penalty factor f_p. For this analysis the default value for f_p was assumed.

3.6   SIMULATION PERMUTATION MATRIX

To account for the variability (or uncertainty) associated with various simulation parameters, while keeping the actual number of simulations within reason, a parameter permutation matrix was created. Whereas the vessel velocity, for example, was kept constant throughout all simulations (to coincide with the velocity obtained using the 2001 AASHTO Specifications), three key parameters were varied: the material properties of the concrete pier (10 samples), the location of the initial contact zone (2 samples), and the angle of attack of the vessel impacting the pier (3 samples). Accordingly, 60 simulations were executed and the impact response was tabulated for each one of them. Parameter values were chosen as follows:

3.6.1   Pier material properties

We assumed a normal (Gaussian) distribution for the compressive strength of the concrete. As per the ACI code (Section 5.3.2.2) we assumed a compressive strength of 4000 psi. Using Equation 3.8, the aforementioned value yields a mean compressive strength of 5200 psi.

$$f_{cr}' = f_c' + 1200 \qquad \text{for } 3000 \leq f_c' < 5000 \text{ psi} \qquad (3.8)$$

We assumed a standard deviation of 10% of the mean, or 520 psi. Using the mean (5200 psi) and the standard deviation (520 psi) we constructed the partitioned normal distribution, which we then sampled randomly at 10 locations. For each one of the 10 compressive strength values we also assigned an elastic modulus, per Equation 3.9.

$$E_c = 57,000\sqrt{f_{cr}'} \qquad \text{(psi)} \quad \text{for normal-weight concrete} \qquad (3.9)$$

54

The resulting values for both parameters are shown in Table 3-2.

Table 3-2 Randomly selected material values from normal distribution

Case #	Probability	f_c' (ksi)	E_c (ksi)
1	0.02605	4.190	3689.6
2	0.14679	4.654	3888.5
3	0.21358	4.787	3943.8
4	0.30727	4.938	4005.5
5	0.40949	5.081	4063.0
6	0.55787	5.276	4140.1
7	0.61057	5.346	4167.6
8	0.77606	5.595	4263.5
9	0.85743	5.756	4324.4
10	0.91391	5.910	4381.9

The procedure described in Section 3.3.4 was applied to each of the material combinations listed in Table 3-2. Subsequently, yield and ultimate values for the smeared properties were entered directly into the material model for the bridge pier. It is important to note that these derived properties are based on purely flexural behavior.

3.6.2 Angle of impact

From initial parametric studies, we determined that the angle at which a vessel collides with a bridge pier is critical to that pier's probability of collapse. Although the 2001 AASHTO Specifications address channel and transit angles for determination of the probability that the vessel will become aberrant, it does not consider the effect an angled impact might have on the impact event itself (for example, compared to a head-on collision). Furthermore, it is important to note the difference between a "glancing" impact and an angled impact. An angled impact implies that, although the vessel approaches the pier at an angle, its

direction of travel passes through the center of the front face of the structural member the vessel will come into contact with. A glancing impact is similar to an angled impact, with the only difference being that the direction of travel does not pass through the center of the impacted member front face. In this study, we considered only angled impact (Fig. 3.13).
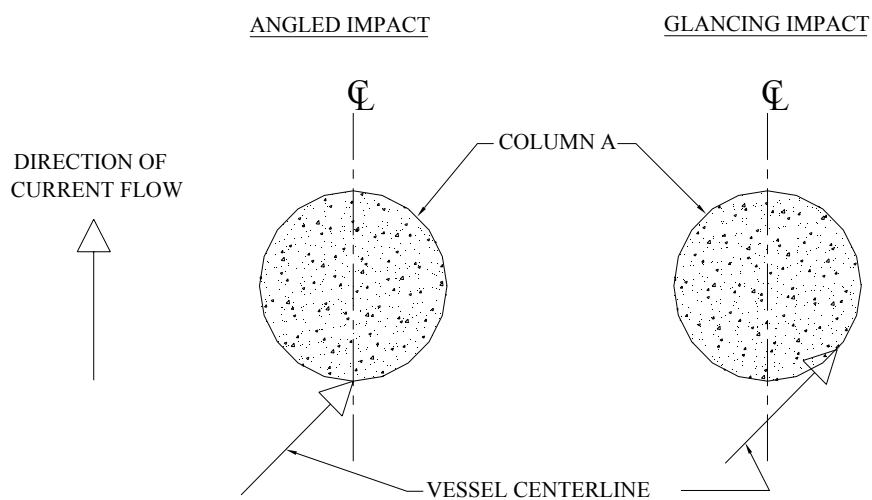
Figure 3.13 Illustration of angled versus glancing impact

The superstructure of the bridge also plays a much larger role for impacts at an angle. Bridge piers are typically about the width of the superstructure in one dimension and as thin as possible in the other dimension. This general criterion for sizing piers reduces the total material needed for the project and allows more space for vessels to pass between them. As a result, piers tend to be stronger in their longitudinal direction than they are in their lateral direction. In this longitudinal direction, parallel to the pier, the deck provides only minimal stiffness to the top of the pier. If the deck includes a joint over that pier, the deck

provides very little stiffness. If the deck is in fact continuous over the pier it will likely provide more support. However, in the lateral direction, perpendicular to the pier, the deck serves as a much stiffer boundary condition, since loads can be transferred longitudinally through the deck cross-section toward the shore.

We note that failure limit states were not considered during this analysis. The bearing length of deck spans on bents can often be very small in proportion to the length of the deck itself. During an impact event the deck could "fail" due to various reasons, such as the deck losing effective bearing length and collapsing. We considered only the lateral resistance in this study.

Additionally, pier columns will typically have a greater effective length in the out-of-plane direction. This is another result of the pier resistance being greater in the direction parallel to the transit path. Lateral beams and shear walls built integrally with the pier columns provide bracing points for the columns. Thus moment resistance values at the ends of the columns in the perpendicular direction are much less than they are in the parallel direction.

In summary and referring to Figure 3.13, we considered the angle of impact values shown in Table 3-3.

Table 3-3 Angle of impact parameter values

Case #	Angle (degrees)
1	0
2	7.5
3	15

3.6.3   Impact zone – contact height

The location of the vessel's point of impact on a bridge element is a critical parameter in the resulting reaction forces. The height of the water surface at the time of impact, and the draft of the vessel, are both included in this parameter. The draft is directly related to the amount of payload that the vessel is carrying. A greater payload means that the barge headlog will be closer to the water surface.

For simplicity, we assumed that the equivalent static load was applied at the water surface. This is a reasonable approximation since the simulations were carried out assuming a full barge load. The maximum loaded draft of a fully-loaded jumbo hopper barge is 9 feet (AASHTO, 1991). Assuming the barge has a 13-foot bow depth, this translates to 4 feet of error in assuming contact at water level.

For our simulations, the impact zone was determined using 2 different water level heights. The mean water level (MWL), and the high water level (HWL) were the two values used. For the San Jacinto Bridge, the mean water level was chosen to be 6.5' above the datum (indicated on the existing drawings), and the high water level was chosen to be the 100-year flood level or equivalently 15.7' above the datum (see Table 3-4).

Table 3-4 Contact height parameter values

Case #	Contact height (ft)
1	6.5
2	15.7

For an actual design case, these values would be obtained from the local Flood Authority; however, for simulation purposes we simply used the values

found on the original drawings. They were collected from the 1973 FEMA Harris County Flood Insurance Study, as indicated on the drawings.
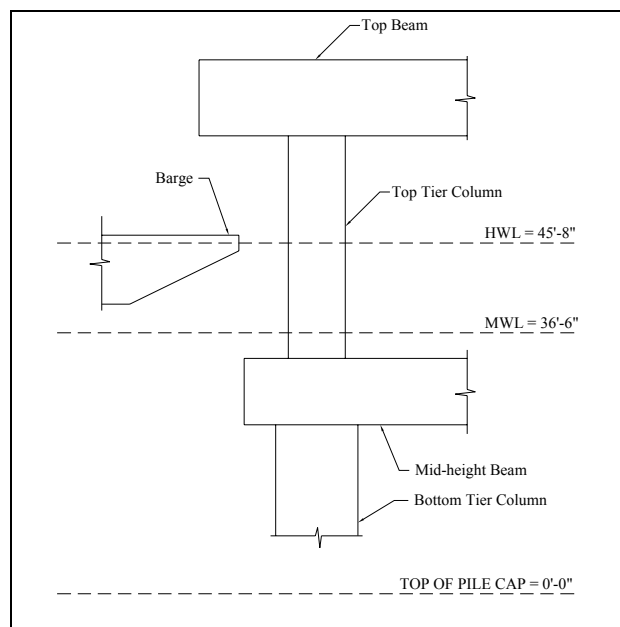
Figure 3.14 Illustration of contact zone for the San Jacinto Bridge Bent 18

The headlog of the barge was centered (vertically) with respect to the top tier columns (Fig. 3.14). The contact locations were both located along Column A at the top tier of columns. The mean water level (MWL) corresponded to a contact point at 7% of the height of Column A (Fig. 3.14). The high water level (HWL) corresponded to a contact point at 51% of the column's height. The location of these points is critical to the response of the bridge element. The high water contact point results in a much more 'flexible' response than the mean water point. Although the cross-section of the column is the same in the 2 locations, much larger bending moments are required to resist the impact forces at

the high water strike point. At the mean water location, the shear at the bottom of the column will be much larger and failure could be of a brittler nature.

3.6.4   Vessel/current speed

The speed of the vessel at the time it passes underneath the bridge plays an important role in determining the probability of collapse. The vessel speed has the greatest effect on the reaction forces when the internal bow trusses do not completely buckle during impact. For the San Jacinto trial case, there was no recorded current component perpendicular to the direction of vessel transit. Thus, the only velocity that was applied to the vessel was in the direction of the current's flow.

The speed of the current in the vessel transit path plays an essential part in the vessel's speed. As a general rule, the *overall* speed of the vessel is determined by the tug operator. However, the *minimum* speed that the vessel travels is directly determined from the current's velocity parallel to the transit path.
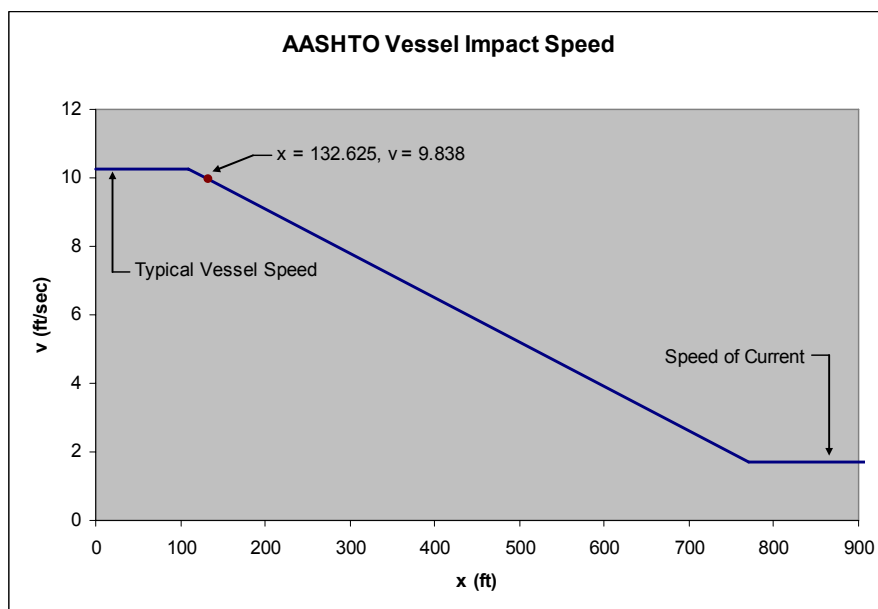
Figure 3.15 AASHTO vessel impact speed calculation for Bent 18

The speed selected for our simulations was based on the 2001 AASHTO Specifications for determining vessel impact speed (Fig. 3.15). The bridge element under investigation, Bent 18 of the San Jacinto Bridge, fell in the linear range between the typical vessel transit speed for the channel (V), 10.1 fps, and the typical speed of the current in the channel (V_{min}), 1.7 fps. The edge of the channel is located 110 ft from the channel centerline. This corresponds to the end of the first plateau in Figure 3.15. The distance 3 times LOA, where LOA represents the overall length of the barge tow (see Section 2.4.1), is located at 771 feet and corresponds to the beginning of the second plateau. Bent 18 is located between these 2 stations as shown in Figure 3.15. The vessel speed is found by interpolating between the two plateaus to arrive at a speed of approximately 9.9 fps. This speed was used for all finite element simulations of this study.

3.6.5 Vessel loading conditions

The load that the vessel carries directly affects its momentum, and in turn, the force exerted on the bridge pier. Typically, vessels heading in one direction are usually fully-loaded while vessels traveling in the opposite direction carry no cargo load. Moreover, the load in the cargo bay affects the draft of the vessel in the water, as discussed in Section 3.6.3. Changing the height of the barge headlog above the waterline alters the location of the contact point on the bridge element. In most cases, this relocation will change the force experienced by the element as well as the probability that it will fail. Thus, whether or not the vessel is loaded is of significance to the impact studies.

To simulate various loading conditions, point masses were included in the vessel model. Specifically, point masses were attached to the four corners of the cargo bay, positioned at bay mid-height, to account for the cargo load.

61

Furthermore, we assumed one fully-loaded vessel (1900 tons) and one tug boat (200 tons) as the sole members in the barge group. The mass of the tug boat was included although it may have been disconnected from the barge tow moments before the collision (this is a conservative assumption). Table 3-5 depicts a typical calculation of the nodal masses needed to simulate a barge (200 tons), its cargo (1700 tons) and a tug boat (200 tons).

Table 3-5 Additional nodal mass sample calculation

Segments	Total Area (ft^2)	Shell Thickness (in)	Volume (ft^3)
Stern	420	0.375	13.1
Rear Sides	4200	0.375	131.3
Forward Sides	280	0.375	8.8
Cargo Bay Bottom	6125	0.375	191.4
Bow Bottom	783	0.375	24.5
Headlog	70	0.375	2.2
Bow Top	1050	0.375	32.8
Bow Stiffeners	3380	0.063	17.6
Total Volume =	421.6	ft^3	
Barge Model Mass =	6421.0	slugs	
Total Mass =	130542.6	slugs	
Required Nodal Mass =	31030.4	slugs/node	

CHAPTER 4
Vessel Impact Simulations

4.1 OVERVIEW

In this chapter we report on the results of the numerical experiments we conducted to simulate the vessel impact. We report the time history of the contact forces developed between the vessel and the pier during the impact. We considered perturbation on the pier material properties, the angle of vessel attack, and the location of the initial impact zone. Of these, as it turns out, the material perturbation have the least effect on the contact forces.

First, we conducted a number of convergence tests to ensure that the meshes for the vessel and the pier were adequate. For example, we kept the pier mesh constant (at 25,506 degrees-of-freedom (DOF)) and refined the vessel's mesh; the details are shown in Table 4-1. Figure 4.1 depicts the time history (for the first 2 seconds) of the contact forces for these meshes. As it can be seen in Figure 4.1 there is only small difference between the mesh we termed "Model" and the finest mesh. Thus, for subsequent simulations we fixed the vessel mesh at 736,608 DOF.

Table 4-1 Vessel mesh densities

Mesh Refinement	Total Nodes	Total DOF	Impact Area DOF
Coarse	47667	572004	24804
Model	61384	736608	28332
Fine	77617	931404	30924
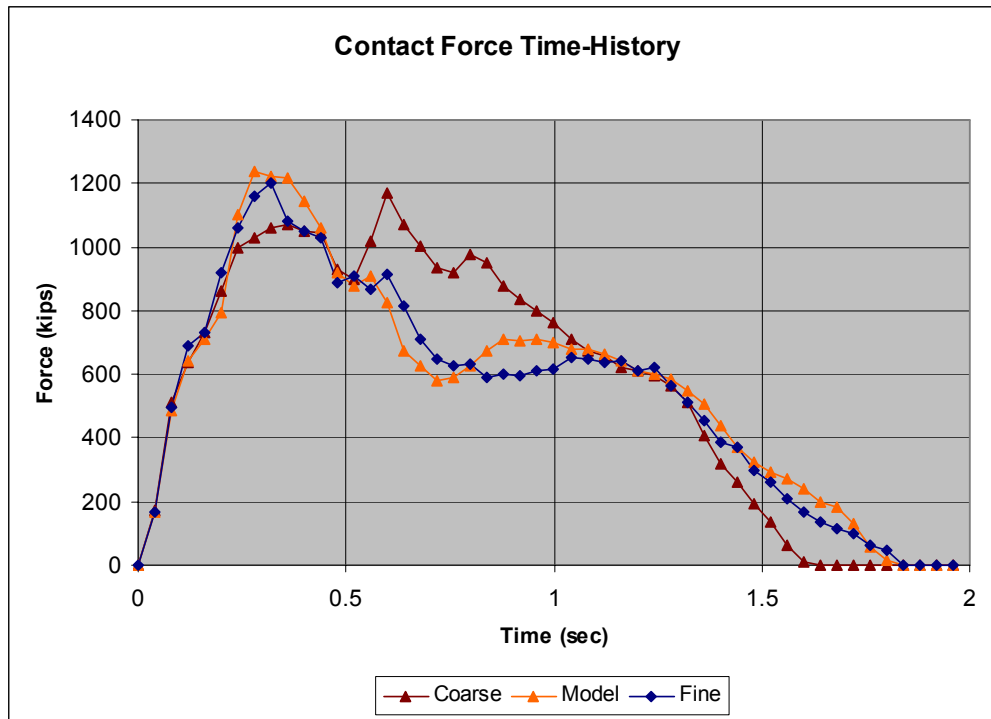
Figure 4.1 Comparison of contact forces for 3 vessel mesh densities

Similarly, we refined the pier mesh as per the details of Table 4-2. Figure 4.2 depicts again the time history of the contact forces for the three pier meshes shown in Table 4-2 (the vessel mesh was kept at "Model" level). Again, as shown in Figure 4.2, there is small difference between the histories corresponding to the fine and "Model" scales; we henceforth fixed the pier mesh at 25,506 DOF.

Table 4-2 Bent 18 mesh densities

Mesh Refinement	Total Nodes	Total DOF	Column A DOF
Model	2834	25506	6192
Fine 1	5271	47439	15093
Fine 2	8801	79209	27279

Contact Force Time-History
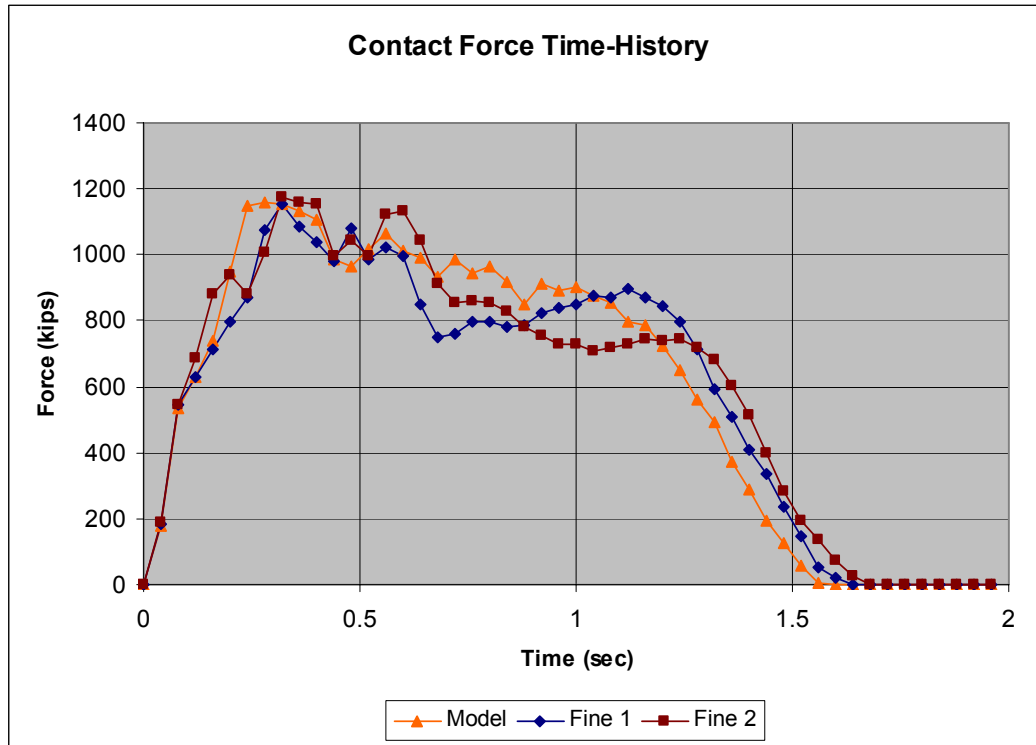
Figure 4.2 Comparison of contact forces for 3 pier mesh densities

We remark that the refinement study as presented here is not rigorous: proper convergence studies are conducted in appropriate global error norms. Furthermore, the contact forces shown in Figures 4.1 and 4.2 are averaged over the contact zone (per ANSYS), which does not remain constant during the impact. The zone also changes somewhat between the mesh refinements. Thus, the refinement study reported here is an imperfect one; nevertheless given the ultimate intent of quantification of the contact forces, from a macroscopic point of view, this refinement study is more than adequate.

The density of the meshes is represented using the number of degrees-of-freedom for the model. For each node in an LS-DYNA SHELL163 element there

are 12 degrees-of-freedom. These degrees represent 3 displacements, 3 velocities, 3 accelerations, and 3 rotations. Thus, the number of degrees-of-freedom for a solid model composed solely of shell elements is equal to the total number of nodes multiplied by 12. Similarly, for an LS-DYNA SOLID164 element, each node possesses 9 degrees-of-freedom. Only the 3 rotational degrees are omitted for this explicit solid element's nodes.

4.2 PARAMETRIC STUDIES

4.2.1 Effect of material properties on contact forces

One of the three parameters chosen for our simulations was the variability of concrete properties. Section 3.6.1 discusses the process used to randomly select values for the concrete and longitudinal reinforcement properties. The section also details the process for determining the smear properties that were used directly in the vessel and pier input files. We report on a subset of our results: Figure 4.3 shows the contact force time history for two different pier material set values (see Appendix B) case 1 and case 10 refer to impact at the mean water level and at an impact angle of 0 degrees. Clearly, there are insignificant differences in the results due to the two materials. Thus, henceforth we conducted all simulations using material set 5 (see Appendix B).
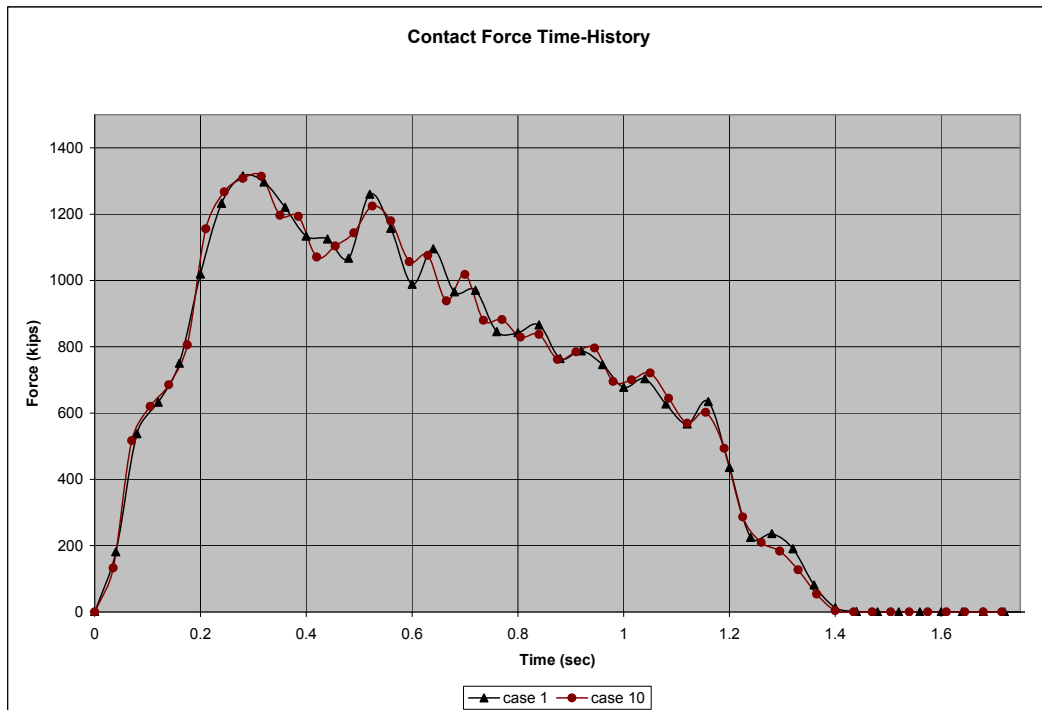
Figure 4.3 Contact force comparison for material sets 1 & 10

4.2.2 Effect of impact angle on contact forces

The simulations also included the possibility that a barge might approach a pier in a manner other than directly from the side. Section 3.6.2 discusses how three different angles were chosen to account for this eventuality. A zero angle represents head-on collision; included were also impact angles of 7.5 degrees, and 15 degrees. Figure 4.4 shows the effect the angle of impact has on the contact forces.
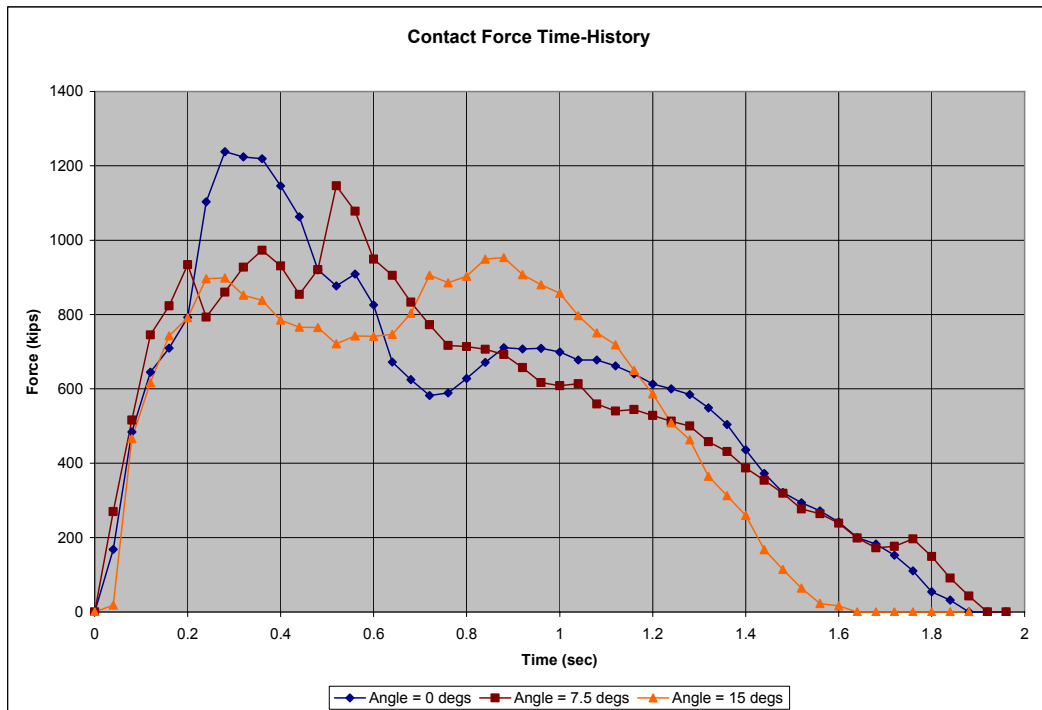
Figure 4.4 Contact force comparison for 3 impact angles

The San Jacinto bent is stiffest in its longitudinal direction, parallel to the channel. The results agree with this fact, since the largest contact force is observed when the pier is struck directly from the front. The lesser angle of impact (7.5°) represents the next highest dynamic reaction force. Overall, the 3 plots are not that dissimilar in an average sense. This is due to the barge's bow stiffness; the strength of the bow is the controlling factor in the magnitude of the contact force.

4.2.3 Effect of contact point location on contact forces

The height at which the vessel impacts the pier is the third parameter varied in this study. Section 3.6.3 discusses how the location of contact has an

effect on the contact forces. Figure 4.5 shows that the case using the lower contact location (case 1, see Table 4-3) has a shorter duration of impact, by approximately 0.2 seconds, and a slightly higher dynamic impact force.
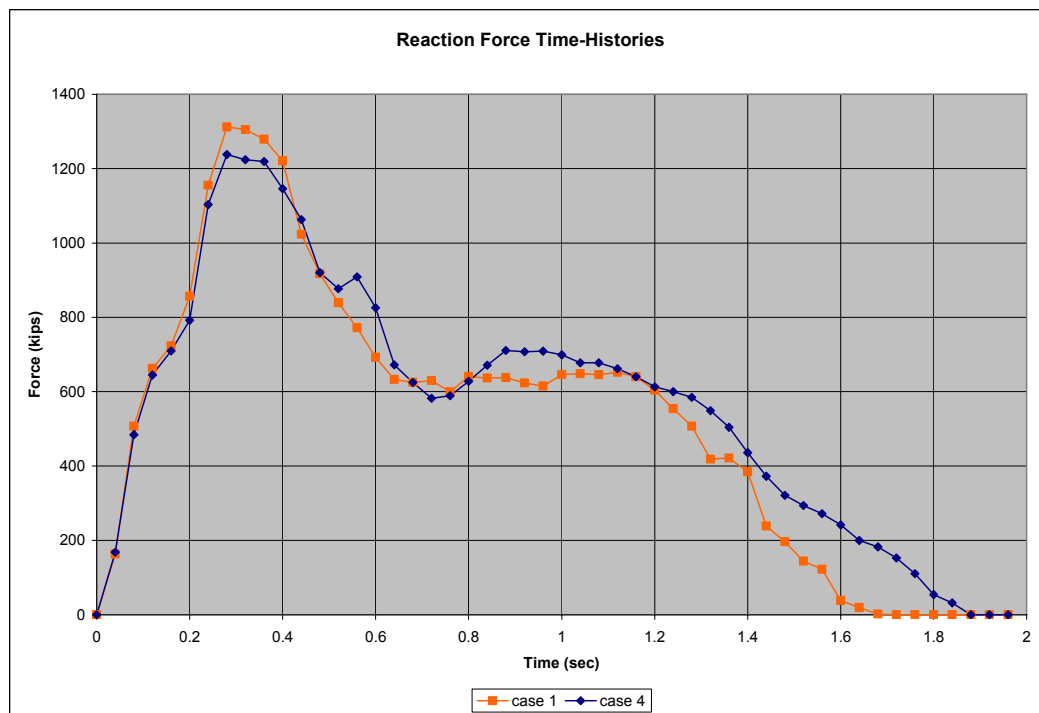
Figure 4.5 Contact force comparison for 2 contact locations

4.3   EQUIVALENT STATIC LOAD (COMPUTATIONAL MODEL)

To allow for a meaningful comparison with the code provisions, that prescribe a static force for design purposes, we too attempted to extract a static force equivalent to the dynamic contact forces. To arrive at an equivalent static force we chose to match the maximum dynamic deformation of the pier in the contact zone with the deformation due to a statically applied load at the center of the contact zone. To this end, we created a static finite element model using the

69

traditional ANSYS solvers (LS-DYNA will only allow for dynamic modeling). The ANSYS solid element (SOLID45) was used in place of the solid element that LS-DYNA uses (SOLID164); we kept the same material model between the two solvers.
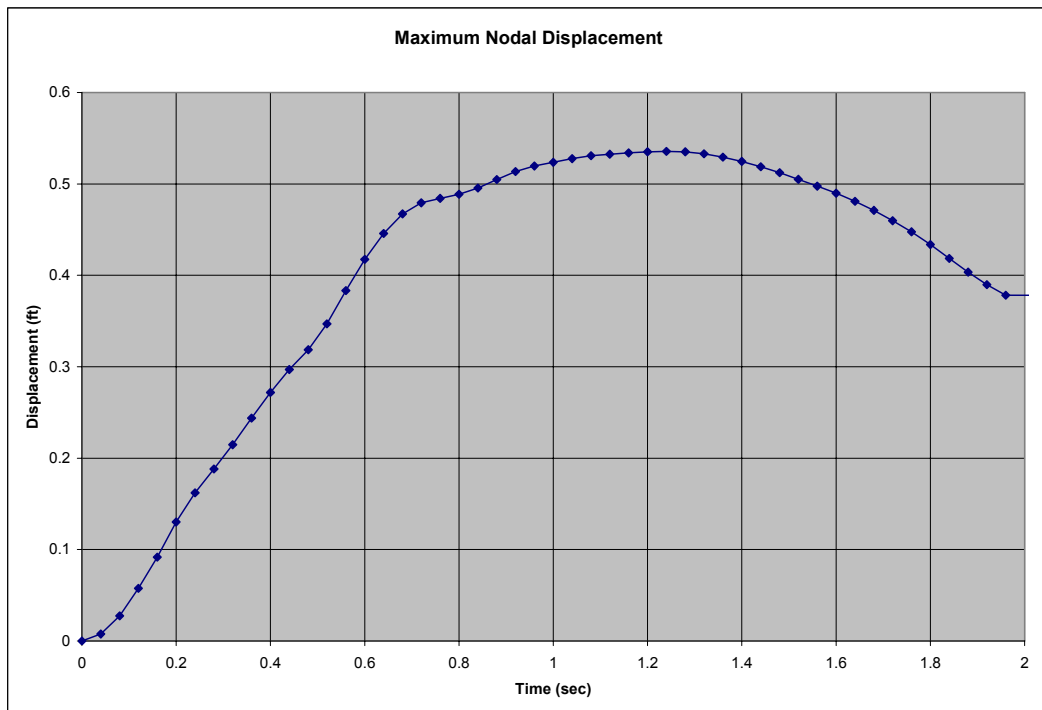
Figure 4.6 Typical nodal displacement for calculating equivalent static load

The maximum displacement, during dynamic loading, was determined by examining the largest nodal displacements in the neighborhood of the impact. Figure 4.6 is a typical time-history of the displacement of a pier node at the contact zone. In this case, the maximum deflection is approximately 0.54 feet or 6.5 inches. This maximum deflection is then recreated in the static model and the corresponding static force is extracted.
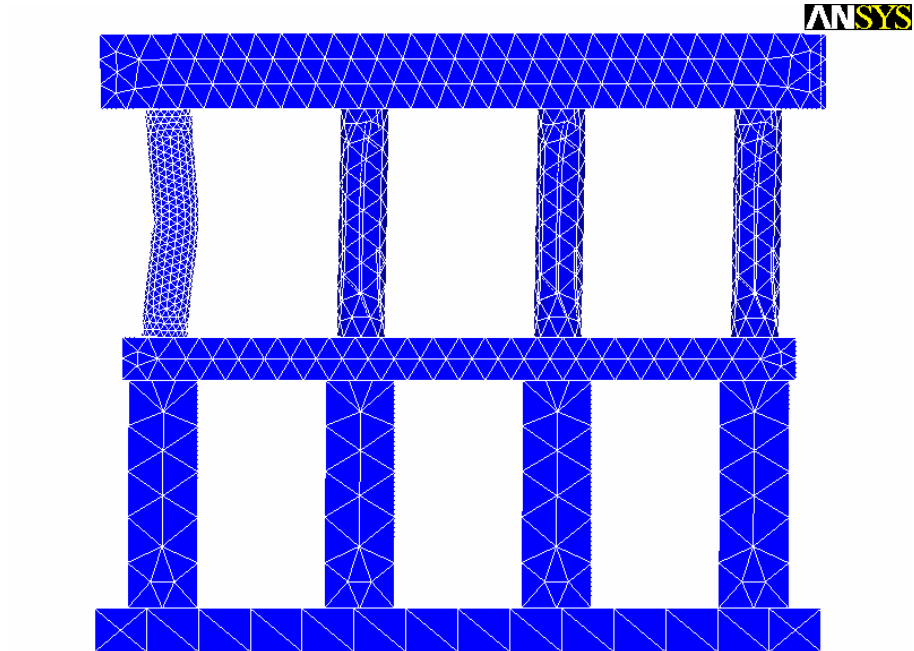
Figure 4.7 San Jacinto Bent 18 under equivalent static loading

Figure 4.7 illustrates Bent 18 under the equivalent static loading that produces the identical maximum deflection to that observed during dynamic response. The resulting equivalent static loads that were calculated using this procedure are shown in the table below for the six cases considered.

Table 4-3 Equivalent static loads for 6 trial cases

Case #	Contact Point	Angle (degs)	ESF (kips)
1	MWL	0	1507.6
2	MWL	7.5	1190.7
3	MWL	15	1318.9
4	HWL	0.0	2139.0
5	HWL	7.5	2042.9
6	HWL	15	2057.4

4.4   STATIC LOAD (2001 AASHTO SPECIFICATIONS)

Section 2.4 outlines the basic procedure for calculating the annual frequency of collapse for a bridge element, based on Method II of the 2001 AASHTO Specifications. In this section we carry out such an analysis for our particular trial case. The majority of the equations in this section are repeated from Section 2.4. The equation for annual frequency of collapse is represented by Equation 4.1.

$$AF = (N)(PA)(PG)(PC) \qquad (4.1)$$

As explained in Section 2.4.2.1, the N parameter represents the number of vessels of a certain class that pass the particular bridge element in a given year. The code instructs that this value include the projected increase in vessel traffic over the expected life of the bridge. The projected frequency of barge passes for the San Jacinto Bridge's Bent 18 was calculated to be 812 trips per year.

4.4.1   Probability of aberrancy

The next task was to calculate the probability of aberrancy for a typical vessel in the channel. This probability is tabulated using Equation 4.2. The first required parameter is the base rate of aberrancy, which for barge traffic is assumed, by the code, to be a value of 1.2×10^{-4}.

$$PA = BR(R_B)(R_C)(R_{XC})(R_D) \qquad (4.2)$$

The R_B variable is the correction factor for the bridge element's location in the waterway. In our case, Bent 18 is located immediately downstream of a bend

region in the waterway. The approximated angle of this bend is 15 degrees. The location correction factor is calculated using Equation 4.3.

$$R_B = \left(1 + \frac{\theta}{45^0}\right) = \left(1 + \frac{15^0}{45^0}\right) = 1.333 \tag{4.3}$$

The parameter R_C represents a correction factor for the influence of the waterway's current parallel to the transit path of the vessel. This calculation is carried out using Equation 4.4, where V_C is the component of the current velocity, in knots, which is parallel to the path.

$$R_C = \left[1 + \frac{V_C}{10}\right] = \left[1 + \frac{1.185}{10}\right] = 1.118 \tag{4.4}$$

Similarly, the R_{XC} variable is included to account for influence of the current in the direction perpendicular to the vessel's transit path. This calculation is carried out using Equation 4.5, where V_{XC} is the component of the crosscurrent velocity, in knots, which is perpendicular to the path.

$$R_{XC} = \left[1 + V_{XC}\right] = \left[1 + 0.593\right] = 1.593 \tag{4.5}$$

The R_D parameter is the traffic density correction factor and is intended to account for waterways that experience higher volumes of vessel traffic at any given time. There are 3 subjective values for this variable which are described in Section 2.4. For the San Jacinto Bridge, the traffic density was assumed to be "low" and thus a value of 1.0 was used.

From Equation 4.2, a probability of aberrancy can be calculated using the parametric values determined in Equations 4.3 through 4.5. The resulting probability of aberrancy is 0.000285 per year or, equivalently, a return period of about 3500 years.

4.4.2 Geometric probability

The code uses a normal distribution to describe how far from the centerline of the transit path the vessel will be when it passes underneath a bridge. Section 2.4.2.3 goes into the details of the method that is used to determine this parameter. Bent 18 is taken to be located 135 feet from the centerline of the vessel's transit path. The centerline is located at the mean of the normal distribution. The standard deviation of the curve is assumed to be 3 times the overall length of the tow. For our trial, the overall length of the tow consists of one barge and one tug or 257 feet total. Using these values, a geometric probability of 0.053714 results.

4.4.3 Probability of collapse

The kinetic energy of the vessel is calculated using Equation 3.14.7-1 of the 2001 AASHTO Specification (Equation 4.6). The derivation of this equation from the Meir-Dornberg experiments is discussed in Section 2.3. The formula requires the entry of 3 parameters.

The first parameter is the hydrodynamic mass coefficient, C_H. Section 2.3.1 describes the origin of this coefficient and how it is directly related to the underkeel clearance of the vessel from the bottom of the channel. In our case, the channel depth was 30.7 feet and the draft of the fully-loaded vessel was 9 feet. The resulting underkeel clearance (21.7 feet) exceeds half of the draft depth (4.5 feet). So, the coefficient is taken as a value of 1.05.

The vessel displacement tonnage W is expressed in units of metric tons, also referred to in European measurements as "tonne". For conversion purposes, 1 tonne is approximately equivalent to 2204.6 lbs. So for 1 fully-loaded barge (1700 tons) and 1 tug boat (200 tons), we calculate a total barge tow displacement weight of 1723.7 tonnes.

$$KE = \frac{C_H W V^2}{29.2} \tag{4.6}$$

$$= \frac{(1.05)(1723.7)(9.838)^2}{29.2}$$

$$= 5999.0 \text{ kip-ft}$$

Once the kinetic energy is found, the barge bow horizontal damage length can subsequently be determined. Section 3.14.12 of the 2001 AASHTO Specifications provides the relationship shown as Equation 4.7.

$$a_B = 10.2\left[\left(1 + \frac{KE}{5672}\right)^{1/2} - 1\right] \tag{4.7}$$

$$= 10.2\left[\left(1 + \frac{5999.0}{5672}\right)^{1/2} - 1\right]$$

$$= 4.43 \text{ ft}$$

The bow damage depth is then translated into an equivalent static force using the 2001 AASHTO Specifications' Equation 3.14.11-2 (Equation 4.8). This equation is applied since the crush depth a_B is greater than 0.34 feet.

$$P_B = 1349 + 110a_B \qquad (4.8)$$

$$= 1349 + 110(4.43)$$

$$= 1836.3 \text{ kips}$$

The probability of collapse can be calculated using the 2001 AASHTO Specifications' Equation 3.14.5.4, shown here as Equation 4.9. Section 2.4.2.4 discusses the idea behind the probability of collapse tabulation. The ultimate lateral resistance, H, value was assumed to be 997 kips for our calculations. This value was determined from preliminary pushover analyses of the pier (similar to what would normally be used for this procedure). The ratio of H/P is thus equal to $997/1836.3 = 0.543$. This value falls in the range from 0.1 to 1.0, so Equation 3.14.5.4-2 was utilized. There results:

$$PC = \frac{1}{9}\left[1 - \frac{H}{P}\right] = \frac{1}{9}\left[1 - \frac{997}{1836.3}\right] = 0.0508 \qquad (4.9)$$

Using Equation 4.1 (repeated below), the annual probability of collapse for our bridge element can be determined.

$$AF = (N)(PA)(PG)(PC)$$

$$= (812)(0.000285)(0.053714)(0.0508)$$

$$= 0.000631 \text{ (1/yr)}$$

According to code, this value would be subsequently added to all of the AF values for the other bridge elements, including both sub- and superstructure elements to determine an AF value for the entire bridge. Based on the importance category of the bridge, it would be assigned a pass/fail designation from the analysis.

76

4.4.4 Comparison

As per Equation 4.8 the 2001 AASHTO Specifications require a static design load of 1836.3 kips. We remark that this value is the same irrespective of the contact point location or the angle of impact. By contrast, notice that the equivalent static loads derived from the dynamic contact forces, as shown in Table 4-3, fall both above and below the 2001 AASHTO Specifications' static load value. Thus, it appears that the code both underestimates, by as much as 16%, and overestimates, by as much as 35%, the computationally determined static forces, for, at least, the cases we considered. This comes as no surprise given the rather simplistic approach associated with the code provisions.

It is also of interest to examine the barge bow deformation (this is a key quantity in the 2001 AASHTO Specifications). For example, for the 4th case, shown in Table 4-3, the displacements of both a headlog edge node and a central headlog node (where most of the deformation occurs) are shown in Figure 4.8. We calculate the bow deformation by computing the amplitude of the vector difference of the two nodal displacements, or, equivalently as $[(\Delta X)^2 + (\Delta Y)^2]^{1/2}$, where ΔX and ΔY are shown in the figure below (at the end of the recorded simulation period).

Accordingly, the bow deformation was calculated as 6.26 ft, approximately 40% larger than the value predicted by the code (Equation 4.7). It is noteworthy, that should one use the computationally derived bow deformation in the code, the estimated static load (per the code) will be 2032.6 kips, much closer to the computationally derived value of 2139.0 kips.

77
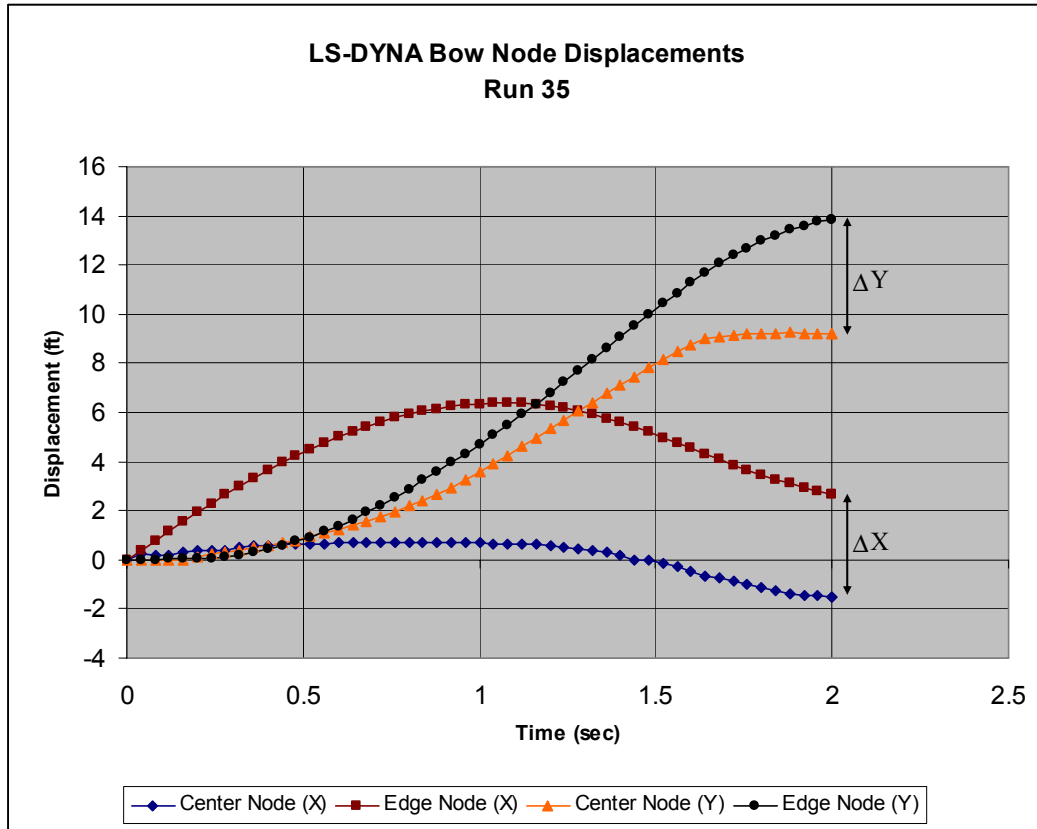
Figure 4.8 Relative nodal displacements for typical bow deformation

4.5   VESSEL-TO-PIER IMPACT VISUALIZATION

There are two simulations depicted in this section. The first set of images are taken from case #1 (Table 4-3)which consisted of a head-on (zero degree) impact at the MWL contact location. The second set of images are from case #6 (Table 4-3) which was carried out using an impact angle of 15 degrees at the HWL contact location.

In viewing the animations, one will notice that the bow of the barge "climbs" up the first column relatively quickly after impact occurs. This effect is

primarily due to the inclined geometry of the bow bottom and the neglect of vertical gravitational forces.
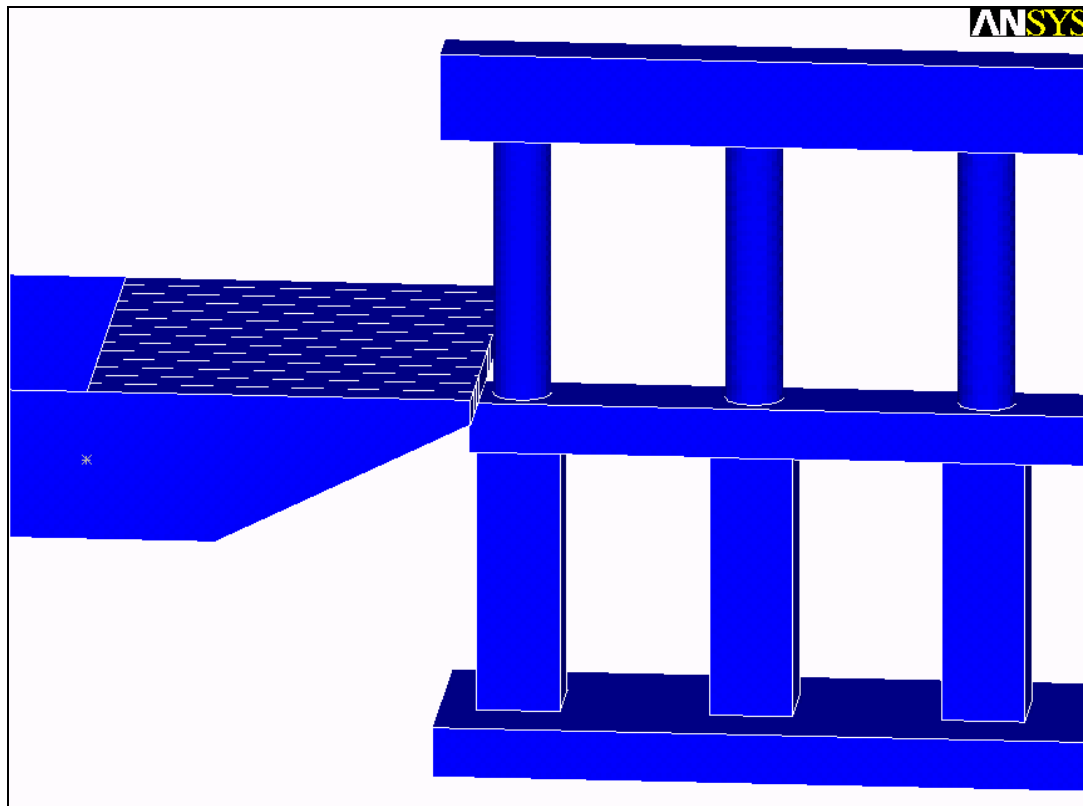
Figure 4.9 ANSYS animation; case #1 impact

It is interesting to note, when viewing the animation in Figure 4.9, that as the barge moves up the first column, a greater amount of stress is distributed to the other 3 top tier columns. At the start of the impact, the majority of the impact force is being distributed down to the mid-beam via shear forces. Toward the end of impact, flexural behavior of the column distributes more of the load to the top

beam which allows the other top tier columns to share the lateral force exerted by the barge.

Figures 4.10-15 are snapshots taken during the collision simulated in case #1 (Table 4-3). Figure 4.10 is captured immediately after impact has occurred. The only stress present in the pier is at the contact location. The gray color that appears on the barge's stress contours (throughout this section) represents stress levels beyond the maximum stresses that the pier experiences, that is, above approximately 3 ksi.
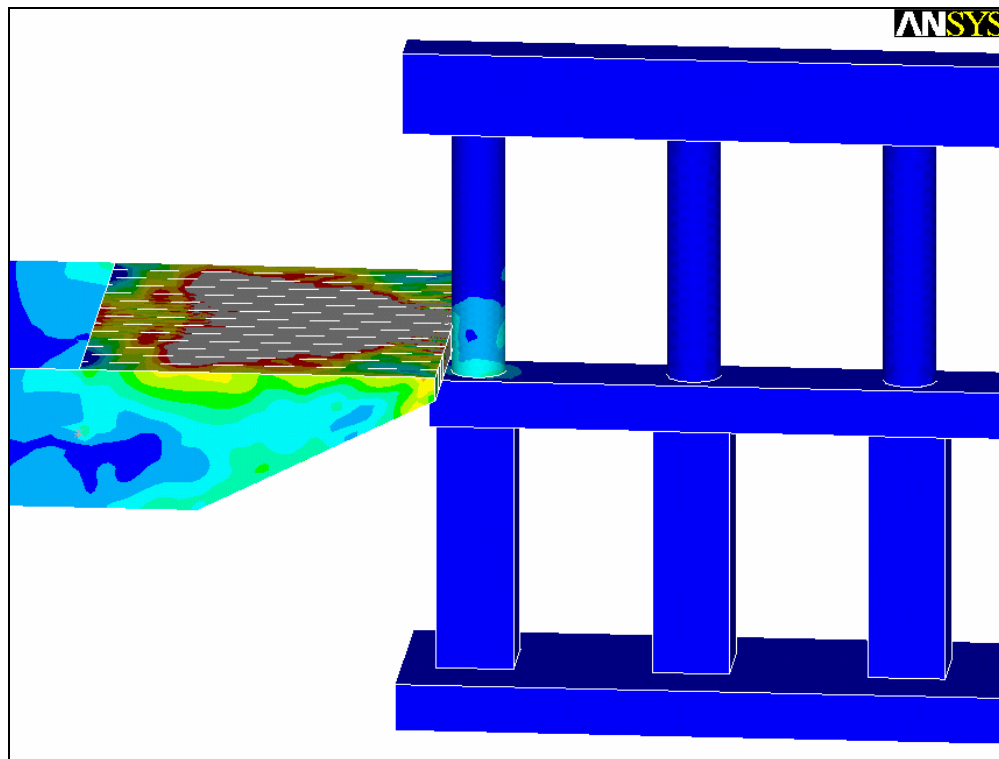
Figure 4.10 Case #1 (t = 0.04 seconds)

In Figure 4.11, crushing of the barge bow has started. Higher stresses are visible at the low end of the first column (and in the mid-beam) as it is dissipating the lateral force via shear to the structure below.
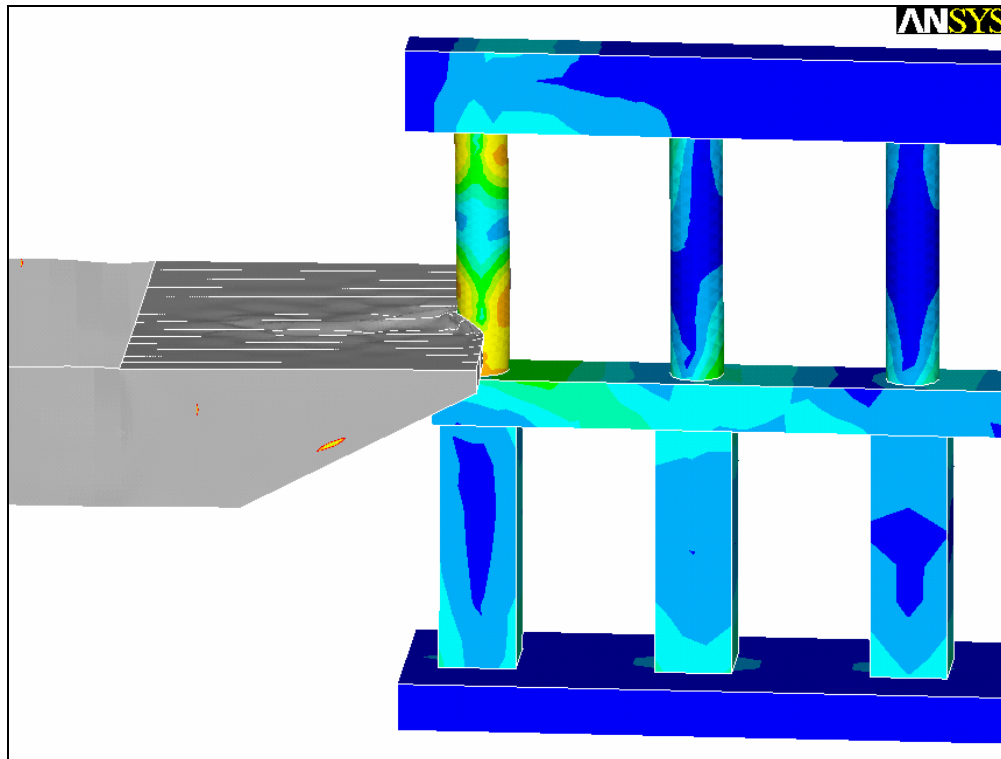
Figure 4.11 Case #1 (t = 0.4 seconds)

Figure 4.12 shows the other three top tier columns starting to carry lateral load.
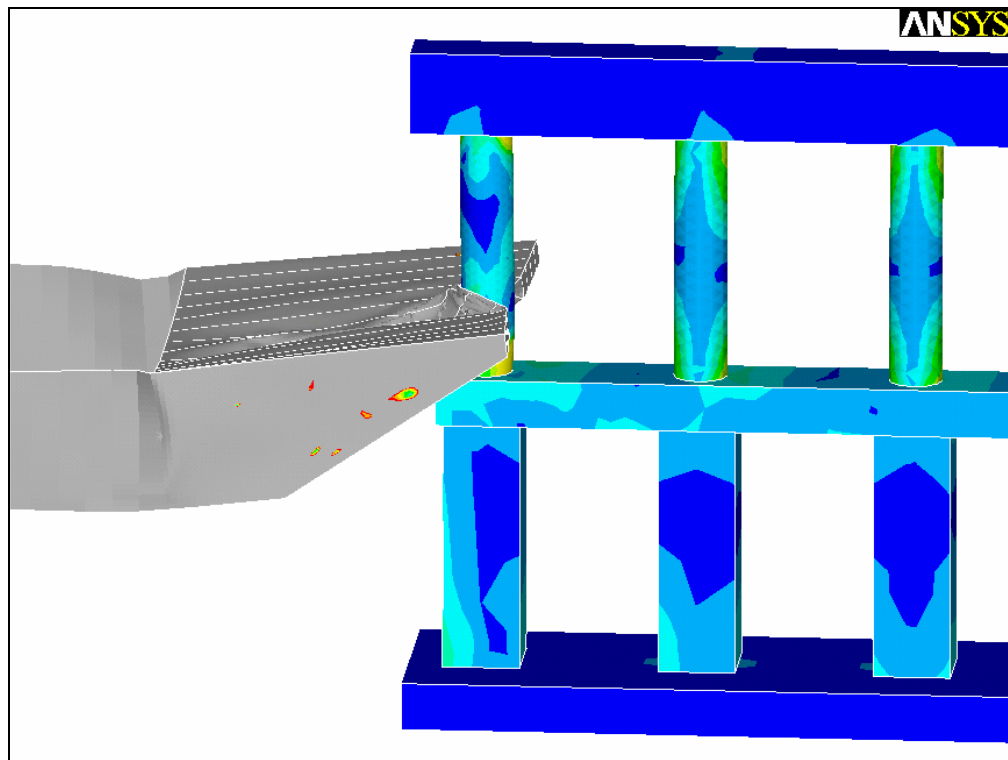
Figure 4.12 Case #1 (t = 0.8 seconds)

It is interesting to note that throughout the case #1 impact, very little force is transferred through the top beam of the bent. Notice that the images from case #6 show much more interaction from the top beam, since the impact is located very close to the center of the first column.
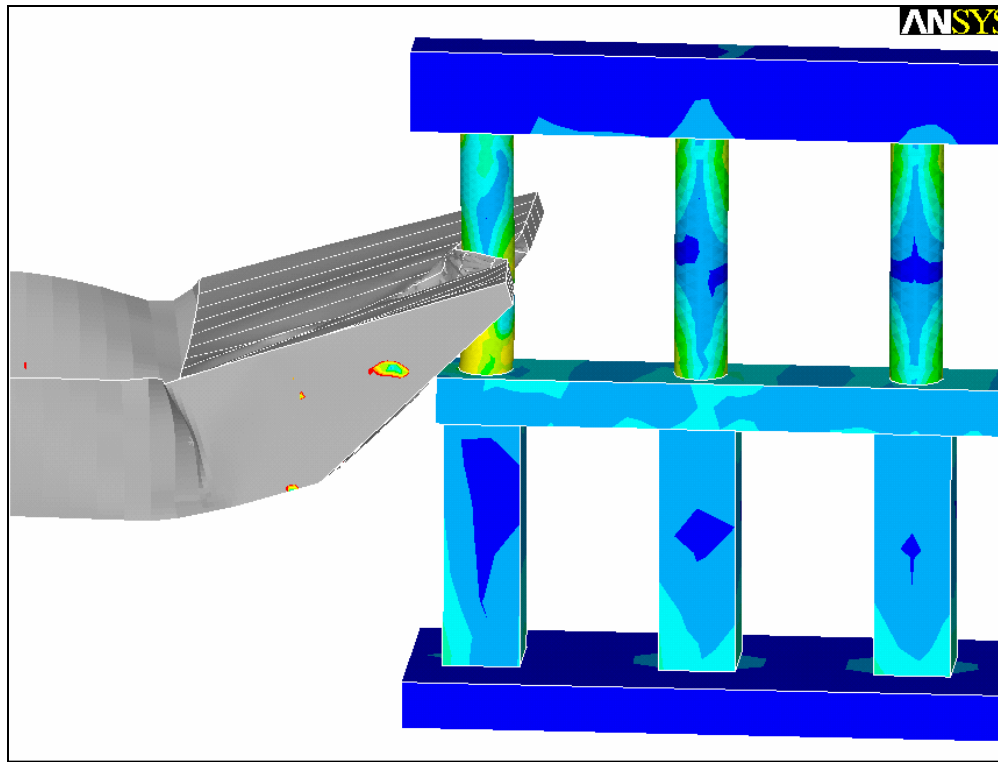
Figure 4.13 Case #1 (t = 1.2 seconds)

In Figure 4.14, the tendency of the vessel to climb the first column becomes evident, as discussed at the beginning of this section. Note that the lateral force imparted by the barge has decreased and stresses have been relieved throughout the pier.

83
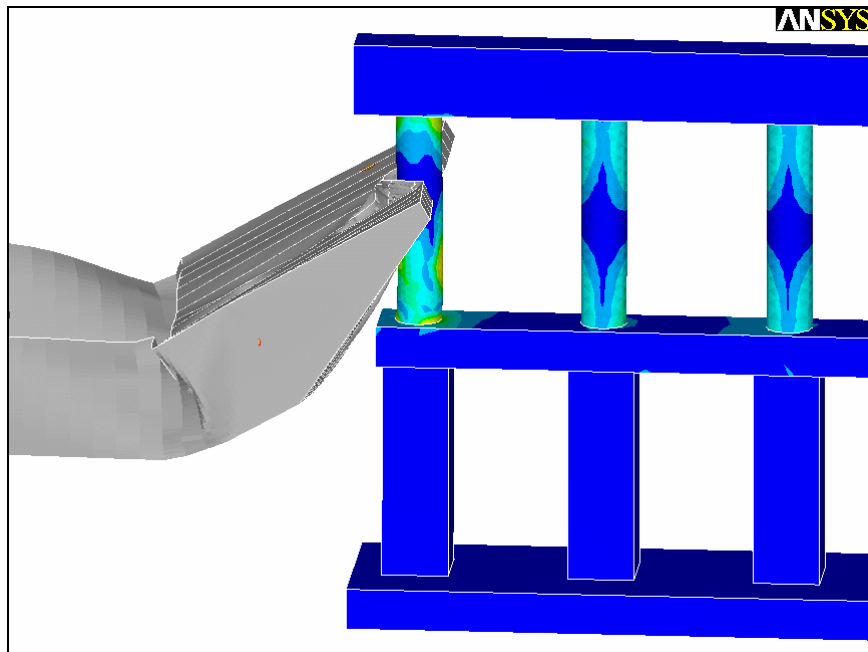
Figure 4.14 Case #1 (t = 1.6 seconds)
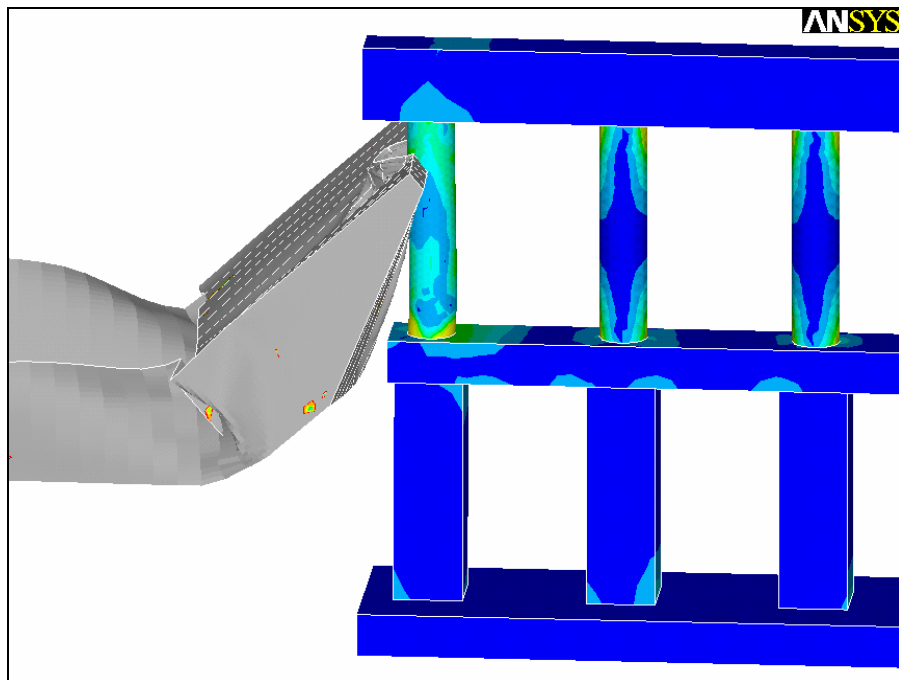
Figure 4.15 Case #1 (t = 2.0 seconds)

Figure 4.16 is a sample animation from case #6. The figures (Figs. 4.17-22) that follow were generated from the same simulation.
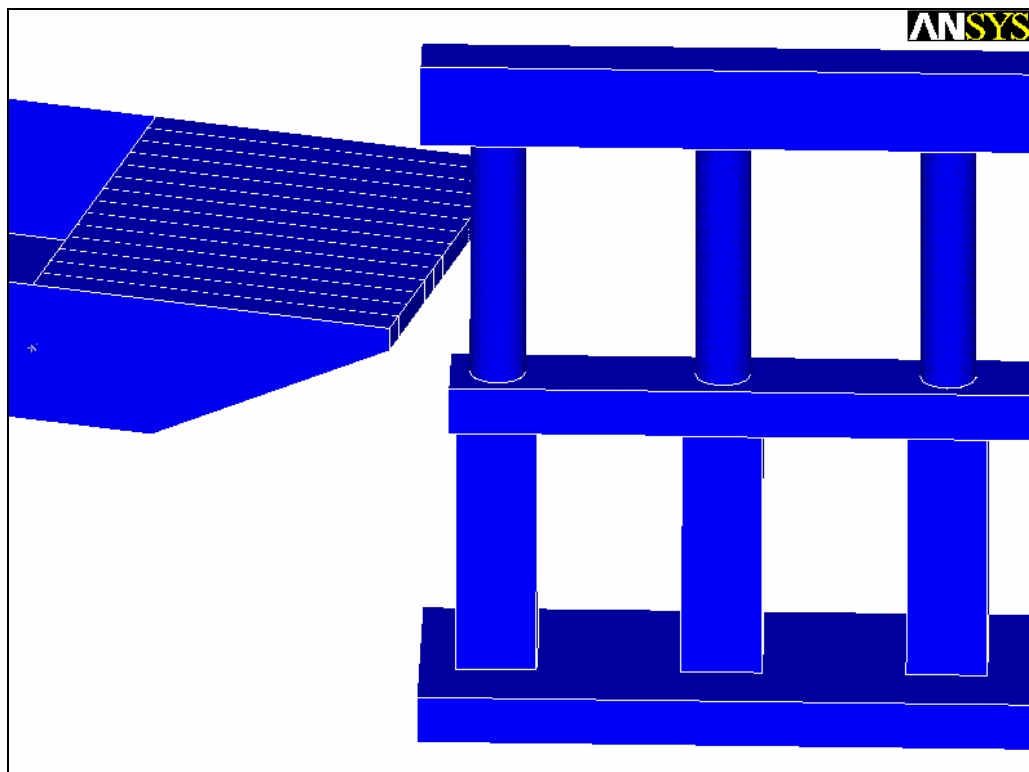
Figure 4.16 ANSYS animation; case #6 impact

Figure 4.17 is captured immediately after vessel impact has occurred. The initial flexural stress (at the center) and shear stresses (at the ends) can be seen in the first column.
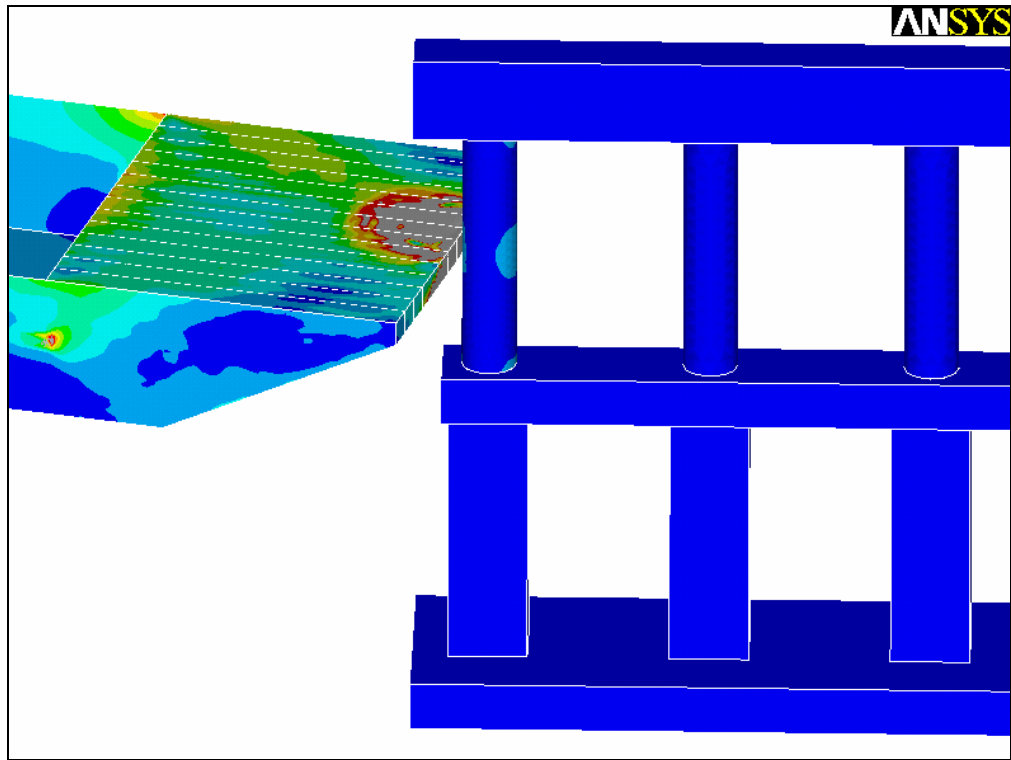
Figure 4.17 Case #6 (t = 0.13 seconds)

In Figure 4.18, stresses in the first column first reach their peak levels. Although the pier is a redundant structure, for this type of excitation, the stress redistribution has yet to reach the back half of the bent.
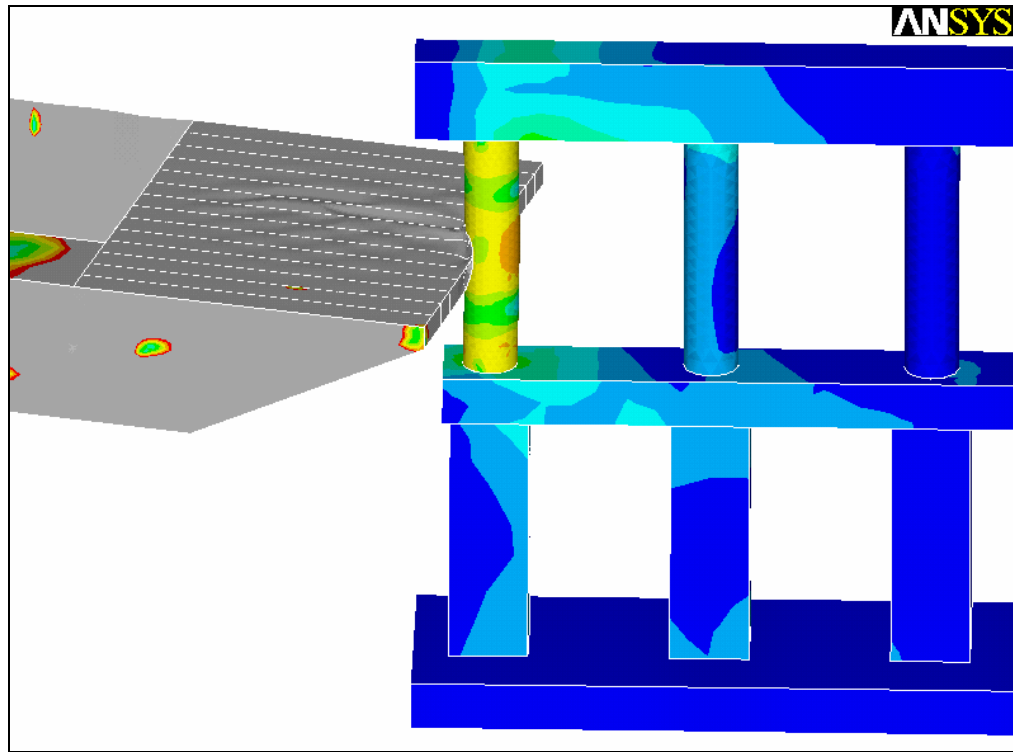
Figure 4.18 Case #6 (t = 0.4 seconds)

In Figure 4.19, stresses distributed more evenly throughout the bent suggest that the lateral impact force has been redistributed throughout the pier. The stresses in the upper tier of columns are higher than they are in the lower tier (as expected) since the lower columns have higher moments of inertia.
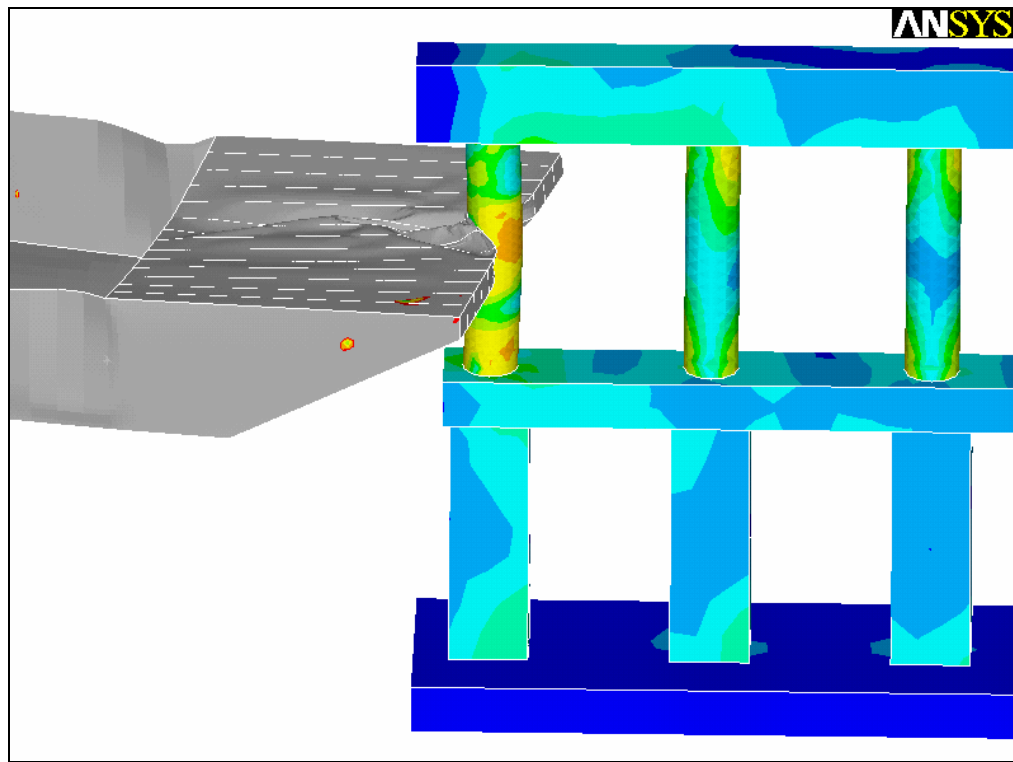
Figure 4.19 Case #6 (t = 0.8 seconds)

In Figure 4.20 there is a visible lateral deflection in the top tier columns, as we expect. This behavior was not seen in case #1, since the contact point was located relatively low on the first column.
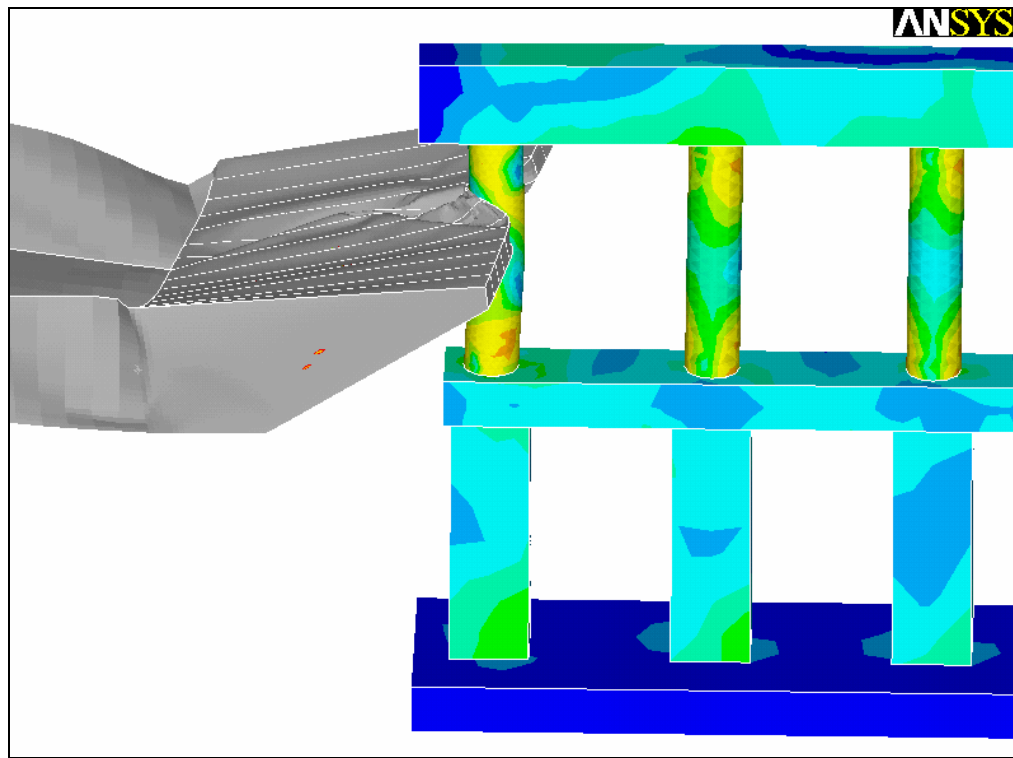
Figure 4.20 Case #6 (t = 1.2 seconds)

Again, Figure 4.21 exhibits the barge models tendency to climb the bent after initial impact.
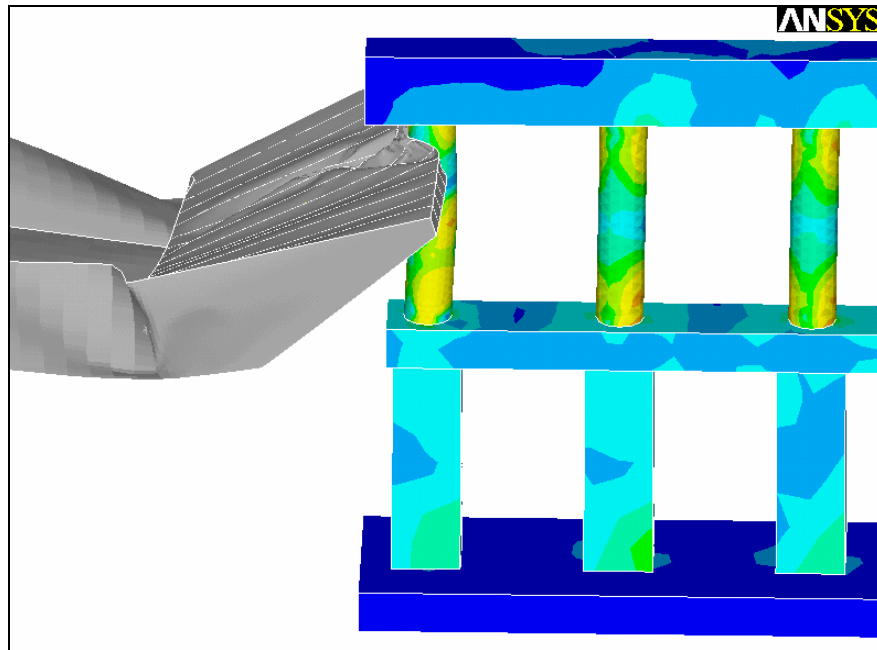
Figure 4.21 Case #6 (t = 1.6 seconds)
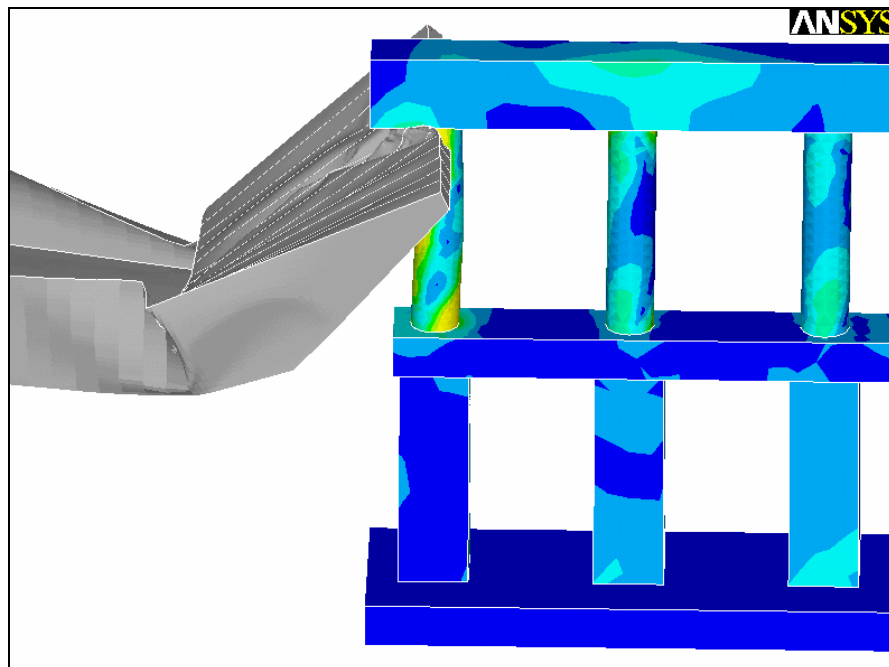
Figure 4.22 Case #6 (t = 2.0 seconds)

4.6   COMPARISON TO UFL MODEL

The calibration of our model using a comparison to the UFL model meant carrying out a simulation as similar to the UFL simulations as possible. The contact parameters, material properties, etc. were matched as closely as possible; our main differences stem from differences in the geometry of the barge.

The UFL model uses connection modeling, that is, models of the actual spot weld strengths and lengths, that may result in lower initial stiffness at impact (although the welds were specified with infinite strength, they allow the attached members to distort and detach from one another in such a way that the overall barge stiffness would be compromised).

In any case, were our model stiffer than an actual barge, the results would be conservative. In general, the stiffer the contact components used for the simulation the higher the contact forces will be. Although this may not be the case for all examples, it appeared to be the case with the preliminary simulations of this study.

Figure 4.1 illustrates the difference in the results from the two models (UFL results were taken from Figure 11-3 in the UFL report (Consolazio 2002)). Our model exhibits large contact forces at the beginning of contact (~ 0.1 sec) which immediately reduce for the remainder of the event. This high initial load carrying capacity can be attributed to the added stiffness that the stiffener plates contribute. Although these plates provide a simple replacement for the internal bow trusses of the UFL model, they represent stiffer internal support than the trusses actually provide. Once these plates buckle, the magnitude of the reaction forces is in the neighborhood of that observed in the UFL simulations. It is important to note that the initial stiffness of the impact is almost identical for the

two cases. Only after the internal trusses of the UFL model buckle, do the two plots separate.
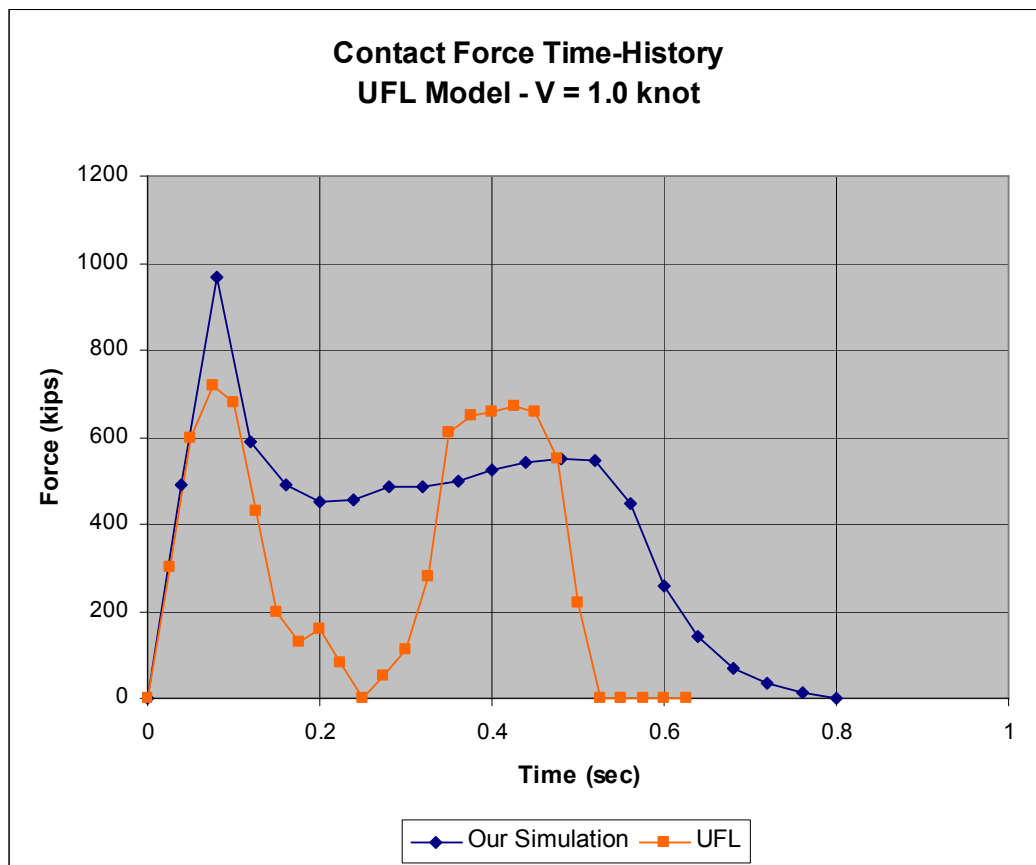
Figure 4.23 Comparison of present study's model versus the UFL model

CHAPTER 5

Concluding Remarks

5.1 SUMMARY

The primary goal of this study was to evaluate computationally the AASHTO code provisions for vessel-to-bridge pier impact. To this end, computational modeling of collision events based on the finite element method allowed for the estimation of static loads equivalent to the dynamic contact forces developed during the impact. The equivalency was based on an equal maximum deformation concept between the static and dynamic cases.

The numerical experiments revealed that the code provisions may underestimate or overestimate the computationally predicted static loads. Depending on the event parameters (vessel velocity, angle of impact, initial contact location, etc.), the static design load that the 2001 AASHTO Specifications require may lead to either an inadequate or a conservative design. For example, for the case of the San Jacinto Bridge prototype case of this study – contact at the high water line mark would have produced deformations and loads on the pier that would have been underestimated at the design phase (about 16% for the loads).

Whereas these observations are of a preliminary nature, the observed differences are nevertheless indicative of the design-for-impact problem. We note that our parametric studies took into account only a subset of physically important problem parameters. Inclusion of those aspects neglected in the present study will allow for greater fidelity between the computational models and the actual vessel-pier-soil-water-bridge physical system. The parametrized models provided in this study form a firm basis on which to build these more sophisticated models. Such

models will allow for the systematic study of the impact problem for the most commonly encountered bridge systems. Design recommendations derived from such simulations of individual bridge systems will result in an improved design tool based on updated code provisions.

APPENDIX A

Smear Properties for Member Sections (Henderson 2005)

IH 10 Eastbound Bridge at San Jacinto River (Bents 18 &19)					
Mat'l Set	M_y (kip-in)	M_p (kip-in)	f_y (ksi)	f_u (ksi)	f_u/f_y
			Bottom Tier Columns		
Specified	126060.0	159900.0	1.06	1.35	1.27
1	126269.6	160287.6	1.06	1.35	1.27
2	126794.4	161269.2	1.07	1.36	1.27
3	126816.0	161570.4	1.07	1.36	1.27
4	126986.4	161967.6	1.07	1.37	1.28
5	127095.6	162350.4	1.07	1.37	1.28
6	127210.8	162913.2	1.07	1.37	1.28
7	127268.4	163101.6	1.07	1.37	1.28
8	127446.0	163804.8	1.07	1.38	1.29
9	127530.0	164244.0	1.07	1.38	1.29
10	127614.0	164612.4	1.08	1.39	1.29
			Top Tier Columns		
Specified	34572.0	42576.0	1.32	1.62	1.23
1	34744.8	42734.4	1.32	1.63	1.23
2	35108.4	43022.4	1.33	1.64	1.23
3	35205.6	43105.2	1.35	1.64	1.22
4	35296.8	43213.2	1.35	1.65	1.22
5	35374.8	43320.0	1.35	1.65	1.22
6	35516.4	43477.2	1.36	1.66	1.22
7	35545.2	43526.4	1.36	1.66	1.22
8	35696.4	43741.2	1.36	1.67	1.23
9	35778.0	43886.4	1.36	1.67	1.23
10	35862.0	44017.2	1.36	1.68	1.23

Notes:
1. Refer to Table 3-2 for the properties of each material set.

Appendix A (cont.) Smear Properties for Member Sections (Henderson 2005)

IH 10 Eastbound Bridge at San Jacinto River (Bents 18 &19)					
Mat'l Set	M_y (kip-in)	M_p (kip-in)	f_y (ksi)	f_u (ksi)	f_u/f_y
		Top Beam & Pile Cap			
Specified	61668.0	86904.0	1.27	1.80	1.41
1	61192.8	87045.6	1.27	1.80	1.42
2	61197.6	87332.4	1.26	1.80	1.43
3	61304.4	87428.4	1.26	1.81	1.43
4	61327.2	87520.8	1.26	1.81	1.43
5	61358.4	87606.0	1.27	1.81	1.43
6	61509.6	87806.4	1.27	1.81	1.43
7	61500.0	87867.6	1.27	1.82	1.43
8	61423.0	88032.0	1.27	1.82	1.43
9	61590.0	88117.2	1.27	1.82	1.43
10	61590.0	88207.2	1.27	1.82	1.43
		Mid-Height Beam			
Specified	42735.6	55396.8	0.88	1.14	1.30
1	42830.4	55515.6	0.88	1.15	1.30
2	42981.6	55837.2	0.89	1.15	1.30
3	43009.2	55941.6	0.89	1.16	1.30
4	43062.0	55971.6	0.89	1.16	1.30
5	43104.0	55989.6	0.89	1.16	1.30
6	43153.2	56032.8	0.89	1.16	1.30
7	43160.4	56050.8	0.89	1.16	1.30
8	43218.0	56100.0	0.89	1.16	1.30
9	43256.4	56138.4	0.89	1.16	1.30
10	43281.6	56175.6	0.89	1.16	1.30

Notes:
1. Refer to Table 3-2 for the properties of each material set.

APPENDIX B

ANSYS Input Files – Simulation Input

```
!---------------------- Contact Preparation --------------------

/PREP7                           !Open Preprocessor
/NOPR

/INPUT,'jhb3.3','txt','Z:\Thesis\ANSYS\Input_Files\',,0

WPOF,-3.75,-28.7,-9             !Position components for contact
!WPRO,,,15                       !Rotate working plane

/INPUT,'pier_sje_final','txt','Z:\Thesis\ANSYS\Input_Files\',,0

ALLSEL,ALL
/REPLOT

EDCGEN,ASTS,STIFFHOPPER,PIER  !Define Auto Surf-to-Surf Contact

FINISH                          !Close Preprocessor

!-------------------------- Solution -------------------------

/SOL                            !Open solver

ASEL,S,,,1002                   !Apply boundary conditions
DA,ALL,ALL,0
ALLSEL,ALL
                                     !Apply initial conditions
EDVE,VELO,STIFFHOPPER,9.838          !0 degree impact angle
!EDVE,VELO,STIFFHOPPER,9.754,,1.284 !7.5 degree impact angle
!EDVE,VELO,STIFFHOPPER,9.503,,2.546 !15 degree impact angle

TIME,2                          !Time at end of load step
EDRST,50                        !Results output interval
```

```
EDHTIME,50                        !Time-history output interval
EDHIST,PIER                       !Component for time-history output

EDOUT,RCFORC                      !Time-history output (ASCII format)
EDDUMP,1                          !Restart file output frequency

/GOPR

SOLVE                             !Obtain solution
FINISH                            !Close solver

----------------------------------------------------------------
```

```
!----------------------- Geometry Input ----------------------

/PREP7                    !Open preprocessor

CSYS,WP                   !Set working plane as coord system
                          !Input keypoints
K,,-195,12,17.5           !Right side (K1 – K7)
K,,-195,0,17.5
K,,-30,12,17.5
K,,-30,0,17.5
K,,-20,0,17.5
K,,0,12,17.5
K,,0,10,17.5


K,,-195,12,-17.5          !Left side (K8 – K14)
K,,-195,0,-17.5
K,,-30,12,-17.5
K,,-30,0,-17.5
K,,-20,0,-17.5
K,,0,12,-17.5
K,,0,10,-17.5
                          !Input areas
A,1,2,4,3,1               !Right side
A,3,4,5,7,6,3
A,8,9,11,10,8             !Left side
A,10,11,12,14,13,10
A,1,2,9,8,1               !Stern
A,2,4,11,9,2              !Back bottom
A,4,5,12,11,4             !Front bottom
A,5,7,14,12,5             !Bow bottom
A,6,7,14,13,6             !Headlog
A,3,6,13,10,3             !Bow top


LSEL,S,,,19,23            !Input bow stiffeners
```

```
LDIV,ALL,,,14
A,79,66,41,28,15
A,78,65,42,29,16
A,77,64,43,30,17
A,76,63,44,31,18
A,75,62,45,32,19
A,74,61,46,33,20
A,73,60,47,34,21
A,72,59,48,35,22
A,71,58,49,36,23
A,70,57,50,37,24
A,69,56,51,38,25
A,68,55,52,39,26
A,67,54,53,40,27


ALLSEL,ALL
AGLUE,ALL                  !Create 1 geometric entity

ASEL,S,,,60,63             !Concatenate 4 areas at contact location
AADD,ALL


!--------------- Element & Real Constant Definitions ------------

ET,1,SHELL163              !Define element type
R,1,,,0.03125             !3/8" Exterior plates
R,2,,,0.00521             !1/16" Bow stiffeners


!--------------------- Material Model Input -------------------

MAT,1                     !Set material pointer
MP,EX,1,4.2624e9          !Young's modulus (psf)
MP,NUXY,1,0.28            !Poisson's ratio
MP,DENS,1,490            !Mat'l density (pcf)
TB,PLAW,1,,,8            !Piecewise linear plasticity mat'l model


TBDATA,6,1               !Define true stress vs. plastic strain
*DIM,strn1,,7            !  curve
*DIM,strs1,,7
```

```
strn1(1)=1e-6,0.002364,0.014191,0.092597,0.219512,0.22,5.0
strs1(1)=5.1902e6,6.9396e6,7.1689e6,1.1563e7,1.5480e7,1,1
EDCURVE,ADD,1,strn1(1),strs1(1)


!------------------------- Meshing -------------------------

TYPE,1                   !Set element pointer
REAL,1                   !Set real constant pointer
MSHAPE,0                 !Set element shape (quadrilateral)
MSHKEY,2                 !Set free meshing (possible mapping opt)


LSEL,S,,,109,113         !Divide lines at center bow stiffeners
LSEL,A,,,129,133         !  to ensure error-free mesh generation
LESIZE,ALL,0.4


LSEL,S,,,67,70           !Divide lines at concatenated contact
LSEL,A,,,54,57           !  area to ensure error-free mesh
LESIZE,ALL,0.28          !  generation


ASEL,S,,,7               !Mesh concatenated contact area


ESIZE,0.28
AMESH,ALL


ASEL,S,,,72,75           !Mesh above & below contact area
ASEL,A,,,48,51
ASEL,A,,,15,19           !Mesh central bow stiffeners


ESIZE,0.4
AMESH,ALL


ASEL,S,,,11,14           !Mesh end stiffeners
ASEL,A,,,20,23


ESIZE,0.5
AMESH,ALL


ASEL,S,,,2               !Mesh right side of barge bow
```

```
ASEL,A,,,24,27
ASEL,A,,,76,79
ASEL,A,,,56,59
ASEL,A,,,44,47
ASEL,A,,,32,35

ASEL,A,,,4                  !Mesh left side of barge bow
ASEL,A,,,28,31
ASEL,A,,,68,71
ASEL,A,,,64,67
ASEL,A,,,52,55
ASEL,A,,,40,43
ASEL,A,,,36,39

ESIZE,0.6
AMESH,ALL

ASEL,S,,,1                  !Mesh sides, bottom, and stern
ASEL,A,,,3
ASEL,A,,,5
ASEL,A,,,6

ESIZE,2.66
AMESH,ALL

ASEL,S,,,11,23             !Modify typ bow stiffener gauge
ESLA
EMODIF,ALL,REAL,2
ALLSEL,ALL

NUMMRG,NODE                 !Merge all nodes

AREFINE,7,,,2.3,3           !Refine concatenated contact area

!----------------------- Point Mass Input ---------------------

ET,2,MASS166                !Define mass element
R,3,31008                   !Fully-loaded barge w/ tug boat
```

```
!R,3,7786               !604 tons (UFL tests)
REAL,3                  !Set real constant pointer
TYPE,2                  !Set element type pointer
E,29833                 !Define point masses
E,31156
E,21506
E,22556


!--------------------- Component Definition -------------------

ESEL,S,TYPE,,1          !Define barge component for contact
ESEL,A,TYPE,,2          !  definition
NSLE,R
CM,STIFFHOPPER,NODE

/NUMBER,0
EPLOT
/REPLOT

/VIEW,1,1,1,1
/ANG,1
/REP,FAST

!--------------------------------------------------------------
```

```
!---------------------- Material Model Input -------------------

/PREP7                            !Open preprocessor
                                  !Bottom Column
MP,EX,2,1.526e8                   !Young's Mod       !mat set 1
!MP,EX,2,1.541e8                                     !mat set 5
!MP,EX,2,1.555e8                                     !mat set 10
MP,NUXY,2,0.15                    !Poisson's Ratio
MP,DENS,2,150                     !Material density (pcf)
TB,PLAW,2,,,8                     !Piecewise linear material model
TBDATA,6,2                        !True stress vs. plastic strain
*DIM,strn2,,3
*DIM,strs2,,3
strn2(1)=0.001,0.002,5.0
strs2(1)=1.5264e5,1.944e5,1.944e5              !mat set 1
!strs2(1)=1.541e5,1.973e5,1.973e5              !mat set 5
!strs2(1)=1.555e5,2.002e5,2.002e5              !mat set 10
EDCURVE,ADD,2,strn2(1),strs2(1)

MP,EX,3,1.901e8                   !Top Column        !mat set 1
!MP,EX,3,1.944e8                                     !mat set 5
!MP,EX,3,1.973e8                                     !mat set 10
MP,NUXY,3,0.15
MP,DENS,3,150
TB,PLAW,3,,,8
TBDATA,6,3
*DIM,strn3,,3
*DIM,strs3,,3
strn3(1)=0.001,0.002,5.0
strs3(1)=1.9008e5,2.347e5,2.347e5              !mat set 1
!strs3(1)=1.944e5,2.376e5,2.376e5              !mat set 5
!strs3(1)=1.973e5,2.419e5,2.419e5              !mat set 10
EDCURVE,ADD,3,strn3(1),strs3(1)
```

```
MP,EX,4,1.2816e8                    !Mid Beam          !mat set 1
!MP,EX,4,1.2816e8                                      !mat set 5
!MP,EX,4,1.2816e8                                      !mat set 10
MP,NUXY,4,0.15
MP,DENS,4,150
TB,PLAW,4,,,8
TBDATA,6,4
*DIM,strn4,,3
*DIM,strs4,,3
strn4(1)=0.001,0.002,5.0
strs4(1)=1.2816e5,1.656e5,1.656e5             !mat set 1
!strs4(1)=1.2816e5,1.670e5,1.670e5            !mat set 5
!strs4(1)=1.2816e5,1.670e5,1.670e5            !mat set 10
EDCURVE,ADD,4,strn4(1),strs4(1)


MP,EX,5,1.8144e8                    !Top Bm            !mat set 1
!MP,EX,5,1.829e8                    !& Pile Cap        !mat set 5
!MP,EX,5,1.829e8                                       !mat set 10
MP,NUXY,5,0.15
MP,DENS,5,150
TB,PLAW,5,,,8
TBDATA,6,5
*DIM,strn5,,3
*DIM,strs5,,3
strn5(1)=0.001,0.002,5.0
strs5(1)=1.8144e5,2.592e5,2.592e5             !mat set 1
!strs5(1)=1.829e5,2.606e5,2.606e5             !mat set 5
!strs5(1)=1.829e5,2.621e5,2.621e5             !mat set 10
EDCURVE,ADD,5,strn5(1),strs5(1)


!------------------------ Geometry Input --------------------

NUMSTR,KP,100000               !Set numbering references
NUMSTR,AREA,1000
NUMSTR,LINE,1000
NUMSTR,ELEM,75000


CSYS,WP                        !Set working plane as coord sys
```

```
BLOCK,0,67,0,4,0,18              !Define pier cap
BLOCK,2.37,64.63,25,29,5.5,12.5   !Define mid beam
BLOCK,0,67,50,57,6.625,11.375     !Define top beam

WPRO,,-90
WPOF,,-9,29
CYL4,6.255,,,,2.25,,21           !Define top tier cols
VGEN,4,4,,,,18.17

WPOF,,,-25
BLOCK,3.005,9.505,-3.25,3.25,0,21  !Define bot tier cols
VGEN,4,8,,,,18.17

WPOF,,9,-4                        !Reset working plane
WPRO,,90

VGLUE,ALL                        !Create 1 geometric entity

!------------------ Element Definition & Meshing -------------

ET,3,SOLID164            !Define element type

TYPE,3                   !Set element pointer
MSHAPE,1,3D              !Set element shape (hexahedral)
MSHKEY,0                 !Set free meshing

VSEL,S,,,4              !Mesh Column A
MAT,3                   !Assign smear mat'l set 3
ESIZE,0.8
VMESH,ALL

VSEL,S,,,5             !Mesh (3) remaining top tier columns
VSEL,A,,,6
VSEL,A,,,7
MAT,3                  !Assign smear mat'l set 3
ESIZE,2.4
VMESH,ALL
```

106

```
VSEL,S,,,14              !Mesh mid-beam
MAT,4                    !Assign smear mat'l set 4
ESIZE,2.4
VMESH,ALL


VSEL,S,,,13              !Mesh top beam
MAT,5                    !Assign smear mat'l set 5
ESIZE,2.4
VMESH,ALL


VSEL,S,,,12              !Mesh pier cap
MAT,5                    !Assign smear mat'l set 5
ESIZE,4.8
VMESH,ALL


VSEL,S,,,8              !Mesh bottom tier columns
VSEL,A,,,9
VSEL,A,,,10
VSEL,A,,,11
MAT,2                    !Assign smear mat'l set 2
ESIZE,4.8
VMESH,ALL


ALLSEL,ALL


NUMMRG,NODE              !Merge all nodes


!------------------------ Component Definition -----------------


ESEL,S,MAT,,2,5          !Define pier component for contact
NSLE,R,
CM,PIER,NODE


EPLOT
/REPLOT


/VIEW,1,1,1,1
```

```
/ANG,1
/REP,FAST

!-----------------------------------------------------------------
```

```
!---------------------- Material Model Input -------------------

/PREP7                          !Open preprocessor

ET,3,SOLID164                   !Define element type

MAT,2                           !Set material pointer
MP,EX,2,5.184e8                 !Young's modulus (psf)
MP,NUXY,2,0.15                  !Poisson's ratio
MP,DENS,2,150                   !Material density (pcf)
TB,PLAW,2,,,8                   !Piecewise linear plasticity model

TBDATA,6,2                      !True stress vs. plastic strain
*DIM,strn,,5
*DIM,strs,,5
strn(1)=0.000304,0.001163,0.002299,0.0025,5.0
strs(1)=3.6036e5,4.3286e5,3.6108e5,1,1
EDCURVE,ADD,2,strn(1),strs(1)


!------------------------- Geometry Input --------------------

NUMSTR,KP,1000                  !Set numbering preferences
NUMSTR,AREA,1000
NUMSTR,LINE,1000
NUMSTR,ELEM,50000

CSYS,WP                         !Set working plane as coord sys
                                !Define keypoints
K,,0,0,0                        !Define top surface keypoints
K,,30.375,0,0
K,,30.375,0,6.572
K,,0,0,6.572
K,,0.958,53,0.958
K,,29.417,53,0.958
```

```
K,,29.417,53,5.614
K,,0.958,53,5.614

K,,7,0,0                        !Define bottom surface keypoints
K,,23.375,0,0
K,,23.375,0,6.572
K,,7,0,6.572
K,,7,46,0
K,,23.375,46,0
K,,23.375,46,6
K,,7,46,6

V,1000,1001,1002,1003,1004,1005,1006,1007 !Define prelim volume
V,1008,1009,1010,1011,1012,1013,1014,1015 !Subtraction volume
VSBV,1,2,,,DELETE                          !Boolean subtraction
ALLSEL,ALL

BLOCK,7,23.375,0,15,1.281,5.124          !Define shear wall
BLOCK,-4.396,34.771,0,-5,-7.219,13.781   !Define pile cap
ALLSEL,ALL

VGLUE,ALL                                !Join all volumes

!------------------- Element Definition & Meshing -------------

TYPE,3                    !Set element pointer
ESIZE,2                   !Set element size
MSHAPE,1,3D               !Set element shape (hexahedral)
MSHKEY,0                  !Set free meshing
VMESH,ALL                 !Mesh pier

EREFINE,56962,,,1,2       !Refine mesh at contact area

!---------------------- Component Definition ----------------

ESEL,S,MAT,,2             !Define pier component for contact
NSLE,R,
CM,FLORIDAPIER,NODE
```
110

```
ALLSEL,ALL

/VIEW,1,1,1,1
/ANG,1
/REP,FAST

EPLOT

!----------------------------------------------------------------
```

References

1. AASHTO. *LRFD Bridge Design Specifications*. Third Edition. American Association of State Highway and Transportation Officials, 1998 (and 2001 Interim Provisions).

2. AASHTO. *Guide Specification and Commentary for Vessel Collision Design of Highway Piers*. American Association of State Highway and Transportation Officials, February, 1991.

3. ACI. *Building Code Requirements for Structural Concrete (ACI 318-02) and Commentary (ACI 318R-02)*, ACI Committee 318, 2002.

4. Basci, Rich. Telephone Interview. 12 Jan 2005.

5. Calzada, Billy. "Shades and Shadows." 2001. 20 Apr. 2005 <http://pages.sbcglobal.net/bcalz/causeway.html>.

6. Chopra, Anil K. <u>Dynamics of Structures</u>. Second Edition. New Delhi: Prentice Hall of India, 2003.

7. Consolazio, G.R., D.R. Cowan. "Nonlinear analysis of barge crush behavior and its relationship to impact resistant bridge design." Computers and Structures 81, 547-557, 2003.

8. Consolazio, G.R., D.R. Cowan, A. Biggs, R.A. Cook, M. Ansley, and H.T. Bollman. *Full-Scale Experimental Measurement of Barge Impact Loads on Bridge Piers*. Transportation Research Board 2005 Annual Meeting CD-ROM, 2005.

9. Consolazio, G.R., R.A. Cook, and G.B. Lehr. "Barge Impact Testing of the St. George Island Causeway Bridge, Phase I: Feasibility Study." UF Report No. 4910-4504-783-12, University of Florida, 2002.

10. Frandsen, A.G. "Accidents Involving Bridges." IABSE Colloquium, Copenhagen, Denmark, Vol. 1, 1983.

11. Henderson, Wyatt. "Modeling and Analysis of Bridges Subjected to Vessel Impact." Masters Thesis, The University of Texas at Austin. May 2005.

12. IABSE Colloquium. "Ship Collision with Bridges and Offshore Structures." 3 Volumes. Copenhagen, Denmark, 1983.

13. Meir-Dornberg, K.E. "Ship Collisions, Safety Zones, and Loading Assumptions for Structures on Inland Waterways." VDI-Berichte No. 496, pp. 1-9, 1983.

14. Modjeski and Masters, Consulting Engineers. 1984. *Criteria for the Design of Bridge Piers with Respect to Vessel Collision in Louisiana Waterways.* Prepared for the Louisiana Department of Transportation and Development and the Federal Highway Adminstration, Harrisburg, PA, November 1984.

15. Saul, R. and Svensson, H. "On the Theory of Ship Collision against Bridge Piers." IABSE Proceedings, pp. 51-82, February, 1980.

16. Woisin, G., Gerlach, W. "On the Estimation of Forces Developed in Collisions Between Ships and Offshore Lighthouses." IALA Conference, Stockholm, 1970.

17. Woisin, G. "Ship-Structural Investigation for the Safety of Nuclear Powered Trading Vessels." Jahrbuch der Schiffbautechnishen Gesellshaft, Volume 65, 225-263, Berlin, 1971.

18. Woisin, G. "The Collision Tests of the GKSS." Jahrbuch der Schiffbautechnishen Gesellshaft, Volume 70, 465-487, Berlin, 1976.

Modeling and Analysis of Bridges Subjected to Vessel Impact

Wyatt R. Henderson
Eric B. Williamson

Executive Summary

Vessel collision is an important consideration in the design of bridges crossing navigable waterways. The American Association of State Highway and Transportation Officials (AASHTO) Load and Resistance Factor Design (LRFD) Bridge Design Specification governs vessel collision design of bridges in the United States. The AASHTO recommended design procedure for vessel collision is a probability-based calculation that returns an annual frequency of collapse for a given bridge.

One of the important calculations in determining the annual frequency of collapse is the ultimate lateral strength of a bridge element, which AASHTO defines as a bridge pier or bridge span. The current AASHTO Design Specification provides little guidance in the calculation of this value. The primary objective of this report is to provide engineers with the necessary tools to calculate the ultimate lateral strength of bridge elements.

This report outlines procedures for modeling and analyzing bridge piers and bridge systems subject to vessel impact loads using a typical structural analysis software package. The methods presented in this report focus on modeling reinforced concrete bridge piers, both with and without shear walls. In addition, the effect of considering system-wide response on the ultimate lateral strength of a bridge is investigated by including the bridge superstructure and adjacent bridge piers in the models.

iv

Table of Contents

List of Figures

x

List of Tables

1. Introduction

1.1 Background on Vessel Collision

Vessel collision is an important consideration in the design of bridges crossing navigable waterways. This section clearly illustrates this importance by showing the consequences of vessel collision accidents. General information on the current state of vessel collision design is outlined along with an analysis of where the current design procedures could be improved.

1.1.1 The Significance of Vessel Collision with Bridges

Recent bridge failures in Texas and Oklahoma resulting from barge collisions indicate that engineers need better methods of design and analysis to counter these catastrophic events. On September 15, 2001, a fully loaded four-barge tow struck a pier on the Queen Isabella Causeway (QIC) in Texas, destroying a 240-foot section of the bridge and killing eight people. Figure 1-1 shows the damage caused by the collision. The accident closed the QIC for over two months, the only road link between South Padre Island and the Texas mainland. Repair costs for the bridge were approximately $4.3 million according to the Texas Department of Transportation (TXDOT press release, 2001)

On May 26, 2002 a towboat pushing two empty barges struck a pier of the I-40 Bridge outside of Webbers Falls, Oklahoma, collapsing a 503-foot section. Figure 1-2 shows the aftermath of the collision. The incident resulted in 14 deaths and an estimated $30 million in damage, including the cost of re-routing traffic while repairs were made, according to the National Transportation and Safety Board Accident Report (NTSB, 2002). These two events clearly show the damage that vessel collision can cause and the importance of carefully considering this load case in the design of bridges crossing navigable waterways.

Figure 1.1: Queen Isabella Causeway Damage

Figure 1.2: Webbers Falls, OK I-40 Bridge Damage

1.1.2 Vessel Collision Design in the United States

Bridge design in the United States is governed by the American Association of State Highway and Transportation Officials (AASHTO) *LRFD Bridge Design Specification* (AASHTO, 2003). Design Section 3.14 of this document covers vessel collision and is based on the AASHTO *Guide Specification and Commentary for Vessel Collision Design of Highway Bridges* (AASHTO, 1991). The AASHTO Guide Specification provides three methods for the evaluation of bridges spanning navigable waterways. Method I provides the simplest procedure for selection of a design vessel and calculation of an equivalent static impact force to apply to a bridge. A structural analysis is then performed to check if the bridge can resist the applied load. Method II is a probability-based procedure that calculates an Annual Frequency of Collapse (*AF*) for a bridge based on waterway characteristics, vessel traffic data, and bridge geometry. AASHTO provides minimum acceptable *AF* values for various bridge types. Method III is a cost effectiveness analysis procedure where the cost of protecting a bridge is compared against the benefits of reducing the risk to a bridge (AASHTO, 1991). Method III is intended for use only in unique cases where the risk acceptance criteria using Method I or II result in designs that are unreasonably expensive (AASHTO, 1991)

The AASHTO Guide Specification recommends the use of Method II. Therefore, the AASHTO Design Specification includes only the Method II procedure. Methods I and III are only found in the AASHTO Guide Specification. A brief review of Method II is given below to provide some essential background on the procedure. All three methods are explained in greater detail in Chapter 3 of this report.

1.1.3 AASHTO Method II Vessel Collision Design Basics

Design Method II is a detailed, probability-based analysis procedure. It requires a wide range of data on the waterway characteristics, the vessels traversing the waterway and the

geometry of the bridge being analyzed. This information is used to compute an annual frequency of collapse for a bridge. A minimum acceptable annual frequency of collapse is given depending on bridge classification. Bridges are classified as 'regular' or 'critical', and the AASHTO Design Specification provides guidance on the factors and parameters that should be considered when determining bridge classification. This topic will be discussed in more detail in Chapter 3.

The annual frequency of collapse calculation is based on the number and type of vessels traversing the waterway, the probability of a given vessel being aberrant, the geometric probability of a collision between an aberrant vessel and a bridge element, and the probability of a bridge collapsing due to a collision with an aberrant vessel. The *AF* is given by the following equation (4.8.3-1 in the AASHTO Guide Specification):

$$AF = (N)(PA)(PG)(PC) \qquad \text{(1-1)}$$

where:

AF = annual frequency of bridge element collapse due to vessel collision

N = annual number of vessels classified by type, size, and loading condition which can strike a bridge element

PA = probability of vessel aberrancy

PG = geometric probability of a collision between an aberrant vessel and a bridge pier or span

PC = probability of a bridge collapse due to a collision with an aberrant vessel

Vessel aberrancy is usually the result of human error, mechanical failure or adverse environmental conditions (AASHTO, 1991). The probability of aberrancy (*PA*) calculation is based on several factors including current speed and direction, location of a bridge within a waterway, and vessel traffic density. The geometric probability (*PG*) that an aberrant vessel will strike a bridge element is based primarily on bridge geometry and vessel traffic data. The probability of collapse (*PC*) from vessel collision is a function of two primary variables, the load imparted to a bridge from the colliding vessel and the lateral capacity of the bridge.

The input data and calculations required to calculate the probability of vessel aberrancy (*PA*) and the geometric probability of a collision between an aberrant vessel and a bridge (*PG*) are clearly defined. For example, the probability of vessel aberrancy is increased if a bridge is located in bend/turn regions of a waterway, or if there is a high density of vessel traffic. The geometric probability of collision increases if there are a greater number of bridge piers exposed in the waterway, or if a barge tow has greater overall length. Calculating the probability of collapse term, however, is less well defined than the other terms.

The probability of collapse term is defined as the probability that a bridge will collapse when an individual bridge element (pier or span) is struck by an aberrant vessel. AASHTO defines the probability of collapse as a function of two variables: the impact force of a vessel and the ultimate strength of a bridge element. Determining the impact forces from a vessel collision requires consideration of many factors, including vessel type, size, mass, speed, location of impact on a bridge, and the direction of the impact against a bridge. AASHTO does provide guidance for the calculation of impact forces, but offers little information on the calculation of bridge element ultimate lateral strength. The probability of collapse is given by a curve defined by the following equations:

For $0.0 \leq H/P < 0.1$, PC shall be computed as:

$$PC = 0.1 + 9\left[0.1 - \frac{H}{P}\right]$$
(1-2)

For $0.1 \leq H/P < 1.0$, PC shall be computed as:

$$PC = \frac{\left[1 - \frac{H}{P}\right]}{9}$$
(1-3)

For $H/P > 1.0$:

$$PC = 0$$
(1-4)

where
$H =$ ultimate bridge element strength (kips)
$P =$ vessel impact force (kips)

These equations are shown as a graph in Figure 1-3.
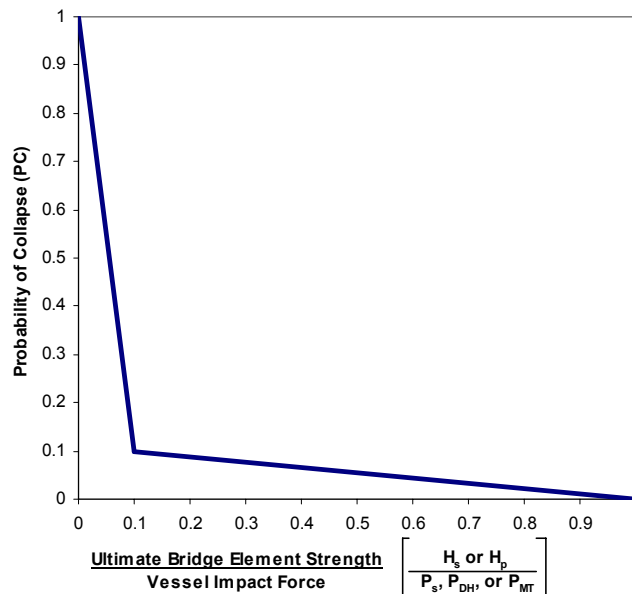
Figure 1.3: Probability of Collapse Curve (Adapted From AASHTO, 1991)

1.1.4 Improving the Probability of Collapse Term

While the basics of the *PC* equations seem reasonable, that is, if the force with which a bridge element is struck increases, the probability of collapse increases, or if the strength of a bridge element being struck increases, the probability of collapse term decreases, looking deeper into the development and background of the equations raises some questions. The AASHTO equations for the *PC* term above are based on historical *ship-to-ship* collision data collected by

4

Fujii in Japan (AASHTO, 1991). How well the damage from ship to ship collisions correlates to ship to bridge or barge to bridge collision damage is questionable.

In addition, current AASHTO guidelines only require the calculation of the ultimate strength of an individual bridge element (defined as either the pier or span). In reality, consideration should be given to system-wide bridge response and strength rather than individual pier or span strengths. Furthermore, AASHTO provides little guidance in the calculation of bridge element, or system ultimate lateral strength. These factors raise further questions about the validity of the probability of collapse term in the recommended AASHTO design procedure for vessel impact.

1.1.5 Summary of the Problem

Vessel collision is a complex problem involving many factors, including the physical characteristics of the waterway, the type and number of vessels traversing the waterway, and the geometric properties of the bridge under consideration. Environmental, human, and mechanical factors can all lead to serious accidents. Characterizing bridge response to vessel collision is an equally complex problem and requires the understanding of both local and system-wide behavior of a bridge pier, nonlinear material behavior and dynamic response of structures. While current design codes attempt to capture all of the variables involved in vessel collision design of bridges, there exists an opportunity to make improvements to the AASHTO design specification. Specifically, the probability of collapse term in the AASHTO Method II annual frequency of collapse equation deserves critical examination. With a better understanding of the ultimate lateral strength of bridge elements and systems, and the loads imparted to a bridge during collision, a more accurate equation for the probability of collapse can be developed that better reflects the actual phenomena of barge to bridge, or ship to bridge impact.

1.2 Objectives

The primary objective of this report is to outline a method for accurately calculating and characterizing the ultimate strength and response of bridge elements or systems subjected to vessel collision forces. AASHTO currently offers no guidance on how to calculate the ultimate strength of a bridge element or system.

In achieving the main objective of this report, emphasis will be placed on improving the probability of collapse (PC) term in the annual frequency of collapse calculation. The calculation of this term is currently based on outdated ship-to-ship collision tests that perhaps do not correlate well to the problem of ship or barge collision with bridges. Additional work undertaken as part of TxDOT Project 0-4650 sought to better understand the loads imparted from a ship or barge to a bridge during vessel collision; that work is described in Volume II of this report. That research, along with the methods presented here (in Volume III) for calculating the ultimate lateral strength of a bridge can be used to improve the PC term.

1.3 Scope

The bridges being investigated for this research are all from inland waterways in the state of Texas and are subject primarily to tug and barge traffic. Two types of bridge piers will be investigated, those with and those without shear walls. Bridge modeling and analysis guidelines will be specifically tailored for use in SAP 2000 (a commercially available structural analysis program), but they should be applicable to other structural analysis software packages with similar features. The analysis results will focus on one representative bridge pier of each type and will compare the results from individual element response and system-wide response.

1.4 Approach

The objectives of this research will be accomplished using computational analysis methods. Computer modeling and analysis guidelines will be presented for two primary bridge pier configurations, those with and those without shear walls. Nonlinear material behavior will be captured using plastic hinges. Further guidance will be given if consideration of system-wide response and redistribution of forces throughout a bridge system, including the effect of the superstructure (deck and girders) and adjacent piers is desired. The outlined procedure will allow a user to calculate a load versus displacement curve and ultimate strength in a straightforward manner using a typical structural analysis software package such as SAP 2000. The simplified modeling and analysis procedures developed will be verified using more detailed, nonlinear finite element analyses

1.5 Organization of Report

A brief summary of previous work and additional background information is provided in Chapter 2. This summary includes work leading up to and influencing the development of the AASHTO Guide Specification and Commentary for Vessel Collision Design in 1991, as well as more recent work that has occurred since the guide specification was completed. Chapter 3 reviews in greater detail the design procedures outlined in the AASHTO Guide Specification for bridges subject to vessel collision, with a heavy emphasis on Method II as it is the AASHTO recommended procedure. In Chapter 4, the modeling procedures used to compute bridge ultimate lateral strengths will be outlined. The modeling of two representative bridges from Texas, one with piers containing shear walls, the other with piers comprised of just beams and columns, will be presented as examples. SAP 2000 (SAP 2000, 2002) will be used to model these bridges. Chapter 5 will present the analysis cases and the ultimate strength analysis results for the two bridges constructed in Chapter 4 and will draw conclusions on the validity of the modeling guidelines. In addition, the affect of considering system-wide response will be examined. Chapter 6 will summarize the work contained in this report and explain how the modeling guidelines from Chapter 4 and the results from Chapter 5 could be used to improve the current AASHTO design procedures for bridges subject to vessel impact. Lastly, future research areas to continue to improve vessel collision design in the United States will be suggested.

2. Historical Background on Vessel Collision Design of Bridges

2.1 Introduction

This chapter reviews the history and development of vessel collision design in the United States. Important events and research that led to the introduction of the *AASHTO Guide Specification and Commentary for Vessel Collision Design of Highway Bridges* in 1991 are presented. A review of research conducted since the development of the AASHTO Guide Specification is also included. An assessment is provided on the direction that research in the area of vessel collision design is going and the areas that need further examination. In addition, work conducted as part of the TxDOT project "Vessel Impact on Bridges" at The University of Texas at Austin is reviewed, along with a discussion of how this work (of which this document is part of) fits into the current spectrum of vessel collision design research, and how this work can be used to further improve vessel collision design in Texas and the rest of the United States.

2.2 Sunshine Skyway Bridge Accident

On May 9, 1980 the freighter Summit Venture, under poor weather conditions, collided with one of the piers of the Sunshine Skyway Bridge crossing Tampa Bay in Florida. The struck pier was destroyed, and a 1300-foot section of the bridge superstructure collapsed into the water. Thirty-five people lost their lives in vehicles that drove off the bridge and into the bay. The extensive damage caused by this event can be seen in Figures 2-1 and 2-2.
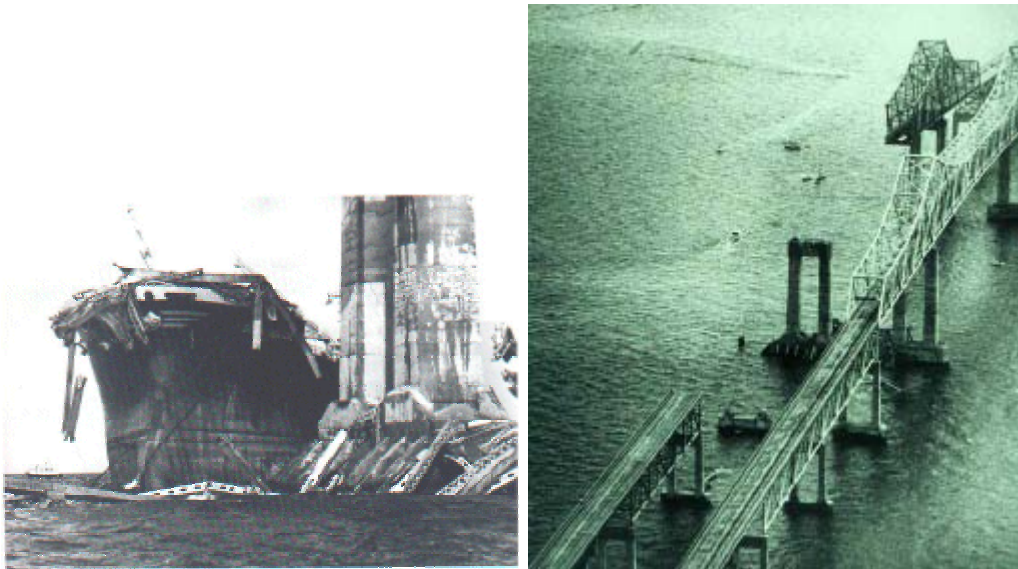
Figure 2.1: Sunshine Skyway Damage

Figure 2.2: Sunshine Skyway Damage

The severe nature of the Sunshine Skyway accident and the large loss of life served to bring significant attention to the problem of vessel collision in the United States and around the world. It is recognized as a "major turning point in the development of vessel collision design criteria for bridges in the United States" (AASHTO, 1991).

2.3 Development of the AASHTO Guide Specification

2.3.1 Introduction

Historically, vessel collision forces have been ignored in the design of bridges (AASHTO, 1991). For many years, it was believed that vessel collision with bridges was a highly unlikely event and it was not possible or economical to protect bridges from serious collision (AASHTO, 1991). However, as accident data grew over the years, it became clear that vessel collision loading needed to be considered in bridge design. Between 1965 and 1989 there occurred, on average, one catastrophic vessel-bridge collision accident per year (AASHTO, 1991). Through the 1980s, attention on vessel collision design grew and significant work was done to develop some basic criteria for vessel collision design. This section seeks to highlight the research that led to the development of the *AASHTO Guide Specification and Commentary for Vessel Collision Design of Highway Bridges* (AASHTO, 1991) which is still the basis for vessel collision design in the United States today.

2.3.2 1983: National Research Council Marine Board

In 1983, the Marine Board of the National Research Council in Washington D.C. appointed a committee to investigate the issue of vessel collision with bridges in the United States. The group was specifically charged with looking into the risk posed by vessel collision and analyzing the consequences of vessel impact with bridges (AASHTO, 1991). Some of the important conclusions reached by the group include the following:

- No one agency is responsible for the protection of bridges subject to vessel collision (AASHTO, 1991).

- Greater coordination between agencies or groups with a vested interest in protecting bridges from vessel collision is needed (Modjeski and Masters, 1984).

- Criteria and standards for the design, protection, and placement of bridges over navigable waterways have not been developed in the United States (Modjeski and Masters, 1984; AASHTO, 1991).

- There exists a large amount of research data in the area of risk assessment, calculation of vessel collision forces, and the design of collision-resistant structures that has yet to be applied in the United States (Modjeski and Masters, 1984).

- Criteria and standards for vessel collision design in the United States needs to be developed by AASHTO (Modjeski and Masters, 1984).

2.3.3 1983: IABSE Colloquium on Ship Collisions with Bridges and Offshore Structures

In 1983, consulting engineers and researchers from around the world gathered in Copenhagen, Denmark to present results from a wide range of vessel collision studies (AASHTO, 1991). Some of the areas covered include historical accident studies, risk assessment studies, determination of collision forces, vessel behavior during collision, design of pier protection systems, and design of motorist warning systems (IABSE, 1983). The work published as part of this colloquium served as an important source of information during the development of the AASHTO Guide Specification (AASHTO, 1991).

2.3.4 1984: Modjeski and Masters Vessel Collision Guidelines

In November of 1984, the consulting engineering firm of Modjeski and Masters completed a document titled, *Criteria for the Design of Bridge Piers with Respect to Vessel Collision in Louisiana Waterways* for the Louisiana Department of Transportation and Development, and the Federal Highway Administration (FHWA). The Louisiana DOT and the FHWA were motivated to sponsor the work based on recognition of the increased occurrence and severity of vessel-bridge collision accidents (Modjeski and Masters, 1984). The document and recommendations contained within were prepared specifically for bridges crossing navigable waterways in Louisiana, but the basic principles and methods developed are applicable for any waterway (Modjeski and Masters, 1984).

The Modejeski and Masters report illustrated the serious nature of the problem posed by vessel collision with bridges and notes the lack of consideration the issue had been given up to that point, especially in the United States. It emphasized the need for the development of a consistent approach to vessel collision design and greater oversight from appropriate governing bodies, such as AASHTO and the United States Department of Transportation (Modjeski and Masters, 1984). Furthermore, they suggested increased research to both better understand the problem of vessel-bridge collision and improve and speed up the development of technology and knowledge to mitigate the problem.

Modjeski and Masters also presented specific methods for bridge design for vessel collision. The report provided guidance for collection of the necessary waterway and vessel traffic data information, determination of the risk of vessel collision and calculation of collision forces. Finally, a design procedure for both deep and shallow waterways was outlined using

those inputs. Many of the basics of the Modjeski and Masters approach to vessel collision design were eventually incorporated into the AASHTO Guide Specification.

2.3.5 1988: FHWA Establishment of a Design Specification

In 1988, eleven states helped to fund a Federal Highway Administration (FHWA) research project to develop a design specification to address vessel collision design (AASHTO, 1991). This work led to the development, in 1991, of the *AASHTO Guide Specification and Commentary for Vessel Collision Design of Highway Bridges*. Method II presented in the Guide Specification was later adopted by the *AASTHTO LRFD Bridge Design Specification* in Section 3.14. Both the Guide Specification and Bridge Design Specification have not seen significant changes related to vessel collision design since their introductions.

2.4 Current Research

2.4.1 Introduction

Research conducted since the introduction of the AASHTO Guide Specification in 1991 has focused on two areas. The first and largest area of ongoing work is in understanding and more accurately characterizing the mechanics of vessel-bridge collision. The second primary area of research is in understanding, implementing and better utilizing the AASHTO Method II design procedure.

2.4.2 Understanding Vessel-Bridge Collision Mechanics

Understanding the mechanics of vessel collision design presents a unique challenge in that conducting actual tests of vessel collisions with existing bridges is not easily accomplished. The current equations in the AASHTO Design Specification related to the mechanics of vessel-bridge collision are based primarily on historic accident data and limited physical testing. In many cases, the AASHTO equations are based on related areas of study. For example, the calculation of the probability of collapse term (*PC*) in AASHTO is based on data from ship to ship collisions. Another example is the determination of impact loads for barges. Current AASHTO equations for barge impact loads are based on laboratory tests on reduced-scale barges conducted by Meir-Dornberg in Germany in the 1980s (AASHTO, 1991).

Recent work, using finite element analyses and expanded physical testing, has sought to better understand the behavior of barges, ships and bridges under the condition of vessel impact. Researchers have focused on improving the ability to calculate the damage to both vessel and bridge from a collision as well as accurately determining the load imparted to a bridge from a colliding vessel. An effort has been made to better understand the influence of both sub- and superstructure elements by considering soil-structure interaction during vessel collision and increased bridge strength from the redistribution of loads through the deck to adjacent piers.

Researchers at the University of Florida and the Florida Department of Transportation have been leaders in vessel collision research. Dr. Gary Consolazio and Dr. Ronald A. Cook have published results from both finite element analyses of barge impacts with bridges (Consolazio, 2003) as well as the first results from actual barge to bridge collision tests (Consolazio, 2005). Both studies have sought to capture barge bow damage and barge impact loads due to collision with a bridge pier, an inherently dynamic problem, and compare those results to the equivalent static load equation suggested by the AASHTO Design Specification (Consolazio, 2003, 2005). Of special interest are the full-scale experiments completed on the St. George Island Causeway Bridge. The bridge was replaced in 2004, allowing for the opportunity

to safely conduct barge collision tests on the old bridge. Test results showed good correlation for barge bow damage equations used in AASHTO, but found that the equations for calculating an equivalent static load were overly conservative. The study found that the load imparted to the bridge by the barge was limited by the plastic capacity of the barge bow.

Other barge impact tests have been carried out by the United States Army Corps of Engineers (Patev, 2003). The Army Corps of Engineers work has focused on understanding the mechanics of barge collision with navigation structures such as lock walls. Two types of full-scale impact tests on barges have been conducted. The first examined barge collision with different types of lock walls and rail systems, and considered various barge speeds and impact angles. The second set of tests involved crushing of the bow of a jumbo hopper barge using a Statnamic load device (typically used for foundation testing) to impart a lateral load (Patev, 2003).

2.4.3 Improving Implementation of the AASHTO Method II Design Procedure

As of 1996, five years after the release of the AASHTO Guide Specification, no inland waterway bridges had been designed using the recommended Method II procedure due to the large amounts of data required to complete that analysis (Whitney, 1996). For the most part, designers used the simple Method I design procedure. Research work in Kentucky and Florida has focused on improving the collection and processing of the necessary waterway and vessel traffic data needed to apply Method II of the AASHTO Guide Specification. M.W. Whitney, I.E. Harik, J.J. Griffin, and D.L. Allen, a team of researchers and engineers from Kentucky and Tennessee, conducted a study of vessel traffic on inland waterways in Kentucky and proposed a method to organize barge and flotilla data for use in the AASHTO Method II design procedure (Whitney, 1996). In 2001, Chunhua Liu and Ton-Lo Wang, from Florida International University, proposed a strategy for collection and analysis of vessel traffic data in Florida so the AASHTO recommended Method II design procedure could be utilized and implemented throughout the state (Liu, 2001).

2.4.4 Work Completed at the University of Texas at Austin as Part of this Study

Research work completed at The University of Texas at Austin, funded by the Texas Department of Transportation (TxDOT Project 0-4650), sought to integrate research in several areas in order to improve vessel collision design in Texas and rest of the United States. This report is part of that project. The work done falls within the current framework of the AASHTO Method II procedure and can be divided into four main areas. An effort has been made to develop a comprehensive database of waterway, vessel traffic and bridge information for the state of Texas. This information is critical for an AASHTO Method II analysis. In addition, a user-friendly, windows-based analysis program has been developed to guide an engineer through the Method II design calculations. With access to the necessary data and a program to run the required calculations, the Texas Department of Transportation will be able to easily analyze and assess the threat of vessel impact for both existing bridges and new bridge designs.

Additional work was focused on accurately characterizing the loads imparted to a bridge during vessel impact. The focus for the impact load study has been on the loads imparted to a bridge pier by a typical barge. Computer simulations have been run to capture the full dynamic effect of a vessel striking a bridge and the loads determined from these analyses compared against the current AASHTO provisions for calculating impact forces.

The last area of research, which this document covers, is focused on the calculation of ultimate strength for bridge elements and bridge systems that are subject to vessel impact. The primary goals of this research are to provide guidelines for modeling the ultimate lateral strength

of a bridge subject to vessel impact in typical structural analysis programs and to investigate the effect of the surrounding bridge system on the strength of an individual element that has been struck by a vessel.

By investigating and calculating impact loads and ultimate lateral strengths for a bridge, a critical examination of the Probability of Collapse term can be made. The calculation of the *PC* term was identified in Chapter 1 as a potential limitation in the Annual Frequency of Collapse equation used in the Method II procedure. This research project proposes an alternate or adjusted method for calculating the Probability of Collapse, which can then be integrated into the vessel impact analysis program.

2.5 Summary

Vessel collision design is a relatively new and still evolving field. It was not until 1991 that a wide-ranging design code was introduced for use in the United States. This chapter has introduced events and research that led to the development of the AASHTO Guide Specification for Vessel Collision Design, which provides a probability and risk-analysis based approach to vessel impact design. Additional works that have been completed since the introduction of the Guide Specification were also reviewed. This research has focused on improving vessel impact design of bridges by staying within the framework of the AASHTO Guide Specification. Research has focused on two primary areas, understanding and characterizing vessel impact mechanics and improving implementation of the AASHTO Method II design procedure. Work completed at the University of Texas at Austin as part of this research project primarily focused on integrating research in both of these areas to improve vessel collision design of bridges.

3. AASHTO Vessel Collision Design

3.1 Bridge Design in the United States

The American Association of State Highway and Transportation Officials (AASHTO) is the leading authority on bridge design in the United States. AASHTO is made up of state department of transportation officials for all fifty states. They are responsible for producing and maintaining a wide range of documents related to bridge design. Primary among these documents is the *AASHTO LRFD Bridge Design Specification* (AASHTO, 2003). AASHTO provides additional documents that offer more detailed information regarding specific design issues. An example is the *AASHTO Guide Specification and Commentary for Vessel Collision Design of Highway Bridges* (AASHTO, 1991). This document will be referred to as the 'AASHTO Bridge Design Specification' throughout the remainder of this report.

3.2 Vessel Collision Design

Section 3.14 of the AASHTO Bridge Design Specification covers vessel collision and is based on the *AASHTO Guide Specification and Commentary for Vessel Collision Design of Highway Bridges* (AASHTO, 1991). This document will be referred to as the 'AASHTO Guide Specification' from this point forward. The AASHTO Guide Specification provides three methods for the evaluation of bridges for vessel collision design. A comprehensive flow chart in Section 1.5 of the AASHTO Guide Specification outlines the analysis steps needed for each of the three evaluation procedures.

A brief review of the three design methods in the AASHTO Guide Specification was presented in Chapter 1. A more detailed review of each is included in this chapter with a focus on Method II as it is the AASHTO recommended design procedure.

3.3 AASHTO Vessel Collision Design Method I

Method I uses a semi-deterministic procedure to select the design vessel for a given waterway. The Method I procedure for design vessel selection is based on bridge design criteria in the *Common Nordic Regulations* used in Scandinavian countries with slight modifications (AASHTO, 1991). With this approach, the design vessel is selected such that a maximum number or percentage of vessels that are larger than the design vessel is not exceeded (AASHTO, 1991). AASHTO states the no more than 50 vessels per year, or 5% of the vessel traffic, can be larger than the design vessel (AASHTO, 1991).

The selected design vessel is used to calculate a design impact force that can be expressed as an equivalent static load at the mean water level. Equations for calculation of design loads based on the design vessel are contained in Chapter 3 of the AASHTO Guide Specification. The procedure and equations used for this calculation are the same for all three design methods. Calculation of impact forces will be discussed in more detail in Section 3.4 of this report, which covers design Method II. Once the design loads have been determined, a linear elastic structural analysis can be completed to check the adequacy of the bridge members.

Method I is intended to be a simple, conservative approach to vessel collision design. Limited vessel traffic and waterway data are required for Method I, and the analysis equations and calculations are less complicated than in Method II. Method I, however, is only applicable in limited situations. The Method I design procedure is not appropriate for bridges classified as

'critical', or for bridges crossing waterways that see a wide distribution of vessel types and sizes, or for waterways that see significant numbers of large ships (AASHTO, 1991). Method I is most appropriate for shallow, inland waterways that are subjected primarily to barge traffic (AASHTO, 1991).

3.4 AASHTO Vessel Collision Design Method II

Method II is the recommended design procedure presented in the AASHTO Guide Specification and is the only method presented in the AASHTO LRFD Bridge Design Specification. Method II is a detailed, probability-based risk analysis procedure. It requires a significant amount of data on the waterway characteristics, the vessels traversing the waterway and the geometry of the bridge being analyzed. The essential data needed for application of Method II are vessel description, speed and loading conditions, waterway geometry, navigable channel geometry, water depths, environmental conditions and bridge geometry (AASHTO, 1991). The specific data requirements can be found in Sections 3 & 4 of the AASHTO Guide Specification and in Sections 3.14.5-3.14.11 of the AASHTO LRFD Bridge Design Specification. The required data are used to compute an annual frequency of collapse for a bridge element. A minimum acceptable annual frequency of collapse for bridges is given based on bridge classification (i.e., regular or critical).

3.4.1 Importance Classification and Acceptance Criteria

Under AASHTO Method II, bridges must be assigned an importance classification as a: 1) Regular or 2) Critical bridge. Bridges are classified based on society/survival demand and security/defense requirements (AASHTO, 1991). Bridges that provide important links for police and fire departments, emergency personnel, hospitals and schools are classified as critical, as well as bridges in areas where few alternate waterway crossings are available.

Heavily traveled bridges can be also be classified as critical, both because of large disruption costs if the bridge is struck by a vessel and because of the possibility of greater loss of motorist life in the event of an accident. The designation of a critical bridge is somewhat subjective, but the AASHTO Guide Specification provides some guidance in the classification process. Bridges not given a critical classification are marked as regular bridges. For critical bridges, the acceptable annual frequency of collapse is less than or equal to 0.0001, or once every ten-thousand years. For regular bridges, the acceptable annual frequency of collapse is less than or equal to 0.001, or once every thousand years.

3.4.2 Annual Frequency of Collapse Calculation

The result of using the AASHTO Method II design procedure is the calculation of an annual frequency of collapse for a given bridge. The equation appears quite simple, but the calculation of each individual term in the equation can be quite complex and may require several levels of calculations. The equation for determining annual frequency of collapse (*AF*) was shown previously in Chapter 1 and is presented below in Equation 3-1. Also shown are the equations for calculating the individual terms in the *AF* calculation as well as some additional information regarding each term and the data required to complete the calculations.

$$AF = (N)(PA)(PG)(PC) \qquad \text{(3-1)}$$

where:

$AF =$ annual frequency of bridge element collapse due to vessel collision

$N =$ annual number of vessels classified by type, size, and loading condition which can strike the bridge element

$PA =$ probability of vessel aberrancy

$PG =$ geometric probability of a collision between an aberrant vessel and a bridge pier or span

$PC =$ probability of a bridge collapse due to a collision with an aberrant vessel

3.4.3 Probability of Aberrancy Calculation

There are three primary causes of vessel aberrancy — pilot error, adverse environmental conditions, or mechanical failure (AASHTO, 1991). The probability of aberrancy (*PA*) calculation attempts to capture the likelihood that if one of these events occur, a vessel will become out of control. AASHTO recommends using a statistical analysis based on historical data on vessel collisions, rammings, and groundings along a waterway to calculate the probability of aberrancy. Given that this information can be difficult to compile, or that there may not be enough information available, AASHTO also provides an equation requiring information on waterway characteristics, bridge location and geometry, and vessel traffic data to compute *PA* (Equation 3-2).

$$PA = BR(R_B)(R_C)(R_{XC})(R_D) \qquad \text{(3-2)}$$

where

$PA =$ probability of aberrancy

$BR =$ aberrancy base rate

$R_B =$ correction for bridge location

$R_C =$ correction factor for current acting parallel to vessel transit path

$R_{XC} =$ correction factor for crosscurrents acting perpendicular to vessel transit path

$R_D =$ correction factor for vessel traffic density

Based on historical accident data on U.S. waterways, AASHTO suggests the following values for aberrancy base rates:

for ships: $BR = 0.6x10^{-4}$
for barges: $BR = 1.2x10^{-4}$

AASHTO provides equations for the calculation of the other variables used in the calculation of the probability of aberrancy. These equations can be found in Section 4.8.3.2 of the AASHTO Guide Specification (AASHTO, 1991), or Section 3.14.5.2 of the AASHTO Bridge Design Specification (AASHTO, 2003).

3.4.4 Geometric Probability of Collision Calculation

The geometric probability is the probability that a vessel will collide with a bridge given that the vessel has already lost control. The geometric probability (*PG*) is computed based on a normal distribution of vessel accidents about the centerline of the vessel transit path (AASHTO,

1991). The graphic in Figure 3-1 illustrates the *PG* calculation. The AASHTO guide specification recommends using a standard deviation value of $\sigma = LOA$. *LOA* is length overall of the design vessel. For ships, length overall is simply the length of the ship. For barges, length overall is the length of the entire barge tow including the towboat. The use of 1 *LOA* as the standard deviation in the geometric probability calculation is based primarily on ship collision data (AASHTO, 1991). Despite the fact that barge collisions are more common in the United States, these accidents have not been as well documented as ship collisions, and less accident data is available. Therefore, AASHTO recommends using the same value for the standard deviation for both barge and ship calculations (AASHTO, 1991).

Because of the assumed normal distribution of accidents about the water navigation channel centerline, by definition, 99.7 percent of accidents will occur within a distance of 3 *LOA* from the centerline. AASHTO states that bridge elements located outside of 3 *LOA* from the centerline need not be considered in the analysis. As Figure 3-1 shows, the *PG* is the area under the normal distribution in the ship/barge impact zone. The impact zone is defined by the pier location and width, plus ½ of the ship/barge width on each side of the pier.
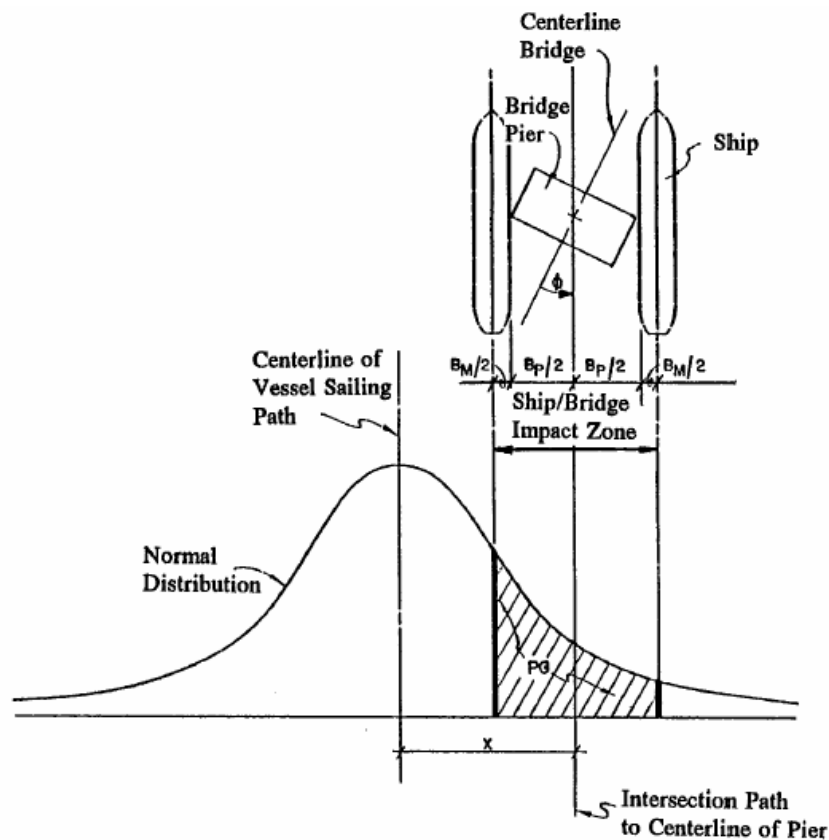
Figure 3.1: Geometric Probability of Pier Collision (AASHTO, 1991)

3.4.5 Probability of Collapse Calculation

The probability of collapse calculation is covered in Section 4.8.3.4 of the AASHTO Guide Specification and in Section 3.14.5.4 in the AASHTO Bridge Design Specification. The probability of collapse is a function of just two variables — the ultimate strength of the bridge

16

element (pier or span) being struck and the load imparted by the vessel. Bridge element ultimate strength and impact force are used in simple equations (shown below as Equations 3-3, 3-4, 3-5) to calculate the *PC* factor. These equations were developed based on historical data from ship to ship collisions collected by Fujii in Japan (AASHTO, 1991). Fujii used data on the damage caused during ship to ship collision events to develop a damage relationship based on the angle at which the two ships collided and the gross tonnage of the two colliding vessels. This damage relationship was used by Conwiconsult to develop the *PC* term for ship to bridge and barge to bridge collisions that was later adopted by AASHTO (AASHTO, 1991).

The calculation of impact loads is covered in Chapter 3 of the AASHTO Guide Specification. AASHTO currently recommends the calculation of an equivalent static load that is applied as a point load, or as a distributed load over the bow length of a barge or ship, at the mean high water level. The actual impact load can be calculated using empirical equations based on vessel velocity and dead weight tonnage (*DWT*). There are separate equations for calculating impact forces for ships or barges. There are also different equations for impact on a bridge pier or against a bridge span. The AASHTO empirical equation for ship impact forces is based on tests performed in the 1970s in Germany by Woisin. The AASHTO equations for barge impact forces are based on work done by Meir-Dornberg in Germany in the 1980s (AASHTO, 1991). It is significant to note that the AASHTO Design Specification does not provide guidance in the calculation of bridge element ultimate strengths.

For $0.0 \leq H/P < 0.1$, *PC* shall be computed as:

$$PC = 0.1 + 9 \left[0.1 - \frac{H}{P} \right]$$

$$\text{(3-3)}$$

For $0.1 \leq H/P < 1.0$, *PC* shall be computed as:

$$PC = \frac{\left[1 - \frac{H}{P} \right]}{9}$$

$$\text{(3-4)}$$

For $H/P > 1.0$:

$$PC = 0 \qquad \text{(3-5)}$$

where
$H =$ ultimate bridge element strength (kips)
$P =$ vessel impact force (kips)

These equations are shown as a graph in Figure 3-2.

17
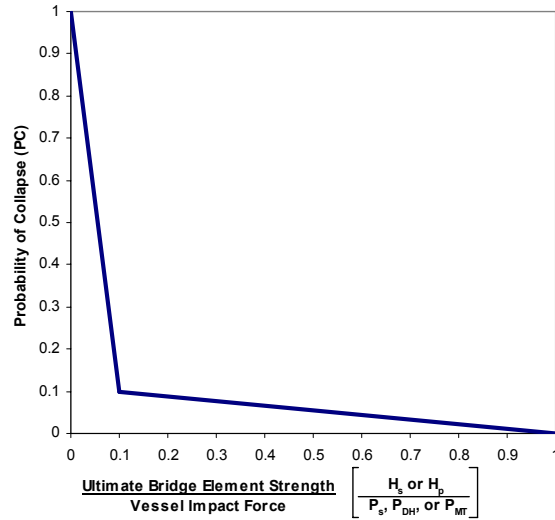
Figure 3.2: Probability of Collapse Curve (Adapted From AASHTO, 1991)

3.5 AASHTO Vessel Collision Method III

Method III is a cost-effectiveness analysis procedure that uses standard engineering economic principles. It was developed for situations where design Method II does not accurately capture the acceptable risk levels for a bridge and results in designs that are cost-prohibitive or not technically feasible (AASHTO, 1991). A possible scenario for this case is a bridge with a large number of piers in the water that are exposed to vessel collision (AASHTO, 1991).

Method III allows a designer to make decisions based on a typical cost/benefit analysis. In this case, the 'costs' represent the present worth of the costs of making a bridge stronger or providing some additional protection for a bridge, while the 'benefits' side of the equation is represented by the present value worth of the avoidable disruption cost. The avoidable disruption costs are equal to whatever losses are expected should a bridge collapse due to vessel collision. Section 4.9.3 of The AASHTO Guide Specification provides an equation for calculation of the disruption costs should a vessel collision accident occur. The equation is as follows:

$$DC = PRC + SRC + MIC + PIC \qquad (3\text{-}6)$$

where:
$DC =$ disruption cost
$PRC =$ pier replacement cost
$SRC =$ span replacement cost
$MIC =$ motorist inconvenience cost
$PIC =$ port interruption cost

The cost/benefit analysis should be carried out over the lifetime of a bridge. A bridge design or improvement to an existing bridge is effective when benefits outweigh costs over the expected life span of the bridge.

18

3.6 Summary

This chapter has outlined the various design methods presented in the *AASHTO Guide Specification and Commentary for Vessel Collision Design of Highway Bridges*. The remainder of this document will focus on the AASHTO recommended Method II design procedure for calculation of an Annual Frequency of Collapse (*AF*) of a bridge. Procedures for computer modeling and analysis of bridges for the calculation of ultimate lateral strengths will be presented. This procedure will be applied to several bridge pier configurations and analysis results will be presented.

4. Bridge Ultimate Strength Modeling

4.1 Introduction

For application of Design Method II, AASHTO requires the calculation of the ultimate lateral strength of a bridge element being impacted by a vessel. This capacity is used in the probability of collapse term (*PC*) in the Annual Frequency of Collapse (*AFC*) calculation. Chapter 3 of this document outlines in detail the AASHTO Method II design procedure and calculation of both the *PC* and *AFC* terms.

While AASHTO requires the calculation of the ultimate lateral strength, it provides virtually no guidance in the determination of this value. The judgment of what represents the ultimate strength of a bridge element is left to the engineer. There are several possible ways to interpret this requirement, and each interpretation could lead to significantly different values of bridge element capacity for the same structure. In addition, for certain bridge geometries, determination of the ultimate lateral strength can require a complex analysis. Furthermore, AASHTO only considers the lateral capacity of an element, which it defines as a single pier or single span, as opposed to the lateral strength of the bridge system as a whole. AASHTO does not consider the interaction between a bridge pier and deck, and the redistribution of forces from one bridge element to the next.

The goal of this chapter is to provide a modeling procedure that is simple, consistent, and conservative that can be used for a design to capture the inelastic behavior and the ultimate or limit strength of a bridge pier or bridge system subject to vessel collision. Special emphasis is placed on developing modeling techniques and procedures that can be used within commonly used structural analysis software packages and will not require the use of more complex finite element analysis programs.

4.2 Scope

The method for determination of ultimate lateral strength outlined in this chapter is intended to be applied to reinforced concrete bridge piers that may or may not contain shear or web walls. Figure 4-1 shows a half-elevation and section drawing of a bridge pier with a web or shear wall extending upwards from the pile cap. Notice that the wall is flush with one edge of the column. This configuration is not typical. Normally, the wall will be centered on the face of the column. Figure 4-2 shows a simple bridge pier, consisting of beams and columns without a wall.

This chapter presents modeling guidelines for use with SAP 2000 (version 8) [SAP 2000, 2002], a commonly used software package for structural analysis. Primary emphasis is placed on modeling bridge piers subject to vessel impact, but additional guidelines to capture system-wide response and the effect of redistribution of forces through the deck to adjacent piers is also considered. As they are presented, the models are not intended to be used as part of a dynamic analysis, although dynamic effects could be considered by applying a dynamic response factor to the static analysis results that will be presented in Chapter 5.
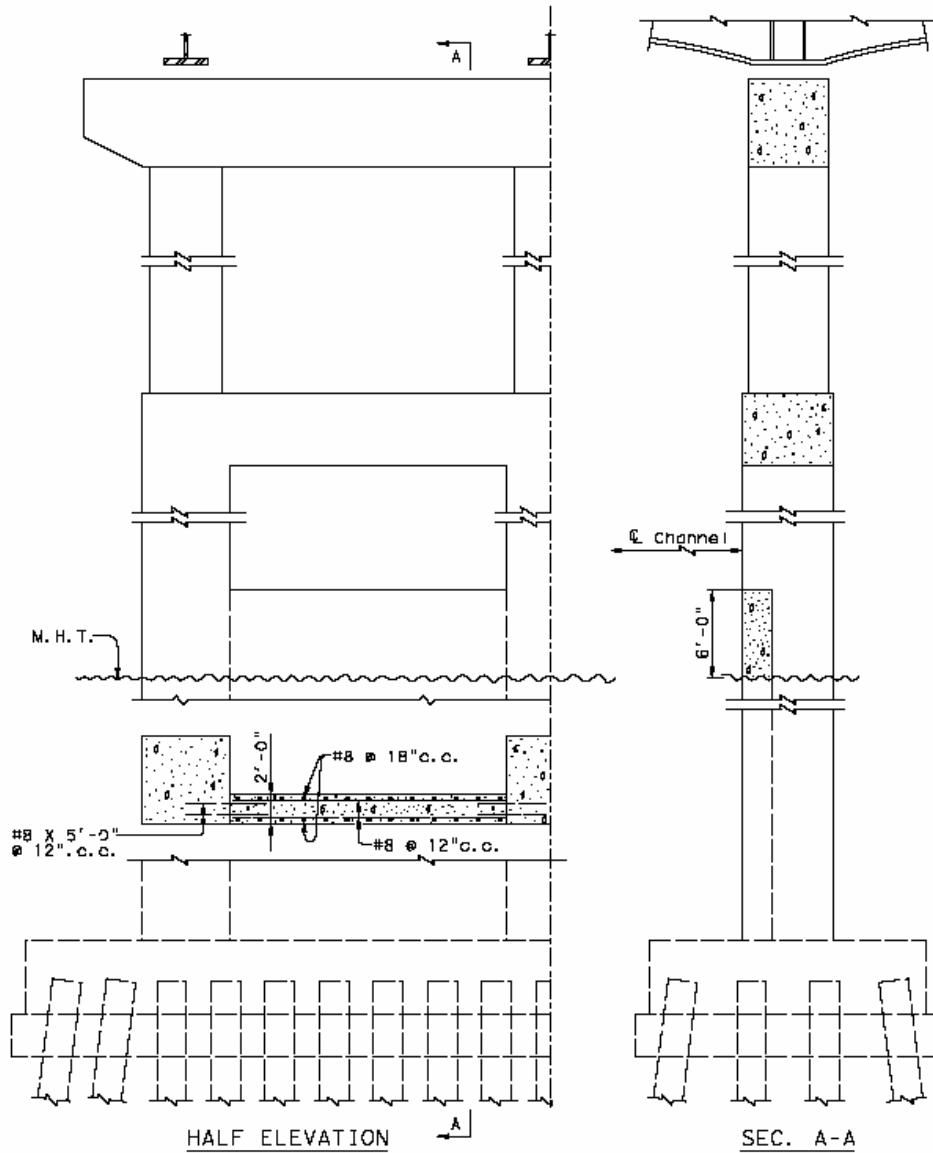
Figure 4.1: Bridge Pier with Shear Wall (TXDOT, 2001)
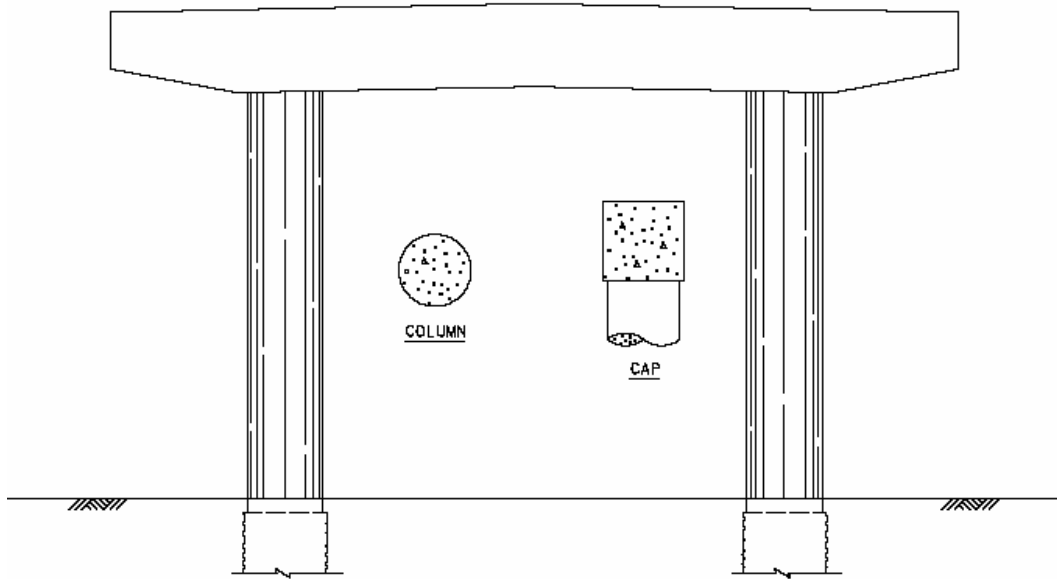
Figure 4.2: Bridge Pier without Shear Wall (TXDOT, 2001)

4.3 Approach

Because SAP 2000 and other typical structural analysis software packages do not have the capability to capture inelastic behavior for wall elements, an approximate method to capture response is presented. The approximate method is verified using ANSYS, a general finite element analysis software package. ANSYS has the capability to capture inelastic response of all types of elements, including shell/wall elements. Other aspects of the SAP 2000 and ANSYS models are defined in a similar manner, so the only variable in the two sets of models is how the wall is being modeled. Once the SAP 2000 approximate wall model has been verified, ultimate lateral strength analyses are conducted for two bridges.

4.4 Modeling Basics in SAP 2000

This section outlines basic background information on the creation of models within SAP 2000 to capture the inelastic behavior and ultimate strength of bridge piers subject to vessel collision. The following sub-sections are intended to provide introductory details on the major areas that need to be addressed within SAP 2000 to build an accurate bridge model. Later sections provide a step-by-step procedure, along with screen shots from SAP 2000, for the construction of specific bridge models.

4.4.1 Defining Bridge Geometry

A wide range of bridge geometries can be easily defined within SAP 2000 by establishing gridlines along the centroid of beam and column members and around the boundaries of wall areas. Walls are defined by shell elements if the wall behaves in a linear elastic manner. To capture inelastic behavior of wall elements, shells cannot be used. Instead, an approximation of the wall needs to be developed. The method proposed in this chapter utilizes a grid of truss

elements to replace the wall. Both rigid and axially deformable members are used in the grid. The specifics of the approximate wall model are discussed in detail in later sections.

4.4.2 Element Types

Two basic element types are used within SAP 2000 (frame elements and shell elements), to construct bridge pier and bridge system models. Other types of elements can be defined in SAP 2000 by modifying frame elements. Rigid members can be used by assigning large stiffness modification factors to the desired elements. Truss elements can be defined by releasing moments at member ends.

4.4.3 Material Model

A simplified approach is used to model reinforced concrete. Smeared material properties, considering the concrete and reinforcing steel as a single material with similar properties in tension and compression are specified for the analyses. Taking this approach, a reasonable determination of strength and stiffness characteristics of the elements in a bridge pier can be made without having to address the difficulties of modeling reinforced concrete material properties directly. Modeling reinforced concrete requires not only accurately capturing the material behavior of steel, which is not especially difficult, and concrete, which is more difficult because it behaves differently in tension and compression, but also the interaction between the two materials. Taking the two materials as a single smeared material, while not as accurate, is considerably easier and more appropriate for design calculations. Using this approach, the key material properties a user needs to input are E, the modulus of elasticity, f_y, the yield stress, and f_u, the ultimate stress.

Defining Modulus of Elasticity

The Modulus of Elasticity is calculated in accordance with American Concrete Institute (ACI) guidelines (ACI 318-02, 2002). Section 8.5.1 of ACI 318-02 (Building Code Requirements for Structural Concrete and Commentary) recommends the following expression to define E:

$$E = 57000\sqrt{f_c'}$$

(4-1)

where
$E =$ Modulus of Elasticity in psi
$f'_c =$ Concrete Strength in psi

Defining fy and fu

Values for the yield stress and ultimate stress can be determined by a reinforced concrete section analysis. Separate values of f_y and f_u must be defined for each element (column, beam, or wall) in a bridge pier. Thus, a separate section analysis must be completed for each element. Several readily available computer programs will perform a reinforced concrete section analysis. An example of such a software package, and the program used for calculations contained in this report, is Response-2000, developed at the University of Toronto (Bentz, 2001). This program allows a user to input the geometric and material properties of a reinforced concrete section, including longitudinal and transverse steel reinforcement, and returns the strength and ductility characteristics of that section in the form of a moment-curvature plot. Figure 4-3 shows the basic section information produced by Response-2000 for a typical circular column section. Note that

geometric properties of the section are shown along with the user specified material properties for concrete and reinforcing steel, as well as the layout of longitudinal and transverse steel.
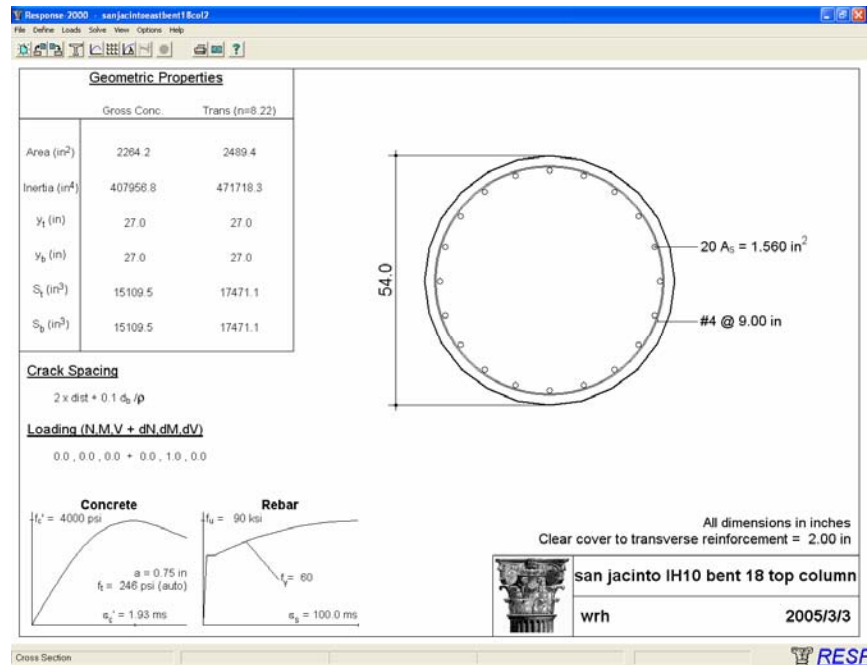
Figure 4.3: Response Section Input

Figure 4-4 shows a moment-curvature plot from the analysis of the 54-inch-diameter column section shown in Figure 4-3. The section analysis results shown are for a section with no axial load. It will be shown later that neglecting axial load will result in material property values that are slightly conservative. On Figure 4-4, values for the yield moment, M_y, and the plastic moment, M_p, have been estimated. Response-2000 returns a value for M_p, and the user will need to estimate a value for M_y, although doing so is straightforward as there is generally a clear point at which the stiffness begins to change. These values will be used to determine the yield stress and ultimate stress using the following equations:

$$f_u = \frac{M_p}{Z} \qquad (4\text{-}2)$$

$$f_y = f_u \frac{M_y}{M_p} \qquad (4\text{-}3)$$

where
$f_u =$ Ultimate Stress
$f_y =$ Yield Stress
$M_y =$ Yield Moment
$M_p =$ Plastic Moment
$Z =$ Plastic Section Modulus

The ultimate stress, f_u is defined based on the plastic section modulus and the ultimate or plastic moment. The yield stress is then defined based on the ratio between the yield and plastic

moment. It is important to note that the definition for the yield stress value is not consistent with the typical definition, which is as follows:

$$f_y = \frac{M_y}{S} \qquad (4\text{-}4)$$
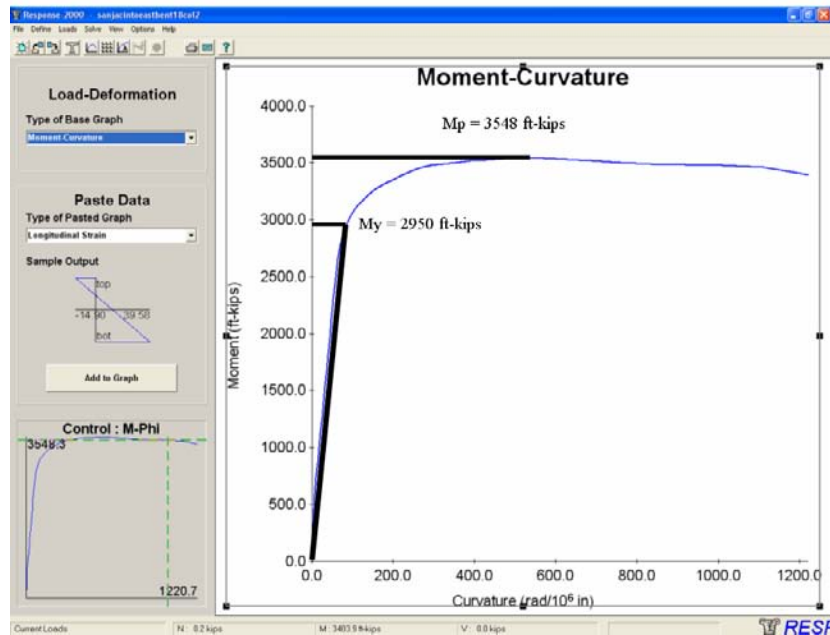
Figure 4.4: Response Moment-Curvature Analysis Results

The expressions shown are being used because they are consistent with how SAP 2000 defines the values of moment at which hinges first form and then reach their ultimate strength capacity. Table 4-1 summarizes the calculation of the smeared material properties for the 54-inch-diameter column section shown previously. The section properties and actual material properties are entered into Response-2000, a sectional analysis is performed, and the results are used to calculate the new, smeared material properties for use within SAP 2000.

Table 4.1: Smeared Material Properties for 54" Diameter Column Section

Section Properties	
Section Diameter, d (in)	54
Section Modulus, Z (in^3)	26244
Real Material Properties	
Concrete Strength, f_c' (ksi)	4
Reinforcing Steel Strength, f_y (ksi)	60000
Response Section Analysis Results	
Yield Moment, M_y (ft-kips)	2950
Plastic Moment, M_p (ft-kips)	3548
Smeared Material Properties	
Ultimate Stess, f_u (ksi)	1.62
Yield Stress, f_y (ksi)	1.35
Modulus of Elasticity, E (ksi)	3605

It was stated earlier that performing a section analysis with zero axial load will result in slightly conservative values for the smeared material properties. The moment-axial interaction diagram shown in Figure 4-5 helps to explain why neglecting axial load on the section is conservative. This plot is for the same 54-inch-diameter column that has been discussed throughout this section. The vertical line represents the value of M_p that was used to calculate the smeared material properties. The plot shows that for axial loads between 0 k and 7750 k, the actual moment capacity for this section is actually greater than the value of M_p used. In addition, an axial load of 7750 k represents approximately 75% of the crush load, P_u. An axial load of this magnitude is not only extremely unlikely, but would also fail to meet code requirements. Realistically, bridge piers will see axial loads much less than 50% of the crush load, and in many cases the axial loads will be closer to 10-15% of the crush load.
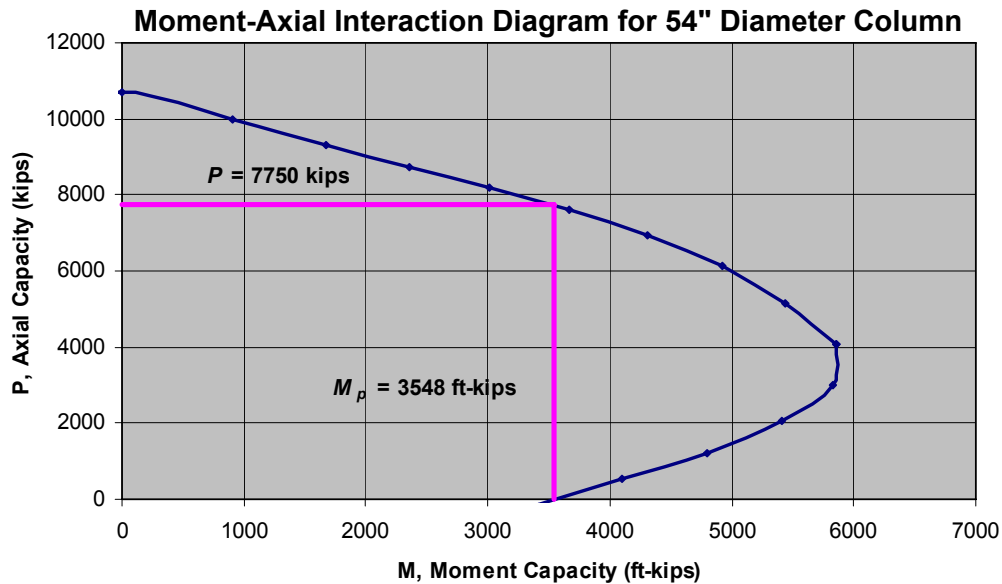
Figure 4.5: Response Moment-Axial Interaction Results

4.4.4 Section Properties

A wide range of user-defined sections can be entered in SAP 2000. Modeling of most reinforced concrete bridge piers will require the use of regular geometries, usually rectangular or circular sections. As the section is being defined, the user needs to assign a material model to that particular section. Figure 4-6 shows the SAP 2000 input for a rectangular section called 'COLUMN', which is made of a material called 'MAT1'. The windows shown in Figure 4-6 were reached through the 'Define-Frame/Cable Sections' menu in SAP 2000. Once elements have been created, the user-defined sections are then assigned to the appropriate members. The shapes required to define the bridge pier geometries are assigned using sections that exactly match the geometry of the actual bridge. SAP 2000 also has the option of applying section modification factors for a specific property. For example, a user could enter a large value for the cross-sectional area modification property, essentially making the element axially rigid. Figure 4-6 also shows that the section 'COLUMN' has been given a large axial modification factor.
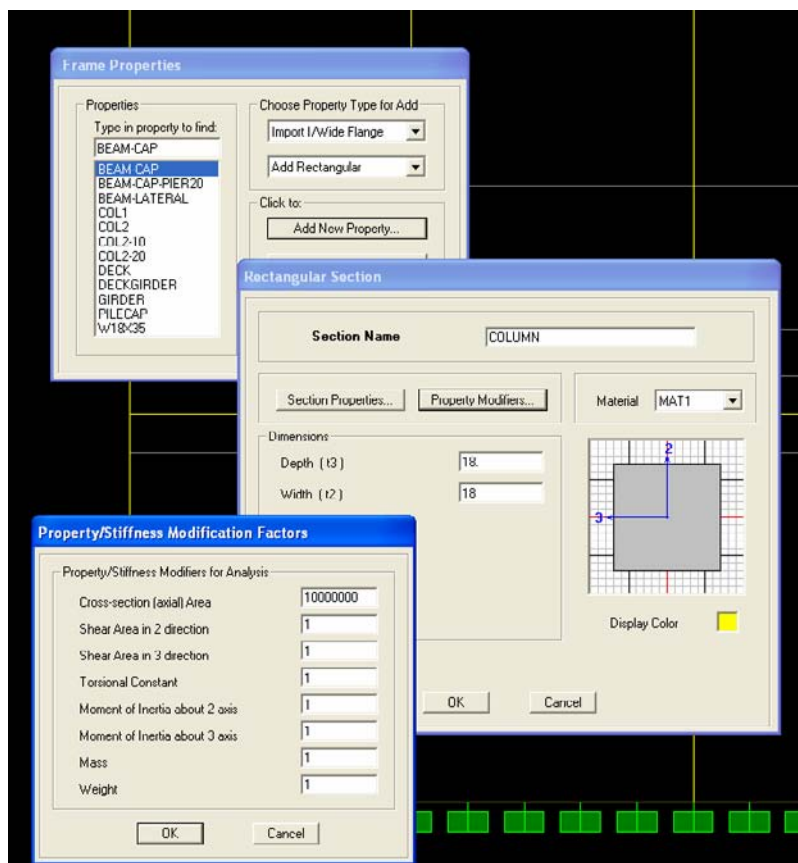
Figure 4.6: Entering Section Properties in SAP 2000

In addition, SAP 2000 has the option of using a 'general' section, which can be defined based only on the section properties such as area and the moment of inertia, without specifically defining the geometry. Figure 4-7 shows the input box for a general section, which SAP 2000 names 'FSEC1' by default. Notice that the section properties are entered directly and no geometrical parameters need to be defined. The general section option is particularly useful for defining section properties for elements to represent the bridge deck and girders. The strength and stiffness of these members can be determined and then applied to a 'general' section rather

28

than explicitly drawing sections to represent the girders and the deck. In the case of the girders it may be necessary to model members with unique geometries such as AASHTO prestressed girder types or steel trapezoidal girders, or in the case of the deck, require the use of shell elements. In either case, the geometry for these elements may not be easily defined using the default shapes in SAP 2000, and use of general sections is favorable.
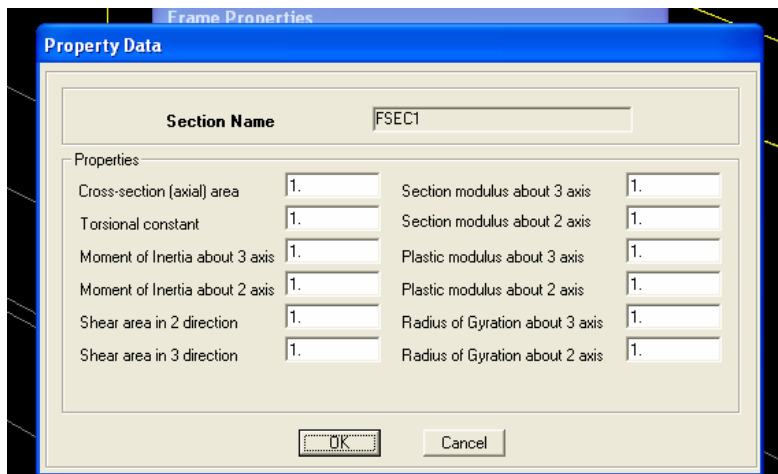
Figure 4.7: General Section Input in SAP 2000

4.4.5 Plastic Hinges

Inelastic behavior and nonlinear material properties are captured with plastic hinges acting at the member ends. Hinges can be defined as axial hinges, shear hinges, moment hinges, or moment-axial interaction hinges within SAP 2000. For the bridges modeled within this report, axial hinges and moment-axial interaction hinges are be used.

Plastic hinge properties are defined in SAP 2000 based on the strength and deformation capacities of the member to which they are assigned. The yield and ultimate strength are based on the material properties from a reinforced concrete section analysis. Therefore, because of the smeared material model approach, different hinge properties must be defined for each column, beam, and grid section. If there are two different column sections in a bridge pier, a different set of hinge properties is needed for each section and must be applied at the ends of members with that section.

For the bridge models in this report, hinges are defined as infinitely plastic, and system ductility will be assessed in the post-analysis phase. This approach was taken to simplify the analyses and to ensure that the bridge models have adequate ductility to form a failure mechanism. Another option would be to define the deformation or rotational capacity of the hinges, either as a multiple of the yield deformation or rotation, or by their actual deformation or rotational limits, in inches or radians. This approach is slightly more difficult than the approach described above given the variation that will be seen in rotational and deformational capacities based on the specific concrete section that is being considered. Figure 4-8 shows the typical hinge profile that is used. Note that the values assigned for the ultimate strength and the rotation when ultimate strength is reached are merely representative of a typical hinge. Exact values for these properties will be determined by the material properties and will vary for each hinge used. Also, a more detailed discussion of the actual plastic hinge inputs, with SAP 2000 screen

captures, is provided in Sections 4.6.1 and 4.6.2, which outline the modeling of two specific bridges.
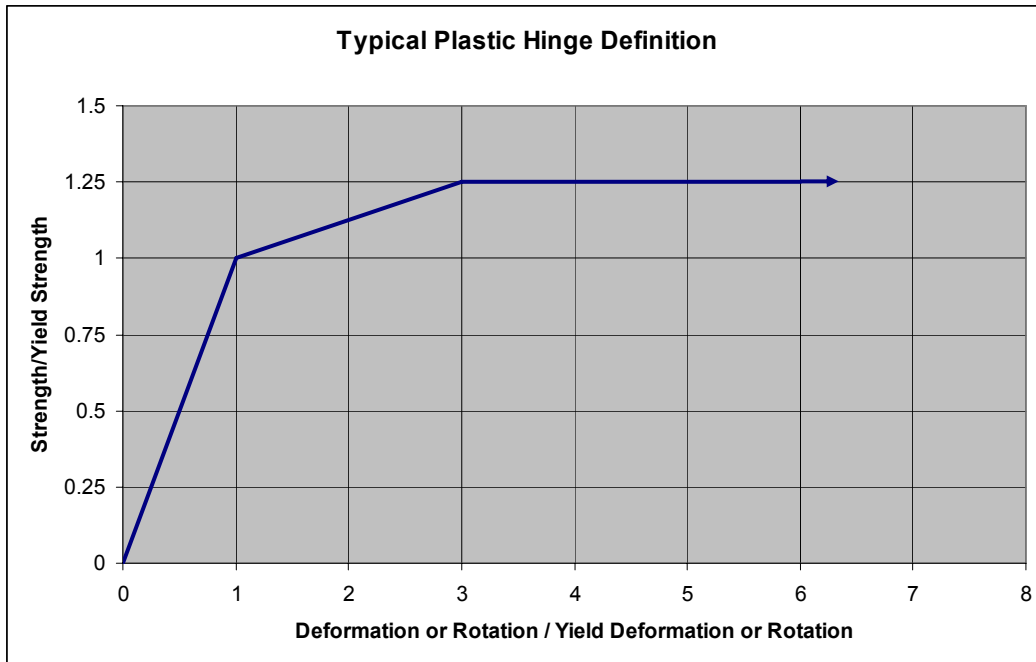
Figure 4.8: Typical Plastic Hinge Definition

To properly capture post-yield behavior in a model, plastic hinges must be assigned to the regions of the model that are subject to inelastic deformation. Therefore, the location of plastic hinges must be carefully selected. Hinges can be placed at any relative distance along the length of a member, but it is often easiest to apply hinges only at the ends of members in SAP. Using this approach, it may be necessary to subdivide elements, such as columns, to assign plastic hinges at locations along the length.

4.4.6 Boundary Conditions

Boundary conditions at the base and at the top of a bridge model need to be considered carefully. The boundary conditions can have a significant effect on the stiffness and strength characteristics of a bridge system. A single base condition is considered at the base of the structure, while several boundary conditions are considered at the top of a pier.

Bridge Pier Base Boundary Condition

The base conditions for all of the bridge piers being modeled for this research are assumed to be fixed. This assumption is reasonable for the connection between the wall and columns of a bridge pier and the foundation cap beam, but it ignores the interaction between the foundation piles or piers and the surrounding soil or water. Figure 4-9 shows a graphical representation of the assumption being made. The resulting system will be less flexible than what actually exists, and there are several important implications to this statement.

First, a stiffer system will attract more loads to the elements in the bridge pier. This observation can be viewed as both conservative and unconservative, depending on how the problem is being considered. If vessel impact loads are known *a priori* and a bridge model with a

30

fixed base is being analyzed for those *known* loads, the forces in the members will be greater than they are in reality. In comparing these loads to member capacities, a conservative approach is being taken. If instead a bridge model with a fixed base is subject to a static nonlinear analysis, in which the load is increased incrementally until failure, the stiffer structure will again attract more load, and an artificially high, or unconservative value of ultimate lateral strength will result. Second, with a stiffer system, the displacements are expected to be underestimated. For systems that are controlled by ductility, the modeling approach used for this research could also result in unconservative ultimate lateral strength results.

　　While the fixed base assumption may not be the most accurate representation of actual bridge base conditions, it is made both for the sake of simplicity and because accurately modeling the base condition with springs or other elements would require data on the soil conditions at a given site, which might not be easily obtained. It is important to know both the strength and ductility limits of the real structure and to understand the effect that the assumed fixed base condition has on the analysis results
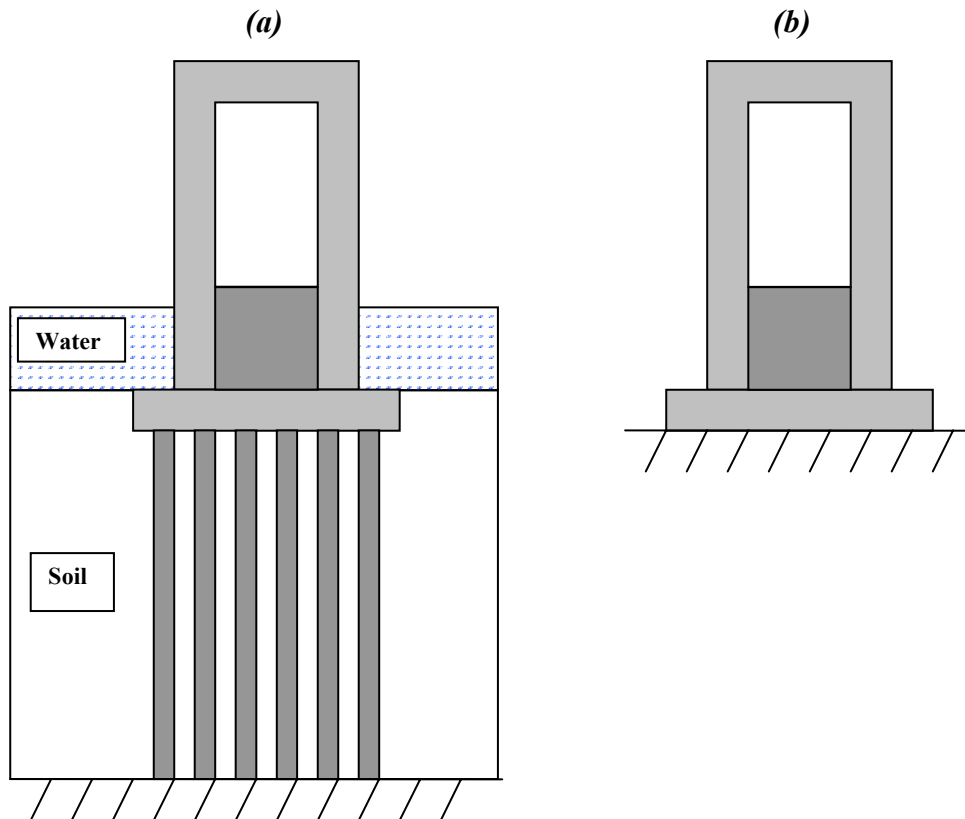
Figure 4.9: Bridge Pier Base Condition: (a) Actual Conditions; (b) Assumed Conditions

Bridge Pier Top Boundary Condition

　　Several boundary conditions are considered at the top of the bridge piers being modeled and analyzed. Currently, AASHTO requires the calculation of ultimate lateral strength of a stand-alone pier. Therefore, an analysis for this case will be considered. At the opposite extreme, the assumption will be made that the bridge deck and girders provide a rigid support at the top of

the pier. Analyses of these two cases will provide a range of possible strengths for the bridge system under consideration. Figure 4-9 shows free and fixed top conditions for a SAP 2000 bridge pier model. To best represent an actual bridge system, a third analysis case is considered with elements at the top of the bridge pier that match the stiffness contributed by the bridge girders and deck. This case is illustrated in Figure 4-10.
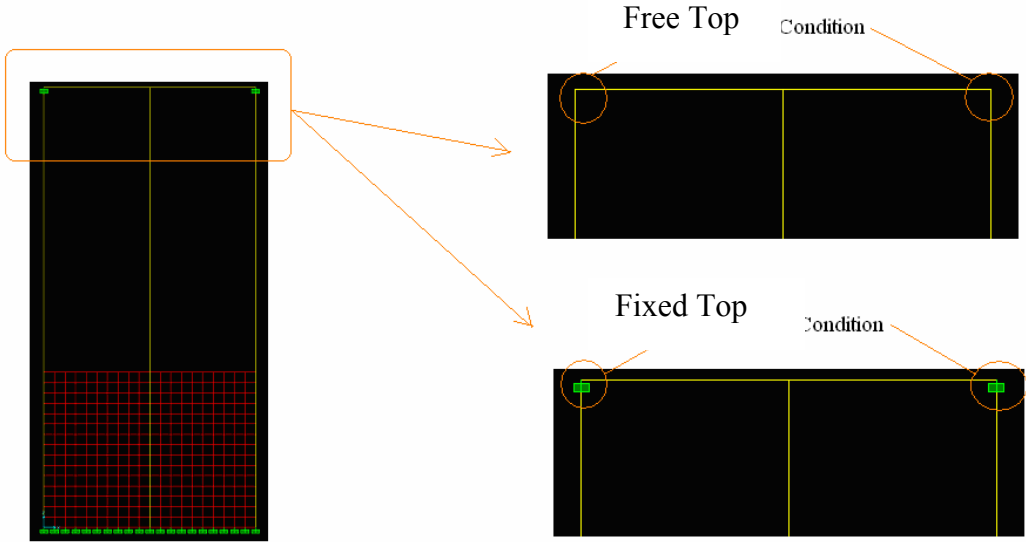
Figure 4.10: Bridge Pier Top Boundary Condition: (a) Free Top, (b) Fixed Top

32

Perpendicular elements representing
bridge superstructure
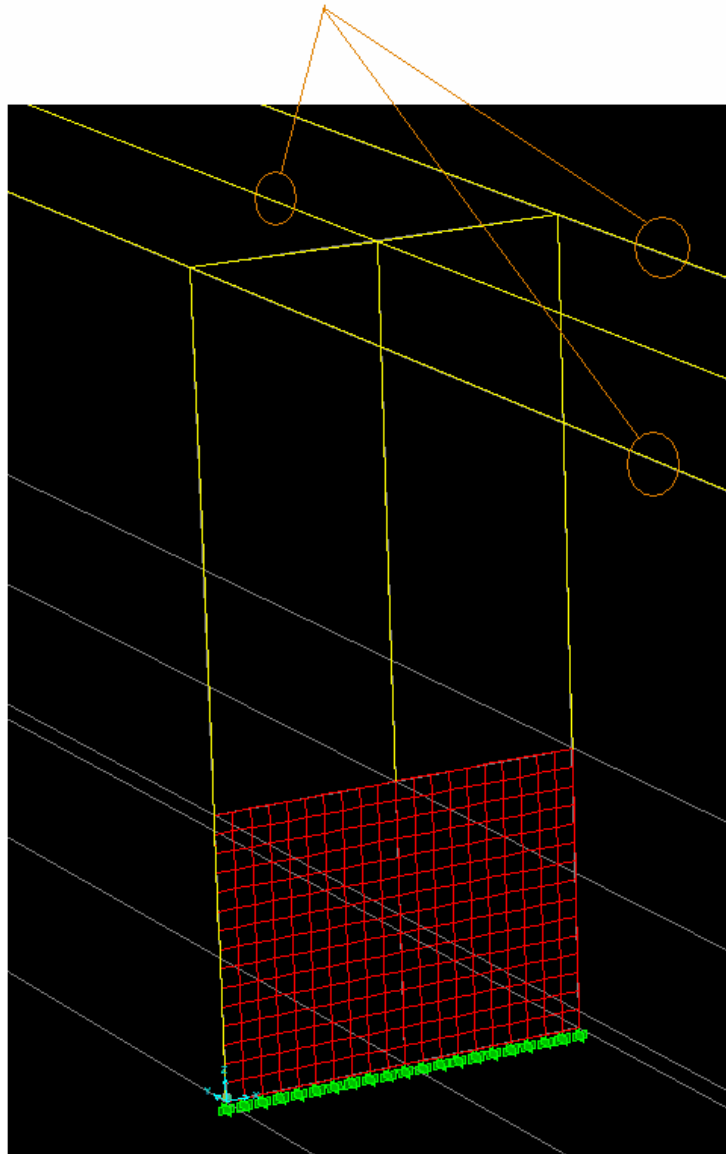
Figure 4.11: Bridge Pier Top Boundary Condition — Superstructure

4.5 Modeling Shear or Web Walls

For a linear elastic analysis within SAP 2000 or other typical structural analysis programs, walls can be modeled using shell elements. These programs, however, usually lack the capability to capture inelastic behavior of these element types. As an alternative, one could build a model using a general finite element software package such as ANSYS. Finite element analysis programs can be rather expensive considering both dollars and computational time. Furthermore, these programs are more difficult to use and increase the chance of user error in the course of an analysis. Because of these reasons, there is a need for a simple, approximate method to capture

the inelastic response of a wall within a structural analysis program like SAP. This section outlines such a method for the purposes of ultimate lateral strength prediction.

A possible solution to the problem of modeling bridge piers with shear walls to is to replace the shear wall with a truss-grid system. Figure 4-12 illustrates two models. The model on the left is comprised of frame elements for the columns and beams and shaded shell elements for the shear wall. In SAP 2000, this model is only capable of capturing linear elastic response. The model shown on the right is made up of frame elements to represent the beams and columns and a grid of truss elements to model the wall.

With the truss-grid model, the wall is replaced by rigid truss members in the vertical and horizontal direction. Non-rigid truss elements are placed on the diagonal between the rigid members. The diagonal truss members are sized such that the response for a linear elastic analysis matches the response of the shell-wall model. Once the linear elastic analysis case has been verified, plastic hinges are applied to the ends of the truss members and the analysis is rerun. Because the horizontal and vertical members are rigid, all of the inelastic deformation in the wall is captured in the diagonal truss elements. Figure 4-13 shows a close-up view of the truss-grid system for the pier shown in Figure 4-12.

Shell Wall   Truss-grid
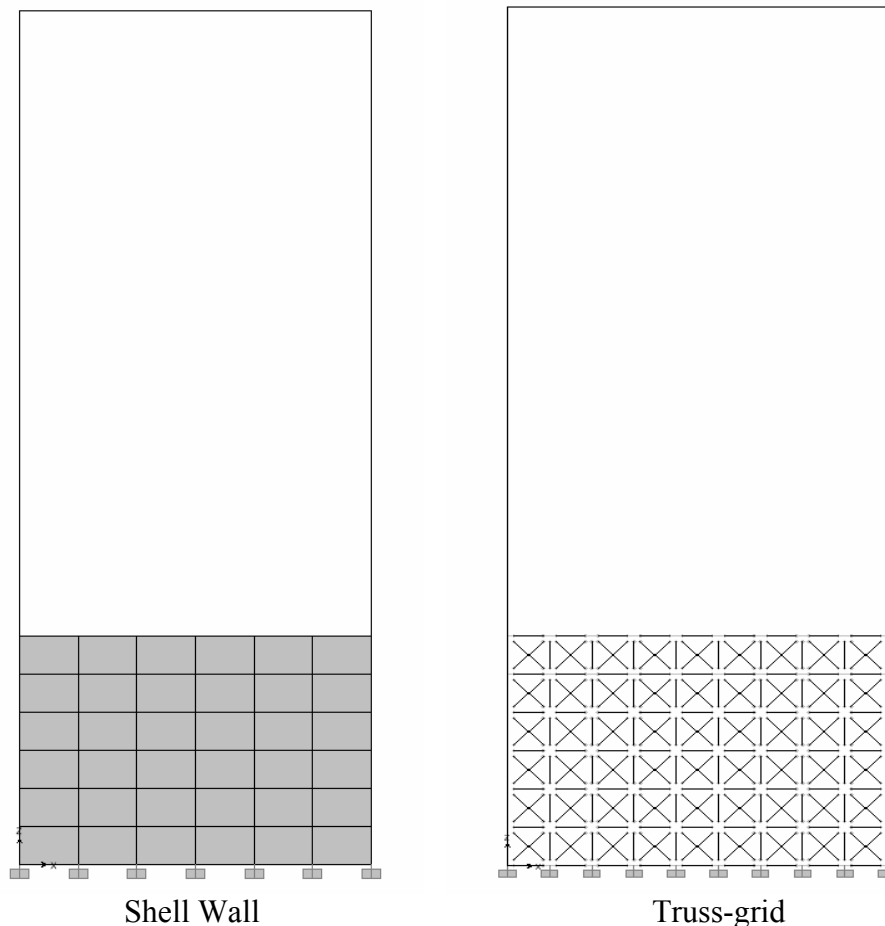
Figure 4.12: SAP 2000 Bridge Pier Models

Column (Frame) Elements
On Exterior

Rigid Horizontal and Vertical Elements on the
Interior

Diagonal Truss Elements

Moment Released for all Interior Elements
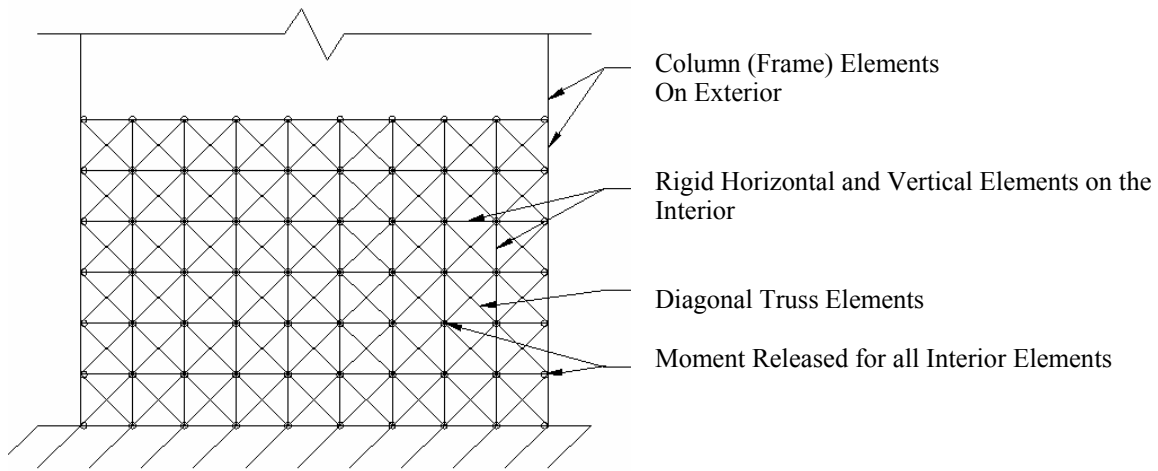
Figure 4.13: Close-up of Truss-Grid Wall Model

4.6 Procedure for Bridge Ultimate Strength Modeling within SAP

This section provides a step-by-step procedure to model bridge piers, both with and without shear walls, within SAP 2000. Along with a written description, images from SAP 2000 are included to show the necessary steps to accurately model the bridge piers and bridge systems under consideration. The bridges being modeled represent actual bridges crossing navigable waterways in the state of Texas that are subject to potential vessel collision.

4.6.1 Bridge Pier without Shear Wall

The representative example selected for this type of bridge pier is the eastbound Interstate Highway 10 (IH-10) bridge over the San Jacinto River outside of Houston, Texas. Bent 18 is one of two identical piers on each side of the main navigation channel that is subject to vessel collision. The bridge superstructure is comprised of 622-foot, 3-span continuous plate girders topped with a 10-inch reinforced concrete deck. Figure 4-14 shows a simple line sketch of the pier and includes the basic dimensions of the structure. Note the member names associated with each beam and column as those same names will be used throughout this section as labels for the material model and section definitions in SAP 2000 for those elements.
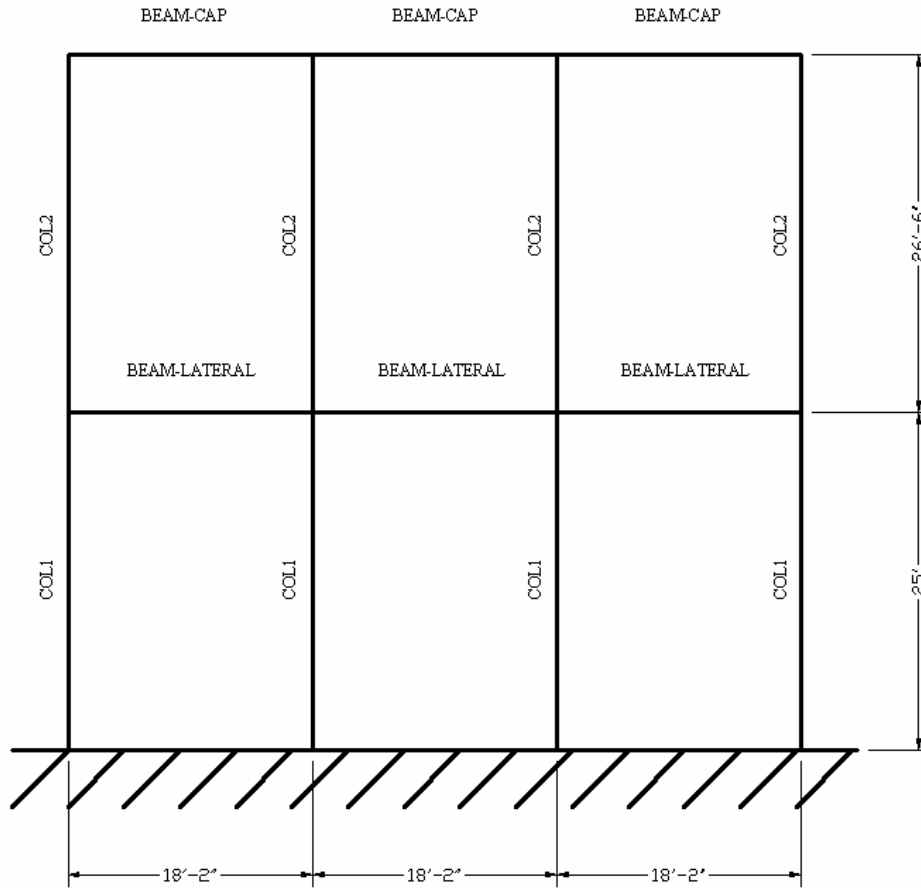
Figure 4.14: IH-10 Bridge Bent 18

Step 1: Define Bridge Pier Geometry

Bent 18 is 51.5-feet tall by 54.33-feet wide and is comprised of four equally spaced columns, connected together by a pile cap at the bottom, a beam at 25 feet above the pile cap and a cap beam at the top of the columns. To define the geometry of this pier in SAP 2000, it is convenient to start with a blank model and define gridlines along the centroids of the columns and beams. Figure 4-15 shows the creation of a grid within SAP 2000.
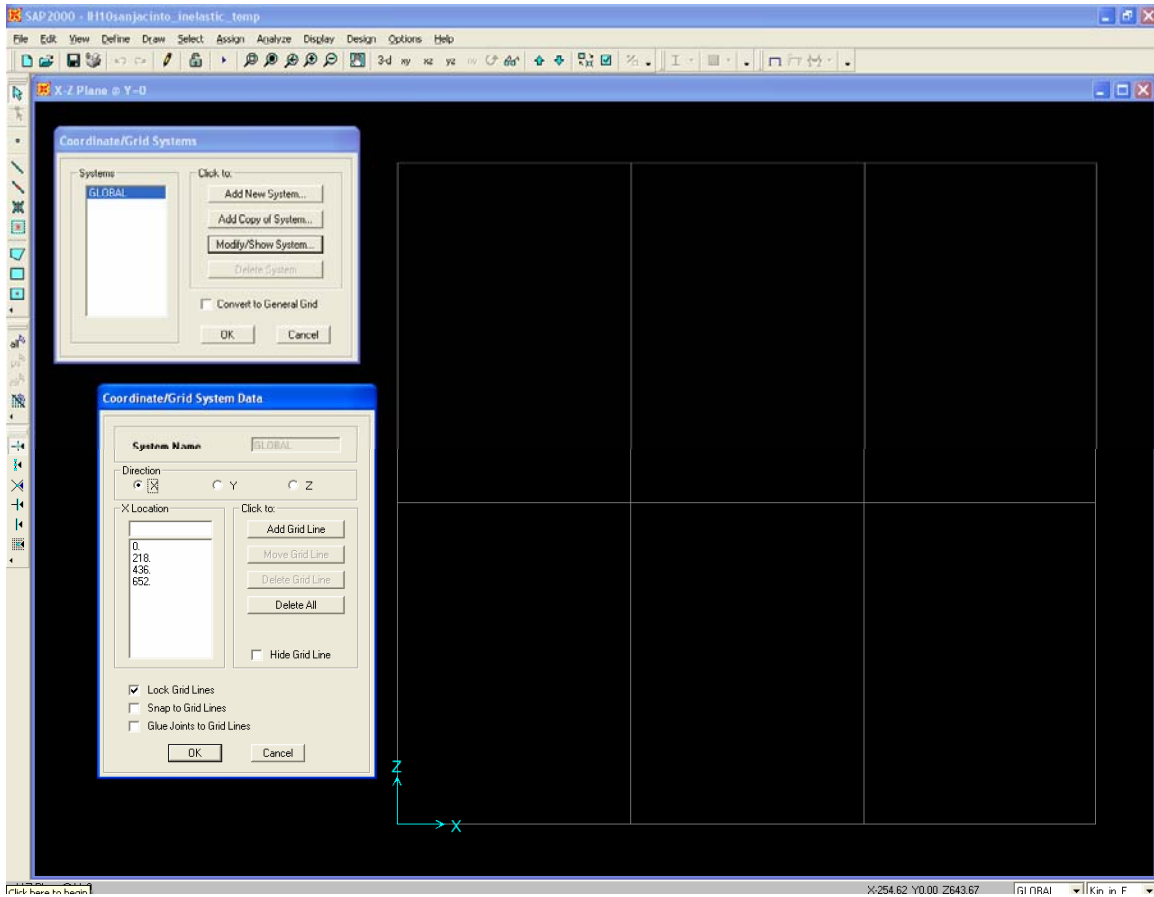
Figure 4.15: IH-10 San Jacinto Bridge Bent 18

Step 2: Define Material Models

Once the basic geometry of the system being analyzed has been established, the next step is to define a set of material properties for each of the bridge elements. As previously described, smeared material properties are being used to represent the modeling of the reinforced concrete elements. To establish the material property sets, a reinforced concrete section analysis was run for each of the bridge pier elements. These results are summarized in Table 4-2.

Table 4.2: IH-10 San Jacinto Pier 18 Material Model Summary

IH10 San Jacinto Eastbound Pier 18 Bottom Column				IH10 San Jacinto Eastbound Pier 18 Lateral Beam			
Basic Section Properties				*Basic Section Properties*			
width (in)	78.00	depth (in)	78.00	width (in)	84.00	depth (in)	48.00
Plastic Modulus (in^3)	118638.00	Section Modulus (in^3)	79092.00	Plastic Modulus (in^3)	48384.00	Section Modulus (in^3)	32256.00
bars	40-#11 bars	stirrups	#4 @ 9"	bars	22-#11	stirrups	#4 @ 9"
Response 2000 Section Analysis				*Response 2000 Section Analysis*			
My (in-kips)	126060.00	fy (ksi)	1.06	My (in-kips)	42732.00	fy (ksi)	0.88
Mp (in-kips)	159900.00	fu (ksi)	1.35	Mp (in-kips)	55392.00	fu (ksi)	1.14
		fu/fy	1.27			fu/fy	1.30
IH10 San Jacinto Eastbound Pier 18 Top Column				IH10 San Jacinto Eastbound Pier Cap Beam			
Basic Section Properties				*Basic Section Properties*			
diameter (in)	54.00			width (in)	84.00	depth (in)	48.00
Plastic Modulus (in^3)	26244.00	Section Modulus (in^3)	15458.99	Plastic Modulus (in^3)	48384.00	Section Modulus (in^3)	32256.00
bars	20-#11	stirrups	#4-9" pitch	bars	22-#11	stirrups	#6 @ 9"
Response 2000 Section Analysis				*Response 2000 Section Analysis*			
My (in-kips)	34572.00	fy (ksi)	1.32	My (in-kips)	61668.00	fy (ksi)	1.27
Mp (in-kips)	42576.00	fu (ksi)	1.62	Mp (in-kips)	86904.00	fu (ksi)	1.80
		fu/fy	1.23			fu/fy	1.41

Figure 4-16 shows the material property input boxes in SAP 2000. SAP 2000 contains default properties for several materials. Figure 4-16 specifically shows the material property input for 'col 1' or the bottom columns in the pier frame. Note that the values under 'Analysis Property Data', the mass, weight, modulus of elasticity, Poisson's ratio, and the coefficient of thermal expansion, are all consistent with reinforced concrete material properties. Also, note that the 'Type of Design' is set to steel. This selection is intentional, despite the fact that a reinforced concrete pier is being modeled. This box must be set to steel in order to define smeared material properties based on a yield and ultimate stress.
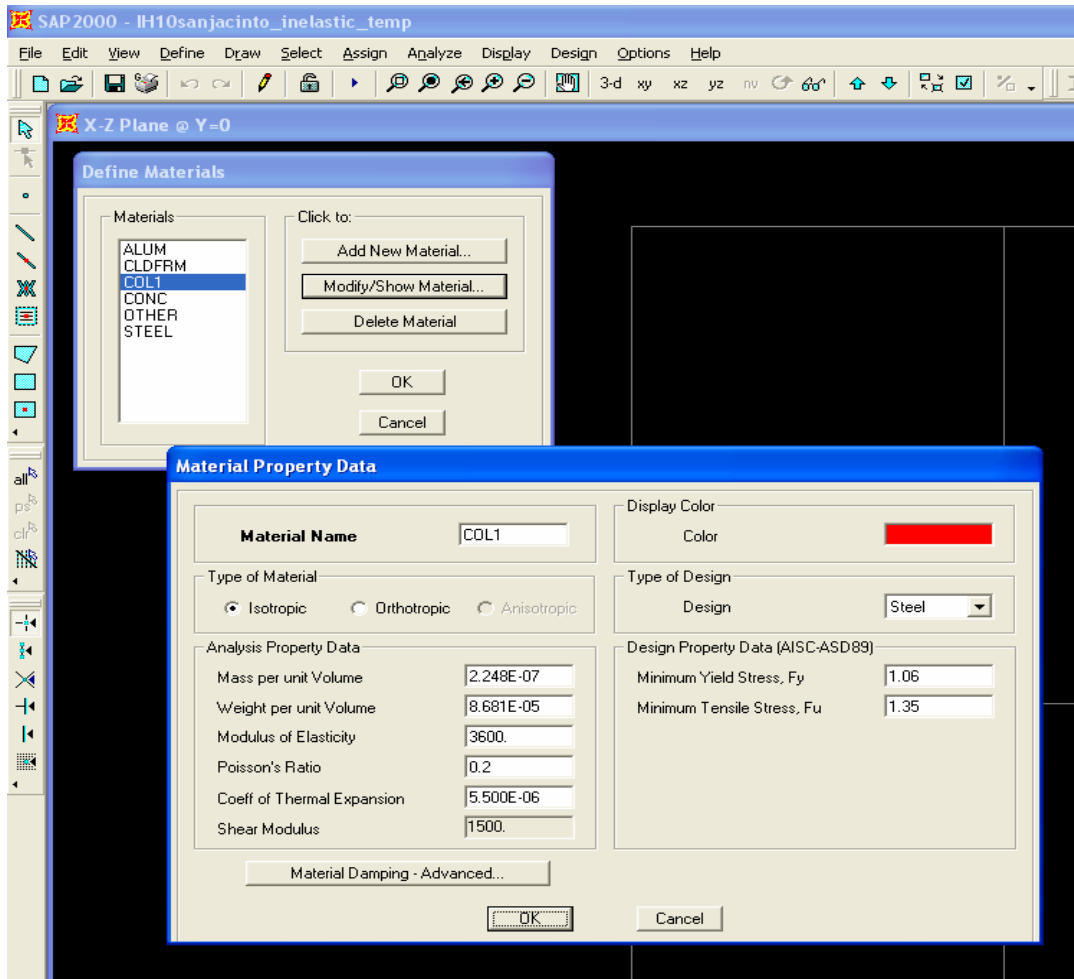
Figure 4.16: Material Property Definition in SAP 2000

Step 3: Define Element Section Properties

Figure 4-17 shows the SAP 2000 screen for entering a new section. Again, input for the bottom column or 'col 1' in the pier frame is shown. A user needs to enter dimensions and assign a material for the section. Also shown in the screen capture are the section properties, which SAP calculates based on the geometry entered by the user.
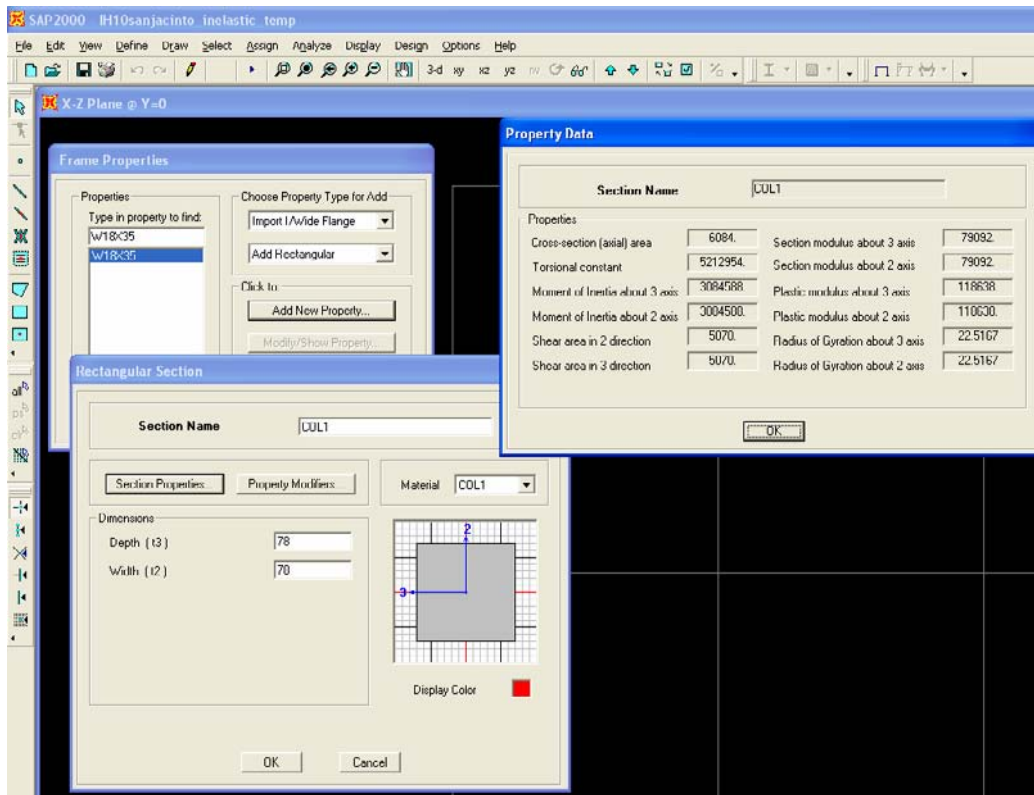
Figure 4.17: Section Input in SAP 2000

Step 4: Draw Bridge Pier Elements

After the material and section properties are entered for each element, the bridge pier can be drawn. Figure 4-18 shows two images of the drawn bridge in SAP 2000, one as line elements and a second comprised of 3-D solids. It is helpful to view the solid model to ensure that sections have been defined properly.
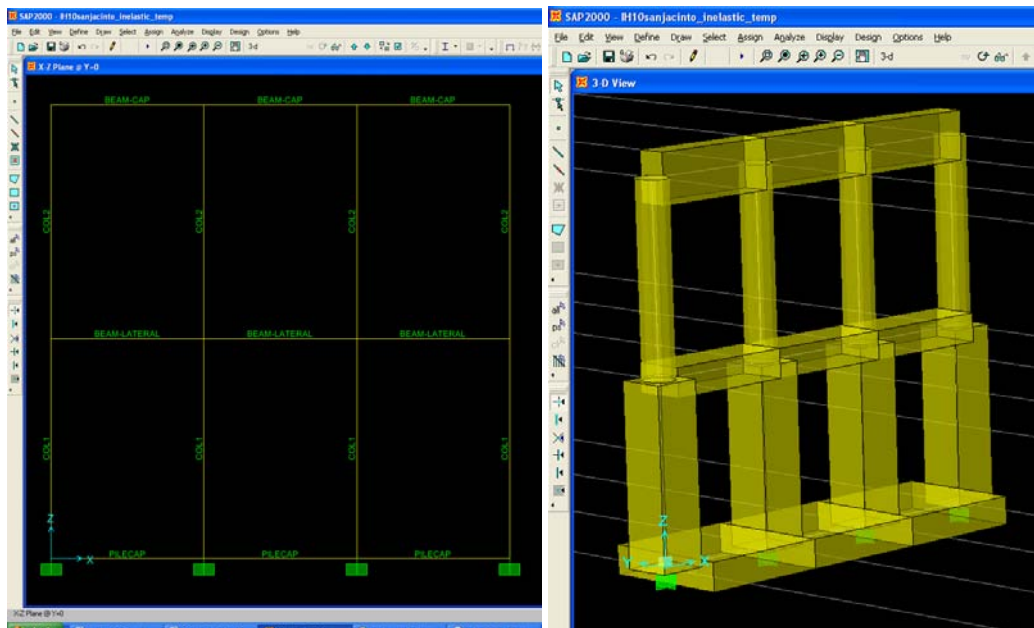
Figure 4.18: SAP 2000 Pier Models

Step 5: Define Plastic Hinge Properties and Assign to Element Ends.

The next step is to define plastic hinges, which will be applied to member ends and will be used to capture the inelastic behavior of the structure. SAP 2000 has several default hinge properties built in including moment, axial, shear, and moment-axial interaction hinges. User-defined hinges can also be defined and are used for this model. Plastic hinge properties are based on the section analyses performed to determine the material properties. The hinges used in these models are defined as moment-axial hinges and are based on the yield stress and the ratio of the yield stress to the ultimate stress. This ratio defines how much additional capacity is available in the hinges after the onset of yield. Figure 4-19 shows the SAP 2000 input boxes for defining hinge properties.

Recall that, in defining the material properties it was assumed that there was zero axial load on the sections. It seems counterintuitive then, that the hinges are defined as moment-axial interaction hinges. Assuming zero axial load in defining the material was shown to be a conservative assumption, given the level of axial load on bridge members. There is, however, axial load in the real structure, and by defining moment-axial hinges, the effect of the axial load on yielding in the structure is taken into consideration. In addition, by defining moment-axial hinges, as opposed to hinges based only on moment, any change in how the material is defined could be easily integrated into the models. For example, a more accurate or detailed reinforced concrete material model could be used or developed.

41
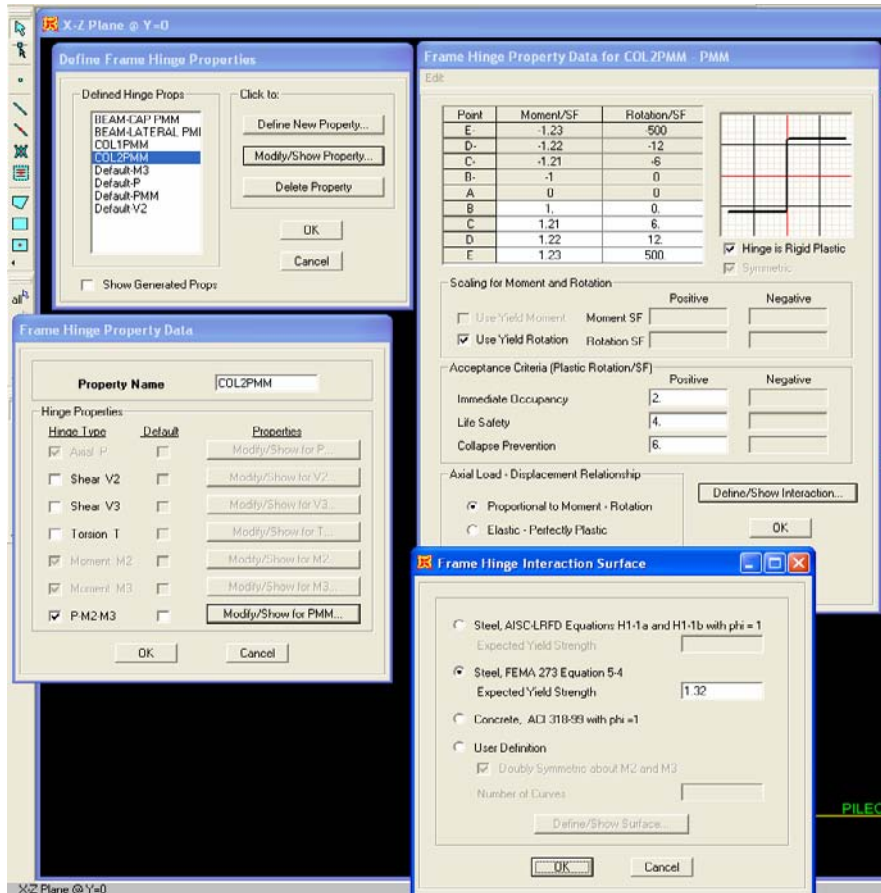
Figure 4.19: SAP 2000 Plastic Hinge Property Input

The 'Define Frame Hinge Properties' window (upper left of Figure 4-19) lists all of the default and user-defined hinges and provides the option to modify, delete or define a new hinge property. The moment-axial hinge for the top column, 'COL2-PMM', has been selected. The 'Frame Hinge Property Data' window (lower left of Figure 4-19) shows that 'COL2-PMM' is a user-defined moment-axial interaction hinge. The 'Frame Hinge Property Data for COL2-PMM' box in the upper right of Figure 4-19 shows the actual strength and deformation properties of the hinge. This hinge is defined based on strength and deformation relative to the yield strength and rotation. The strength characteristics of the hinge are defined by the left column. The values entered are based on the ratio of the plastic moment to the yield moment for this section, M_p/M_y = 1.23. The deformation capacity of the hinge is defined by the right column. In this case, a large value has been assigned for the ultimate rotation capacity, essentially making the hinge capable of infinite plastic deformation or rotation once the plastic strength has been reached. A real plastic hinge would not be capable of infinite deformation or rotation, but this definition is acceptable if the deformation capacity of the member or structure as a whole is assessed in the post-analysis phase.

For user defined moment-axial interaction hinges, an interaction surface must be defined. The lower right window in Figure 4-19 shows that 'Steel FEMA 273 Equation 5-4' has been selected as the yield surface. A steel interaction surface has been defined even though the bridge sections being defined are reinforced concrete because of the smeared material approach that has been taken. When using the 'Steel FEMA 273 Equation 5-4', the yield strength of the section

42

that the hinge is being used for must be re-entered. Figure 4-19 shows that for the top column the yield stress was entered as 1.32, which is consistent with how this value was previously defined.

Once plastic hinges have been defined for each member, they need to be assigned to the proper elements. Hinges can be defined at any relative point along the length of a beam, but it is often easiest to assign hinges just to the ends of members. Therefore, it may be necessary to subdivide an element to place hinges at the desired locations. It is important to note that static nonlinear analysis results in SAP 2000 are very sensitive to the number and location of hinges used. In order to capture the inelastic response at given point in a system, a hinge must be assigned to that location. If a static nonlinear analysis case is setup in SAP 2000, but no hinges are assigned to the model, the analysis results will show the system acting in a linear elastic fashion. While possible hinge locations could vary widely depending on the specifics of a given structure, it is generally sufficient to place hinges at member ends and at points where loads are applied to a structure. Other portions of a structure that are subject to high moment or axial forces should also have hinges assigned. If necessary, several configurations of hinges may need to be tried to be certain that SAP 2000 is accurately capturing the inelastic response of the system being analyzed. Figure 4-20 shows the hinge assignment process for a specific case of the IH-10 Bridge in SAP 2000. For the results presented in Chapter 5, different hinge patterns are considered for each particular load case. Figure 4-20 is presented only as an example of assigning hinges to the model.
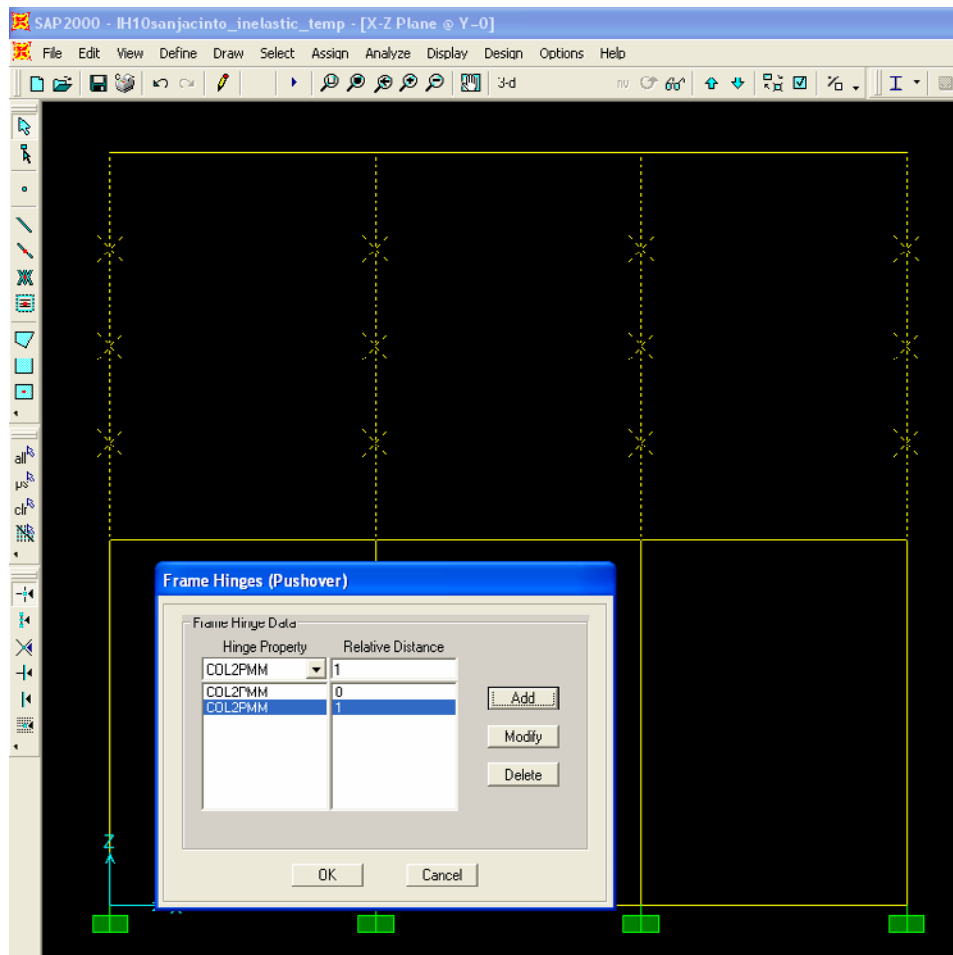
Figure 4.20: Assigning Hinges in SAP 2000

43

Step 6: Modeling Bridge Superstructure and Adjacent Piers

The current AASHTO specifications consider only the strength of a stand-alone pier and do not account for the redistribution of forces through a cap beam and deck to adjacent piers. By modeling the adjacent piers of a bridge, as well as the bridge deck and girders, these factors can be considered. Adding adjacent piers can be done by adding grid planes in the direction perpendicular to the pier that has already been drawn. Rather than redrawing an identical pier, a user can also simply copy and paste elements onto a new grid plane. Figure 4-21 shows the IH-10 Bridge with all of the piers connected to the 3-span continuous plate girder that spans the main navigational channel. It is assumed that the adjacent piers will behave linear elastically during a vessel collision event, so there is no need for the material model and plastic hinge property definitions described above. The pier and section geometry, along with a simple material model that accurately reflects the stiffness of reinforced concrete, needs to be defined.
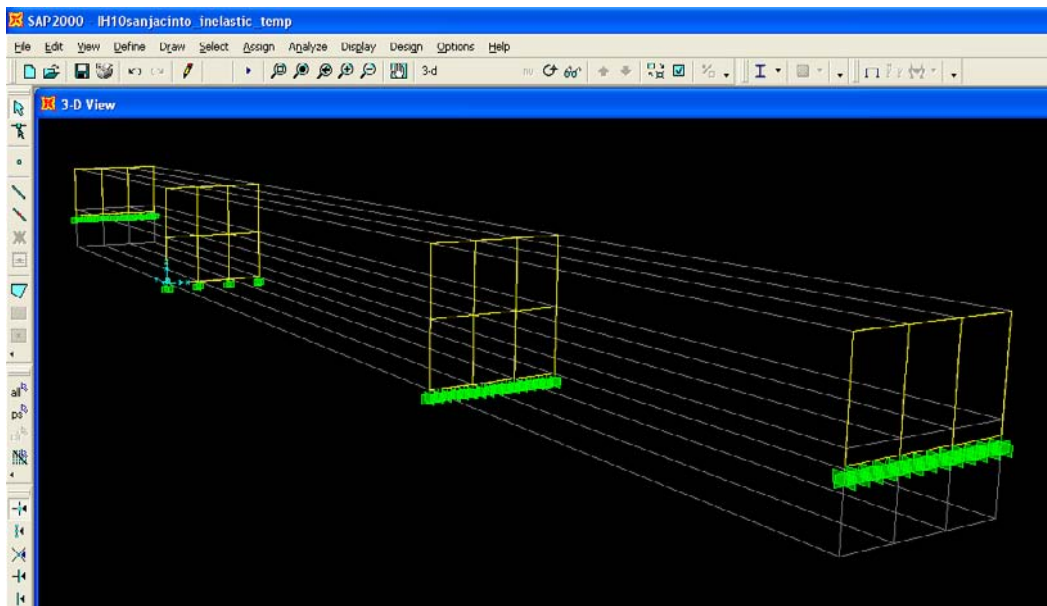
Figure 4.21: Bridge Model with Adjacent Piers

Rather than model the exact geometry of the bridge superstructure, general elements are defined that match the stiffness characteristics of the bridge deck and girders. In order to model the superstructure this way, geometric and stiffness properties of the superstructure must be determined. Table 4-3 shows the section properties for the deck and girders of the IH-10 Bridge. It is assumed that the deck and girders do not act as a composite system, so the section properties of each are merely added together to get the final section properties shown. Note that Table 4-3 also shows the dead load of the deck and girders. This information will be used in chapter 5 when loads are assigned to the model.

Table 4.3: Deck and Girder Properties

Member	Description	Modulus of Elasticity (ksi)	Cross Section Area (in^2)	Moment of Inertia (in^4)		Dead Load Contribution to Pier (kips)
				xx	yy	
Deck	7.25" Thick Deck 60' Roadway Width	3600.00	5220.00	22864.69	225504000.00	1212.60
Girder	3-span Cont Plate Girder 6 Individual Girders 84" Depth, 30" Flange Width 1" Plate Thickness	29000.00	852.00	895723.98	27041.00	586.47
Transformed Girder	Girder Properties Transformed to Account for Difference in Modulus of Elasticity	3600.00	6816.00	7165791.84	216327.98	586.47
Total	Entire Superstructure Properties--Deck and Transformed Girder Together	3600.00	12036.00	7188656.53	225720327.98	1799.07
Total/4	4 Elements will be used to represent the deck in SAP 2000	3600.00	3009.00	1797164.13	56430082.00	449.77

Once the section properties have been determined, the bridge and deck can be modeled together as a series of elements with a general section. SAP 2000 allows a user to input section properties such as area and moment of inertia without entering the exact section geometry. Figure 4-22 shows the input for a general section that is used to represent the superstructure of the IH-10 Bridge model. For this model, four elements are used to represent the deck and girders. Therefore the section properties entered reflect ¼ of the moment of inertia, *I*, and cross-sectional area, *A*, for the superstructure in each direction. Lastly, property modification factors are assigned. This step is shown in Figure 4-23. Large modification factors have been applied to the area properties, making the section axially rigid, to the torsion properties to prevent twist, and to the shear properties, so that shear deflections will be negligible. Also note that a modification factor of *0.0* has been applied to the weight and mass for these elements. The dead load of the girders and deck were determined earlier, but will not be applied directly to the general elements being defined here. Instead, the dead load as well as the live load from the bridge and deck will be applied directly to the top of the piers. Application of in-place loads is addressed in more depth in Chapter 5. These factors are used to ensure that the line elements representing the superstructure behave in a similar fashion to the actual deck.
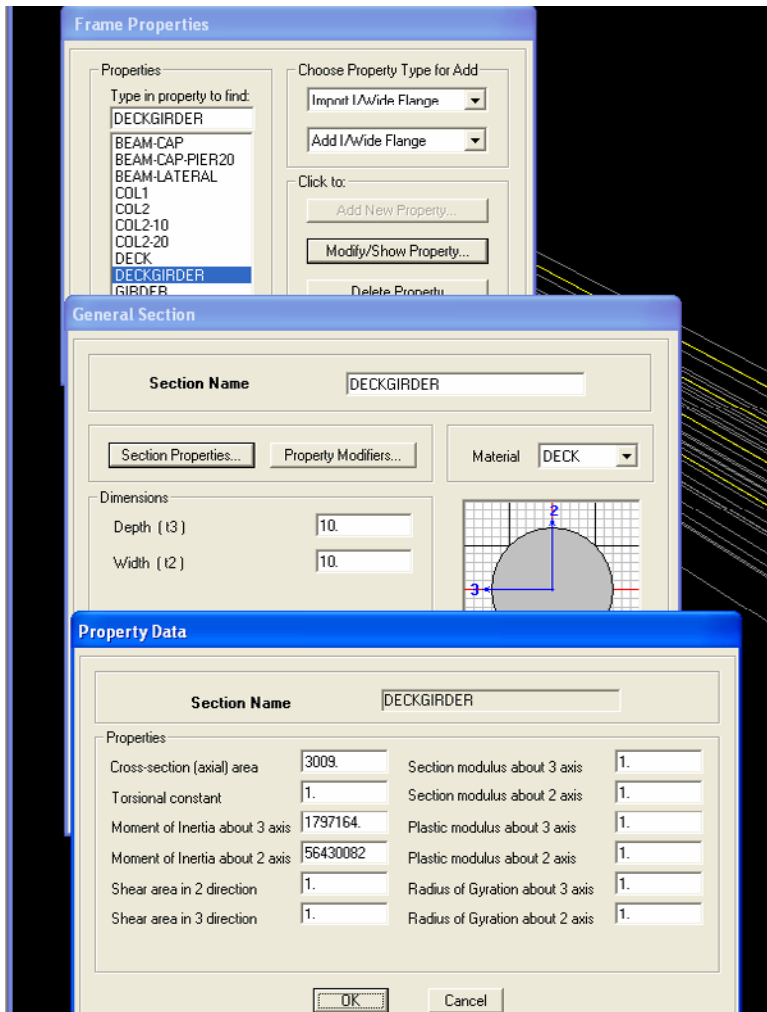
Figure 4.22: General Section Properties
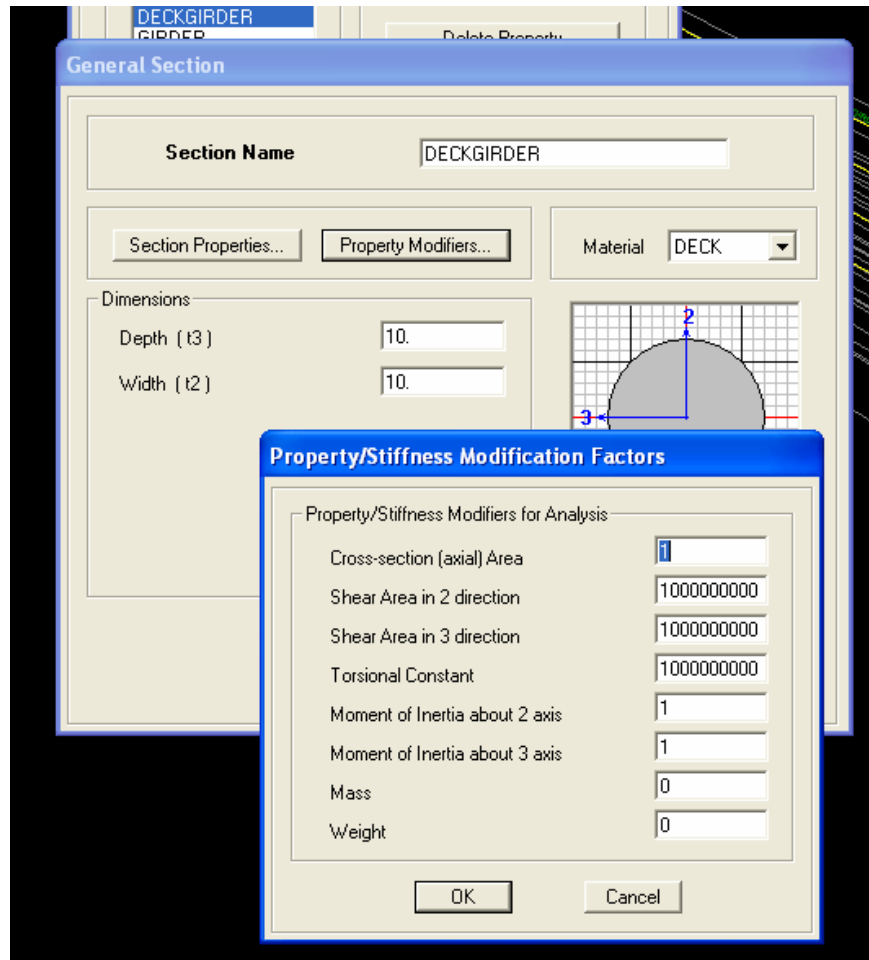
Figure 4.23: Section Modification Factors

Once a general section has been defined for the superstructure, line elements, representing the superstructure can be drawn into the model. This step is shown in Figure 4-24. At this point, it is crucial to assess and understand the connection detail between the bridge superstructure and bridge pier. Take for example a bridge with simply supported precast concrete 'I' girders between the bridge piers with a continuous deck poured over the top. One needs to be careful in assuming how much redistribution is possible. The girders and deck will certainly provide some type of support condition at the top, but the effect may be limited if the girders are simply sitting on bearing pads on the cap beam of the pier. The IH-10 Bridge superstructure is continuous over the main channel piers. For the IH-10 Bridge being modeled for this research, the 3-span superstructure is assumed to be fully connected over the two interior piers and simply supported at the two exterior piers. After the superstructure elements have been drawn, moments can be released at the far ends of the elements.

47
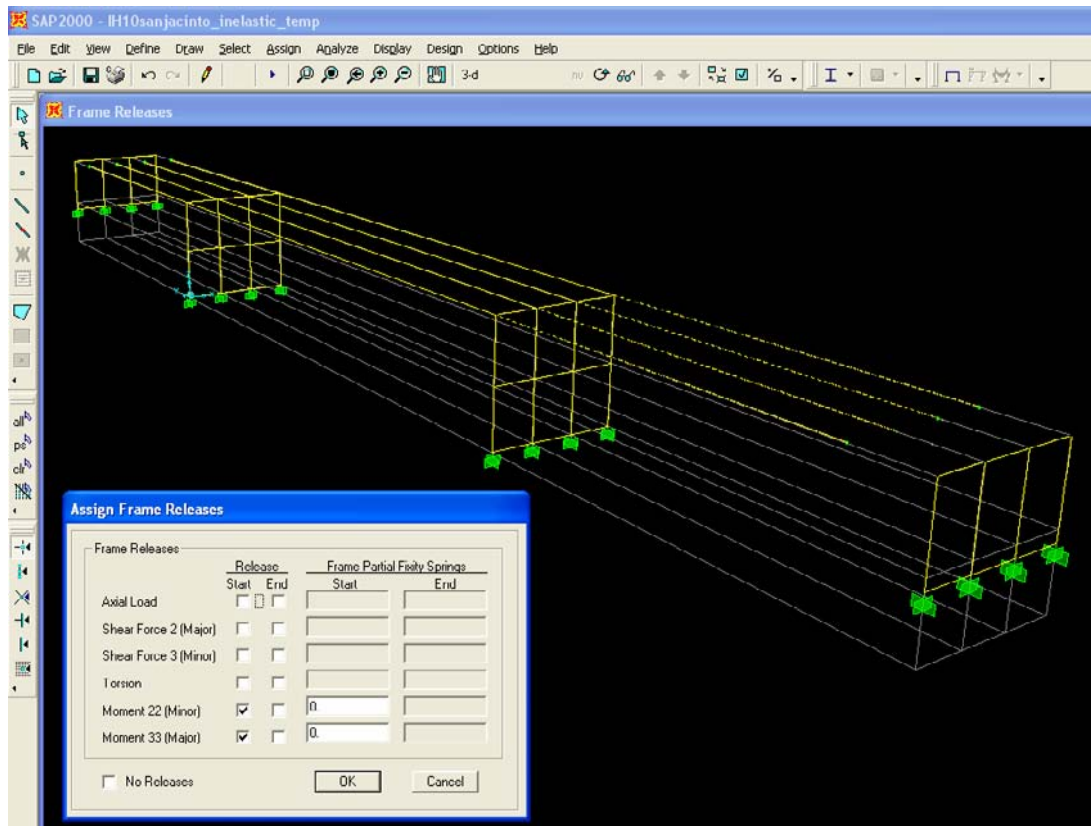
Figure 4.24: Releasing End Moments in Superstructure Elements

At this stage, the structure is ready to be analyzed. Chapter 5 of this report outlines the loads applied and the analysis cases performed for this model to assess the structural performance when subjected to vessel impact.

4.6.2 Bridge Pier with Shear Wall

The representative examples selected for this type of bridge pier are bents 21 and 22 of the State Highway 87 (SH-87) bridge over the Gulf Intracoastal Waterway (GIWW), constructed in 1969. Bents 21 and 22 are two identical piers on each side of the main navigation channel that are subject to potential vessel collision. The bridge superstructure over the waterway is a 680-foot, 3-span continuous steel plate girder unit. An elevation of the SH87 Bridge is shown in Figure 4-25. The drawing is shown to give an idea of what the SH-87 bridge profile looks like, the specific notes on the bridge are not important.

Bents 21 and 22 of the SH-87 Bridge are 3-column piers, and measure 88-feet high by 42-feet wide. A 2-foot wide shear or web wall extends 31 feet up from the pile cap. Figure 4-26 shows the construction drawing for these piers. Notice that the column sections change 27 feet above the shear wall, from a 66-inch square column to a 48-inch circular section. Again, the specific notes in the figure are not relevant to the current discussion.

The following section outlined the procedure for the modeling of bridge piers with shear walls. Many of the required steps have already been described in detail in Section 4.6.1 and will only be touched on briefly. The emphasis is on modeling of the shear wall using the truss-grid model described earlier.

48

Figure 4.25: SH87 Bridge over the GIWW Elevation
(TXDOT Construction Documents, 1969)

49

Figure 4.26: SH87 Bridge Pier (TXDOT Construction Documents, 1969)

Part A: Shell Wall Model

Step 1: Define Bridge Pier Geometry

The bridge geometry for this model can be established in the same fashion as described earlier for the IH-10 Bridge. Gridlines should be spaced and drawn to correspond with the centroids of the beams and columns. In addition, gridlines should be defined at the boundaries of the wall.

Step 2: Define Material Models

The shell-wall model being constructed in this section will only be used for a linear elastic analysis. Therefore, the lengthy process for defining material properties for each individual member in the frame described in Section 4.6.1 does not need to be completed. Instead, only the proper Modulus of Elasticity, E, needs to be defined. The Modulus of Elasticity used here is based on the ACI 318-02 equation given earlier (Equation 4-1). This value can be entered into either the SAP 2000 default concrete material property (CONC), or a new user-defined material property, as was done previously. From the construction drawings, it is known that the specified concrete compressive strength for this bridge, f_c', is 1200 psi. Therefore, the corresponding modulus of elasticity, E, is 1975 ksi.

Step 3: Define Element Section Properties

Section properties can be assigned in the same manner for the beams and columns as described earlier. Additional properties need to be defined for the wall/area section. Figure 4-27 shows the definition of an area section in SAP2000. Note that the section has been titled 'WALL' and is defined as a 'Shell'. SAP 2000 defines a shell as an area element that has both

50

translational and rotational degrees of freedom and is capable of supporting both forces and moments (SAP2000 user manual, 2004). SAP 2000 also has sub-types for a shell element. In this case, the sub-type used is also called 'Shell' with the 'Thick Plate' option checked. The 'Shell' subtype again means that the element is capable of supporting both forces and moments. The 'Thick Plate' option is used to include shear deformations in the elements. The defined thickness values used should correspond to the dimensions of the actual shear wall being modeled.
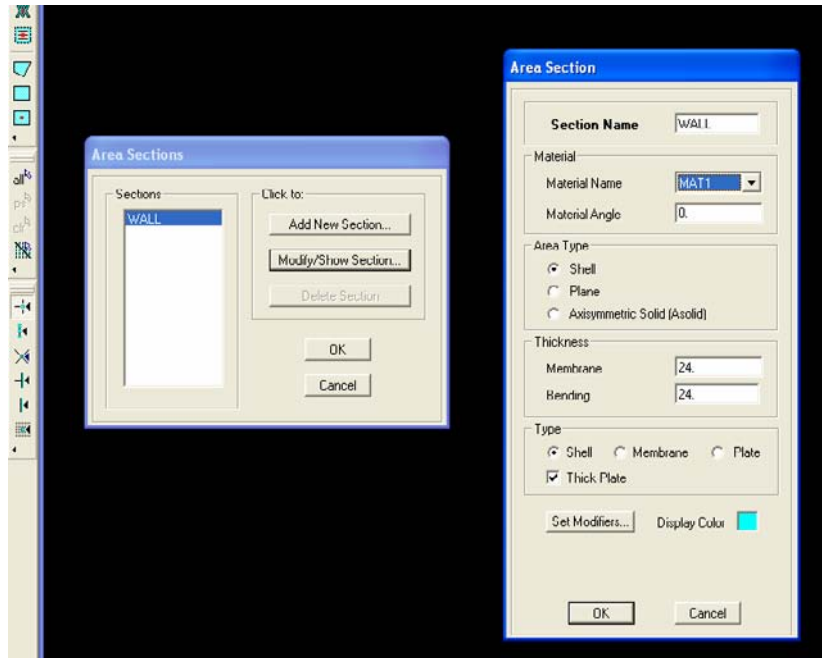
Figure 4.27: Defining Area Sections

Step 4: Draw Bridge Pier Elements

Much of the process for building the SAP 2000 model for bents 21 and 22 is the same as described for the IH-10 Bridge. The only difference is the addition of a shear wall. The wall is added by drawing two area elements between the three columns up to a height of 31 feet. Next, the user needs to mesh the large areas into a series of smaller elements. It is best to break the areas down into elements that are approximately square. In this case, each area representing the walls between the three columns is divided into a 10 by 16 mesh of elements, each 25.2 inches × 25.2 inches. After the area has been meshed, the joints at the bottom of the pier need to be fixed. Figure 4-28 shows the two wall areas drawn and ready to be meshed. Figure 4-29 shows the final meshed model.

51
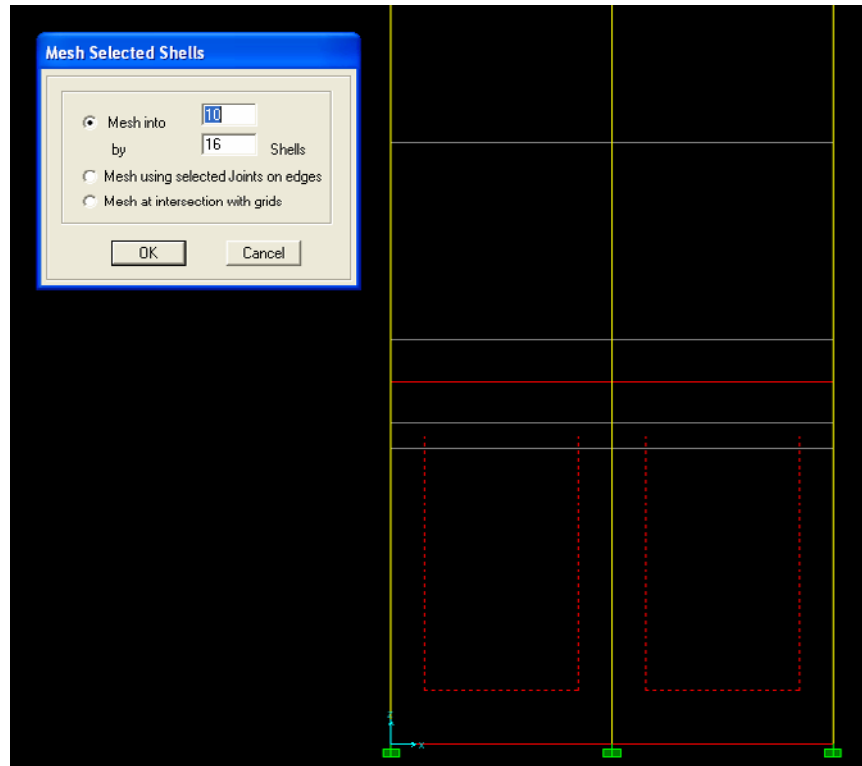
Figure 4.28: Meshing Shell Wall in SAP 2000
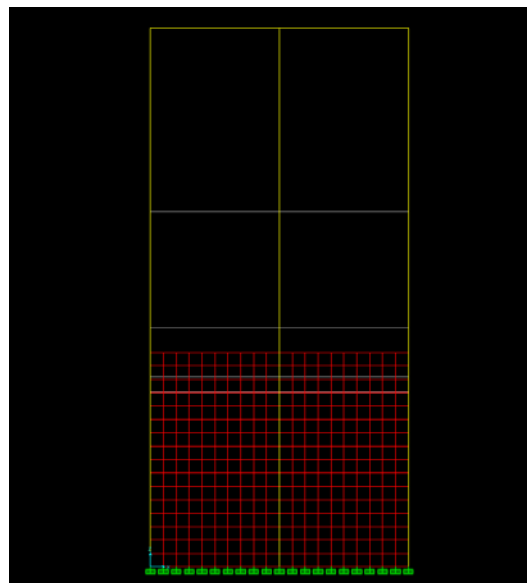
Figure 4.29: Meshed Wall

To check if the wall mesh is adequate, at least two different meshes need to be investigated. If they both models give the same solution (displacement) under the same loads, then the coarser mesh is acceptable. If the solutions are not close, a finer mesh must be used. For this model, the 10 by 16 element mesh has been verified to be adequate.

Step 5: Modeling Bridge Superstructure and Adjacent Piers

This step can be completed as previously described. However, due to a lack of information, the two exterior piers at the ends of the 3-span continuous plate girder unit are not modeled. Instead, simple pin supports are placed at the ends of the superstructure. Figure 4-30 shows the SH-87 Bridge Model with identical piers 21 and 22 defining the main navigation channel and both subject to potential vessel collision. Table 4-4 summarizes the section and material properties needed to define the superstructure elements shown in Figure 4-30.
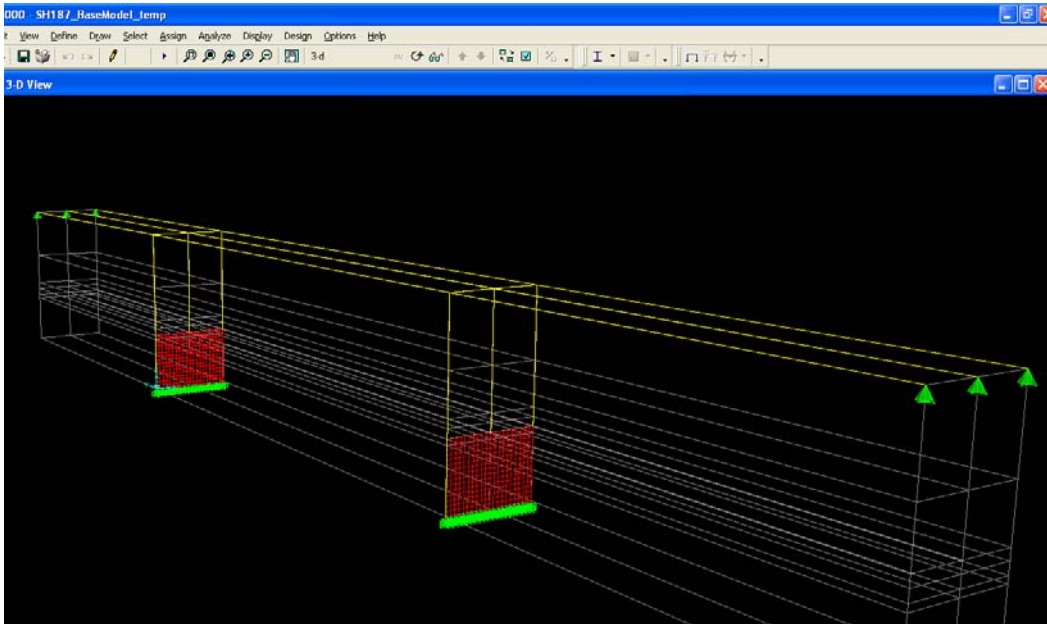
Figure 4.30: SH87 Bridge Model in SAP 2000

Table 4.4: SH87 Superstructure Properties

Member	Description	Modulus of Elasticity (ksi)	Cross Section Area (in^2)	Moment of Inertia (in^4)		Dead Load Contribution to Pier (kips)
				xx	yy	
Deck	10.5" Thick Deck 50.3' Roadway Width	3600.00	6337.80	58228.54	192422452.00	1584.53
Girder	3-span Cont Plate Girder 6 Individual Girders 72" Depth, 20" Flange Width 1.5" Plate Thickness	29000.00	490.50	346885.80	6058.20	523.16
Transformed Girder	Girder Properties Transformed to Account for Difference in Modulus of Elasticity	3600.00	3924.00	2775086.40	48465.60	523.16
Total	Entire Superstructure Properties--Deck and Transformed Girder Together	3600.00	10261.80	2833314.94	192470917.60	2107.69
Total/3	3 Elements will be used to represent the deck in SAP 2000	3600.00	3420.60	944438.31	64156972.53	702.56

Step 6: Apply Load

At this stage, the model is ready for loads to be applied for analysis. Again, this step is being done in order to calculate the linear elastic response of the shell wall bridge pier model to an arbitrary load at any given load location. The lateral displacement from this load is then used

to size the truss members in the truss-grid wall model. The following list describes the type and location of all the loads that are considered. The loads are also illustrated in Figure 4-31.

Linear Elastic Load Cases for Shell-Wall Model:

- Load Location 1: Point load at the top of the wall

- Load Location 2: Point load 48 inches above the top of the wall

- Load Location 3: Point load 96 inches above the top of the wall

- Load Location 4: Distributed Load 30 inches above and below the wall
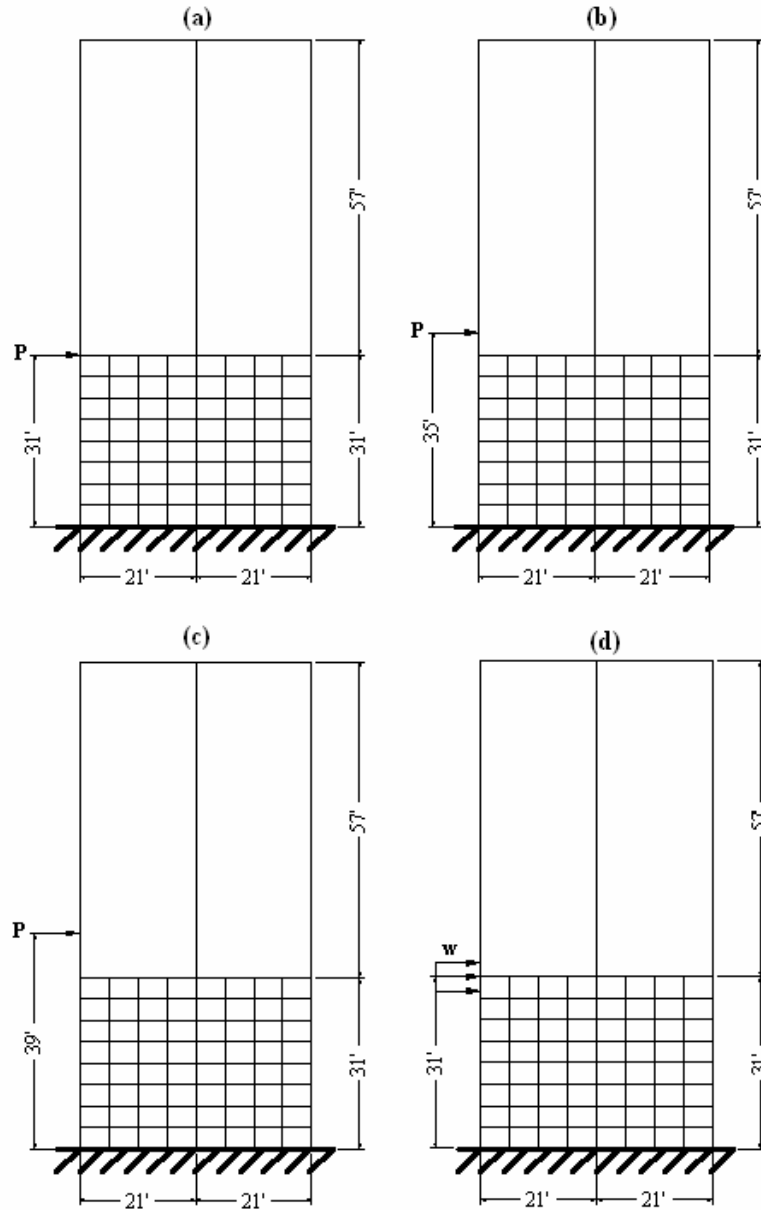
Figure 4.31: SH-87 Impact Loads:
(a) Load Location 1: Point Load at Top of Wall, (b) Load Location 2: Point Load 48 inches
Above Wall, (c) Load Location 3: Point Load 96 inches Above Wall, (d) Location 4: 60-inch
Wide Distributed Load at Wall

It should be noted that the load cases selected here represent a set of possible cases for this bridge based on a range of water levels, not the exact cases that are required by the AASHTO specification. They have also been selected in part to provide the opportunity to make some reasonable conclusions regarding the validity of the truss-grid model. In addition, presenting multiple load cases for multiple boundary conditions emphasizes the requirement that the diagonal truss members in the truss-grid model need to be sized separately for each load and boundary condition configuration. It is important to reiterate that the load cases presented here

55

only represent the lateral loads being used to match the response of the shell wall model and the truss-grid wall model to a linear elastic analysis. Chapter 5 discusses the loads applied to the bridge to determine the capacity to potential vessel collisions

Step 7: Run Linear Elastic Analysis

Table 4-5 summarizes the results from a linear elastic analysis on the SH87 shell-wall model built above.

Table 4.5: Shell Wall Linear Elastic Analysis Results

Load Description	Top Boundary Condition	Total Load Applied	Lateral Displacement at Point of Load
Point Load at Top of Wall	free	1000 k	0.108"
Point Load at Top of Wall	fixed	1000 k	0.103"
Point Load at Top of Wall	superstructure	1000 k	0.106"
Point Load 48" above Top of Wall	free	1000 k	0.235"
Point Load 48" above Top of Wall	fixed	1000 k	0.210"
Point Load 48" above Top of Wall	superstructure	1000 k	0.224"
Point Load 96" above Top of Wall	free	1000 k	0.472"
Point Load 96" above Top of Wall	fixed	1000 k	0.394"
Point Load 96" above Top of Wall	superstructure	1000 k	0.436"
Distributed Load 30" above and below wall	free	1000 k	0.107"
Distributed Load 30" above and below wall	fixed	1000 k	0.101"
Distributed Load 30" above and below wall	superstructure	1000 k	0.104"

Part B: Truss-Grid Wall

Step 1: Define Bridge Pier Geometry

The geometry and grid layout defined previously in Section 4.6.2.1 is also be used for the truss-grid model. The model geometry, including the wall boundary dimensions, remains the same; however, the shell wall is replaced with a truss-grid wall. Replacing the shell wall with the truss-grid wall will is discussed in detail in Step 4.

Step 2: Define Material Models

The procedure to define the material properties for the various sections of the SH-87 Bridge is carried out in the same fashion as previously described for the IH-10 Bridge. In addition to performing a reinforced concrete section analysis for the beams and columns, an

additional analysis is needed for the wall section. The following lists the assumed material properties for piers 21 and 22 of the SH87 Bridge:

- Concrete Compressive Strength, $f_c' = 1200\ psi$

- Modulus of Elasticity, $E = 1975\ ksi$

- Steel Reinforcing Yield Strength, $f_y = 40\ ksi$

These values were input into Response, along with the section geometry and reinforcing bar layout, to develop the material models summarized in Table 4-6.

Table 4.6: SH87 Material Properties

SH 87 Intracoastal Piers 21 &22 Top Column Section				SH 87 Intracoastal Piers 21 &22 Bottom Column Section			
Basic Section Properties				*Basic Section Properties*			
diameter (in)	48.00			*width (in)*	66.00	*depth (in)*	66.00
Plastic Modulus (in^3)	18432.00	*Section Modulus (in^3)*	10857.34	*Plastic Modulus (in^3)*	71874.00	*Section Modulus (in^3)*	47916.00
bars	24-#11	*stirrups*	#3 @ 6"	*bars*	28-#11	*stirrups*	# 4 @ 12"
Response 2000 Section Analysis				*Response 2000 Section Analysis*			
My (in-kips)	22178.40	*fy (ksi)*	1.20	*My (in-kips)*	46820.40	*fy (ksi)*	0.65
Mp (in-kips)	27290.40	*fu (ksi)*	1.48	*Mp (in-kips)*	61653.60	*fu (ksi)*	0.86
		fu/fy	1.23			*fu/fy*	1.32
SH 87 Intracoastal Piers 21 &22 Cap Beam Section				SH 87 Intracoastal Piers 21 &22 Wall Section			
Basic Section Properties				*Basic Section Properties*			
width (in)	51.00	*depth (in)*	54.00	*width (in)*	252.00	*depth (in)*	24.00
Plastic Modulus (in^3)	37179.00	*Section Modulus (in^3)*	24786.00	*Plastic Modulus (in^3)*	36288.00	*Section Modulus (in^3)*	24192.00
bars	12-#11	*stirrups*	#5 @ 17"	*bars*	12-#11	*stirrups*	#5 @ 17"
Response 2000 Section Analysis				*Response 2000 Section Analysis*			
My (in-kips)	17707.20	*fy (ksi)*	0.48	*My (in-kips)*	26781.60	*fy (ksi)*	0.74
Mp (in-kips)	23161.20	*fu (ksi)*	0.62	*Mp (in-kips)*	39825.60	*fu (ksi)*	1.10
		fu/fy	1.31			*fu/fy*	1.49

Step 3: Define Element Section Properties

Section information for the beams and columns in the SH-87 Bridge is entered as previously described. For models with shear walls, two additional sections need to be defined in order to use the truss-grid wall model — a 'rigid' element and a 'truss' element. The rigid element can be defined in several ways. A general section could be used, as was done to model the bridge superstructure, and a large value for the cross-sectional area could be used. Otherwise, a simple section, such as a square or circle can be used and large section modification factors could be applied. The latter of these is shown in Figure 4-32. A 12-inch × 12-inch section is defined and called 'RIGID', then the property modification box is opened and a large value is entered for the cross-section area modifier. All of the rigid elements in the model are pinned, so it is only necessary to make certain that the model is axially rigid.
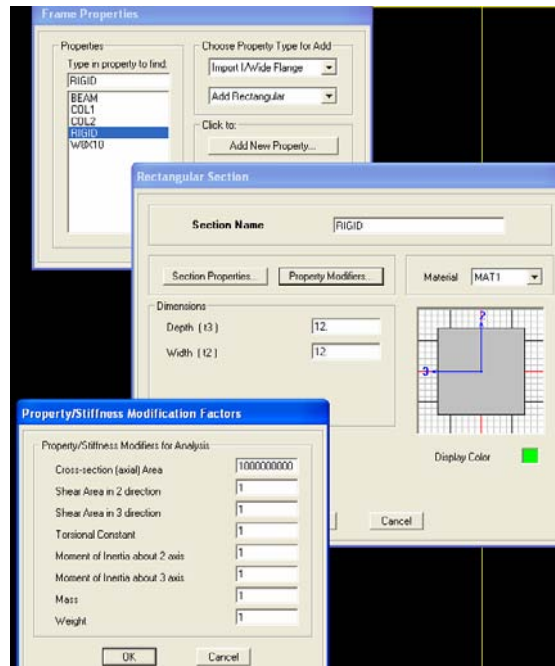
Figure 4.32: Rigid Member Section Properties

The truss members can also be defined as a general section, or by choosing a specific geometry. At this stage in building the model, the cross-sectional area of this element is not known. As an initial guess, a 12-inch × 12-inch section has been defined for the truss members. The truss section dimensions will be changed as needed to match the elastic response of the shell wall model. Once the truss and rigid sections have been defined, the truss-grid can be drawn for the model. The next step outlines this procedure.

Step 4: Draw Bridge Pier Elements

The truss-grid model is built by modifying the existing shell wall model. To start the process, the shell elements making up the shear wall are deleted. With only the pier frame composed of the beam and column elements remaining, a grid of vertical and horizontal rigid members are drawn. Each of the individual elements or panels in the grid should be approximately square. This step is important and will greatly improve the inelastic analysis results. Beyond this requirement, there are no firm rules for establishing the size of the grid. It will be easier to build the model, and the analyses performed will run quicker with fewer elements used to make up the grid. However, the grid needs to be sufficiently subdivided to properly capture the inelastic behavior of the system. It may be necessary to run several analyses to be sure that the selected grid is adequate and the SAP 2000 results are converging toward a unique solution. For the SH 87 Bridge, a 4 × 6 grid for each of the two wall segments was found to be suitable. The grid is added by drawing a rigid element across the top of the wall, and dividing it by the number of grid lines in that direction. Next, the columns are divided by the number of gridlines in the horizontal direction. Finally, the vertical and horizontal rigid elements are drawn. Pictures of the pier model, before and after the addition of the rigid elements, are shown in Figure 4-33.

58
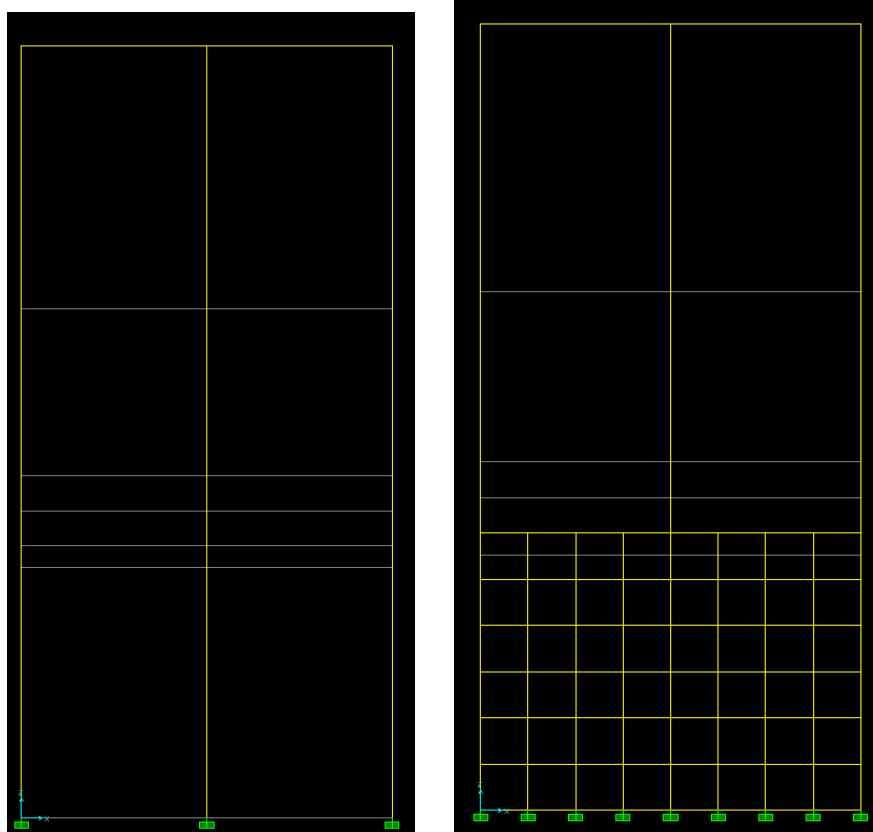
Figure 4.33: SH87 Before and After Rigid Grid Elements

Next, all of the vertical and horizontal members of the grid are divided into smaller elements at the points of intersection. Dividing elements is done under the 'Edit' menu in SAP 2000. At this stage, the rigid elements need to be classified as being pin connected to each other and to the columns, thus making the grid a truss-grid as opposed to a frame-grid. Truss elements are defined in SAP 2000 by releasing the moments at the member ends as discussed earlier.

Once the horizontal and vertical grid has been established, the diagonal truss members are drawn. Again, these members are pinned at the ends. Figure 4-34 shows the finished bridge pier geometry for the truss-grid model with the moments released on all of the interior members, as well as a 3D version of the model with shaded sections to give a better pictorial representation of the pier being modeled.
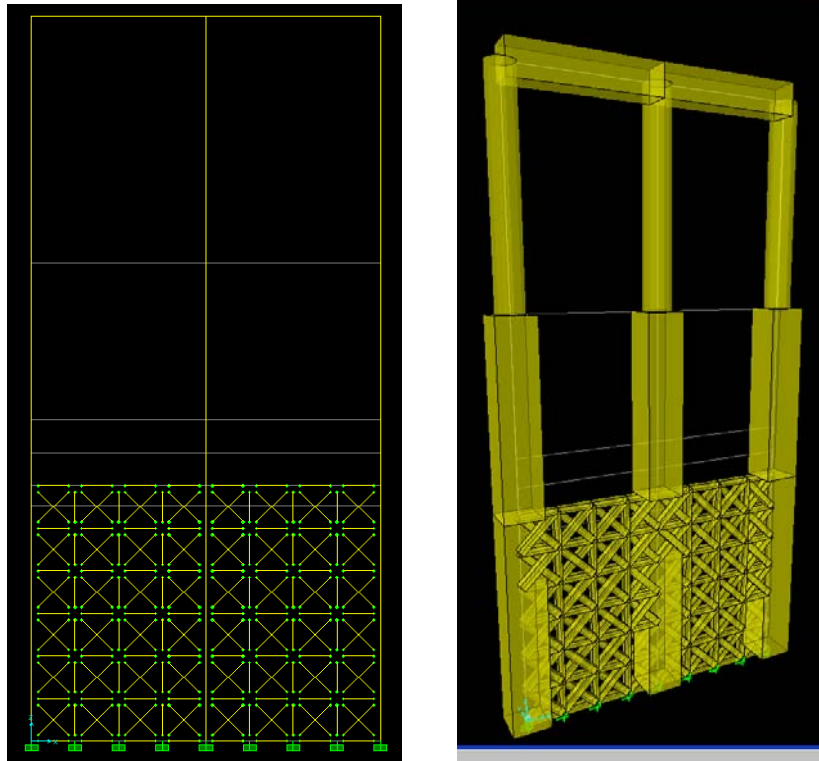
Figure 4.34: SH87 Bridge Pier with Truss-Grid Wall

Step 5: Modeling Bridge Superstructure and Adjacent Piers

The same procedure described previously in the shell wall modeling section is used to model the adjacent piers and superstructure for the truss-grid model.

Step 6: Apply Loads

The same lateral load cases described previously are applied to the truss-grid model.

Step 7: Size Truss Members

Two methods to size the diagonal truss members are presented in this section. The first is a more rational approach to sizing the truss members, using simple structural analysis tools. The second utilizes an iterative approach. Both methods are based on matching the stiffness of the truss-grid wall model with the initial linear elastic stiffness of the shell wall. The size of the truss members needs to be adjusted for each combination of load location and boundary conditions that one wishes to consider. For the SH-87 Bridge model, four load configurations and three top boundary conditions are being considered, so truss element sizes need to be determined for twelve cases.

Method I

The approach with this method is to determine the lateral stiffness contribution that the truss elements need to make in order to match the elastic response of the shell wall model. To start, linear elastic analysis results from the shell wall model are needed. As opposed to applying an arbitrary load, a linear elastic static 'pushover' analysis should be run, with a defined displacement limit at the load location. In this type of analysis, instead of applying a given load, SAP 2000 will increment the load up until a displacement limit is reached at a specified location.

A more detailed description of a static pushover analysis is provided in Chapter 5. The SAP 2000 load output is used along with the specified displacement at the point of the load, to calculate the stiffness of the system, k = Load/Displacement.

Once the stiffness of the shell wall model is known, the stiffness of the truss-grid model needs to be determined. The stiffness of the truss-grid model depends upon the stiffness of the diagonal truss members, and the beam, column and rigid members. The size of the beams, columns, and rigid members are known before the analysis begins; therefore, the stiffness of this system is known. To calculate the contribution of the beams, columns and rigid members to the overall stiffness of the system, all of the truss members are removed from the model, leaving only the columns, beams, and horizontal and vertical rigid elements. A linear elastic analysis is run for this model. Using the applied load and corresponding displacement, the stiffness of the frame and rigid elements can be determined. The difference in the stiffness of the two systems represents the required stiffness of the truss members in order for the two models to be equivalent. The required truss element stiffness is illustrated in Figure 4-35. The plot is for a typical bridge pier that is pushed so that there is a 1-inch displacement at the load location.
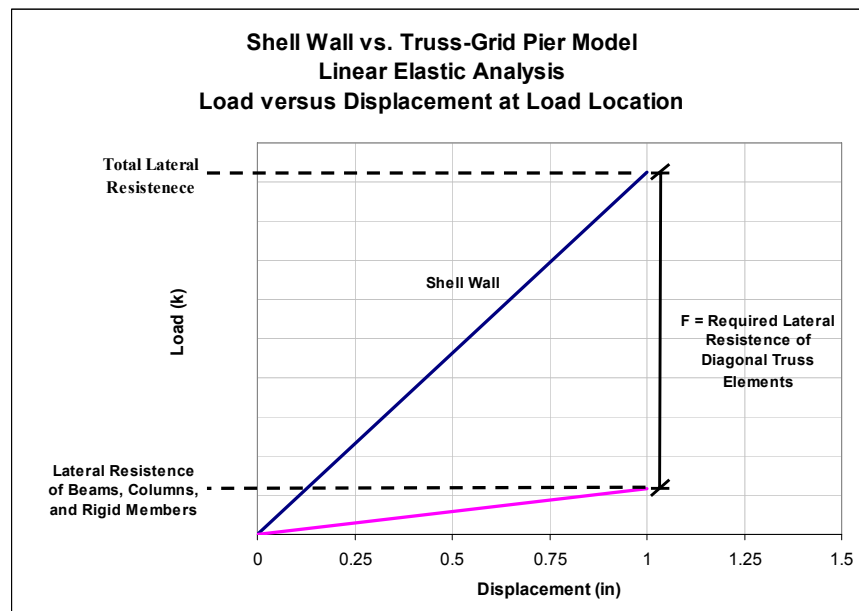
Figure 4.35: Required Stiffness of Truss Members

Once the information in Figure 4-35 is known, the required stiffness for the truss members can be calculated using known relationships between force, stiffness, and displacement. For the most basic case of replacing a shell wall with a single rigid element and a single truss element, these calculations result in Equation 4-5. This equation can be used to solve for the required truss member area. Figure 4-36 illustrates the variables needed from a model to apply Equation 4-5.

$$A = \frac{F * L}{E * \Delta}$$
(4-5)

where
F = Total Lateral Force Truss Elements Need to Resist (see Figure 4-30)
L = Length of Wall Diagonal
E = Modulus of Elasticity of Wall Material
Δ = Displacement along Wall Diagonal
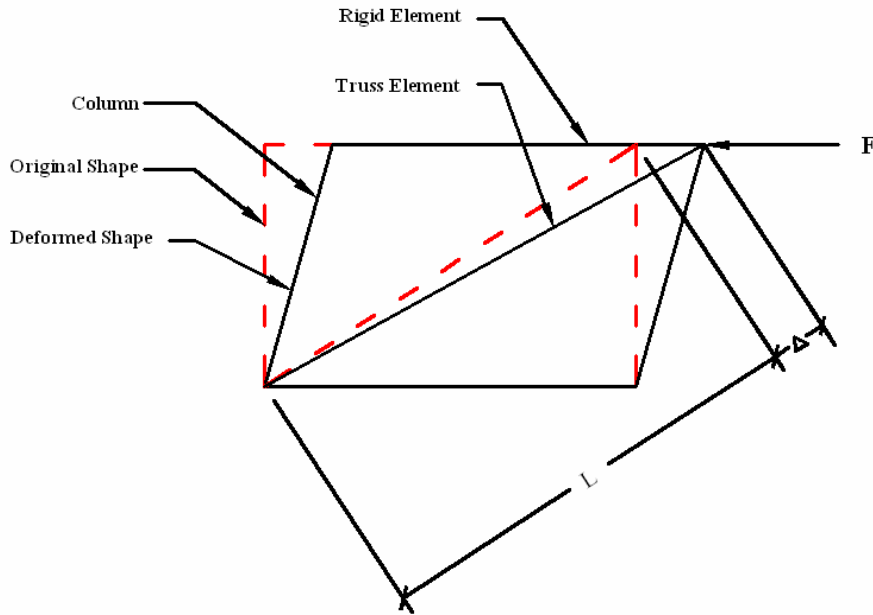
Figure 4.36: Determining Truss Size

Method I is useful in that it provides a procedure for sizing truss members that is based on basic structural analysis concepts. However, applying this method becomes more difficult when sizing truss elements that are part of a large grid, as is required for the SH-87 Bridge that is being modeled in this chapter. As the complexity of the wall and pier geometry increases, so does the difficulty of correctly sizing the truss elements. To work around this problem, a second method for sizing truss elements is presented.

Method II
Method II is essentially a guess and check approach to determining the proper size for the truss elements to match the linear elastic response of the truss-grid model to the linear elastic response of the shell wall model. This method is suggested because of its ease of use within SAP 2000. The diagonal truss members will be given an arbitrary size and an initial linear elastic analysis will be conducted for each load and boundary condition configuration. The truss member sizes will be adjusted for each load case until the linear elastic response is matched. Using this approach will result in the same size truss elements as would be found using Method I. Method II was used to size the truss elements for the SH-87 Bridge Models.

Table 4-7 summarizes the first run of linear elastic analyses on the truss-grid model. Note that the truss elements are 12-inches × 12-inches for all of the analysis cases. The size of the

truss elements will be adjusted based on the results shown below, to match the analysis results presented earlier. The next step outlines this procedure.

Table 4.7: Initial Linear Elastic Analysis Results

Load Description	Top Boundary Condition	Total Load Applied	Truss Dimensions	Lateral Displacement at Point of Load
Point Load at Top of Wall	free	1000 k	12" x 12"	0.196"
Point Load at Top of Wall	fixed	1000 k	12" x 12"	0.175"
Point Load at Top of Wall	superstructure	1000 k	12" x 12"	0.184"
Point Load 48" above Top of Wall	free	1000 k	12" x 12"	0.316"
Point Load 48" above Top of Wall	fixed	1000 k	12" x 12"	0.258"
Point Load 48" above Top of Wall	superstructure	1000 k	12" x 12"	0.285"
Point Load 96" above Top of Wall	free	1000 k	12" x 12"	0.551"
Point Load 96" above Top of Wall	fixed	1000 k	12" x 12"	0.409"
Point Load 96" above Top of Wall	superstructure	1000 k	12" x 12"	0.477"
Distributed Load 30" above and below wall	free	1000 k	12" x 12"	0.196"
Distributed Load 30" above and below wall	fixed	1000 k	12" x 12"	0.175"
Distributed Load 30" above and below wall	superstructure	1000 k	12" x 12"	0.183"

Once the initial analysis results have been tabulated, the dimensions of the diagonal truss elements can be adjusted to match the previously determined linear elastic analysis results. If the results from the initial truss-grid model, with 12-inch × 12-inch truss elements, result in a smaller displacement, the truss element dimensions should be decreased. If a larger displacement is seen, the member size needs to be increased. Table 4-8 summarizes the results from this process.

Table 4.8: Adjusted Linear Elastic Analysis Results

Load Description	Top Boundary Condition	Total Load Applied	Truss Dimensions	Lateral Displacement at Point of Load	Shell Wall Model Lateral Displacement at Point of Load
Point Load at Top of Wall	free	1000 k	17.1" x 17.1"	0.108"	0.108"
Point Load at Top of Wall	fixed	1000 k	17.1" x 17.1"	0.103"	0.103"
Point Load at Top of Wall	superstructure	1000 k	17.0" x 17.0"	0.106"	0.106"
Point Load 48" above Top of Wall	free	1000 k	14.9" x 14.9"	0.235"	0.235"
Point Load 48" above Top of Wall	fixed	1000 k	14.2" x 14.2"	0.210"	0.210"
Point Load 48" above Top of Wall	superstructure	1000 k	14.5" x 14.5"	0.224"	0.224"
Point Load 96" above Top of Wall	free	1000 k	13.8" x 13.8"	0.472"	0.472"
Point Load 96" above Top of Wall	fixed	1000 k	12.1" x 12.1"	0.394"	0.394"
Point Load 96" above Top of Wall	superstructure	1000 k	13.2" x 13.2"	0.436"	0.436"
Distributed Load 30" above and below wall	free	1000 k	17.2" x 17.2"	0.107"	0.107"
Distributed Load 30" above and below wall	fixed	1000 k	17.1" x 17.1"	0.101"	0.101"
Distributed Load 30" above and below wall	superstructure	1000 k	17.1" x 17.1"	0.104"	0.104"

Step 10: Define Plastic Hinge Properties

The process within SAP 2000 to define hinge properties is the same as previously described. The truss-grid model, however, requires the use of two types of hinges. In addition to the moment-axial interaction hinges used for models without shear walls, the truss-grid model requires axial hinges. The axial hinges are placed at the ends of the diagonal truss members, and are used to capture the inelastic deformation in the wall. Moment-axial interaction hinges are used as they were before, on the beam and column members in the pier.

While the basics of defining and using plastic hinges for models with shear walls remains the same, a slightly different definition for the plastic hinge properties is used. Again, in SAP 2000, hinges are defined based on strength and deformation capacity. In Section 4.6.1, when modeling of the IH-10 Bridge (a bridge without shear walls) was discussed, the strength characteristics of the moment-axial hinges were based on the yield and plastic moment, M_y and M_p, determined by a section analysis. It is suggested that both the moment-axial hinges and axial hinges for a truss-grid model be based solely on yield moment. The hinge profile is then elastic, perfectly plastic, as opposed to the previously defined hinge, which had an area of transition from the yield to ultimate capacity. Figure 4-37 shows the two hinge definitions on the same plot, with the previous definition drawn as a dashed line.
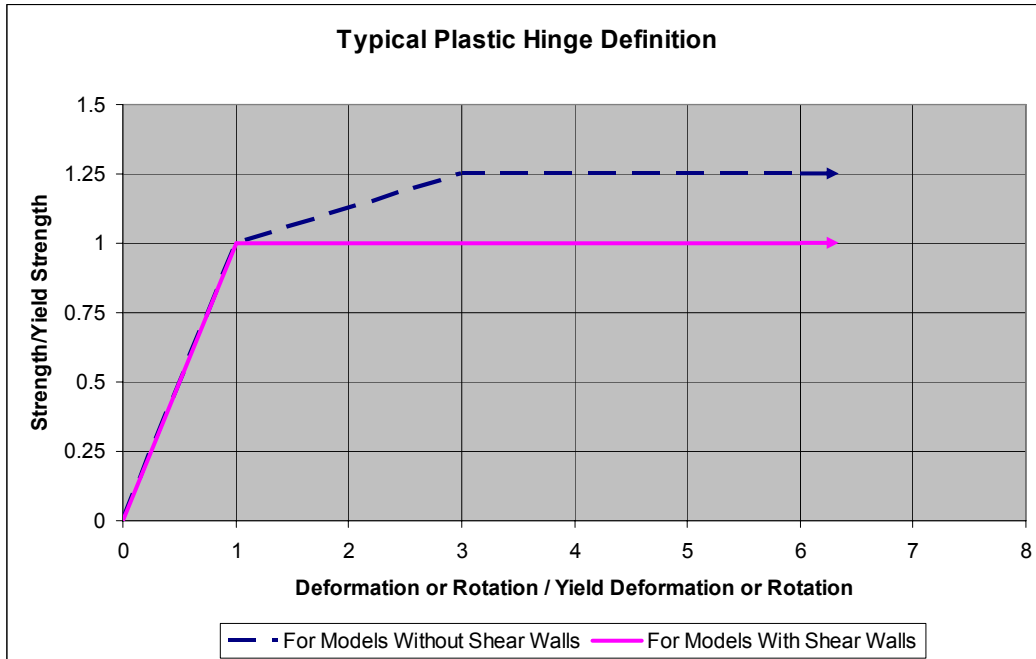
Figure 4.37: Plastic Hinge Definition Comparison

By using rigid elements in the truss-grid wall model, the forces that are transferred into the wall are distributed in a relatively even fashion throughout the diagonals in the grid. In reality, much of the inelastic behavior due to a large vessel impact force would be concentrated in a smaller local area near the point of impact. Because of the rigid members, the truss-grid model does not capture this behavior very well, and the truss-grid model is an inherently stiffer model when inelastic behavior is considered. Initial analysis results from SAP 2000 of the truss-grid pier model showed a 20-30% greater ultimate strength when compared to a finite element model analysis of the same pier with shell elements capable of plastic behavior. Coincidently, the ratio of M_p/M_y for most of the reinforced concrete sections used in the bridge piers that were examined was between 1.2 and 1.3. While the inelastic response of the truss-grid pier models result in higher (unconservative) ultimate strength results due to the modeling method, adjusting the material model provides a simple way to compensate for the error.

Step 11: Assign Plastic Hinges to Pier Elements
Plastic hinges should be assigned in the same manner as discussed in Section 4.6.1. Axial Hinges should be assigned at each end of all of the diagonal truss members. Moment-axial interaction hinges should be assigned at the ends of column and beam members, as well as at key locations along the length, such as at a load location or change in section.

4.7 Modeling Reduced Section Capacity in Area of Vessel Impact

It is likely that during a vessel collision event the area of the bridge being struck will be subject to some local crushing and spalling of the concrete due to the dynamic nature of the impact. At a minimum, it is expected that the cover concrete will be lost, and the possibility exists that some of the confined concrete could crush as well. It has been found that merely losing the cover concrete does note have a significant effect on the capacity of the section or the strength of the bridge as a whole. However, if any of the confined concrete core is lost, or if the

65

longitudinal reinforcing bars are lost, the section capacity and bridge strength could be affected significantly. This section outlines a procedure to account for reduced section capacity within the context of the modeling approach outlined earlier. Further investigation on local behavior in the impact zone is needed in order to better estimate what kind of section loss should be considered in bridge ultimate lateral strength calculations.

For the purposes of the models and analyses contained in this report, two reduced sections are considered, a 10% loss and a 20% loss of cross-sectional area. These values are somewhat arbitrary, but are believed to be reasonable. They are being used primarily to illustrate the effect reduced sections have on overall strength if loss of section is considered. Chapter 5 examines the analysis results for models with and without reduced sections in the impact zone, and assesses the effect of a reduced section on the ultimate lateral strength. It is assumed that the concrete will be lost as shown in Figure 4-38. Examples are shown for an arbitrary loss of cross-sectional area for both circular and square column sections. The straight-line assumption shown is made for ease of analysis, although, concrete is not likely to crush and spall in such a fashion.
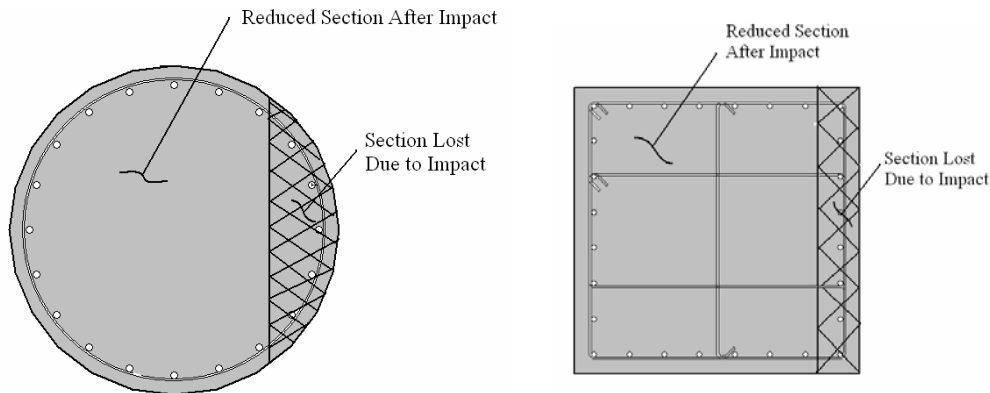
Figure 4.38: Reduced Section Shapes

To account for the reduced cross-section areas in the regions of impact, only slight modifications need to be made to the analysis steps outlined earlier. Rather than trying to determine a reduced section shape in SAP 2000, the approach taken is to use a modified material model for elements near the impact area. The modified material properties are developed using Response-2000. Using Response-2000, the geometry of the section is modified to reflect the reduced cross section. This process involves removing any concrete and steel that falls within the lost area. New values of M_y and M_p are taken from the section analysis output. Figure 4-39 shows screen captures from Response-2000 that illustrate this procedure. Based on these values and the original section properties, f_y and f_u are determined in the same manner as previously described. Table 4-9 shows the original and the reduced section properties for the top column section of the IH-10 Bridge.
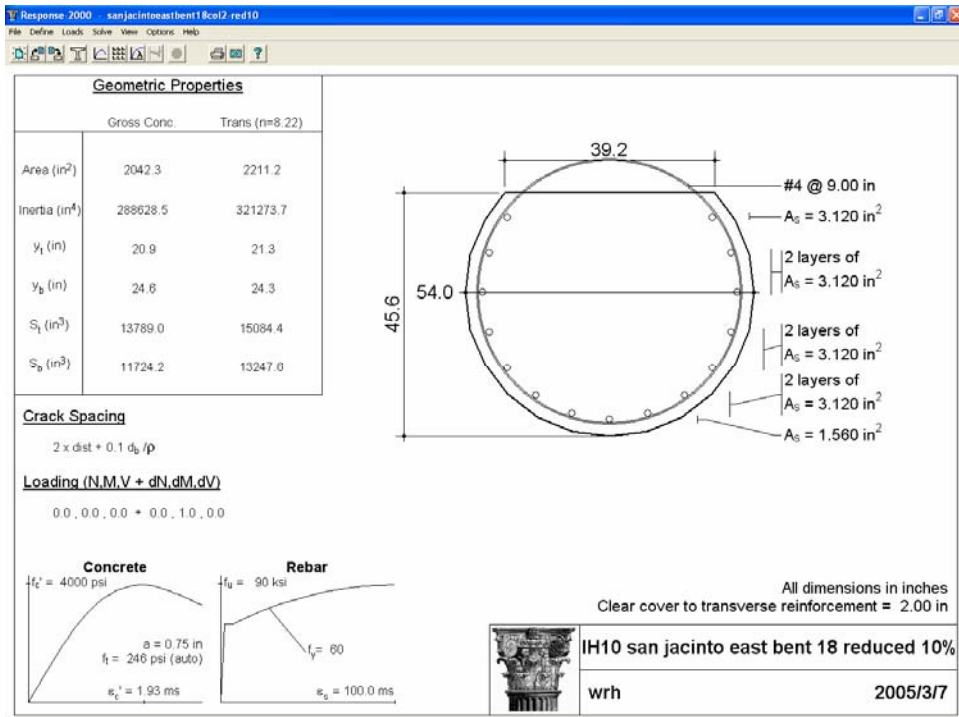
Figure 4.39: Reduced Section Input Response-2000
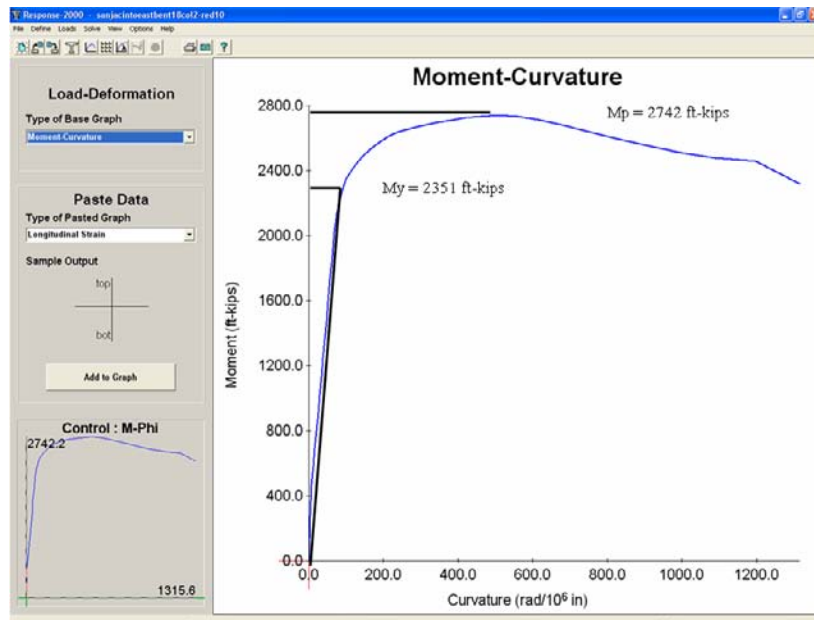
Figure 4.40: Reduced Section Analysis Results in Response-2000

Table 4.9: Full and Reduced Section Material Properties

IH10 San Jacinto Eastbound Pier 18 Top Column - Full Section Properties			
Basic Section Properties			
diameter (in)	54.00		
Plastic Modulus (in^3)	26244.00	Section Modulus (in^3)	15458.99
bars	20-#11	stirrups	#4-9" pitch
Response 2000 Section Analysis			
My (in-kips)	34572.00	fy (ksi)	1.32
Mp (in-kips)	42576.00	fu (ksi)	1.62
		fu/fy	1.23

IH10 San Jacinto Eastbound Pier 18 Top Column - 10% Section Reduction				IH10 San Jacinto Eastbound Pier 18 Top Column - 20% Reduced Section			
Basic Section Properties				**Basic Section Properties**			
diameter (in)	54.00			diameter (in)	54.00		
Plastic Modulus (in^3)	26244.00	Section Modulus (in^3)	15458.99	Plastic Modulus (in^3)	26244.00	Section Modulus (in^3)	15458.99
bars	20-#11	stirrups	#4-9" pitch	bars	15-#11	stirrups	#4-9" pitch
Response 2000 Section Analysis				**Response 2000 Section Analysis**			
My (in-kips)	28212.00	fy (ksi)	1.07	My (in-kips)	22950.00	fy (ksi)	0.87
Mp (in-kips)	32906.40	fu (ksi)	1.25	Mp (in-kips)	26493.60	fu (ksi)	1.01
		fu/fy	1.17			fu/fy	1.15

After the reduced section material properties have been computed, new section properties, material models and hinge properties are defined in SAP 2000. Table 4-9 shows that the section geometry is not changing, but an identical section is defined with the new material model that reflects the reduced section properties. Figure 4-40 shows the new material model definition in SAP 2000 and Figure 4-41 shows the new section definition.
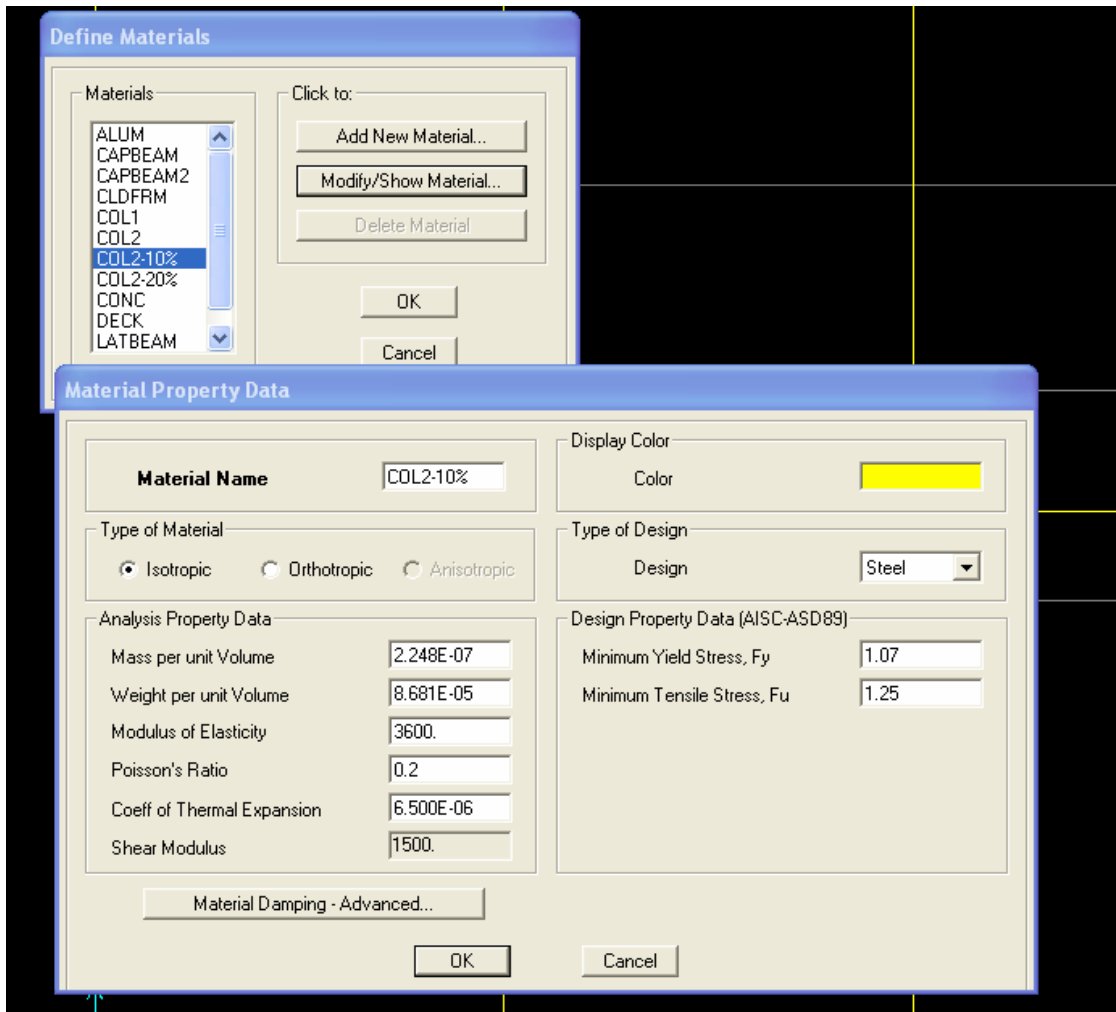
Figure 4.41: Defining Reduced Section Material Properties in SAP 2000
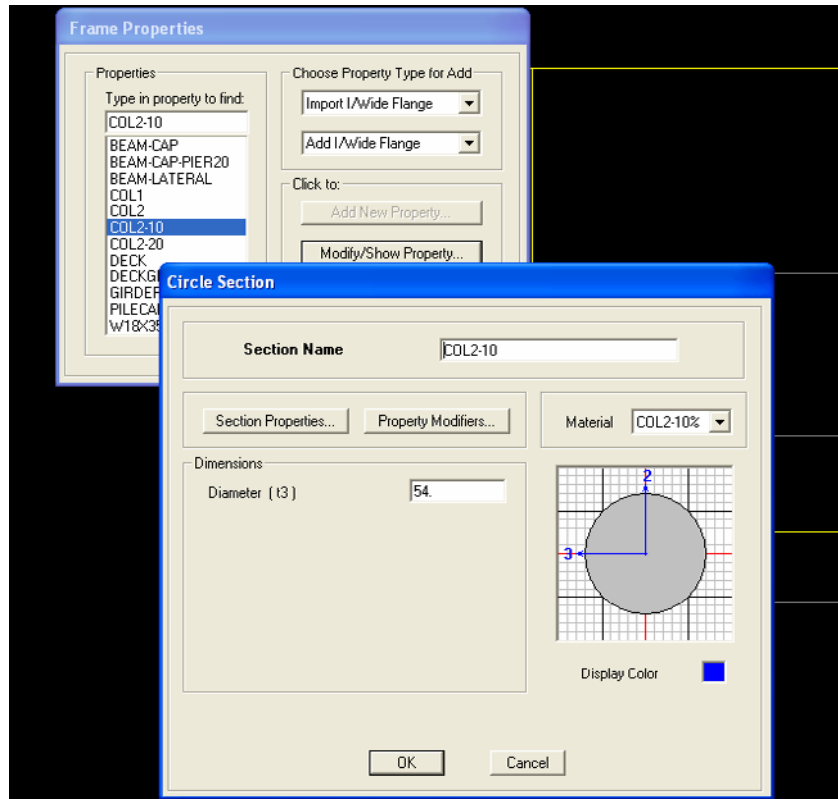
Figure 4.42: Reduced Section Definition in SAP 2000

Next, the new material and hinge properties are assigned to the elements adjacent to the area where the impact load is being applied. The location of impact loads are discussed in greater detail in Chapter 5. It is assumed that impact will result in a lost section over a depth that is equal to the length of the vessel bow. The elements within this region are assigned the reduced section properties. After section properties have been assigned, reduced section hinge properties need to be added as well. The last two steps can be seen in Figure 4-42.
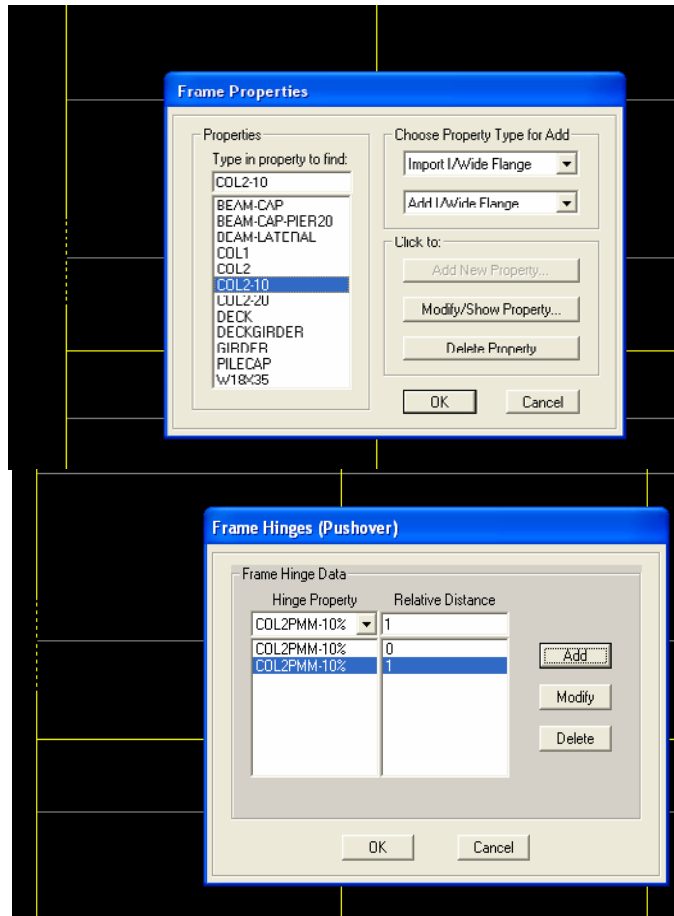
Figure 4.43: Assigning Reduced Sections and Hinges to Elements in SAP 2000

If a column or other structural member loses material due to impact, it is expected that there will be a gradual transition from the area with the most severe damage to an area where the full section is still intact. Therefore, when considering the effect of a larger loss of section, it may be necessary to phase this effect in over several elements. For example, if it is estimated that 20% of the section will be lost due to impact, the appropriate material, section and hinge properties for a 20% section reduction are applied to the elements that are immediately adjacent to the impact point. The next two elements on either side are given properties associated with a smaller reduction in section, for example, 10%. The two elements beyond this location are assumed to have the full section present. This approach can easily be implemented in SAP 2000 by dividing the member of the pier being struck into several elements. Figure 4-43 illustrates the idea of gradually changing the properties of elements around the point of impact.
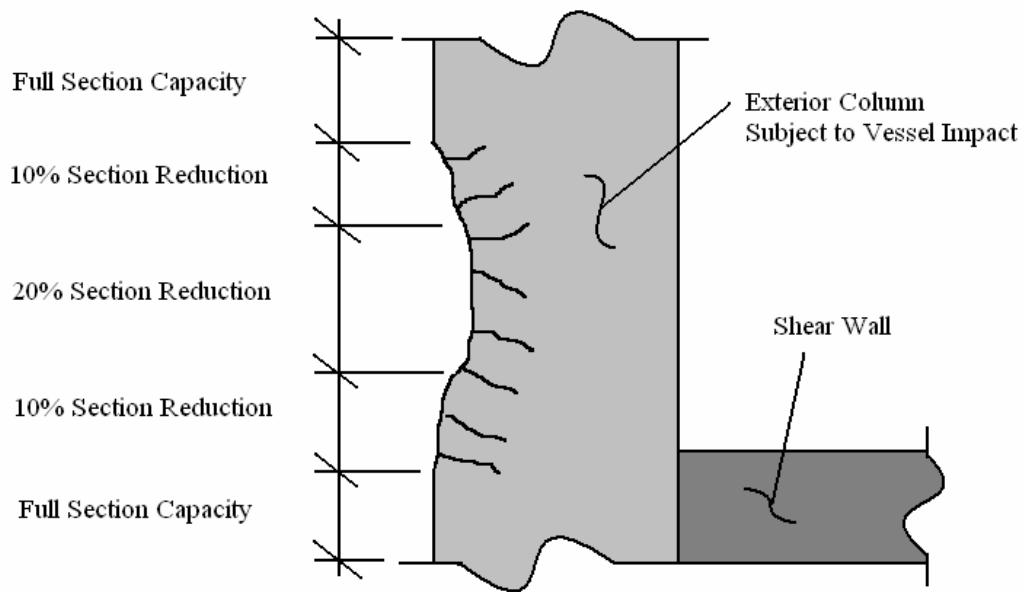
Figure 4.44: Gradual Change in Properties for Reduced Section

4.8 Limitations

In using the approximate methods for bridge modeling presented in this chapter, it is important to understand the limitations that these models have. By recognizing when these models will provide an accurate assessment of bridge lateral ultimate strength, and more importantly, situations where the models' response fails to capture the actual behavior of the system being analyzed, they can be used effectively. The following list describes some of the important assumptions and limitations of the models outlined in this chapter:

- *Assumed fixed base condition.* This assumption ignores the behavior of the bridge pier foundation and the soil-structure interaction and results in a model that has a greater stiffness then the actual structure.

- *Truss-grid model forces inelastic behavior to be evenly distributed through the wall.* It does not capture local response of the wall in the area of an impact as well as a non-linear finite element analysis would. This issue is dealt with indirectly by changing the hinge definition as shown in Step 10 of Section 4.6.2.

- *Hinges are defined as being nearly infinitely plastic.* A plastic hinge region in a real structure will have a rotational or deflection limit. This issue will be addressed in the post-analysis phase.

- *Use of smeared material properties.* While the guidelines presented are for reinforced concrete bridge piers, the material is not being modeled directly. The smeared material model approach, based on a section analysis and the conservative assumption of zero axial load, should provide a reasonable representation of a real reinforced concrete pier, but this assumption does represent a possible source of error.

In many cases, the limitations in these models can be overcome by making some slight modifications or making additional assessments in the post-analysis phase. Additional investigation could also serve to eliminate the some of the potential issues presented in the list above. For example, soil-structure interaction could be captured in SAP 2000 by using frame elements to represent the foundation and springs to represent the surrounding soil. However, such an investigation is beyond the scope of this document.

4.9 Summary

This chapter has outlined general modeling techniques that can be used in accordance with simple structural analysis programs to calculate the ultimate lateral strength of bridge piers, both with and without shear walls, subject to vessel impact loads. The guidelines presented allow for strength calculations based on both the individual pier and the entire bridge system. In addition to the general modeling guidelines, step-by-step procedures for two representative bridges from the state of Texas were presented. Chapter 5 outlines the necessary loads and analysis cases for these models and presents the ultimate strength analysis results, along with finite element verification models.

5. Analysis of Bridge Ultimate Strength Models

5.1 Introduction

The bridge models constructed in Chapter 4 are intended to be analyzed using a nonlinear static analysis in SAP 2000. This chapter outlines the analyses needed to determine the ultimate lateral strength of the SH-87 and IH-10 bridge models. A discussion of how to assess the analysis results follows, with an emphasis on determining which parameters control the limit state of the bridge models. The focus is on strength and ductility limit states with some additional discussion of structural stability. Finally, the analysis results for the IH-10 Bridge and the SH-87 Bridge are presented. The primary goals of the analyses are to evaluate the validity of the truss-grid model, and to determine the effect of considering system-wide response in analyzing a bridge for ultimate lateral strength. Additional results consider the effects of a reduced section in the area of impact as well as the loss of an exterior column in a multi-column bridge pier.

All of the goals outlined above fall within one of the primary objectives of this document, which is to provide bridge engineers with the necessary tools to accurately assess the ultimate lateral strength of a bridge pier, both as an individual element or as part of a larger bridge system, for use within the existing AASTHO Vessel Collision Design Specification. Currently, AASHTO does not provide any guidance in calculating the capacity of a bridge element and this report seeks to address that limitation. In addition, by improving confidence in the calculation of bridge ultimate lateral strength, the opportunity exists to examine critically the probability of collapse term in the current AASHTO Method II vessel collision annual frequency of collapse equation.

5.2 Applied Loads

The structural analyses for the models built in Chapter 4 need to be carried out in multiple steps. The initial analysis considers the effects of loads that are already on the structure prior to vessel collision. The existing, or in-place loads, come primarily from the self-weight of the bridge itself. Once the effects of these loads are known, a lateral load representing vessel impact is applied as a static load case. Both point load and distributed load configurations are considered. The distributed load is applied over a length that is intended to represent the contact area dimensions of a vessel striking a bridge element.

5.2.1 Existing Loads on the Structure

As discussed previously, AASHTO currently defines bridge ultimate lateral strength as the strength of an individual element, either a pier or span. In analyzing a single element, little consideration is likely to be given to the existing loads on the structure and AASHTO makes no mention of these loads. In analyzing the bridge system as whole, it makes sense to consider the in-place loads. At a minimum, the self-weight of the bridge superstructure is present during a vessel collision event, and it should be accounted for when determining the ultimate lateral strength of a bridge system. For the IH-10 and SH-87 Bridge models built in Chapter 4, the self-weight of the bridge deck and girders were determined from construction drawings. An additional 20% of this load was added to account for any other superimposed loads on the structure that could not be estimated from the bridge plans. This estimate of the additional load is believed to be conservative. A lower value could be used if a more detailed investigation were

conducted. Table 5-1 summarizes the existing loads on piers 18 & 19 of the IH-10 Bridge and piers 21 & 22 of the SH-87 Bridge.

Table 5.1: Existing Loads on Bridge Models

IH-10 Piers 18 & 19		SH-87 Piers 21 & 22	
Cap Beam Geometry		*Cap Beam Geometry*	
Width (in)	48	Width (in)	51
Depth (in)	84	Depth (in)	54
Length (in)	654	Length (in)	504
Volume (in^3)	2,636,928	Volume (in^3)	1,388,016
Existing Pier Loads		*Existing Pier Loads*	
Cap Beam Self Weight (kips)	229	Cap Beam Self Weight (kips)	120
Superstructure Self Weight (kips)	1799	Superstructure Self Weight (kips)	2108
Superstructure Load to Each Pier (kips)	645	Superstructure Load to Each Pier (kips)	723
Additional Loads (kips)	129	Additional Loads (kips)	145
Total Load (kips)	1003	Total Load (kips)	988
Material Properties		*Material Properties*	
Old Unit Weight (k/in^3)	8.681E-05	Old Unit Weight (k/in^3)	8.681E-05
New Unit Weight (k/in^3)	3.803E-04	New Unit Weight (k/in^3)	7.116E-04

Using the in-place loads calculated in Table 5-1, the unit weight for the cap beam of the pier is changed so that the entire in-place load is accounted for in this member. As a result, the load is evenly distributed across the member, as it would likely be in the real structure. A slightly more accurate representation could be achieved by distributing the load through the superstructure elements by changing the unit weight for these members. The load would then be transferred to the bridge pier at the points where the general elements connect to the pier. However, this task is more difficult than assigning the load directly to the cap beam because of the general section type that is being used in SAP 2000 to model the superstructure. Table 5-1 shows both the old and new unit weight values for the cap beam.

5.2.2 Impact Loads

Impact loads are applied as static loads with a small arbitrary load value, usually 1 k or 1 k/ft, assigned initially. This load is increased during the static nonlinear analysis by SAP 2000 until a limit state is reached. When performing a vessel collision design using the Method II procedure, AASHTO specifies in Section 3.14.14 that vessel impact forces should be applied either as a point load at the mean high-water level or as a uniform distributed load with a length equal to the depth of the vessel bow at the point on the pier where impact is expected given the draft of the vessel (AASHTO, 2004). When using the analysis and modeling guidelines outlined in the current chapter of this report and in Chapter 4 for use in an actual AASHTO Method II analysis, these locations should be considered for vessel impact. However, for purposes of this chapter, several impact load distributions are considered. The lateral load cases were previously described and shown in Chapter 4 (Section 4.6.1 and Figure 4-31) for the SH-87 Bridge and are reviewed below. Also listed are the loads that will be considered for the IH-10 Bridge. Figures 5.1 and 5.2 show the load locations for each bridge.

For the IH-10 Bridge over the San Jacinto River:

- Load Location 1: Point load at the lateral beam

- Load Location 2: Point load at normal-water level

- Load Location 3: Point load at high-water level

- Load Location 4: 60-inch wide distributed load centered on the lateral beam
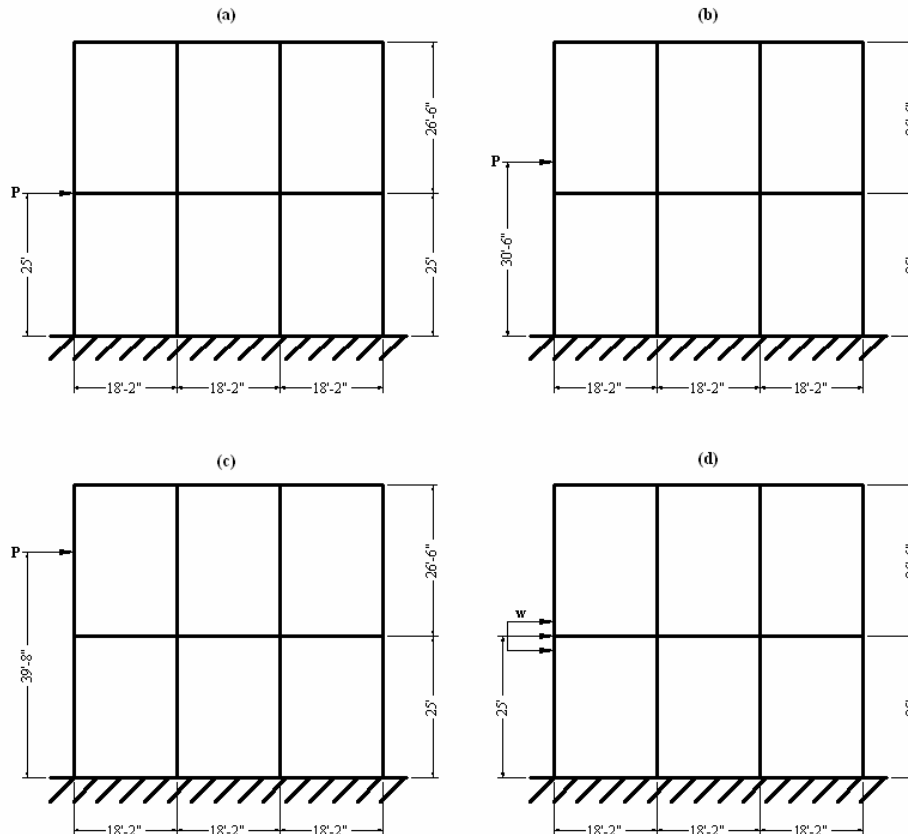
Figure 5.1: IH-10 Impact Load Locations:
(a) Load Location 1: Point Load at Beam, (b) Load Location 2: Point Load at Normal Water Level, (c) Load Location 3: Point Load at High Water Level, (d) Location 4: 60-inch Wide Distributed Load at Beam

For the SH-87 Bridge over the GIWW:

- Load Location 1: Point load at the top of the shear wall

- Load Location 2: Point load 48 inches above the top of the shear wall

- Load Location 3: Point load 96 inches above the top of the shear wall

- Load Location 4: 60-inch wide distributed load centered at the top of the shear wall
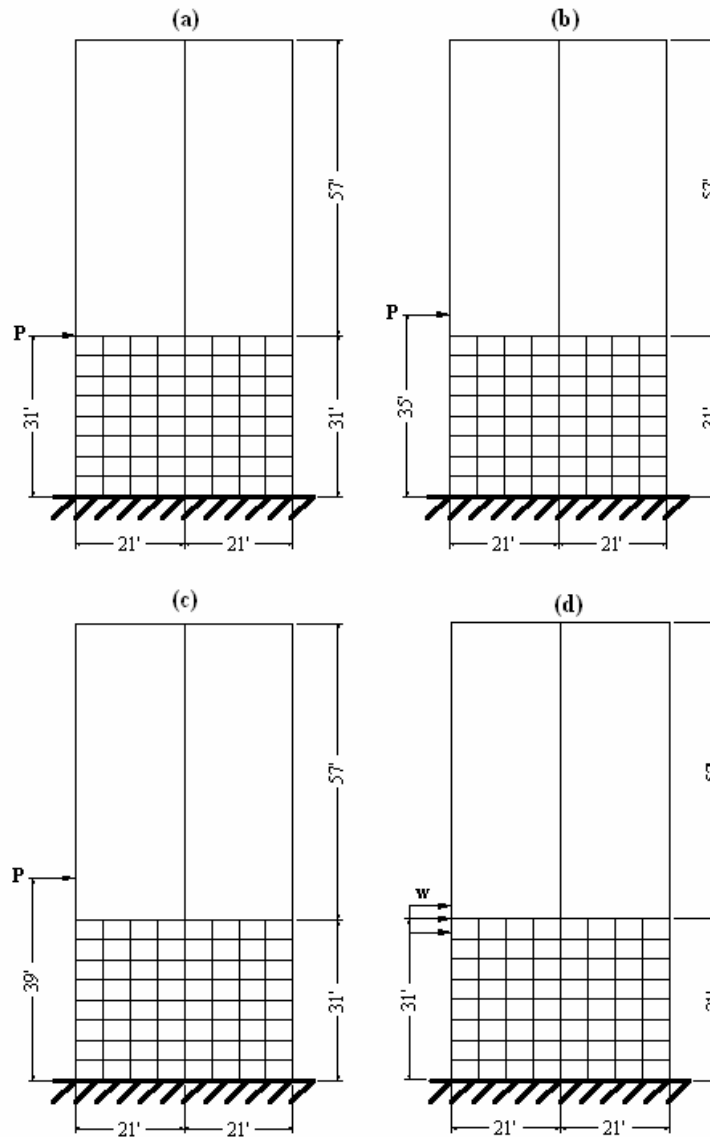
Figure 5.2: SH-87 Impact Load Locations:
(a) Load Location 1: Point Load at Top of Wall, (b) Load Location 2: Point Load 48 inches
Above Wall, (c) Load Location 3: Point Load 96 inches Above Wall, (d) Location 4: 60-inch
Wide Distributed Load at Wall

The cases that were chosen represent a reasonable range of possible water levels for those specific bridges. By considering load situations outside of those that are explicitly defined by AASHTO, a greater understanding of how to better design bridges can be gained. In addition, considering a range of load locations could yield information on when it is appropriate to use simplified models that do not require representing the entire bridge system for acceptably accurate results.

78

5.3 Analysis Cases

The primary analysis case for assessing the ultimate lateral strength of the bridges modeled in Chapter 4 is a nonlinear static pushover analysis. The basics of a pushover analysis are straightforward. The load on a structure is increased in user-defined increments, and the displacement at a specified point is calculated for each of the load increments. In general, the displacement is tracked at the point where the load is applied, although any point of interest could be used. The analysis stops when a specified load or displacement limit is reached.

There is a wide range of possible outputs from a SAP 2000 pushover analysis. Of greatest interest is a load-displacement curve, which plots the total lateral load versus the displacement at a user-defined point. The bridge models built in Chapter 4 are being 'pushed' into the inelastic range. Thus, the resulting load-displacement curves show an initial slope for the linear elastic range, and as different areas of the model reach their strength limit, plastic hinges form and the slope of the curve decreases. If a structure has sufficient ductility, the curves eventually plateau after a mechanism has formed. The load value at which the curve plateaus is defined as the ultimate lateral strength. A load versus displacement curve for a structure with a clearly defined ultimate strength plateau is shown in Figure 5.3. It is also possible that some sort of structural instability could occur before a mechanism has formed. Recall that the hinges in Chapter 4 were defined as being nearly infinitely plastic. In order to determine if a structure has adequate ductility to reach the strength plateau, additional assessments need to be made. It is necessary to consider strength, stability, and ductility when assessing the ultimate strength of a bridge pier or bridge system.
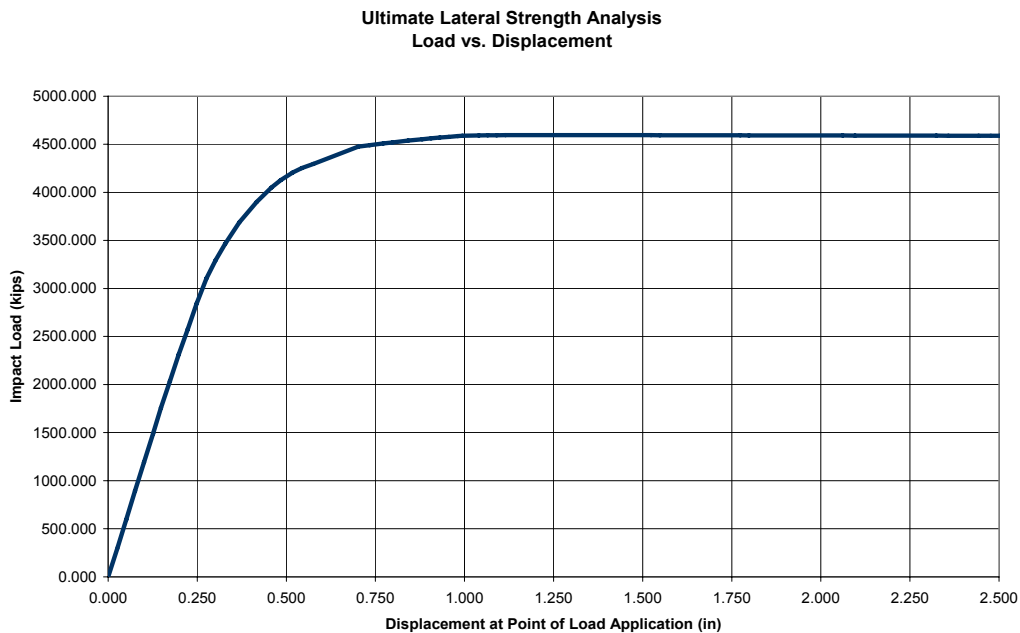
Figure 5.3: Determining Ultimate Strength from a Load versus Displacement Plot

Additional analysis cases take the initial pushover analysis a step further by assessing if a bridge can redistribute forces if a single column in a multi-column bent is destroyed. This analysis is carried out using some of the special features of a SAP 2000 static nonlinear analysis.

The procedure for setting up the various analysis cases for the models built in Chapter 4 are presented in the next section.

5.4 Ultimate Lateral Strength Analysis in SAP 2000

The following section outlines the necessary steps to set up a nonlinear static pushover analysis in SAP 2000. As an example, the analysis setup for the SH-87 Bridge modeled in Chapter 4 is shown. The steps shown outline the process for considering various load configurations and make use of most of the options available within the pushover analysis feature of SAP 2000. Note that terms that appear in **bold** type represent option headings that are shown on the SAP 2000 screens, and terms that appear as *italic* type represent user input or selections.

5.4.1 Define Load Cases

A two-step process is required to set up any structural analysis in SAP 2000. First, load cases need to be defined, and then the load cases need to be assigned to an analysis case. Any number or type of loads, in any direction, can be applied for each load case. It is possible to have all of the loads on a structure applied under one load case. When load cases are assigned to an analysis case, however, only a single scale factor can be applied for all the loads in the load case. Therefore, it is often easier to define multiple load cases based on the type (dead load, live load, wind load, etc.) of load that is applied. For the bridge models analyzed for the current study, two load cases are considered. They are shown in the **Define Loads** box in SAP 2000 shown in Figure 5.4. The first case considers loads that are likely to be present during vessel impact. This case is called *DEAD*, because it is primarily dead load from the superstructure. Note that the self-weight multiplier is set to *1* for this load, because all of the in-place loads have been captured by adjusting the material property for the cap beam of the pier. If the self-weight factor were zero, the in-place loads would be ignored. The second load case, called *IMPACT,* contains the static lateral load that represents vessel impact.
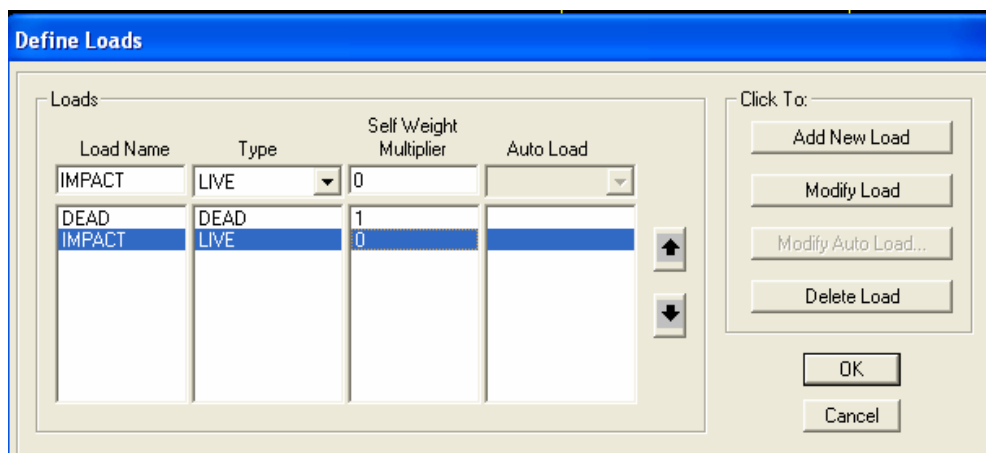
Figure 5.4: Defining Load Cases in SAP 2000

Once all of the load cases are defined, individual loads can be assigned to their appropriate case. For this problem, no loads are directly applied to the *DEAD* case, because the in-place loads are captured by the beam self weight. Loads need to be assigned to the *IMPACT*

case however. As an example, Figure 5.5 shows a 100-kip point load being applied to the top of the wall in the SH-87 Bridge model.
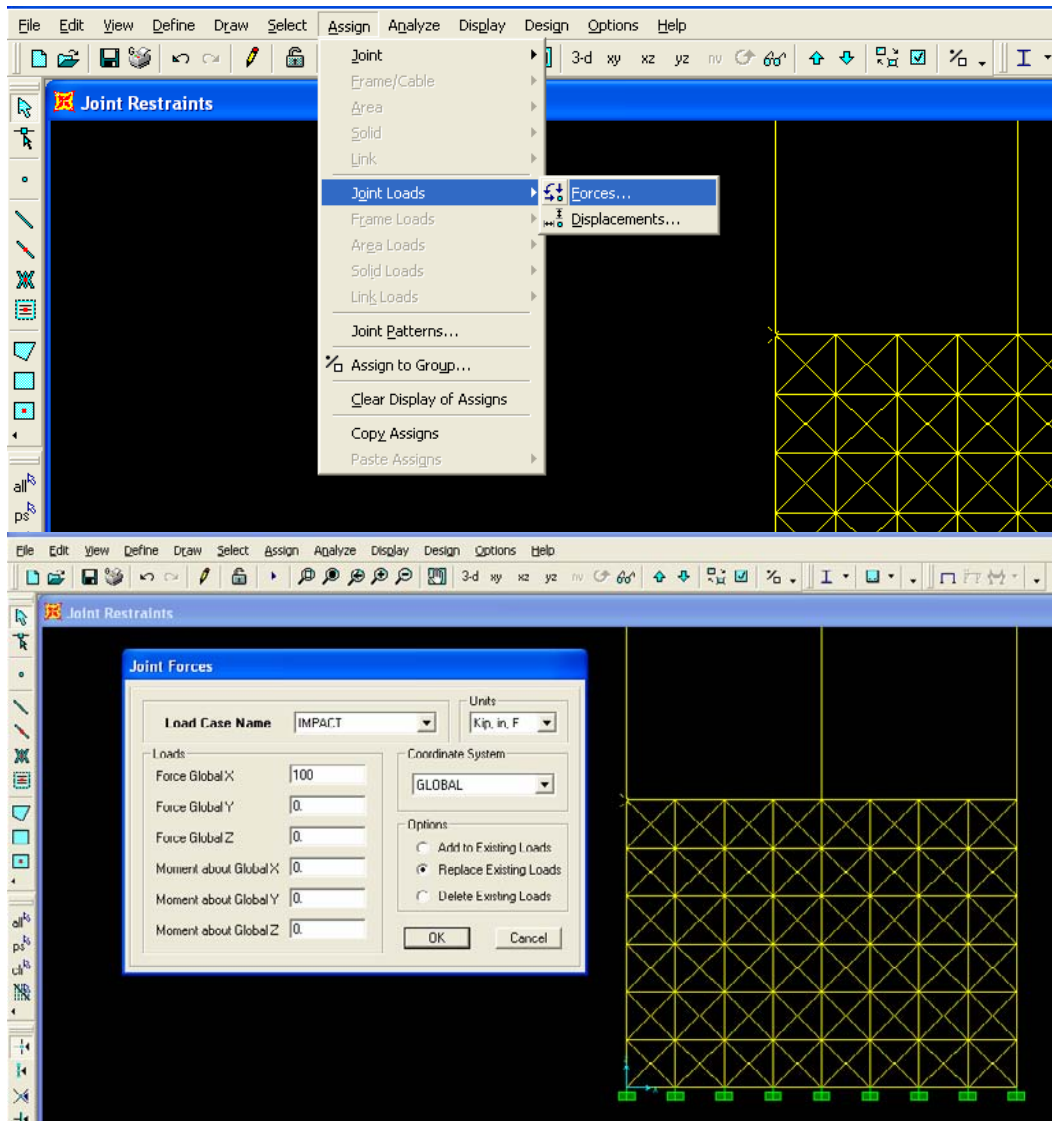
Figure 5.5: Assigning Loads to Load Cases in SAP 2000

5.4.2 Define Analysis Cases

After loads have been applied to a model in SAP 2000, analysis cases need to be defined. SAP 2000 is capable of a variety of analysis types, including dynamic analyses, as well as buckling and modal analyses. In keeping with the goal of providing a simple, user-friendly approach to determining the ultimate lateral strength of bridges, only static load cases are used with the bridge models built in Chapter 4. This approach also fits within the framework of the existing AASHTO design specifications, which uses a series of equations to express dynamic impact loads as equivalent static loads. Calculating the ultimate strength of a bridge element or system based on a static analysis provides a consistent basis on which to compare the strength of

the structure being analyzed to the impact load calculated in the AASTHO Method II design procedure.

If a more detailed investigation, outside the parameters of the AASHTO Method II procedure, were desired, a dynamic response factor could be applied to a static load solution for prediction of ultimate lateral strength under impact loads. Another approach to make a consistent comparison between applied impact loads and ultimate lateral strength of a bridge would be to take a dynamic load profile from an impact event and convert that loading to a static equivalent load. Detailed discussions of those options are beyond the scope of this report.

For the SH-87 and IH-10 Bridge Models, both static linear and static nonlinear analysis cases are needed to determine the ultimate lateral strength. Figure 5.6 shows the analysis cases for the SH-87 Bridge. Note the options to add, delete, or modify analysis cases on the right side of the pop-up window.
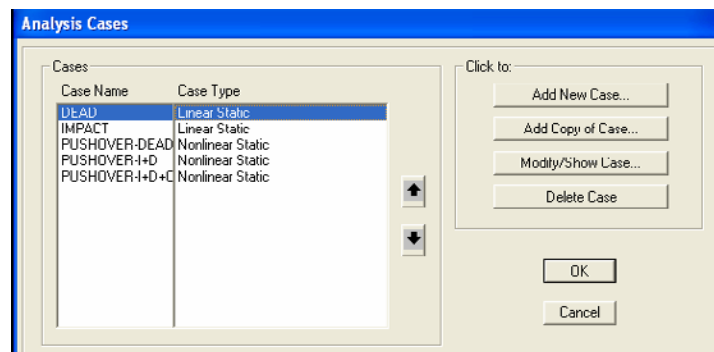
Figure 5.6: Defining Analysis Cases in SAP 2000

The analysis cases shown in Figure 5.6 are the actual cases that are used to determine the ultimate lateral strength of the SH-87 Bridge model from Chapter 4. A total of five cases are shown, two linear static cases, and three nonlinear static, or pushover cases. The linear static cases are automatically created by SAP 2000 for each of the load cases that were defined earlier. In addition, SAP 2000 requires a linear elastic analysis for each of the load cases that are included in a nonlinear static pushover, as is the case with the *DEAD* and *IMPACT* load cases. The next two sections outline the options that are available within each type of analysis case that is run.

Linear Static Analysis Options

A linear static analysis is the least complicated case to run in SAP 2000. Because of this fact, there are limited options a user can change. Figure 5.7 shows how to define a linear static analysis in SAP 2000. The options shown on the right side define the type of analysis being run. Under **Analysis Case Type**, *Static* is selected, and under **Analysis Type,** *Linear* is chosen. The left side of the box shows the options that can be modified based on the selections made for **Analysis Case Type** and **Analysis Type**. For a linear static analysis, only the **Loads Applied** options can be modified by changing which loads are applied and the corresponding scale factor for each load. All of the loads applied to Chapter 4 bridge models are selected to have a scale factor of *1*.

82
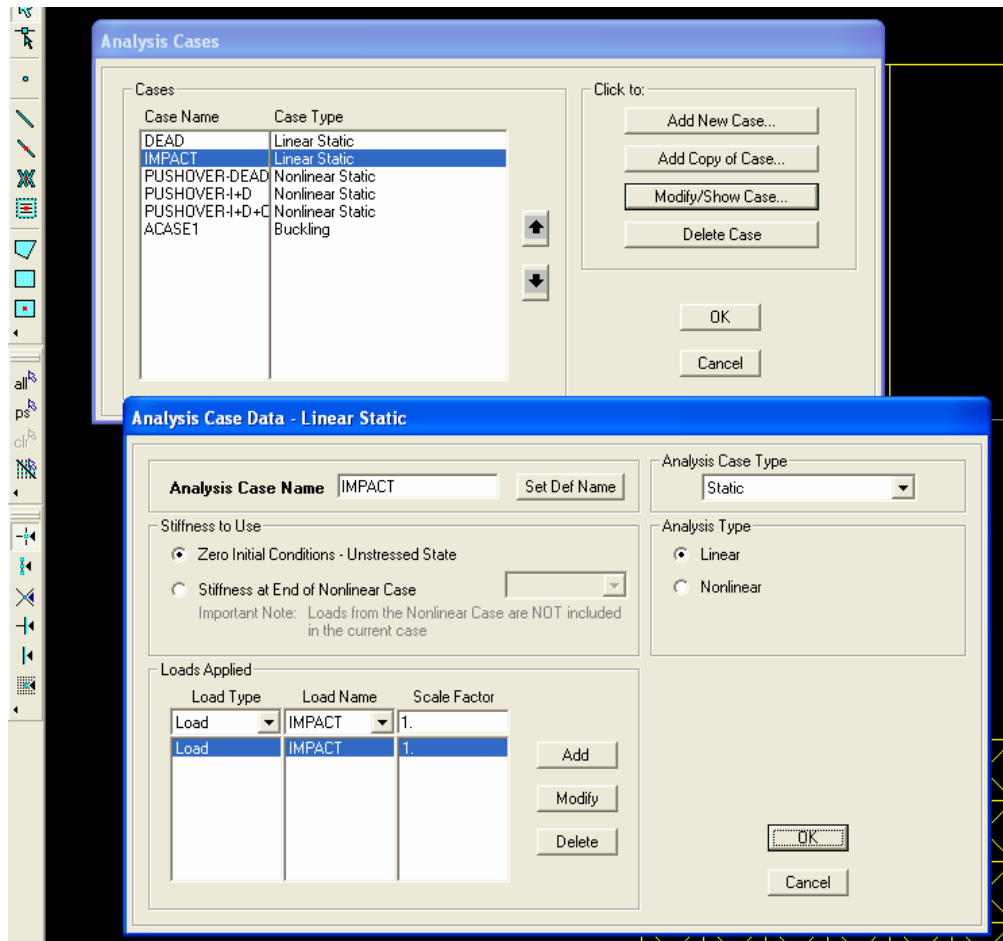
Figure 5.7: Defining Linear Static Analysis in SAP 2000

Nonlinear Static Pushover Analysis Options

Defining a nonlinear static analysis requires the specification of significantly more input parameters than a linear static analysis. The basic settings that are used for analysis of the SH-87 and IH-10 Bridges are presented in SAP 2000 screen shots below, but they only represent the settings that were used for those particular models. The values and options selected may need to be adjusted for each individual model. In addition to the screen shots, a brief explanation of the analysis settings is presented, but that discussion is somewhat limited. For more detailed descriptions of the nonlinear static pushover analysis options, it is recommended that the SAP 2000 user manual be consulted (SAP 2000, 2002).

Figure 5.8, a screen shot from the SH-87 Bridge model, shows the settings for a nonlinear static analysis case called 'PUSHOVER I+D'. This analysis case is defined to capture the effects of both the dead and impact loads on the SH-87 Bridge. The 'PUSHOVER I+D' case is described in greater detail in Section 5.4.3.2 of this report. Note on the right side of the box that the **Analysis Case type** is set to *Static,* and the **Analysis Type** is set to *Nonlinear*. The left side of the box in Figure 5.8 shows the options that can be changed for a static nonlinear analysis. Three groups of options can be adjusted, **Initial Conditions**, **Loads Applied** and **Other Parameters**.

83

Two options exist under the **Initial Conditions** box. The first option is to run the analysis from an unstressed state, or with *Zero Initial Conditions*. The second option is to run an analysis that continues from the end of a previous nonlinear analysis case. Selecting the second option allows a user to perform an analysis on a structure that has already been stressed in some fashion. For example, the dead load on a bridge could be applied before impact is considered. Once the analysis with the dead load has been run, a second case can be run with the impact loads. Figure 5.8 shows that for the 'PUSHOVER I+D' analysis case, the **Initial Conditions** box is set to *Continue from State at End of Nonlinear Case—'PUSHOVER-DEAD'*.

Below the **Initial Conditions** settings are the **Loads Applied** options. The settings here are the same as previously described for a static linear analysis. The desired loads and corresponding scale factors need to be specified. This step is also shown in Figure 5.8.
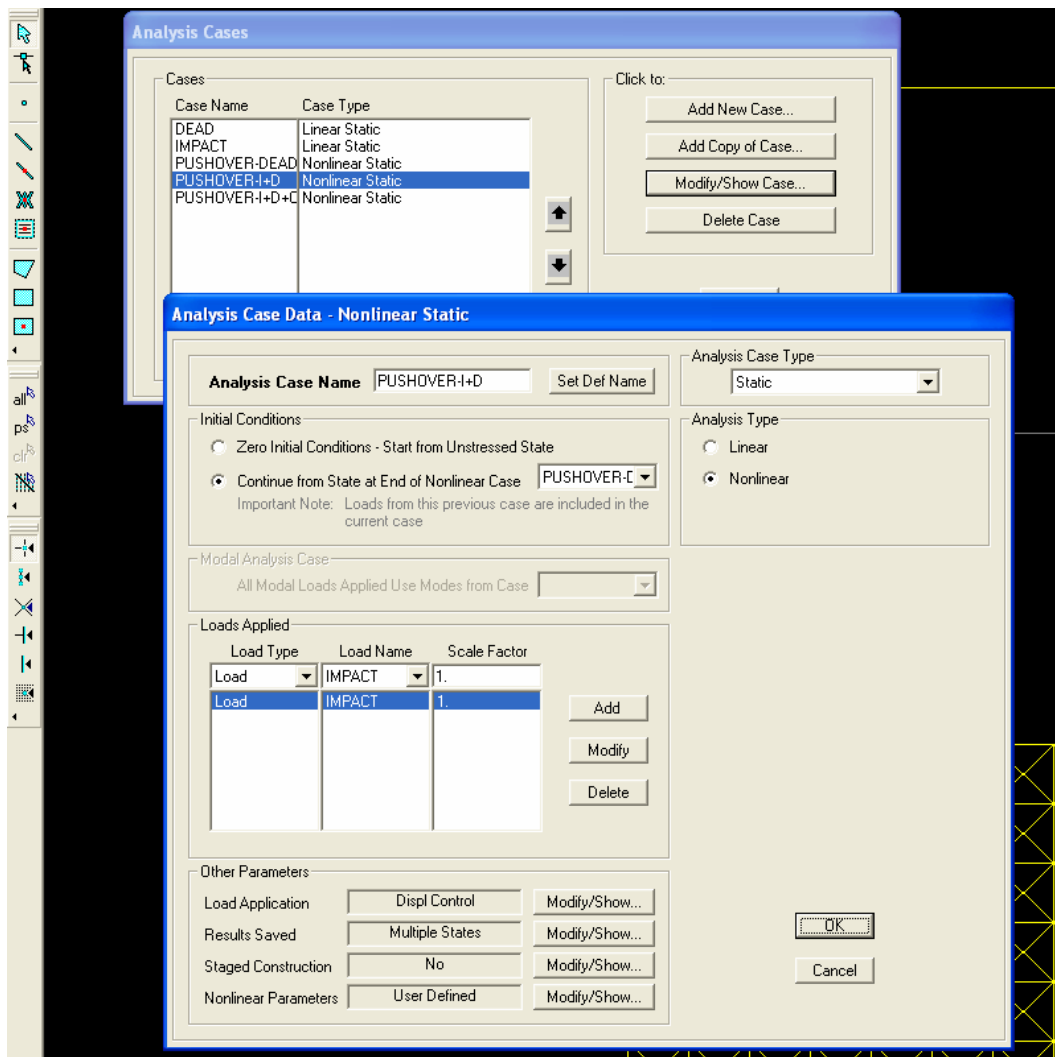
Figure 5.8: Nonlinear Static Analysis Options

The third group of settings for a nonlinear static analysis are listed under the heading **Other Parameters**, which is broken into four sets of options: **Load Application**, **Results Saved**, **Staged Construction** and **Nonlinear Parameters**. There are separate input boxes for each of these options, which are accessed by selecting the *Modify/Show* buttons shown in Figure

84

5.9. Each of the four options listed above is described in more detail, along with additional screen captures, in the paragraphs below.

Figure 5.9 shows the **Load Application** options for a nonlinear static analysis. Nonlinear static pushover analyses can be controlled in one of two ways: by specifying either a maximum load to be applied to a model, or by specifying a maximum displacement at a given point that a model can reach. Using the *Full Load* option, SAP 2000 takes the applied loads, sub-divides them, and applies them in user-specified increments until the entire load has been applied to the model. With the *Displacement Control* option, the load applied to the model is automatically increased until a specified displacement is reached at a specified location.

If the *Displacement Control* option is used, the displacement limit needs to be entered. The limits are set under the **Control Displacement** option shown in Figure 5.9. The models in this report use the *Monitored Displacement* option. When using the monitored displacement option, it is also necessary to specify which joint in the model the displacement should be tracked and in what direction the displacement limit should be enforced. For the example case shown in Figure 5.9, the analysis is set to run until a *4*-inch displacement limit is reached at joint *221* in the *U1* direction. This case represents a 4-inch lateral displacement at the point of impact for this model. In general, for the analysis cases that consider impact loads, tracking the lateral displacement at the point of impact is of the most interest, although other cases may be considered as well. The appropriate joint number is determined by looking at the model drawing in the regular SAP 2000 window.
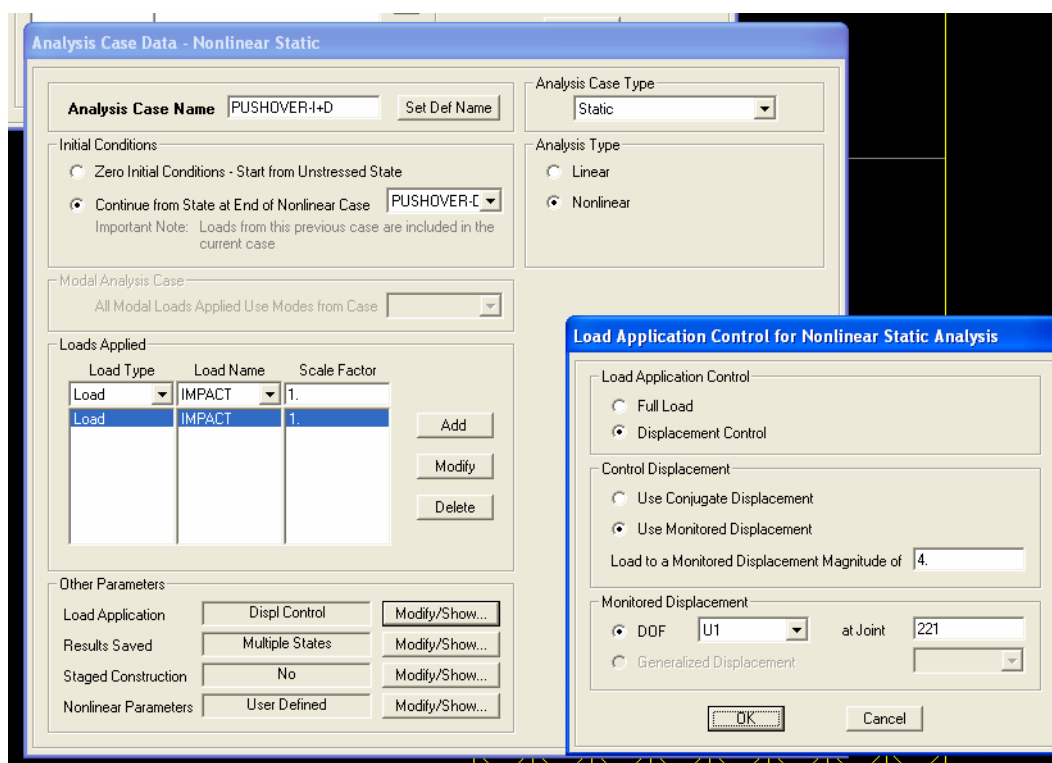
Figure 5.9: Nonlinear Static Analysis Load Application Option

Next, the **Results Saved** options need to be set (Figure 5.10). Two primary options are available: saving only the final results of the nonlinear static analysis, or saving the results for each step of the analysis. If *Multiple States* is selected as is shown in Figure 5.9, the minimum

and maximum number of analysis steps must be specified. These values indicate the smallest and largest increment of load or displacement that each step can be. The initial increment that SAP 2000 uses is based on the minimum number of steps specified by the user. For example, if a 4-inch displacement limit is set with a 100-step minimum and 400-step maximum, SAP 2000 saves the analysis results at increments of 0.04-inch to start and adjusts the increments based on the computed results. In carrying out the analysis, it uses at least 100 steps and no more than 400 steps. Using larger values for the number of saved steps results in greater solution accuracy, but it also results in longer analysis run times.
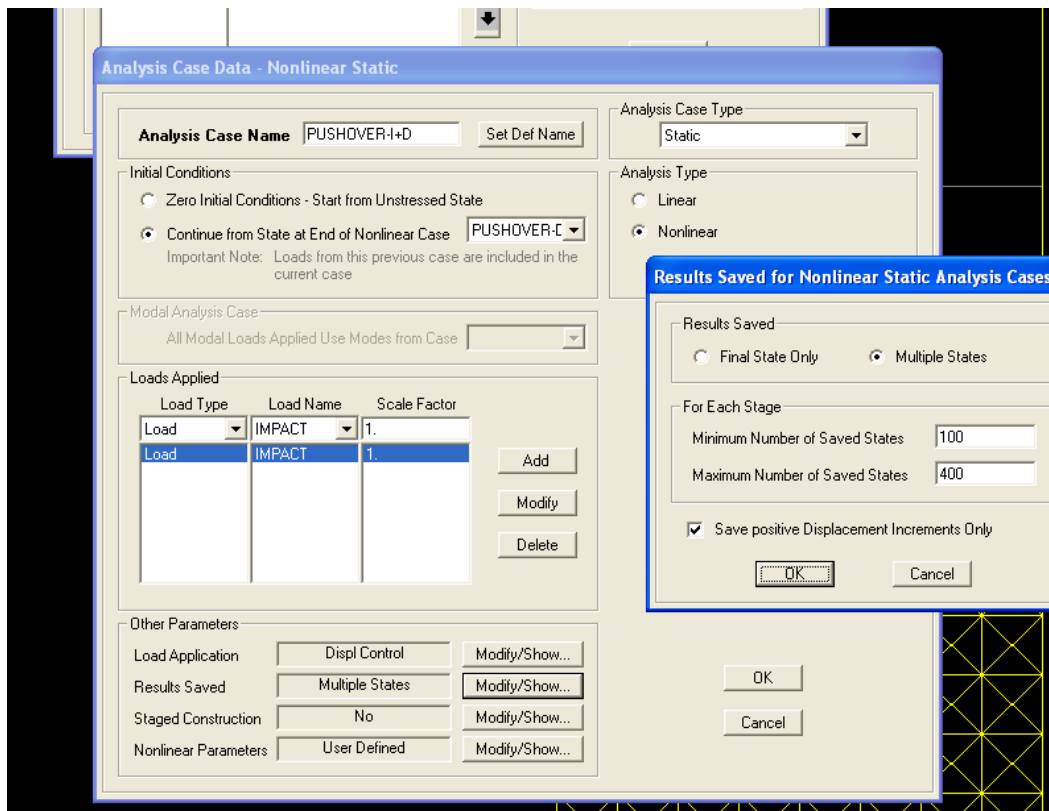
Figure 5.10: Nonlinear Static Analysis Results Saved Option

Figure 5.11 shows the **Staged Construction** options for a nonlinear static analysis. The staged construction option allows a user to add or remove specific groups of elements in a model. This feature is used to consider the effect on the bridge as a whole of losing an exterior column in a multi-column bridge pier. This option is used by selecting whether elements are to be added or removed from the model. Next, the group of elements to add or remove is selected. Groups are defined from the *Assign* menu in the main SAP 2000 window.
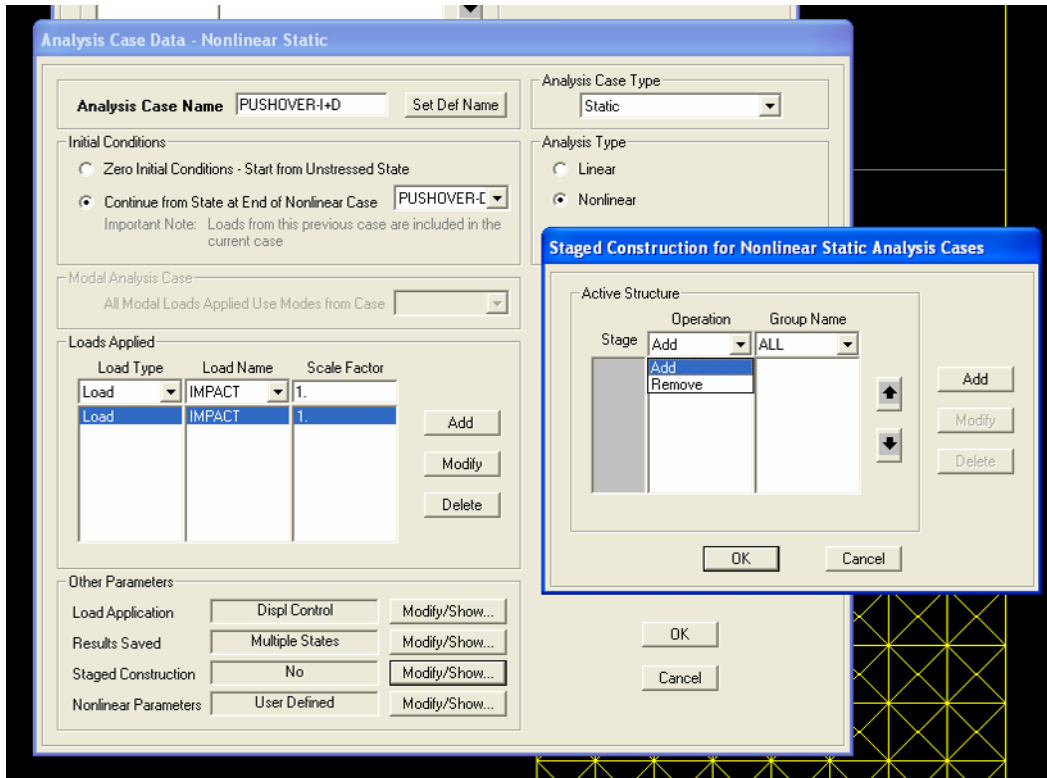
Figure 5.11: Nonlinear Analysis Staged Construction Options

The final group of options to set in a SAP 2000 nonlinear static analysis is the **Nonlinear Parameters**. In the **Nonlinear Parameters** box, the **Solution Control** settings, **Geometric Nonlinearity Parameters** and the **Hinge Unloading Method** parameters are set. Example input data are shown in Figure 5.12. Simple descriptions of the settings in Figure 5.12 are provided below. A detailed description of the items in the nonlinear parameter box can be found in the SAP 2000 user manual (SAP 2000, 2002).

Under the **Geometric Nonlinearity Parameters**, the *P-Delta* option is selected. This option indicates that, in the analysis of a model, the equilibrium equations are set up and solved in the deformed shape. Considering this effect usually results in larger member forces and displacements. Several guidelines can be used to determine whether geometric nonlinearity or 'P-Delta' effects need to be considered in an analysis. Generally, this determination can be made based on the magnitude of the lateral displacement relative to the overall length of the structure from a first-order analysis. For the specific bridges modeled in this report, geometric nonlinearity was not found to have a significant effect on the results. It is quite possible, however, that for other bridge geometries, P-Delta effects could be important. Therefore, it is recommended that this option be considered in a SAP 2000 analysis. The *P-Delta plus Large Displacements* option is intended primarily for SAP 2000 models that use frame elements to model cables (SAP 2000, 2002).

The **Hinge Unloading Method** is set to *Unload Entire Structure*. This setting is recommended by SAP 2000. The **Solution Control** inputs are used to set the tolerance for solution convergence and the maximum number of steps that can be used to get a model to converge at any point of the analysis. If the solution at any point does not converge, the analysis will terminate before the displacement or load limit is reached. There is a variety of reasons for the analysis not converging, ranging from some instability in the structure to a numerical

87

solution problem. The input values shown in Figure 5.12 were found to produce good results for most of the models being analyzed in this chapter. It is strongly recommended, however, that the SAP 2000 user manual (SAP 2000, 2002) or other reference be consulted to learn more about nonlinear analysis settings.
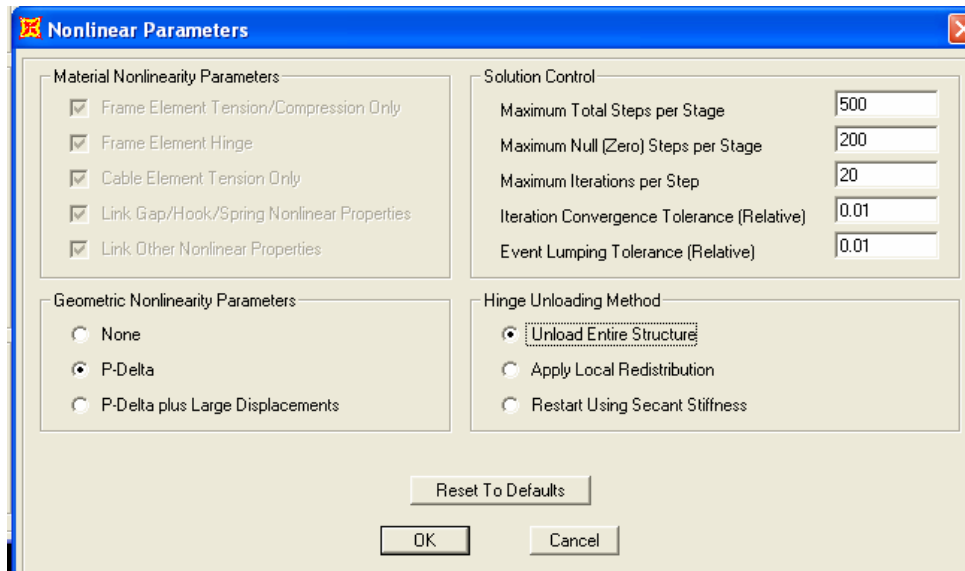
Figure 5.12: Nonlinear Static Analysis Nonlinear Parameter Options

5.4.3 Analysis Cases for Determination of Bridge Ultimate Lateral Strength

This section describes the three nonlinear static analysis cases that are used to analyze the bridge models from Chapter 4. Each of the three analysis cases builds on the previous case. The specifics of the nonlinear static analysis settings, described in detail in Section 5.4.2.2, are outlined for each of the three nonlinear static analysis cases.

Nonlinear Static Pushover Analysis—Dead Load

The first analyses of the SH-87 and IH-10 Bridge models capture the effects of the in-place or existing loads on the structure. This analysis case is called 'PUSHOVER-DEAD' and can be seen in Figure 5.6. Figure 5.13 shows the basic nonlinear static analysis settings for this case. The analysis is run with zero initial conditions. The only load applied is the dead load case, which captures the in-place loads on the structure. The analysis is run until the full load has been applied. The staged construction feature is not used. Similar nonlinear parameters as those shown in Figure 5.12 are used. Notice that this case is a nonlinear static analysis case even though it is not expected that the structure will behave inelastically. It is necessary to run the analysis as a nonlinear static case, however, in order to use the results from this analysis for later cases.

88
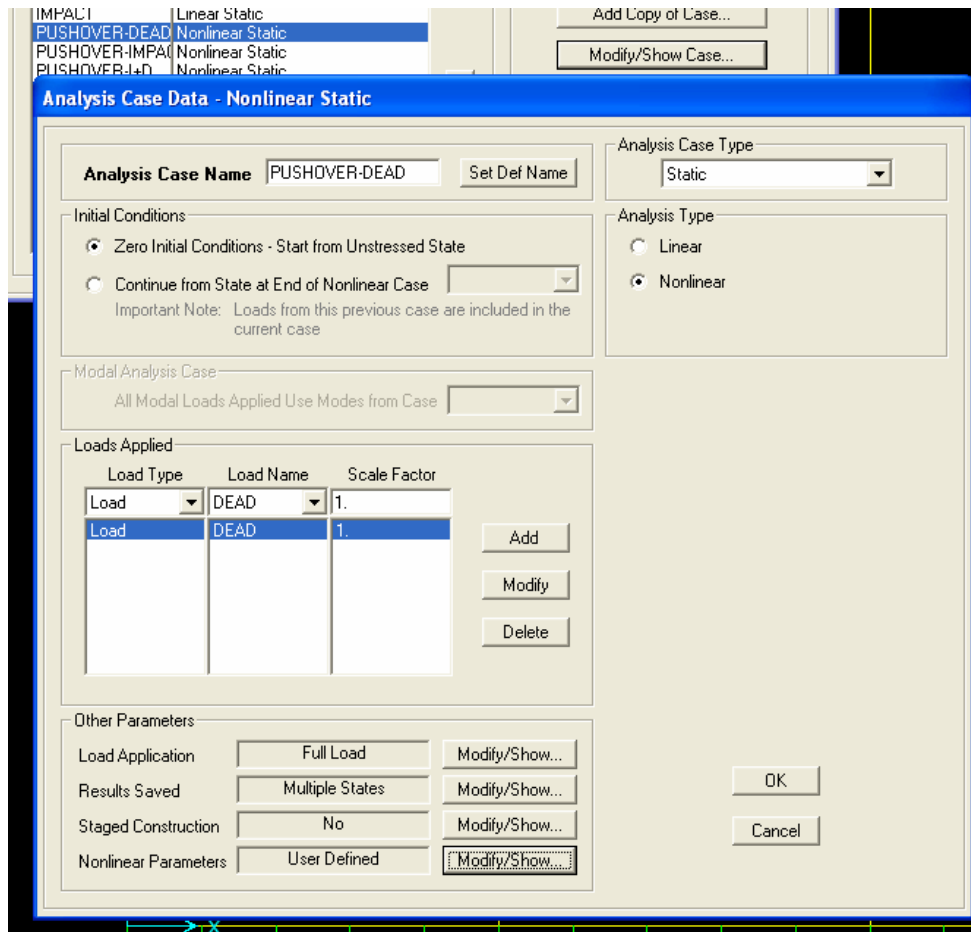
Figure 5.13: Nonlinear Static Pushover Analysis—Dead Load

Nonlinear Static Pushover Analysis—Impact + Dead Load

The second analysis case, called 'Pushover-I+D', starts with the conditions at the end of the 'PUSHOVER-DEAD' analysis. A lateral load is applied to represent vessel impact, and the analysis is run. Figure 5.14 shows the nonlinear static analysis settings for this case. This analysis is controlled by a specified displacement at the point that the load is applied. The displacement limit needs to be entered by the user. There are no specific rules for determining this value, so some adjustments may be required. The displacement limit needs to be large enough so that the load versus displacement plot reaches a plateau, representing a mechanism in the model. If the limit is too large though, the analysis may not yield an accurate solution, or may not be able to converge to a solution. Several iterations on the displacement limit may be required. For the impact load case, multiple steps are saved in order to plot the load versus displacement at the end of the analysis. The staged construction feature is not used. Similar nonlinear parameters as those shown in Figure 5.12 are used.

89
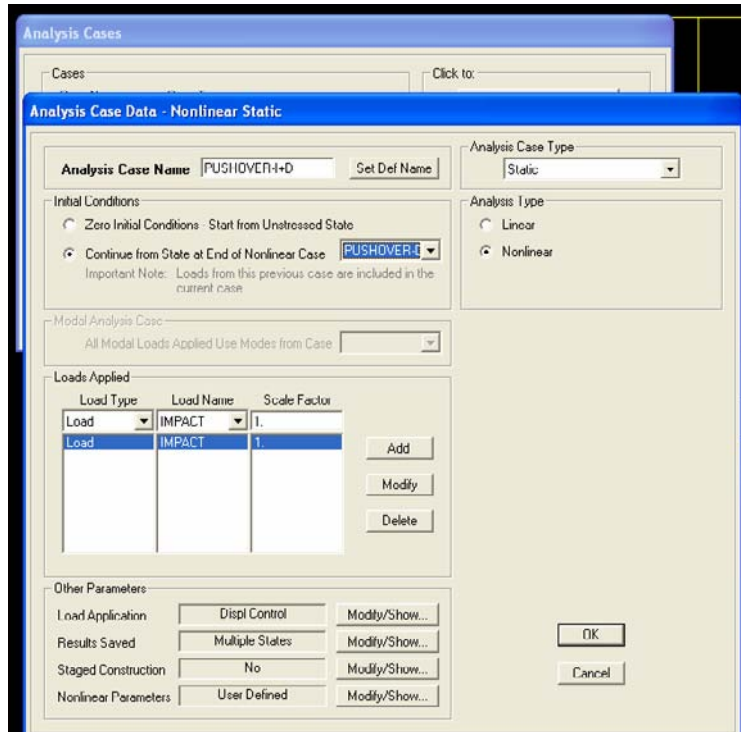
Figure 5.14: Nonlinear Static Pushover Analysis—Impact + Dead Load

Nonlinear Static Pushover Analysis—Impact + Dead Load + Column Removed

The final analysis case continues from the end of the previous case (described in Section 5.4.3.3) and considers the effect of losing a single column due to vessel impact in a multi-column bridge pier. While the analysis of a bridge pier after a single column has been lost does not clearly fit into the current AASHTO Method II design procedure, understanding this type of analysis could prove to be useful in the design of multi-column bridge piers. The results of a column removal analysis could help an engineer to better design the other elements in a pier so that the failure of a single column does not result in a more catastrophic failure of the entire pier. An in-depth investigation into this analysis case has not been conducted. The analysis steps and results presented in this chapter for a column-removal analysis are intended to introduce the topic. Further research in this area is needed in order to draw any wide-ranging conclusions.

A column removal analysis was run for a single load case for both the SH-87 and IH-10 Bridge models, which are comprised of three- and four-column bridge piers, respectively. It is assumed that a two-column bridge pier will not be able to sustain the loss of a column, so this analysis is not necessary. In addition, the column removal analysis should only be run if the impact analysis determines that a mechanism has formed in the column, which is only likely for load configurations where impact occurs directly on the column.

To consider the effects of removing a failed column from a bridge model, the staged construction feature of a SAP 2000 nonlinear static analysis is used. Figure 5.15 shows the nonlinear static analysis settings for the IH-10 Bridge model.
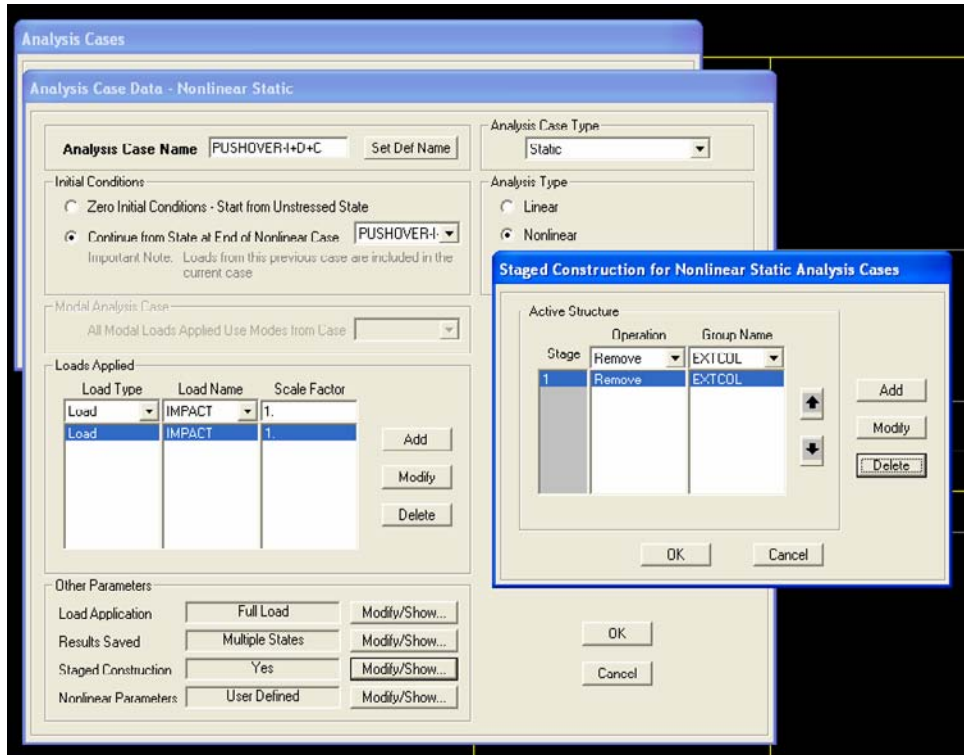
Figure 5.15: Nonlinear Static Pushover Analysis—Impact + Dead Load +
Column Removed Settings

Notice that this analysis starts from the end of the PUSHOVER-I+D analysis described in Section 5.4.3.2. At this point, the in-place loads and impact loads have already been applied to the structure. For the current example, a lateral point load has been applied at mid-height of the top column in the IH-10 Bridge (Load Location 3 in Figure 5.1). Figure 5.16 shows the (exaggerated) deformed shape of the model after the nonlinear static analysis has been run for the in-place and impact loads. Notice that a mechanism has formed in the top column. At this stage, the column removal analysis begins.
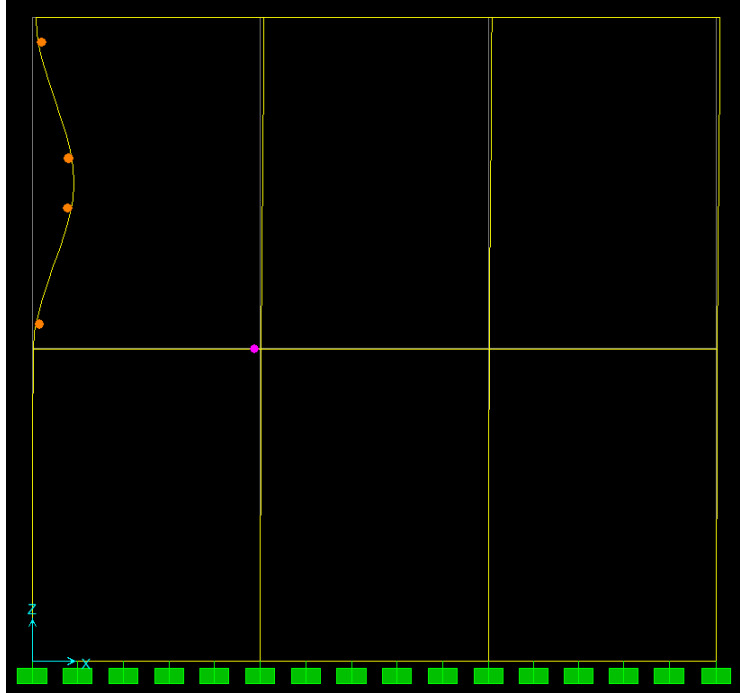
Figure 5.16: IH-10 Bridge Column Failure

The column removal analysis is run as a load control analysis, which is the only option permissible for the staged construction feature (SAP 2000 Analysis Reference, 2002). The elements from the failed exterior column in the IH-10 model were selected and assigned to a group called *extcol*. Under the **Staged Construction** option, the *extcol* group was assigned to be removed. These settings can be seen by looking at Figure 5.15. When the staged construction option is used and a group of elements is removed, SAP 2000 removes the stiffness and mass of these elements and replaces them with equivalent forces, which are reduced to zero as they get distributed through the remaining elements in the structure (SAP 2000 Analysis Reference, 2002).

5.4.4 Run Analysis

After all of the necessary load and analysis cases have been defined, the model is ready to be analyzed. Figure 5.17 shows the run options available in SAP 2000. The user can specify which analysis cases to run or can simply run all of the cases. To initiate the analysis, the *Run Now* button must be selected.
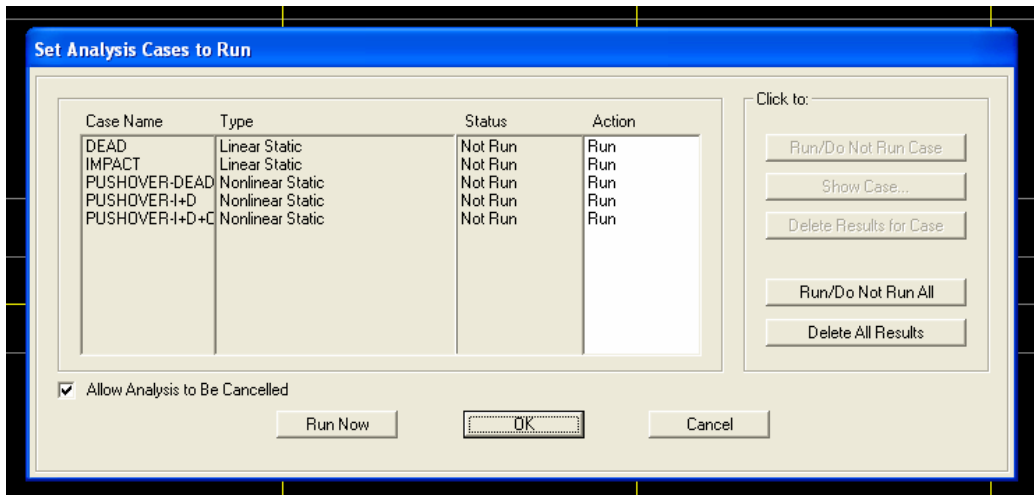
Figure 5.17: Running an Analysis in SAP 2000

5.5 Assessing Analysis Results

One of the key modeling issues discussed in Chapter 4 was the decision to define plastic hinges as being essentially infinitely plastic. A discussion of this choice can be found in Section 4.4.5. Real structures, of course, are not capable of infinite rotation or deformation after yield. A wide range of guidelines exist on ductility and displacement limits for structures subject to large lateral forces, such as earthquake, blast, and impact loads, and this information can be used to assess the rotational or deformational capacities of the bridge systems that are being analyzed in this chapter. The first method presented focuses on the overall ductility of the system and is based on the Federal Emergency Management Agency (FEMA) NEHRP Guidelines (FEMA-302, 1997). The second method considers rotational or deformational limits for specific members and is based on guidelines published by the American Society of Civil Engineers (ASCE, 1999).

5.5.1 Limit State Based on Ductility Ratio

One possible approach is to consider a system-wide ductility limit state by assuming that the structure is capable of a set level of deformation beyond the point of first yield. This approach is appropriate for structures or systems where inelastic response is evenly distributed throughout the structure (Moehle, 1992). While vessel impact is likely to cause significant localized damage, the analysis results presented later in Section 5.6 shows that, for an impact near a wall or beam providing lateral support for a bridge pier, there is significant redistribution of forces throughout the entire system. For typically reinforced concrete structures, a ductility limit of four times the deformation at first yield is a reasonable assumption (FEMA-273, 1997). Making this assumption means that if a structure reaches a plateau in the load versus displacement curve at a displacement beyond four times the yield deformation, then the structure does not have sufficient ductility to reach that strength. Consequently, a ductility limit state controls the strength of the structure. Figure 5.18, a typical load versus displacement plot for a bridge pier, illustrates this point.

Ultimate Load Capacity Based on Ductility Limit
Load vs. Displacement Curve
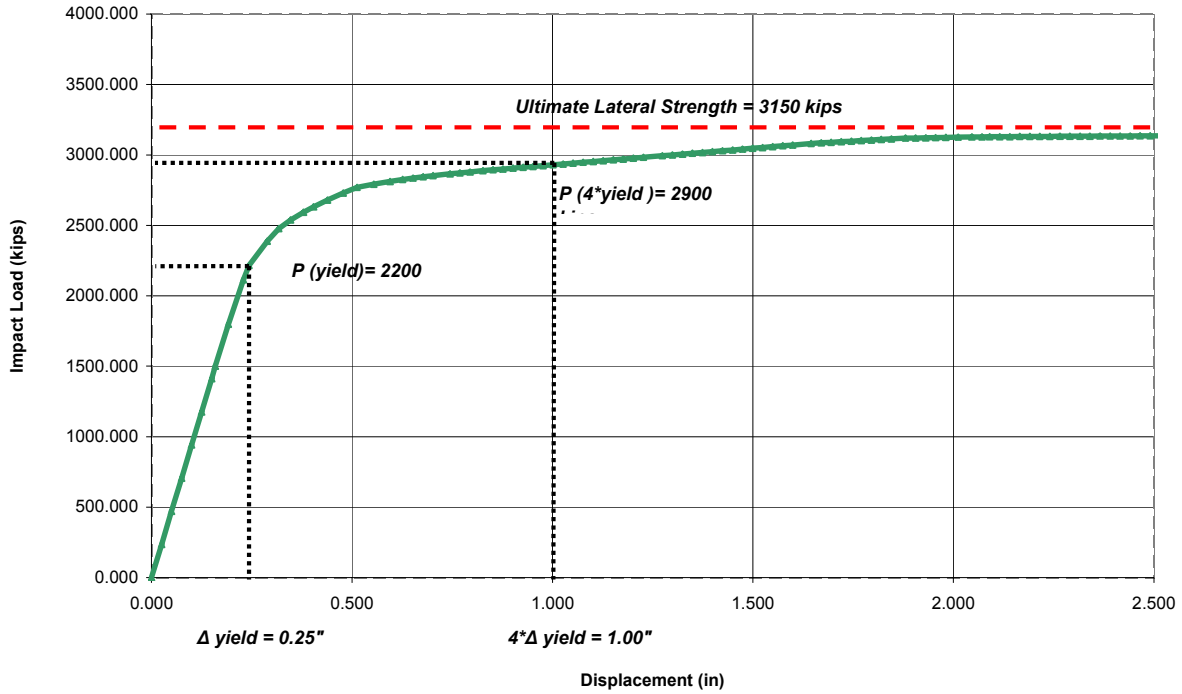
Figure 5.18: System Ductility Limit State

Figure 5.18 shows a point of first yield at a deformation of approximately 0.25 inch. At a ductility ratio of four, the applied load is 2900 kips, which is less than the peak load of 3150 kips. Therefore, the limit state and ultimate lateral strength of this structure are controlled by the ductility of the system.

5.5.2 Member Ductility Limit

A second approach to assess the ultimate lateral strength analysis results would be to consider the rotational or deformational capacity of an individual element or member in the structure. This method is useful for situations where vessel impact is being considered at some point along the length of a column as opposed to impact at a wall or other lateral support element. In this situation, inelastic behavior is more likely to be contained within the column. The results presented in Section 5.6 illustrate this point. For typical reinforced concrete members, a mid-span displacement limit of 4% of the span length is a reasonable assumption (ASCE, 1999). The mid-span displacement limit corresponds to a rotational limit at the ends of the member of 4.57 degrees. This value can used to determine the displacement limit at a distance, *x*, along the length of a column by Equation 5-1 and is illustrated in Figure 5.19.

$$\Delta_{max} = x * \sin(4.57^o) \quad \text{(5-1)}$$
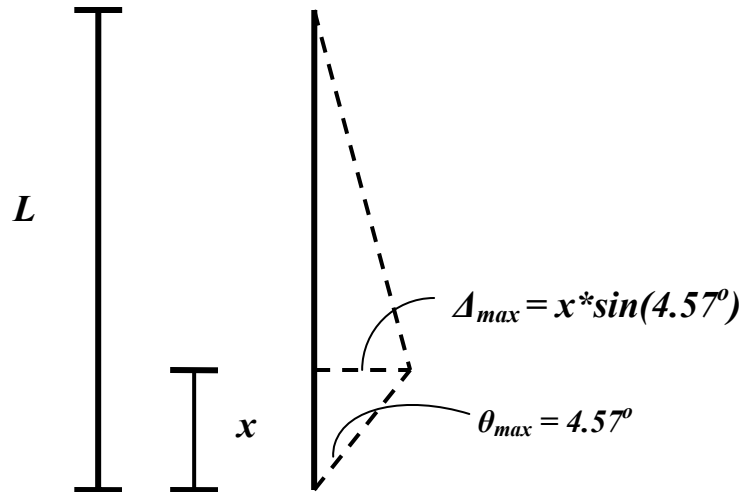
Figure 5.19: Column Displacement Limits

5.6 Analysis Results

This section presents the analysis results for the IH-10 and SH-87 Bridge models presented in Chapter 4. Additional results are presented to determine the effect of considering a reduced section size in the vessel impact area of a model and the effect of losing one column in a multi-column bridge pier.

5.6.1 Truss-Grid Wall Model Verification

The focus of this section is to confirm the validity of the truss-grid wall model used to capture the shear wall behavior in the SH-87 Bridge. A finite element model constructed in ANSYS provides the basis for comparison. A full description of this model follows below. The SAP 2000 truss-grid wall model and the ANSYS model are compared against each other for a range of load configurations and boundary conditions.

Finite Element Verification Models

To verify the accuracy of the SAP 2000 models presented in Chapter 4, finite element models were constructed, and comparable analyses were run using ANSYS. Specifically, models were developed for the piers of the SH87 Bridge, which contain shear walls. ANSYS has the ability to capture inelastic behavior of shell elements, a feature that SAP 2000 and many other typical structural analysis programs lack. While ANSYS and other finite element analysis programs have the ability to model the response of a bridge pier or bridge system to vessel collision, they are not practical for most design situations, primarily due to their cost, both for the software package and in terms of computational time. In addition, ANSYS is not tailored directly for structural engineering use and is not as user friendly when compared to SAP 2000 or other common structural analysis programs.

The ANSYS models were used strictly to verify the inelastic behavior of the truss-grid model developed in Chapter 4 for use within SAP 2000. Other aspects of the ANSYS model were defined in a similar manner to the Chapter 4 SAP 2000 models. Columns and beams were defined using frame elements that appear as lines in ANSYS, just as they do in SAP 2000. The pier geometry, section properties, and material properties were defined as they were in Chapter

95

4. Identical boundary conditions were used for both sets of analyses. The base of the pier was assumed fixed for all analysis runs, and two boundary conditions at the top of the pier were considered (free and fixed). These two cases provide the range of possible strengths for the pier. Comparing the analysis results for the two extreme cases provides a clear assessment of the accuracy of the truss-grid wall model for the wide range of support conditions at the top that may be seen in real bridges. A third condition, using elements that would accurately reflect the properties of the deck and girders, was not considered No ANSYS models were constructed for the IH-10 Bridge piers because they do not contain a shear wall.

SAP 2000 vs. ANSYS Bridge Pier Model Results

The following plots compare the analysis results from SAP 2000 and ANSYS for pier 18 of the SH-87 Bridge. Results for four load configurations, with two different boundary conditions at the top of the pier for each load, are presented for a total of eight plots. They are shown in Figure 5.20 through Figure 5.23. The title of each individual plot describes the exact load and boundary conditions for those results. Table 5-2 summarizes the plot results. A consistent approach to compare the SAP 2000 truss-grid wall model and the ANSYS shell wall model was used by comparing the ultimate lateral strength from each at the same value of displacement.

Truss Grid Model Verification-SAP 2000 vs. ANSYS
Load vs. Disp Plot
Top of Pier Boundary Condition: *Free*
Load Description: *Point Load at Top of Wall*
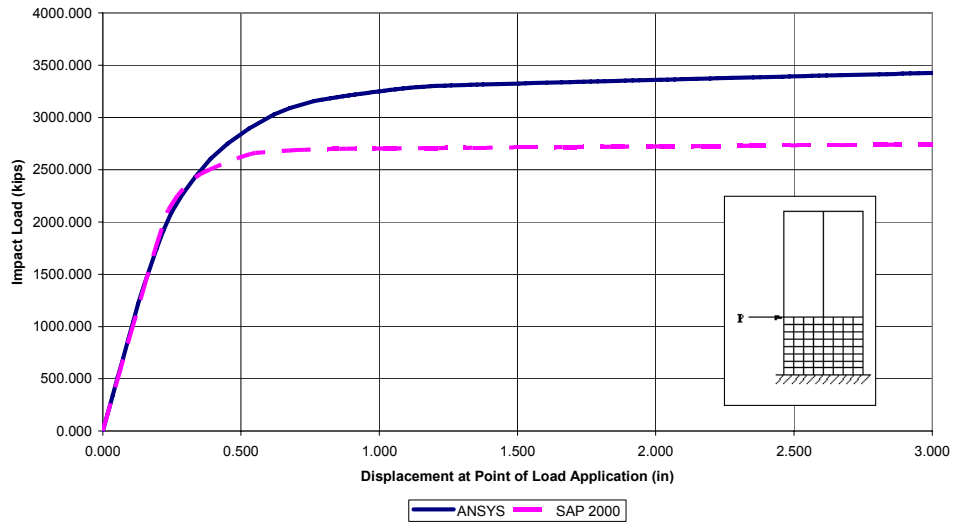
Truss Grid Model Verification-SAP 2000 vs. ANSYS
Load vs. Disp Plot
Top of Pier Boundary Condition: *Fixed*
Load Description: *Point Load at Top of Wall*
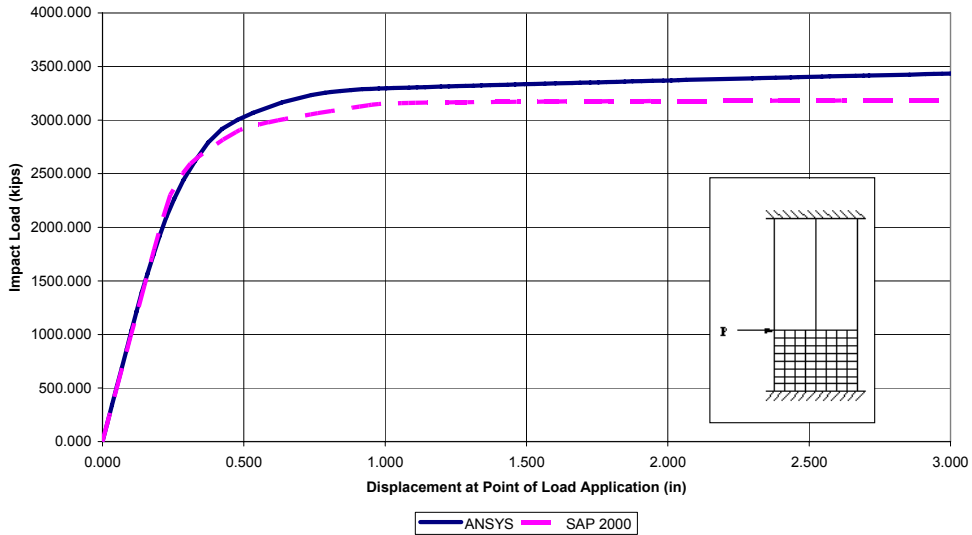
Figure 5.20: Wall Model Comparison SAP 2000 vs. ANSYS—Load Location 1

Truss Grid Model Verification-SAP 2000 vs. ANSYS
Load vs. Disp Plot
Top of Pier Boundary Condition: *Free*
Load Description: *Point Load 48″ Above Wall*
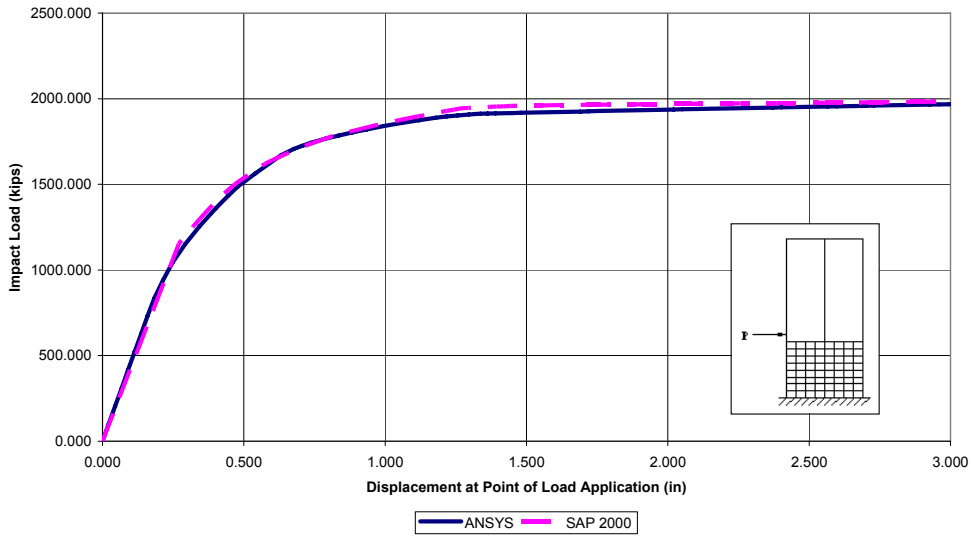
Truss Grid Model Verification-SAP 2000 vs. ANSYS
Load vs. Disp Plot
Top of Pier Boundary Condition: *Fixed*
Load Description: *Point Load 48″ Above Wall*
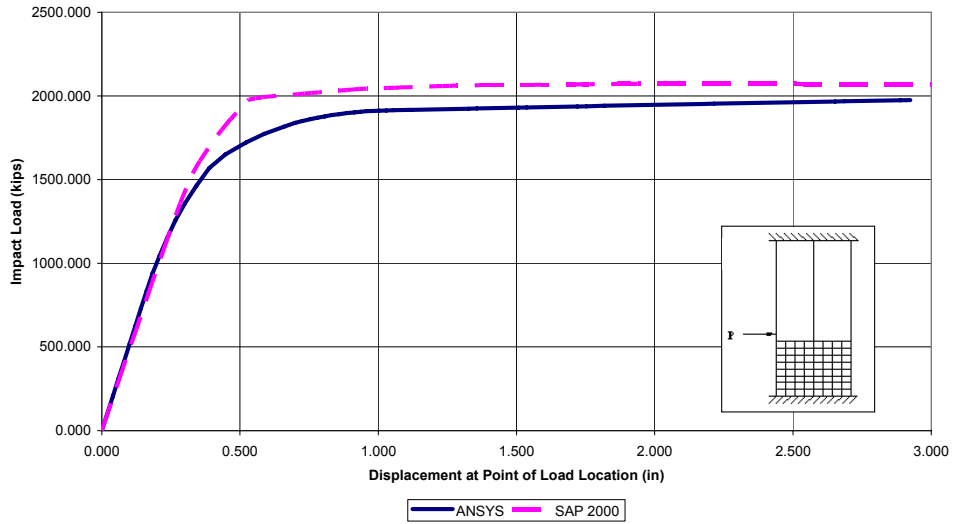
Figure 5.21: Wall Model Comparison SAP 2000 vs. ANSYS—Load Location 2
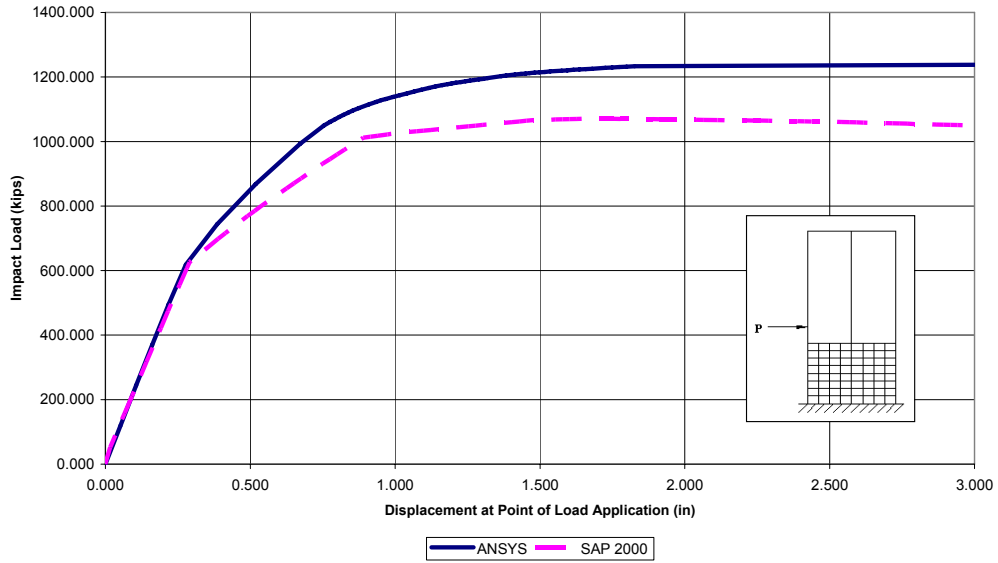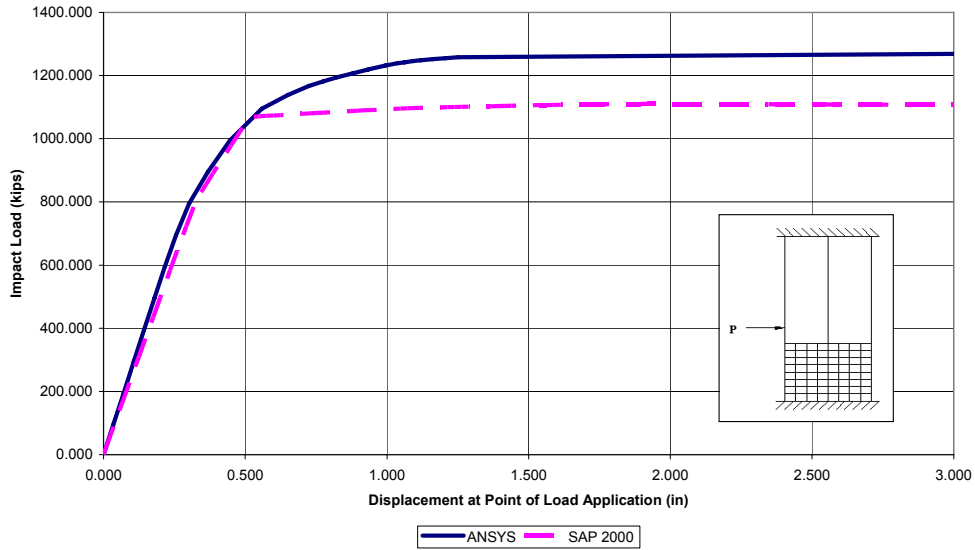
Figure 5.22: Wall Model Comparison SAP 2000 vs. ANSYS –Load Location 3
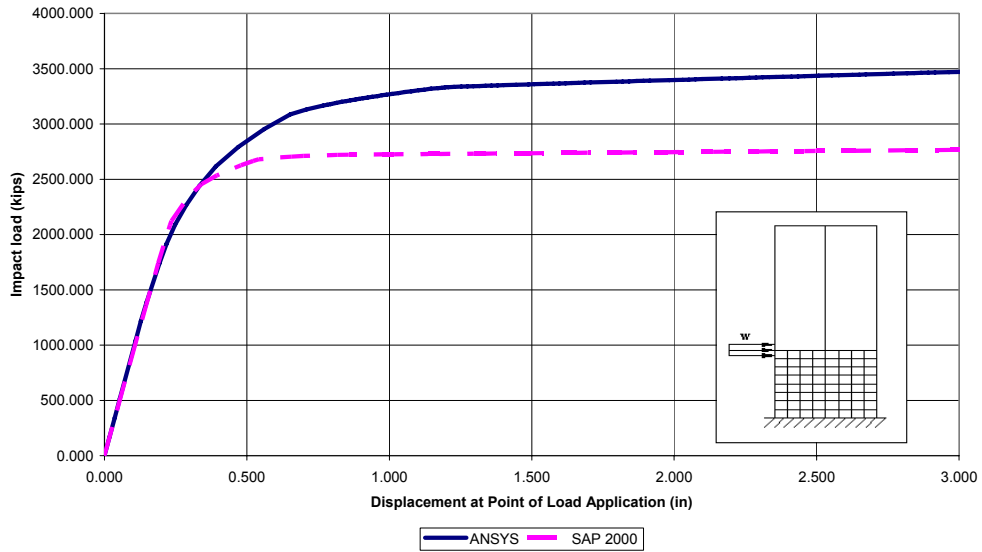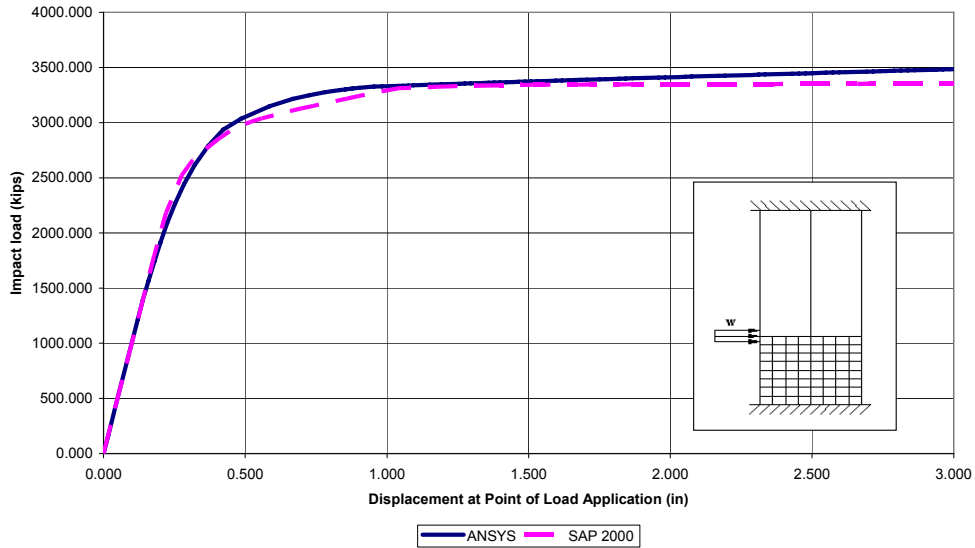
Figure 5.23: Wall Model Comparison SAP 2000 vs. ANSYS—Load Location 4

Table 5.2: Wall Model Comparison Results

SH-87 Bridge Ultimate Lateral Strength Wall Model Comparison Results					
Load Location	Load Description	Boundary Condition at Top of Pier	ANSYS Shell Wall Model Lateral Strength (kips)	SAP 2000 Truss Grid Model Lateral Strength (kips)	% Error
1	Point Load at Top of Wall	Free	3425.0	2742.0	19.94
2	Point Load 48" above Top of Wall	Free	1968.0	1982.0	0.71
3	Point Load 96" above Top of Wall	Free	1238.0	1050.0	15.19
4	Distributed Load 30" above and below wall	Free	3472.0	2765.0	20.36
1	Point Load at Top of Wall	Fixed	3433.0	3185.0	7.22
2	Point Load 48" above Top of Wall	Fixed	1975.0	2070.0	4.81
3	Point Load 96" above Top of Wall	Fixed	1268.0	1107.0	12.70
4	Distributed Load 30" above and below wall	Fixed	3485.0	3353.0	3.79

Figure 5.20 through Figure 5.25 and Table 5-2 show a mixed range of results. Clearly, the initial linear portion of the ANSYS load versus displacement curve matches the SAP 2000 load versus displacement curve. This observation verifies that the dimensions of the truss elements, which were sized in Chapter 4 specifically to match the linear elastic response of an equivalent model with a shell wall, were determined correctly. As the plots move into the inelastic range, however, differences between the SAP 2000 and ANSYS models begin to develop. Several of the SAP 2000 results show very good correlation to the ANSYS results, while others have errors of up to 20%. It is worth noting that for the load cases with higher error, the SAP 2000 values are conservative.

Close examination of the results reveal some interesting observations about the variation in the results based on the configuration of the load. Therefore, it is useful to separate the discussion of the results based on where the load is applied. It makes sense to compare the results from Load Locations 1 and 4 independent from the results of Load Locations 2 and 3. See Table 5-2 or Section 5.2.2 for clarification on load locations.

Loads at or Centered on the Top of the Shear Wall (Load Locations 1 & 4)

Load Locations 1 and 4 are located at or centered on a point at the top of the shear wall. Table 5-3 shows the analysis results for just these two load configurations. The values in Table 5-3 are taken directly from Table 5-2. They are separated only for ease of comparison. The plots for these cases are shown in Figure 5.20 and Figure 5.23, respectively. Table 5-3 indicates that the ultimate lateral strength results for Load Locations 1 and 4 are very similar, which is expected given that they are applied in the same area near the wall. Interestingly, the accuracy of the SAP model is very sensitive to the boundary condition at the top for these two models. With a fixed boundary condition, the SAP 2000 truss-grid wall model results match quite well with the ANSYS shell wall model results. However, the largest errors for any of the load locations are seen in the results from the same models with a free top.

Table 5.3: Wall Model Comparison Results Load Locations 1 and 4

SH-87 Bridge Ultimate Lateral Strength *Wall Model Comparison Results Load Locations 1 and 4*					
Load Location	*Load Description*	*Boundary Condition at Top of Pier*	*ANSYS Shell Wall Model Lateral Strength (kips)*	*SAP 2000 Truss Grid Model Lateral Strength (kips)*	*% Error*
1	Point Load at Top of Wall	Free	3425.0	2742.0	19.94
1	Point Load at Top of Wall	Fixed	3433.0	3185.0	7.22
4	Distributed Load 30" above and below wall	Free	3472.0	2765.0	20.36
4	Distributed Load 30" above and below wall	Fixed	3485.0	3353.0	3.79

Loads Applied on the Column (Load Locations 2 & 3)

Load Locations 2 and 3 are located at points along the exterior column of the pier and do not have any contact with the wall. Table 5-4 shows the comparison between the ANSYS and SAP 2000 models for these two load locations. The values from Table 5-4 are also taken directly from Table 5-2.

Table 5.4: Wall Model Comparison Results Load Locations 2 and 3

SH-87 Bridge Ultimate Lateral Strength *Wall Model Comparison Results Load Locations 2 and 3*					
Load Location	*Load Description*	*Boundary Condition at Top of Pier*	*ANSYS Shell Wall Model Lateral Strength (kips)*	*SAP 2000 Truss Grid Model Lateral Strength (kips)*	*% Error*
2	Point Load 48" above Top of Wall	Free	1968.0	1982.0	0.71
2	Point Load 48" above Top of Wall	Fixed	1975.0	2070.0	4.81
3	Point Load 96" above Top of Wall	Free	1238.0	1050.0	15.19
3	Point Load 96" above Top of Wall	Fixed	1268.0	1107.0	12.70

The results from Table 5-4 show that there is greater error in the Load Location 3 model when compared to the Load Location 2 model. For both cases, however, there is little difference between the results when the top boundary condition is changed, for both the SAP 2000 and the ANSYS models.

Also note that the SAP 2000 load versus displacement curves in Figure 5.21 and Figure 5.22 for loads 2 and 3 show sharp changes in the slope, whereas Figure 5.20 and Figure 5.23 for Load Locations 1 and 4 show a relatively smooth change in the slope. These observations can be explained by examining how plastic hinges were defined in Chapter 4, how hinges form in SAP 2000, and where hinges are forming for the particular load being applied.

Recall that the hinges for the SH-87 model were defined as being nearly elastic perfectly plastic, with little hardening after the hinge formed (see Figure 4-37). Also recall that Load Locations 2 and 3 were applied to a column away from elements of lateral support. Thus, there is a strong likelihood that hinges are forming at the column ends and at the point where the load is being applied (this observation will be verified later in this chapter). The inelastic response of the structure is being concentrated in just a few locations. Furthermore, SAP 2000 does not consider gradual yielding of a section in determining when a hinge forms. In reality, plasticity starts at the extreme fiber in a section and gradually yields through the depth of the section. In SAP 2000, when the yield moment or force has been reached, the hinge forms instantly. Taking all of these facts into consideration, the sharp changes in the load versus displacement plot for Load Locations 2 and 3 are reasonable. When the load is applied at or near the wall, plasticity is likely to spread through many elements in the wall, as opposed to a single column element, and the change in stiffness in the structure is much more gradual. Figure 5.20 and Figure 5.23 show smooth load versus displacement curves for the SAP 2000 models. As analysis results are

presented throughout this chapter, it is essential to keep this discussion in mind. The trend of sharp changes in the load versus displacement curves for bridges with loads applied along the column is seen in the results for both the SH-87 and IH-10 Bridges.

Summary of Truss-Grid Verification Models

The plots and tables shown above verify that the truss-grid wall model captures the nonlinear strength and deformation characteristics of the shell wall model with reasonable accuracy. The greatest error is around 20%, and the mean error for all of the load configurations and boundary conditions is approximately 11%. Given the simplifying assumptions that were made in developing the truss-grid model, this error is considered acceptable. In addition, while there is a significant spread in the error depending on the load location and boundary conditions at the top of the pier, nearly all of the SAP 2000 models resulted in conservative estimates of the ultimate lateral strength, with only two exceptions, which only slightly exceeded the ANSYS estimate of ultimate lateral strength.

5.6.2 System-Wide Response Analysis Results

One of the goals in analyzing the IH-10 and SH-87 Bridge models is to compare system-wide response to individual element response. The AASHTO LRFD Design Specification currently requires that ultimate lateral strength be calculated for single elements, which it defines as a bridge pier or a bridge span. This report has focused on calculating the ultimate lateral strength of bridge piers, and the results presented in this section compare the analyses of the main piers of the IH-10 and SH-87 Bridges. In the models for these two bridges, system-wide response is captured by adjusting the boundary conditions at the top of the bridge pier. In assessing the individual pier response, the pier is left free at the top. To consider system-wide response, elements representing the bridge superstructure are used, and the adjacent piers in the bridge are included as well. Recall from Chapter 4 that the superstructure elements for both the IH-10 and SH-87 represent 3-span continuous steel plate girders and a concrete deck. Therefore, for both bridges, the superstructure is continuous over the bridge piers that are subject to vessel impact. The connection at the other adjacent pier is pinned.

This section compares the ultimate lateral strength of the IH-10 and SH-87 Bridges for three top boundary conditions: free, fixed, and with the superstructure in-place. The free and fixed top cases provide a range of possible strengths for the system. The results from the system-wide models will fall somewhere in this range. Furthermore, by comparing all three of the top boundary conditions described, insight into when it is necessary to model the entire superstructure can be gained.

IH-10 Bridge Analysis Results

Figures 5.24 through Figure 5.27 show the ultimate lateral strength analysis results for the IH-10 Bridge model. The load locations under consideration were described in Chapter 4 and in Section 5.2.2 of this chapter and were shown in Figure 5.1. Diagrams on the plots show where the load is being considered and what the top boundary condition is for each curve.
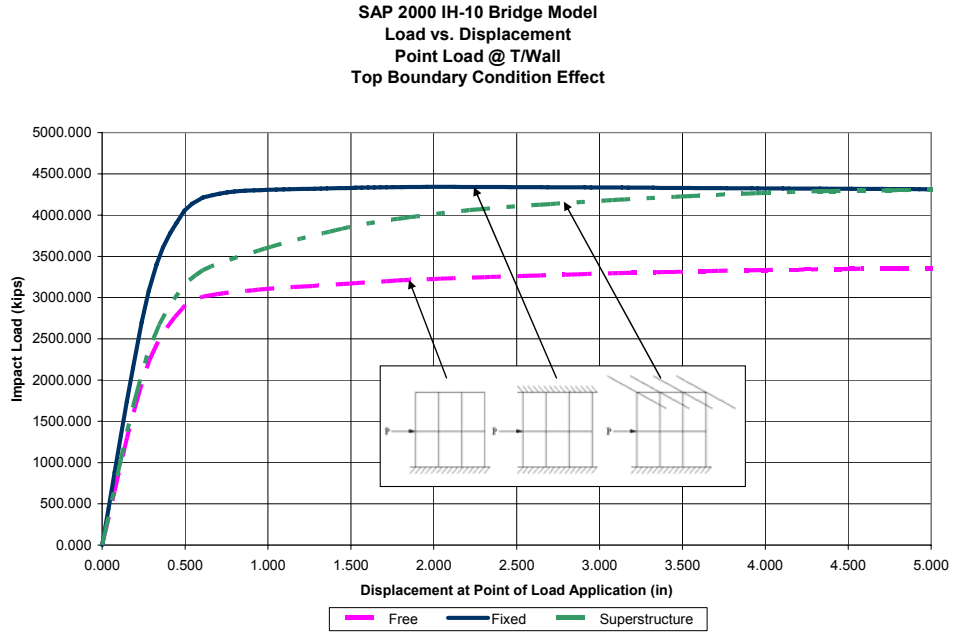
Figure 5.24: IH-10 Bridge Ultimate Strength Analysis Results-Load Location 1
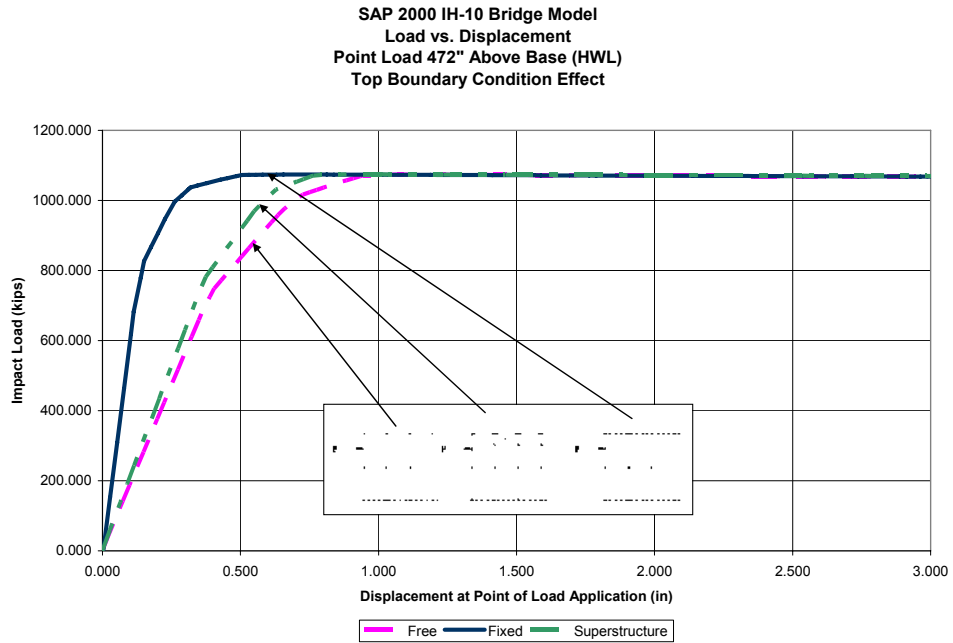
Figure 5.25: IH-10 Bridge Ultimate Strength Analysis Results-Load Location 2

SAP 2000 IH-10 Bridge Model
Load vs. Displacement
Point Load 366" Above Base (MWL)
Top Boundary Condition Effect
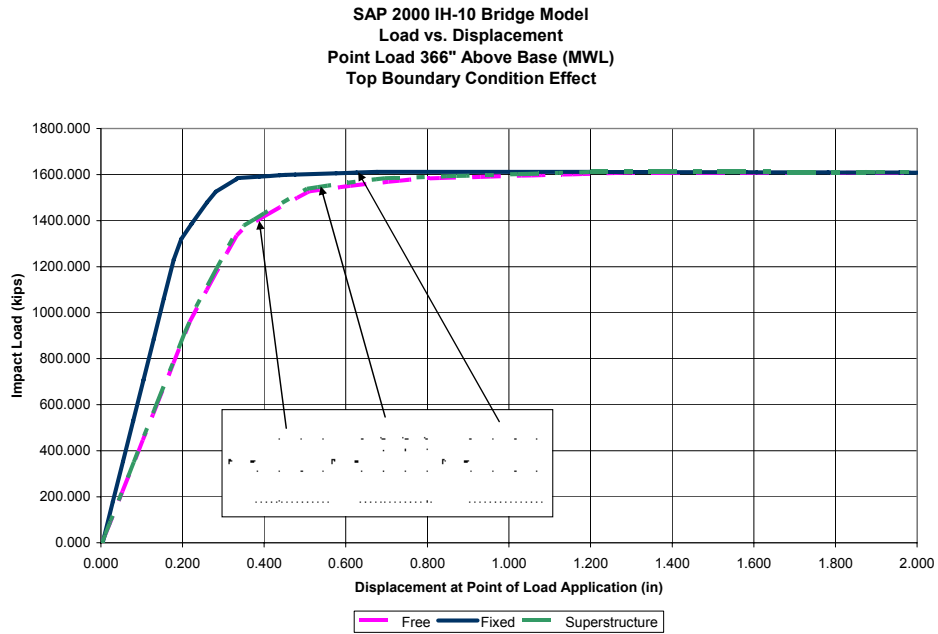
Figure 5.26: IH-10 Bridge Ultimate Strength Analysis Results-Load Location 3

SAP 2000 IH-10 Bridge Model
Load vs. Displacement
60" Distributed Load Centered on Lateral Beam
Top Boundary Condition Effect
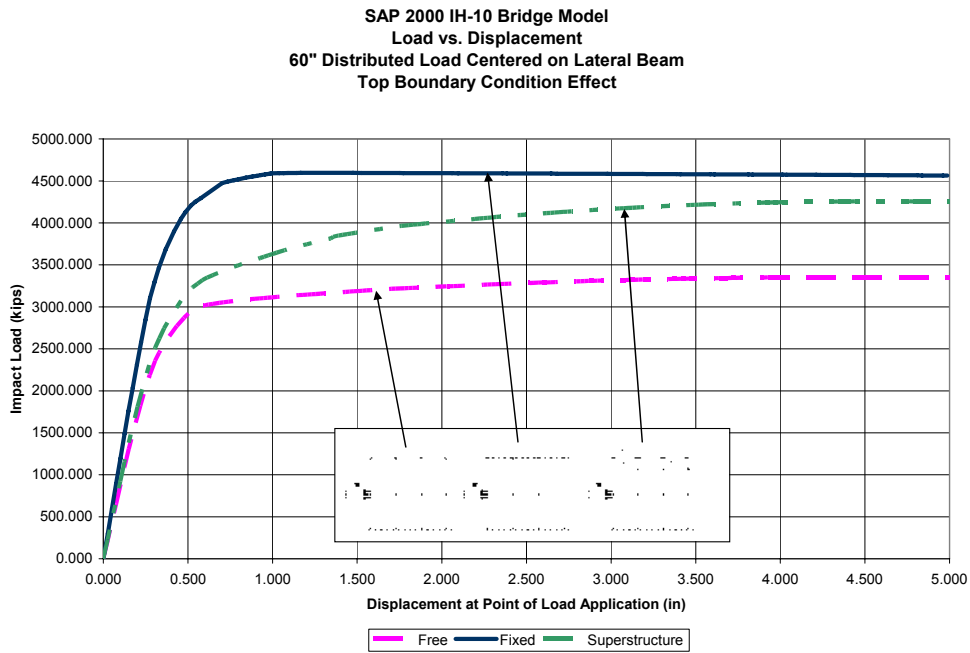
Figure 5.27: IH-10 Bridge Ultimate Strength Analysis Results-Load Location 4

The load versus displacement plots for the IH-10 Bridge model show interesting trends, and several conclusions can be drawn regarding the effect of including the superstructure when modeling a bridge for ultimate lateral strength calculation. First, there are some clear differences in the results between the models with loads applied at or around the lateral beam in the pier and those models with loads applied at some point along the column away from the beams. Results

from Load Locations 1 and 4 (Figure 5.24 and Figure 5.27) have loads applied directly at or around the location where the lateral beam frames into the column. Results from Load Locations 2 and 3 (Figure 5.25 and Figure 5.26) have loads applied along the column, away from the beams. Separate discussions for Load Locations 1 & 4 and Load Locations 2 & 3 can be found below, but first it is necessary to outline the trends that are consistent for all of the load configurations.

Considering the effect of the superstructure, all load cases show very little effect on the response in the initial linear elastic portion of the load versus displacement plots. Including the superstructure slightly increases the stiffness of the system, but it still remains close to the free top condition. In addition, the superstructure does appear to have a large effect the point of first yield. Again, a slight increase in the yield point is seen, but the superstructure results are still closer to the results from the free top case than the fixed case. The effect of the superstructure appears to increase as the model moves further into the inelastic range. For all of the results presented, including the superstructure allows the model to reach, or nearly reach, the same ultimate lateral strength as a fixed top condition. Keep in mind that adequate ductility is required for this result to occur. Table 5-5 summarizes the analysis results of the IH-10 Bridge. Results for the initial stiffness, yield strength, and ultimate strength are shown along with the percent increase as compared to the free top case.

Table 5.5: IH-10 Ultimate Strength Analysis Results

IH-10 Bridge Ultimate Lateral Strength Analysis Results Top Boundary Condition Comparison								
			Initial Stiffness (kips/in)		Yield Strength (kips)		Ultimate Strength (kips)	
Load Location	Load Description	Boundary Condition at Top of Pier	Value	% Increase (Relative to Free)	Value	% Increase (Relative to Free)	Value	% Increase (Relative to Free)
1	Point Load at Beam	Free	8523.0	-	2915.0	-	3349.0	-
1	Point Load at Beam	Superstructure	8981.0	5.4	3171.0	8.8	4301.0	28.4
1	Point Load at Beam	Fixed	11501.0	34.9	4055.0	39.1	4316.0	28.9
2	Point Load at MWL	Free	4027.0	-	1365.0	-	1608.0	-
2	Point Load at MWL	Superstructure	4447.0	10.4	1378.0	1.0	1608.0	0.0
2	Point Load at MWL	Fixed	6057.0	50.4	1525.0	11.7	1608.0	0.0
3	Point Load at HWL	Free	1985.0	-	748.0	-	1073.0	-
3	Point Load at HWL	Superstructure	2164.0	9.0	782.0	4.5	1073.0	0.0
3	Point Load at HWL	Fixed	5461.0	175.1	827.0	10.6	1073.0	0.0
4	60" Dist'd Load Centered at Beam	Free	8491.0	-	2921.0	-	3349.0	-
4	60" Dist'd Load Centered at Beam	Superstructure	8945.0	5.3	3166.0	8.4	4326.0	29.2
4	60" Dist'd Load Centered at Beam	Fixed	11509.0	35.5	4206.0	44.0	4566.0	36.3

Loads Applied Near the Beam (Load Locations 1 & 4)

Figure 5.24 and Figure 5.27 show the load versus displacement plots for the IH-10 Bridge with loads applied at or near the location of the beam. The analysis results of these models indicate that the superstructure has a significant effect on the strength of the pier, but as previously indicated, there is little change in the initial stiffness and yield point. Table 5-5 shows that for Load Location 1, there is less than a 10% change in the initial stiffness and yield point, while the increase in ultimate strength is nearly 30%. The results from the analysis with Load Location 4 are similar.

Figure 5.25 and Figure 5.26 show the load versus displacement plots for the IH-10 Bridge with loads applied away from the pier beams at some point along the column above the beam. The top exterior column is 318-inches long, measured from the beam near the middle of the pier frame up to the cap beam. Load Location 2 is 66 inches above the beam, or about one-fifth of the way up the column. Load Location 3 is 176.4 inches above the beam or just beyond the midpoint of the column. The results for these cases are summarized in Table 5-5. The results indicate that it is not necessary to consider the effect of the top boundary condition, or to even model the entire bridge pier. The ultimate lateral strength is governed almost entirely by the strength of the individual column being struck. The boundary condition at the top affects the initial stiffness and point of first yield, but the ultimate strength plateaus at the same value for all of the models.

SH-87 Bridge Analysis Results

The results presented below for the SH-87 Bridge show trends similar to the IH-10 Bridge analysis results. Figure 5.28 through Figure 5.31 show the ultimate lateral strength analysis results for four different load configurations, each with three different boundary conditions at the top of the model. The load locations under consideration have been described and shown previously in Figure 5.2. Table 5-6 summarizes the results of the analyses. Discussion of the results can again be broken down into two groups—loads applied at or around the top of the wall, and loads applied along the column.
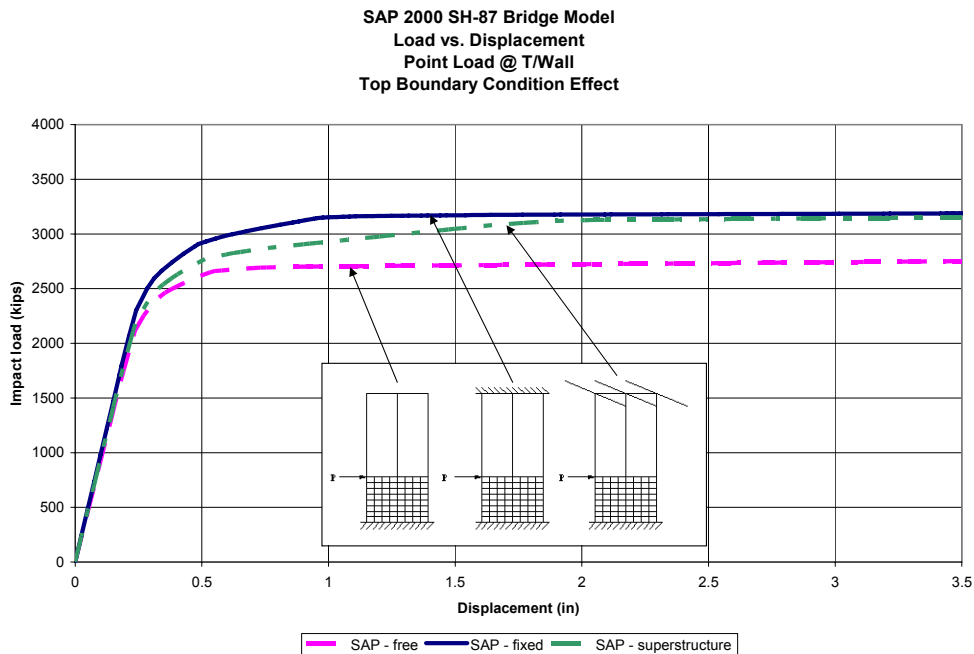
Figure 5.28: SH-87 Bridge Ultimate Strength Analysis Results 1
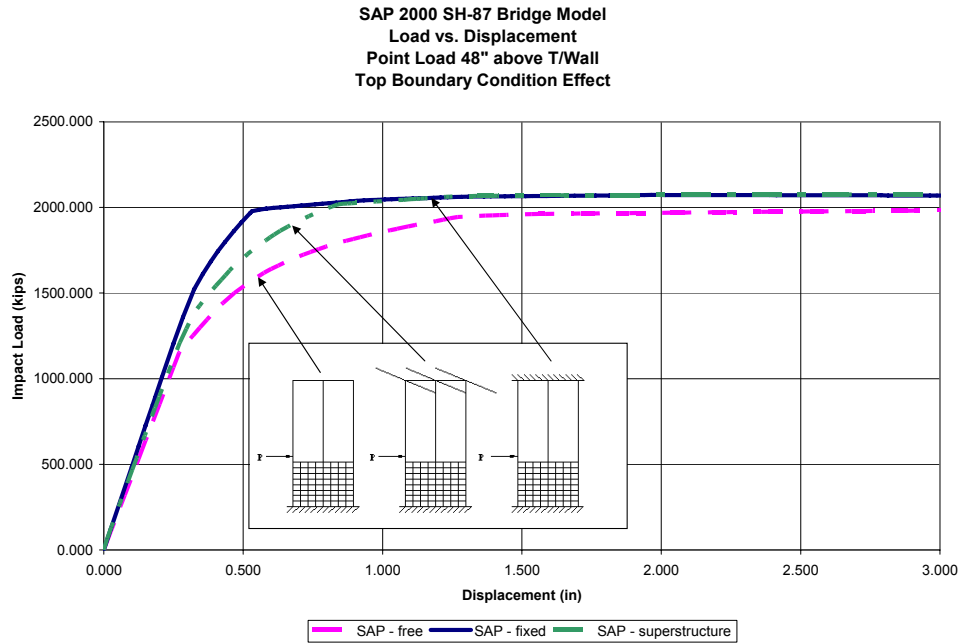
Figure 5.29: SH-87 Bridge Ultimate Strength Analysis Results 2
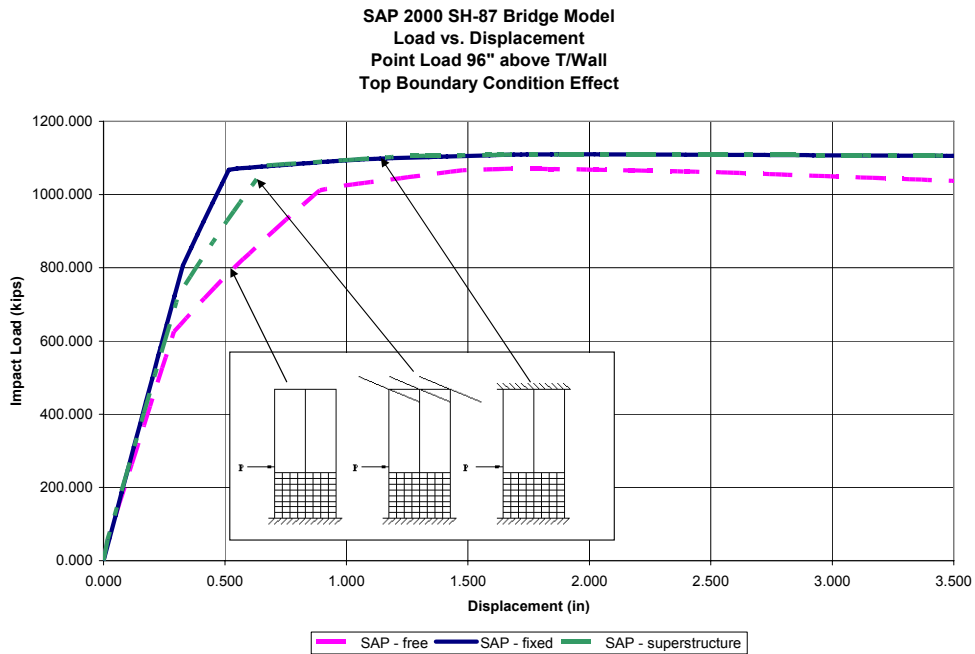
Figure 5.30: SH-87 Bridge Ultimate Strength Analysis Results 3
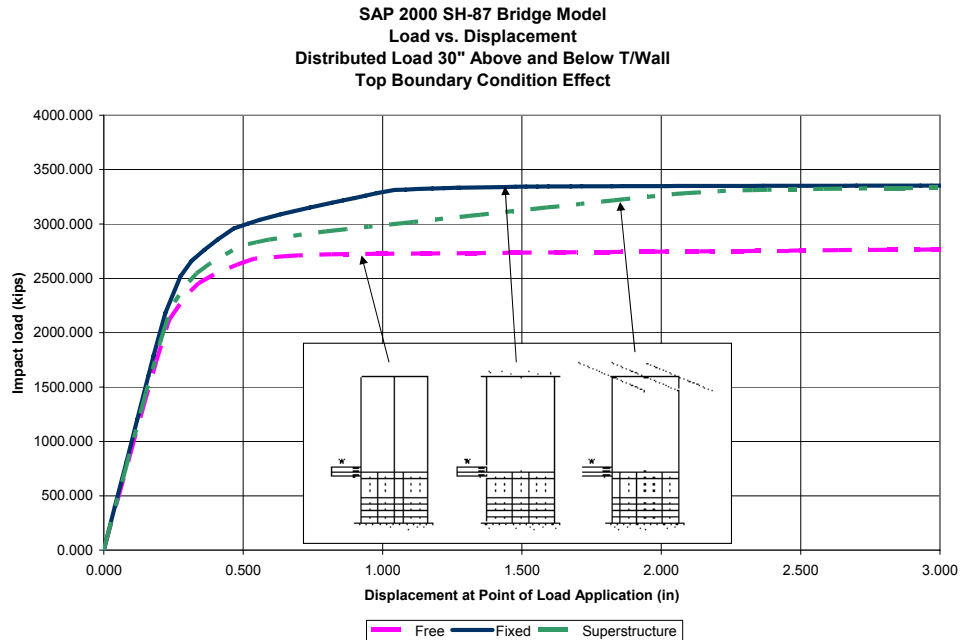
Figure 5.31: SH-87 Bridge Ultimate Strength Analysis Results 4

Table 5.6: SH-87 Ultimate Strength Analysis Results

SH-87 Bridge Ultimate Lateral Strength Analysis Top Boundary Condition Comparison								
Load Location	Load Description	Boundary Condition at Top of Pier	Initial Stiffness (kips/in)		Yield Strength (kips) (estimated)		Ultimate Strength (kips)	
			Value	% Increase (Relative to Free)	Value	% Increase (Relative to Free)	Value	% Increase (Relative to Free)
1	Point Load at Top of Wall	Free	9203.0	-	2335.0	-	2742.0	-
1	Point Load at Top of Wall	Superstructure	9410.0	2.2	2386.0	2.2	3137.0	14.4
1	Point Load at Top of Wall	Fixed	9803.0	6.5	2504.0	7.2	3185.0	16.2
2	Point Load 48" above Top of Wall	Free	4264.0	-	625.0	-	1974.0	-
2	Point Load 48" above Top of Wall	Superstructure	4450.0	4.4	724.0	15.8	2074.0	5.1
2	Point Load 48" above Top of Wall	Fixed	4849.0	13.7	806.0	29.0	2074.0	5.1
3	Point Load 96" above Top of Wall	Free	2174.0	-	1152.0	-	1070.0	-
3	Point Load 96" above Top of Wall	Superstructure	2353.0	8.2	1341.0	16.4	1107.0	3.5
3	Point Load 96" above Top of Wall	Fixed	2483.0	14.2	1523.0	32.2	1107.0	3.5
4	Distributed Load 30" above and below wall	Free	9291.0	-	2122.0	-	2765.0	-
4	Distributed Load 30" above and below wall	Superstructure	9557.0	2.9	2232.0	5.2	3322.0	20.1
4	Distributed Load 30" above and below wall	Fixed	10007.0	7.7	2518.0	18.7	3353.0	21.3

Loads Applied at, or Centered on the Top of the Wall (Load Locations 1 & 4)

The analysis results for the SH-87 models with loads at or around the wall are shown in the load versus displacement plots in Figure 5.28 through Figure 5.31 and are summarized in Table 5-6. The results show similar trends when compared to the IH-10 Bridge results for loads applied near the beam. While the geometries of the two bridges are quite different, the load locations are both located at or near the main lateral support elements in the pier. As with the IH-

10 Bridge, the SH-87 results show little increase in the initial stiffness and yield strength when the superstructure is included in the model, but there is a significant increase in the ultimate strength.

Examining the displaced shapes of the SH-87 Bridge pier at the limit state also provides insight into the behavior of the system. The displaced shape for Load Locations 1 and 4 are shown in Figure 5.32. The small dots at member ends represent locations where hinges have formed. Both models show extensive inelastic behavior throughout the system. Clearly, forces are being redistributed throughout the pier, and pier-wide response is dominating.
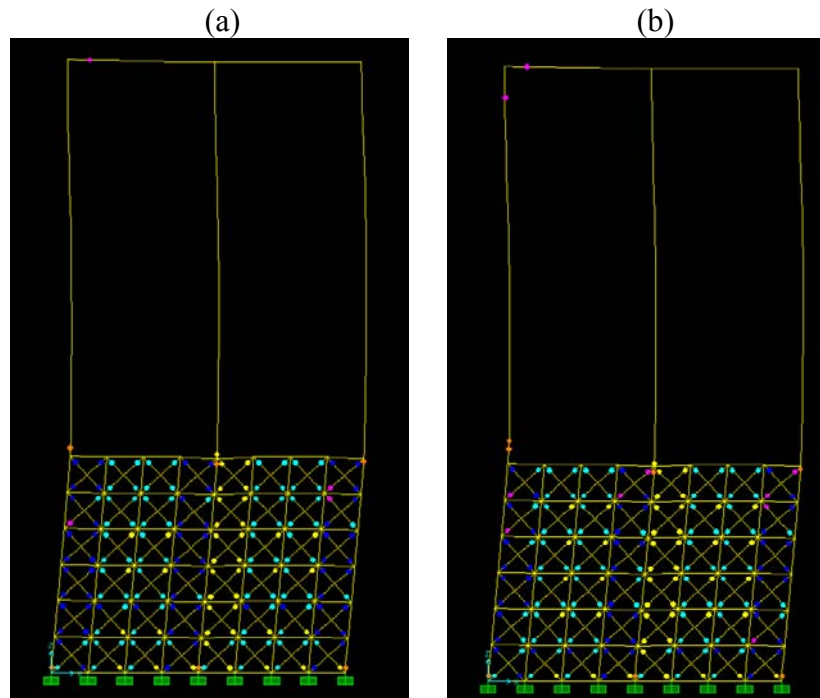
Figure 5.32: SH-87 Displaced Shape at Limit State:
(a) Load Location 1; (b) Load Location 4

Loads Applied on the Column (Load Locations 2 & 3)

The results from an analysis of the SH-87 Bridge with loads applied to the column at 48 inches and 96 inches above the wall are shown in Figure 5.29 and Figure 5.30, respectively. These plots and the results summarized in Table 5-6 show patterns that are somewhat similar to the IH-10 Bridge results for loads applied to the column. The results from both bridges show little increase in the initial stiffness of the system when the superstructure is included. Unlike the IH-10 Bridge, however, the SH-87 results show that the superstructure affects both the yield strength and the ultimate strength. This trend was also found for loads applied to the SH-87 Bridge at points higher than 96 inches above the wall. These results indicate that it is not possible to draw a conclusion on the effect of including the superstructure on the yield strength for loads applied to a column based on the analysis results presented. Further investigation into this matter is required.

Figures 5.33 and 5.34 show the model setup and displaced shape (after the ultimate lateral strength has been reached) for the SH-87 Bridge pier model for Load Locations 2 and 3,

respectively. The small dots represent locations where plastic hinges have formed. In both models, a mechanism has formed in the exterior column to which the load is being applied. There are hinges at each end of the column, as well as two hinges along the length. The hinges along the length are on each side of the point load and physically represent a single hinge location.
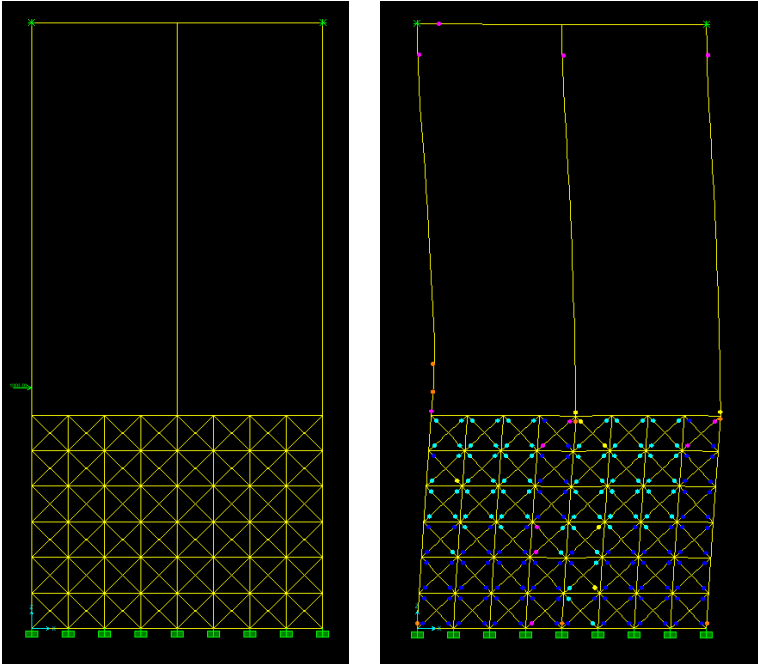
Figure 5.33: Load Location 2 Model and Displaced Shape
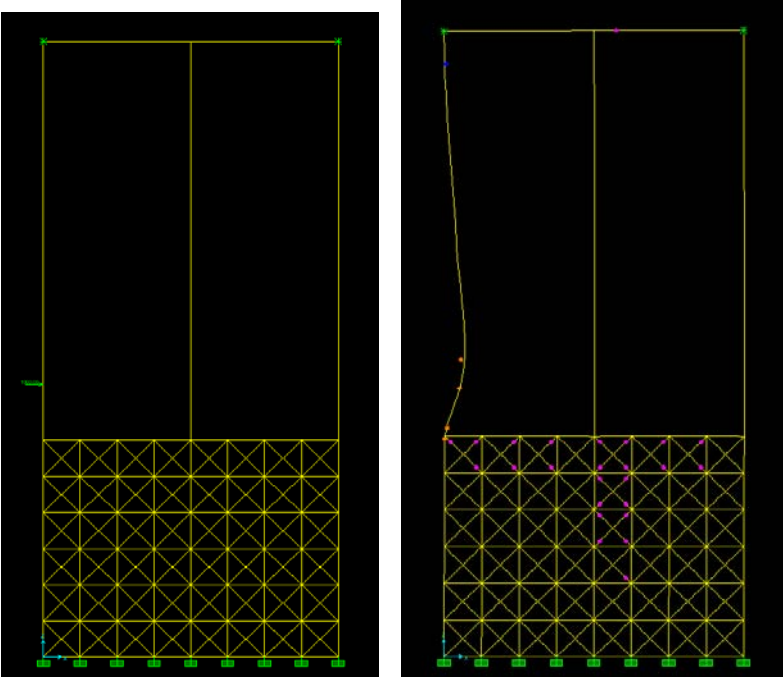
Figure 5.34: Load Location 3 Model and Displaced Shape

Load Location 2 is a point load 48 inches above the top of the wall, or about 7% up the length of the column, and Load Location 3 is a point load 96 inches above the wall, or about 14% up the length of the column. Despite the small difference in load location relative to the overall length of the column (684 inches), there is a significant difference in the displaced shapes. Figure 5.33 shows that with a point load 48 inches above the wall, there is still noticeable deformation in the wall, and the wall is clearly having a significant contribution to the response of the system. Figure 5.34 shows smaller deformations in the wall. Only a few of the truss elements have yielded by the time a mechanism has formed in the column. Figure 5.34 also suggests that it may not be necessary to consider the wall if this point is where vessel impact is expected. The response of the column clearly dominates for Load Location 3, and a simple plastic analysis of this member should provide a reasonably accurate estimate of the ultimate lateral strength of the pier. The displaced shape at the limit state for Load Location 2 looks very similar to Figure 5.32, which shows the displaced shape for Load Locations 1 and 4. The response of the system is less localized than with Load Location 3.

Summary of System-Wide Response Analyses

Despite significantly different bridge pier geometries, the IH-10 and SH-87 Bridge models show similar trends based on the load location when the effect of system-wide response is considered in an ultimate lateral strength analysis. Based on the results presented in this chapter, the following conclusions can be drawn about the effect of including the superstructure to capture system-wide response.

- *Conclusion 1:* Modeling the superstructure has little impact on the initial stiffness for all load cases considered.

- *Conclusion 2:* If impact occurs at a distance greater than 10% of the column length away from the lateral support element on a single column, local response dominates. The rest of the bridge pier has little effect on the analysis results, and a simple plastic analysis of the column would produce a reasonable estimate of the ultimate lateral strength. This conclusion assumes that there is adequate stiffness in the lateral support elements to allow a column mechanism to form, which is believed to be a reasonable assumption

- *Conclusion 3:* If impact occurs in close proximity to a lateral support element in a pier (i.e., a wall or beam), system-wide response dominates, and accurately modeling and analyzing the entire bridge pier is necessary.

- *Conclusion 4:* If impact occurs in close proximity to a lateral support element in a pier, inclusion of the superstructure in the analysis results in an increase in the ultimate lateral strength. For some cases, this increase can be significant (up to a 30% increase).

5.6.3 Reduced Section Analysis Results

Section 4.7 covered the modeling procedure to capture the effect of some loss of cross-sectional area in the regions of a bridge pier where impact is being considered. This section outlines the analysis results using the Chapter 4 guidelines for section loss modeling on the IH-10 Bridge. The same four load cases that have been used throughout this chapter are used. The superstructure and adjacent piers have been included in the model. A 10% and 20% loss of cross sectional area in the impact region are considered. Use of these values is not to suggest that they

represent the expected section loss due to impact; instead, they merely represent possible section losses. Determining these values exactly would require a detailed finite element model and dynamic analysis of the bridge pier and vessel, or some sort of physical testing, both of which are beyond the scope of this document. This section is presented to show how the ultimate lateral strength would change if the modeling procedure described in Section 4.7 was used and a section loss of 10% or 20% was assumed. Table 5-7 shows the ultimate lateral strength analysis results, including the effect of cross section loss, for the IH-10 Bridge.

Table 5.7: IH-10 Bridge Reduced Cross Section Analysis Results

IH-10 Bridge Ultimate Lateral Strength Analysis Results Affect of Cross Section Loss due to Impact					
				Ultimate Strength (kips)	
Load Location	*Load Description*	*% of Cross-Section Area Lossed*	*Boundary Condition at Top of Pier*	*Value*	*% Decrease*
1	Point Load at Beam	Full Section	Superstructure	4301.0	-
1	Point Load at Beam	10% Loss	Superstructure	4197.0	2.4
1	Point Load at Beam	20% Loss	Superstructure	4154.0	3.4
2	Point Load at MWL	Full Section	Superstructure	1608.0	-
2	Point Load at MWL	10% Loss	Superstructure	1437.0	10.6
2	Point Load at MWL	20% Loss	Superstructure	1168.0	27.4
3	Point Load at HWL	Full Section	Superstructure	1073.0	-
3	Point Load at HWL	10% Loss	Superstructure	956.0	10.9
3	Point Load at HWL	20% Loss	Superstructure	872.0	18.7
4	60" Dist'd Load Centered at Beam	Full Section	Superstructure	4326.0	-
4	60" Dist'd Load Centered at Beam	10% Loss	Superstructure	4262.0	1.5
4	60" Dist'd Load Centered at Beam	20% Loss	Superstructure	4101.0	5.2

The results shown in Table 5-7 reinforce some of the conclusions that have already been made regarding both the IH-10 and SH-87 Bridge. Table 5-7 shows that for the loads applied near the lateral support element in the pier (Load Locations 1 and 4), considering a loss of cross sectional area due to impact results in little change in the ultimate lateral strength. Because the load is applied near a lateral support element, forces can be redistributed through the system with a minimal decrease in the overall strength. System-wide behavior dominates the response. For Load Locations 2 and 3, modeling a cross-sectional area loss in the area of impact causes a significant decrease in the ultimate lateral strength. The local behavior of the column dominates the response for these two load cases, and assigning reduced section properties has a noticeable effect on the strength of the column.

5.6.4 Column Removal Analysis Results

For cases where vessel impact is expected to occur at a point along the length of the column, it may be useful to consider the effect of losing that single column on the response of the rest of the bridge. This section presents an analysis of the IH-10 Bridge and SH-87 Bridge with an exterior column removed for one of the previously outlined load cases. The results

presented here are intended to be an introductory example into this type of analysis. An in-depth investigation has not been conducted on the effect of losing a single column in a multi-column bent. While the analysis procedure and results produced in this chapter for a column removal analysis are limited, they are still important. Gaining a better understanding of system behavior after failure of a single element could allow engineers to design bridge structures that can withstand the loss of individual elements without catastrophic failure of the entire system.

IH-10 Bridge Column Removal Analysis

For the IH-10 Bridge model, a column removal analysis was performed for Load Location 3 (a point load located 476 inches above the base of the pier at the high water level). For this load case, hinges form at the column ends and at the point where the lateral load is applied. The displaced shape of the IH-10 Bridge with a mechanism formed at the point of impact was shown previously in Figure 5.16. Figure 5.35 shows the bridge pier after the column removal analysis has been performed, using the staged construction option. Notice that no hinges (represented by small dots) have formed at the end of the now cantilevered cap beam. Based on the analysis results presented here, the response suggests the remaining portion of the structure will not fail.
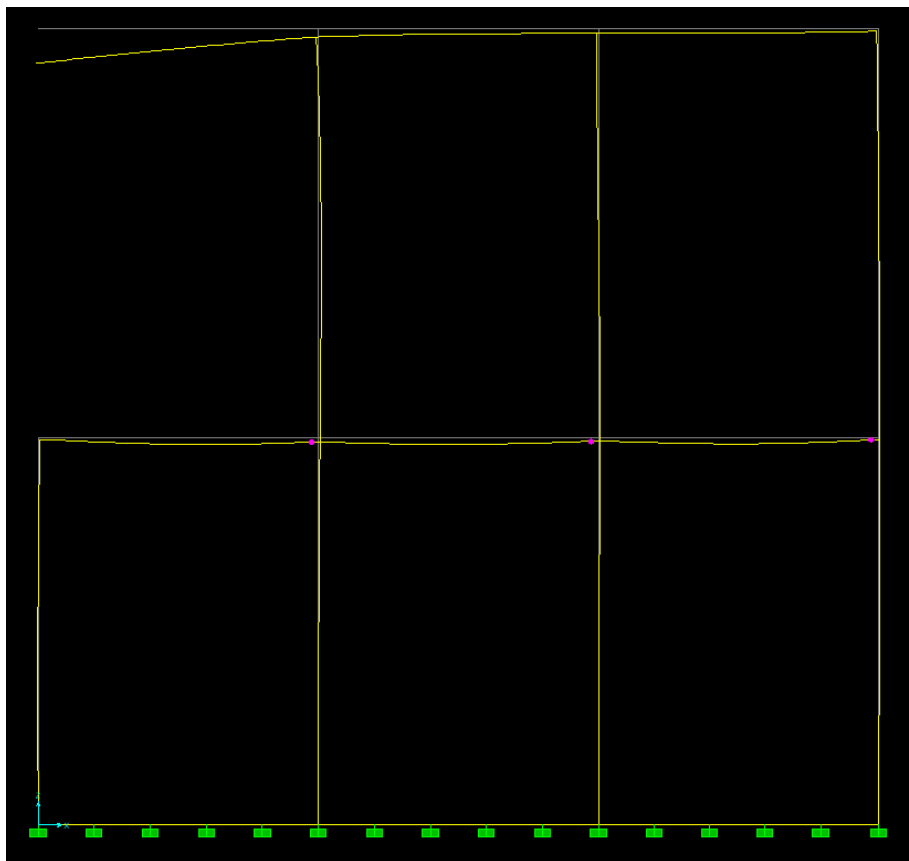
Figure 5.35: IH-10 Bridge Column Removal Analysis

SH-87 Bridge Column Removal Analysis

For the SH-87 Bridge model, a column removal analysis was also performed for Load Location 3 (a point load located 96 inches above the shear wall). For this load case, hinges form at the column ends and at the point where the lateral load is applied, creating a failure mechanism. Figure 5.36 shows the SH-87 bridge pier after the column removal analysis is performed. Notice that a hinge (represented by a small dot) has formed at the end of the now cantilevered cap beam. Figure 5.37 shows a three-dimensional view of the SH-87 Bridge after the failed column has been removed from the structure. For this case, the column removal analysis was not able to complete due to excessive deformations at the end of cap beam. Thus, it is possible to conclude that this bridge has insufficient strength and ductility to support the deck elements framing into the cap beam, and the loss of a single exterior column leads to a progressive failure in the bridge system.
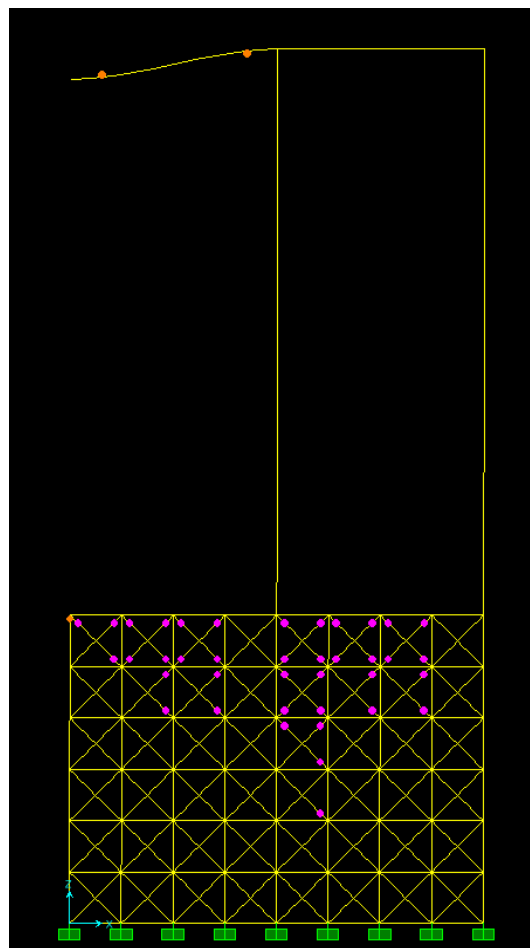
Figure 5.36: SH-87 Bridge Column Removal Analysis-1
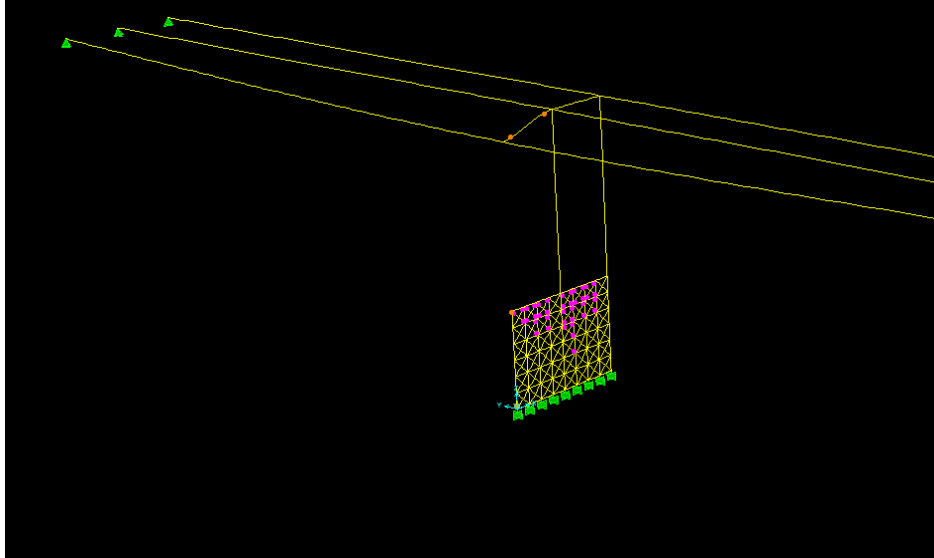
Figure 5.37: SH-87 Bridge Column Removal Analysis-2

5.7 Analysis and Results Summary

This chapter presented the analysis results of the IH-10 and SH-87 Bridge models that were constructed in Chapter 4. Several static nonlinear analysis cases, for use within SAP 2000, were outlined as a means to calculate the ultimate lateral strength of bridge elements and bridge systems. Tools for assessing analysis results were also presented. Research findings presented in this chapter demonstrated that a truss-grid model is adequate for modeling the response of bridge piers with shear walls. In addition, the effect of modeling system-wide behavior on the ultimate lateral strength was illustrated. Additional guidelines were presented to account for reduced cross-sectional areas due to impact and the failure of a single member in a multi-column bridge pier. Chapter 6 summarizes the work in this document and reviews the major conclusions that were drawn based on the research completed for TxDOT Project 0-4650.

6. Summary and Conclusions

6.1 Introduction

This document has investigated the problem of vessel collision with bridges and has attempted to provide engineers with useful tools to deal with this issue by examining the calculation of the ultimate lateral strength of bridges subject to impact loads. The importance of considering vessel impact loads for bridges over navigable waterways was illustrated by showing the consequences of vessel collision accidents with bridges using specific examples from the last twenty-five years. A thorough review of the events, groups, and research work that lead to the development of the *AASHTO Guide Specification for Vessel Collision Design of Bridges* was provided. In addition, a detailed review and critical examination of the AASHTO Guide Specification was made. Several areas in need of improvement for the AASHTO recommended Method II design procedure were identified. Calculation of the Probability of Collapse term was emphasized as an area in need of examination. This calculation is based on the impact load from a vessel and the ultimate lateral strength of a bridge element. AASHTO provides little guidance in the calculation of the ultimate lateral strength and does give any consideration to the strength of bridge system as a whole.

6.2 Summary of Work

The research in this report has focused on the modeling and analysis of bridge piers and bridge systems subject to impact loads. Chapter 4 focused on the modeling of these systems, and Chapter 5 presented results from the analyses of those models. One of the primary goals of this report has been to provide easy-to-use guidelines and procedures to calculate the ultimate lateral strength of these structures using typical structural analysis software packages. Reinforced concrete bridge piers, both with and without shear walls, were investigated. Guidelines for modeling reinforced concrete using a smeared material model based on a sectional analysis were presented. The use of plastic hinges to capture the inelastic behavior in bridge systems was discussed. A truss-grid model was introduced to capture the inelastic response of shear walls in a bridge pier. Modeling examples for two representative bridges from Texas, the IH-10 Bridge over the San Jacinto River and the SH-87 Bridge over the Gulf Intracoastal Waterway, were shown using SAP 2000, a typical structural analysis program.

Additional work focused on investigating the effect of system-wide bridge response to impact loads. Further guidelines outlined a procedure to account for a reduced section size in the regions of a bridge pier where vessel impact occurred. Analysis methods to capture the response of a multi-column bridge pier, given the failure of a single column, were also introduced.

Several conclusions were reached based on the results presented in Chapter 5, and they are summarized below. For a more detailed discussion, refer to Chapter 5.

6.2.1 Important Conclusions Based on Ultimate Lateral Strength Analysis Results

Modeling Conclusions

- *Truss-Grid Model.* A comparison of two models of the same SH-87 Bridge pier, one built in SAP-2000 using a truss-grid model for the wall and the other built in

ANSYS using shell elements for the wall, showed similar load versus displacement responses for a range of load locations and boundary conditions. Based on these results, it is believed that the truss-grid model outlined in Chapter 4 can capture the inelastic response of a shear wall with acceptable accuracy for the purposes of design.

- *Localized Response.* Results from Chapter 5 showed that, for loads applied along the length of a column away from lateral support elements, the response of an individual column controlled the ultimate lateral strength, and extensive modeling of the entire structure is not required. Based on the IH-10 and SH-87 Bridge results, it is suggested that a simple plastic analysis on a column is appropriate if the impact load is being applied at a point greater than 10% of the column length away from a lateral support. For both bridges, the lateral support elements at the top and bottom of the column provide enough stiffness so that a mechanism can form in the column. Given the differences in geometry between the piers of the IH-10 and SH-87 Bridges, it is believed that this rule could be applied across a variety of bridge piers

- *Pier-Wide Response.* When impact loads were considered at or near locations of beams or walls providing lateral support for a pier, forces were distributed throughout the entire bridge pier and inelastic response spread through the structure.

System-Wide Response Conclusions

- *Initial Stiffness.* Including elements to represent the bridge superstructure and modeling adjacent bridge piers had little effect on the initial response of a bridge system subject to lateral loads.

- *Point of First Yield.* The effect of including elements to represent the bridge superstructure and of modeling adjacent bridge piers on the initial strength of the bridge system varied. For the IH-10 Bridge, little change in the initial strength was found when the superstructure was modeled; however, a slight increase in the yield point was seen in the SH-87 Bridge.

- *Ultimate Lateral Strength.* For cases where impact loads acted at or near lateral support elements, including the bridge superstructure and adjacent bridge piers had a noticeable effect on the ultimate lateral strength of the bridge systems being studied. For cases where impact loads were applied along the length of a column, the top boundary condition had little impact on the ultimate lateral strength of the systems considered.

It is also important to note the limitations of the models and procedures presented in Chapters 4 and 5. These issues have been addressed previously and are summarized below:

- *Local Response of Wall.* The truss-grid model has been shown to accurately capture the overall response of a shear wall in a bridge pier. However, because of the rigid grid, inelastic behavior is spread through the truss elements more evenly than in a real wall, which would see more localized damage near the point of impact.

- *Base Boundary Condition.* A fixed condition was assigned to the base of the bridge pier models. In reality, these structures have some flexibility at the base. By

accurately modeling the soil-structure interaction, a better representation of the base condition can be made.

- *Material Model.* This report focused on reinforced concrete bridge piers. Instead of modeling the concrete and steel directly, a smeared material model approach was taken. In doing so, a level of ductility was assumed for all of the members, which in turn assumed that the bridge pier elements were properly detailed. This assumption greatly simplified modeling and analysis of the bridge piers, but a more accurate representation of the material is possible.

- *Limited Results.* One of the clear limitations of the research contained in this report is that results have been presented for only two bridges. The IH-10 and SH-87 Bridges were selected because they are representative of bridge piers found in Texas. While they did provide the opportunity to examine two different bridge pier geometries, investigating more bridges would likely allow further and more distinct conclusions to be drawn on the issues addressed in this report.

6.3 Integration with Other Research to Improve AASHTO Vessel Collision Design Specifications

This report is one part of a larger research project undertaken at the University of Texas at Austin. Another aspect of this research, conducted by Adam Cryer under the supervision of Dr. Loukas Kallivokas, investigated actual loads imparted to a bridge from barge impact. The probability of collapse term in the AASHTO Method II is based on the impact load and the ultimate lateral strength. With improved understanding of bridge strength provided in this report and a more accurate determination of loads imparted during a vessel impact (Volume II of this report), a critical examination of the probability of collapse term can be made. This work was part of the third aspect of the research that was completed by Kenny Berlin under the supervision of Dr. Lance Manuel (and discussed in Volume I of this report).

6.4 Future Research Opportunities

Vessel collision design is an evolving field. The first design code in the United States was not introduced until the early 1990s. Implementation of the AASHTO recommended Method II design procedure has been slow, and many states lack access to the necessary information to effectively use this procedure in designing and analyzing bridges subject to vessel collision. Furthermore, little physical testing has been done to investigate the mechanics of vessel impact on bridges, mostly due to the impractical nature of testing full-scale vessel-bridge impact. In short, there exists a wide range of future research opportunities that could be explored in order to improve bridge design for vessel collision in the United States. This section outlines some of these areas, with a focus on how the research presented in this document could be expanded.

One area for future research would be to repeat the same analyses presented in Chapter 5 over a wider range of bridge types. Different pier geometries should be considered. In addition, a more thorough investigation into the effect of including superstructure elements in an analysis could be conducted by considering a range of deck and girder types and configurations. Loading types and locations could also be carried out across a wider range. A more accurate model for reinforced concrete could also be developed for use in the analyses presented in this report. In addition, future research could focus on determining the effect of soil-structure interaction and behavior during vessel impact, in order to better model bridge pier base conditions. The research

possibilities outlined here could lead to more detailed guidelines and rules for calculating ultimate lateral strength of bridges.

Several other areas of possible research were discussed in this report, but not investigated fully. For example, the basics of a column removal analysis were outlined, but this research was limited. A more detailed look into progressive collapse of bridge elements or bridge systems could yield valuable information. Research into the mechanics of vessel-bridge impact, through physical testing or detailed finite element modeling, could lead to a better understanding of the dynamic effects of vessel impact and could produce guidelines on how much damage impact causes on bridge pier sections. This research would also provide information for dynamic load cases that could be applied to bridge models.

6.5 Final Remarks

This report has outlined modeling and analysis procedures that can be used to calculate the ultimate lateral strength of bridge elements and systems. It is the hope of the author that the methods and tools presented in this document will assist engineers in designing or analyzing bridge piers and bridge systems that are subject to vessel collision so that the catastrophic accidents of the last 25 years are not seen in the future.

References

AASHTO, (1991). *Guide Specification and Commentary for Vessel Collision Design of Highway Bridges*, American Association of State Highway and Transportation Officials, Washington, D.C.

AASHTO, (2004). *LRFD Bridge Design Specifications*, American Association of State Highway and Transportation Officials, Washington, D.C.

ACI 318-02, (2002). *Building Code Requirements for Structural Concrete and Commentary*, American Concrete Institute, Farmington Hills, MI.

ASCE, (1999). *Structural Design for Physical Security State of Practice,* American Society of Civil Engineers, Reston, VA.

Bentz, E.C., Collins, M.P., (2001). *RESPONSE-2000 User Manual*, University of Toronto, Toronto, Ontario Canada.

Consolazio, G.R., Cowan, D.R., (2003). "Nonlinear Analysis of Barge Crush Behavior and its Relationship to Impact Resistant Bridge Design", Computers and Structures, Vol. 81, No. 8-11, 547-557.

Consolazio, G.R., Cowan, D.R., Biggs, A., Cook, R.A., Ansley, M., Bollmann, H.T., (2005). "Full-Scale Experimental Measurement of Barge Impact Loads on Bridge Piers", Transportation Research Board (TRB) Annual Meeting CD-ROM, Washington, D.C.

FEMA 302, (1997). *NEHRP Recommended Provisions for Seismic Regulations for New Buildings and Other Structures*, Federal Emergency Management Agency, Washington, D.C.

Fujii, Y., (1978). "The Estimation of Losses Resulting from Marine Accidents", Journal of Navigation, Vol. 31, No. 1, 117-125.

Knott, M., Prucz, Z., (2000). *Vessel Collision Design of Bridges: Bridge Engineering Handbook*, CRC Press LLC, Washington D.C.

Liu, C. and Wang, T., (2001). "Statewide Vessel Collision Design for Bridges", Journal of Bridge Engineering, ASCE, Vol. 6, No. 3, 213-219.

Moehle, J.P., (1992). "Displacement-Based Design of RC Structures Subjected to Earthquakes", Earthquake Spectra, Vol. 8, No. 3, 403-428.

Modjeski and Masters Consulting Engineers, (1984). *Criteria For: The Design of Bridge Piers with Respect to Vessel Collision in Louisiana Waterways*, Prepared for the Louisiana Department of Transportation and Development and the Federal Highway Administration, Harrisburg, PA.

Patev, R.C., (2005). "Development of USACE Engineering Guidance for the Barge Impact Design of Navigation Structures", Transportation Research Board (TRB) Annual Meeting CD-ROM, Washington, D.C.

SAP 2000, (2002). *SAP 2000 Analysis Reference Manual,* Computers and Structures, Inc., Berkeley, CA.

TxDOT*, (2001). *Bridge Design Manual*, Texas Department of Transportation, Austin, TX.

TxDOT, (1969). Intracoastal Canal Bridge State Highway 87 Construction Plans, Texas Department of Transportation.

Whitney, M.W., Harik, I.E., Griffin, J.J., Allen, D.L., (1996). "Barge Collision Design of Highway Bridges", Journal of Bridge Engineering, ASCE, Vol. 1, No. 2, 47-58.

Data Collection for the Model for Vessel Impact on Bridges

Michael Bomba

Table of Contents

List of Tables

Chapter 1. DATA COLLECTION FOR THE MODEL FOR VESSEL IMPACT ON BRIDGES

The following sections describe the methodology used to collect relevant data on waterways, vessels, and bridges for this research project. The focus was on data related to thirty-one Texas Department of Transportation (TxDOT) bridges that span the Gulf Intracoastal Waterway (GIWW) as well as a number of inland waterways including the Houston Ship Channel, the Neches River, and the Victoria Barge Canal.

In an internal study previously undertaken, TxDOT engineers relied upon contacts within the barge industry to self-report their vessel activity. During the first meeting for this project, TxDOT personnel suggested that the researchers also use this methodology for collecting the project data. The researchers made some initial attempts to collect data in this manner and quickly concluded that it would not lead to the level of detail required for the model for several reasons. First, there are literally hundreds of thousands of barge movements along the Texas portion of the GIWW and the state's inland waterways each year. Although a few large barge operators account for the majority of these movements, there are hundreds of smaller operators that also make up a large number of the total trips. Second, when the project was discussed with barge operators, they generally were not interested in contributing to this study. Third, port operators were originally thought to be a rich source of information on barge movements, but this turned out not to be the case. When ports were able to provide data on barge activity, it was very generalized and inadequate for the researchers' use. Finally, collecting information from the individual operators would be-time intensive and beyond the resources allocated for this project

Given these limitations, the researchers chose to gather the vessel movement data from a source that was precise and reproducible, which was a vessel dataset obtained from the U.S. Army Corps of Engineer's (hereafter referred to as the "Corps") Waterborne Commerce Statistics Center (WCSC), which collects and releases data on domestic shipping movements in aggregated form. Because this study required data that are not normally released to the public, a special request was made to the appropriate office of the WCSC. It should also be noted that the WCSC was the provider of the data for the Florida vessel-bridge collision study. The responsible personnel at the WCSC for this information are listed below and Ms. Peggy Galliano should be the first person contacted if there are future data requests. See Attachment 1 to this memorandum for the layout of the data provided by the Corps.

Ms. Peggy Galliano
Waterborne Commerce Statistics Center
U.S. Army Corps of Engineers
7400 Leake Avenue
New Orleans, LA 70118
Phone: (504) 862-1424
Fax: (504) 862-1423
E-Mail: Peggy.A.Galliano@mvn02.usace.army.mil

Mr. James Lambert
Waterborne Commerce Statistics Center
U.S. Army Corps of Engineers
P.O. Box 61280
New Orleans, LA 70161-1280
Phone: (504) 862-1465
E-mail: james.j.lambert@USACE.ARMY.MIL

The data provided by the Corps gives a description of every vessel passing a mile marker on the GIWW during 2002, including the number of trips made by the vessel. In the case of inland waterways, the data provided movements for entire waterway and not for any particular point. Vessels are described as ships, towboats, and barges. All vessels in the dataset are domestic vessels and data for foreign vessels were not collected for this study.

The Corps was unable to provide data for each of the requested thirty-one bridges, simply because the data are not collected and/or reported at many of these points. Data were available for each of the bridges crossing the GIWW, but not for many of bridges crossing inland waterways, even at major facilities. Table 1.1 provides a list of the bridges for which the Corps was unable to provide data. Project resources did not permit an attempt to build a dataset for the missing bridges. During the study, TxDOT also asked the researchers to request data for every mile marker along the GIWW. This request was passed along to the Corps, but the data was not readily available.

Table 1.1: Bridges without Vessel Movement Data from the U.S. Army Corps of Engineers.

Bridge No.	Roadway	Water Body
1	S.H. 288	Dow Barge Canal
2	S.H. 36	Brazos River
5	F.M. 523	Dow Barge Canal
9	S.H. 146	Dickinson Bayou
13	S.H. 146	Clear Creek Channel
15	I.H. 10	Mouth of the San Jacinto River
17	S.H. 35	Victoria Barge Canal
20	F.M. 521	Colorado River
21	U.S. 181	Corpus Christi Ship Channel
28	S.H. 82	Mouth of the Sabine River
29	I.H. 10	Neches River

In addition to being unable to obtain data for these bridges from the Corps, in a few cases, it did not appear that barges passed beneath the bridges at all. The crossing of the Clear Creek Channel by S.H. 146 is one example. While there is a substantial amount of vessel traffic from Clear Lake into Galveston Bay, after examining digital aerial photography of the location, all of this traffic appears to be recreational boats. There is also a very sharp turn in the channel that would make navigating it with one or more barges very difficult. Further north on S.H. 146, where the roadway crosses Dickinson Bayou, there is a similar situation. A review of the digital aerial photography and a visit to the site in July 2004 did not reveal any commercial barge traffic to the east of the bridge, although there were several commercial facilities to the east that could generate barge traffic. However, none of these facilities would require a vessel to pass underneath the bridge. There is also a parallel rail bridge with a relatively narrow opening that would make it difficult for barge groups to navigate through. In other cases, it was unclear whether a bridge even had piers in the water with which a barge could collide, such as where I.H. 10 crosses the Neches River.

Barges
Among other pieces of information, the WCSC dataset provided information on barge sizes, types, length, width, loaded and unloaded draft, tonnage capacity, number of trips, and whether it was loaded or unloaded. Although the Corps data did not provide any information on the vessels empty displacement, it did provide information on its cargo capacity in tons. The empty displacement for barges was estimated using the equation from the American Association of State Highway and Transportation Officials (AASHTO) guidelines and the block coefficient value assumed to be 0.861.

All data for the individual barges was categorized according to Table 1.2 below. A review of the barge data tables revealed a wide variety of possible barge dimensions, even if the lengths of the barges were the same. This is because barge sizes are not standardized in any meaningful way and barge builders frequently custom build barges for clients or use their own design. Thus, while a 195-foot dry cargo barge may be the standard length for a jumbo hopper barge; this does not mean that all 195-foot jumbo hopper barges will have identical dimensions. Thus, the barges in the dataset were placed into one of four categories, according to size, so that the dataset could

be used with the existing model. These four categories are small, standard, jumbo, and oversize and barges were assigned to one of these classifications according to their total length.

Table 1.2: Categorization of Barge Data

Barge Type	Barge Size	Barge Length	Barge Type	Barge Size	Barge Length
Dry Cargo	Small	62' to 174'	Tanker	Small	62' to 174'
Dry Cargo	Standard	175' to 194'	Tanker	Standard	175' to 194'
Dry Cargo	Jumbo	195' to 199'	Tanker	Jumbo	195' to 199'
Dry Cargo	Oversize	200' or more	Tanker	Oversize	200' or more

Because there was a wide range of possible barge dimensions (length, width, draft, etc.), the barges were reduced to the eight categories shown in Table 1.3.   The assumed length, width, empty draft, loaded draft, empty displacement, and loaded displacement for each category was based upon a weighted average (based upon the number of total trips) of barges within each category. The final assumed values of these variables are shown in Table 1.3.

Table 1.3: Assumed Barge Characteristics

Type	Size	FEET				TONNAGE	
		Length	Width	Empty Draft	Loaded Draft	Empty Displacement	Loaded Displacement
Dry Cargo	Small	67	32	2	9	105	530
Dry Cargo	Standard	178	48	2	10	428	2,458
Dry Cargo	Jumbo	198	35	2	9	337	2,350
Dry Cargo	Oversize	272	53	2	11	720	4,076
Tanker	Small	149	47	2	9	352	2,023
Tanker	Standard	181	49	2	9	449	2,212
Tanker	Jumbo	196	36	2	9	346	1,904
Tanker	Oversize	284	53	2	11	830	5,096

Not all of the data requested was available from the WCSC dataset. For example, the documentation of the model distinguishes between different types of dry cargo barges, such as deck barges and hopper barges. Because the Corps data did not make any distinction between these two types, it simply reported all dry cargo barges as "Dry Cargo". Similarly, there was not distinction for different types of tanker barges; all were reported as "Tanker". The WCSC also did not report vessel speed; therefore, after conversations with an industry expert, the assumption was made that all vessels operated at 5 miles per hour in either the GIWW or one of the inland waterways (Butler, 2005). Additional information was requested for the depth of the vessel, depth of the bow, bow rake length, head log capacity, and cargo capacity. However, with the exception of cargo capacity, no data were provided by the Corps for any of these variables and the researchers could not identify any reliable method of estimating these values.

Towboats
As with the barge data, the WCSC dataset provided information for several required variables of the towboat data, such as vessel length, width, and draft. However, two important pieces of information were missing: towboat horsepower and tonnage displacement, hence, the researchers were required to arrive at an estimation of these values.

The first step to estimating the horsepower variable was to build a database of all towboats operating within the Texas segment of the GIWW. This was done by assembling and merging two datasets from the Corps. The first dataset was formed by identifying all towboat operators who reported that they provide service in the Texas segment of the GIWW or one of the inland waterways. Unfortunately, Gulf of Mexico operators and Mississippi River operators are within the same dataset, so the relevant operators had to be chosen manually, based upon a field that described their area of operation. It was important not to use data from operators along the Mississippi River, because they often use significantly larger towboats than do Texas GIWW and inland waterway operators. The second database was developed by extracting all towboats that are based in Texas. The two databases were merged and redundant observations were removed. The final database was then sorted and grouped by towboat length. The average horsepower of all towboats within each foot increment was used to estimate the horsepower of all towboats (See Table 1.4). Prior to this exercise, explanatory statistics were used to determine that vessel length was the single most important factor to predict towboat horsepower. The tonnage displacement of towboats was based upon the previously referenced equation in the AASHTO guidebook, using a block coefficient of 0.612.

Table 1.4: Assumed Towboat Characteristics

Type	Horsepower	Length	Width	Draft	Displacement
Harbor Boat	502	44	17	7	84
Line Haul	808	54	22	7	136
Line Haul	956	60	23	7	176
Line Haul	1369	68	26	7	233
Line Haul	1737	82	28	8	318
Line Haul	2122	83	29	8	341
Line Haul	3395	102	32	11	652
Line Haul	8141	144	36	12	1,103

Barge Groups

The data describing the movement of barges and towboats in the GIWW was unavailable from the Corps. Because of this limitation and because data for the configuration of barge groups is absolutely necessary to use the model, the researchers developed a Monte Carlo-based matching program, which randomly assigns barge trips to towboat trips at each bridge (Users should note that because the barges and towboats are randomly assigned to each other, it could take thousands or even millions of subsequent attempts to reproduce the exact dataset). The program, written in QuickBASIC, rapidly reads in datasets of barge and towboat trips, matches them according to five rules that are exogenously entered by the user, and writes an output file that shows a simulated configuration of all barges and towboats. These five rules were developed after multiple discussions with the project engineers and an industry expert and are as follows:

1. All barges within a barge group are of the same type (dry cargo or tanker)
2. All barges within a barge group are the same size (small, standard, jumbo, or oversize)
3. All barges within a barge group are either loaded or empty
4. Barge groups can exist in one of four configurations: a single barge, two barges side by side, two barges end to end, and four barges—two by two. All barge groups only have one towboat

5. There are minimum horsepower requirements for the towboats moving a two-barge barge group and a four-barge barge group.

Rules 1, 2, and 3 were requested by the project engineers so that the dataset would be compatible with the existing collision model. Rules 4 and 5 were based upon discussions with the industry expert who advised the researchers on the most likely pairing of towboats and barges[1]. The suggested percentage breakdown of the four configurations of barge groups were: 5 percent single barge, 70 percent for two barges, and 25 percent for four barges. It was also suggested that 30 percent of the two-barge groups would be side by side while 70 percent would be end to end. A towboat's horsepower determines the number of barges that can be safely pushed, therefore, it was suggested that two-barge groups be pushed by a towboat with at least 1,200 horsepower and four-barge groups be pushed by a towboat with at least 1,800 horsepower.

One important assumption that the matching program makes is that all available barge trips will be used. In other words, every barge will be matched with a barge group so that after the match program has finished, there are no remaining barge trips. Unfortunately, the assumed barge configurations sometimes resulted in a large number of unused towboat trips. Another limitation to the program is that sometimes it is not possible reach a solution using all five of the rules listed above. When this occurs, the user will have to relax the assumptions of Rules 4 and 5 so that the program can reach a solution. The program does not provide any guidance on how these rules should be relaxed and so the user must simply use trial and error until a solution is reached.

To match the barges with the towboats, users must run the Corps data in two or three groups, according to the water body. If the mile marker is on the GIWW, then the Corps reports the vessel data as either upbound or downbound and so two groups of data are produced. The matching program must allocate the data for each direction separately since, for example, it would not be possible for a downbound towboat to push upbound barges. In the case of inland waterways like the Houston Ship Channel or the Neches River, the Corps reports the vessel traffic in three categories: local, shipping, and receiving. The output of these three categories was later combined to produce "upbound" and "downbound" datasets at the request of the project engineers.

The program produces two output files. The first file describes the various barge groups. The second file describes the unmatched towboats. Both of these files are necessary to describe the vessel fleets that pass beneath a bridge. The first file is also used to produce detailed descriptions of the barge group characteristics. The program output does not occur in the format that can be immediately entered into the MathCAD program so a second program was developed using SAS to summarize and reformat the data so that they can be used in the collision model. While the matching algorithm is an imperfect solution to the problem of unmatched barges and towboats, the researchers concluded that there was no other opportunity to develop a solution to this problem.

Ships
Many, if not the vast majority, of ships passing underneath the bridges along important inland waterways like the Houston Ship Channel and the Neches River are foreign flagged ships, which

---

[1] Raymond Butler. Executive Director – Gulf Intracoastal Canal Association. 2004. Personal communication.

are not included in the WCSC database. The omission of foreign flagged ships in the GIWW is less of a problem, because its depth and width constrain the size of ship that could safely operate within it. However, since most foreign ships operating within the deeper ship channels are large bulk carriers or container ships, it is likely that this missing data has some effect on the model results and underestimates the risk and, possibly, the consequences of a vessel-bridge collision.

The model requires a number of vessel characteristics, such as a ship's ballasted drafts at the stern and bow, which were not provided in the WCSC data. A review of various sources did not reveal any means of calculating these variables with the available data. Therefore, as a simplifying assumption, each ship was assigned the characteristics given for a typical dry bulk or tanker ship in the AASHTO documentation. Ships were assigned the maximum characteristics of the data range. In other words, ships of less than 1,000 deadweight tonnes (DWT) were assigned the typical characteristics of a 1,000 DWT ship, while ships between 1,000 DWT and 3,000 DWT were assigned the typical characteristics of a 3,000 DWT ship and so on.

Digital Aerial Photography
Although it was not identified in the project proposal as a data need, digital aerial photography was obtained for each of the thirty-one bridges identified for this study. This data was useful in a number of ways. First, it was necessary to have some type of basemap to identify which mile markers along the GIWW would be used for the data request. The mile marker coordinates can be downloaded from the Corps website (See link below), but they must then be imported into a GIS program like ArcGIS, so that the desire markers can be identified. Second, the aerial photography gives the researcher some information about vessel traffic in the area surrounding the bridge and whether other nearby channels could contribute barge traffic. The data can be downloaded from the Texas Natural Resource Information System's website (See link below). The data are available in a range of resolutions, but the 1.0 meter resolution is probably most appropriate, since it provides the greatest amount of detail. To reduce the size of the digital files, they have been compressed into a format called "MrSID". Unfortunately, with earlier versions of this program, a noticeable amount of detail is lost from the compression but they are still adequate for this project. Once downloaded, the compressed files must be viewed using ArcGIS or a MrSID viewer.

http://www.iwr.usace.army.mil/ndc/data/dictionary/ddmile.htm

www.tnris.state.tx.us/digital.htm

Water Current Data
The availability of current data for points along the GIWW was extremely limited but as many points as possible were collected from existing sources (See Table 5). The Texas Water Development Board (TWDB) collected current data for various points in bays and estuaries located along the Texas Gulf Coast, between 1988 and 2003 (See link below). With the exception of a measurement site near the Queen Isabella Memorial Causeway, all the current meters reported data along one axis, which was the parallel current. The TWDB reported the meter readings in feet per second but this measure was converted into miles per hour. The original data was also reported as positive and negative values to indicate the direction of the flow. The estimates of parallel current velocities provided in Table 1 of the dataset were

calculated by finding the absolute value of each observation and dividing it by the total number of observations. This produced an average speed of the current over the observed period. The TWDB usually provided the data for various depths of each channel so the researchers used the shallowest reported depth for the current estimates. This allowed the potential effects of the water currents on unloaded barges to be captured.

http://hyper20.twdb.state.tx.us/data/bays_estuaries/surveypage.html

Table 1.5: Sources of Water Current Data from the Texas Water Development Board

Bridge No.	Roadway	Water Body	Study	Meter Site	Data Period
3	S.H. 322	GIWW	1992 Christmas Bay Study	GIWW near Surfside	06/12/92-06/15/92
8	S.H. 124	GIWW	1989 Galveston Bay Study	GIWW near Oyster Bayou	05/07/89-05/10/89
10	I.H. 45	GIWW	1989 Galveston Bay Study	GIWW at I.H. 45 Causeway	05/07/89-05/10/89
11	U.S. 90-A	Houston Ship Channel	1989 Galveston Bay Study	Houston Ship Channel at Baytown Tunnel	05/07/89-05/10/89
12	Loop 610	Houston Ship Channel	1989 Galveston Bay Study	Houston Ship Channel at Baytown Tunnel	05/07/89-05/10/89
14	F.M. 146	Houston Ship Channel	1989 Galveston Bay Study	Houston Ship Channel at Baytown Tunnel	05/07/89-05/10/89
16	Loop 8	Houston Ship Channel	1989 Galveston Bay Study	Houston Ship Channel at Baytown Tunnel	05/07/89-05/10/89
18	F.M. 2031	GIWW	1993 Matagorda Bay Study	GIWW East of Matagorda	06/12/93-07/03/93
22	P.R. 22	GIWW	1995 Upper Laguna Madre Study	JFK Causeway at GIWW	06/12/95-06/15/95
23	S.H. 361	GIWW	1995 Aransas Bay Study	GIWW near Cove Harbour	09/29/95-10/01/95
30	Queen Isabella Memorial Causeway	GIWW	1997 Lower Laguna Madre Study	Queen Isabella Causeway	06/19/97-06/22/97

Source: Texas Water Development Board, 2005.

Traffic Density Data

The AASHTO documentation provided little guidance into what constitutes light, medium, and heavy vessel traffic. Most of the bridges in the study have either high volumes of barge traffic, many thousands of trips like the Houston Ship Channel, or very light vessel traffic, only few barges per week, month, or year like the San Jacinto River. Mile markers that fell somewhere in between these extremes were considered medium (See Table 1.6).

Table 1.6: Reported Number of Vessel Trips at Study Area Bridges

Bridge No.	Roadway	Water Body	Barge Group	Tugs	Domestic Ship	Assumed Traffic Density
3	S.H. 332	GIWW	7,422	866	1,558	1.6
4	F.M. 1495	GIWW	6,616	1,734	506	1.6
6	F.M. 521	San Bernard River	248	112	0	1.0
7	F.M. 2611	San Bernard River	248	112	0	1.0
8	S.H. 124	GIWW	10,170	551	587	1.6
10	I.H. 45	GIWW	7,203	2,134	491	1.6
11	U.S. 90-A	Houston Ship Channel	218	97	0	1.0
12	Loop 610	Houston Ship Channel	10,705	4,023	705	1.6
14	S.H. 146	Houston Ship Channel	14,634	1,431	578	1.6
16	Beltway 8	Houston Ship Channel	14,474	6,069	778	1.6
18	F.M. 2031	GIWW	6,338	907	574	1.6
19	F.M. 457	GIWW	6,338	907	574	1.6
22	P.R. 22	GIWW	1,204	347	150	1.0
23	S.H. 361	GIWW	4,186	321	791	1.3
24	I.H. 10	Trinity River	2	4	0	1.0
25	S.H. 73	Neches River	8,003	417	143	1.6
26	S.H. 87	GIWW	14,390	1,338	704	1.6
27	S.H. 82	GIWW	14,390	1,338	0	1.6
30	Queen Isabella Memorial Causeway	GIWW	2,101	119	323	1.3
31	F.M. 106	Arroyo Colorado	295	32	0	1.0

Source: U.S. Army Corps of Engineers Waterborne Commerce Statistics Center, 2002.

Conclusion

A very significant effort was undertaken to collect the data required by the researchers so that they could simulate the probability and effect of vessel collisions on bridges along the GIWW and Texas' inland waterways using the most realistic dataset that could be produced. When actual data could not be obtained from the Corps, simulations were performed, as outlined here, based on realistic assumptions to create a usable dataset.

Appendix A

Institute for Water Resources

US Army Corps
Of Engineers

Reply To:

Waterborne Commerce Statistics Center
P. O. Box 61280
New Orleans, LA 70161-1280
(504) 862-1424   FAX (504) 862-1423
ceiwr-ndc-qc@mvn02.usace.army.mil

BRIDGE STUDY DATA

FIELD DESCRIPTIONS / FILE LAYOUT

Field 1*DIRECTION	Text(10)	Upbound: Traffic that moves in an upstream direction. For waterways without a characteristic monodirectional flow (e.g. the Gulf Intracoastal Waterway), "upbound" means in a northerly or easterly direction.
		Downbound: Traffic that moves in a downstream direction. For waterways without a characteristic monodirectional flow, "downbound" means in a southerly or westerly direction.
Field 2*TRANSFER TYPE	Text(10)	1 = cargo, 2 = tonmiles, 3 = trips
Field 3*VESSEL TYPE	Text(2)	1 = Self-Propelled, Dry Cargo
		2 = Self-Propelled, Tanker
		3 = Towboat
		4 = Non-Self Propelled, Dry Cargo
		5 = Non-Self Propelled, Tanker
		6 = Other (undefined)
Field4*NRT	Text(6)	The volume of space available for the accommodation of passengers and the stowage of cargo, expressed in units of 100 cubic feet for each net register ton.
Field 5*CAP_TONS	Text(10)	Capacity Tons specify the full load capacity in short tons (2000)
Field 6*LENGTH	Text(10)	Specifies the register length of the vessel reported in units of feet to the nearest tenth.
Field 7*BREADTH	Text(10)	Specifies the breadth of a vessel at its widest part measured from the outer side of the planking or plating on one side to the corresponding point on the opposite side.
Field 8*DRAFT	Text(3)	Specifies the draft of the vessel when loaded or light, reported in units of feet to nearest tenth.
Field 9*TRIPS	Text(10)	A vessel movement. For self-propelled vessels, a trip is logged between every point of departure and every point of arrival. For loaded barges, a trip is logged from the point of loading of the barge to the point of unloading of the barge. For empty barges, trips are logged from point of unloading to the point of loading counting the fleeting areas in between.
Field 10*TONS	Text(10)	Short tons in thousands (0 means less than 500 tons)
Field 11*LOAD_DRAFT	Text(10)	Specifies the draft of the vessel when fully loaded, reported in units of feet to nearest tenth.
Field 12*LIGHT_DRAFT	Text(10)	Specifies the draft of the vessel when it is empty, reported in units of feet to nearest tenth.
Field 13*LIGHT	Text(1)	0 = loaded move
		1 = light move/trip only
Field 14*H-F-POINT	Text(10)	Specifies the height of the highest fixed point on the vessel in units of feet to the nearest tenth.
Field 14*YEAR	Text(2)	Calendar year the movement took place based on date of unloading.
Field 15*CONTAINERIZED	Text(1)	

Appendix B

BRIDGE_NUMBER	NAME	MILE_MARKER	VESSEL_FLEET	PARCURRENT	PERPCURRENT	TRAFFIC_DENSITY	MINIMUM_IMPACT_SPEED
3	GIWW	394	VF3D	1.078	N/A	1.6	2.080
3	GIWW	394	VF3U	1.078	N/A	1.6	2.080
4	GIWW	398	VF4D	N/A	N/A	1.6	N/A
4	GIWW	398	VF4U	N/A	N/A	1.6	N/A
6	SAN BERNARD RIVER	10	VF6D	N/A	N/A	1.0	N/A
6	SAN BERNARD RIVER	10	VF6U	N/A	N/A	1.0	N/A
7	SAN BERNARD RIVER	11	VF7D	N/A	N/A	1.0	N/A
7	SAN BERNARD RIVER	11	VF7U	N/A	N/A	1.0	N/A
8	GIWW	319	VF8D	0.196	N/A	1.6	0.627
8	GIWW	319	VF8U	0.196	N/A	1.6	0.627
10	GIWW	357	VF10D	0.703	N/A	1.6	1.500
10	GIWW	357	VF10U	0.703	N/A	1.6	1.500
11	HOUSTON SHIP CHANNEL	52	VF11D	0.336	N/A	1.0	1.091
11	HOUSTON SHIP CHANNEL	52	VF11U	0.336	N/A	1.0	1.091
12	HOUSTON SHIP CHANNEL	47	VF12D	0.336	N/A	1.6	1.091
12	HOUSTON SHIP CHANNEL	47	VF12U	0.336	N/A	1.6	1.091
14	HOUSTON SHIP CHANNEL	27	VF14D	0.336	N/A	1.6	1.091
14	HOUSTON SHIP CHANNEL	27	VF14U	0.336	N/A	1.6	1.091
16	HOUSTON SHIP CHANNEL	38	VF16D	0.336	N/A	1.6	1.091
16	HOUSTON SHIP CHANNEL	38	VF16U	0.336	N/A	1.6	1.091
18	GIWW	441	VF18D	0.901	N/A	1.6	1.780
18	GIWW	441	VF18U	0.901	N/A	1.6	1.780
19	GIWW	418	VF19D	N/A	N/A	1.6	N/A
19	GIWW	418	VF19U	N/A	N/A	1.6	N/A
22	GIWW	553	VF22D	0.313	N/A	1.0	0.600
22	GIWW	553	VF22U	0.313	N/A	1.0	0.600
23	GIWW	533	VF23D	0.305	N/A	1.3	0.716
23	GIWW	533	VF23U	0.305	N/A	1.3	0.716
24	TRINITY RIVER	13	VF24D	N/A	N/A	1.0	N/A
24	TRINITY RIVER	13	VF24U	N/A	N/A	1.0	N/A
25	NECHES RIVER	40	VF25D	N/A	N/A	1.6	N/A
25	NECHES RIVER	40	VF25U	N/A	N/A	1.6	N/A
26	GIWW	289	VF26D	N/A	N/A	1.6	N/A
26	GIWW	289	VF26U	N/A	N/A	1.6	N/A
27	GIWW	286	VF27D	N/A	N/A	1.6	N/A
27	GIWW	286	VF27U	N/A	N/A	1.6	N/A
30	GIWW	665	VF30D	0.039	0.188	1.3	0.216
30	GIWW	665	VF30U	0.039	0.188	1.3	0.216
31	ARROYO COLORADO	23	VF31D	N/A	N/A	1.0	N/A
31	ARROYO COLORADO	23	VF31U	N/A	N/A	1.0	N/A